GDAŃSK UNIVERSITY OF TECHNOLOGY
FACULTY OF CHEMISTRY

The author of the PhD dissertation: Daria Biernacka
Scientific discipline: Chemical Sciences

DOCTORAL DISSERTATION

Title of PhD dissertation: Regulation of LPS assembly via controlled proteolysis and sensing of LPS stress in *Escherichia coli.*

Title of PhD dissertation (in Polish): Regulacja składania LPSu poprzez kontrolowaną proteolizę oraz wykrywanie stresu komórkowego w odpowiedzi na defekty LPSu u *Escherichia coli.*

Supervisor *signature*
Prof. dr. Satish Raina

Gdańsk, 2021

GDAŃSK UNIVERSITY OF TECHNOLOGY
FACULTY OF CHEMISTRY

STATEMENT

The author of the PhD dissertation: Daria Biernacka

I, the undersigned, agree that my PhD dissertation entitled:
Regulation of LPS assembly via controlled proteolysis and sensing of LPS stress in *Escherichia coli*
may be used for scientific or didactic purposes.[1]

Gdańsk,..... .....
signature of the PhD student

Aware of criminal liability for violations of the Act of 4th February 1994 on Copyright and Related Rights (Journal of Laws 2006, No. 90, item 631) and disciplinary actions set out in the Law on Higher Education (Journal of Laws 2012, item 572 with later amendments),[2] as well as civil liability, I declare, that the submitted PhD dissertation is my own work.

I declare, that the submitted PhD dissertation is my own work performed under and in cooperation with the supervision of Prof. dr Satish Raina.

This submitted PhD dissertation has never before been the basis of an official procedure associated with the awarding of a PhD degree.

All the information contained in the above thesis which is derived from written and electronic sources is documented in a list of relevant literature in accordance with art. 34 of the Copyright and Related Rights Act.

I confirm that this PhD dissertation is identical to the attached electronic version.

Gdańsk,..... .....
signature of the PhD student

I, the undersigned, agree to include an electronic version of the above PhD dissertation in the open, institutional, digital repository of Gdańsk University of Technology, Pomeranian Digital Library, and for it to be submitted to the processes of verification and protection against misappropriation of authorship.

Gdańsk,..... .....
signature of the PhD student

[1] Decree of Rector of Gdansk University of Technology No. 34/2009 of 9th November 2009, TUG archive instruction addendum No. 8.

[2] Act of 27th July 2005, Law on Higher Education: Chapter 7, Criminal responsibility of PhD students, Article 226.

GDAŃSK UNIVERSITY OF TECHNOLOGY
FACULTY OF CHEMISTRY

DESCRIPTION OF DOCTORAL DISSERTATION

The Author of the PhD dissertation: Daria Biernacka

Title of PhD dissertation: Regulation of LPS assembly via controlled proteolysis and sensing of LPS stress in *Escherichia coli*

Title of PhD dissertation in Polish: Regulacja składania LPSu poprzez kontrolowaną proteolizę oraz wykrywanie stresu komórkowego w odpowiedzi na defekty LPSu u *Escherichia coli*

Language of PhD dissertation: English

Supervision: Prof. dr Satish Raina

Date of doctoral defense:

Keywords of PhD dissertation in Polish: lipopolisacharyd, LapB, LapC, YejM, LpxC, HslV/U, RpoE

Keywords of PhD dissertation in English: lipopolysaccharide, LapB, LapC, YejM, LpxC, HslV/U, RpoE

Summary of PhD dissertation in Polish: Biosynteza lipopolisacharydu (LPSu) wymaga niezbędnego dla żywotności bakterii białka LapB w celu regulacji, za pośrednictwem proatezy FtsH, ilości enzymu LpxC katalizującego pierwszy nieodwracalny etap syntezy LPSu. Aby lepiej zrozumieć podstawowe funkcje LapB oraz jego rolę w regulacji LpxC, zanalizowano wielokopijne supresory mutanta Δ*lapB,* ujawniając rolę proteazy HslUV w regulacji LpxC, definiując po raz pierwszy alternatywny szlak degradacji LpxC. Izolacja i charakterystyka pozagenowych mutacji supresorowych, które zapobiegają śmiertelności Δ*lapB* przez przywrócenie normalnej syntezy LPS, zidentyfikowała mutację przesunięcia ramki odczytu w niezbędnym genie oznaczony jako *lapC*. Sugerowało to, że LapB i LapC mogą działać antagonistycznie. Ten sam gen *lapC* zidentyfikowano podczas poszukiwań mutacji, które jednocześnie indukują transkrypcję z promotora *rpoE*P3, który odpowiada na defekty LPSu, nadają wrażliwość na inhibitor LpxC CHIR090 i wykazują fenotyp wrażliwy na temperaturę. Mutacje supresorowe zidentyfikowanych mutantów *lapC*, które odtwarzały wzrost w podwyższonych temperaturach, zmapowane zostały w genach *lapA/lapB*, *lpxC* i *ftsH*. Mutacje te przywracały normalne poziomy LPSu i zapobiegały proteolizie LpxC w mutantach *lapC*. Dodatkowo wykazano, że można skonstruować delecję *lapC* w szczepach, które albo nadprodukują LpxC, albo mają delecję *lapB*, ujawniając, że FtsH, LapB i LapC wspólnie regulują syntezę LPS poprzez kontrolowanie ilości LpxC.

Summary of PhD dissertation in English: Lipopolysaccharide (LPS) assembly requires the essential LapB protein to regulate LpxC enzyme that catalyzes the first committed step in the LPS synthesis by FtsH-mediated degradation. To further understand the molecular basics LapB essential function and its role in LpxC turnover, multicopy suppressors analysis of Δ*lapB* revealed the role of HslUV protease in LpxC regulation, providing the first alternative pathway of LpxC degradation. Isolation and characterization of an extragenic suppressor mutation that prevents lethality of Δ*lapB* by restoration of normal LPS synthesis identified a frame-shift mutation after 377 aa in the essential gene designated *lapC*, suggesting LapB and LapC act antagonistically. The same *lapC* gene was identified during search for mutations that simultaneously induce transcription from *rpoE*P3 promoter that responds to LPS defects, confer sensitivity to LpxC inhibitor CHIR090 and exhibit a temperature-sensitive phenotype. Suppressors of isolated *lapC* mutants that restored growth at elevated temperatures mapped to *lapA*/*lapB*, *lpxC* and *ftsH* genes. Such mutations restored normal levels of LPS and prevented proteolysis of LpxC in *lapC* mutants. Additionally, it was shown that a *lapC* deletion could be constructed in strains that either overproduce LpxC or have *lapB* deletion, revealing that FtsH, LapB and LapC together regulate LPS synthesis by controlling LpxC amounts.

Acknowledgments

First and the foremost, I would like to express my deepest gratitude to my supervisor, Professor dr. Satish Raina, who has a substance of a genius, knowing Escherichia coli like no other person in this world. I could not be more grateful for shared expertise, valuable guidance, dedicated time and the constant encouragement to be professional and the best of myself. Thank you, Professor, for providing me with invaluable wealth of your knowledge.

I am also highly indebt to Professor dr hab. Gracjana Klein-Raina for sharing her phenomenal laboratory experience, for her meaningful and patient assistance and admirable commitment to the highest standards of research.

I would also like to thank other members of Laboratory of Bacterial Genetics, Ania and Paweł, for your help, companionship and a wonderful atmosphere when working together.

Last, but not least, I would like to express my warm and heartfelt thanks to my family, friends and my partner whose constant love and support keep me motivated and confident.

This research was funded by National Science Center (NCN) Grant 2017/25/B/NZ6/02021 granted to Prof. dr. Satish Raina.

CONTENTS

STRESZCZENIE

Lipopolisacharyd (LPS) to złożony pod względem budowy glikolipid, niezbędny dla życia bakterii. Wspólnie z fosfolipidami stanowi główny amfifilowy składnik błony zewnętrznej większości bakterii Gram-ujemnych, w tym bakterii *Escherichia coli*. Cząsteczki LPSu czynią z błony zewnętrznej bakterii selektywnie przepuszczalną barierę oraz odgrywają kluczową rolę w interakcjach między bakteriami a środowiskiem zewnętrznym. Synteza LPSu i fosfolipidów jest ściśle regulowana i utrzymywana w stałym wzajemnym stosunku. Wszelkie zmiany w równowadze pomiędzy tymi składnikami nie są tolerowane przez bakterie i powodują śmierć komórki. W celu utrzymania tej równowagi pomiędzy szlakami biosyntetycznymi oraz w celu odpowiedniej dystrybucji wspólnego ich prekursora, *R*-3-hydroksymirystynianu, ilości białek FabZ (dla fosfolipidów) i LpxC (dla LPSu), które katalizują pierwsze reakcje stanowiące rozgałęzienie pomiędzy szlakami, są skorelowane *in vivo*. Regulowana proteoliza białka LpxC, które odpowiedzialne jest za katalizę pierwszego nieodwracalnego etapu biosyntezy LPSu, jest punktem kontrolnym zapewniającym balans pomiędzy składnikami błony zewnętrznej. LpxC to niestabilny enzym, a jego ilość regulowana jest za pomocą białka LapB, które przeznacza LpxC do degradacji przez proteazę FtsH. Aby lepiej zrozumieć mechanizm działania białka LapB oraz jego rolę w regulowaniu ilości LpxC, poszukiwano wielokopijnych supresorów przywracających żywotność mutanta Δ*lapB*. Przyczyniło się to do ujawnienia roli proteaz HslUV w regulacji ilości LpxC, determinując po raz pierwszy alternatywny szlak degradacji LpxC. Ponadto postanowiono scharakteryzować nowe pozagenowe mutacje supresorowe, które zapobiegałyby śmiertelności mutanta Δ*lapB*, dzięki przywróceniu normalnej syntezy LPSu. W ten sposób zidentyfikowano mutację przesunięcia ramki odczytu w niezbędnym dla życia bakterii genie nazwanym jako *lapC*. Odkrycie sugerowało, że białka LapB i LapC mogą działać w sposób antagonistyczny. Ten sam gen *lapC* zidentyfikowano podczas poszukiwań mutacji, które jednocześnie indukują transkrypcję z promotora *rpoE*P3 aktywowanego w odpowiedzi na defekty LPSu, nadają bakterii wrażliwość na inhibitor enzymu LpxC, CHIR090, oraz wykazują wrażliwość na wysoką temperaturę. Zdefiniowano także mutacje supresorowe, które przywracały żywotność bakterii ze zmutowanym genem *lapC*, zmapowane w genach *lapA/lapB*, *lpxC* i *ftsH*. Mutacje odtwarzały normalne poziomy LPSu i zapobiegały proteolizie LpxC w mutantach *lapC*. Pokazano również, że gen *lapC*, mimo jego niezbędności, można usunąć w szczepach nadprodukujących LpxC lub z usuniętym genem *lapB.* Wyniki przedstawionych badań dowiodły, że białka FtsH, LapB i LapC oddziałują ze sobą i wspólnie regulują syntezę LPSu poprzez kontrolowanie ilości enzymu LpxC.

Słowa kluczowe: lipopolisacharyd, LapB, LapC, YejM, LpxC, HslV/U, RpoE

ABSTRACT

Lipopolysaccharide (LPS) is a complex glycolipid, essential for the bacterial viability and along with phospholipids, it constitutes the major amphiphilic component of outer membrane (OM) in most of the Gram-negative bacteria, including *Escherichia coli*. LPS molecules confer an effective permeability barrier to the OM and play a crucial role in bacteria-environment and -host interactions. The synthesis and accumulation of this highly heterogeneous in the composition molecule are controlled by abundance of regulatory factors and growth conditions. Furthermore, the synthesis of LPS and phospholipids is tightly co-regulated and held at a nearly constant ratio. Any alterations in the balance of phospholipids and LPS are not tolerated by bacteria and cause cell death. This balance is achieved by tightly regulated turnover of unstable LpxC enzyme to maintain the flux of common precursor for the utilization in either LPS or phospholipid biosynthetic pathways. It constitutes an essential branch point in the biosynthesis of phospholipids and the lipid A part of LPS and simultaneously determines the first committed step in LPS biosynthetic pathway. It has been reported that LPS assembly requires the essential LapB protein to regulate FtsH-mediated proteolysis of LpxC protein. To further understand the function of LapB and its role in LpxC turnover, multicopy suppressor screening of Δ*lapB* was employed and it revealed a role for HslUV proteases in regulating LpxC amounts, providing the first alternative pathway of LpxC degradation. Isolation and characterization of an extragenic suppressor mutation that prevents lethality of Δ*lapB* by restoration of normal LPS synthesis identified a frame-shift in the essential gene designated *lapC*, suggesting LapB and LapC act antagonistically. The same *lapC* gene was identified during selection for mutations that induce transcription from LPS defects-responsive *rpoE*P3 promoter, confer sensitivity to LpxC inhibitor CHIR090 and exhibit a temperature-sensitive phenotype. Suppressors of *lapC* mutants that restored growth at elevated temperatures mapped to *lapA*/*lapB*, *lpxC* and *ftsH* genes. Such suppressor mutations restored normal levels of LPS and prevented excessive proteolysis of LpxC in *lapC* mutants. Interestingly, a *lapC* deletion could be constructed in strains either overproducing LpxC or in the absence of LapB, revealing that FtsH, LapB and LapC together regulate LPS synthesis by controlling LpxC amounts.

Keywords: lipopolysaccharide, LapB, LapC, YejM, LpxC, HslV/U, RpoE

LIST OF MAJOR DESIGNATIONS AND ABBREVIATIONS

Δ	-	indication of the absence of the gene
ATP	-	adenosine triphosphate
ADP	-	adenosine diphosphate
bp	-	base pair(s)
σ^{32} (RpoH)	-	heat shock sigma factor
σ^{E} (RpoE)	-	extracytoplasmic stress sigma factor
CAMP	-	cationic antimicrobial peptide
CHIR090	-	*N*-aroyl-L-threonine hydroxamic acid
Gal	-	galactose
Glc	-	glucose
GlcN	-	glucosamine
GlcN-6-P	-	glucosamine-6-phosphate
GlcUA	-	glucuronic acid
Hep	-	heptose
IM	-	inner membrane
IPTG	-	isopropyl 1-thio-*β*-D-galactopyranoside
Kdo	-	3-deoxy-*α*-D-*manno*-oct-2-ulosonic acid
Lac up	-	increased *β*-galactosidase activity
L-Ara4N	-	4-amino-4-deoxy-L-arabinose
LPS	-	lipopolysaccharide
ncRNA (sRNA)	-	non-coding RNA, small regulatory RNA
nt	-	nucleotide
OM	-	outer membrane
P-EtN	-	phosphoethanolamine
TCS	-	two-component system
UDP-GlcNAc	-	uridine diphosphate *N*-acetylglucosamine
wt	-	wild type

1. INTRODUCTION

Bacteria, like any other living organism, need to interact with the surrounding environment. In order to persist in dynamically changing settings, and function accurately, microorganisms like *Escherichia coli* evolved complex mechanisms providing rapid and exact response to different external and internal stimuli. The cell envelope is the first barrier that separates majority of bacteria from environment. It ensures cellular integrity, serves as a protection barrier, but also functions as a transport and communication structure[1]. Cell envelope is subjected to the intensive research as it is an increasingly popular target for novel compounds that act as antibiotics and are expected to help combat rising microbial multidrug resistance[2]. In Gram-negative bacteria, lipopolysaccharide (LPS) is one of the critical components that executes envelope functionality.

1.1. LPS emplacement within envelope components of E. coli

The envelope of *E. coli*, a Gram-negative model bacterium, consists of three main layers: an inner membrane (IM), a periplasm with thin peptidoglycan, and the distinctive for Gram-negative bacteria outer membrane (OM), whose outer leaflet main constituent is lipopolysaccharide[3]. All these components are illustrated in the model of *E. coli* envelope in Figure 1.1. below, and further described.

The inner membrane is a symmetric bilayer of phospholipids surrounding aqueous cytoplasm. In *E. coli*, the IM primary consists of phosphatidyl ethanolamine and phosphatidyl glycerol phospholipids. Other minor lipids include phosphatidyl serine, cardiolipin and polyisoprenoid carriers[4]. Proteins and lipoproteins are embedded within the bilayer structure of the IM, either anchored with *α*-helical transmembrane domains or through lipid modifications of terminal amino acids, accordingly[3]. The periplasmic space is the compartment that is surrounded by the inner and outer membranes. It is oxidizing in nature and much more viscous and protein-rich than the cytoplasm. Within the periplasm a thin 2-7 nm layer of peptidoglycan (cell wall) is enclosed[5,6]. It is reported that *E. coli* periplasm encompasses more than 300 different proteins that perform a vast array of functions, starting with a fundamental protein folding, nutrients governance or different proteins manipulations[7]. The cell wall component

provides bacteria with shape, rigidity, and protection from turgor. The durability of peptidoglycan is based on its mesh-like structure formed with alternating glycan strands of *N*-acetylglucosamine (GlcNAc) and *N*-acetylmuramic acid (MurNAc) that are cross-linked by short peptides[8,9].

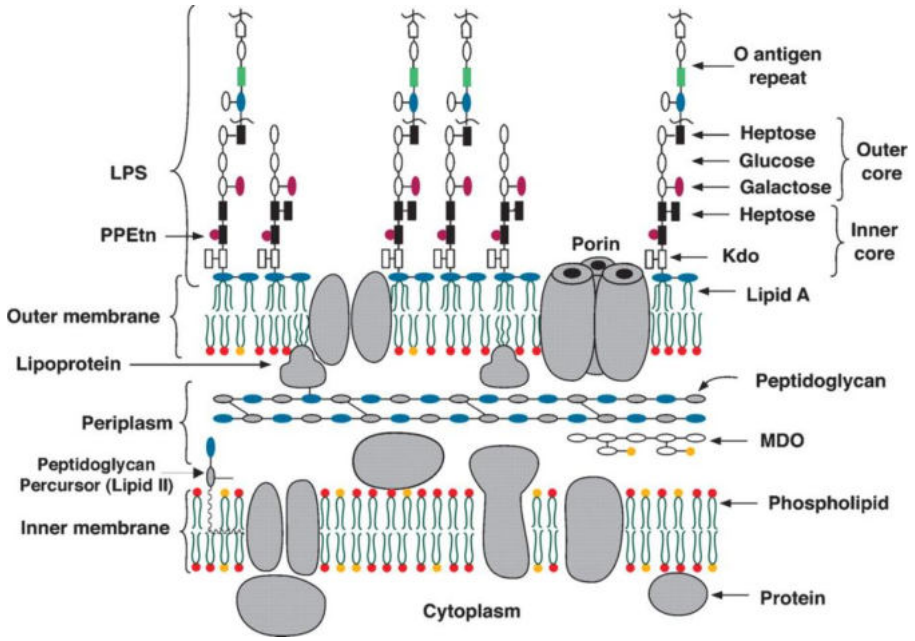

Fig. 1.1. Schematic structure of *E. coli* envelope[10]

The outermost structure, the outer membrane, is an asymmetric lipid bilayer that is also essential for bacterial viability. Its inner leaflet is composed of phospholipids, in similar manner like within the IM, and LPS is the most abundant molecule of the outer leaflet[3]. Structure and architecture of OM is overall conserved among Gram-negative bacteria[11] and LPS contributes to many characteristic features of OM, like selective permeability of membrane, signal transduction, interaction with host immune system and other, which will be described later in greater detail[12,13]. Among the other OM components, there can be distinguished outer membrane proteins (OMPs) and lipoproteins. Most of OMPs are transmembrane proteins adopting *β*-barrel conformation and their main function is to allow passive diffusion of small compounds across the membrane, as well as the contribution to membrane transport machinery as porins channels or receptors[3]. The most prominent among lipoproteins is Lpp that is known to be the most numerically abundant protein reaching over 500,000 molecules per cell[11]. Lpp is covalently attached to the peptidoglycan and plays important role in sustaining the OM structure and integrity[14,15].

1.2. Structure of lipopolysaccharide of E. coli

Lipopolysaccharide determines most of the outer monolayer of nearly all Gram-negative bacteria and has a great influence on maintaining envelope functionality[16]. In *Escherichia coli*, 75% of its surface is covered with LPS that is equal to approximately two million molecules of this glycolipid per cell[17].

1.2.1. Composition of LPS

LPSs are complex glycolipids but share overall common architecture and are composed of three main elements presented in Figure 1.2.: the most conserved is the lipid A part, then core oligosaccharide (core OS) and optional, present in 'smooth' type bacteria, *O*-antigen (*O*-polysaccharide, *O*-PS)[18].

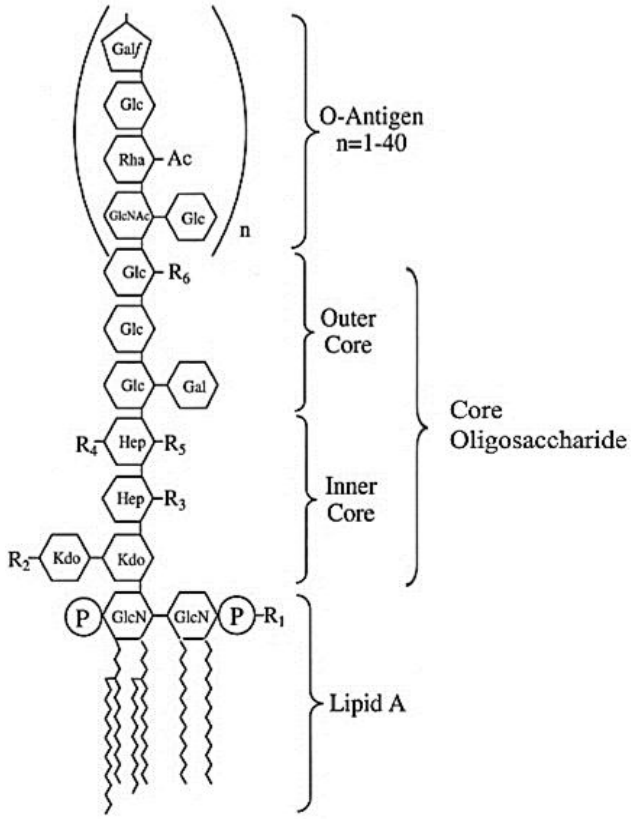

Fig. 1.2. Schematic representation of *E. coli* K-12 LPS, modified based on[19]
Abbreviations used in the figure: GlcN: D-glucosamine; Kdo: 3-deoxy-*α*-D-*manno*-oct-2-ulosonic acid; Hep: L-*glycero*-D-*manno*-heptose; Glc: D-glucose; Gal: D-galactose; GlcNAc: *N*-acetyl-D-glucosamine; Rha: L-rhamnose; Galf: D-galactofuranose; P: phosphate; Ac: acetate. R groups mark common chemical modifications. R1: phosphate; R2: Kdo, rhamnose, or phosphoethanolamine; R3: phosphate or ethanolamine pyrophosphate; R4: phosphate; R5: heptose; R6: heptose or GlcNAc.

1.2.2. Structure of lipid A

The primary component of LPS, lipid A, which is depicted in detail in Figure 1.3., structurally is a phosphorylated at positions 1 and 4', and acylated with *R*-3-hydroxymyristate at positions 2, 3, 2' and 3', *β*(1→6)-linked glucosamine (GlcN) disaccharide that anchors LPS in the outer membrane. Its two *R*-3-hydroxy-acyl groups of the nonreducing glucosamine are further esterified, most commonly with laurate ('12' in Fig. 1.3.) and myristate ('14' in Fig. 1.3.)[18,20–23].

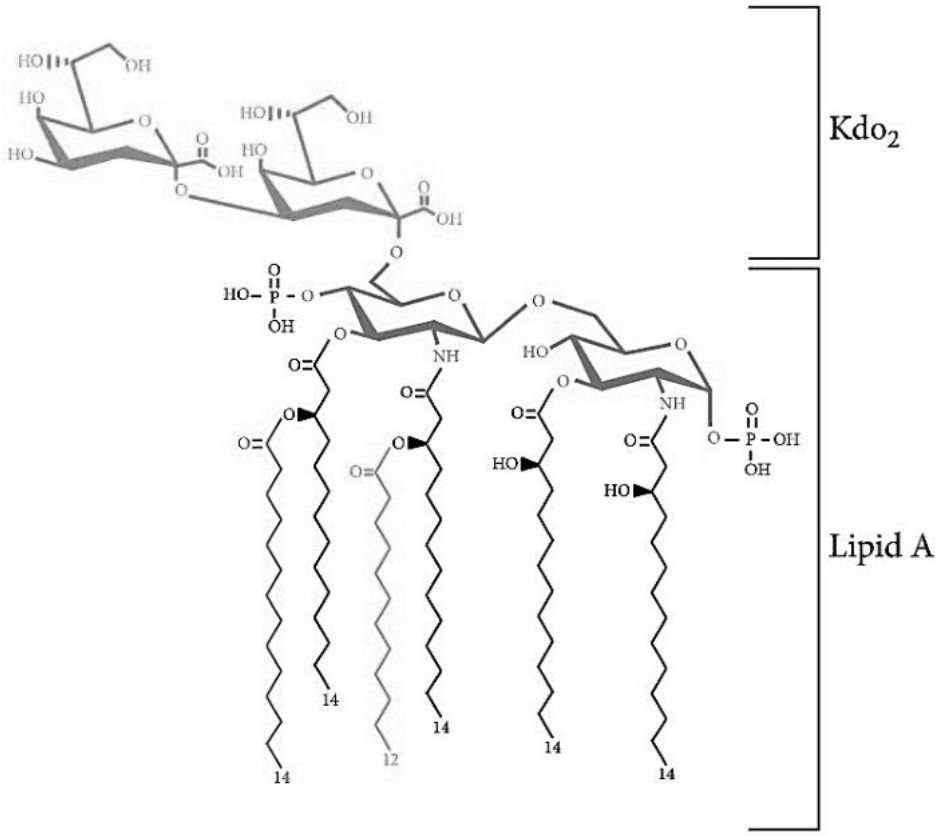

Fig. 1.3. Covalent structure of *E. coli* K-12 lipid A-Kdo$_2$[24]
Numbers 12 and 14 indicate carbon atoms quantity in fatty acyl moiety decorating lipid A; 12 - lauroyl group, 14 - myristoyl group.

A glycosidic linkage between the O-6' position of the lipid A and the sugar, a 3-deoxy-*α*-D-*manno*-oct-2-ulosonic acid (Kdo I), forms the connection of lipid A with the next LPS segment, the core oligosaccharide[18,25]. Presented in Figure 1.3. arrangement of hexaacylated lipid A with two first saccharides, which are two Kdo moieties (lipid A-Kdo$_2$), represents the first known minimal LPS

structure sufficient for *E. coli* survival up to 42°C[18]. It was established later by Professor Raina's group that it was possible to construct viable and suppressor-free strains that synthesize even smaller structures composed of only tetraacylated lipid A (lipid IV_A) or lipid IV_A-Kdo_2 under slow growing conditions (minimal medium at 23°C)[26]. However, strains that synthesize such minimal LPSs are characterized with very narrow growth range, defects in cell division, hyper-induced RpoE-regulated stress response and Cpx signal transduction pathway, without requirement for suppressors to be present in order to maintain *E. coli* viability under such growth conditions[26].

1.2.3. Structure of core oligosaccharide

The core OS component of LPS that starts with Kdo disaccharide is conventionally divided into the inner core that is proximal to lipid A and more conserved in nature, and the outer core that exhibits greater variability in composition. In addition to Kdo residues, the inner core usually contains L-*glycero*-D-*manno*-heptoses (Hep in Fig. 1.2.) and can be modified with additional, non-stoichiometric substituents including phosphate groups (R2-R4 in Fig. 1.2.)[27,28]. The outer core is more exposed to environment on the cell's surface portion of LPS and that is one of the reasons that it is characterized by greater variability in structure than the inner region. Composition of outer region of core OS is based on common saccharides such as glucose, galactose, heptose, *N*-acetylglucosamine or *N*-acetylgalactosamine[26,28,29]. Both lipid A-Kdo_2 and core region are relatively dynamic structures and are subjected to varied modifications in response to activation of two-component systems, non-coding RNAs and stress-induced pathways resulting in formation of so far known seven different LPS glycoforms[24] that will be described in detail in further subsections.

1.2.4. O-antigen

The most outwards directed part of LPS, *O*-antigen, is an often branched polysaccharide composed of numerous repeating oligosaccharide units (*O*-units) that contain two to seven sugars and sugar derivatives[30,31]. *O*-antigen structure varies between strains, with over 160 different known *O*-polysaccharide variants produced by *E. coli* alone[12]. The parental strain of *E. coli* K-12, utilized in this study, was first isolated almost 100 years ago and it lost the ability to synthesize

its *O*-antigen due to a mutation in *rfb* gene cluster. It was probably a result of passaging and human manipulations, as there was no advantage to produce metabolically demanding component, unnecessary in laboratory conditions[32]. Although this dissertation does not refer to *O*-antigen of LPS, it is important to mention that the diversification of polysaccharide presented by bacteria allows them to introduce different surfaces that offer specific advantages in different niches[33]. Human body can be considered such a niche, and among commensal and pathogenic strains of *E. coli*, with latter causing severe infectious diseases, *O*-antigen became a standard in categorizing the strains for taxonomical and epidemiological purposes[31]. Additionally, the presence or absence of *O*-chain is used to categorize LPS molecules as 'rough' or 'smooth'. Full-length *O*-polysaccharide render oval 'smooth' bacterial colonies, whereas the reduction or absence of LPS structure resulted in colonies with irregular 'rough' edges, and often more susceptible to environmental challenges, such as hydrophobic antibiotics[34].

1.3. Overview on lipopolysaccharide biosynthesis

Lipopolysaccharide is synthesized continuously as bacteria grow and divide. There are more than 100 genes involved in LPS formation and functioning, some of them being essential for bacterial viability and unique for the species.

1.3.1. The Raetz pathway of lipid A-Kdo$_2$ formation and regulation of the first committed step in LPS biosynthesis

The biosynthesis of minimal LPS and further lipid A–Kdo$_2$ was organized in nine sequential enzymatic steps named Raetz pathway that is presented in Figure 1.4.[35].

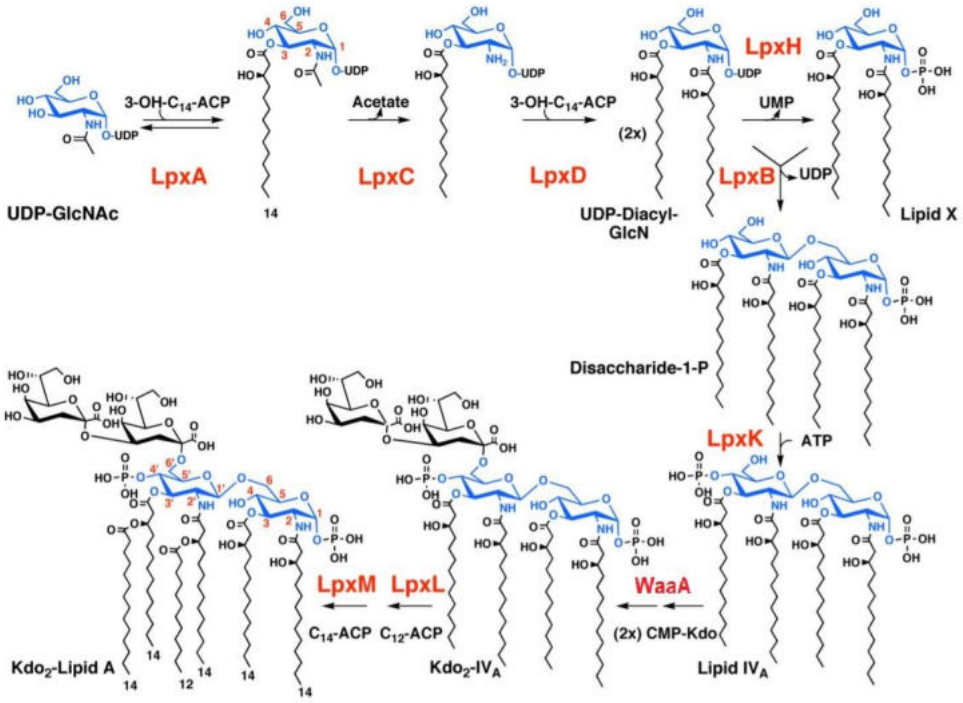

Fig. 1.4. The Raetz pathway for constitutive biosynthesis of *E. coli* K-12 lipid A-Kdo$_2$[35], modified

In blue the glucosamine disaccharide backbone of lipid A is marked. The Kdo$_2$ is black. In red letters enzymes involved in the pathway are depicted. LpxA, C and D are soluble cytoplasmic proteins, and LpxH and B are peripheral membrane proteins. LpxK and remaining enzymes of the pathway are IM proteins with the active sites facing the cytoplasm. The red numbers refer to the glucosamine ring positions of lipid A and its precursors. The predominant fatty acid chain lengths found in *E. coli* lipid A are indicated by the black numbers.

The process of lipid A-Kdo$_2$ biosynthesis starts at the interface between cytosol and the IM and begins with the fatty acylation of uridine diphosphate *N*-acetylglucosamine that is catalyzed by LpxA protein. LpxA enzyme is an acyl transferase that requires thioester *R*-3-hydroxymyristoyl acyl carrier protein

(ACP) as its donor substrate. Its active site precisely recognizes C14 hydroxyacyl chains of *R*-3-hydroxymyristate and incorporates them selectively two orders of magnitude faster than C12 or C16 chains[35–37]. The *R*-3-hydroxymyristoyl-ACP is also a substrate for FabZ dehydrase as a precursor for phospholipids biosynthesis[36]. Common substrate links the LPS and phospholipids pathways, whose biosynthesis is strictly coupled with a nearly constant ratio of 0.15:1.0 that must be preserved to maintain bacterial cell viability (Fig. 1.5.)[38]. LpxA-driven acylation, besides being the first biochemical step at the branchpoint of two biosynthetic pathways, has a highly unfavorable equilibrium constant, therefore the actual first committed step in LPS biosynthesis is the consecutive deacetylation of UDP-3-*O*-(acyl)-GlcNAc catalyzed by LpxC deacetylase (Fig. 1.5. and Fig. 1.6.)[39,40].

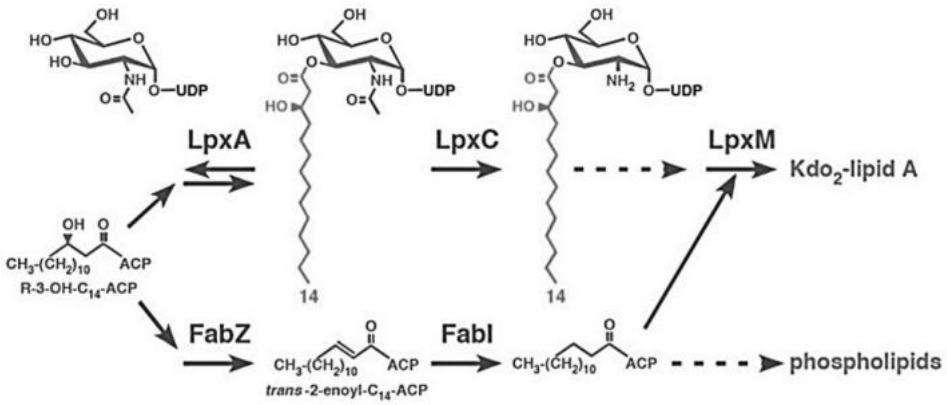

Fig. 1.5. The *R*-3-hydroxymyristoyl-ACP as a common precursor of LPS and phospholipids biosynthesis pathways[41]

The *R*-3-hydroxymyristoyl-ACP is common substrate for lipid A-Kdo_2 and phospholipids biosynthetic pathways. The main branchpoint constitutes of reaction performed by FabZ dehydrase, for phospholipids biosynthesis, and the deacetylation of UDP-3-*O*-(acyl)-GlcNAc catalyzed by LpxC deacetylase, as preceding step of the fatty acylation of UDP-GlcNAc is unfavorable.

LpxC is metalloenzyme encoded by a conserved among various Gram-negative bacteria single-copy gene[39,42]. It was originally categorized as Zn^{2+}-dependent deacetylase based on its reversible inhibition by metal chelators (for example incubation with ethylene diamine tetraacetic acid, EDTA) and its co-purification with Zn^{2+} ions under aerobic conditions (Fig. 1.5.)[42]. Following studies identified that the replacement of the Zn^{2+} with Fe^{2+} enhances the catalytic activity of LpxC approximately 6-fold and alters its affinity for ligands[43]. However, such substitution with different cofactor rendered the enzyme more susceptible to

oxidation *in vivo* and LpxC was characterized by essentially higher affinity for zinc than iron[43,44]. The model was proposed where LpxC could switch the active site metal depending on the cellular ion availability and under different environmental conditions which could constitute a regulatory and/or adaptative mechanism[43,44].

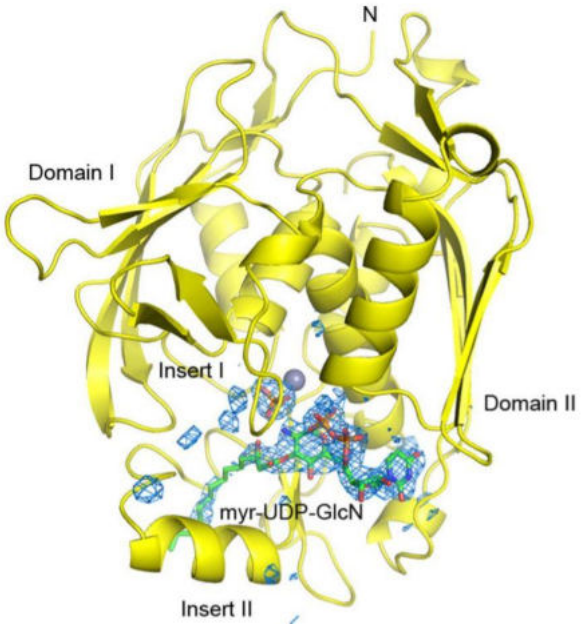

Fig. 1.6. Structure of *E. coli* LpxC bound to myr-UDP-GlcNAc[45]
Figure presents LpxC domain and fold architectures (in yellow). Myr-UDP-GlcN (UDP-(3-*O*-(*R*-3-hydroxymyristoyl))-*N*-acetylglucosamine) and phosphate are depicted in sticks molecular representation and blue mesh corresponds to electron densities for substrate and phosphate groups. Zn^{2+} ion in catalytic site is shown as silver sphere[45].

LpxC is a globular protein that contains two domains of similar *α*+*β* fold that are sandwiching the Zn^{2+}-containing active site (Fig. 1.6.)[45,46]. The Insert I and Insert II unique structures are elements that distinguish the two domains (Fig. 1.6.)[45]. The catalytic site of LpxC is located in a cleft formed at the base of the domain interface and Inserts I and II that form a hydrophobic tunnel known to bind fatty acids[45]. During deacetylation catalyzed by LpxC, enzyme removes the acetyl group from the amino moiety on UDP-(3-*O*-(*R*-3-hydroxymyristoyl))-*N*-acetylglucosamine. Reaction produces acetate and UDP-(3-*O*-(*R*-3-hydroxymyristoyl))-glucosamine (myr-UDP-GlcN in active site in Fig. 1.6.) that is further converted by subsequent enzymes[35,45].

Available amounts of LpxC determine the further rate of LPS biosynthesis, therefore this catalytic step is strictly regulated. It has been reported that in the presence of sublethal concentrations of LpxC inhibitors, the specific activity of enzyme increases up to 10-fold[47]. Similarly, when the amounts of cellular FabZ

change, cells increase or decrease the LpxC activity, accordingly[48]. Abundance of LpxC UDP-3-*O*-acyl-*N*-acetylglucosamine deacetylase is regulated in response to bacterium need for lipid A and occurs due to the proteolytic activity of FtsH[47,49]. FtsH is an IM-anchored and zinc-dependent metalloendoprotease that is essential for bacterial viability[50]. FtsH degrades number of cellular proteins, including heat shock sigma factor RpoH[51,52]. In the model of post-translational regulation of this heat shock sigma factor, DnaK chaperone binds to RpoH, preventing its interaction with RNA polymerase and activation of sigma 32-responsive genes. RpoH, captured by a chaperone, remains in a competent state for degradation by FtsH protease and the levels of RpoH are maintained low[53]. However, when DnaK machinery is occupied by substrates such as misfolded proteins that accumulate during stress response, chaperone is not available to bind RpoH to limit its activity through proteolysis and in this manner, sigma H activity is coupled directly with the level of misfolded proteins in the cell[54]. Despite participating in such an important cellular process, the essentiality of FtsH protease was found to rely on its key role in degradation of LpxC to prevent excessive LPS biosynthesis at the expense of synthesis of phospholipids[55]. Up to date, it is known that FtsH becomes dispensable only in the Δ*waaA* background at 21°C, which is attributed to the overall reduced level of LPS in the absence of WaaA transferase[56]. Moreover, it was found that the rate of LpxC proteolysis is regulated in cell growth manner - it accelerates during slow growth, and is stabilized under fast growing conditions as the LPS demand is high in order to maintain the membrane equilibrium in growing cells[57]. The proteolysis of deacetylase was discovered to require a C-terminal degradation signal within the final 11 amino acid residues and additional interaction between the proteins that could possibly explain the regulation of crucial process that still remained unclear[58].

Suspected additional interactions in FtsH-dependent LpxC degradation were confirmed further, when it was discovered that the mechanism hinge on another essential IM-anchored protein - the LPS assembly heat shock protein LapB[41,59]. Results published previously by Professor Raina's laboratory established that FtsH and LapB work together to regulate LpxC proteolysis (Fig. 1.7.). LpxC levels were highly increased in mutants where either the *lapB* or *ftsH* genes were deleted and the data showed that these proteins co-purify,

suggesting *in vivo* interaction between molecules. Mutations in either *lapB* or *ftsH*, or both of the genes also resulted in the increased amounts of LpxC, which led to overproduction of LPS at the expense of phospholipids due to deficiency of their common precursor, the *R*-3-hydroxymyristoyl-ACP[41]. As a reinforcement of above evidence, it was also established that the *lapB* or *ftsH* deletions in strains carrying either a hyperactive allele of the *fabZ* gene, *sfhC21,* or when the LPS synthesis is dampened due to mutations in either *lpxA* or *lpxD* genes, were much more tolerated by bacteria due to restoration of the ratio between OM components[41,59].

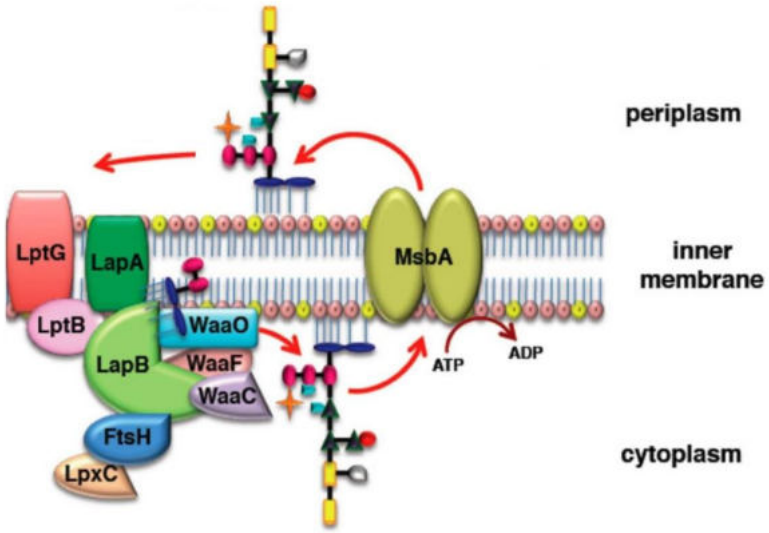

Fig. 1.7. Model of LPS biosynthesis and translocation machinery within envelope of *E. coli,* based on[41]

LapB is thought to function as a scaffold for the LPS biosynthetic enzymes and control point of LPS amounts. It could coordinate LPS synthesis on both leaflets of IM and direct LpxC to degradation by FtsH protease accordingly to demand for LPS molecule.

LapB (YciM), in parallel with its operon partner LapA (YciS), were discovered during the search for mutants with the elevated levels of envelope stress response in study concerning periplasmic folding factors[60]. Subsequent in-depth analysis revealed that these two proteins play an important role in LPS assembly, hence their names lipopolysaccharide assembly proteins LapA and LapB[41]. Detailed mutational study unveiled that single Δ*lapA* deletion was tolerated in many tested *E. coli* backgrounds[41]. Meanwhile, Δ(*lapA lapB*) or Δ*lapB* suppressor-free mutants could be obtained only in the BW25113 parental strain on M9 medium at 30°C after prolonged (72 h) incubation, and these mutants formed very small size colonies. In other commonly used wild-type strains such

as W3110 or BW30207, Δ(*lapA lapB*) and Δ*lapB* transductants were only obtained in the presence of plasmid carrying *lapA* and *lapB* genes[41]. Thus, it was concluded that the *lapB* gene is essential under standard laboratory growth conditions, and its deletion results in a severe growth defects[41]. In addition to already described results, the lethal phenotype of Δ*lapB* or Δ(*lapA lapB*) could be alleviated, if either the LPS synthesis was impaired due to mutation in the *waaC* gene or when non-coding sRNA SlrA (MicL), a translational repressor of the Lpp lipoprotein was overproduced[41,61]. The *lapA/B* transcription unit has three distinct promoters. The sequence of proximal promoter resembles house-keeping promoters, the middle promoter is recognized by heat shock sigma factor RpoH and the most distal promoter is located upstream of *pgpB* gene[41]. PgpB is one of three phosphatidylglycerophosphatases, which catalyze the dephosphorylation of phosphatidylglycerol phosphate to phosphatidylglycerol, an essential phospholipid of the inner and outer membrane in *E. coli*[62]*.* It was suggested that *lapA/B* and *pgpB* co-transcription can be another mechanism that couples transcription of *lapA*/*B* genes with phospholipid metabolism[41].

Despite showing that LapA and LapB interact with FtsH protease and LPS, it was still unclear what is the mechanism by which LapB regulates the LpxC proteolysis in response to LPS status. Modelling and crystal structure studies revealed that LapB contains three major structural motifs: the N-terminal transmembrane helix, nine tetratricopeptide repeats (TPRs) in its N-terminal domain and a C-terminal rubredoxin-like domain (Fig. 1.8.)[41,63]. The transmembrane helix anchors LapB to the IM with the soluble domain in the cytoplasm and the latter two structures were found to be bound together. This association of rubredoxin metal binding properties and scaffold-folding of TPR motifs of LapB is essential to mediate protein–protein interactions and enables the assembly of multiprotein complexes, necessary for the assembly and recruitment of LpxC and various LPS biosynthetic enzymes, aiding the general *E. coli* growth *in vivo*[41,63].

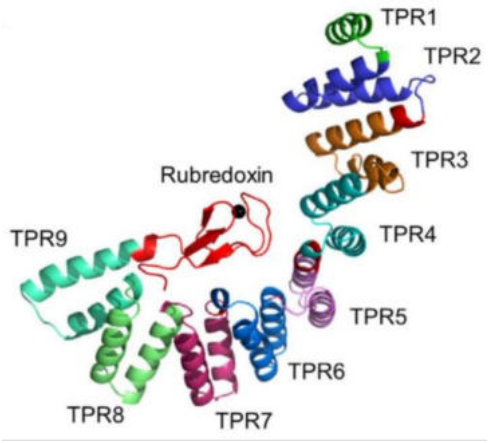

Fig. 1.8. Crystal structure of LapB monomer[63]
Nine TPR motifs are highlighted in the figure, rubredoxin domain is shown in red and bound zinc atom is indicated by black sphere.

The Raetz pathway of LPS biosynthesis relies on the formation of intermediate precursors. The lipid X is the first to be synthesized and it requires, besides LpxA and LpxC, two other essential enzymes: LpxD and LpxH, as depicted in Fig. 1.4.[35]. LpxD adds *R*-3-hydroxymyristate chain to deacetylated UDP-3-*O*-(acyl)-GlcNAc to make UDP-2,3-diacyl-GlcN[64], whose pyrophosphate linkage is cleaved by LpxH, by attacking of water on the *α*-phosphorus atom of the UDP moiety[65,66]. As a result, the first intermediate, 2,3-diacyl-GlcN-1-phosphate (lipid X) is formed. Lipid X undergoes condensation with UDP-2,3-diacyl-GlcN due to LpxB activity[67]. Resultant disaccharide structure, which is very characteristic for lipid A, becomes secondarily phosphorylated by LpxK and the most minimal structure of LPS sustaining *E. coli* viability of lipid IV_A is formed[26,68,69]. Subsequently, WaaA (KdtA), the 3-deoxy-*α*-D-*manno*-oct-2-ulosonic acid transferase, catalyzes the addition of two Kdo residues to glucosamine disaccharide backbone of lipid A, resulting into synthesis of lipid IV_A-Kdo_2 precursor[18,70]. Lastly, final steps of *E. coli* lipid A-Kdo_2 formation involve the LpxL and LpxM enzymes, which are responsible for the addition of the secondary lauroyl and myristoyl chains, accordingly, to the Kdo-linked glucosamine unit[71]. It was established previously that LpxL and LpxM require within their substrates the presence of the Kdo disaccharide moiety prior to transfer of acyl groups, however the most recent data reports that it is possible for lipid IV_A to act as an acceptor for acylation by LpxL/M transferases under slow-growth conditions, without the prior incorporation of Kdo[56,72]. The described above enzymes of the

pathway are encoded by highly conserved genes in Gram-negative bacteria[12]. First three catalytic steps are carried by soluble proteins, formation of lipid A 1-P-disacharide is executed by peripheral IM proteins LpxB and LpxH and, the IM integral proteins LpxK, WaaA, LpxL and LpxM involved in remaining stages, complete the formation of lipid A-Kdo_2[35].

1.3.2. Diversified biosynthesis of core and O-antigen regions

Core biosynthesis relies on membrane-associated glycosyltransferases that sequentially transfer nucleotide sugar precursors. Genes encoding core biosynthetic enzymes are encoded within *waa* locus depicted in the bottom of Figure 1.9. The *waa* locus is divided in three operons: *gmhD*, *waaQ* and *waaA*[73–76], latter encoding already described enzyme WaaA, the 3-deoxy-*α*-D-*manno*-oct-2-ulosonic acid transferase. The *gmhD* operon contains *waaC* and *waaF* genes necessary for the addition of Hep residues. Within the long *waaQ* operon there are encoded genes required for the biosynthesis of the outer core and for core modifications. In *E. coli* strains, *waaQ* operon also contains the *waaL* gene, whose product is required to link *O*-polysaccharide to the completed core[12]. Figure 1.9. presents exemplary glycoform of *E. coli* K-12 W3110 core that was established by Müller-Loennies *et al*[77,78], however *E. coli* can be characterized by several known core structures, depending on varied gene expression and regulation in response to different stimuli.

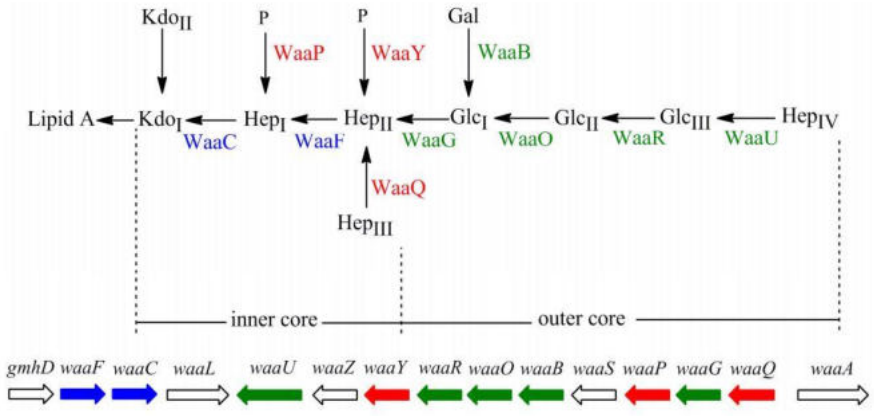

Fig. 1.9. Organization of *waa* locus and core structure of *E. coli* K-12 W3110 strain[78]
In blue there are marked glycosyltransferases of the inner core backbone and the genes encoding these enzymes; enzymes modifying the inner core structure and their corresponding genes are shown in red. Outer core enzymes and encoding them genes are presented in green.

In pathogenic or commensal strains of *E. coli*, completion of the smooth LPS molecule involves the addition of *O*-polysaccharide to the nascent lipid A-core. *O*-antigen is synthesized independently of other two LPS components. Saccharide polymer is assembled on a carrier lipid, undecaprenyl phosphate (Und-P), which is situated in the IM on the cytoplasmic side. *O*-antigen polymerization takes place at the reducing end of the growing chain, forming Und-PP-linked saccharide. The ligation of *O*-PS and lipid A-core occurs at the periplasmic face of the IM, after both elements are flipped across the membrane[12,18,79].

1.4. LPS translocation across the envelope and assembly on cell's surface

After the completion of LPS synthesis on the cytoplasmic-facing leaflet of IM, lipid A-core is flipped across the membrane to the periplasmic side by the ABC transporter, MsbA flippase (Fig. 1.10.)[80–82]. The essential *E. coli msbA* gene was originally discovered as a multicopy suppressor that suppressed the temperature sensitive phenotype of Δ*lpxL* bacteria[83]. When MsbA is either depleted or substituted with the loss-of-function mutation, it results in increased accumulation of LPS and phospholipids in the IM[80,81]. The overexpression of flippase-encoding gene relieves such accumulation as well as suppresses the lethal phenotype of mutant with impaired Kdo synthesis[84,85].

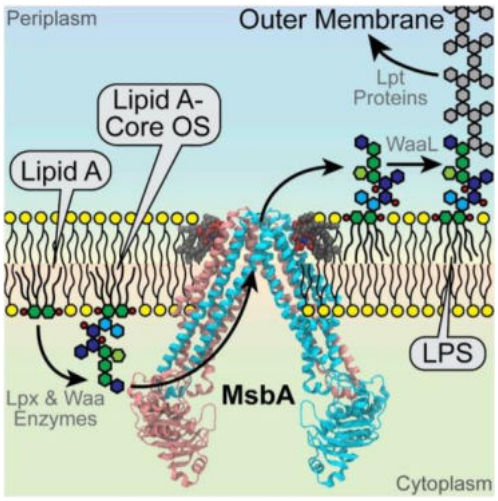

Fig. 1.10. Schematic representation of MsbA activity in LPS transmembrane transport[86]
MsbA is a lipid flippase anchored in the IM that transports lipid A with or without core sugars from the cytoplasmic leaflet to the periplasmic IM leaflet.

MsbA functions as a homodimer that consists of two transmembrane domains (TMDs) and each contains six transmembrane helices and two nucleotide binding domains located in the cytoplasm (Fig. 1.10.)[86,87]. Based on comparison of existing MsbA structures from different species, Padayatti *et al*. in 2019 proposed the model of sequential conformational changes in homodimer that occur along the LPS transport[86]. It is presumed that LPS may enter the flippase chamber through lateral opening of the membrane portals of inward-facing MsbA (Fig. 1.11. A). At the interface of monomers in inward-facing conformation, positively charged residues are exposed that could provide the recognition and affinity for hydrophilic part of LPS (Fig. 1.11. B)[86]. Subsequent or

concurrent binding of ATP molecule dimerizes the nucleotide binding domains and propels the switch of dimeric protein in open outward-facing conformation (Fig. 1.11. C)[86,88]. Upon ATP hydrolysis and the reset of transporter a switch back to inward-facing conformation can occur that releases LPS in the outer leaflet of the IM (Fig. 1.11. D)[86]. Figure 1.11. illustrates the described model extended by possible explanation of LPS flipping and release mechanism presented by Ho *et al.* 2018[89]. Upon opening of the periplasmic gate in outward-facing MsbA, hydrophobic acyl-chain exposure to the aqueous periplasm and concomitant opening of a lateral gate provides a possible pathway for LPS to exit MsbA and become flipped into the outer leaflet of the bilayer (Fig. 1.11. C and D)[89].

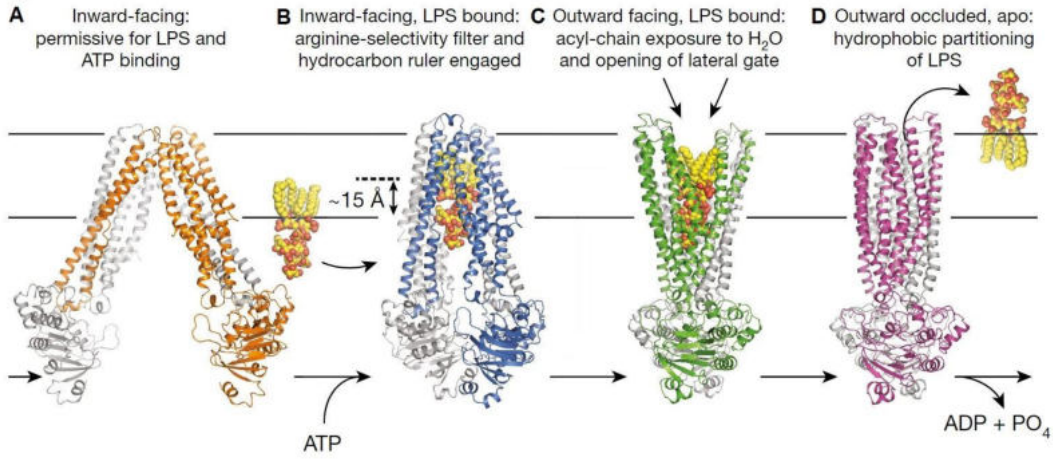

Fig. 1.11. Conformational changes of MsbA during LPS transport, adapted from[89]. MsbA is represented as ribbon with A- *E. coli* MsbA (PDB accession 3B5W), B- G907 inhibitor–LPS–EcMsbA complex as a proxy for the LPS-bound inward-facing state, C- StMsbA (PDB accession 3B60); D- ADP–vanadate–EcMsbA-cryo (PDB accession 5TTP). LPS is depicted in yellow and orange in sphere molecular representation. Black lines symbolize inner and outer leaflets of IM.

MsbA-mediated transfer of LPS plays a crucial role in quality control of LPS structure, due to the poor recognition of underacylated precursors. Such unrecognized by flippase LPS intermediates accumulate in the IM and are unavailable for the periplasmic enzymes[80,82]. It is critical for the survival of the mutant bacteria synthesizing minimal LPS like lipid IV_A, which must be translocated to the outer membrane, especially under fast-growing conditions. Lipid IV_A, due to underacylation and lack of Kdo_2, is a poor substrate for the flippase in comparison with penta- and hexaacylated derivatives[90]. Suppressors that allow for the growth of bacteria with minimal LPS under fast growing conditions, often require overexpression of late acyltransferases or, reciprocally, mutations mapping to MsbA itself[26,83,85,91]. Recently, in the study published by

Professor Raina's group, new suppressor mutations were found that mapped to the predicted lipid A-binding domain of MsbA and to the domain that provides MsbA in the selection of the acyl chain length of lipid A[56]. Suppressor mutations facilitated the transfer of LPS across the membrane of either glycosylation-free underacylated species or strains synthesizing pentaacylated LPS in the absence of LpxM and cardiolipin synthase A[56]. It emphasizes again the importance of the proper composition of the most conserved part of LPS for functionality of bacteria[56]. Of significant interest is also the discovery of a previously unknown requirement of cardiolipin (IM lipid) biosynthesis in Δ*lpxM* and Δ*lpxL* bacteria lacking either myristoyl or lauroyl acyl chains, as it can point the more complex connection between LPS and cardiolipin biosynthetic pathways[56,92].

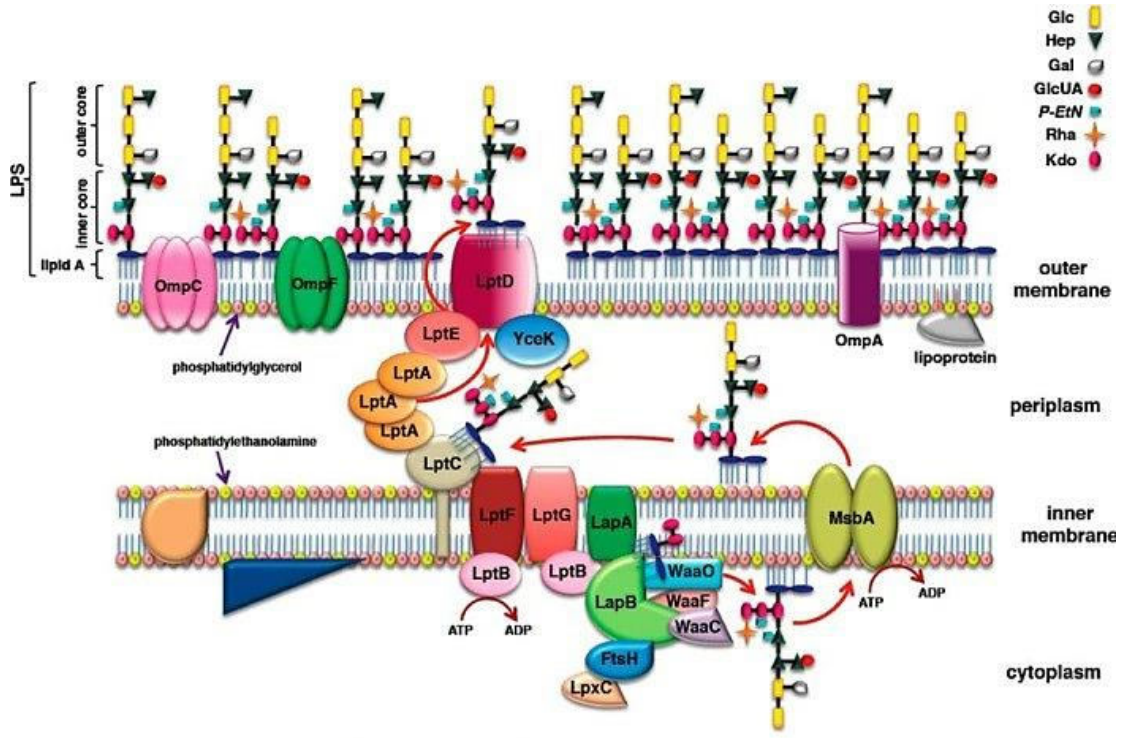

Fig. 1.12. Model of LPS biosynthesis and translocation machinery within envelope of *E. coli*[41]

Mature LPS flipped by MsbA, and in subsequent steps LapA and LapB could function together with transenvelope Lpt complex to transfer LPS to outer leaflet of OM.

After lipid A-core is flipped across the IM, if it is relevant for particular strain, the ligation of lipid A–core with independently synthesized *O*-antigen is performed by WaaL ligase on the periplasmic site of IM[93–95]. In laboratory strains of *E. coli* K-12, transported through the inner membrane LPS molecules are then substrate for the ATP-driven Lpt system presented in Figure 1.12. that delivers LPS through periplasmic space to the outer membrane[96,97]. Lpt (LPS transport) proteins form

a bridge between inner and outer membranes. LptB, LptF and LptG are assembled in ABC transport protein complex, to whom extraction of LPS from the IM is attributed[98,99]. Process of LPS extraction by Lpt machinery is compared to removal of substrates by some efflux pumps – LptB serves as a nucleotide binding component and provides the energy by ATP-binding, and LptF and LptG act as two transmembrane domains[17,100]. LptBFG complex interacts with the essential IM-anchored protein LptC[101]. In the hypothetical model of periplasmic bridge formed by Lpt machinery, LPS is thought to bind LptC at the IM, from where it is transferred through filament of LptA proteins to cross the periplasm, and is inserted into the OM outer leaflet by LptDE complex[98,99,102,103]. LptC, LptA and the N-terminal domain of LptD were each found to have a *β*-jellyroll domain, which assemble into a continuous slide for LPS molecules, insulating hydrophobic lipid A region from aqueous periplasm[104,105]. In the outer membrane, LptD C-terminal domain and LptE form stable complex. LptD forms a 26 *β*-stranded barrel, while LptE forms a plug located inside the LptD barrel and aids its assembly[102,106,107]. Lipid A travels via hydrophobic core of LptD N-terminal domain across intramembrane hole and is inserted into the OM, while the hydrophilic core oligosaccharide (as well as *O*-antigen) pass the channel formed by LptD C-terminal domain and LptE[108]. YceK is a lipoprotein that was found to suppress the essentiality of *lapB* when introduced in multicopy. In a screen for genetic interaction maps, the interaction between *lptD* and *yceK* was reported and it suggested its potential function in the transport of LPS[109]. Deletion of *yceK* gene results in impaired outer membrane integrity, but the exact function remains to be established[41,110].

1.5. Regulated alterations of LPS

Lipopolysaccharide is not only structurally heterogenous molecule among the species, but also its structure dynamically changes in response to different stimuli. Each region of LPS molecule undergo modifications that are tightly regulated in order to accommodate the cell to specific environmental niches or challenges. LPS alterations respond and contribute to bacterial virulence, resistance to antimicrobial agents, survival upon stress stimuli like temperature, pH, osmolarity, the presence of detergents and many other[111].

1.5.1. Modifications of lipid A

Under standard laboratory growth conditions lipid A of *E. coli* K-12 is a hexaacylated and biphosphorylated disaccharide *β*-D-Glc*p*N4P-(1→6)-*α*-D-Glc*p*N1P (Figure 1.13.), as described in subsection 1.2.2[18,20]. In response to different external conditions, each region of lipid A component can undergo modifications. For example, changes within the acylation pattern of lipid A provide bacteria with resistance to some cationic antimicrobial peptides (CAMPs) and affect the endotoxic properties of lipid A. Lipid A is a long-known active component of LPS endotoxin. When it is recognized in human by TLR4-MD2-CD14 system, it induces the signal cascade that leads to the production of cytokines, chemokines and other antimicrobial agents that activate the innate immune response to overcome bacterial infection[112]. The inflammatory reaction is essential to eliminate the pathogen, but is also the reason for some main pathophysiological symptoms associated with infections, with the sepsis as an extreme example[113]. It is known that bacteria can modulate the structure of its lipid A to attenuate the inflammatory response and evade recognition by immune system[113]. One of such alterations is incorporation of additional palmitate chain to the hydroxyl group of 3-hydroxymyristic acid at C-2 position of reducing-end of hexaacylated lipid A, catalyzed by PagP enzyme (Fig. 1.13.)[114]. PagP is an OM protein that is usually enzymatically inactive. Its activation is induced when permeability of outer membrane is disturbed. The *pagP* gene transcription is subject to regulation by the PhoP/Q two-component system (TCS), EvgAS TCS and in biofilm form, RcsB cascade with aid of GadE auxiliary regulator[115,116]. The PhoP/Q two-component system senses low Mg^{2+} or Ca^{2+} ions concentration, or

the presence of cationic antimicrobial peptides that alter Mg^{2+} distribution at the membrane surface, via PhoQ that is a histidine kinase found in the cytoplasmic membrane. PhoQ responds to the changes in ionic concentrations through altering its conformation resulting in autophosphorylation of its conserved histidine residue. Subsequently, the phosphorylated histidine kinase transfers phosphate group to the PhoP response regulator, which consecutively activates transcription of genes within its regulon, in this example the *pagP* gene[117–119]. The next TCS, EvgS/A, confers acid resistance in *E. coli*. The activation of EvgS sensor initiates the cascade of transcription factors, including its response regulator EvgA and GadE acid-responsive regulator, inducing transcription of many acid resistance genes. EvgS/A enhances activity of PhoP/Q TCS, thus activating the *pagP* gene transcription[115]. The adaptative feature of lipid A modifications with importance for pathogenesis is emphasized by the fact that PagP enhanced synthesis occurs, when in biofilm state, due to the activation by another signal cascade Rcs phosphorelay. RcsB is a response regulator that belongs to the multicomponent RcsF/RcsC/RcsD/RcsA/RcsB system. It was found to be involved in the regulation of the various processes, like synthesis of colanic acid capsule, cell division, periplasmic proteins control, motility and biofilm formation[120]. In biofilm state, due to the osmolarity changes, Rcs system induces changes in LPS structure, but in planktonic culture it is also able to sense LPS defects and activate RpoE-dependent stress response[116,121]. In each signal cascade, the activation of PagP occurs that generates the heptaacylated lipid A. Such modification not only help bacteria to attenuate the production of CAMPs by infected host due to not being recognized by TLR4 pathway, but it also probably directly protects bacterial cells from certain CAMPs. Latter assumption is based on the theory that lipid A palmitoylation presumably changes the fluidity of the bacterial OM that interferes with CAMP insertion and translocation across the membrane bilayer[122].

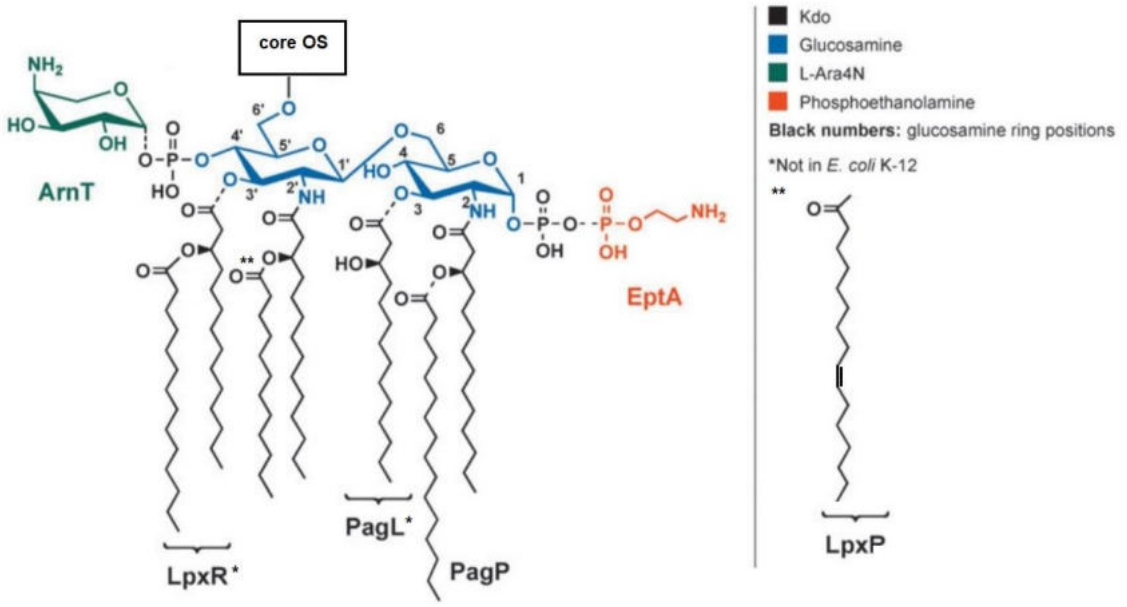

Fig. 1.13. Modifications within lipid A (modified)[35]
Enzymes ArnT and EptA catalyze incorporation of L-Ara4N and *P*-EtN, respectively. Acylation of glucosamine is regulated by several proteins: PagP, PagL, LpxR and LpxP. Asterisks indicate modification enzymes not found in *E. coli* K-12. PagP and PagL are under control of two-component systems. LpxR deacylase is negatively regulated by MicF sRNA. LpxP incorporates a palmitoleoyl chain into lipid A instead of the secondary laurate chain regularly added by LpxL at low temperatures.

Evading the host response by alteration of lipid pattern can also be observed through deacylation of lipid A. Discovered first in *Salmonella,* with its homolog in *E. coli*, protein PagL, is a lipid A 3-*O*-deacylase, whose gene is another member for the PhoP/Q regulon[123]. Catalyzed by PagL deacylation of lipid A was shown to significantly decrease ability of modified LPS molecules to induce TLR4-mediated signaling, thus help bacteria evade the host immune response[124]. Similar mechanism is also established for pathogenic *Escherichia coli*, where another lipid deacylase, LpxR (Fig. 1.13.), was found to remove 3′-acyloxyacyl residue of lipid A and contribute to the low inflammatory response of infected host cells[125]. What is interesting, the expression of *lpxR* gene is negatively regulated by non-coding RNA MicF (Fig. 1.14. B). MicF ncRNA is a *trans*-acting molecule that base-pairs within the coding sequence of *lpxR* mRNA and promotes its degradation by RNase E[126]. The levels of expression of *micF* itself depends on various environmental conditions and stresses, including osmolarity changes or membrane perturbations. It was discovered as an important regulator of outer membrane porin OmpF, and the interactions between

these two molecules were found to increase antibiotic resistance of bacterial cells, as well as resistance to killing by macrophages[127,128].

Escherichia coli K-12 genome does not contain *pagL* or *lpxR* genes, probably because as a laboratory strain, it does not require mechanisms responding to host environment. However, its lipid A modifications relying on acylation are not limited only to PagP activity. Under cold-shock or at low temperatures (12°C) *E. coli* exploits also other acyltransferase, LpxP, palmitoleoyl-acyl carrier protein (ACP)-dependent acyltransferase that acts on the lipid A precursor, Kdo_2-lipid IV_A. LpxP incorporates a palmitoleoyl chain into nascent lipid A in place of the secondary laurate chain, regularly added by LpxL. It is believed that the presence of palmitoleate in place of laurate may contribute to maintaining the optimal membrane fluidity at low temperatures[72,129]. Furthermore, transcription of the *lpxP* gene is activated upon RpoE induction[26].

The commonly observed modifications of lipid A are also situated within the glucosamine part of the molecule. These include incorporation of phosphoethanolamine (*P*-EtN) at C1 and or C4', and 4-amino-4-deoxy-L-arabinose (L-Ara4N) at C4' of glucosamine (Fig. 1.13. and Fig. 1.14. B). These non-stoichiometric substitutions are catalyzed by EptA and ArnT transferases, respectively, which reside in the inner membrane, facing the periplasm[35]. Additions of *P*-EtN and/or L-Ara4N to lipid A were found to contribute to resistance of *E. coli* to cationic antimicrobial peptides and, similar to *pagP/L* genes, genes encoding EptA and ArnT transferases are also regulated by PhoP/Q TCS. PhoP/Q TCS also enhances activity of yet another signaling cascade – BasS/R two-component system[130,131]. BasS becomes phosphorylated in response to high concentration of iron ions or mild acidity, and activates the BasR response regulator that induces transcription of genes involved in modification of lipopolysaccharide to prevent excessive Fe(III) binding[131]. Additionally, in *E. coli* and in *Salmonella*, BasS/R TCS is induced also due to response of PhoP/Q system to decreased concentration of Mg^{2+} and Ca^{2+} ions, which requires adaptor protein PmrD to mediate the signal between these two signal transduction pathways[132]. Such cross-talking between different signaling cascades allows bacteria to expand the signal sensing and fine-tune the response to win the advantage in the environment. Glucosamine modification of carbons C1 and C4' of lipid A relies also on another enzyme, LpxT (Fig. 1.14. B). C1 and C4' of lipid A

are frequently presented as phosphorylated due to LpxH and LpxK activities within the Raetz pathway of lipid A-Kdo_2 biosynthesis[35]. Notwithstanding, it is estimated that approximately one third of lipid A molecules from *E. coli* K-12 is biphosphorylated at C1 position[133]. The enzyme responsible for incorporation of second phosphate group, LpxT, transfers a phosphate group from undecaprenyl-pyrophosphate to the position 1 phosphate and contributes to increased negative charge of lipid A[134]. Upon exposure of bacteria to low concentration of divalent cations or cationic antimicrobial peptides, when the coupled PhoP/Q and BasS/R TCSs signaling occurs, the expression of short polypeptide PmrR is induced, which binds to LpxT and inhibits its activity[135]. Then, depending on the environmental signal, either further *P*-EtN or L-Ara4N addition in the place of second phosphate group is favored in order to maintain appropriate membrane permeability[111].

LPS biosynthesis and its modifications remain in complex relations with major regulator of extracytoplasmic (envelope) stress response, sigma factor RpoE (sigma E, sigma 24)[136]. Strains that synthesize only minimal LPS structure, mutants with underacylated lipid A or bacteria where the imbalance between phospholipids and LPS synthesis occurs, are characterized with often hyper-elevated levels of RpoE[26,41,137]. Concerning only the modifications of lipid A region of lipopolysaccharide, it is worth noticing that some of RpoE-regulated components participate in this process. In this instance, RpoE stress response affects mainly the PhoP/Q two-component system. The sigma E-regulated ncRNA MicA base pairs with the *phoP* mRNA and restrain its translation, consequently inhibiting the lipid A modifications orchestrated by the TCS, while stress response is activated[138]. MicA sRNA was also predicted to base-pair with the *lpxT* mRNA[139]. The MicA-dependent LpxT inhibition and its effects on the LPS structure has not been directly studied yet, however the structural analysis of LPS mutants from strains with RpoE and BasS/R simultaneously induced, revealed the absence of second phosphate group on C1 that can be attributed to MicA activity (Fig. 1.14. B)[29]. Another ncRNA that participates in the lipid A modifications through PhoP/Q repression is GcvB sRNA[140]. Binding of either small RNA MicA or GcvB to the *phoP* mRNA is sufficient to inhibit ribosome binding and induce mRNA degradation. GcvB is not reported to be induced by sigma E activity, but it has been shown during the study on mutagenic break

repairs that it strongly affects levels of RpoE response, though the exact mechanism is not known[141]. The most recent data published by Professor Raina's group reported that overexpression of GcvB sRNA was found to repress the accumulation of LpxC and suppress the lethality of Δ*lapA/B* mutant[56]. This previously unknown contribution of GcvB non-coding RNA to regulation of first committed step of LPS biosynthesis could explain its link to RpoE-dependent envelope stress response activation. It is clear that there are present variety of mechanisms responsible for modification of only lipid A part of LPS. The involvement of several signaling cascades, non-coding RNAs and the RpoE sigma factor of extracytoplasmic stress response emphasize the importance of lipopolysaccharide molecule in bacterial homeostasis and pathogenicity as lipid A constitute the major portion of outer membrane leaflet.

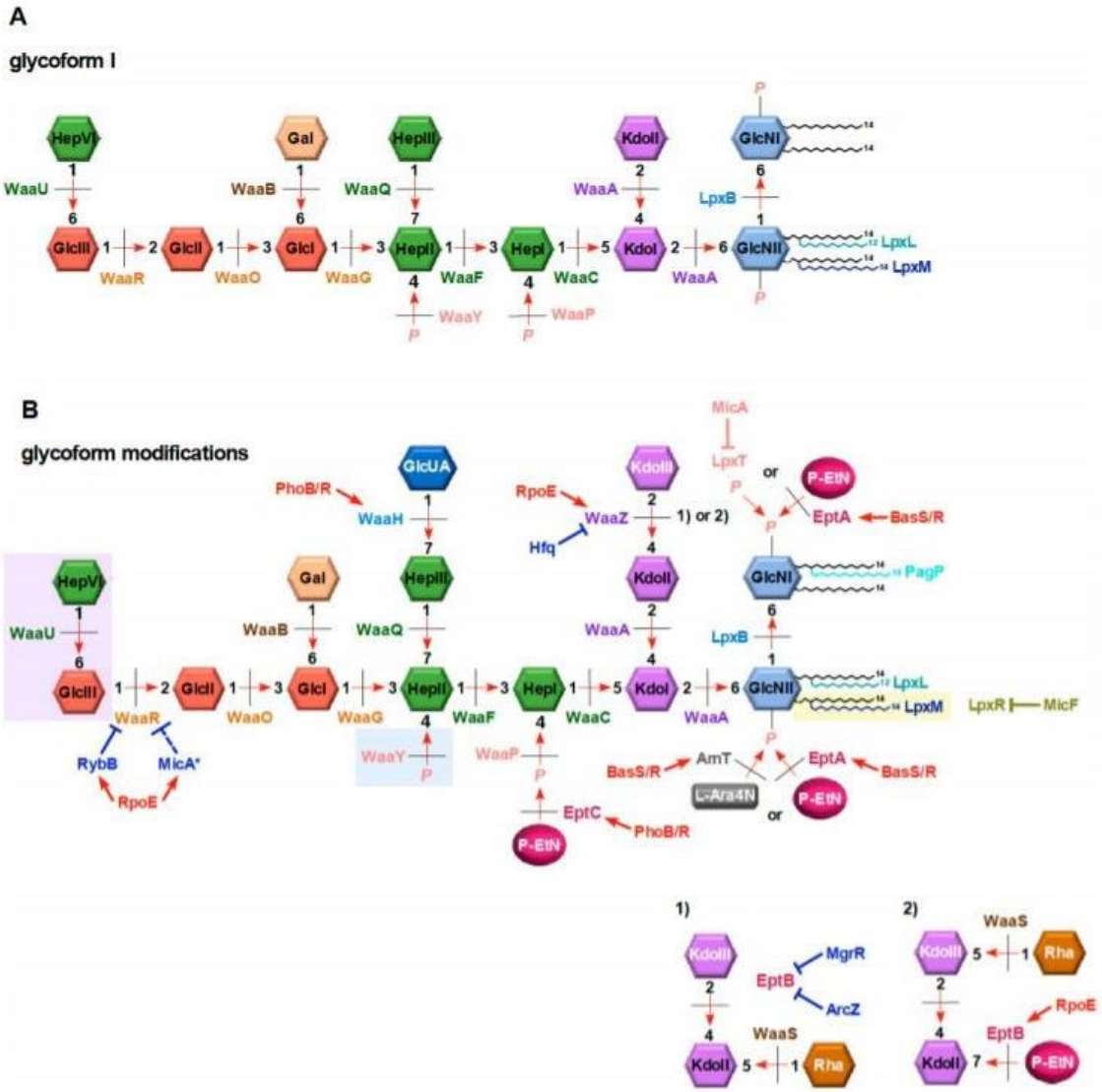

Fig. 1.14. Schematic representation of hexaacylated lipid A-core structure of *E. coli* K-12 (glycoform I) and its modifications in response to different signals[111]

Enzymes, which catalyze biosynthesis of subsequent steps, are indicated along with non-coding RNAs, two-component systems and RpoE sigma factor that all have an impact on glycoforms composition. (A) Under non-stress conditions glycoform I is the main composition of LPS found in *E. coli.* (B) PagP activity generates heptaacylated lipid A. On the contrary, LpxR removes the 3′-acyloxyacyl residue. Lipid A part can be modified by EptA and ArnT enzymes that catalyze incorporation of *P*-EtN and L-Ara4N at position 1 and 4', respectively. Induction of envelope stress RpoE sigma factor results in the incorporation of the Kdo III moiety by enhanced synthesis of WaaZ and inhibition of WaaR by RybB ncRNA. It favors the attachment of Rha on Kdo III and enhancement of EptB activity that overcomes its MgrR-dependent inhibition, decorates *P*-EtN on Kdo II (panels 1 and 2). Simultaneously, the truncation of the terminal Glc III-Hep IV disaccharide occurs. Activation of PhoB/R TCS results in the addition of GlcUA on Hep II regulated by WaaH and *P*-EtN moiety on Hep I by EptC.

1.5.2. Diversification of core oligosaccharide

Along with the distance from the outer membrane, the diversification of LPS molecule increases. The composition of the inner core is still relatively well conserved among Gram-negative bacteria. In *E. coli*, inner core consists of *α*-(2-4)-linked Kdo disaccharide to which three L-*glycero*-D-*manno*-heptose residues are attached (Fig. 1.14. A)[12]. The Kdo residue is the only component found in all known cores, although in some cases its derivative, D-*glycero*-D-talo-oct-2-ulosonic acid, is present[23]. All components of the inner core are subjected to modifications orchestrated by two-component systems, ncRNAs, ppGpp alarmone and RpoE sigma factor, in order to ensure OM permeability, antibiotic resistance and diversity in the LPS composition, depending on external signals[111]. Similar to lipid A part, one of the most common modification within the core is its decoration with *P*-EtN that occurs on the second Kdo residue (Fig. 1.14. B)[142]. The phosphoethanolamine transferase that catalyze *P*-EtN incorporation is encoded by the *eptB* gene, which was found to be induced in the presence of Ca^{2+} ions in the medium[125,143]. No direct signal cascade was found so far to control this phenomenon, however the regulation of *P*-EtN incorporation on Kdo II can be explained by cross-talking of RpoE stress response and PhoP/Q TCS. Transcription of the *eptB* gene is negatively regulated by PhoP-dependent non-coding RNA MgrR (Fig. 1.14. B panel 1)[144]. Under standard growth conditions MgrR base-pairs with the *eptB* mRNA and silences its expression. The *mgrR* transcription is induced by PhoP/Q cascade, therefore under normal conditions, it directly inhibits the activity of EptB and *P*-EtN incorporation[145]. The opposite course of events can be explained by RpoE activity (Fig. 1.14. B panel 2). Under conditions that induce envelope stress response, for example as found in the case of Δ*waaC* or Δ*waaF* mutants with LPS defects, the RpoE-dependent MicA ncRNA represses the PhoP/Q signaling and as a consequence, the activity of MgrR sRNA is also hindered[26,56,138,140]. In addition, the *eptB* gene itself is transcribed from a sigma E-recognized promoter, therefore its activity is not only not repressed but also induced upon envelope stress conditions, and that explains enhancement of the EptB-dependent *P*-EtN modification of the second Kdo upon activation of RpoE[29]. This model was confirmed by recent studies published by Professor Raina's group, where suppressor mutations that

overcome the Ca^{2+} sensitivity of a Δ(*waaC eptB*) mutant were found to map to the *basS* and *basR* genes[56]. Suppressor mutations in *basS/R* caused a constitutive incorporation of *P*-EtN in the lipid A part and were able to abolish the sensitivity of Δ(*waaC eptB*) mutant to Ca^{2+} through compensation for *P*-EtN absence on the second Kdo[56]. The data reassured that incorporation of *P*-EtN on the Kdo II is due to the higher level of induction of the *eptB* gene, whose transcription responds to the RpoE-dependent envelope stress response. Another non-coding RNA that inhibits translation of *eptB* mRNA via base-pairing is ArcZ sRNA[144]. ArcZ is negatively regulated by oxygen-responsive two-component system ArcB/A[146]. Thus, under normal aerobic conditions ArcZ functions freely and inhibits EptB activity (Fig. 1.14. B panel 1). The combined effects of MgrR and ArcZ ncRNAs, when *E. coli* growth is undisturbed, Mg^{2+} and Ca^{2+} levels are relatively low and oxygen is available, hinder *P*-EtN addition by EptB. It is under microaerobic or anaerobic conditions when Mg^{2+} or Ca^{2+} levels are high, and/or when *E. coli* is exposed to cationic antimicrobial peptides, like polymyxin B that in all cases lead to envelope stress induction, when this and other LPS modifications are necessary for bacteria to survive and acquire resistance. *E. coli* genome encodes one more phosphoethanolamine transferase, designated as EptC. This enzyme is necessary for the incorporation of *P*-EtN on phosphorylated Hep I[147]. EptC undergoes regulatory control by PhoB/R TCS that responds to phosphate levels in the bacterial surrounding and it is activated under phosphate-limiting conditions (Fig. 1.14. B)[147,148]. EptC-mediated *P*-EtN incorporations are absent on the LPS of *E. coli* grown under phosphate-rich conditions but are present in the LPS of cells grown under phosphate-limiting conditions, when PhoB/R TCS is induced[147]. This modification serves as an adjustment of OM permeability, as mutants that lack the *eptC* gene exhibit increased sensitivity to sublethal concentration of Zn^{2+} or to the presence of SDS detergent in the medium[147]. The same TCS contributes also to the addition of glucuronic acid (GlcUA) on Hep II regulated by WaaH (Fig. 1.14. B)[29,147]. This modification coincides with the absence of phosphate on the second heptose.

Extracytoplasmic stresses that induce activity of RpoE, despite the favoring of *P*-EtN addition to the second Kdo, result also in several other changes within core region. Under envelope stress, there is observed an increase in the incorporation of the third Kdo residue linked to Kdo disaccharide, catalyzed by

WaaZ lipopolysaccharide biosynthesis protein (Fig. 1.14. B)[29,149]. Kdo III residue is further decorated with rhamnose by reaction controlled by WaaS rhamnosyl transferase[29]. Under normal growth conditions WaaS catalyzes the addition of Rha to the second Kdo, as EptB-dependent *P*-EtN incorporation there is inhibited (Fig. 1.9. B panels 1 and 2)[111]. Simultaneously, RpoE-inducing conditions harbor RybB sRNA together with, to some extent, MicA ncRNA, to repress the synthesis of WaaR glycotransferase responsible for the addition of the third glucose (Glc III) to the second glucose (Glc II) in the outer core of *E. coli* K-12 LPS (Fig. 1.14. B)[29,75]. It results in truncated LPS, lacking terminal saccharides, with three Kdo residues alternated with rhamnose and *P*-EtN, and possible *P*-EtN residue on Hep I. Such core variant was designated as glycoform V.

1.5.3. Switching of glycoforms

Up to current knowledge, one can distinguish at least seven different glycoforms of *E. coli* K-12. The study upon structural analysis of oligosaccharides from LPS revealed that under optimal growth conditions, the majority of *E. coli* K-12 LPS was found to correspond to glycoform I, with two Kdo residues, four heptoses and four hexoses attached in specific order as presented in Figure 1.14. A and 1.15. below[77]. Glycoform I accounts for approximately 70% of total LPS and other observed species under normal conditions are glycoforms II, III and IV (Fig. 1.15.)[77]. In comparison to glycoform I, glycoform II contains an additional residue of *N*-acylated *β*-D-GlcN (GlcAc) 1→7 linked to Hep IV and it contributes only in 5% to total lipopolysaccharide amount. In the same study, another minor amount of molecules, with approximate same 5% input, was found to lack the terminal L-*α*-D-Hep in the outer core but otherwise identical to the major oligosaccharide that was designated as glycoform III. Glycoform IV, which was identified as 20% of total LPS, contained a branched tetrasaccharide of three Kdo residues and rhamnose connected to lipid A with concurrent truncation within the outer core missing terminal disaccharide (Hep IV-Glc III)[77].

The molecular switch that leads to accumulation of different LPS glycoforms can be defined as a shift in conditions activating specific signaling cascades that have impact on LPS composition. It was discovered that glycoform IV is the most abundant LPS species when TCSs PhoB/R and BasS/R are induced, but there is no enhancement of RpoE activity[29]. Thus, external

signals activating the switch to glycoform IV are the limiting phosphate conditions, mild acidity or excess of external Fe(III) in the environment, as it was described earlier. The accumulation of glycoform IV is a result of MgrR sRNA-dependent repression of *eptB* mRNA, when *P*-EtN does not occupy place on Kdo II for rhamnose to be attached by WaaS (Fig. 1.14. B panel 2)[24,145]. On the contrary, when RpoE sigma factor-inducing conditions arise, either naturally or due to mutations like for example, deletion of RpoE anti-sigma factor (Δ*rseA* mutants), the accumulation of LPS glycoform V occurs[29]. Glycoform V (Fig. 1.15.) contains rhamnose on Kdo III and *P*-EtN moiety on Kdo II as the RpoE-driven transcription overrides MgrR sRNA-dependent repression of the EptB synthesis due to the hyperinduction of RpoE-recognized promoter of the *eptB* gene[24,29]. Interestingly, each known glycoform that contains three Kdo residues (glycoform IV, V and VII), is characterized by truncation of the core due to WaaR inhibition (Fig. 1.14. B and Fig. 1.15.). The *waaR* mRNA translation is silenced due to RpoE-induced activity of two non-coding RNAs – MicA and RybB[29,75]. Consistent with these findings, the *waaR* mutants were discovered to synthesize derivatives of glycoform IV without the requirement of sigma E induction[24]. Therefore, signal in form of RpoE stress response results in the switch to LPS glycoforms IV, V and VII. Glycoform IV accumulation is dependent on predominant repression of the *eptB* gene by MgrR sRNA. However, when the RpoE activity is utmost, σ^E-induced EptB synthesis overrides the MgrR-mediated repression, resulting in the synthesis of glycoform V. The glycoform VII becomes major LPS form, when in concert with RpoE-induction, *E. coli* is grown under phosphate-limiting conditions with sub-millimolar concentrations of Zn^{2+} and Fe^{3+}, which are the WaaH glucuronic acid transferase-inducing conditions[111,147]. Lastly, difference between switches to glycoform VI and VII is based on the fact that no stress response activation is required in the case of glycoform VI[147].

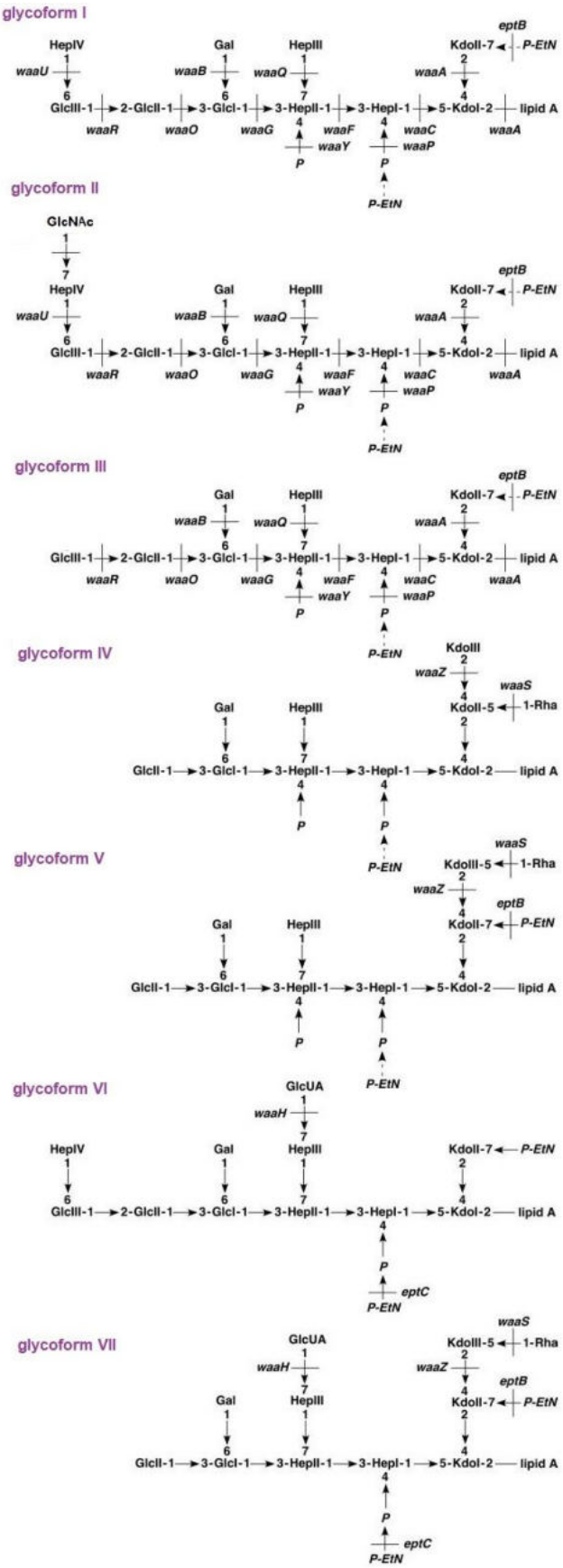

Fig. 1.15. Schemas of *E. coli* K-12 LPS glycoforms I-VII, based on[77,147]

Seven known glycoforms of *E. coli* K-12 are presented in the figure along with the indicated genes, whose products are responsible for the addition of particular moieties.

1.5.4. Regulation of transcription of long LPS-related operons

The significant amount of genes that encode proteins necessary for LPS biosynthesis and its alterations are located within long transcription units like *waaQ* or *rfb* operons. The *waaQ* is the major core-oligosaccharide assembly operon in *E. coli* and *rfb* products are involved in *O*-antigen biosynthesis[12]. It was found that both of these genomic locations undergo regulation by a global-acting RfaH transcription antiterminator[150,151]. RfaH inhibits the Rho-dependent termination of *waaQ* and *rfb* operons and its activity allows to bypass downstream termination signals and to transcribe long mRNAs[152,153]. RfaH is a paralog of universally conserved family of NusG transcription factors[154]. It exhibits the unique specificity of recognition for only the operons that contain its binding *ops* (operon polarity suppressor) sequence, encoded as a part of so-called JUMPstart (just upstream of many polysaccharide-associated gene starts), located in the 5' UTR[151,155]. Such RfaH-recognized sequences were found not only upstream of *waaQ* or *rfb* operons, but also in operons with genes encoding proteins necessary for haemolysin, capsule synthesis and for conjugation[154]. The RfaH protein that is not bound to the *ops* site remains in its inactive closed conformation with the C-terminal domain (CTD) in form of *α*-helical hairpin that is tightly packed against its N-terminal domain (NTD). Closed conformation prevents the interactions of NTD with DNA and RNA polymerase. Upon binding to *ops* sites, in the presence of RNA polymerase, the CTD changes its conformation into a *β*-barrel, exposing NTD and allowing for the recruitment of ribosomal proteins to couple transcription with translation and also to enhance transcriptional elongation[156]. The LPS-associated *waaQ* and *rfb* operons contain an 8-nt *ops* site and the JUMPstart site in their 5′ UTR and they also lack a ribosome-binding site[121]. It was shown that in Δ*rfaH* mutants LPS is significantly shorter and such mutants have elevated envelope stress response, they exhibit permeability defects and pathogenic strains of *E. coli* become avirulent due to the mutation[111,121].

In 2016 Professor Raina's group published identification of a new non-coding RNA RirA sRNA (RfaH interacting RNA) as a potential regulator of the *waaQ* regulon[121]. The expression of the *rirA* gene induced from the multicopy plasmid led to the increased *β*-galactosidase activity on 5-bromo-4-chloro-3-indolyl-*β*-D-galactopyranoside (X-gal) supplemented medium in strain with the

lacZ gene fusion with *rpoE*P3 promoter that specifically responds to LPS defects. RirA sRNA is 73-nt long and located in the 5' UTR of *waaQ* gene. It is transcribed in the same direction as *waaQ* and the 5' end mapping showed that it shares the transcription start site with the *waaQ* operon. Overexpression of RirA causes similar disruptions as in the Δ*rfaH* bacteria – it abolishes synthesis of *O*-antigen, causes truncation of the LPS core and reduces overall amounts of LPS. It is known that RirA ncRNA directly interacts with RfaH in the presence of RNA polymerase. Potential interpretation of RirA role can be explained by RfaH-tittering function. It is possible that the accumulation of RirA in the cell might serve as an internal checkpoint for balanced LPS synthesis[111,121].

1.6. Envelope stress systems in response to LPS defects

It has already been emphasized in this thesis how maintaining the homeostasis within bacterial envelope is crucial for growth and viability of bacteria. In order to protect the functioning of the envelope, which is the first structure separating the cell from environment, bacteria have evolved the signaling pathways not only to introduce the environment-dependent alterations, as described above, but also to detect and cope with malfunctions and repair the damage by controlling the expression of appropriate genes. *E. coli* envelope stress response systems have been studied extensively, but only recently the steps of exact mechanisms of sensing the defects of LPS which is one of the major contributors to envelope stresses, were established.

1.6.1. RpoE sigma factor

Since early studies upon heat shock stress response and RpoE-regulated extracytoplasmic stress response, it was repeatedly reported that disruptions within lipopolysaccharide-related genes induce the expression of the *rpoE* gene itself or genes recognized by RpoE sigma factor–RNA polymerase complex[60,136,157]. Hyper-elevated levels of RpoE were also detected in strains that synthesize the minimal LPS variants of Kdo_2-lipid IV_A or free lipid IV_A and the activity of σ^E is also induced when there is an imbalance in the ratio between LPS and phospholipids[26,41]. It is also known that mutant strains synthesizing heptoseless LPS exhibit a constitutive induction of the *rpoE* expression[26,157].

RpoE is regulated by products of the genes of its own operon, *rseA*, *rseB* and *rseC* genes (Fig. 1.16. A). RseA is the anti-sigma factor of sigma E. Under normal conditions it binds to sigma subunit via its N-terminal domain and sequesters RpoE, titrating it and hence reduction in its activity[158]. When the extracytoplasmic stress occurs, activated proteases, like for example DegS or RseP (EcfE), degrade inhibitor and relieve σ^E[159]. RseA interacts with another negative regulator of RpoE, RseB[158]. This protein facilitates the RseA-RpoE binding and prevents the cleavage of RseA by proteases[160,161]. The third member of the operon, RseC, is a positive regulator of sigma E, however the *ΔrseC* mutants do not exhibit any effect on σ^E activity, unless coupled with the deletion of *rseB*[158]. Along with the discovery of the *rpoE* gene, it was already established

in two complementary studies that the sigma E-encoding gene has its two promoters and that its transcription is positively autoregulated from its adjacent promoter (called *rpoE*P2) as it is recognized by $E\sigma^E$ and its activity is induced when the disturbance in OMPs conjuncture occurs. The regulation of distal promoter region (called the *rpoE*P1) remained unclear (Fig. 1.16. A)[136,162].

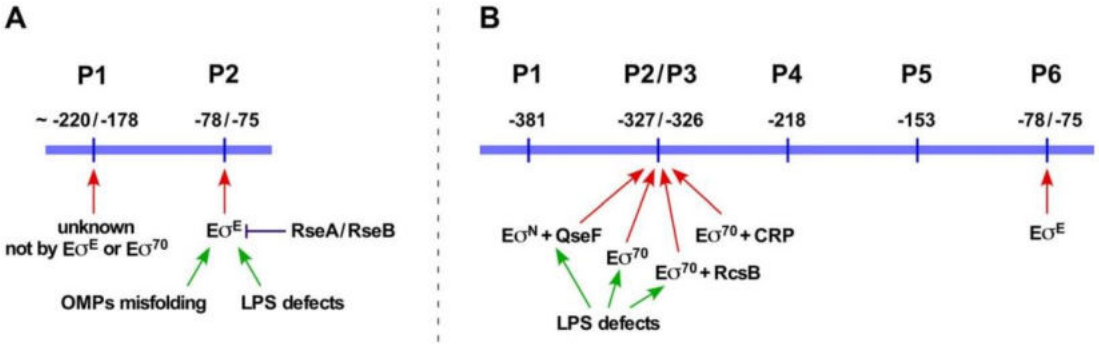

Fig. 1.16. Transcriptional regulation of the *rpoE* gene[121], modified
Schematic presentation of transcriptional start sites of the *rpoE* gene known previously, since gene discovery (A) and identified by Professor Raina's group by mapping of transcription start sites and verification by *in vitro* run-off assays (B). Different established in later study sigma factors and regulatory proteins that affect the activity of certain promoters are presented. Black numbers below each TSS refer to number of base pairs upstream of +1 position of the *rpoE* gene.

During the research in our group from Professor Raina's laboratory, addressed to understand mechanisms of induction of RpoE-driven stress response to LPS defects in *E. coli,* it was discovered that the transcription of the *rpoE* gene is initiated from six start sites and that transcription of two of its newly established promoters *rpoE*P2 and *rpoE*P3 is specifically induced when LPS is defective (Fig. 1.16. B)[121]. Among these, the most pronounced was the transcription from the *rpoE*P3 promoter when LPS core biosynthesis was disrupted, the assembly of LPS misfunctioned or when bacteria were challenged with LPS-binding antibiotic polymyxin B. The activity of the same *rpoE*P3 promoter was found to be highly induced in mutants lacking RfaH transcription antiterminator and by the overexpression of described RirA sRNA. Similar effect was observed when *E. coli* was treated with ammonium metavanadate (AMV) that non-specifically activates different TCSs[121].

1.6.2. Rcs signaling cascade is activated by defective LPS

The first evidence in establishing signal transduction in response to LPS defects was observed when the 7-fold induction of the *rpoE*P3 promoter detected

in Δ*waaC* mutant was nearly abolished in double mutant of Δ(*waaC rcsB*). It suggested that Rcs TCS is required to activate RpoE-dependent envelope stress response[121]. This was further confirmed by the *in vitro* DNA binding assays with purified RcsB response regulator that established the presence of RcsB binding motif in the *rpoE*P3 promoter region[121]. The transcription run-off assays demonstrated the authenticity of P3 promoter recognition by the house-keeping sigma factor RpoD and analysis of mutated RcsB-binding sequence reinforced the results that this response regulator acts as a transcription factor in response to LPS defects[121].

The possibility of function of Rcs pathway in sensing LPS defects was considered earlier, during the examination of deep-rough LPS mutant strains. The *rfa-1* strains synthesize truncated LPS composed of two first heptose residues in the core region and they are characterized by the induction of *cps* genes leading to overexpression of exopolysaccharide. It was found that signal transmission from defective LPS to induction of *cps* operon relied on the outer membrane lipoprotein RcsF, as it was abolished when the *rcsF* gene was deleted[163]. RcsF lipoprotein was later found to exists in complexes with outer membrane proteins and that these RcsF/OMP complexes are required for sensing OM outer leaflet stress. When such stress, including disturbance within the LPS structure happens, this information is transduced to the RcsF C-terminal signaling domain located in the periplasm, to activate the stress response[164]. Such activation of Rcs phosphorelay resulted in activated RcsB response regulator which in turn induced transcription from the *rpoE*P3 promoter (Fig. 1.17.).

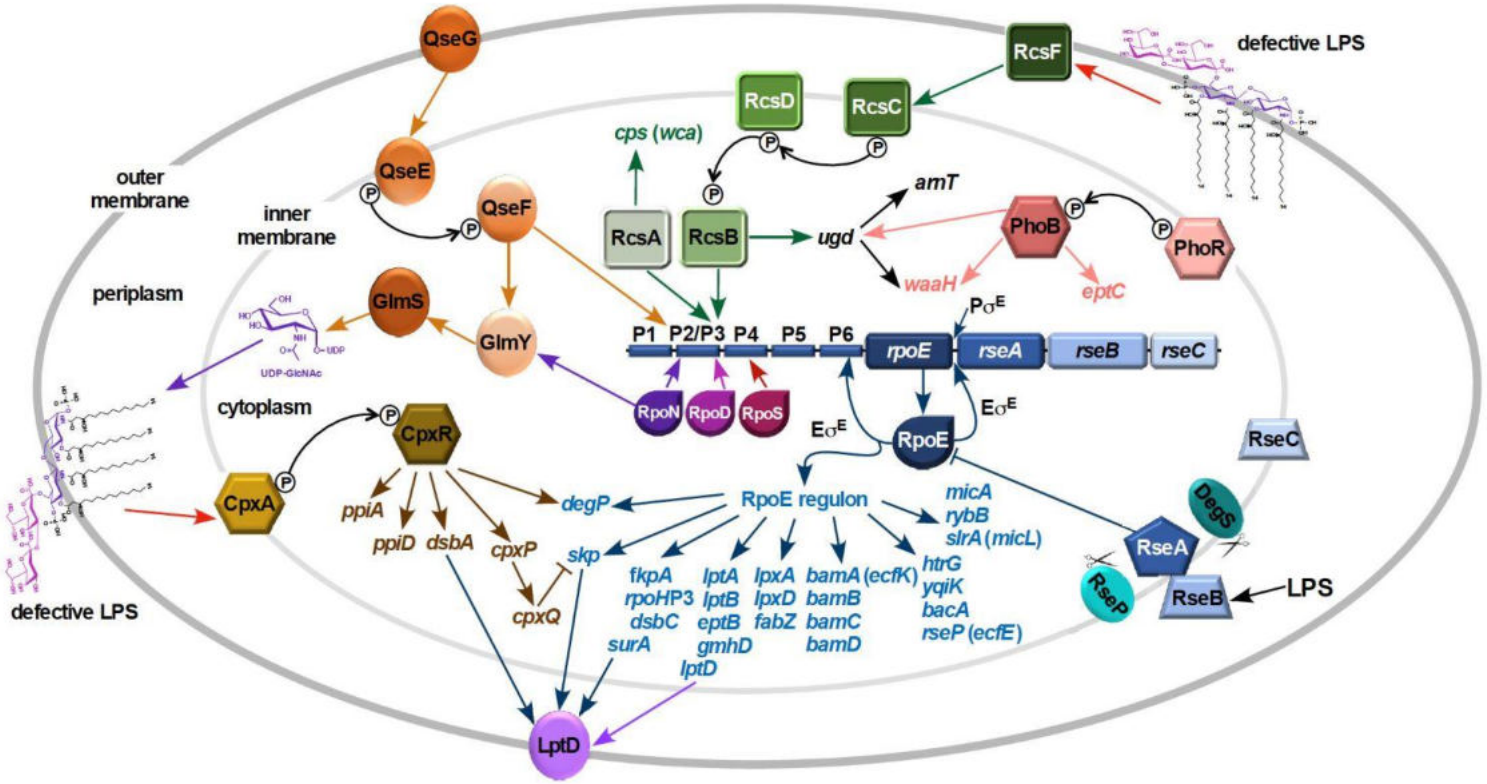

Fig. 1.17. Signal transduction in response to LPS defects[111]

LPS defects can be sensed by Rcs signaling cascade, whose activation results in induced transcription from the RpoD-recognized *rpoE*P3 promoter requiring RcsB as an activator. The overlapping promoter *rpoE*P2 also responds to LPS but to a lower extent. This promoter is regulated by RpoN sigma factor and it utilizes QseF as an activator. CpxR/A TCS is activated when LPS is severely defective, however the pathway is unknown. The free LPS accumulated in the periplasm when Lpt translocation pathway malfunctions, can bind to RseB. Such binding inhibits RseB role of protecting RseA from proteolysis and RseA does not hinder RpoE. Activity of RpoE sigma factor and RpoE-dependent extracytoplasmic stress response is necessary to maintain the envelope stability. RpoE regulates expression of genes of molecules involved in crucial for the process protein folding in the periplasm, assembly of OMPs and certain genes whose products are involved in LPS biosynthesis and regulated modifications.

1.6.3. Free LPS competes for binding with RseB

The another model of detecting LPS defects and launching adequate stress response is based on competition between LPS and RseA for binding RseB[165]. Authors of this study have shown that binding of free LPS in the periplasm to RseB endures the protective function of RseB-RseA binding and allows for the increased proteolysis of RseA anti-sigma factor. Hindering of RseA functioning results in the release of RpoE and the auto-induced *rpoE* gene transcription, as described in the beginning of subsection[158]. The support for this trade-off model, came from the experiment where the presence of filament-forming LptA molecules that form crossbridge for LPS translocation through periplasm (Fig. 1.12.), prevented the RseA-RseB dissociation by LPS. It suggested that the accumulation of LPS in the periplasm due to release from Lpt machinery constitute a signal that initiates the RpoE-dependent stress response through the suspension of functioning of anti-sigma factor (Fig. 1.17.)[165]. The model requires further validation, however the analysis of distribution between free RpoE and IM-bound RpoE in Δ*waaA* mutants indicated that in such strains, where LPS is composed of only lipid IV_A, enhanced RpoE expression can be caused by elevated release rate of RpoE from the IM[166]. Furthermore, the Δ(*lapA lapB*) mutants, quite like Δ*waaA* bacteria, were also characterized with constitutive induction of RpoE, as the lack of assembly factors leads to reduced amounts of LptD in the OM with simultaneous overproduction of LPS due to stabilization of LpxC, and accumulation of LPS precursors with incomplete core and defective acylation (Fig. 1.17.)[41].

1.6.4. Qse TCS-dependent and RpoN-regulated rpoEP2 promoter responds to LPS defects

Induction of RpoE-dependent response when there are defects in LPS present is also dependent on the RpoN-regulated *rpoE*P2 promoter. This phenomenon occurs to a significantly lower extent than the activation of the *rpoE*P3 promoter and mainly upon entry into the stationary phase[121]. Two promoters that are affected by perturbations within LPS biosynthesis share the same transcription initiation start site at -327 position, but the *rpoE*P2 exhibits homology to RpoN-recognized promoters with the presence of conserved −12

and −24 RpoN recognition sites. It was discovered that this promoter is activated by QseF protein by a nearly 20-fold induction upon overexpression of the OM protein QseG (Fig. 1.17.)[121]. QseF is a response regulator of QseE/F two-component regulatory system. In non-pathogenic *E. coli*, it is involved mostly in the regulation of GlcN6P synthase (GlmS) biosynthesis. GlmS catalyzes the conversion of fructose-6-phosphate into GlcN6P, together with GlmM and GlmU enzymes and it is the first step in the biosynthesis of UDP-GlcNAc, which is a substrate for peptidoglycan, as well as for LPS biosynthesis (Fig. 1.4. and Fig. 1.17.)[167]. QseE/F TCS is present in many bacteria species. In enterohaemorrhagic (EHEC) strains of *E. coli,* this system is involved in sensing human hormones in order to form lesions in the large intestine[168]. The *qseG* gene, which encodes another described outer membrane lipoprotein, is co-transcribed with *qseE* and *qseF* genes. The phosphorylation state of QseE/QseF is strictly dependent on interaction with QseG lipoprotein in response to an envelope signal[169]. However, there is no exact mechanism established yet on how the Qse TCS senses LPS.

1.6.5. Cpx two-component system is induced in LPS mutants

The integrity and homeostasis of OM, beside correctly synthesized and assembled LPS, requires functional assembly of OMPs and a balance between synthesis of peptidoglycan, phospholipids and LPS. It is ensured by mechanisms that need execution of not only RpoE-dependent response, but also the function of Cpx two-component system. The Cpx TCS responds principally to misfolded proteins in the periplasm and it regulates the expression of genes encoding proteases and chaperons. It is known that these two signaling cascades overlap and that some of the envelope stress-related genes undergo regulation by both of the systems, like in the case of *degP (htrA)* gene encoding periplasmic heat shock protease[170,171]. Within this TCS, CpxA protein serves as the histidine kinase and CpxR functions as the response regulator (Fig. 1.17.). The signal transduction pathway is extended by regulatory protein, CpxP, that in the absence of stress signal binds to the periplasmic domain of histidine kinase and participates in the feedback inhibitory circle[172,173]. Along with CpxR response regulator, the pathway utilizes another executor molecule, the CpxQ ncRNA that is formed by RNase cleavage of *cpxP* mRNA from its 3' UTR[174]. Its main function

is the inhibition of protein synthesis in the cytoplasm. The Cpx system responds to both types of stimuli, internally, to excessive synthesis of membrane proteins, and to external stresses such as alkaline pH, ethanol, adhesion, cationic antimicrobial peptides, heavy metals, and metal chelators[175]. It is not known exactly what is the signal pathway between defective LPS and Cpx system induction. However, mutants described above, Δ(*lapA lapB*) or Δ*waaA* bacteria, as well as mutants that produce tetraacylated derivatives synthesizing Kdo_2-lipid IV_A like Δ(*waaC lpxL*) or Δ(*waaC lpxL lpxM lpxP*) exhibit significant induction of both RpoE and Cpx pathways. It is possible that Cpx TCS somehow detects LPS malfunctions independently, as it is known to respond to the outer membrane lipoprotein NlpE that was found to specifically monitor two essential envelope processes - lipoprotein sorting and oxidative folding, in similar manner as RcsF activates Rcs phosphorelay[176,177]. It should be noted that a joint signaling to amplify RpoE induction by different models can be considered hence these models are not mutually exclusive[121].

1.7. LPS genetics

The overview of distribution and positioning of LPS-related genes on *E. coli* map emphasize the importance and complexity of lipopolysaccharide molecules.

Bacterial evolution studies prove that genes encoding proteins involved in common pathways are often found in close proximity of each other along bacterial chromosomes and there are several hypotheses explaining such occurance[178]. It is speculated that clustering of genes is favored due to increased efficiency of coregulation of genes concentrated in one genomic location and further, that clustered arrangements of genes are transferred to other species with higher probability, thus improving the chance for survival of the cluster. Other explanation for clustering takes into consideration that genes that are in close proximity are less likely to be disrupted by deletions[178]. Genetic studies upon bacterial complex carbohydrate pathways often report the tendency of gene clustering among genes encoding the molecules that participate in biosynthetic pathways[179]. In line with such observations, LPS genes that encode the core and *O*-antigen components of LPS are also found in organized locations of clusters of contiguous genes[179]. This study is focused on LPS found in laboratory strains of *E. coli*, like *E. coli* K-12 derivatives, therefore considerations upon *O*-antigen genetics is not further described beside the *O*-antigen attachment. However, considering the biosynthetic pathways of saccharides that are common building blocks for lipid A-core as well as *O*-antigen (Fig. 1.2.), the clustering phenomenon can be already observed. One of such examples is *rfb* L-rhamnose biosynthetic operon, encoding *rfbA, rfbB, rfbC* and *rfbD* genes[79].

Table 1.1. enlists LPS-related genes that were selected from *E. coli* K-12 MG1655 genome based on information provided by Profiling of *Escherichia coli* chromosome (PEC) database Version: 4.10.7 and EcoCyc bioinformatics database[180]. Enlisted genes are categorized in groups as follows: genes related to lipid A-core biosynthesis (red), related to lipid A-core transport and translocation (orange), LPS-related sigma and anti-sigma factors (yellow), genes whose products are involved in signal transduction in LPS biosynthesis and assembly (green), genes encoding proteases involved in LPS biosynthesis and assembly (blue), genes of LPS biosynthesis/assembly proteins (pink) and genes

of non-coding RNAs involved in LPS biosynthesis/assembly (purple). Specific colors correspond to a schematic genetic map presented in Figure 1.18. below that shows approximate locations of the majority of genes involved in LPS synthesis, assembly and regulation that were listed in Table 1.1. and described within this work. Among the species that are studied within this dissertation, the most prominent is example of gene's clustering exhibited by *waa* (*rfa*) locus described above in subsection 1.3.2. This locus distinguishes three operons: *gmhD*, *waaQ* and *waaA*[73–76]. The *E. coli* K-12 *waa* cluster is known to consists of more than 17 genes (see National Center for Biotechnology Information, *Escherichia coli* str. K-12 substr. MG1655, complete genome, GenBank accession number: U00096.3)[183,184]. Sharing of common genetic location can be also observed in the case of the genes encoding some participants of Raetz pathway (*lpxA, lpxB* or *lpxD*) with the *fabZ* gene, encoding critical for phospholipids biosynthesis FabZ dehydrase, underlining the importance of maintaining the balance between these outer membrane components. Similarly, forming of smaller clusters occurs in the case of genes encoding proteins involved in other essential aspects of LPS homeostasis, and examples are: genetic connection of part of LPS transportation system *lptCAB* with gene encoding other relevant protein for *E. coli* viability, *rpoN*; colocalization of two-component systems executors responding to LPS defects, like *qseEF* and *qseG* or *basSR* and *eptA*; and lastly, forming operons like *lapA/B* or *hslUV*, that are of primary interest in this study. As it can be observed in Figure 1.18., the genome of *E. coli* is enriched in clustered LPS-related genes and their occurrence is noticeably dispersed throughout the genome. It is also important to underline that among approximately 4,500 known genes of *E. coli,* only little over 300 are essential for survival of this microorganism. Within this group, as many as 39 of *E. coli* genes that are involved in LPS biosynthesis, assembly and regulation are indispensable, essential for bacterial viability at high temperature and required for thermotolerance (Table 1.1.)[181,185,186]. This again emphasizes the importance of complete elucidation of LPS function in bacterial viability.

Table 1.1. List of LPS-related genes, names of encoded products and the information of essentiality for bacterial survival in *E. coli* K-12 substr. MG1655
Table based on information from Profiling of *Escherichia coli* chromosome (PEC) database Version: 4.10.7 and EcoCyc bioinformatics database[180]

Gene	Product	Essentiality
	genes related to lipid A-core biosynthesis	
arnA	UDP-4-amino-4-deoxy-L-arabinose formyltransferase/UDP-glucuronate dehydrogenase	not essential
arnB	UDP-4-amino-4-deoxy-L-arabinose aminotransferase	not essential
arnC	undecaprenyl phosphate-L-Ara4FN transferase	not essential
arnD	undecaprenyl phosphate-*α*-L-Ara4FN deformylase	not essential
arnE	undecaprenyl phosphate-*α*-L-Ara4N exporter	not essential
arnF	undecaprenyl phosphate-*α*-L-Ara4N exporter	not essential
arnT	lipid IV_A 4-amino-4-deoxy-L-arabinose transferase	not essential
cdsA	CDP-diglyceride synthase	essential
clsA	cardiolipin synthase I	not essential
clsB	cardiolipin synthase II	not essential
clsC	stationary phase cardiolipin synthase III	not essential
eptA	lipid A phosphoethanolamine transferase	not essential
eptB	Kdo phosphoethanolamine transferase	not essential
eptC	LPS core phosphoethanolamine transferase	not essential
fabZ	(3*R*)-hydroxymyristol acyl carrier protein dehydratase	essential
galE	UDP-galactose-4-epimerase	not essential
glmM	phosphoglucosamine mutase	essential
glmS	L-glutamine:D-fructose-6-phosphate aminotransferase	essential
glmU	fused *N*-acetyl glucosamine-1-phosphate uridyl transferase/ glucosamine-1-phosphate acetyl transferase	essential
gmhA	D-sedoheptulose 7-phosphate isomerase	required for thermotolerance[181]
gmhB	D-*glycero*-*β*-D-*manno*-heptose-1,7-bisphosphate 7-phosphatase	required for thermotolerance[181]
hldD (htrM)	ADP-L-*glycero*-D-*manno*-heptose-6-epimerase	essential>42°C[157], required for thermotolerance[181]
hldE (gmhC)	fused heptose 7-phosphate kinase/heptose 1-phosphate adenyltransferase	required for thermotolerance[181]
kdsA	3-deoxy-D-*manno*-octulosonate 8-phosphate synthase	essential
kdsB	3-deoxy-D-*manno*-octulosonate cytidylyltransferase	essential
kdsC	3-deoxy-D-*manno*-octulosonate 8-phosphate phosphatase	essential
kdsD	D-arabinose 5-phosphate isomerase	not essential
lpxA	UDP-*N*-acetylglucosamine acetyltransferase	essential
lpxB	lipid A disaccharide synthase	essential
lpxC	UDP-3-*O*-acyl *N*-acetylglucosamine deacetylase	essential
lpxD	UDP-3-*O*-(3-hydroxymyristoyl)-glucosamine *N*-acyltransferase	essential
lpxH	UDP-2,3-diacylglucosamine pyrophosphatase	essential
lpxK	lipid A 4'-kinase	essential
lpxL	lauryl-acyl carrier protein (ACP)-dependent acyltransferase	essential>33°C[182]
lpxM	myristoyl-acyl carrier protein (ACP)-dependent acyltransferase	not essential

lpxP	palmitoleoyl-acyl carrier protein (ACP)-dependent acyltransferase	not essential
lpxT	lipid A-core phosphotransferase	not essential
pagP	lipid A palmitoyltransferase	not essential
pgpA	phosphatidylglycerophosphatase A	not essential
pgpB	phosphatidylglycerophosphatase B	not essential
pgpC	phosphatidylglycerophosphatase C	not essential
pgsA	phosphatidylglycerophosphate synthetase	essential
psd	phosphatidylserine decarboxylase	essential
pssA	phosphatidylserine synthase	essential
rfbA	glucose-1-phosphate thymidylyltransferase	not essential
rfbB	dTDP-glucose-4,6-dehydratase	not essential
rfbC	dTDP-4-deoxyrhamnose-3,5-epimerase	not essential
rfbD	dTDP-4-dehydrorhamnose reductase subunit	not essential
waaA	3-deoxy-*α*-D-*manno*-oct-2-ulosonic acid transferase (Kdo transferase)	essential
waaB	UDP-D-galactose:(glucosyl)lipopolysaccharide-1,6-D-galactosyltransferase	not essential
waaC (rfaC)	ADP-heptose:LPS heptosyltransferase I	essential>42°C[26], required for thermotolerance[181]
waaF	ADP-heptose:LPS heptosyltransferase II	required for thermotolerance[181]
waaG	glucosyltransferase I	required for thermotolerance[181]
waaH	UDP-glucuronate:LPS(HepIII) glycosyltransferase	not essential
waaJ	UDP-D-glucose:(galactosyl)lipopolysaccharide glucosyltransferase	not essential
waaL	*O*-antigen ligase	not essential
waaP	lipopolysaccharide core heptose (I) kinase	not essential
waaQ	lipopolysaccharide core heptosyltransferase III	not essential
waaR	UDP-D-glucose:(glucosyl)LPS *α*-1,3-glucosyltransferase	not essential
waaS	lipopolysaccharide core biosynthesis protein, WaaS rhamnosyltransferase	not essential
waaU	ADP-heptose:LPS heptosyltransferase 4	not essential
waaY	lipopolysaccharide core heptose (II) kinase	not essential
waaZ	lipopolysaccharide core biosynthesis protein (Kdo III attachment)	not essential
genes related to lipid A-core transport and translocation		
lptA	periplasmic LPS-binding protein	essential
lptB	lipopolysaccharide transport system ATP-binding protein LptB	essential
lptC	lipopolysaccharide transport system protein LptC	essential
lptD	lipopolysaccharide assembly protein LptD, *β*-barrel component	essential
lptE	lipopolysaccharide assembly protein LptE, lipoprotein component	essential
lptF	lipopolysaccharide transport system protein LptF	essential
lptG	lipopolysaccharide transport system protein LptG, ABC permease	essential
msbA	ATP-dependent lipid A-core flippase	essential
yceK	outer membrane integrity lipoprotein	not essential

LPS-related sigma and anti-sigma factors		
rpoE	RNA polymerase, sigma 24 (sigma E) factor	essential
rseA	anti-sigma factor of sigma 24	required for thermotolerance[181]
rseB	negative regulator of sigma E factor, binds RseA	not essential
rseC	σ^E factor regulatory protein RseC	not essential
rpoN	RNA polymerase, sigma 54 (sigma N) factor	not essential
genes involved in signal transduction in LPS biosynthesis and assembly		
arcA	DNA-binding transcriptional dual regulator ArcA	not essential
arcB	sensor histidine kinase ArcB	not essential
basR	DNA-binding transcriptional dual regulator BasR	not essential
basS	sensor histidine kinase BasS	not essential
pmrD	signal transduction protein PmrD	not essential
pmrR	small regulatory membrane protein PmrR	not essential
phoP	DNA-binding transcriptional dual regulator PhoP	not essential
phoQ	bifunctional sensor histidine kinase PhoQ	not essential
cpxA	sensor histidine kinase CpxA	not essential
cpxP	periplasmic protein CpxP	not essential
cpxR	DNA-binding transcriptional dual regulator CpxR	not essential
evgA	DNA-binding transcriptional activator EvgA	not essential
evgS	sensor histidine kinase EvgS	not essential
gadE	DNA-binding transcriptional activator GadE	not essential
qseE	histidine kinase QseE	not essential
qseF	DNA-binding transcriptional activator QseF	not essential
qseG	outer membrane lipoprotein QseG	not essential
phoB	DNA-binding transcriptional dual regulator PhoB	not essential
phoR	sensor histidine kinase PhoR	not essential
rcsA	DNA-binding transcriptional activator RcsA	not essential
rcsB	DNA-binding transcriptional activator RcsB	not essential
rcsC	histidine kinase RcsC	not essential
rcsD	RcsD phosphotransferase	not essential
rcsF	sensor lipoprotein RcsF	not essential
genes encoding proteases involved in LPS biosynthesis and assembly		
hslU	molecular chaperone and ATPase component of HslUV protease	not essential
hslV	peptidase component of the HslUV protease	not essential
ftsH	ATP-dependent zinc-metalloprotease	essential
LPS biosynthesis/assembly proteins encoding genes		
lapA	lipopolysaccharide assembly protein A	not essential
lapB	lipopolysaccharide assembly protein B	essential[41], required for thermotolerance[181]
lapC	lipopolysaccharide assembly protein C	essential[188]
rfaH	DNA-binding transcriptional antiterminator	not essential
genes of non-coding RNA involved in LPS biosynthesis/assembly		
arcZ	small regulatory RNA ArcZ	not essential
cpxQ	small regulatory RNA CpxQ	not essential

gcvB	small regulatory RNA GcvB	not essential
glmY	small regulatory RNA GlmY	not essential
glmZ	small regulatory RNA GlmZ	not essential
mgrR	small regulatory RNA MgrR	not essential
micA	small regulatory RNA MicA	not essential
micF	small regulatory RNA MicF	not essential
rirA	small regulatory RNA RirA	not essential
rybB	small regulatory RNA RybB	not essential
slrA	small regulatory RNA SlrA	not essential

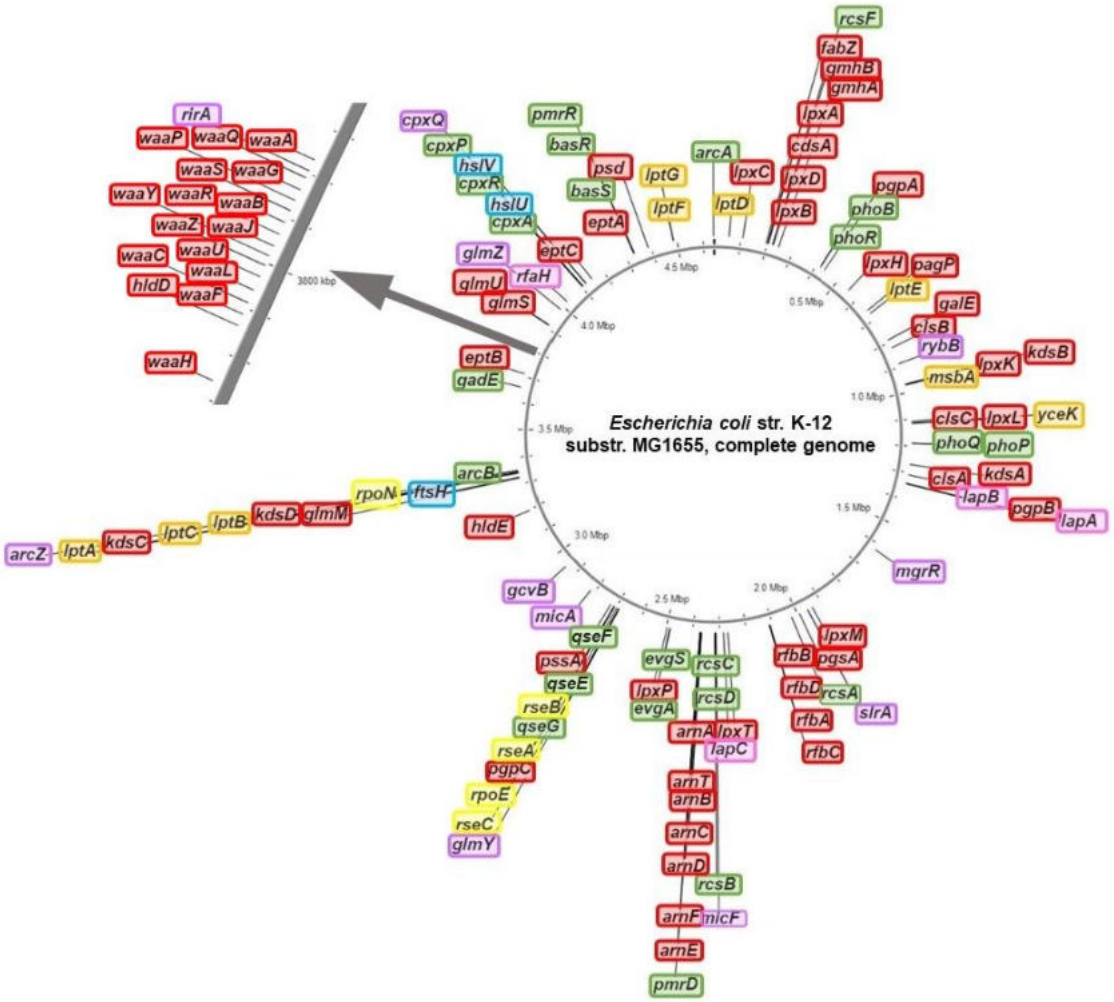

Fig. 1.18. Schematic genetic map showing locations of majority of genes involved in LPS synthesis assembly and regulation, identified in *E. coli* K-12 substr. MG1655

Map was created using the CGView Server[187] and further modified. Genes marked in red color are related to lipid A-core biosynthesis. Orange indicates genes of products related to lipid A-core transport and translocation. LPS-related sigma and anti-sigma factors are marked with yellow. Genes whose products are involved in signal transduction in LPS biosynthesis and assembly are presented in green and genes encoding proteases involved in LPS biosynthesis and assembly are marked as blue. LPS biosynthesis/assembly protein-encoding sequences are indicated with pink and lastly, genes of non-coding RNA involved in LPS biosynthesis/assembly are encircled in purple. These colors correspond to Table 1.1. that lists depicted LPS-related genes, names of encoded products and the information of essentiality for bacterial survival.

2. AIM AND SCOPE OF WORK

2.1. Aim of the work

The purpose of this research was to broaden the understanding of regulation and assembly of *Escherichia coli* lipopolysaccharide by examining the molecular basis of LapB essentiality and its role in turnover of LpxC that catalyzes the first committed step in LPS biosynthesis. In addition, the investigation was undertaken to establish if there are any undiscovered interacting partners of LapB present, and if the possible alternative mechanism of LpxC regulation exists.

Results presented in this dissertation are published in the form of manuscript: Biernacka, D. *et al*. (2020) 'Regulation of the first committed step in lipopolysaccharide biosynthesis catalyzed by LpxC requires the essential protein LapC (YejM) and HslVU protease' published in the *International Journal of Molecular Sciences*[188].

2.2. Rationale and scope of the work

As it was repeatedly mention in the introduction, the connection between the synthesis of phospholipids and LPS is well established and two pathways are tightly co-regulated, maintaining the ratio of 1.0:0.15 in undisturbed cells of wild-type *E. coli*[189]. The imbalance within the LPS biosynthesis without compensation in phospholipids pathway is poorly countenanced by bacterial cell and it predominantly results in cell death[41,49]. Maintaining of the balance between these two outer membrane components depends on strict regulation of LpxC enzyme turnover that constitutes the first committed step in LPS biosynthesis (Fig. 1.4.)[190]. Although the branching of two pathways occurs at earlier step (Fig. 1.5.), where they share the common precursor, *R*-3-hydroxymyristoyl-ACP, the unfavorable equilibrium constant of LpxA-driven reaction results in LpxC and FabZ to be the key enzymes propelling two processes[190]. Abundance of LpxC UDP-3-*O*-acyl-*N*-acetylglucosamine deacetylase is regulated in response to the bacterium need for lipid A and occurs due to the degrading activity of FtsH protease[47,49]. The FtsH-dependent LpxC degradation relies on the LPS assembly heat shock protein LapB[41,59]. Results published previously by Professor Raina's laboratory established that FtsH and LapB work together to regulate LpxC

proteolysis[41]. LapB (YciM) and its operon partner LapA (YciS) were discovered during the search for mutants with the elevated levels of envelope stress response in study concerning periplasmic folding factors[60]. Several non-polar deletions, Δ*lapA*, Δ*lapB*, and Δ(*lapA lapB*), were constructed and examined in detail for the LPS content and transduced in well-characterized *E. coli* strain backgrounds W3110, BW30207 (MG1655 derivative), and BW25113 on minimal M9 and rich LA medium at 23, 30, 37, and 42°C. The examination of growth phenotype under different conditions revealed that single Δ*lapA* deletion was tolerated in all backgrounds, unless when such strains were grown on MacConkey agar at 43°C that confers mild permeability defects and temperature sensitivity when grown on bile salt-containing medium[41]. Meanwhile, Δ(*lapA lapB*) or Δ*lapB* suppressor-free mutants could be obtained only in the BW25113 parental strain on M9 medium at 30°C after prolonged (72 h) incubation, and these mutants formed very small size colonies. In the parental strains W3110 or BW30207, Δ(*lapA lapB*) and Δ*lapB* transductants were only obtained in the presence of plasmid carrying *lapA* and *lapB* genes[41]. Thus, it was concluded that the *lapB* gene is essential under standard laboratory growth conditions, and its deletion results in severe growth defects.

Despite showing that LapA and LapB interact with FtsH protease and LPS, it is still unclear what is the mechanism by which LapB regulates the LpxC proteolysis in response to LPS status. Based on previously reported studies by Professor Raina's group, LapB was assumed to act as a scaffold in the inner membrane, where LPS biosynthetic enzymes are recruited[41]. During this process, LapB could monitor the accumulation of LPS in the IM and direct LpxC to proteolysis via FtsH to prevent unwanted excess of LPS biosynthesis over phospholipids pathway. Consistent with this presumption, it was already shown that LapB co-purifies with LPS and FtsH[41]. However, it remained unknown how LPS amounts are sensed by LapB and if FtsH is the sole protease that regulates LpxC turnover. There are many examples throughout the research of unstable proteins that undergo proteolytic regulation by more than one protease. One of the relevant examples described earlier is the case of RpoH sigma factor that is a substrate of FtsH and also of the heat shock-inducible HslVU (ClpQY) proteolytic complex[52,191,192]. The similar example is RcsA transcriptional activator component of Rcs phosphorelay, whose amounts are limited both by its rapid

degradation by Lon ATP-dependent protease, and HslVU[193]. In this study, experiments were undertaken to address if any additional interacting partners of LapB exist and if there is the possibility of alternative mechanism of LpxC proteolysis aside from known FtsH-mediated degradation.

Thus, several approaches were undertaken to gather the evidence that answers given questions. First, in order to identify if additional proteases are involved in the degradation of LpxC, the multicopy suppressor approach was used to investigate if there are additional factors that can bypass the lethality of Δ*lapB* or Δ*lapA/B* mutants (Fig. 2.1. A). This experiment led to identification of the HslVU protease complex to participate in the turnover of LpxC. Overexpression of *hslV* alone or *hslVU* was found to repress the elevated accumulation of LpxC in Δ*lapB* mutants, which was validated by pulse-chase experiments revealing an alternative pathway of LpxC degradation. In the second approach, the isolation of extragenic suppressors of Δ*lapB* strain that restored normal LPS biosynthesis and bypassed *lapB* deletion lethality, identified a unique frame-shift mutation in the essential *yejM* gene causing truncation of its periplasmic domain (Fig. 2.1. B). Next, it was assumed that if LapB is interacting with the additional partner, the deletion of such a gene could be lethal. At the same time, if the point mutations in an appropriate gene would be introduced, such mutant should exhibit the elevated transcriptional response of RpoE sigma factor, similar like observed with *lapB* mutants or in strains where LPS synthesis is severely disrupted[26,41]. Based on this assumption, in the complementary study, Tn*10* transposon-linked point mutations were analyzed that met simultaneously three requirements: i) mutants exhibited the elevated *rpoE*P3 promoter activity, ii) the sensitivity of such mutants to CHIR090 LpxC inhibitor was observed to different extents, and iii) mutated strains manifested membrane permeability defects. Juxtaposition of above conditions led to the identification of three significant point mutations again in the essential *yejM* gene: one having a frame-shift mutation resulting in truncation after 377th amino acid residue (isolated three times), the second mutation introduced a stop codon after amino acid residue 190, and another resulting into a single amino acid F349S substitution (Fig. 2.1. C). During the completion of this work, YejM has been speculated to either maintain lipid homeostasis or be involved in the transport of cardiolipin or

exhibit a metal-dependent phosphatase activity[194–200]. YejM was designated as LapC based on identified genetic and biochemical interactions of LapC with LapB.

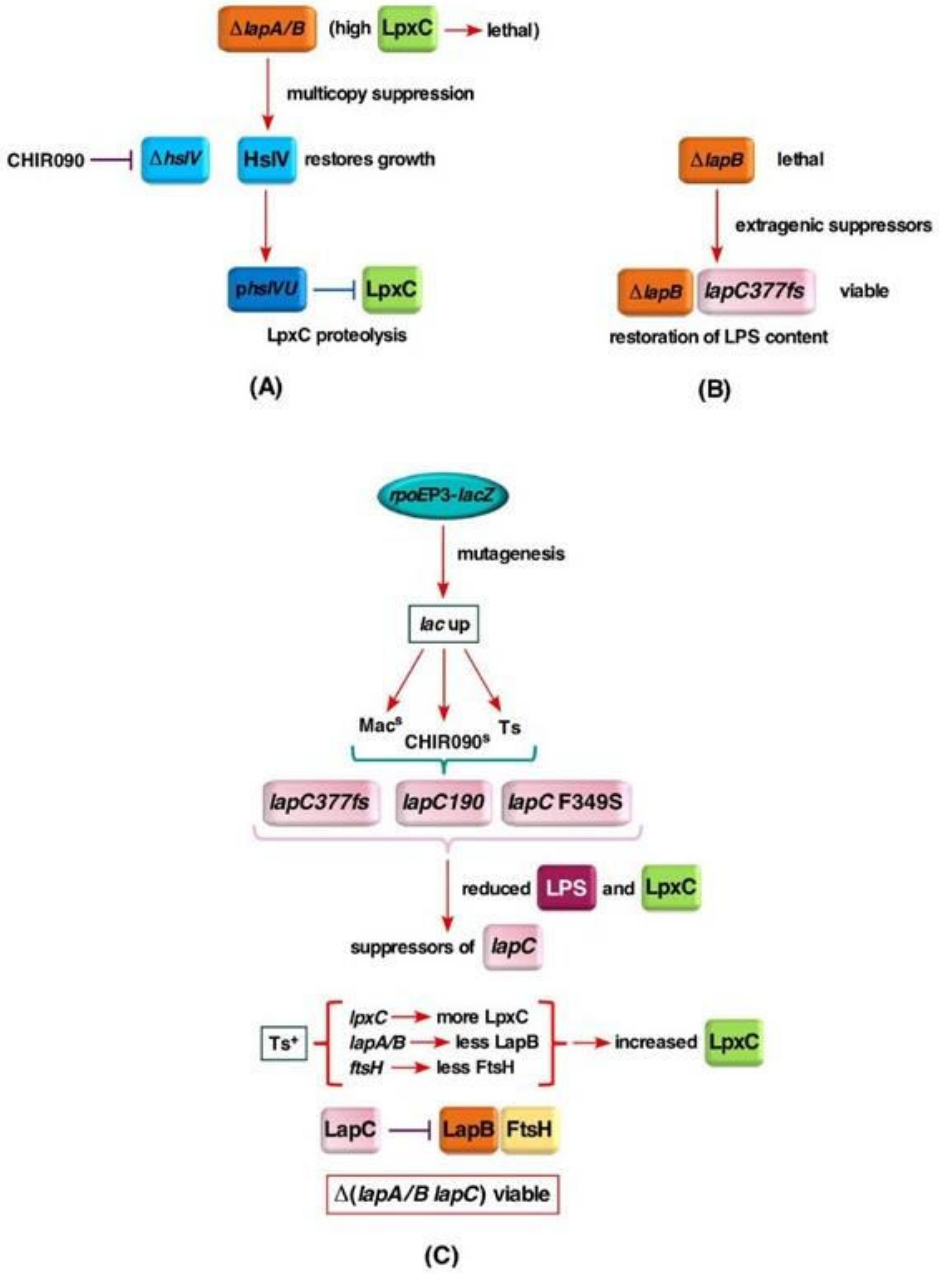

Fig. 2.1. Illustration of three major approaches that identified additional players in the regulation of LPS assembly

Three main approaches used in this research to characterize LapB additional partners and its role in LpxC regulation. (A) Multicopy suppressor analysis of *ΔlapA/B* lethal phenotype. The search led to discovery of HslVU-dependent proteolysis of LpxC. (B) Identification of extragenic suppressors of *ΔlapB* that restored the normal LPS synthesis and the viability of bacteria revealed mutation mapped in 377th aa of LapC. (C) Screening for Tn*10* transposon-linked point mutations that are CHIR090- and temperature-sensitive and have defects in LPS identified essential *lapC* gene, whose product was found to interact with LapB/FtsH to regulate LpxC proteolysis.

During the research on LapB protein, Professor S. Raina and Professor G. Klein isolated LPS derived from wild-type *E. coli*, Δ*lapB* and different Δ*lapB* derivatives to analyze their composition on the charge-deconvoluted mass spectra in the negative ion mode. One of isolated Δ*lapB* suppressor mutation was found to contain a frame shift mutation in the newly characterized *lapC* gene with genotype of (Δ*lapB lapC377fs).* In Figure 2.2., mass spectra of LPS from wild-type *E. coli*, Δ*lapB* and (Δ*lapB lapC377fs)* are presented in panels A, B and C, accordingly, which were recently published by our group[188]. Consistent with the results published in Klein *et al.* 2014, mass spectra of LPS of Δ*lapB* mutant reveal the mass peaks corresponding to early LPS intermediates and the complete LPS molecules (Fig. 2.2. panel B)[41]. Pre-mature LPS forms of LapB-deficient strain correspond to peaks with mass ranging from 2428.9 to 3770.7 Da that comprise mostly of predicted LA_{hexa} + Kdo_2 + Hep (2428.9 Da) and LA_{penta} + Kdo_2 + Hep_2 + Hex_2 + *P* (2815.4 Da), and their modifications. Interestingly, when the *lapC377fs* mutation is introduced in Δ*lapB* strain (Fig. 2.2. panel C), none of the early intermediates can be observed and the accumulation of LPS with the complete core with hexaacylated lipid A is restored. The further similarities of wild type and (Δ*lapB lapC377fs*) derivative spectra constitute mass peaks of LPS glycoforms with 2 Kdo or 3 Kdo residues with *P*-EtN and L-Ara4N non-stoichiometric modifications. Thus, mass peaks at 3936.8 Da and its derivatives with mass peaks at 4139.9 and 4489.9 Da correspond to the glycoform I with 2 Kdo residues with different additional non-stoichiometric substitutions that are observed in panel A and C in Fig. 2.2. Glycoforms IV and V of LPS that represent derivatives with 3 Kdo residues and rhamnose with corresponding peaks of 3948.8, 4071.7, 4202.8 and 4298.9 Da are also prominent for wild type and (Δ*lapB lapC377fs*) but are absent in the spectra of LPS obtained from Δ*lapB*. Therefore, it is evident that suppression of Δ*lapB* by *lapC377fs* mutation restores the normal LPS composition and it suggests that the truncation within the C-terminal domain of LapC could prevent the excessive synthesis of LPS in a Δ*lapB* background, which is consistent with the reduced LPS synthesis in the *lapC* mutant observed in LPS profiles presented further in this thesis. These results significantly indicated that LapB and LapC cooperate to regulate the LpxC level and the amounts of LPS.

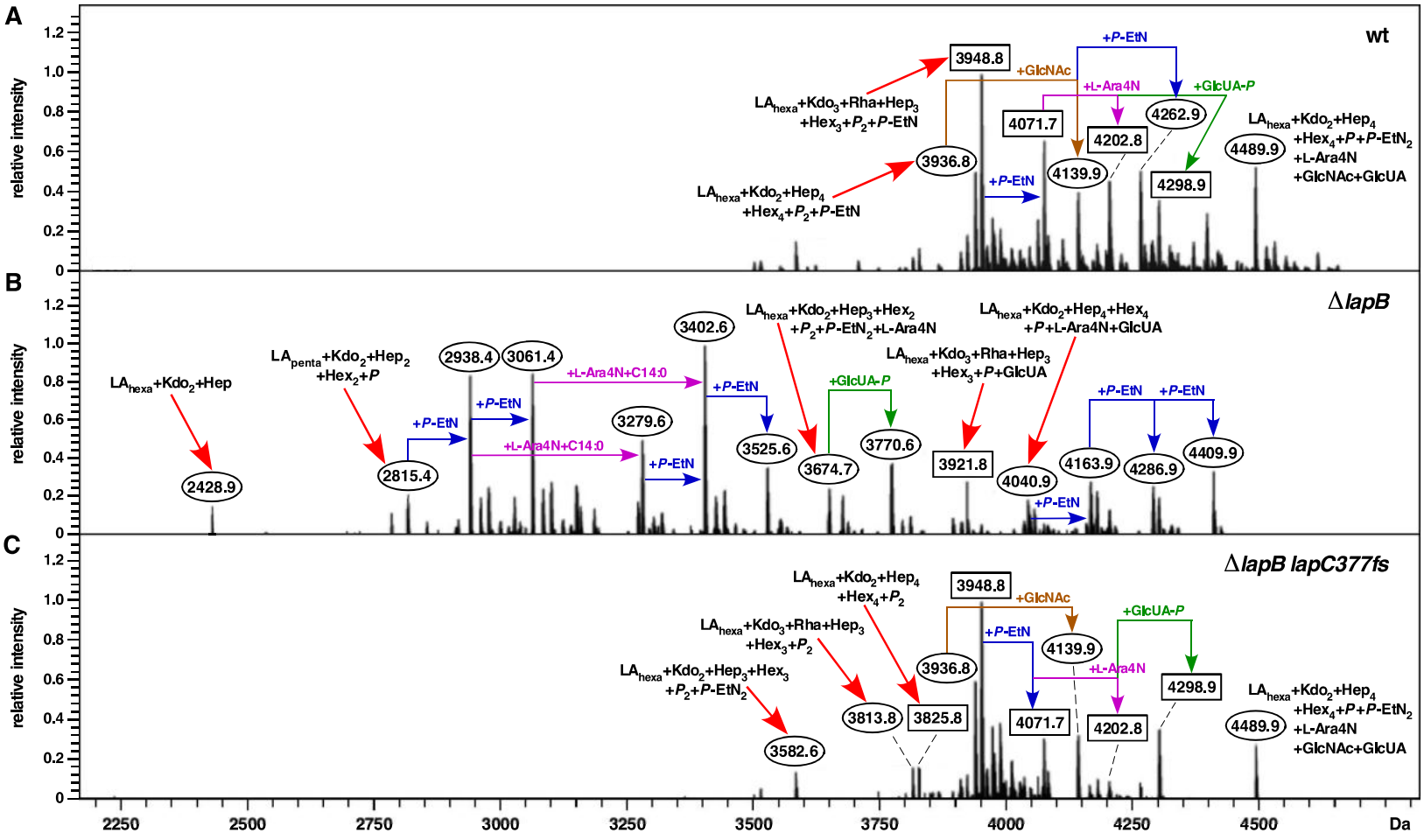

Fig. 2.2. Charge-deconvoluted mass spectra in the negative ion mode of LPS derived from the wild-type *E. coli* (A), Δ*lapB* (B) and (Δ*lapB lapC377fs)* (C)[188]

Mass numbers refer to monoisotopic peaks. Rectangular boxes correspond to the glycoform containing the third Kdo. Mass numbers in ovals are the derivatives with two Kdo residues with either complete or incomplete core.

3. MATERIALS AND METHODS

3.1. Materials

3.1.1. Bacterial strains and plasmids

Table 3.1. contains a list of strains used in this study with their genetic characteristics and indicated source.

Table 3.1. Strains used in this study

Strain	Characteristics	Reference/source
DH10B	F$^-$ mcrA Δ(*mrr-hsd*RMS-*mcr*BC) Φ80d*lac*ZΔM15 *lac*X74 *end*A1 *rec*A1 *deo*R (*ara*,*leu*)7697 *ara*D139 *gal*U *gal*K *nup*G *rps*L λ$^-$	Professor S. Raina collection
BL21	*fhuA2 [lon] ompT gal (λ DE3) [dcm] ΔhsdS λ DE3 = λ sBamHIo ΔEcoRI-B int::(lacI::PlacUV5::T7 gene1) i21 Δnin5*	Professor S. Raina collection
BW25113	*lacI^q rrnB*$_{T14}$ Δ*lacZ*$_{WJ16}$ Δ*araBAD*$_{AH33}$ Δ*rhaBAD*$_{LD78}$	[201]
T7 Express *lysY/I^q*	MiniF *lysY fhuA2 lacZ::T7 gene1 [lon] ompT*	NEB
GK1942	BW25113 (pKD46)	[41]
SR7753	BW25113 (*lapB*)<>*aph*	[41]
SR9523	BW25113 (*lapB*)<>*frt*	[41]
SR8348	SR7753 *lapC377fs*	[188]
SR16087	BW25113 *lapA-lapB*<>*cat*	[41]
SR17187	BW25113 *lapA-lapB*<>*aph*	[41]
SR19796	SR17187+p*hslV*$^+$	[188]
SR17432	BW25113 Φ (*rpoE*P6-*lacZ*)	[41]
SR18868	BW25113 Φ (*rpoE*P2/P3-*lacZ*)	[121]
SR18987	BW25113 Φ (*rpoE*P2*-*lacZ* -12 and -24 mut)	[121]
SR19041	SR18987 *lapC190*	[188]
SR19750	SR18987 *lapC377fs*	[188]
SR22861	SR18987 *lapC377fs*	[188]
SR22862	SR18987 *lapC* F349S	[188]
GK6075	BW25113 Δ*lapC190*	[188]
GK6078	GK6075 *lpxC* K270T	[188]
GK6093	GK6075 *lpxC* V37G	[188]
SR22727	GK6075 *lpxC* R230C	[188]
SR22728	GK6075 *lpxC* R230C	[188]
SR22729	GK6075 *lpxC* R230C	[188]
SR22731	GK6075 *lpxC* V37G	[188]
SR22732	GK6075 *lpxC* V37G	[188]

SR22738	GK6075 *lpxC* V37L	[188]
SR22739	GK6075 *lpxC* V37G	[188]
GK6094	GK6075 *lpxC fs306* stop codon	[188]
GK6085	GK6075 *lapA* IS after 34 nt	[188]
GK6089	GK6075 *lapA fs* 137 nt	[188]
GK6090	GK6075 *lapA* IS after 103 nt	[188]
GK6097	GK6075 *lapA* L8 to TGA stop codon	[188]
SR22734	GK6075 *lapA* IS after 34 nt	[188]
SR22736	GK6075 *lapA fs* after 69 nt	[188]
SR22737	GK6075 IS at -106 in *lapA/B* promoter region	[188]
GK6084	GK6075 *lapB* D124Y	[188]
GK6087	GK6075 *lapB* R125L	[188]
SR22724	GK6075 *lapB* H325P	[188]
SR22725	GK6075 *lapB* H325L	[188]
SR22726	GK6075 *lapB* A88V	[188]
SR22733	GK6075 *lapB* R115H	[188]
GK6095	GK6075 *ftsH* A296V	[188]
SR22766	BW25113 Δ*hslUV<>aph*	[188]
SR22776	SR18987 *lapC190*	[188]
SR22777	SR17432 *lapC190*	[188]
SR22433	SR18987 *lapC377fs*	[188]

Table 3.2. contains a list of plasmids used in this study with their characteristics and indicated source.

Table 3.2. Plasmids used in this study

Plasmid	Characteristics	Reference/source
pET24b	expression vector	Professor S. Raina collection
pET28b	expression vector	Professor S. Raina collection
pDUET	expression vector	Professor S. Raina collection
pCP20	ts replicon with inducible FLP recombinase	[201]
pKD3	*oriR6K*$_g$, *bla* (Amp^R), *kan*, *rgnB* (Ter), *cat*	[201]
pKD13	*oriR6K*$_g$, *bla* (Amp^R), *kan*, *rgnB* (Ter)	[201]
pKD46	*araBp-gam-bet-exo*, *bla* (Amp^R), *repA101*(ts)	[201]
pCA24N	IPTG-inducible expression vector Cm^R	[202]
pSR19788	*hslV*$^+$ in pCA24N	[188]

pSR19796	*hslVU*$^{+}$ in pCA24N	[188]
JW2176	*lapC*$^{+}$ in pCA24N	[202]
pSR22763	*hslVU*$^{+}$ in pET24b	[188]
pSR22821	*hslVU*$^{+}$ in pET28b	[188]
pSR22901	*lapC*$^{+}$ in pET28b	[188]

3.1.2. Oligonucleotides

Table 3.3. lists the oligonucleotides used in this study with their application and sequences indicated.

Table 3.3. Oligonucleotides used in this study

Name	Sequence
For gene disruption	
lapC For	5′-CTC TAT CAA CGA AGA CAA AGC GCA CTA AGG GAA ACA GAT AAC AGG TTA TGA TTC CGG GGA TCC GTC GAC CC-3′
lapC Rev	5′-AGA TAT TTC GCT AAC TGA TTT ATA ATT AAT CAG TTA GCG ATA AAA CGC TTT GTA GGC TGG AGC TGC TTC G-3′
For cloning and overexpression	
lapC For	5′-CCG CAT CCC ATG GCT AAA ATT AAA CAT CAC CAT CAC CAT CAC CAC CAT CAC CAT ATG GTA ACT CAT CGT CAG C-3′
lapC Rev	5′-GCA AGT AAG AGA ATT CGC TAA CTG-3′
hslV For	5′-AGG GGT CAG CAT ATG ACA ACT ATA GTA AG-3′
hslU Rev	5′-GAT TGA ACG CTC GAG TCA TTA ATG ATG ATG GTG ATG ATG TAG GAT AAA ACG GCT CAG-3′
For sequencing and PCR amplification	
lapC For	5′-GCG CCT TAC AGT CCT CTA TCA AC-3′
lapC Rev	5′-CGT TTT CCA CAC CGA TTG CAA G-3′
lapA For	5′-GTT GAT TTC GTG GGC GCT GGT G-3′
lapB Rev	5′-GTC GTT GCC GGA GCA CAA TGG-3′
ftsH For	5′-GGA TAT AGA GTA TCC TGA CGC-3′
ftsH Rev	5′-CGG TAC AAA TAC AGT CAT CTG-3′
For qRT-PCR	
q*lapC* For	5′-ATT CGC AAG GTC AGG ATT TG-3′
q*lapC* Rev	5′-GCG ATA AAA CGC TTC TCG TC-3′

3.1.3. Media

Media used in this study are presented below. The composition, manufacturers and recipes are included.

LB medium (Difco)

per liter:

10 g tryptone
5 g yeast extract
10 g NaCl
25 g of LB powder dissolved in 1000 mL of Millipore quality (MQ) water, sterilized by autoclaving for 30 min at 121°C 1.5 atm.

LB agar (Difco)

per liter:

10 g tryptone
5 g yeast extract
10 g NaCl
15 g agar-agar
40 g of LB agar powder dissolved in 1000 mL of MQ water, sterilized by autoclaving for 30 min at 121°C 1.5 atm.

LB soft agar

per liter:

25 g LB powder (Difco)
7.5 g agar-agar (Difco)
Dissolved in 1000 mL of MQ water, sterilized by autoclaving for 30 min at 121°C 1.5 atm.

M9 minimal medium

per liter:

200 mL 5x M9 salts (Difco)
1 mL 1 M $MgSO_4$
1 mL 0.01 $FeCl_2$
100 µl 1 M $CaCl_2$
1 mL B1 (10 mg/mL)
5 mL 10% casamino acids
15 mL 20% glucose
876.9 mL H_2O

M9 minimal agar

per liter:

500 mL 2x agar
200 mL 5x M9 salts (Difco)
1 mL 1 M $MgSO_4$
1 mL 0.01 $FeCl_2$
100 µl 1 M $CaCl_2$
1 mL B1 (10 mg/mL)
5 mL 10% casamino acids
15 mL 20% glucose
376.9 mL H_2O

MacConkey agar (Difco)

per liter:

50 g of MacConkey agar powder boiled in 1000 mL of MQ H_2O until dissolved and aliquoted in sterile Petri dishes.

MOPS medium:

per liter:
10 g MOPS powder (Sigma-Aldrich)
30g tryptone (Difco)
20 g yeast extract (Difco)

Dissolved in 1000 mL of MQ water, pH adjusted with NaOH to 7.0, sterilized by autoclaving for 30 min at 121°C 1.5 atm.

SOC medium:

per liter:

20 g bacto-tryptone (Difco)
5 g yeast extract (Difco)
0.5 g NaCl
1.86 g KCl
19 g $MgCl_2$
1.2 g $MgSO_4$
18 g glucose
pH adjusted to 7.0, MQ water added to 1000 mL. Sterilized by autoclaving for 30 min at 121°C 1.5 atm.

3.1.4. Antibiotics

Media were supplemented with ampicillin (100 µg/mL), kanamycin (50 µg/mL), tetracycline (10 µg/mL), chloramphenicol (20 µg/mL) and CHIR090 (0.004 or 0.008 µg/mL), when needed.

3.1.5. Enzymes

Table 3.4. presents enzymes used in this study and their manufacturers.

Table 3.4. List of enzymes used in this study

Enzyme	Manufacturer
Lysozyme	Sigma-Aldrich
Proteinase K	QIAGEN
Benzonase	Merck
T4 DNA ligase	Thermo Scientific
Reverse transcriptase	Bio-Rad
RQ1 DNase	Promega
Platinum SuperFi II DNA Polymerase	Thermo Scientific
NdeI	Thermo Scientific
XhoI	Thermo Scientific
NcoI	Thermo Scientific

3.1.6. Buffers, gels and solutions

Table 3.5. lists the buffers used during this study and their composition.

Table 3.5. Buffers used in this study

Buffer	Composition
50xTAE	per liter: 242 g Tris 18.61 g Disodium EDTA 57.1 mL Acetic Acid Glacial MQ water up to 1000 mL
Z-buffer	per liter: 16.1 g $Na_2HPO_4 \cdot 7H_2O$ 5.5 g $NaH_2PO_4 \cdot H_2O$ 0.75 g KCl 0.246 g $MgSO4 \cdot 7H_2O$ 2.7 mL *β*-mercaptoethanol pH adjusted to 7.0
1x SDS-PAGE running buffer	14.4 g glycine 3.03 g Tris 1 g SDS

1 M Tris pH 6.8	per liter: 121 g Tris Base in 808 mL of MQ water, pH adjusted to 6.8, water added to total volume of 1000 mL
1 M Tris pH 8.8	per liter: 121 g Tris Base in 808 mL of MQ water, pH adjusted to 8.8, water added to total volume of 1000 mL
8x phosphate buffer	0.16 M sodium phosphate, 4M NaCl, pH 7.4
2x binding buffer (20 mM imidazole)	per 10 mL: 2.5 mL 8x phosphate buffer 0.1 mL 2 M imidazole 7.4 mL MQ water
elution buffers for protein purification	Elution buffers (10 mL) for protein purification were prepared by mixing appropriate volume of 2 M imidazole solution with 1.25 mL of phosphate buffer and equivalent volume of sterile MQ water up to 10 mL. If necessary, binding and elution buffers were supplemented with appropriate volume of 10% octyl *β*-D-glucopyranoside
gel buffer for LPS	3 M Tris, 0.3% SDS, pH 8.45
6x lysis buffer	0.001% bromophenol blue, 10% glycerol, 2% SDS, 0.0625 M Tris-HCl pH 6.8, 5% *β*-mercaptoethanol
10x top buffer for LPS	1 M Tris pH 8.35, 1% SDS, 1M Tricine
10x bottom buffer for LPS	2 M Tris, pH 8.9
transfer buffer for Western blotting	per liter: 14.4 g Glycine 3.026 g Tris base 200 mL methanol MQ water added to total volume of 1000 mL
Blocking buffer for Western blotting	Thermo Scientific™ StartingBlock™ (TBS) Blocking Buffer
Washing buffer for Western blotting	Thermo Scientific™ Pierce™ 20X TBS Buffer
6x DNA loading buffer	30% glycerol, 0.25% bromophenol blue, 0.25% xylene cyanol FF, MQ quality sterile water

Table 3.6. presents composition of gels used in this study.

Table 3.6. Gels used in this study

Type of gel	Composition
SDS-PAGE 4% stacking gel	1.47 mL H_2O 260 µl 30% acrylamide:Bis solution (37.5:1) 250 µl buffer (1 M Tris pH 6.8) 20 µl 10% sodium dodecyl sulfate (SDS) 20 µl 10% ammonium persulfate (APS) 4 µl N,N,N',N'-tetramethylenediamine (TEMED)
SDS-PAGE 12% resolving gel	1.905 mL H_2O 1.8 mL 30% acrylamide:Bis solution (37.5:1) 750 µl buffer (1 M Tris pH 8.8) 45 µl 10% sodium dodecyl sulfate (SDS) 22.5 µl 10% ammonium persulfate (APS) 2.25 µl N,N,N',N'-tetramethylenediamine (TEMED)
SDS-PAGE 12.5% resolving gel	1.83 mL H_2O 1.875 mL 30% acrylamide:Bis solution (37.5:1) 750 µl buffer (1 M Tris pH 8.8) 45 µl 10% sodium dodecyl sulfate (SDS) 22.5 µl 10% ammonium persulfate (APS) 2.25 µl N,N,N',N'-tetramethylenediamine (TEMED)
14% Tricine-SDS resolving gel for LPS	1.142 mL H_2O 0.410 mL 49.5% acrylamide:Bis solution 1.494 mL gel buffer (3 M Tris, 0.3% SDS, pH 8.45) 0.468 mL 100% glycerol 12 µl 10% ammonium persulfate (APS) 7.2 µl N,N,N',N'-tetramethylenediamine (TEMED)
16% Tricine-SDS resolving gel for LPS	1.084 mL H_2O 0.468 mL 49.5% acrylamide:Bis solution 1.494 mL gel buffer (3 M Tris, 0.3% SDS, pH 8.45) 0.468 mL 100% glycerol 12 µl 10% ammonium persulfate (APS) 7.2 µl N,N,N',N'-tetramethylenediamine (TEMED)
stacking gel Tricine-SDS for LPS	1.260 mL H_2O 0.150 mL 49.5% acrylamide:Bis solution 0.465 mL gel buffer (3 M Tris, 0.3% SDS, pH 8.45) 30 µl 10% ammonium persulfate (APS) 13 µl N,N,N',N'-tetramethylenediamine (TEMED)

Table 3.7. lists the solutions used during this study.

Table 3.7. Solutions used in this study

Solution	Description
X-Gal 5-bromo-4-chloro-3-indolyl-β-D-galactopyranoside	X-Gal indicator dye of β-galactosidase activity was used at a final concentration of 40 or 60 µg/mL in the agar medium
IPTG isopropyl β-D-1-thiogalactopyranoside	IPTG reagent was prepared as 1 M H_2O solutions and added accordingly to indicated concentration when induction of expression from lactose-induced promoter was needed
1 M sodium citrate	Sodium citrate was prepared as 1 M water solution, sterilized by autoclaving for 30 min at 121°C 1.5 atm and added accordingly to indicated concentration when needed during bacteriophages-involved experiments
20% glucose	Glucose was prepared as 20% water solution, sterilized by filtration, added accordingly to indicated concentration when needed as a carbon source or catabolic repressor
10x M9 salts	Composition per liter: 60 g Na_2HPO_4, 30 g KH_2PO_4, 10 g NH_4Cl, 5 g NaCl. Salts dissolved in Millipore Quality water and sterilized by autoclaving for 30 min at 121°C 1.5 atm
2x agar	Per liter 20g of agar-agar powder (Difco) were dissolved in 1000 mL of MQ H_2O and sterilized at 121°C, under 1.5 atm pressure for 30 minutes
1 M $MgSO_4$	Magnesium sulfate was prepared as 1 M water solution, sterilized by autoclaving for 30 min at 121°C 1.5 atm and added accordingly to indicated concentration or diluted with sterile MQ water to obtain concentrations indicated in methods
1 M $MgCl_2$	Magnesium chloride was prepared as 1 M water solution, sterilized by autoclaving for 30 min at 121°C 1.5 atm and added accordingly to indicated concentration or diluted with sterile MQ water to obtain concentrations indicated in methods
10 mM $FeCl_2$	Iron (II) chloride was prepared as 10 mM water solution, sterilized by autoclaving for 30 min at 121°C 1.5 atm, stored in the dark and added accordingly to indicated concentration
1 M $CaCl_2$	Calcium chloride was prepared as 1 M water solution, sterilized by autoclaving for 30 min at 121°C 1.5 atm and added accordingly to indicated concentration or diluted with sterile MQ water to obtain concentrations indicated in methods
10 mg/mL B1	Vitamin B1 was prepared as a 10 mg/mL water solution and sterilized by filtration
10% casamino acids	Casamino acid were prepared as 10% water solution, sterilized by autoclaving for 30 min at 121°C 1.5 atm and added accordingly to indicated concentration
80% glycerol	Glycerol was prepared as 80% water solution, sterilized by autoclaving for 30 min at 121°C 1.5 atm and added accordingly to indicated concentration or diluted with sterile MQ water to obtain concentrations indicated in methods
10% SDS sodium dodecyl sulfate	SDS was prepared as 10% water solution
4 mg/mL ONPG 2-nitrophenyl-β-D-galactopyranoside	ONPG was prepared as a 4 mg/mL solution in Z-buffer
1 M Na_2CO_3	Disodium carbonate was prepared as 1 M solution in MQ water
Benzonase® endonuclease	EMD Millipore Enzyme in 20 mM Tris-HCl (pH 8.0), 2 mM $MgCl_2$, 20 mM NaCl, 50% glycerol
B-PER Bacterial Protein Extraction Reagent	Pierce In 20 mM Tris buffer (pH 7.5)
2 M imidazole	Imidazole was prepared as 2 M solution in MQ water

Lysozyme	Lysozyme was prepared as 20 mg/mL solution in sterile MQ water
fixing solution for silver staining	40% ethanol, 5% acetic acid

3.1.7. Other chemicals

The kits and other chemicals used in this study are listed in Table 3.8. below.

Table 3.8. List of other chemicals and kits used in this study

Name	Manufacturer
Acetic acid	POCH
Ethanol	POCH
Isopropanol	POCH
Methanol	POCH
Chloroform	POCH
GeneRuler 1kb DNA Ladder	Thermo Scientific
SeaKem™ LE Agarose	Lonza
Ethidium Bromide	Sigma-Aldrich
InstantBlue	Expedeon
SuperSignal™ West Pico PLUS Chemiluminescent Substrate	Thermo Scientific
Plasmid DNA Extraction GPB Kit	GenoPlast Biochemicals
GenElute™ Bacterial Genomic DNA Kit	Sigma-Aldrich
GeneJET Gel Extraction Kit	Thermo Scientific
GeneJET PCR Purification Kit	Thermo Scientific

3.2. Methods

3.2.1. Calcium chloride competent cells

The overnight culture was diluted in ratio 1:100 (or higher, if necessary) in LB or M9 medium supplemented with appropriate antibiotic. Diluted culture was incubated with shaking at 30 or 37ºC until value of OD_{595} reached approximately 0.4. After, culture was transferred to sterile, pre-cooled centrifuge tube and centrifuged for 15 min at 7,000 rpm at 4ºC. Supernatant was discarded and pellet was resuspended in half of the initial culture volume of ice-cold 10 mM $MgCl_2$. Immediately after, the tube was centrifuged for 10 min at 7,000 rpm, 4ºC. This step was repeated twice, and after the second centrifugation, supernatant was removed and pellet was resuspended in half of the initial culture volume of ice-cold 100 mM $CaCl_2$, followed by 20 min incubation on ice. After that time, sample was centrifuged for 10 min at 7,000 rpm at 4ºC to remove calcium solution and recentrifuged for 3 min for all of the liquid to be eliminated. Cells prepared in such manner were resuspended in desired volume of ice-cold 100 mM $CaCl_2$ and aliquoted by 100 µl to pre-cooled Eppendorf tubes with 15 µl o 80% glycerol for immediate freezing at -80ºC (for storage) or to tubes without glycerol for upcoming transformation.

3.2.2. Transformation of calcium chloride competent cells

To 100 µl (or less) of prepared competent cells 1-2 µl of plasmid DNA was added. Tube was incubated on ice for 45 min and heat-shocked at 43ºC for 45 s. Immediately after the reaction tube was incubated on ice for 2 min, up to 700 µl of M9 or LB medium (supplemented with glucose, if needed) was added. Cells were incubated in culture medium for 1 h at 30 or 37ºC. After the time passed, culture was centrifuged for 3 min at 7,000 rpm, at room temperature (RT), the supernatant was discarded. Pellet was resuspended in the desired volume of M9 or LB medium and cultures were plated on solid medium supplemented with necessary additives. Plates were incubated overnight at 30, 37 or 42ºC.

3.2.3. Plasmid DNA isolation

Isolation of plasmid DNA was performed using Plasmid DNA Extraction GPB Kit (GenoPlast Biochemicals) according to the protocol provided by the

manufacturer. If necessary, isolation process was confirmed by agarose gel electrophoresis.

3.2.4. Chromosomal DNA isolation

The volume of 1.5 to 3 mL overnight culture was centrifuged at maximum speed for 3 min to pellet the cells. Isolation of chromosomal DNA was performed using GenElute™ Bacterial Genomic DNA Kit (Sigma-Aldrich) according to the protocol provided by the manufacturer. If needed, isolation process was confirmed by agarose gel electrophoresis.

3.2.5. DNA agarose gel electrophoresis

Electrophoretic DNA separation was carried out in an agarose gel with a concentration of 0.8 to 1.2%, depending on the size of the analyzed DNA fragments. DNA samples were prepared by adding the appropriate amount of 6x DNA loading buffer and applied to the wells of a prepared gel containing ethidium bromide at a final concentration of 0.5 µg/mL. For the electrophoretic separation, 1x TAE buffer and a voltage adequate to the size of the gel were used. The time of separation was chosen individually. The gel was observed using a UV transilluminator to visualize the DNA fragments.

3.2.6. PCR amplification

For 100 µl of total reaction mixture, 50 µl of 2x Master Mix, 43 µl of H_2O, 2.5 µl of each forward and reverse primer, 2 µl of template chromosomal DNA and 0.5 µl of high fidelity polymerase were mixed and subjected to PCR amplification using standard procedure with cycling parameters according to manufacturer's protocol.

After the PCR amplification, amplified DNA was resolved by agarose gel electrophoresis on 1% agarose gel and excised.

3.2.7. Elution of DNA products from agarose gel

Excision of PCR products and other DNA fragments from agarose gels was performed using GeneJET Gel Extraction Kit (ThermoFisher Scientific) according to the protocol provided by the manufacturer.

3.2.8. Enzymatic digestion

For 20 µl of digestion mixture, 2 µl of 10x Fast Digestion buffer, 1 µl of enzymes, and appropriate volumes (due to the concentration of DNA) of DNA fragment/plasmid and H_2O were added to the Eppendorf tube. The mixture was incubated at 37ºC for 60 min, centrifuged briefly, separated on the agarose gel and the DNA excised when required.

3.2.9. Ligation

The ligation mixture contained 8 µl of H_2O, 4 µl of 5x reaction buffer, 3 µl of DNA insert, 4 µl of vector and 1 µl of T4 DNA ligase. The ligation reaction was incubated at 23ºC for 45 min.

3.2.10. Bacteriophage P1 lysates

To obtain bacteriophage P1 lysates, 1 mL of overnight culture carrying the appropriate mutation marked with antibiotic resistance cassette was inoculated in 7 mL of LB with 5 mM $CaCl_2$ in ratio that allowed for OD_{595} ~ 0.1. Cultures were incubated with shaking at 30 or 37°C for at least 20 min or until the exponential growth phase was reached at OD_{600} ~ 0.3. Next, 100 µl of bacteriophage P1 stock (collection of Professor Raina) was added and culture was incubated for 20 min at 30 or 37°C for the P1 bacteriophage to be absorbed. Afterwards, the incubation, with shaking, at 30 or 37°C was continued until cultured lysed. In order to kill any resistant bacteria, 300 µl of chloroform was added and cultures were incubated with shaking at 37°C for 20 min to make sure all bacteria are lysed. Subsequently, sample was transferred to the centrifuge tubes without chloroform and centrifuged for 5 min at 7,000 rpm at 4°C. Supernatants (bacteriophage P1 lysates) were carefully collected to the pre-cooled tubes and stored at 4°C.

3.2.11. Bacteriophage P1-mediated transduction

Overnight culture of recipient strain was diluted 1:100 ratio in LB medium with 5 mM $CaCl_2$ and cultivated at 30 or 37°C until culture reached appropriate optical density of OD_{595} ~ 1.0. Subsequently, to 1.2 mL of culture, bacteriophage P1 lysate was added at multiplicity of infection (MOI) of 1 and the mixture was incubated at 37°C for 20 min. Next, 130 µl of 1 M sodium citrate was added to prevent readsorption of bacteriophage and the culture was centrifuged for 3 min

at 7,000 rpm at RT. Bacterial pellet was resuspended in desired liquid medium supplemented with 10 mM sodium citrate and incubated for 22 min at 30 or 37°C, allowing the resistance genes to be expressed. In case of kanamycin resistance cassette, such incubation was omitted. Culture was centrifuged again at the same parameters, resuspended in the appropriate volume of M9/LB with 10 mM sodium citrate and plated on M9/LA plates supplemented with 10 mM sodium citrate and appropriate antibiotic and/or additive like IPTG. Plates were incubated overnight or longer at 30 or 37°C. Depending on the aim of experiment, colonies were counted or passaged on the same type of 10 mM sodium citrate-supplemented plates and handled accordingly to next experiment procedures.

3.2.12. SDS-PAGE electrophoresis

Equivalent amounts of whole cell lysates or protein samples prepared with the addition of 6x lysis buffer and, if necessary water, were boiled at 95°C for 10 min. Next, samples were incubated on ice for 2 min and briefly centrifuged. Samples were separated on appropriate gel, using Bio-Rad SDS-PAGE Mini-PROTEAN® Tetra Cell apparatus. Electrophoresis was carried at 200 V. The time of separation was chosen individually. Gels were washed with water for 1 min and either stained using InstantBlue® Coomassie Protein Stain (Expedeon) according to the protocol provided by the manufacturer or used in Western blotting.

3.2.13. Western blotting

Samples were separated on acrylamide gels using SDS-PAGE technique according to protocol described above. Proteins from SDS-PAGE gel were transferred on methanol-activated PVDF membrane using 90 min electrotransfer at 100 V. After electrotransfer was finished, membrane was incubated in blocking buffer overnight at 4°C. Blocking was followed by 1 h incubation with specific primary antibodies. To remove antibodies that did not bound, membrane was washed 3 times with washing buffer, each time with 15 min incubation with gentle agitation. Afterwards, secondary antibodies were added to the membrane for 1 h incubation. Lastly, membrane was washed 5 times with washing buffer, each time with 10 min incubation with gentle agitation. Blots were revealed by chemiluminescence kit from Thermo Scientific as per manufacturer's instructions.

LPS amounts were detected using the WN1 222-5 monoclonal antibody (kindly gifted by Prof. S. Müller-Loennies) at a dilution of 1:10,000[201]. Anti-LpxC (1:20,000) and anti-FtsH antibodies (1:2,000) were kind gifts of Professors F. Narberhaus and K. Ito. Custom made LapB-specific antibodies were made by Cusabio (Wuhan, China) and used at a dilution of 1:5,000.

3.2.14. Electrocompetent cells

An overnight culture of GK1942 strain was diluted in MOPS medium to OD_{595} of 0.05. Cells were further cultivated at 30°C in the presence of L-arabinose, until culture reached mid-exponential phase and optical density OD_{595} of 0.6. Such cultures were transferred into pre-cooled centrifuge tubes and incubated on ice for 30 min. Next, cultures were centrifuged for 15 min at 4°C at 5,000 rpm. Supernatant was discarded and pellet was resuspended in the initial volume of ice-cold H_2O. After 15 min centrifugation with the same parameters, pellet was resuspended in half of the initial volume of ice-cold H_2O. Centrifugation was repeated and cells were resuspended in 1/20 of the initial volume of ice-cold 10% glycerol. The last centrifugation lasted 15 min at 4°C at 5,000 rpm. All the supernatant was removed and cells were resuspended in ice-cold 10% glycerol so that they were concentrated approximately 350 times. Such prepared electrocompetent cells were used directly for electroporation.

3.2.15. Electroporation

To the electrocompetent cells, less than 100 ng of DNA was added. Contents were mixed gently and mixture was let to sit on ice for 1-2 minutes and it was transferred into a chilled cuvette. Next, the cuvette was placed in the MicroPulser Electroporator (Bio-Rad) and the electroporation was performed. After electroporation, cells were recovered in SOC medium. Transformed cells were incubated for 75 min at 30 or 37ºC in a shaking incubator and plated on LA plate supplemented with 20 µg/mL of chloramphenicol. Plates were incubated overnight at 30 or 37°C.

3.2.16. Gene disruption strategy

Strains with gene deletions of *hslV*, *hslU*, *hslV/U*, *lapB* and *lapA/B* used in this study have been constructed and used in previously published research[41,192]. The Δ*lapC190* strain was constructed using λ-Red mediated recombineering, according to method described by Datsenko and Wanner, 2000, as followed[199]. PCR primers to construct Δ*lapC190* deletion were designed in such a manner to contain upstream and downstream regions of homology flanking the sequence encoding the periplasmic domain of LapC. Simultaneously, these oligonucleotides carried 20 nt of homology to *aph* kanamycin resistance cassette. DNA fragment was PCR amplified using pKD13. Product of PCR reaction was verified on agarose gel, excised from the gel and electroporated in electrocompetent cells of wild-type *E. coli* BW25113 transformed prior with λ-Red recombinase-expressing pKD46 plasmid (GK1942). Transformants were selected for kanamycin on LA medium at 30°C. Colonies of transformants were passaged in parallel on LA plate supplemented with ampicillin and LA plate with kanamycin and incubated at 30°C, to confirm temperature-induced loss of pKD46 plasmid. Additionally, constructed strains were verified for carrying a Δ*lapC190* deletion by PCR amplification, using isolated chromosomal DNA from mutants as a template. The Δ*lapC190* deletion was further transduced using bacteriophage P1-mediated transduction in BW25113 resulting into the construction of GK6075, which was retained for further experiments.

3.2.17. Multicopy suppressor screening to identify genes whose overexpression restore viability of ΔlapA/B bacteria

Search for the genes that overcome phenotypic defects of tested mutants, when present in multicopy was based on transformation of calcium chloride generated competent cells of SR17187 Δ*(lapA lapB)* strain with a complete library of all cloned open reading frames (ORFs) from ASKA collection[202]. In this collection, genes are cloned in pCA24N and are expressed from the P_{T5}-*lac* promoter that is IPTG-inducible. Transformants were plated on LA rich medium at 37 and 42°C (non-permissive growth conditions for SR17187) in the presence of 75 μM IPTG to induce gene expression. Based on the colony size and appearance of transformants, colonies of strains carrying potential multicopy

suppressors were chosen to start the liquid culture for the isolation of plasmid DNA. Plasmids with DNA fragments encoding suppressor genes were isolated and used to retransform SR17187 strain to confirm suppression. Confirmation of suppression was performed by cultivation of transformants in parallel, on growth-permissive M9 medium at 30°C and non-permissive conditions on LB agar at 42°C. The identification of multicopy suppressor genes was obtained by sequence analysis of plasmid DNA of confirmed suppressors. DNA sequencing was performed by Eurofins company.

To validate the suppression by overexpression of either the *hslV* gene alone or by co-expression of *hslVU*, pSR19788 (*hslV*$^{+}$ in pCA24N) and pSR19796 (*hslVU*$^{+}$ in pCA24N) were used that were derived from plasmids constructed in the previous study from Professor Raina's laboratory[192].

3.2.18. Isolation of extragenic mutations that prevent ΔlapB mutants lethality

Bacteriophage P1 lysate grown on SR17187 (Δ*lapA/B*) was used to transduce *lapA/B* deletion in *E. coli* W3110 background, where it was known that such deletion is only tolerated, if an extragenic suppressor is present[41]. Transductions were carried on M9 minimal medium at 30°C. After prolonged incubation, colonies of strains with potential extragenic mutation that restored *E. coli* W3110 Δ*lapA/B* mutants viability were cultivated. In parallel, as most of the extragenic suppressors of *E. coli* W3110 Δ*lapA/B* strain map either to *waaC* or *gmhA* genes and thus, synthesize deep-rough LPS, during this screening isolated Δ*lapA/B* derivatives in W3110 were examined if they synthesize normal LPS based on reactivity with WN1 222-5 antibodies. It conjointly resulted in the construction of one strain that met both conditions, SR8348. The suppressor mutation was marked by Tn*10,* as described below, and further transduced in the wild-type strain. Subsequently, the complementation study was performed, using the plasmid DNA from the ASKA library of *E. coli* ORFs[202]. Plasmids that could restore the growth of mutants were isolated and used for subcloning and DNA sequencing of cloned inserts. The position of Tn*10* mutation was established by DNA sequencing of PCR-amplified product determined by complementation. PCR amplification of region with determined Tn*10* mutation, using chromosomal DNA of SR8348 strain and DNA sequencing, revealed that SR8348 had a mutation in the *lapC* (*yejM)* gene. This mutation caused an insertion of

C residue at 1133 nt position and resulted in the frame-shift after 377th amino acid (*lapC377fs*) and the addition of 13 amino acid residues after Thr377, which led into the truncation of periplasmic C-terminal domain.

3.2.19. Isolation of extragenic mutations that induce transcription from the rpoEP3 promoter, which led to identification of the lapC gene

The screening for additional partners involved in LpxC turnover regulation was based on two initial assumptions: mutations in such potential genes should induce transcription from *rpoE*P3 promoter, as its activity is induced during envelope stress response, specifically when LPS biosynthesis or assembly is severely compromised[121]; and by analogy to defects exhibited by other mutations in essential genes involved in LPS homeostasis, potential mutants should be characterized by sensitivity to elevated temperatures. Therefore, saturated pools of mini-Tn*10* Kan transposon mutants were generated in wild-type BW25113 strain in rich medium at 30°C. Bacteriophage P1 was cultivated on these pools, subjected to chemical mutagenesis and used to transduce strains SR18868 (BW25113 Φ *rpoE*P2/P3-*lacZ*) and SR18987 (BW25113 Φ (*rpoE*P2*-*lacZ* -12 and -24 mut) that were constructed during other research in Professor Raina's laboratory upon regulation of the *rpoE* gene[121]. Among transductants, the deep blue colonies that exhibited a Lac up phenotype on LA X-Gal-supplemented plates, were patched simultaneously at 30 °C as a control, and at 42°C to select Ts mutants. Approximately more than 80,000 Lac up colonies were replica plated in such manner. At this point, only Tn*10*-linked point mutations that were unable to grow at 42°C and were simultaneously inducing the activity of the *rpoE*P3 promoter were retained. Next, in order to narrow down the pool of candidates, to the fraction of strains that would have mutations in genes whose products are involved in LpxC regulation with higher probability, two more conditions were tested. Lac up and Ts isolates were tested by streaking on MacConkey agar at 37°C and on LA agar with the addition of the LpxC inhibitor CHIR090 (0.008 µg/mL) at 30°C. Only those mutants that were unable to grow or grew poorly on MacConkey agar and were sensitive to growth inhibition by the sublethal concentration of the CHIR090 compound, were selected for further testing. Isolated candidates were verified by bacteriophage P1-mediated transductions and measurement of *β*-galactosidase activity of the *rpoE*P3-*lacZ*

fusion. To identify the gene, in which mutation took place, the position of insertion linked with Tn*10*, was determined by inverse PCR on candidates chromosomal DNAs and sequencing of amplified fragments or by sub-cloning of Tn*10* from recombinant cosmid clones that complement the mutation causing LPS defects, as further described. Mutations in the genes that mapped to the main biosynthetic *waa* locus or other known LPS-related genes, were not followed.

3.2.20. Mapping and complementation of mutations that allowed for the identification of lapC gene

The complementation studies that allowed for the identification of isolated mutated genes was performed using cosmid library in the single-copy vector to transform the mutants. This protocol was based on strategy published by Raina *et al.* 1995[136]. Complementing cosmids were selected by searching for the restoration of mutants growth at 42°C on MacConkey agar. Plasmids that could recombine mini-Tn*10* and restore growth of Ts mutants on MacConkey agar were isolated and used for subcloning and DNA sequencing of cloned inserts. Five Tn*10*-linked Ts mutants mapping at 49 min on the genetic map of *E. coli* with the *rpoE*P3-*lacZ* Lac up phenotype and unable to grow on MacConkey agar that identified the *lapC* gene were further followed. In addition, to identify the mutation, the isolated from candidates chromosomal DNA was used as a template to PCR amplify the *lapC* gene and its adjoining regions, using appropriate oligonucleotides. Amplified DNA fragments were sequenced and analyzed. Presented approach resulted in mutant strains designated as SR19041, SR19750, SR22861 and SR22862.

3.2.21. Isolation of extragenic suppressors of *lapC377fs* and *lapC190*

Strains isolated in the approaches described above, with the mutations mapping to the *lapC* gene, were characterized by the temperature-sensitive phenotype (above 42°C) and intolerance to MacConkey agar, due to the strategy of their isolation. These features were used to identify extragenic suppressor mutations that would restore the growth defects of *lapC377fs* and *lapC190* bacteria. Thus, several independent cultures of each strain were cultivated in LB at 30°C (permissive growth conditions) and portions of each plated on non-permissive growth conditions at 43°C, to search for temperature-resistant

colonies. Simultaneously, in a similar manner, suppressors that restore growth on MacConkey agar were selected by directly plating *lapC* derivatives cultures from LB at 30°C on MacConkey agar medium. Obtained colonies were verified for suppression by passaging in the same non-permissive growth conditions. Potential extragenic suppressor mutations in confirmed candidates were marked with mini-Tn*10* Kan and verified by complementation analysis using cosmid library, as described above. Cosmid clones that could recombine Tn*10*-linked suppressor mutation, were used to group 26 out of 29 suppressors in three complementation groups. Additional transductions with defined linked mutations were performed to reinforce verification. Furthermore, to specifically define isolated extragenic mutations, chromosomal DNA of all 29 suppressor strains was isolated and used as a template to PCR amplify candidate genes that were chosen based on complementation. PCR amplified regions, using appropriate oligonucleotides, were defined as followed: the coding and adjoining regions covering the *lpxC* gene, the promoter region and structural genes of *lapA/B* operon, and the *ftsH* gene.

3.2.22. Bacterial growth measurement by spot-dilution

For the analysis of bacterial growth and comparison of suppression under varied conditions that were considered, the spot-dilution assay was used. First, exponentially grown cultures were adjusted to an optical density OD_{595} of 0.1. Ten-fold serial dilutions of cultures in sterile 10 mM $MgSO_4$ were prepared starting from 10^0 (undiluted cultures) up to 10^{-6}. Five µl drops of each dilution were spot-tested on agar plates supplemented with appropriate antibiotic/compound at different temperatures. Bacterial growth was analyzed after incubation at indicated temperatures.

3.2.23. Measurement of β-galactosidase activity

In order to measure the effect of *lapC* mutations on the expression of the *rpoE* gene from its LPS defects-responsive promoter, isogenic cultures of the wild-type *E. coli* and its derivatives with a *lapC* mutations carrying chromosomal fusions of *rpoE*P3-*lacZ* were grown overnight under permissive growth conditions. Next, OD_{595} of each culture was measured and adjusted to OD_{595} of 0.05. Rejuvenated cultures were allowed to grow at 30°C for another 45 min. After

this time, every 30 min interval, two sets of samples were taken from each culture: 500 µl to establish the OD_{595} and 200 µl to measure *β*-galactosidase activity. The 200 µl sample was placed in previously prepared vial with 800 µl of Z-buffer. To such mixture subsequently added were: 20 µl of 10% SDS, 20 µl of chloroform and 200 µl of ONPG substrate (4 mg/mL). Next, vials were incubated at 30ºC for 10 min and 500 µl of 1 M Na_2CO_3 was added to stop the reaction. Before the final measurement, samples were incubated for 3 min in the dark (RT) and then transferred to cuvettes to establish the absorbance with 420 and 550 nm wavelengths. *β*-Galactosidase activity of examined strains was calculated in Miller Units, using the equation presented below:

$$\textbf{Miller Units} = 1000 \frac{A_{420} - (1.75 \times A_{550})}{V \times OD_{595}}$$

where:

A_{420} - absorbance measured with 420 nm wavelength

A_{550} - absorbance measured with 550 nm wavelength

V - volume of sample [mL]

OD_{595} - optical density of culture measured with 595 nm wavelength

For each assay, three independent cultures were used and average of each were plotted.

3.2.24. LPS extraction and measurement of LPS amounts

In order to analyze LPS levels in different strains from this study, cultures were grown at permissive growth conditions up to an OD_{595} of 0.5 and harvested by centrifugation. To obtain the whole cell lysates, pellets were resuspended in 1x lysis buffer, boiled for 10 min at 95°C, incubated on ice for 2 min and briefly centrifuged. Subsequently, lysates were treated with Proteinase K. As described in SDS-PAGE method, equivalent portions of such whole cell lysates were applied to a 14% or 16% SDS-Tricine gel. After the electrophoresis, LPS was either silver-stained or transferred by Western blotting. Immunoblots were probed for LPS amounts using the WN1 222-5 monoclonal antibody.

3.2.25. Purification of proteins

For the induction and purification of HslVU proteins, using the chromosomal DNA from the *E. coli* BW25113, the minimal coding region of the

operon was amplified using PCR and cloned in the expression vector pET24b (pSR22763). To co-purify LapA and LapB proteins, the minimal coding region of *lapA/B* operon was cloned into the low-copy T7 promoter-based pDUET expression vector (Novagen) in a way that LapA was tagged with in-frame deca-His tag at the N-terminus. The BL21(DE3) derivative was transformed with the constructed vector. The expression of *lapA/lapB* genes was induced in 1 L of culture medium at an OD_{595} of 0.2 by the addition of either 100 or 500 µM IPTG. For the purification of LapC, the *lapC* gene was cloned in the T7 promoter-based pET28b vector and the expression induced with the addition of 200 µM IPTG. Cells were harvested by centrifugation at 4°C, 10,000 rpm for 20 minutes. Pellet was frozen overnight at -80°C. Next, pelleted cells were resuspended in B-PER reagent (Pierce) and adjusted to contain 50 mM NaH_2PO_4, 300 mM NaCl, 10 mM imidazole (buffer A), supplemented with lysozyme to a final concentration of 200 µg/mL. A cocktail of protease inhibitors (Sigma) was added as per manufacturer's instructions. The mixture was incubated on ice for 15 min with gentle mixing. To this lysate 30 units of benzonase (Merck) were added, incubated with gentle mixing at 4°C for another 45 min. The mixture was centrifuged at 45,000 x g for 90 min at 4°C. LapA/B and LapC proteins were extracted using 2% octyl-*β*-D-glucoside for solubilization of inner membrane proteins in the presence of PMSF and a cocktail of protease inhibitors. Solubilized IM proteins were applied over nickel-nitrilotriacetic acid beads (Qiagen) and LapA/B and LapC proteins eluted, as described in Klein *et al*. 2014[41]. For HslUV purification, soluble proteins fraction was applied over nickel-nitrilotriacetic (Ni^{2+}-NTA) acid beads columns, washed and eluted with buffers with increasing concentration (50 mM - 500 mM) of imidazole.

3.2.26. Isolation of RNA and qRT-PCR analysis

To measure the *lapC* mRNA amounts at different temperatures, the BW25113 wild-type culture was grown at 30°C in LB medium to an OD_{595} of 0.1. To induce heat shock, aliquots of culture were shifted to prewarmed medium held at 43°C and incubated for 15 min. Equivalent amounts of samples from cultures grown at 30°C and 43°C were harvested by centrifugation. Total RNA was extracted by hot phenol extraction as established in methods published by Professor Raina in previous study[204]. The purification of total RNA was performed

according to original protocol with additional steps of digestion of possible chromosomal DNA contamination with RQ1 DNase (Promega) and ethanol precipitated. Next, pellets were resuspended in DEPC-treated water. RNA amounts were quantified and RNA integrity confirmed by agarose gel electrophoresis. To quantify changes in the *lapC* gene expression in response to temperature shift qRT-PCR was used. For each sample, 2 µg of purified mRNA was reverse transcribed to cDNA using iScript Reverse Transcription Supermix (Bio-Rad). qRT-PCR was performed using CFX Connect Real-Time PCR Detection System (Bio-Rad). According to protocol published previously[205], reactions were carried out for 40 cycles in an optical 96 well plate with 20 µl reaction volumes containing 10 µl PowerUp SYBR® Green PCR Master Mix (ThermoFisher Scientific), 0.5 µl cDNA, 0.6 µl each of the 10 µM forward and reverse primers, and 8.3 µl of RNase-free water. In addition, samples lacking cDNA in above reaction served as a control for any DNA contamination. Data were analyzed by software Bio-Rad CFX Maestro. For each condition, three biological replicates were used.

4. RESULTS

4.1. Multicopy suppressor screening of genes that overcome ΔlapB lethal phenotype at high temperature in rich media

It was previously shown by Klein *et al.* 2014 that the *lapB* gene is essential in *E. coli* under normal laboratory growth conditions and that Δ*lapB* mutants can survive only under specific settings in few strain backgrounds at 30°C on minimal medium after prolonged incubation, unless an extragenic suppressor is present[41]. Performed previously by Professor Raina's laboratory multicopy suppressor analysis showed that overexpression of genes encoding enzymes involved in the phospholipid and fatty acid biosynthesis (*fabZ*, *fabB*), peptidoglycan synthesis (*murA*), and envelope stress response regulators (*rcsF*, *slrA* ncRNA, and toxin/antitoxin system *hicA*) and genes of unknown function: *yceK*, *yeaD*, *yffH*, and *ydhA* that are predicted to function in the envelope biogenesis, can bypass the lethality of a *lapB* deletion derivative at 37°C in rich LA media[41]. The essential function of LapB is attributed to its role in LPS biosynthesis by regulating turnover of LpxC in concert with the essential metalloprotease FtsH[41,63]. In this work, it was intended to find additional genes that overcome Δ*lapB* lethal phenotype at 42°C on LA media when present in multicopy, aiming to identify if any alternative proteolytic pathway exists for LpxC enzyme. Therefore, a complete library of all cloned open reading frames (ORFs), where genes are expressed from the IPTG-inducible P_{T5}-*lac* promoter from ASKA collection in the vector pCA24N[202], was introduced into the Δ*(lapA lapB)* strain SR17187 and plated on LA medium at 42°C in the presence of 75 μM IPTG as an inducer for the gene expression. Subsequently, plasmid DNA was isolated from such transformants and used to retransform the Δ*(lapA lapB)* strain to confirm that the plasmid-mediated suppression generates viable cells. Confirmed plasmid DNAs were analyzed by sequencing in order to identify which gene present in multicopy in the Δ*(lapA lapB)* mutant rescue the lethality of such a deletion. Analysis of sequenced DNAs revealed that most of the suppressors overlap with results published in Klein *et al.* 2014, except for the set of plasmids that encoded the *hslV* gene[41]. HslV is the peptidase component of HslVU (ClpQY) protease complex[192,206]. It forms a double ring that is associated with one or two of hexameric rings of HslU that

has the ATPase activity[207,208]. HslV exhibits homology to the *β*-subunits of the eukaryotic 20S proteosome, while HslU is highly homologous to the ClpX protein of *E. coli*, which is known to present large polypeptides to its partner, the ATP-independent proteolytic enzyme ClpP and it resembles ATP-stimulated process similar to that of the chymotrypsin-like activity of the eukaryotic proteasome[192,209]. HslV is also characterized by its own proteolytic function, which is enhanced by HslU in the presence of ATP to a much greater extent[192,209]. Compatible with the set high temperature of experiment HslVU are known heat shock proteases that also contribute to regulation of the heat shock sigma factor RpoH to some extent[191].

To verify the contribution of HslV in the LapB-deprived bacteria, the set of controlled transductions was performed. Transformants of BW25113 wild-type *E. coli* strain derivatives carrying either the vector alone, or the plasmid carrying either only the *hslV* gene or with cloned *hslVU* genes in the presence of 75 μM IPTG, were transduced with Δ*lapA/B* (P1 SR17187) and Δ*lapB* (P1 SR7753) deletions using bacteriophage P1 cultivated on mutant strains. Transductions were carried at 30°C on M9 medium. Results from transductions are presented in Table 4.1. below.

Table 4.1. Number of colonies of transductants

Donor	**Recipient strain BW25113**		
	+ vector	**+ p*hslV*$^+$**	**+ p*hslUV*$^+$**
P1 SR17187 Δ*lapA/B* Kan^R	35 Kan^R, small colonies	1112 Kan^R	3230 Kan^R
P1 SR7753 Δ*lapB* Kan^R	43 Kan^R, small colonies	1230 Kan^R	2980 Kan^R

Results presented in Table 4.1. demonstrate that overexpression of the *hslV* allows for the deletion of the *lapB,* and the transduction frequency is even enhanced by approximately 3-fold, when the *hslVU* genes were overexpressed simultaneously. It should be noted that the Δ*lapB* transductants appear only after prolonged incubation, when vector alone is present and with very low numbers of colonies that are much smaller in size.

4.2. Monitoring of LpxC degradation under overexpression of the hslV gene in LapB-independent manner

It was presumed that overexpression of *hslV* or *hslUV* genes encoding proteases could bypass the Δ*lapB* lethality due to regulation of LpxC amounts. In attempt to resolve the molecular basis of this suppression, the levels of LpxC protein in the Δ*lapA/B* mutant derivative transformed with the plasmid containing the *hslV* gene under the control of a tightly regulated inducible P_{T5}-*lac* promoter, were measured using Western blotting technique. Cultures of mutant strain with the *hslV* gene on a plasmid were cultivated in M9 medium and adjusted to the starting OD_{595} of 0.2 in LB medium at 42°C. Induction of the *hslV* expression was achieved by the addition of 75 μM IPTG to the broth. During experiment, the equal amount of culture was sampled after 10 min intervals. Proteins from whole cell lysates were resolved on a 12% SDS-PAGE. Analysis of LpxC amounts with LpxC-specific antibodies was performed using Western blotting. It was shown in Klein *et al.* 2014 that in the absence of LapB, LpxC is stabilized and its levels are increased in a Δ*lapA/B* mutant, which results in the bacterial lethality due to increased synthesis and accumulation of LPS[41]. Analysis of Western blot showed a progressive reduction in amounts of LpxC in the time of experiment (Fig. 4.1.).

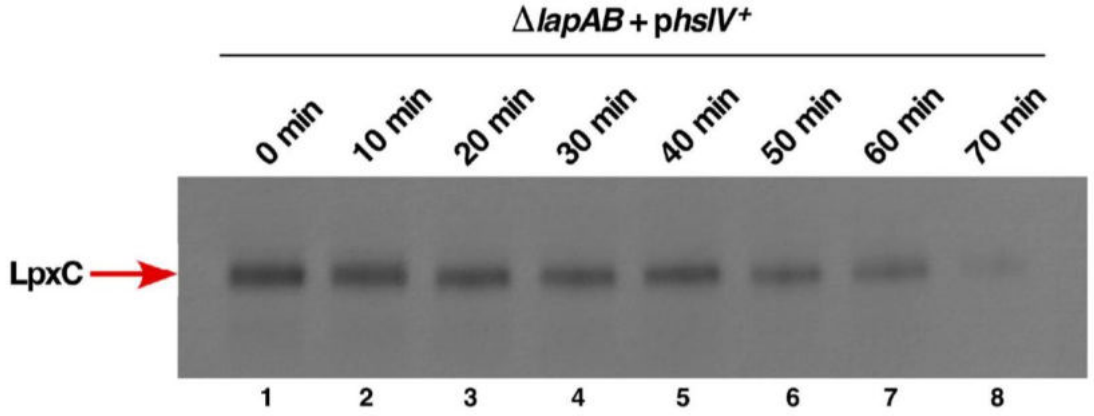

Fig. 4.1. Immunoblot of LpxC amounts during incubation at 42°C in the Δ*lapA/B* strain with the *hslV* overexpressed from the plasmid

Lanes 1-8 in Western blot picture represent the position of LpxC indicated by red arrow, which was detected with anti-LpxC primary antibody using cell lysates from Δ*lapA*/*B* mutant transformed with the plasmid containing the *hslV* gene under control of inducible P_{T5}-*lac* promoter, sampled in 10-minute intervals. Each lane is described with time of sample collection starting with 0 min in lane 1 that corresponds to the beginning of induction of *hslV* expression by the addition of 75 μM IPTG. A progressive reduction in amounts of detected LpxC in the time of experiment can be observed.

After only 20 min of incubation, less than half of the initial amount of LpxC was detected and within 70 min of incubation LpxC signal could be barely detected (Fig. 4.1. lanes 3 and 8, accordingly). It should be noted that in LapB-deficient mutant the amounts of LpxC in the cell are elevated under all conditions, as LpxC cannot be directed to LapB/FtsH-mediated proteolysis[41]. Results presented in Figure 4.1. show that LpxC can be subjected to degradation, even when LapB is absent, establishing an alternative mechanism of LpxC levels adjustment. These results help to explain the identification of the HslV subunit encoding gene as a suppressor of Δ*lapB* lethality, when expressed at higher levels.

4.3. Impact of co-overexpression of hslVU genes on LpxC amounts in the wild-type background

As HslV peptidase is known to hydrolyze some proteins alone albeit at very low rate that is significantly increased by HslU ATPase[210,211]. Thus, it was decided to examine the fate of LpxC in the wild-type background, when *hslVU* genes are co-overexpressed, using pulse chase experiments. The T7 polymerase expression-based derivative of *E. coli* strain was transformed with a pET24b plasmid DNA carrying *hslUV* genes under control of T7 promoter. Cultures were grown in LB at 30°C up to OD_{595} of 0.1. The induction of both genes overexpression was initiated by the addition of 75 μM IPTG for 15 min. Next, cultures were washed to remove the inducer and shifted to 42°C. Next immediately, transcription of host genes was stopped by the addition of 200 μg/mL of rifampicin and the chase incubation at 42°C initiated. The equivalent amount of aliquots were collected after 10 min intervals. Proteins from total-cell extracts were resolved on a 12% SDS-PAGE gel and analyzed by immunoblotting, using anti-LpxC antibodies. Results from the pulse chase experiment are presented in Figure 4.2.

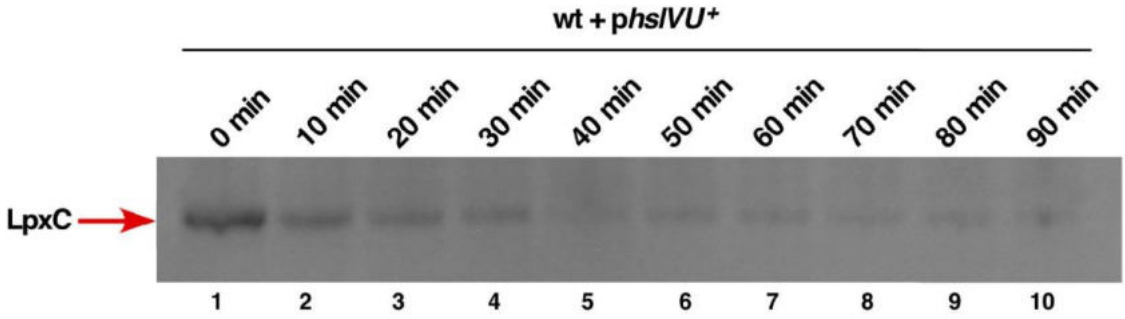

Fig. 4.2. LpxC during chase after co-overexpression of *hslUV* in the wild-type *E. coli*
Image of Western blot is shown. Lanes 1-10 marked in the picture represent protein corresponding to LpxC (red arrow), which was detected with anti-LpxC primary antibodies using total protein extracts of wild-type *E. coli* transformed with the plasmid containing the *hslVU* genes under control of inducible P_{T7}-*lac* promoter, sampled in 10-minute intervals. Each lane is described with time of sample collection after chase start (0 min in lane 1) that corresponds to the beginning of induction of *hslUV* expression by the addition of 75 μM IPTG and stopping of host transcription by the addition of 200 μg/mL of rifampicin and the chase incubation at 42°C. A progressive reduction in amounts of detected LpxC in the time of experiment can be observed.

It can be observed that during the chase time, LpxC signal rapidly declines. Since the addition of rifampicin shuts down the host transcription, results from Fig. 4.2. confirm that HslUV protease degrades LpxC in the LapB/FtsH-independent manner. Even after 10 min following the chase (Fig. 4.2. lane 2),

LpxC amounts are approximately five times reduced, with background level detection after only 40 min chase (Fig. 4.2. lane 5). Therefore, these results provide a convincing evidence of alternative LpxC proteolysis, where HslV can degrade LpxC in the absence of LapB/FtsH and this degradation is enhanced, when HslU is also present.

4.4. Purification of HslUV

In order to investigate the overexpression of *hslUV* genes in the wild-type *E. coli* and purify the complex of HslUV proteases, the pSR22763 plasmid carrying His-tagged *hslU* and non-tagged *hslV* under control of T7 promoter was transformed into the T7 Express *lysY/I*^{q} *E. coli*. Transformant colonies were cultivated in LB medium at 30°C and induction of expression was initiated by the addition of 0.5 mM IPTG. After 2 h of incubation, all host transcription was stopped with the addition of 200 µg/mL of rifampicin and incubated at 37°C for additional 2 h. Cells were harvested and proteins were purified using the Ni^{2+}-NTA chromatography. Selected fractions were resolved by SDS-PAGE electrophoresis (Fig. 4.3.). As it can be observed, the expression system delivers substantial amounts of protein. The interaction between proteins is observable as non-tagged HslV co-purifies with HslU and elutes mostly with lower concentrations of imidazole (lanes 1-3).

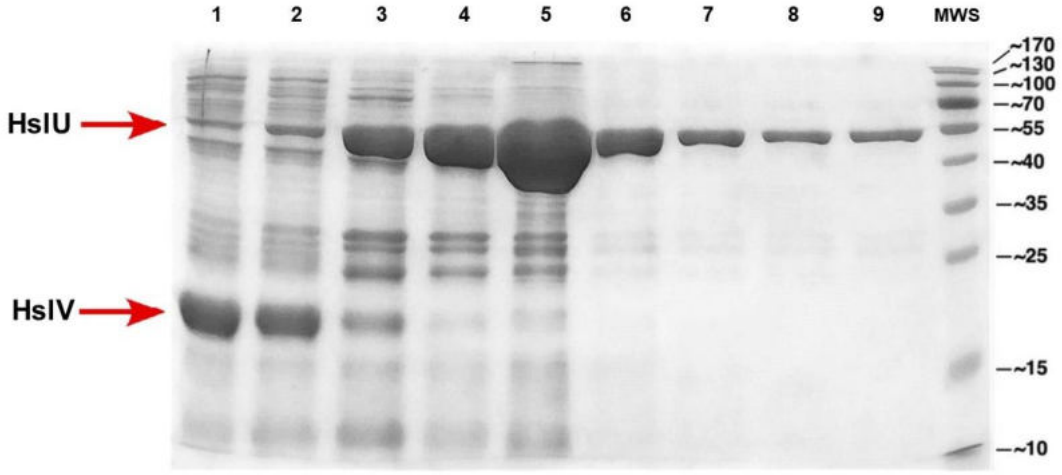

Fig. 4.3. SDS-PAGE gel of the elution profiles of overexpressed and purified HslU and HslV

Lanes 1-9 correspond to HslUV protein samples resolved by SDS-PAGE electrophoresis, eluted with appropriate concentration of imidazole (1 – 50 mM second fraction, 2 - 50 mM third fraction, 3 - 100 mM second fraction, 4 – 250 mM first fraction, 5 – 250 mM second fraction, 6 – 250 mM fourth fraction, 7 – 250 mM fifth fraction, 8 – 500 mM first fraction, 9 – 500 mM second fraction). In lane 10 the prestained molecular weight standard PageRuler™ Prestained Protein Ladder (Thermo Scientific) was added. After electrophoresis proteins were visualized by staining with InstantBlue® (Expedeon) Coomassie protein detection reagent.

4.5. Testing the sensitivity of ΔhslV, ΔhslU and ΔhslUV mutants to the LpxC inhibitor CHIR090

Based on the discovery that HslUV regulates the amounts of LpxC in *E. coli,* it was suspected that mutants lacking the genes encoding subunits of protease complex, can exhibit altered sensitivity to CHIR090 LpxC inhibitor. CHIR090 (*N*-aroyl-L-threonine hydroxamic acid) is the most potent inhibitor of the LpxC isolated up to date and it exhibits antibiotic activity against most Gram-negative bacteria, including *E. coli* and *Pseudomonas aeruginosa*, as effectively as ciprofloxacin or tobramycin[212,213]. Its described in detail characteristic, promising antimicrobial activity and specificity towards LpxC, made CHIR090 ideal compound to complement the study upon LpxC regulation. Therefore, isogenic strains of wild-type BW25113 and its derivatives lacking HslU and HslV protease subunits were tested by spot dilution on LA agar with or without supplementation of CHIR090 at a sublethal concentration that is not deleterious to the wild-type strain. Results are presented in Figure 4.4. below.

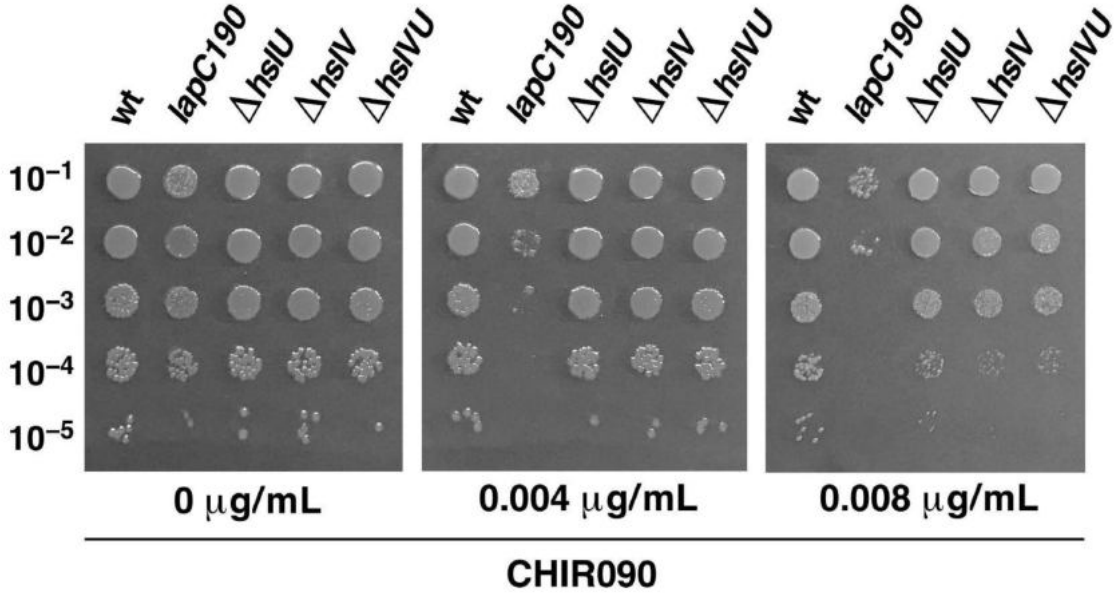

Fig. 4.4. Spot-testing of wild-type *E. coli* and its *lapC190,* Δ*hslU*, Δ*hslV* and Δ*hslUV* derivatives on LA agar with or without CHIR090

Figure presents pictures of plates with spotting of serial dilutions of exponentially grown cultures of the wild-type strain and its isogenic derivatives lacking genes encoding HslVU protease subunits. Cultures were adjusted to an OD_{595} of 0.1, serially diluted and spotted at 30°C on LA agar supplemented with or without varying concentrations of CHIR090 as indicated in the bottom of the pictures. The isogenic CHIR090-sensitive strain with the *lapC190* mutation was included as a control. Plates were photographed after 24 h incubation. Presented results are from one of the representative experiments.

Presented results indicate that deletion of *hslV* gene or both genes encoding HslUV protease subunits, impacts the resistance ability of mutants by reducing their viability by 100-fold in comparison to the wild-type strain, when exposed to 0.008 µg/mL of CHIR090. The reduction of colonies size is observed in the case of all derivatives. The Δ*hslU* mutants, although more sensitive than the parental strain, exhibit only a moderate sensitivity to CHIR090. The strain with the *lapC190* mutation was included as a control in this experiment, as it was established in the experiment described in subsection 4.9. that it is characterized by significant sensitivity to inhibitor. Thus, it can be concluded that consistent with a role for HslUV protease in the regulation of LpxC amounts, a deletion of either both genes encoding subunits of this protease complex or the *hslV* gene alone that encodes catalytic subunit, enhances the sensitivity to CHIR090, which is a specific inhibitor of LpxC.

4.6. Search for the extragenic mutations that prevent lethality of ΔlapB mutants

It was described earlier in this thesis that under normal laboratory growth conditions *lapB* is an essential *E. coli* gene and its deletion is only tolerated under specific conditions, unless an extragenic suppressor is present[41]. To understand the molecular basis of LapB essentiality and its function, the screening for supplementary extragenic suppressors was undertaken. Transduction of *lapB* deletion in *E. coli* W3110 resulted in the identification of a novel mutation that suppressed the Δ*lapB* and Δ*lapA/B* lethality. The constructed strain carrying the mutation was designated as SR8348. The suppression mutation was marked with Tn*10* and used to transduce the mutation in the Δ*lapA/B* strain in BW25113 background on LA rich medium at 30°C. This resulted in obtaining of viable Δ*lapA/B* in BW25113 background with the extragenic suppressor mutation. It proved that this isolated suppressor mutation of Δ*lapB* was not only specific for W3110 strain. The DNA sequencing and complementation experiments revealed that obtained mutation arose due to a frame-shift in the *yejM* gene. Based on further experiments on its genetic interaction it was designated as the *lapC* gene. This mutation caused an insertion of C residue at nucleotide position 1133 resulting into frame-shift after 377 amino acid (referred from now on as *lapC377fs*), with the addition of 13 aa residues after Thr377, leading into the truncation of C-terminal periplasmic domain. LapC (YejM) structures have been described recently revealing five IM-spanning helices in the N-terminus and a large C-terminal globular domain connected by a linker domain[195,197,214,215]. Thus, the experiments were undertaken to understand the role of the LapC inactivation in suppression of Δ*lapB* and Δ*lapA/B* mutants lethality.

4.7. Examination of the molecular basis of suppression by the lapC377fs mutation

Based on the data published before by Professor Raina's group that lethality of LapB-deprived strains is strongly connected to excessive accumulation of LPS, it was decided to examine the LPS content of Δ*lapB*, *lapC377fs* and (Δ*lapB lapC377fs*) mutants, in order to address the molecular effects of the *lapC377fs* mutation[41]. The whole cell lysates from the wild-type *E. coli* and its Δ*lapB*, *lapC377fs* and (Δ*lapB lapC377fs*) derivatives were treated with Proteinase K to remove proteins and further obtain LPS. Equivalent amount of extracts were resolved on a 14% SDS-Tricine gel and LPS was revealed by silver staining. Figure 4.5. below presents the LPS profiles of tested strains.

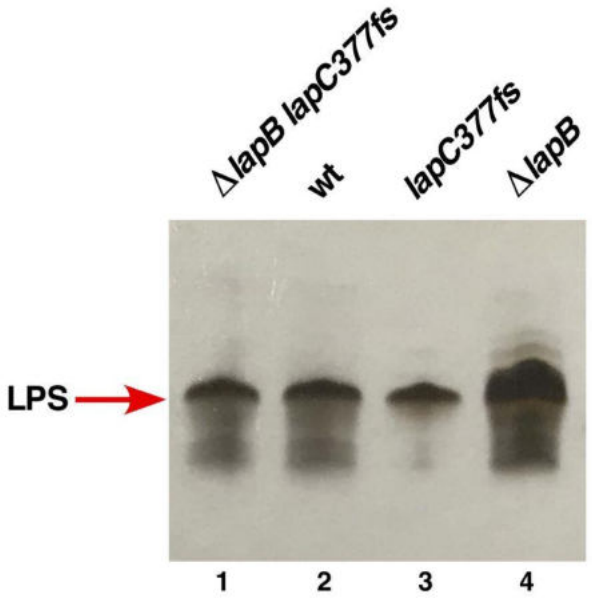

Fig. 4.5. LPS profiles of (Δ*lapB lapC377fs*), wild-type *E. coli*, *lapC377fs* and Δ*lapB* derivatives

Lanes 1-4 show LPS from equivalent amounts of Proteinase K-treated whole cell lysates of isogenic *E. coli* derivatives: 1 – (Δ*lapB lapC377fs*), 2 – wild-type strain, 3 - *lapC377fs* mutant and 4 – Δ*lapB* bacteria. Samples were resolved on a 14% SDS-Tricine gel and the presence of LPS was detected by silver staining. The red arrow indicates the position of LPS.

The comparison of LPS profiles clearly indicates that combination of *lapC377fs* mutation with Δ*lapB* deletion restores the wild-type LPS content (Fig. 4.5. lanes 1 and 2) that is otherwise significantly increased in the Δ*lapB* derivative (Fig. 4.5. lane 4) and visibly reduced when LapC is defective (Fig. 4.5. lane 3). These results clearly correspond and support the mass spectra results presented in Fig. 2.2. that were obtained earlier by Professor S. Raina and Professor G. Klein.

4.8. Identification of additional partners in LpxC turnover using transposon-mediated mutagenesis

In order to expand the search for additional proteins that could regulate LpxC turnover, therefore sense the accumulation of LPS in the envelope or respond to defects in LPS biosynthesis, the temperature-sensitive (Ts) Tn*10* transposon-linked point mutations that conferred the increased activity of single-copy *rpoE*P3-*lacZ* promoter were isolated. The assumptions of this experiment were based on the fact that previously identified proteins that play key roles in LPS maintenance, as for example LapB or FtsH, were found to be essential for bacterial viability. The *lacZ* fusion with *rpoE*P3 promoter was chosen as, according to researches published by Professor Raina's group, its activity is induced specifically when LPS biosynthesis or assembly are severely compromised[121]. Among isolated mutants that are characterized by temperature sensitivity and induction of *rpoE*P3 promoter, only isolates that were simultaneously unable to propagate on MacConkey agar and that were sensitive to the CHIR090 inhibitor, were retained. Mapping and complementation analysis of Tn*10*-linked mutations identified four independent Ts mutants with permeability defects with a mutation linked > than 95% to the *bcr* gene located at 49 min and were designated SR19041, SR19750, SR22861 and SR22862. Subcloning and further complementation approach led to the cloning of the *lapC* gene, which reversed the Ts phenotype, restored growth on MacConkey agar plates as well as restored the nearly wild-type activity of the *rpoE*P3-*lacZ* fusion. Next, the *lapC* gene was PCR amplified from the chromosomal DNA isolated from identified mutants. Analysis of the DNA sequence revealed that SR19041 has a stop codon (TGA) replaced with the tryptophane-coding TGG (*lapC190*), SR19750 and SR22861 carry the same frame-shift mutation *lapC377fs* that was identified during search for the extragenic mutations that prevent lethality of Δ*lapB* mutant (subsection 4.6.), and SR22862 contains a single amino acid change resulting into substitution of 349F to 349S (*lapC* F349S). Among the isolated Ts mutations, the *lapC190* is identical to a mutation found in strain LH530 that is characterized with membrane permeability defects[194,216]. It lacks the entire periplasmic domain and expresses only the IM domain that consists of five predicted TM helices[217]. SR22862 mutant carries the mutation in highly conserved 349 amino acid residue

that is located in the Mg^{2+}-binding pocket of the pseudo-hydrolase domain and in the putative phosphatase active site of the enzyme[195,197]. However, the most frequent mutation found in the course of this study is the *lapC377fs* that results in the truncation of C-terminal periplasmic domain and it has been not described up to date.

4.9. Comparison of lapC mutants sensitivity to CHIR090 LpxC inhibitor

To characterize isolated mutation further and recognize their relevance to regulation of LpxC, specific sensitivity to sublethal concentrations of CHIR090 was examined for each type of mutation. The wild-type *E. coli* culture and its isogenic derivatives with point mutations in the *lapC* gene, described in previous subsection, were exponentially grown, adjusted to an OD_{595} of 0.1 and serially spot diluted at 30°C on LA agar supplemented with or without varying concentrations of CHIR090 as indicated in Figure 4.6.

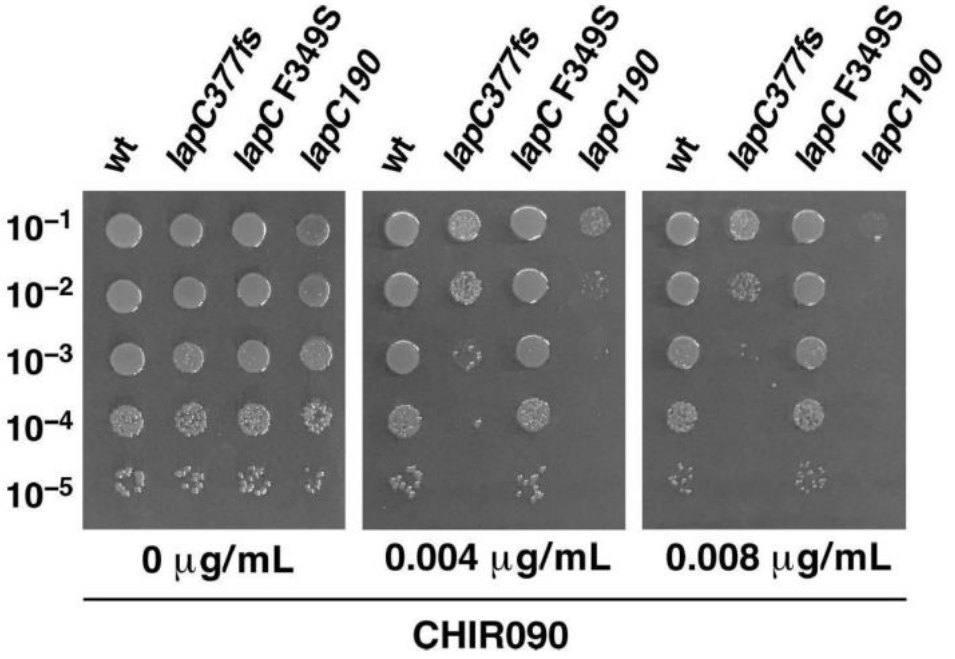

Fig. 4.6. Spot-testing analysis of wild-type *E. coli* and its isogenic derivatives *lapC377fs*, *lapC* F349S and *lapC190* sensitivity to CHIR090

Figure presents spot dilution of exponentially grown cultures of the wild-type strain and its isogenic derivatives carrying the isolated mutations in the *lapC* gene. Cultures with genotypes indicated above each figure, were adjusted to an OD_{595} of 0.1 and serially spot diluted at 30°C on LA agar supplemented with or without varying concentrations of CHIR090 as indicated in the bottom of the pictures. Plates were incubated overnight and the photograph of each plate was taken.

Comparison of sensitivity profile of each *lapC* mutant to CHIR090 showed that the most severely affected by the CHIR090 concentration, when growth of the parental strain is not affected, is the strain with *lapC190* mutation that does not express the periplasmic domain (Fig. 4.6.). It is followed by *lapC*377*fs* that is able to grow to only slightly higher extent, forming suppressor colonies. In the case of the *lapC* F349S derivative, only a small decrease in the colony size was observed upon the exposure to CHIR090.

4.10. Induction of transcriptional activity of rpoE in lapC mutant strains

Simultaneously, besides sensitivity to CHIR090, it was decided to evaluate exact impact of each point mutation on the *rpoE*P3 promoter activity that is responsive to LPS defects. Thus, cultures carrying the single-copy chromosomal *rpoE*P3-*lacZ* fusion of wild type and *lapC* mutants, were grown exponentially, adjusted to an OD_{595} of 0.05 and allowed to grow in LB medium at 30°C. Aliquots of cultures were drawn after different time points and used to measure the *β*-galactosidase activity. To prevent the read-through of stop codon in the original *lapC190* derivative, it was decided that for further comparative analysis and verification of results, a Δ*lapC190* derivative (GK6075) will be used. GK6075 was constructed in a manner to express the 190 amino acids of N-terminal part of protein (IM anchor), but the periplasmic domain was replaced by recombineering with an excisable antibiotic cassette. SR19041 (*lapC190*) and GK6075 were both used in this assay for comparison. Figure 4.7. presents a comparative of *β*-galactosidase activity expressed in Miller Units (MU) for wild type and each mutation carrying strains at two optical densities – OD_{595} of 0.15 and 1.5. Error bars represent the standard error of three independent measurements.

Analysis of *β*-galactosidase activity of *lapC* mutants revealed the most pronounced difference (6 to 8-fold induction of *rpoE*P3 promoter activity) in comparison to wild-type when examined during growth in stationary phase at OD_{595} of 1.5 in *lapC190* or Δ*lapC190* and *lapC377fs* derivatives. The *lapC* F349S mutation had lower impact on expression from LPS defects-responsive promoter. These results correlate with the examination of *lapC* mutants sensitivity to the CHIR090 LpxC inhibitor as described in the subsection 4.9. Taken together, the induction of transcription from the *rpoE*P3 promoter that responds to LPS defects accompanied by the Ts phenotype, the sensitivity to the CHIR090 inhibitor and membrane permeability defects allowed to conclude that LapC is required for the bacterial envelope integrity and the regulation of LPS biosynthesis. It is consistent with the suppression of lethality and the restoration of wild-type LPS content in LapB-deprived bacteria by *lapC* loss-of-function mutations (subsection 4.7. and Figure 2.2.). These results establish that LapC has to be essential for the regulation of LpxC. Among three isolated mutants of LapC, *lapC190* and

lapC377fs showed a strict temperature sensitive phenotype, the hypersensitivity to CHIR090 and these two mutations were further characterized as they conferred a tighter phenotype.

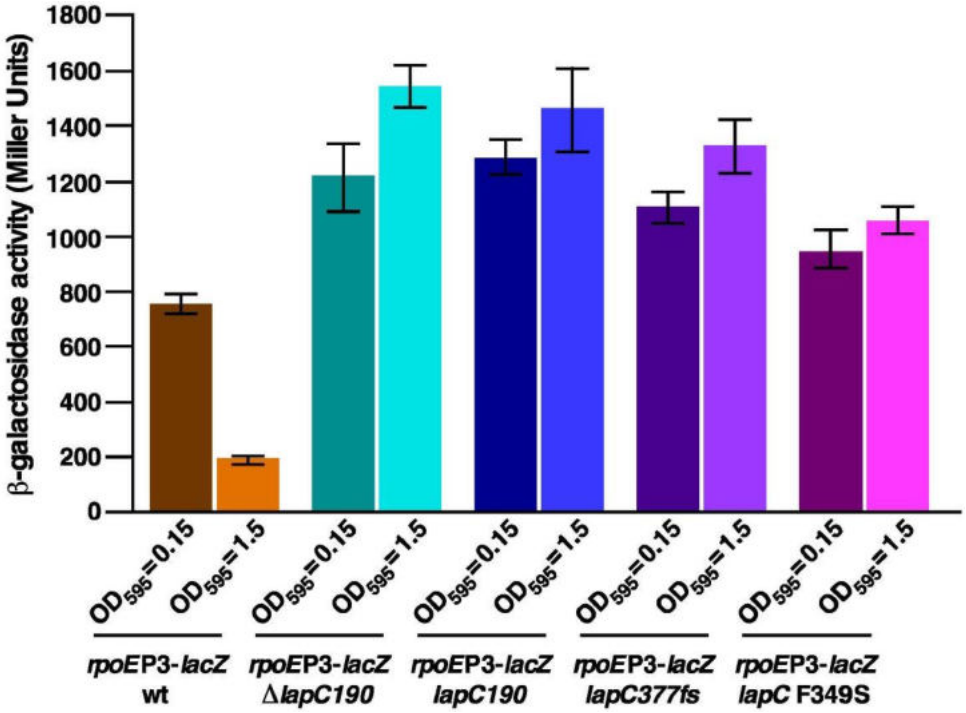

Fig. 4.7. Induction of RpoE activity from its LPS-responsive promoter in the wild-type *E. coli* and its isogenic derivatives Δ*lapC190, lapC190, lapC377fs* and *lapC* F349S carrying a single-copy chromosomal *rpoE*P3-*lacZ* fusion for OD_{595} of 0.15 and 1.5

Chart presents the *β*-galactosidase activity measured from isogenic cultures of wild type and mutation carrying strains having a single-copy chromosomal fusion of *rpoE*P3-*lacZ* at two optical densities – OD_{595} of 0.15 and 1.5. Genotypes are indicated in the bottom of the figure. Three independent measurements were taken for each strain and error bars represent a calculated standard error.

4.11. Mapping of extragenic suppressors of lapC mutants

Taking the advantage of phenotypes such as the sensitivity to high temperature and the inability to grow on MacConkey agar of strains with the *lapC190* and *lapC377fs,* it was decided to search for extragenic suppressors that either restored growth on LA agar at 42°C or allowed growth on MacConkey agar. Cultures were plated under non-permissive growth conditions and that led to isolation of several strains with spontaneous suppressor mutations. Twenty-nine of such strains were cultivated and mutations were marked with Tn*10* transposon according to protocol by Raina *et al.* 1995[136]. The positions of Tn*10* insertions were directly sequenced from recombinant cosmid clones. Among mapped extragenic mutations, 26 suppressor mutations could be grouped into three complementation groups: *zab*::Tn*10* (10 suppressors), *pyrF*::Tn*10* (15 suppressors) and *greA*::Tn*10* (1 suppressor). These map positions suggested that suppressor mutations linked to *zab*::Tn*10* could have a mutation in the *lpxC* gene, those linked to *pyrF*::Tn*10* mapping to the *lapA/B* locus and the last one linked to the *greA* gene could be having a mutation in the *ftsH* gene. Therefore, the chromosomal DNA from all 26 mutants was isolated and DNA region that encompass these four genes of interest and their flanking regions was sequenced. Table 4.2. below presents the results of DNA sequencing analysis.

The most frequently isolated suppressor (4 independent isolations) had a single exchange in 37th amino acid in the coding region of the *lpxC* gene of valine to glycine. Alteration of the same amino acid position, but V37L, was also isolated. The isolation of five independent mutants with the substitution of the same Val37 residue is consistent with recent identification of LpxC V37G as a stable variant in *Klebsiella pneumoniae*[218]. It can be assumed that strains with substituted variants can have the LpxC that is also resistant to proteolysis. The next three of the mutant strains had an exchange of R230C residue, one strain with single amino acid alteration of K270T and another suppressor revealed a frame-shift mutation due to the deletion of 2 nt in the stop codon that results in the extension of LpxC wild-type sequence by 20 amino acids. Such addition of 20 amino acids to the C-terminal domain can result in the stabilization of LpxC, as the C-terminal part of LpxC was found to be involved in the recognition of enzyme by FtsH protease[219]. DNA sequence analysis revealed also eight strains

with suppressor mutations within the *lapB* gene. All eight suppressors contain single amino acid substitutions located in highly conserved regions defining TPR elements required for mediation of protein–protein interactions. It is also worth noticing that *lapA* and *lapB* genes are co-transcribed and their translation is coupled, therefore all 7 isolates with the mutations disturbing the *lapA* expression have a possible impact on LapB amounts. Lastly, during search for extragenic suppressors of *lapC* mutants, one strain was found that contain the mutation in the Second Region of Homology (SRH) domain of FtsH protease. Mutations in this domain are associated with the loss of ATPase activity, which is critical for the proteolytic activity of enzyme, therefore should also result in the stabilization of LpxC protein[220]. In order to understand the function of LapC, it was decided to investigate further each of isolated strains that carry extragenic suppressors of *lapC* mutants.

Table 4.2. Extragenic suppressors of *lapC190* and *lapC377fs* mutations

Gene	Mutation Position	Amounts of Isolates
lpxC	V37G (GTC → GGC)	4
	V37L (GTC → CTC)	1
	R230C (CGT → TGT)	3
	K270T (AAA → ACA)	1
	a frame-shift by the deletion of 2 nt TA from the stop codon resulting into the addition of 20 aa at the C-terminus	1
lapB	A88V (GCT → GTT) TPR2	2
	R115H (CGT → CAT) TPR3	1
	D124Y (GAC → TAC) TPR3	1
	R125L (CGC → CTC) TPR3	1
	H181R (CAT → CGT) TPR5	1
	H325L (CAC → CTC) TPR9	1
	H325P (CAC → CCC) TPR9	1
lapA	IS element after 34 nt	2
	IS element after 103 nt	1
	IS element after -107 nt - 2 nt after P2hs promoter of the *lapA* gene	1
	a frame-shift by the insertion of G after 69 nt (23 aa from LapA wt and 7 aa new followed by the stop codon)	1
	a frame-shift by the deletion of 137 nt C (45 aa from LapA wt and 12 aa new followed by the stop codon)	1
	LapA L8 (TTA → TGA) stop codon	1
ftsH	A296V (GCG → GTG) in the SRH domain	1

4.12. Comparison of lapC mutants extragenic suppressors ability to reverse Ts phenotype and permeability defects conferred by LapC C-terminal domain truncation

Results presented up to this point strongly suggested that LapC has a specific role in the regulation of LPS biosynthesis and/or assembly. The *lapC* mutants are characterized by severe sensitivity to the sublethal concentration of the LpxC inhibitor CHIR090 (Fig. 4.6.), they excessively induce the *rpoE*P3 promoter, whose activation occurs in response to defects in LPS (Fig. 4.7.) and they were found to restore the LPS composition of a Δ*lapB* mutant strain (Fig .4.5. and Fig. 2.2.). Such phenotypes, associated often with LPS-related function, resulted also in the sensitivity to high temperature and permeability defects that hinder growth of bacteria on MacConkey agar. This set of features attributed to *lapC* mutants allowed for the isolation of various suppressor mutations that alleviate the susceptibility of bacteria to challenged conditions (Table 4.2.). To further gain information about the function of LapC, firstly growth of the *lapC190* and *lapC377fs* extragenic suppressor-carrying strains on LA and MacConkey agar was measured to compare the extent of suppression effects. Exponentially grown cultures with indicated in Figure 4.8. genotypes were grown in M9 at 30°C, adjusted to an OD_{595} of 0.1 and spot diluted on LA and MacConkey agar at 30, 37 and 42°C. The spot-testing analysis presented in Fig. 4.8. indicates the degree of suppression of *lapC190* phenotype.

Among the suppressors that harbor the mutation of V37 single amino acid residue that were independently isolated as suppressor strains that restored growth at 42°C on LA medium and also allowed growth to some extent on MacConkey agar (Table 4.2.), the strain with LpxC V37G suppressor grows poorly on MacConkey agar as compared to the LpxC V37L suppressor-containing strain in the *lapC190* background, although both of mutations suppress the Ts phenotype of the *lapC* mutant. The suppressor mutations that restored growth of either *lapC190* or *lapC377fs* mutant strains and had an exchange of R230C or K270T in the coding region of the *lpxC* gene allow for the nearly wild type-like growth of the *lapC190* mutant, with K270T less pronounced effect and forming smaller size colonies. Mutations in FtsH SRH domain and the frame-shift mutation within LpxC C-terminal domain in combination with *lapC190*

encoding the periplasmic domain-deficient LapC, also results in complete restoration of growth, with FtsH A296V forming small colonies.

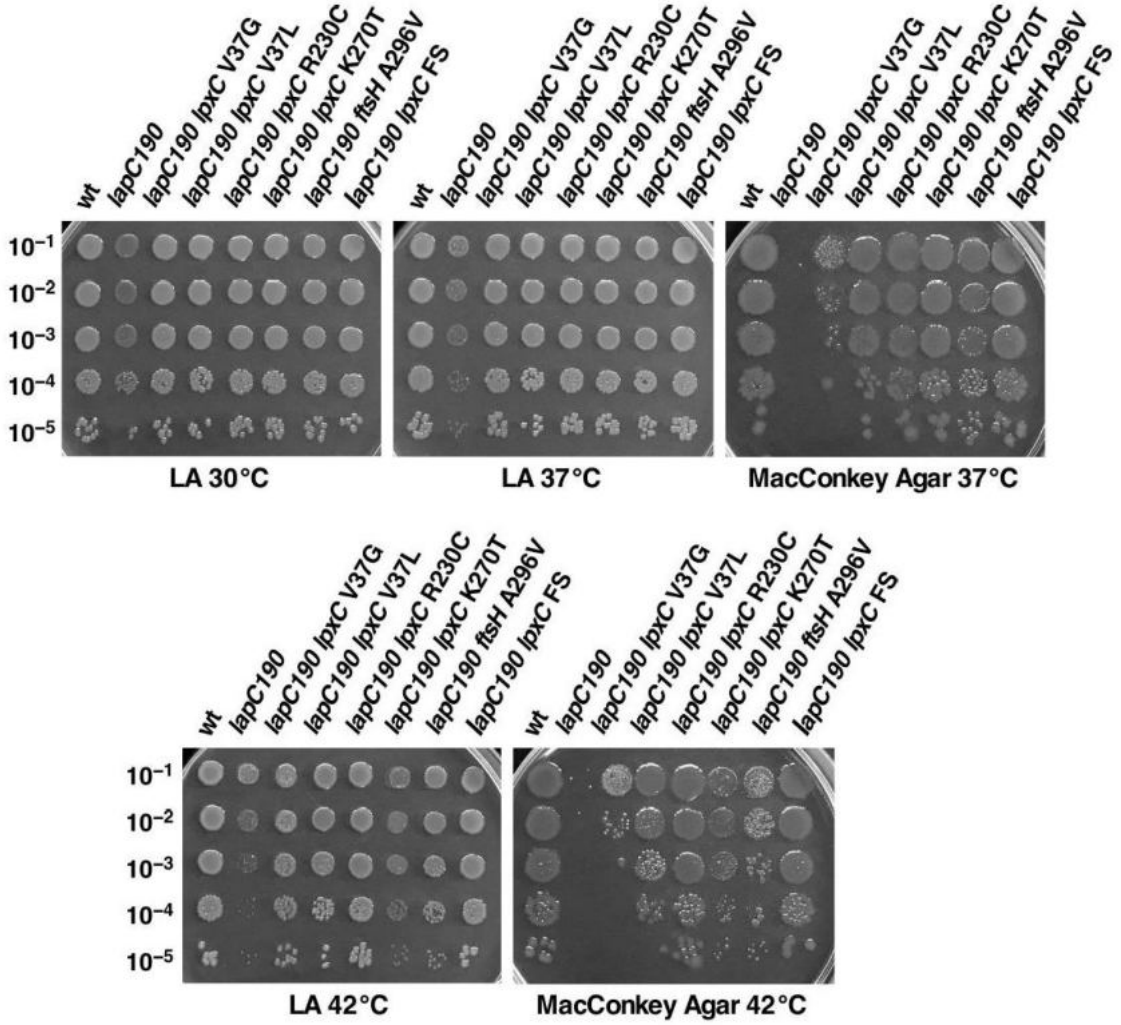

Fig. 4.8. Spot-testing analysis of wild-type *E. coli* and its isogenic derivatives of *lapC190,* and isolated strains that carry the extragenic suppressor mutations of *lapC190* and *lapC377fs* phenotypes on LA rich media and MacConkey agar

Exponentially grown cultures of the wild type and *lapC190* mutant and its isogenic derivatives with suppressor mutations that are indicated in the figure were grown at permissive conditions (M9, 30°C) adjusted to an OD_{595} of 0.1 and serially spot diluted on LA and MacConkey agar at 30, 37 and 42°C. Plates were incubated at designated temperatures overnight, growth of different strains compared and the photographs were taken. Presented results are from one of the representative experiments.

4.13. Effect of lapC190 and lapC377fs suppressor mutations on LpxC amounts

As a next step, it was decided to investigate what is the effect of suppressor mutations on LpxC amounts. Among three *lapC* mutations identified in this work a *lapC190* mutation exhibits the most stringent phenotype as reflected by the sensitivity to CHIR090 (Fig. 4.6.). Thus, the levels of LpxC from cellular extracts obtained from exponentially grown cultures of the isogenic wild type and its *lapC190* derivative were analyzed. As controls, the mutants with *lapA*/*B* deletion and a strain carrying a suppressor mutation of Δ*lapA*/*B* mapping to the *lpxC* gene (Δ*lapA/B lpxC186*) were also included[41]. Cultures were grown under permissive growth conditions in M9 at 30°C. To measure LpxC amounts whole cell extracts were analyzed by Western blot technique, using anti-LpxC antibodies. In Figure 4.9. results from one of representative experiments are presented.

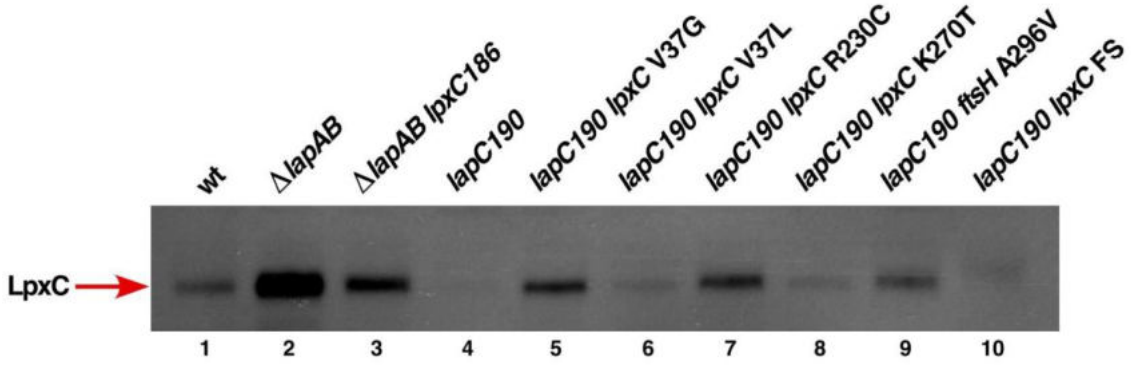

Fig. 4.9. Western blot revealing LpxC amounts in the isogenic wild type, its *lapC190* derivative and as controls Δ*lapA*/*B*, (Δ*lapA/B lpxC186*) in comparison to derivatives with suppressor mutations

Lines 1-10 in Western blot picture shows detected LpxC levels (red arrow) using anti-LpxC primary antibodies from total protein extracts obtained from equivalent amount of cultures of exponentially grown wild type, its *lapC190* derivative and strains with suppressor mutations (genotypes indicated in the figure). As controls, the mutants with *lapA*/*B* deletion and a confirmed in other study strain carrying a suppressor mutation of Δ*lapA*/*B* mapping to the *lpxC* gene (Δ*lapA/B lpxC186*) were included. Cultures were grown under permissive growth conditions on M9 at 30°C, the whole cell extracts were prepared and equivalent amounts resolved on a 12.5% SDS-PAGE and analyzed by Western blotting technique.

It should be noted that *lapC190* bacteria reveal almost undetectable levels of LpxC in comparison to the isogenic parental strain (Fig. 4.10. lanes 1 and 4). It contrasts significantly with elevated LpxC levels in a Δ*lapA*/*B* derivative and its partial reduction in the *lpxC186* derivative of *lapA/B* mutation (Fig. 4.10. lanes 2 and 3). In the case of all extragenic suppressors of *lapC* mutants, the amounts of

LpxC are visibly higher than in strain with LapC mutation (Fig. 4.10. lanes 4-10). The most prominent examples are strains with LpxC V37G, LpxC R230C and with a frame shift causing the extension of LpxC C-terminal domain. This is consistent with the considerations upon increased stability of LpxC due to mutations in described regions (subsection 4.12.). Taken together, these results allow to conclude that truncation of the C-terminal periplasmic domain of LapC destabilizes LpxC and suppressors mapping to the *lpxC* gene that restore growth at high temperature render LpxC more stable to balance the LPS synthesis.

4.14. Comparison of LPS levels in strains with different suppressor mutations of lapC190 and lapC377fs

As the altered LpxC amounts should correlate with different LPS accumulation in examined mutants, the levels of LPS were measured using Proteinase K-treated whole cell lysates of the isogenic bacterial cultures of the wild-type *E. coli*, the *lapC190* mutant and its derivatives with the indicated genotypes were grown up to an OD_{595} of 0.5 at 30°C. The equivalent portions of whole cell lysates were applied to a 14% SDS-Tricine gel. LPS was analyzed by Western blotting with detection using the LPS-specific WN1 222-5 monoclonal antibody[201]. Results that are presented in Figure 4.10. indicate that the *lapC190* mutant has reduced amounts of LPS that reacted with the WN1 222-5 monoclonal antibody, as in comparison to wild-type strain and even more reduced compared to the Δ*lapA/B* strain (Fig. 4.10. lanes 1-3). It clearly suggests the role of LapC in regulating LpxC turnover by controlling LPS synthesis that is in line with the results presented in subsection 4.7. Mutations that suppress the *lapC190* strain defects are all characterized by increased accumulation of LPS as compared to the original *lapC190* mutant (Fig. 4.10. lanes 3-10). These results provide an explanation of decreased LPS synthesis due to the destabilization of LpxC, when LapC function is impaired, and the restoration of LPS synthesis in the presence of suppressors mapping either to the *lpxC* gene or to the *lapAB* operon, which results in stabilization of LpxC.

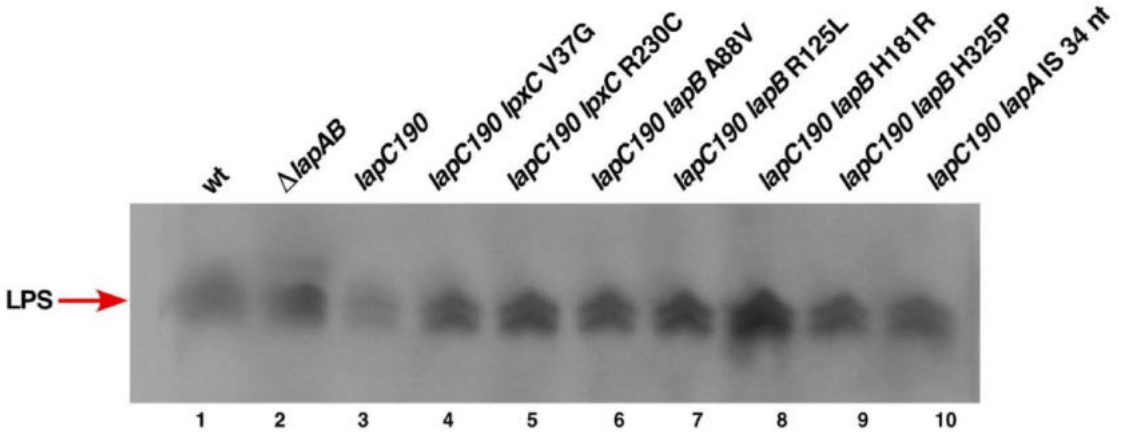

Fig. 4.10. Immunoblot revealing LPS levels in the isogenic wild type, its Δ*lapA*/*B* and *lapC190* derivative and derivatives with suppressor mutations of LapC mutants

Immunoblot compares LPS content of wild-type *E. coli* (lane 1), in lane 2 Δ*(lapA/B)* mutant and in the lane 3 the *lapC190* bacteria and its derivatives with suppressor mutations with relevant genotypes indicated in the figure (lanes 4-10). Cultures were grown up to an OD_{595} of 0.5 at 30°C and the Proteinase K-treated whole cell extracts were resolved on 14% SDS-Tricine gel and immunoblotted using LPS-specific WN1 222-5 monoclonal antibody. LPS detected in samples is indicated by the red arrow.

4.15. Verification of the extragenic suppressor mutations of lapC190 and lapC377fs mapping to the lapA/B operon

Mapping of extragenic suppressors of *lapC190* and *lapC377fs* mutants resulted in the isolation of more than half out of 26 suppressors that had a mutation either in the coding region of the *lapB* gene, or an insertion sequence element (IS) in the *lapA* gene or in the promoter region of *lapA/B* operon, or a stop codon within the sequence of *lapA* gene. Two mutations were also identified that caused frame shifts in the *lapA* gene, which can disrupt the co-translation of downstream *lapB* mRNA (Table 4.2.). Figure 4.12. shows the position of suppressor mutations in the *lapA* gene.

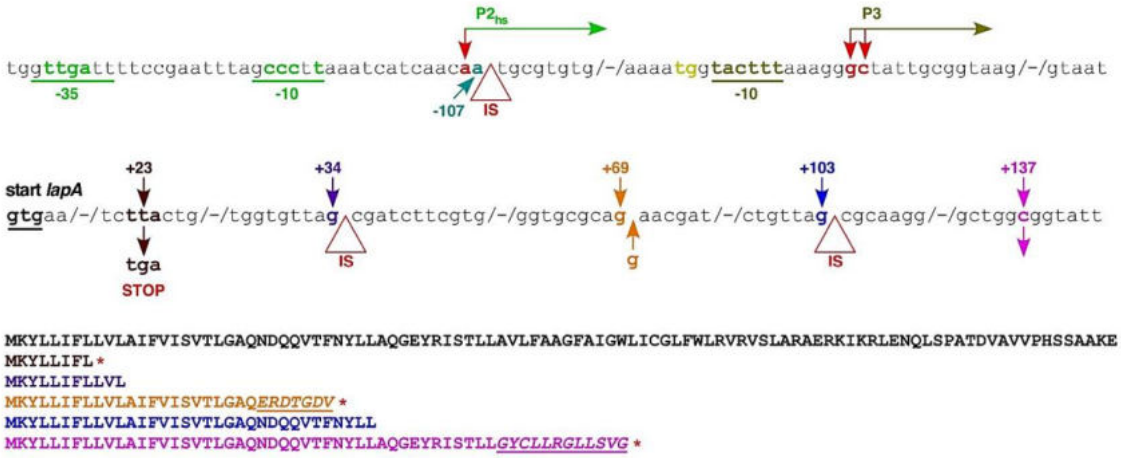

Fig. 4.11. Illustration of position of suppressor mutations within the *lapA* gene
Figure shows position of mapped suppressor mutations in the *lapA* gene within the sequence flanking TSS. Triangle indicates IS elements at the specific nucleotide positions. Mutations that cause frame shifts or introduce stop codons are marked with the arrows with defined exact nt positions of mutations. In corresponding color to the arrow, the alternated by mutations amino acid sequences are enlisted. Introduction of stop codon is marked as an asterisk (*) symbol.

In Figure 4.11. the presence of IS element in either the coding region or the promoter region is indicated by a triangle at the specific nt position. Other mutations causing frame shifts or introducing stop codons, resulting into either truncation of LapA or alterations in the amino acid sequence, are marked according to the description provided in the legend to figure (Fig. 4.11). It is important to remember that these mutation in *lapA* coding region have the direct impact on the expression of the essential downstream *lapB* gene, since they are transcribed as an operon and their translation is coupled[41]. Therefore, such mutations, either in the coding region of the *lapB,* or within *lapA* sequence, could result in the increased stability of LpxC, as its proteolysis by FtsH in the absence

of functional LapB, would be prevented. It was published already by Klein *et al.* 2014 that LpxC becomes stabilized when the LapB is absent and that is the reason of lethality of Δ*lapB* bacteria, as LpxC stabilization leads to excessive accumulation LPS. The same research demonstrated that suppressors mapping to the *lpxC* gene and reducing the synthesis or accumulation of LpxC, can allow a deletion of the *lapB* gene[41]. However, the results presented in this work suggested that LapC could act as an antagonist of LapB, as a loss-of-function mutations in LapC have reduced LpxC stability and less LPS, which is the opposite phenotype to Δ*lapB* bacteria. Additionally, the combination of mutations (Δ*lapB lapC377fs*) restores the normal LPS synthesis. Therefore, the characterization of isolated suppressors of the *lapC190* and *lapC377fs* mutations mapping to the *lapA/B* operon should allow to explain how LapB and LapC interact.

First, to confirm the suppression and estimate the degree of phenotypic restoration, suppressor mutations in the *lapA*/*B* operon that restore bacterial growth at high temperature of *lapC190* and *lapC377fs* mutant derivatives were analyzed by spot-dilution on LA medium and MacConkey agar at 37 and 42°C and on LA at 30°C as a control. Results are presented in Figure 4.12. below. All tested suppressor strains restore the growth of strain with a *lapC190* mutation on LA rich media at all temperatures tested. Similar results are observed for growth on MacConkey agar, with slight differences in the extent of suppression.

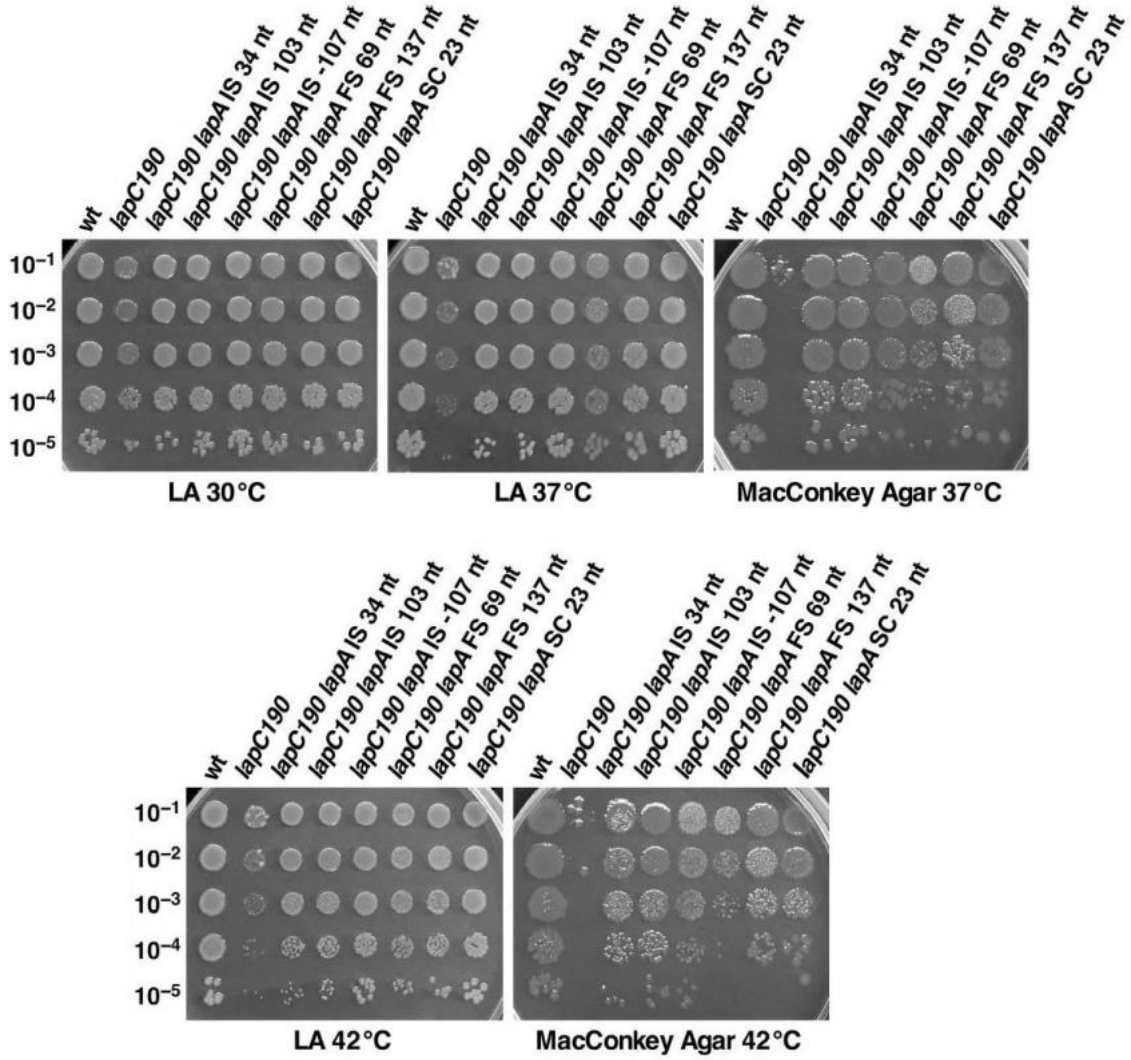

Fig. 4.12. Measurement of bacterial growth by spot-dilution analysis of cultures of wild-type *E. coli* and its isogenic derivatives of *lapC190,* and isolated strains that carry the extragenic suppressor mutations of *lapC190* and *lapC377fs* within *lapA*/*B* operon

Cultures of the wild-type strain, *lapC190* mutant and its isogenic derivatives with suppressor mutations in *lapA*/*B* operon (genotypes indicated in the figure) were grown exponentially at permissive conditions (M9, 30°C) and adjusted to an OD_{595} of 0.1. Serially diluted cultures were spotted on LA and MacConkey agar at 37 and 42°C and on LA agar at 30°C as a control. Plates were incubated at designated temperatures overnight, growth of different strains compared and the photographs were taken. Presented results are from one of the representative experiments.

4.16. Measurement of LapB levels in isolated suppressors of the lapC190 mutants mapping to the lapA gene

To verify the molecular mechanism of suppression of *lapC* mutants defects by the mutations that map to the *lapA* gene region, the LapB amounts were compared in cell extracts of such suppressor-containing strains to the isogenic wild-type *E. coli*, its *lapC190* derivative and to strain with a deletion of *lapA/B*. As a positive control, the purified LapB protein was used due to courtesy of Professor Raina[41]. As already described, the equivalent amount of total proteins from whole cell lysates of strains with indicated mutations in the *lapA* gene or its promoter region were examined by Western blotting using anti-LapB antibodies to measure LapB amounts. Results of this immunoblot are presented in Figure 4.13.

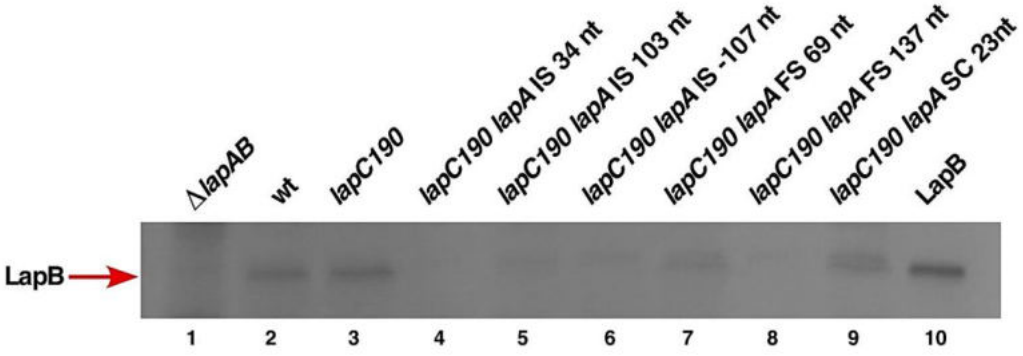

Fig. 4.13. Immunoblot analysis of extracts obtained from the wild-type *E. coli*, its isogenic derivatives of *lapC190,* and isolated strains that carry the extragenic suppressor mutations of *lapC190* and *lapC377fs* mapping to the *lapA* gene and its promoter region
Lanes 1-10 in immunoblot picture show detected LapB amounts (red arrow) using anti-LapB primary antibodies. LapB levels were compared in obtained strains that carry the extragenic suppressor mutations of *lapC190* and *lapC377fs* mapping to the *lapA* gene and its promoter region with the wild type, Δ*lapA/B* and *lapC190* mutants. Prior to Western blotting, cultures of such strains were grown under permissive growth conditions, the whole cell extracts were prepared and its equivalent amounts resolved on SDS-PAGE along with the purified LapB protein as a positive control (lane 10).

Analysis of LapB immunoblot reveals that the presence of mutation within the *lapA* structural gene or its promoter region results either in the complete abolishment of LapB accumulation or it reduces synthesis of this scaffold protein, when comparing to the wild-type strain or the *lapC190* mutant. It supports the assumption that transcription and translation of *lapA* and *lapB* genes is coupled and that the suppression mechanism of mutations of *lapC* derivatives that map to the *lapA* gene, rest on blocking the LapB synthesis. Reduced amounts of LapB, again, cause the enhanced stability of LpxC, which suppress *lapC* mutants that have less LPS and less LpxC.

4.17. Verification of the extragenic suppressor mutations of lapC mutants with the substitutions in the coding sequence of the lapB gene

Nearly one third of isolated strains with extragenic suppressor mutations that restore the growth of either the *lapC190* or *lapC377fs* mutants on LA and MacConkey medium at 42°C, map to the *lapB*-coding sequence (Table 4.2.). To validate the isolation of suppressor mutations within this essential gene, the degree of suppression by all point mutations was quantified. Thus, exponentially grown cultures of *lapC190* mutant strain and its derivatives with A88V, R115H, D124Y, R125L, H181R, H325L and H325P amino acid substitutions in LapB sequence, were cultivated in M9 at 30°C, adjusted to an OD_{595} of 0.1 and spot diluted on LA and MacConkey agar at 30, 37 and 42°C. Results from this spot-testing analysis are shown in Fig. 4.14.

Presented results reveal that amino acid substitutions in the *lapB* coding sequence restore the temperature sensitive growth of *lapC190* mutant on LA medium at 37 and 42°C, but the permeability defects reflected by the sensitivity towards MacConkey medium were alleviated only when suppressor mutations D124Y, H181R and H325P were present. All tested suppressor-containing strains have a single amino acid substitution in the highly conserved residues in TPR elements of LapB. Such mutations could result in ceased interaction with proteins such as FtsH or the interaction with its own rubredoxin domain, therefore inhibit LapB activity that rescues *lapC* mutants.

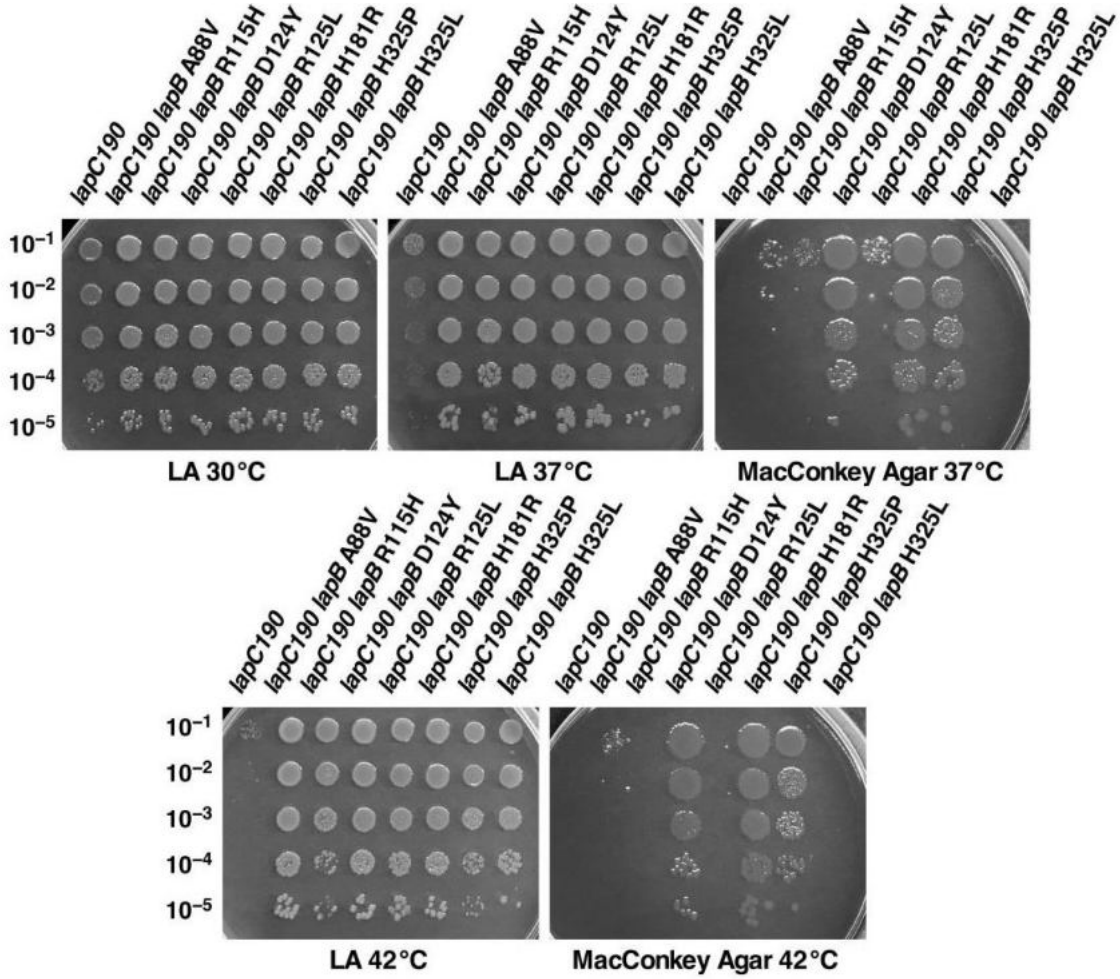

Fig. 4.14. Spot-dilution analysis of *lapC190* mutant and its isogenic derivatives that carry the extragenic suppressor mutations within *lapB* sequence

Cultures of the wild-type strain, *lapC190* mutant and its derivatives with A88V, R115H, D124Y, R125L, H181R, H325L and H325P amino acid substitutions in LapB sequence (genotypes indicated in the figure) were grown exponentially at permissive conditions (M9, 30°C) and adjusted to an OD_{595} of 0.1. Serially diluted cultures were spotted on LA and MacConkey agar at 30, 37 and 42°C. Plates were incubated at designated temperatures overnight, growth of different strains compared and the photographs were taken. Presented results are from one of the representative experiments.

4.18. Measurement of LapB amounts in isolated suppressors of the lapC190 mutants with alterations in LapB sequence

In order to investigate if isolated suppressor mutations mapping to the *lapB* structural gene have an impact on accumulation of protein itself, the immunoblotting of total cellular proteins from strains used in experiment described above was performed. The isogenic bacterial cultures of the wild-type *E. coli*, the *lapC190* mutant and its *lapB* derivatives were grown up to an OD_{595} of 0.5 at 30°C and the equivalent amounts of cell extracts were resolved on a 12% SDS-PAGE and proteins analyzed by Western blotting. To detect relative amounts of LapB, immunoblots were probed with LapB-specific antibodies. As a positive control, purified LapB protein was used as described in subsection 4.16. Results are presented in Figure 4.15.

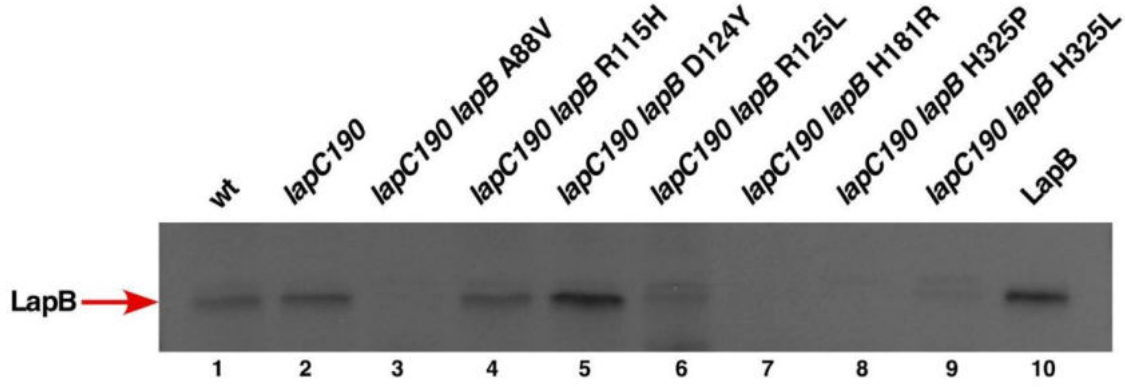

Fig. 4.15. Immunoblot of LapB detected in the wild-type *E. coli* and its isogenic derivatives of *lapC190* and isolated strains that carry its suppressor mutations within *lapB* gene coding sequence

Picture of immunoblot shows detected LapB amounts (indicated with red arrow) using anti-LapB primary antibodies. LapB levels were compared in the wild-type strain (lane 1), the *lapC190* mutant (lane 2) and its derivatives with A88V, R115H, D124Y, R125L, H181R, H325P and H325L amino acid substitutions (lanes 3-9) in LapB sequence. Purified LapB protein was used as a positive control (lane 10). Cultures of these strains were grown under permissive growth conditions, the whole cell extracts were prepared and its equivalent amounts resolved on SDS-PAGE. Proteins were transferred by Western blotting and probed with LapB-specific antibodies.

Examination of LapB levels by immunoblotting revealed that most of the strains with mutations mapping to the *lapB* gene are characterized by a significant reduction in the amounts of protein as compared to the wild-type strain. The exception is the LapB D124Y that most likely undergoes some conformational change due to mutation, which inactivates protein. Consistent with this assumption are the results of spot-testing analysis of *lapC190* mutant and its growth restoration by extragenic suppressor mutations within *lapB* (Fig. 4.14.),

where the D124Y substitution in LapB is one of mutations that restore the growth defects of the *lapC190* mutation on LA as well as on MacConkey agar. It can be concluded that the examined changes in LapB amino acids result in its reduced accumulation or misfolding of protein, which could be due to an enhanced proteolysis and/or its dysfunction due to aberrant folding. These results are in line with the data presented in Fig. 4.10, as the amounts of LapB protein in the cells corelate with LPS accumulation measured using the WN1 222-5 monoclonal antibody. The availability of functional LapB determines the rate of LPS synthesis and the reason for Δ*lapB* strain lethality is based on the fact that in such strain LpxC protein is stable and it causes the increased synthesis of LPS that results in depletion of pools of the common precursor for both phospholipid and LPS biosynthesis (Fig. 1.5.)[41]. LPS immunoblots show that the LPS synthesis is restored in all investigated variants of either LapA or LapB mutations (Fig. 4.10., lanes 6 to 10). As suppressor mutations strains exhibit the increased accumulation of LPS and decreased levels of LapB, in comparison to the *lapC* mutants with the highly reduced LPS content, these results provide the molecular explanation of suppression of *lapC190* mutant that lacks the C-terminal periplasmic domain. Thus, it allows to conclude that LapC and LapB jointly regulate the LPS synthesis by acting in an antagonistic manner.

4.19. Measurement of relative abundance of FtsH in lapC190 ftsH A296V bacteria

Lastly, among suppressor mutations that were found to restore the growth of *lapC* mutants on LA medium at 42°C, one such strain contained a suppressor mutation that was mapped to the *ftsH* gene in a region that encodes the SRH domain of FtsH protease (Table 4.2.). The mutation caused the substitution of 296th alanine by valine residue. It is known that mutations in SRH domain are associated with the abolishment of ATPase activity of FtsH[220]. The immunoblot presented in Fig. 4.10. indicates that *lapC190 ftsH* A296V strain accumulates significantly more LpxC protein as compared to the isogenic *lapC190* mutant (Fig. 4.10. lane 9 and 4). According to results published by Professor Raina's group in Klein *et al.* 2014 and confirmed throughout this research, LapB acts in concert with FtsH to regulate LpxC proteolysis to prevent unwanted excess of LPS biosynthesis over phospholipids[41]. Therefore, it was decided to examine the levels of FtsH in the strain with *lapC190 ftsH* A296V genotype and compare its amounts to the *lapC190* isolate, using Western blotting technique. As described earlier, equivalent amounts of total cellular extracts of strains with indicated genotypes were resolved on a 12% SDS-PAGE gel and immunoblots were treated with anti-FtsH antibodies. As a positive control, the cellular extract of isogenic wild-type *E. coli* was used and cell lysates from Δ*ftsH* mutant bacteria that are viable due to the *sfhC21* suppressor mutation, served as a negative control[221]. Results are depicted in Figure 4.17. below.

The results from Western blot experiment demonstrate that the *lapC190 ftsH* A296V bacteria are characterized by considerably reduced amounts of FtsH protein that reacted with antibodies, as compared to the parental *lapC190* mutant, as well as to the wild type (Fig. 4.16. lane 3 versus 1 and 2). It allows to deduce that A296V amino acid substitution in FtsH restores *lapC190* bacteria growth defects due to decreased amounts of FtsH protease and location in SRH ATPase-regulating domain that hinder degradation of LpxC and restore the LPS synthesis in bacteria with defective LapC.

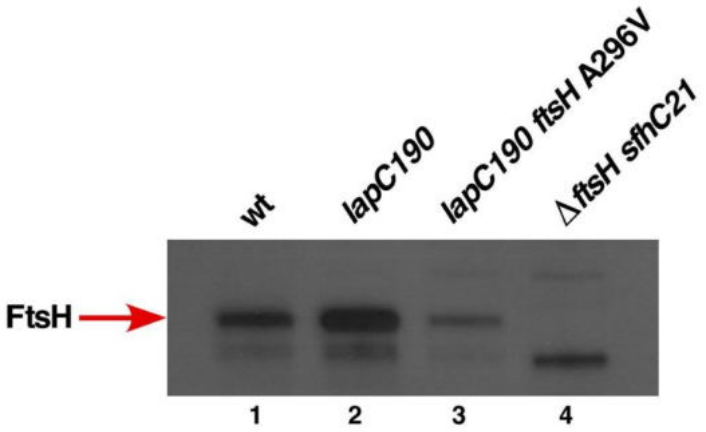

Fig. 4.16. Western blot analysis to detect FtsH amounts in the wild-type *E. coli* and its isogenic derivatives of *lapC190, lapC190 ftsH* A296V and (Δ*ftsH sfhC21)* mutant as a control

Picture presents comparison of FtsH protein levels (red arrow) detected in total cellular extracts obtained from the wild type (lane 1), the *lapC190* mutant (lane 2) and the *lapC190 ftsH* A296V derivative (lane 3). As the negative control, the isogenic strain with Δ*ftsH sfhC21* mutations was used (lane 4). Similarly, as described before, cultures of indicated strains were grown up to an OD_{595} of 0.5 at 30°C and the equivalent amounts of whole cell extracts were resolved on SDS-PAGE gel, transferred by Western blotting and probed with FtsH-specific antibodies.

4.20. Verification of lapB gene essentiality in lapC loss-of-function mutants

The reasoning to address the details of LapB and LapC interaction was supported by several lines of evidences described in this thesis. First, it has been shown that the suppressors of Δ*lapB, lapC377fs* and further isolated *lapC190* are characterized by reduced amounts of LPS that is an opposite phenomenon to what can be observed in Δ*lapB* mutants. Among the isolated extragenic suppressor mutations of *lapC377fs* and *lapC190,* more than half mapped to the *lapA/B* operon and resulted in restoration of the lipopolysaccharide content. Lastly, the Δ*lapB lapC377fs* mutations combination recovered the viability of Δ*lapB* bacteria, while showing the restoration of wild type-like composition of the LPS in the analyzed mass spectra. Based on the presented data, it can be assumed that if LapC and LapB cooperate to regulate the LPS synthesis in an antagonistic manner, the essential *lapB* gene could be dispensable when LapC is dysfunctional. Therefore, using bacteriophage P1 grown on strains with deletions of *lapA/B* or *lapB* alone, the transductions were performed that attempted to introduce deletions in either the *lapC190* or in the *lapC377fs* backgrounds. The numbers of obtained transductants are shown in Table 4.3.

Table 4.3. Number of transductants with selection for kanamycin resistance

Donor	**Recipient strain**		
	BW25113	**BW25113 *lapC190***	**BW25113 *lapC377fs***
P1 Δ*lapA/B* Kan^R	33 Kan^R, small colonies	2930 Kan^R, normal size	3470 Kan^R, normal size
P1 Δ*lapB* Kan^R	36 Kan^R, small colonies	3154 Kan^R, normal size	3696 Kan^R, normal size

Results from transductions presented in Table 4.3 fortify the thesis that the deletions of *lapB* gene or *lapA/B* deletion can be introduced in strains carrying a mutation in the *lapC* gene that renders LapC inactive, with high efficiency. Transductants of Δ*lapB* or Δ*lapA/B* in the wild-type strain appear to the extremely

low frequency and form very small colonies and are obtained after the prolonged incubation. As it was described earlier, the *lapB* gene is essential in most of wild-type *E. coli* backgrounds, however its deletion is tolerated at very low efficiency on M9 minimal medium at 30°C, and such strains grow very poorly, if the extragenic suppressor mutations are not introduced[41]. Presented results support the original isolation of *lapC377fs* as an extragenic suppressor of Δ*lapB* (subsection 4.6.). Taken together, it can be concluded that LapB becomes dispensable, when LapC is dysfunctional, consistent with the model of antagonistic function of LapB and LapC in the regulation of LpxC.

4.21. Verification of lapC gene essentiality in the presence of overexpressed lpxC

It was shown that the suppressor mutations of *lapC* mutants phenotype that map to the *lpxC* gene render LpxC variants resistant to proteolysis and that leads to increased accumulation of LpxC in such cells, which results in the restoration of LpxC amounts otherwise limiting in *lapC* mutant bacteria. Hence, with the similar rationale as presented in previous subsection, experiments were performed to verify if the presence of *lpxC* gene in multicopy will allow for introduction of *lapC* deletion. Firstly, the Δ*lapC* derivative of wild-type *E. coli* was constructed in a strain with a low-copy cosmid clone expressing the *lapC* gene. In such background, the Δ*lapC* derivative is maintained viable due to the extrachromosomal expression of the *lapC* gene and it can serve as a donor in bacteriophage P1-mediated transduction. Next, the recipient strain was constructed by transformation of wild-type *E. coli* with a plasmid expressing the *lpxC* gene under the inducible P_{T5}-*lac* promoter. Using controlled bacteriophage P1-mediated transductions, it was attempted to introduce the *lapC* gene deletion in a *lpxC*-expressing recipient.

Table 4.4. Number of Δ*lapC* transductants with/without overexpression of *lpxC*

Donor	Recipient BW25113 + p*lpxC*$^{+}$	
	no IPTG	**50 μM IPTG**
P1 Δ*lapC* Kan^{R}	none	754

Results presented in Table 4.4. confirm that the *lapC* deletion can be introduced when the *lpxC* gene is induced by the addition of 50 μM IPTG, but not when the *lpxC* gene is repressed by supplementation of 0.2% glucose and without IPTG. Obtained results are in line with the fact that extragenic suppressor mutations of *lapC* mutants were characterized by increased accumulation of LpxC amounts. Therefore, again, it supports the conclusion that LapC and LapB act in the antagonist manner to maintain the turnover of LpxC enzyme, as a deletion of the essential *lapC* gene can be introduced in either the LapB-deprived bacteria or when the *lpxC* gene is mildly overexpressed.

4.22. Co-purification of LapC and LapB

Taking into consideration all genetic evidence for LapB and LapC interaction, the pull-down experiments were performed to verify these data. LapA and LapB proteins were co-overexpressed from a plasmid carrying both genes, with N-terminally His_{10}-tag LapA used as a bait. The inner membrane fractions were subjected to Ni^{2+}-NTA chromatography, eluted and resolved on a 12% SDS-PAGE gel. The identity of isolated polypeptides from SDS-PAGE were revealed using MALDI-TOF mass spectrometry. In parallel, the pull-down experiment was performed with His_6-LapC protein induction that was subjected for affinity purification. Results of pull-down experiments are depicted in Figure 4.17.

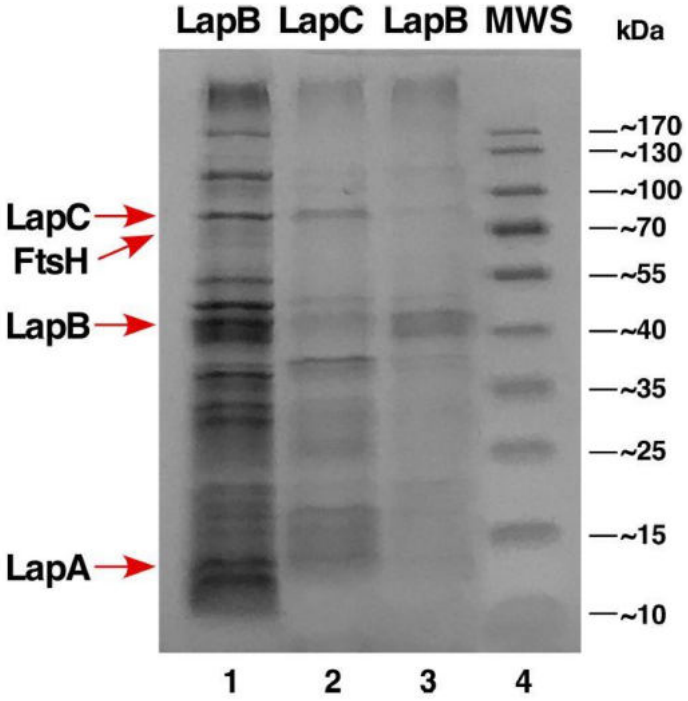

Fig. 4.17. SDS-PAGE gel of elution profiles of proteins from IM fractions after the induction of *lapA* and *lapB* transcription, and *lapC* transcription

Figure presents purification profiles of proteins from IM fractions after the induction of *lapA* and *lapB* transcription with 100 μM and 500 μM IPTG addition (lanes 1 and 3). Lane 2 shows elution profile of hexahistidine-tagged LapC. Proteins were resolved on a 12% SDS-PAGE and visualized using InstantBlue stain. The identification of isolated polypeptides was performed using MALDI-TOF mass spectrometry. The position of identified proteins (LapC, FtsH, LapB and LapA) is indicated by red arrows.

In Figure 4.17., lanes 1 and 3 present the elution profile of proteins that co-purify with His-tagged LapA with LapB. Lane 2 shows the profile of proteins that co-elute with His_6-LapC. The bands corresponding to LapC, LapB, LapA and FtsH are indicated by arrows. The evidence for co-purification of LapA, LapB and

FtsH was published by Klein *et al.* in 2014[41]. Consistent with LapA and LapB co-purification, presented experiment allowed to also identify LapC as one of the proteins that could be part of this complex. In pull-down experiments using His_6-LapC, it was also possible to identify LapB protein. Thus, presented reciprocal co-purification of LapB and LapC provide the additional evidence of interaction of these proteins, supporting data showing their interaction at genetic level.

4.23. Measurement of lapC transcript abundance under heat shock conditions

Although the *lapC* gene was found to be essential under all growth conditions, the fact that it is involved in the regulation of LPS synthesis, which is a major envelope component, allowed to presume that the expression of this gene might vary under stress conditions. What is more, the expression of its interacting partners, LapA, LapB and FtsH are known to be heat shock-inducible[41]. To further characterize this molecule and address if its transcription is altered upon exposition to high temperature, the relative abundance of *lapC* transcripts was measured by qRT-PCR using total RNA extracted from the wild-type *E. coli* grown at 30°C and after a transient shift for 15 min to 43°C.

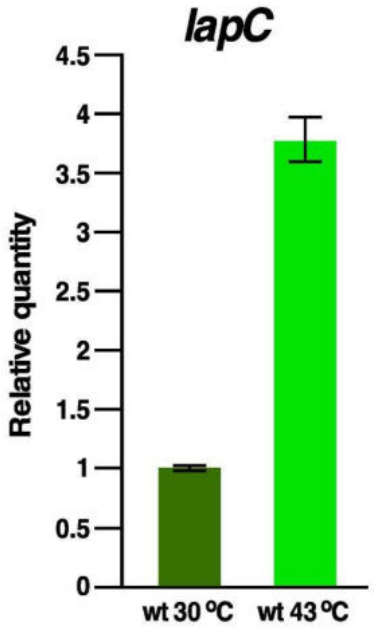

Fig. 4.18. Relative quantity of *lapC* transcripts in the wild-type *E. coli* at 30°C and after a 15-min shift to 43°C

Bars present the relative quantity of *lapC* transcripts in qRT-PCR analysis isolated from wild-type bacteria grown up to an OD_{595} of 0.2 in M9 minimal medium at 30°C and after shift to 43°C. Data presented are from RNA isolated from three biological replicates and bars indicate standard error of experiments.

Comparison of gene expression pattern based on the relative quantity of *lapC* transcripts in qRT-PCR analysis, revealed a 3.5-fold higher amounts of *lapC* mRNA after transient exposure to heat shock conditions. Thus, it should be noted that transcription of *lapC* is not only sustained at high temperature but is rather induced.

5. DISCUSSION

Balanced LPS biosynthesis is critical to maintain the OM integrity and bacterial viability. Regulation of its first rate-limiting step that determines the ratio between phospholipids and LPS outer membrane component, greatly relies on the tight control of LpxC, UDP-3-*O*-acyl-*N*-acetylglucosamine deacetylase, amounts[41,48,49,111]. Up to date, it was known that the FtsH protease and LapB protein play a critical role in the regulation of LpxC turnover, directing its degradation in response to variable demand of lipid A synthesis[41,49,59]. However, the mechanism of how LapB interacts with FtsH during this process and if there are any additional proteins involved in control of LpxC, remained unclear. Both, LapB and FtsH, are essential for *E. coli* viability and a deletion of either of encoding them genes can be tolerated by bacteria only when suppressor mutations or when complementing gene is provided ectopically. Thus, a deletion of *lapB* or *ftsH* genes can be achieved in bacterial backgrounds alternated by mutations in genes, whose products are required in lipid A or early LPS core biosynthesis that results in reduction of LPS biosynthesis or intercept the accumulation of LPS in the inner membrane. One of such examples is the presence of *sfhC21* mutation that results in hyperactive allele of the *fabZ* gene that shifts the utilization of *R*-3-hydroxymyristoyl-ACP common precursor to phospholipid biosynthesis[24,41,49]. The *lapB* gene deletion was found to be poorly tolerated under specific conditions in certain genetic backgrounds, like in BW25113 strain, where after prolonged incubation on minimal medium at 30°C, the Δ*lapB* mutants can be obtained with very low efficiency[41]. This circumstance was fundamental for employed within this research approaches, to expand the knowledge about the LpxC regulation and how LapB participates in its proteolysis.

In the first place, the multicopy suppressor approach was implemented to search for the genes whose presence in high dosage allow for the deletion of *lapB* or *lapA/B* genes at elevated temperatures. These experiments, besides identifying previously published multicopy suppressors, resulted in the isolation of the *hslV* gene. The *hslV* gene encodes ATP-dependent subunit (HslV) of HslVU proteasome-like degradation complex. HslVU (ClpQY) is one of ATP-dependent proteases in *E. coli* that are involved in general cellular protein quality

control. It has been proven to drive the proteolysis of several unstable proteins (RpoH, RcsA, SulA), had a role in degradation of the defective peptides produced in the presence of puromycin and, as a heat shock-inducible protease, lessen the elevated heat shock response in bacterial cells[191–193,222]. Results described in this dissertation experiments show that elevated LpxC levels that contribute to either Δ*lapB* or Δ*lapA/B* derivatives lethality, can be reduced by overexpression of *hslV* gene from the plasmid (subsection 4.1. and 4.2.). This effect is enhanced by co-overexpression of *hslU* gene, as it has been shown in pulse chase experiments when they together synergistically enhance LpxC proteolysis at elevated temperatures. Thus, under conditions when the synthesis of all bacterial proteins is blocked by the addition of rifampicin, the *hslUV* genes under control of T7 promoter expressed from the plasmid contributed to almost complete degradation of LpxC within first 20 min of experiment (subsection 4.3.). In 2016 Emiola *et al.*, in the computational and system biology-based study upon the relationship between bacterial phospholipid biosynthesis and LPS regulation, predicted that LpxC can be regulated by an additional unidentified protease[223]. Presented results demonstrate for the first time such FtsH-independent degradation of LpxC *in vivo* and that this speculated proteolytic activity is due to HslUV complex. Furthermore, it was shown that Δ*hslV* and Δ*hslUV* mutants are sensitive to sublethal concentrations of CHIR090 LpxC inhibitor, which is in line with the discovered role of protease complex in the regulation of LpxC amounts (subsection 4.5.). The uncovering of HslUV complex role in LpxC turnover can be of relevance, particularly at high temperatures. In *Escherichia coli*, the expression of HslU and HslV enzymes is known to increase approximately 10-fold at high temperatures and furthermore, the proteolytic activity of complex is triggered directly by heat-induced conformational changes[192,206,224]. As LpxC degradation is inversely corelated with the doubling time of bacteria, it is possible that the HslUV-dependent LpxC proteolysis becomes mostly relevant at high temperatures and serves as a back-up mechanism to regulate the levels of LpxC and LPS under stress conditions[57]. It can be supported by the data published by Chang *et al.* 2016, where at 41°C the more rapid degradation of RcsA by HslUV was observed than at 30°C[225]. It is one of the examples when HslUV fills the role of the Lon protease under specific conditions[193]. Similarly, it was found that overproduction of HslVU reduced RpoH levels in strains that were otherwise

expected to accumulate heat shock sigma factor[191]. Although FtsH is the primary regulator of RpoH degradation under normal growth conditions, HslUV can be harbored as an additional regulatory proteolytic complex, when the stress conditions-induced misfolded peptides titer FtsH. In the same study, Δ*hslUV* mutant was established to display growth defects only at very high temperatures (>44°C) in rich medium[191]. This could also be reason why HslUV are not essential for bacterial growth like FtsH, since it seems that its proteolytic function comes into play mostly at high temperature. Thus, in similar manner, the HslUV-dependent proteolysis could also constitute a back-up mechanism to fine tune levels of LpxC under stress conditions to maintain the balance between phospholipids and LPS.

Unlike in *E. coli* BW25113, the Δ*lapB* mutation is not viable in other commonly used wild-type strains such as W3110[41]. Therefore, the second approach used in this study, rested on attempt to identify suppressor mutations that would allow for introduction of the *lapB* gene deletion in W3110 strain. It led to isolation of a novel frame-shift mutation in an essential gene *yejM.* The *yejM* was designated as *lapC* upon further characterization of its genetic interactions and the strain with the suppressor mutation that resulted in the frame shift after 377th amino acid in *yejM* was referred as *lapC377fs* mutant. Isolated mutation causes the truncation of C-terminal periplasmic domain that has probably a significant role in LapC functioning. Further experiments verifying LPS content of Δ*lapB*, *lapC377fs*, (Δ*lapB lapC377fs*) in comparison to the wild type, allowed to establish a significant explanation for LapC function in the restoration of Δ*lapB* mutant viability. As previously shown by Klein *et al.* 2014, *E. coli* Δ*lapB* mutants synthesize excessive amounts of LPS and excessive presence of its precursor species. Such aberrant LPS species could accumulate in the IM or may not be targeted to the OM correctly, which can account for the observed toxicity[41]. In this study, it was shown upon comparison of LPS profiles that combination of *lapC377fs* mutation with *lapB* deletion restores the wild-type LPS content (subsection 4.7.). Most importantly, mass spectrometry analysis of LPS from the (Δ*lapB lapC377fs*) derivative revealed the restoration of normal LPS composition and suppression of accumulation of early intermediates as is observed in the spectra of LPS of strains lacking LapB (Fig. 2.2.). Obtained results suggested

that LapB and LapC could act as antagonists and co-operate to adjust the LPS amounts in cell at the level of regulation of LpxC.

In the third approach, to complement the gathered results, the genetic screen was designed to identify the Tn*10* transposon-linked Ts point mutations that induce the envelope stress response, cause LPS defects and simultaneously, confer the sensitivity of such mutant bacteria to sublethal concentration of LpxC inhibitor CHIR090. The rationale for such a screen based on the activation of *rpoE*P3 promoter of *rpoE* gene, whose product is a major responder to envelope stress, was supported by the data published by Professor Raina's group that transcription directed from this particular promoter is known to be specifically induced upon defects in LPS[121]. Additionally, mutant strains with disturbed LPS synthesis and/or assembly are characterized by permeability defects that render them sensitive to bile salt-containing MacConkey agar. And lastly, inclusion of LpxC inhibitor CHIR090 sensitivity criteria allowed for selection of mutants that potentially fail to interact with LpxC deacetylase[48,226]. Combination of these requirements led to isolation of several mutant strains with mutations that mapped to the *lapC* gene (subsection 4.8.). This gene, previously designated *yejM*, was known to be essential for *E. coli* viability and the loss-of-function mutations in *yejM* were characterized by imbalance in outer membrane components, although the molecular basis of this effect was not fully understood[194,216]. Among isolated strains, three mutations in *lapC* were identified: one with a stop codon (TGA) replacing the tryptophane-coding TGG resulting into truncation after amino acid residue 190 (*lapC190*), two that carried the same frame-shift mutation *lapC377fs* that suppressed the Δ*lapB* strain lethality, and one that contained a single amino acid change resulting into substitution of 349F to 349S (*lapC* F349S). The *lapC190* and *lapC377fs* conferred a tight Ts phenotype, the hypersensitivity to CHIR090 and the inability to grow on MacConkey agar and were further investigated.

To further examine the function of LapC and possibly identify its partners, the search for extragenic suppressors that could restore growth of *lapC190* or *lapC377fs* mutants at elevated temperatures or when such mutants were plated on MacConkey agar at 42°C were employed. Isolated extragenic suppressor mutations mapped either to the promoter region of the *lapA*/*B* operon or within the structural genes of *lapA*, *lapB*, *lpxC* and *ftsH*. Suppressor-containing strains

isolated in this dissertation work were characterized by the increased synthesis of LPS as well as the restoration of LpxC amounts. On the contrary, the examination of LPS content of *lapC190* revealed a drastic reduction in LpxC and LPS amounts. It suggested that LapC can regulate the degradation of LpxC. Furthermore, all of the isolated within this experiment suppressors of *lapC* mutants that mapped to the *lpxC* structural gene, were shown to accumulate higher amounts of LpxC, indicating that isolated LpxC variants are resistant to FtsH-mediated proteolysis (subsection 4.13.). It has been reported that C-terminal residues of deacetylase are crucial for recognition by FtsH, and indeed one of the LpxC mutations was found to introduce a frame-shift mutation at the stop codon resulting into the addition of 20 amino acids[219]. Such a LpxC variant obviously would not be recognized by FtsH. The most frequently isolated mutation had a single exchange in V37 amino acid (four independent isolations V37G and one V37L). Similarly, to the aforementioned mutation, structural analysis predicts that this V37G substitution results in a structural change in LpxC that leads to the stabilization of LpxC. Consistent with these results, a Val37 substitution mutation in *Klebsiella pneumoniae* has been reported to render LpxC more stable and resistant to the LpxC inhibitor[218]. The second most frequently mapped LpxC mutation was R230C residue alteration. It was isolated three times independently and confirmed that this change results in elevated levels of LpxC in comparison to the *lapC* mutant.

Consistent with assumed model that LapC, LapB and FtsH co-operate to regulate LpxC turnover, the significant amount of isolated extragenic suppressors of *lapC* mutants had mutations that reduced the LapB abundance or its activity. The impairing of LapB expression in analyzed mutants was observed to be achieved in many different manners. Some of mutations blocked transcription or prevented translation of *lapB* as a member of *lapA/B* operon, which was evident from the identification of suppressor mutation due to IS elements in the *lapA*-coding region and its translational stop codon. This was further confirmed by immunoblotting examination of LapB levels, where all mutants with the IS element or mutations in the *lapA* gene, revealed a pronounced or complete reduction in the detected amounts of LapB. In addition, 8 out of 26 extragenic suppressor mutations identified, mapped within the coding region of *lapB* gene itself, more precisely in highly conserved residues of various LapB TPR domains. It is known

that TPR domains are involved in the governance of protein-protein interactions and multiprotein complex mediators[227–229]. Thus, such LapB variants could be misfolded or be unable to interact with its partners, resulting in nonfunctional variant. The analysis of computed LapB model suggest that isolated A88V substitution disrupts all side-chain H-bonds. Another mutation that stands out during analysis of DNA sequences of suppressors within LapB, is H181R substitution. The mutation of H181 residue was reported in earlier studies by Prince *et al.* to be a loss-of-function mutation in LapB[63]. It can be deduced that all isolated LapB mutants, as they result into its loss of function, thus they mimic the Δ*lapB* mutants phenotype with the excessive accumulation of LPS and the reduced levels of LapB. Therefore, by analogy to described isolation of *lapC377fs* loss-of-function mutation as suppressor of Δ*lapB* growth defects, LapB inactive derivatives rescue the *lapC* mutants phenotype. These findings again support the model, in which LapC and LapB act antagonistically and LapC could either inhibit the interaction of LapB with FtsH or forestall the LapB functioning as a scaffold in the IM that directs the LpxC degradation by FtsH.

After the completion of this manuscript, five independent groups using complementary genetic or structural approaches reported results that support proposed model of LapC and LapB interaction emanating from this work[196, 198-200, 230]. However, none of these studies were aimed to directly address regulation of either LPS biosynthesis or that of turnover of LpxC and sensing of LPS defects, unlike the work undertaken in this thesis. Nonetheless, similar sets of *lapA*, *lapB*, *lpxC* and *ftsH* suppressors has been characterized with nonsynonymous polymorphisms that suppressed the defects in OM integrity, rifampin resistance, survival in macrophages, and colonization of mice only in *Salmonella enterica* serovar Typhimurium bacteria[196]. Research was focused on LapC (PbgA) homolog with a truncated periplasmic domain in a similar manner as in the *lapC190* mutant isolated in this study and it was the first evidence reported that linked PbgA to LPS biosynthesis[196]. The role of LapC in OM homeostasis in *E. coli* was also revealed in the studies involving iron uptake since truncation of LapC periplasmic domain suppressed growth defects of *E. coli tonB* mutant on a medium low in iron[230]. It was found that the analyzed *yejM1163* strain with the truncated LapC periplasmic domain after 388th amino acid is characterized with an increased OM permeability that suppressed a *tonB* mutants phenotype by

allowing iron to enter the cell. Further testing of *yejM1163* strain while searching for suppressors to bulky antibiotics, identified mutations in LapB and FtsH that were identified in this study as well[200]. LpxC and LapA/B suppressors of the Δ*lapC* mutant with a *lapC*-carrying suicide vector were also reported by Fivenson and Bernhardt 2020[199]. In parallel, the search for suppressors was performed that alleviate growth defects of *yejM*569 mutant, expressing a truncated version of LapC lacking its globular and linker domains, on SDS and EDTA-containing media or at 42°C. Suppressors were mapped to *lapB* and *lpxC* genes and measured LPS levels demonstrated lowered LPS amounts in the mutant were restored in the suppressor-carrying strains[196]. It should be noted that among extragenic suppressors of *lapC190* and *lapC377fs* mutations mapped in this research (Table 4.2.), there can be found suppressor mutations of either V37 or R230 amino acids that were reported in two of mentioned manuscripts, after the completion of this research and during the publication of Biernacka *et al.* 2020 manuscript[188,198,199]. It is of significant importance that different approaches led to the identification of the same mutations, which suggests the relevance of described amino acids in LpxC-LapC dynamics. However, in this work a broader and saturated spectrum of suppressor mutations were isolated, mapping to the *lapA/B* operon and *lpxC* gene. Thus, many of the isolated additional mutations mapping to either the *lpxC* gene, or to the *lapA* gene, or the *lapB* gene that suppress *lapC190* and *lapC377fs* mutations, were not reported earlier in other mentioned complementary studies. Hence, this study provides a broader background for the model of LpxC regulation and helps to establish the function of LapC.

The reciprocal co-purification of LapB and LapC presented in this research, constitute a direct proof of interaction between LapB and LapC and supports the model derived from genetic experiments. Additionally, a finding published during completion of this dissertation, has reported that FLAG-tagged LapC can pull-down LapB[195]. The most recent study of Lee *et al.* 2021 reports, based on bacterial two-hybrid assay, that it is the transmembrane domain of LapC that inhibits LapB through protein-protein interaction and that this interaction requires transmembrane domain of LapB[231].

Considering these antagonistic interactions and the fact that a vast number of isolated suppressors of *lapC* mutants that mapped to the *lapA/B* region were

in fact synthesizing very limited amounts of LapB, it was reasoned that the deletion of essential *lapB* gene could be feasible in background where LapC is defective. This was indeed accomplished by the successful transduction of the *lapA*/*B* deletion into strains with *lapC190* and *lapC377fs* mutations (subsection 4.22.). These results were successfully reproduced later by Lee *et al.* 2021, where they were able to construct double deletion of *lapC* and *lapB* genes in the cells with extra chromosomal copy of *lapB* gene under the control of an arabinose inducible promoter[231]. In line with the explanation why LapB becomes dispensable when LapC is dysfunctional, are the results that established the LPS content in various suppressor backgrounds that revealed the elevation in the LPS accumulation in mutants despite the presence of *lapC190* mutation. Thus, the absence of LapB would stabilize LpxC and increase the LPS synthesis that compensate for the reduction in LPS levels in *lapC* mutants. Based on the same reasoning, the extrachromosomal expression of the *lpxC* gene allowed for successful transduction of *lapC* deletion. Taken together, the findings presented in this doctoral dissertation research, support a proposed model wherein the newly established interaction partner, LapC, inhibits the LapB/FtsH-driven proteolysis of LpxC and allows for the accumulation of LpxC and increased LPS biosynthesis. This inhibition could be relieved, when higher levels of the LPS are not physiologically required. Additionally, as a safety mechanism which could be recruited at high temperatures, HslUV proteolytic complex prevents disadvantageous accumulation of LpxC and LPS by promoting proteolytic degradation of LpxC.

6. CONCLUSIONS

The aim of this research was to broaden the understanding of regulation and assembly of *E. coli* LPS, specifically by examining the molecular basis of LapB role in mediating the turnover of LpxC. LpxC is essential for bacterial growth as its product mediates the first committed step in the LPS biosynthetic pathway. The undertaken investigation allowed to identify the role of additional interacting LapB partner, LapC. Based on the presented data, the model was established where LapC cooperate with LapB and FtsH to regulate the turnover of LpxC by the controlled proteolysis in order to ensure dynamically changing demand for the balanced LPS synthesis in relation to phospholipids synthesis and growth condition of bacteria. The multicopy suppressors of Δ*lapB* provided the first evidence for an alternative pathway of LpxC degradation based on HslUV-dependent proteolysis that could constitute a back-up mechanism to fine tune levels of LpxC under stress conditions to maintain the balance between phospholipids and LPS. However, it remains for further investigation to determine the circumstances leading to LapB and LapC interaction that promotes LpxC stability, or how such LapC-dependent inhibition of LapB is disrupted to direct LpxC to degradation. One possible explanation could be that stress conditions, like for example elevated temperature, which were shown to induce the expression of the *lapC* gene, can be a signal to repress the proteolytic activity of LapB/FtsH. This model is supported by independent findings that LpxC degradation is inversely correlated with the *E. coli* doubling time[57]. Such mechanism would allow for the enhanced synthesis of LPS under stress conditions. However, when the accumulation of LPS under stress condition becomes toxic and the LapB/FtsH-mediated proteolysis of LpxC is the limiting factor, the HslUV proteolytic complex could shift the equilibrium, as its expression and proteolytic activity are significantly induced at high temperatures that would result in the rapid degradation of excess LpxC to restore the balance between LPS and phospholipids biosynthesis. Another explanation of LapC and LapB dynamic can be considered when the unwarranted accumulation of LPS intermediates in the IM or before/during the LPS delivery to the OM by Lpt machinery. During such occurrences LapB function becomes limiting and that might signal to relieve the inhibitory effect of LapC and direct LpxC for

degradation by FtsH, again allowing a balance between phospholipid and LPS biosynthesis. This explanation is reinforced by a crystal structure of LapC from *E. coli* that was published by Clairfeuille *et al.* 2020, during the completion of this dissertation[195]. In the manuscript, the group reported an additional density within LapC that could fit a modelled lipid A molecule and designed synthetic peptides that mimicked the potential LapC lipid A-binding domain were found to interact with LPS[195]. Furthermore, during the completion of this dissertation, Professor Raina's laboratory reported negative control of LpxC synthesis by non-coding sRNA, GcvB[56]. Upon overexpression of GcvB sRNA, the reduction in LpxC quantities was observed and strains with GcvB in multicopy were able to partially suppress the lethality of Δ*lapA/B* bacteria. In addition, Δ*gcvB* mutants exhibited increased sensitivity to CHIR090 inhibitor[56]. It remains to be elucidated if *lpxC* mRNA base-pairs with GcvB sRNA, adding another level of control of LpxC amounts along with LapC and LapB/FtsH-mediated regulation.

REFERENCES

(1) Silhavy, T. J.; Kahne, D.; Walker, S. The bacterial cell envelope. *Cold Spring Harbour Perspectives in Biology* **2010**, *2* (5), a000414.

(2) Kleanthous, C.; Armitage, J. P. The bacterial cell envelope. *Philosophical transactions of the Royal Society of London. Series B, Biological sciences* **2015**, *370* (1679), 20150019.

(3) Nikaido, H. Molecular basis of bacterial outer membrane permeability revisited. *Microbiology and molecular biology reviews: MMBR* **2003**, *67* (4), 593–656.

(4) Raetz, C. R., Dowhan, W. Biosynthesis and function of phospholipids in *Escherichia coli*. *Journal of Biological Chemistry* **1990**, *265*(3):1235-1238.

(5) Mullineaux, C. W.; Nenninger, A.; Ray, N.; Robinson, C. Diffusion of green fluorescent protein in three cell environments in *Escherichia coli*. *Journal of Bacteriology* **2006**, *188* (10), 3442–3448.

(6) Van Wielink, J. E.; Duine, J. A. How big is the periplasmic space? *Trends in Biochemical Sciences* **1990**, *15* (4), 136–137.

(7) Weiner, J. H.; Li, L. Proteome of the *Escherichia coli* envelope and technological challenges in membrane proteome analysis. *Biochimica et biophysica acta* **2008**, *1778* (9), 1698–1713.

(8) Vollmer, W.; Blanot, D.; Pedro, M. A. D. Peptidoglycan structure and architecture. *FEMS Microbiology Reviews* **2008**, *32* (2), 149–167.

(9) Koch, A. L.; Woeste, S. Elasticity of the sacculus of *Escherichia coli*. *Journal of Bacteriology* **1992**, *174* (14), 4811–4819.

(10) Raetz, C. R.; Guan, Z.; Ingram, B. O.; Six, D. A.; Song, F.; Wang, X.; Zhao, J. Discovery of new biosynthetic pathways: the lipid A story. *Journal of Lipid Research* **2009**, *50*, 103–108.

(11) Vaara, M. Agents that increase the permeability of the outer membrane. *Microbiology and Molecular Biology Reviews* **1992**, *56* (3), 395–411.

(12) Raetz, C. R.; Whitfield, C. Lipopolysaccharide endotoxins. *Annual Review of Biochemistry* **2002**, *71* (1), 635–700.

(13) Savage, P. B. Multidrug-resistant bacteria: overcoming antibiotic permeability barriers of Gram-negative bacteria. *Annals of Medicine* **2001**, *33* (3), 167–171.

(14) Braun, V.; Rehn, K. Chemical characterization, spatial distribution and function of a lipoprotein (murein-lipoprotein) of the *E. coli* cell wall. *European Journal of Biochemistry* **1969**, *10* (3), 426–438.

(15) Suzuki, H.; Nishimura, Y.; Yasuda, S.; Nishimura, A.; Yamada, M.; Hirota, Y. Murein-lipoprotein of *Escherichia coli*: a protein involved in the stabilization of bacterial cell envelope. *Molecular Genetics and Genomics* **1978**, *167* (1), 1–9.

(16) Sutcliffe, I. C. A phylum level perspective on bacterial cell envelope architecture. *Trends in Microbiology* **2010**, *18* (10), 464–470.

(17) Whitfield, C.; Trent, M. S. Biosynthesis and export of bacterial lipopolysaccharides. *Annual Review of Biochemistry* **2014**, *83* (1), 99–128.

(18) Raetz, C. R. H. Biochemistry of endotoxins. *Annual Review of Biochemistry* **1990**, *59* (1), 129–170.

(19) Kadrmas, J. L.; Raetz, C. R. H. Enzymatic synthesis of lipopolysaccharide in *Escherichia coli*: purification and properties of heptosyltransferase I. *Journal of Biological Chemistry* **1998**, *273* (5), 2799–2807.

(20) Takayama, K.; Qureshi, N.; Mascagni, P.; Nashed, M. A.; Anderson, L.; Raetz, C. R. H. Fatty acyl derivatives of glucosamine 1-phosphate in *Escherichia coli* and their relation to lipid A. Complete structure of a diacyl GlcN-1-P found in

a phosphatidylglycerol-deficient mutant. *Journal of Biological Chemistry* **1983**, *258* (12), 7379–7385.

(21) Neidhardt, F. C., Curtiss III R., Ingraham, J. L., Lin, E. C. C., Low, K. B., Magasanik, B., Reznikoff, W. S., Riley, M., Schaechter, M., Umbarger, H. E., editors. *Escherichia coli* and *Salmonella*: cellular and molecular biology. 2nd ed. Washington, D.C.: ASM Press; **1996**.

(22) Rietschel, E. T.; Kirikae, T.; Schade, F. U.; Mamat, U.; Schmidt, G.; Loppnow, H.; Ulmer, A. J.; Zähringer, U.; Seydel, U.; Di Padova, F. Bacterial endotoxin: molecular relationships of structure to activity and function. *FASEB Journal* **1994**, *8* (2), 217–225.

(23) Brade, H. *Endotoxin in Health and Disease*; CRC Press, 2020.

(24) Klein, G.; Raina, S. Regulated control of the assembly and diversity of LPS by noncoding sRNAs. *BioMed Research International* **2015**, *2015*, e153561.

(25) Strain, S. M.; Fesik, S. W.; Armitage, I. M. Characterization of lipopolysaccharide from a heptoseless mutant of *Escherichia coli* by carbon 13 nuclear magnetic resonance. *International Journal of STD and AIDS* **1983**, *258* (5), 2906–2910.

(26) Klein, G., Lindner, B., Brabetz, W., Brade, H., Raina, S. *Escherichia coli* K-12 suppressor-free mutants lacking early glycosyltransferases and late acyltransferases: minimal lipopolysaccharide structure and induction of envelope stress response. *Journal of Biological Chemistry* **2009**, *284* (23), 15369-15389.

(27) Holst, O. The structures of core regions from enterobacterial lipopolysaccharides – an update. *FEMS Microbiology Letters* **2007**, *27* (1), 3-11.

(28) Heinrichs, D. E.; Yethon, J. A.; Whitfield, C. Molecular basis for structural diversity in the core regions of the lipopolysaccharides of *Escherichia coli* and *Salmonella enterica*. *Molecular Microbiology* **1998**, *30* (2), 221–232.

(29) Klein, G.; Lindner, B.; Brade, H.; Raina, S. Molecular basis of lipopolysaccharide heterogeneity in *Escherichia coli*: envelope stress-responsive regulators control the incorporation of glycoforms with a third 3-deoxy-*α*-D-*manno*-oct-2-ulosonic acid and rhamnose. *Journal of Biological Chemistry* **2011**, *286* (50), 42787–42807.

(30) Merino, S.; Gonzalez, V.; Tomás, J. M. The first sugar of the repeat units is essential for the Wzy polymerase activity and elongation of the *O*-antigen lipopolysaccharide. *Future Microbiology* **2016**, *11*, 903–918.

(31) Liu, B.; Furevi, A.; Perepelov, A. V.; Guo, X.; Cao, H.; Wang, Q.; Reeves, P. R.; Knirel, Y. A.; Wang, L.; Widmalm, G. Structure and genetics of *Escherichia coli* O antigens. *FEMS Microbiology Reviews* **2020**, *44* (6), 655–683.

(32) Stevenson, G.; Neal, B.; Liu, D.; Hobbs, M.; Packer, N. H.; Batley, M.; Redmond, J. W.; Lindquist, L.; Reeves, P. Structure of the *O* antigen of *Escherichia coli* K-12 and the sequence of its *rfb* gene cluster. *Journal of Bacteriology* **1994**, *176* (13), 4144–4156.

(33) Reeves, P. R. Variation in *O*-antigens, niche-specific selection and bacterial populations. *FEMS Microbiology Letters* **1992**, *100* (1–3), 509–516.

(34) Hitchcock, P. J.; Makela, P. H.; Morrison', D. C. Lipopolysaccharide nomenclature-past, present, and future. *Journal of Bacteriology* **1986**, *166* (3), 699–705.

(35) Raetz, C. R.; Reynolds, C. M.; Trent, M. S.; Bishop, R. E. Lipid A modification systems in Gram-negative bacteria. *Annual Review of Biochemistry* **2007**, *76*, 295–329.

(36) Anderson, M. S.; Bull, H. G.; Galloway, S. M.; Kelly, T. M.; Mohan, S.; Radika, K.; Raetz, C. R. H. UDP-*N*-acetylglucosamine acyltransferase of *Escherichia coli*. The first step of endotoxin biosynthesis is thermodynamically unfavorable. *Journal of Biological Chemistry* **1993**, *268* (26), 19858–19865.

(37) Wyckoff, T. J.; Lin, S.; Cotter, R. J.; Dotson, G. D.; Raetz, C. R. H. Hydrocarbon rulers in UDP-*N*-acetylglucosamine acyltransferases. *Journal of Biological Chemistry* **1998**, *273* (49), 32369–32372.

(38) Nikaido, H. Outer membrane. In: Neidhardt, F. C.; Curtiss, III R.; Ingraham, J. L.; Lin, E. C. C.; Low, K. B. Jr.; Magasanik, B.; Reznikoff, W. S.; Riley, M.; Schaechter, M.; Umbarger, H. E., editors. *Escherichia coli* and *Salmonella:* cellular and molecular biology. 2nd ed. Washington, D.C: *American Society for Microbiology;* **1996***,* 29–47*.*

(39) Young, K.; Silver, L. L.; Bramhill, D.; Cameron, P.; Eveland, S. S.; Raetz, C. R.; Hyland, S. A.; Anderson, M. S. The e*nvA* permeability/cell division gene of *Escherichia coli* encodes the second enzyme of lipid A biosynthesis. UDP-3-*O*-(*R*-3-hydroxymyristoyl)-*N*-acetylglucosamine deacetylase. *Journal of Biological Chemistry* **1995**, *270* (51), 30384–30391.

(40) Anderson, M. S.; Robertson, A. D.; Macher, I.; Raetz, C. R. H. Biosynthesis of lipid A in *Escherichia coli*: identification of UDP-3-*O*-[(*R*)-3-hydroxymyristoyl]-alpha-D-glucosamine as a precursor of UDP-N^2,O^3-bis[(*R*)-3-hydroxymyristoyl]-alpha-D-glucosamine. *Biochemistry* **1988**, *27* (6), 1908–1917.

(41) Klein, G.; Kobylak, N.; Lindner, B.; Stupak, A.; Raina, S. Assembly of lipopolysaccharide in *Escherichia coli* requires the essential LapB heat shock protein. *Journal of Biological Chemistry* **2014**, *289* (21),14829-14853.

(42) Jackman, J. E.; Raetz, C. R.; Fierke, C. A. UDP-3-*O*-(*R*-3-hydroxymyristoyl)-*N*-acetylglucosamine deacetylase of *Escherichia coli* is a zinc metalloenzyme. *Biochemistry* **1999**, *38* (6), 1902–1911.

(43) Hernick, M.; Gattis, S. G.; Penner-Hahn, J. E.; Fierke, C. A. Activation of *E. coli* UDP-3-*O*-(*R*-3-hydroxymyristoyl)-*N*-acetylglucosamine deacetylase by Fe^{2+} yields a more efficient enzyme with altered ligand affinity. *Biochemistry* **2010**, *49* (10), 2246–2255.

(44) Gattis, S. G.; Hernick, M.; Fierke, C. A. Active site metal ion in UDP-3-*O*-((*R*)-3-hydroxymyristoyl)-*N*-acetylglucosamine deacetylase (LpxC) switches between Fe(II) and Zn(II) depending on cellular conditions. *Journal of Biological Chemistry* **2010**, *285* (44), 33788–33796.

(45) Clayton, G. M.; Klein, D. J.; Rickert, K. W.; Patel, S. B.; Kornienko, M.; Zugay-Murphy, J.; Reid, J. C.; Tummala, S.; Sharma, S.; Singh, S. B.; Miesel, L.; Lumb, K. J.; Soisson, S. M. Structure of the bacterial deacetylase LpxC bound to the nucleotide reaction product reveals mechanisms of oxyanion stabilization and proton transfer. *Journal of Biological Chemistry* **2013**, *288* (47), 34073–34080.

(46) Lee, C.J.; Liang, X.; Gopalaswamy, R.; Najeeb, J.; Ark, E. D.; Toone, E. J.; Zhou, P. Structural basis of the promiscuous inhibitor susceptibility of *E. coli* LpxC. *ACS Chemical Biology* **2014**, *9* (1), 237–246.

(47) Sorensen, P. G.; Lutkenhaus, J.; Young, K.; Eveland, S. S.; Anderson, M. S.; Raetz, C. R. H. Regulation of UDP-3-*O*-[*R*-3-hydroxymyristoyl]-*N*-acetylglucosamine deacetylase in *Escherichia coli*: the second enzymatic step of lipid A biosynthesis. *Journal of Biological Chemistry* **1996**, *271* (42), 25898–25905.

(48) Zeng, D.; Zhao, J.; Chung, H. S.; Guan, Z.; Raetz, C. R. H.; Zhou, P. Mutants resistant to LpxC inhibitors by rebalancing cellular homeostasis. *Journal of Biological Chemistry* **2013**, *288* (8), 5475–5486.

(49) Ogura, T.; Inoue, K.; Tatsuta, T.; Suzaki, T.; Karata, K.; Young, K.; Su, L. H.; Fierke, C. A.; Jackman, J. E.; Raetz, C. R.; Coleman, J.; Tomoyasu, T.; Matsuzawa, H. Balanced biosynthesis of major membrane components through regulated degradation of the committed enzyme of lipid A biosynthesis by the AAA protease FtsH (HflB) in *Escherichia coli*. *Molecular Microbiology* **1999**, *31* (3), 833–844.

(50) Jayasekera, M. M.; Foltin, S. K.; Olson, E. R.; Holler, T. P. *Escherichia Coli* requires the protease activity of FtsH for growth. *Archives of Biochemistry and Biophysics* **2000**, *380* (1), 103–107.

(51) Herman, C.; Thévenet, D.; D'Ari, R.; Bouloc, P. Degradation of sigma 32, the heat shock regulator in *Escherichia coli*, is governed by HflB. *Proceedings of National Academy of Science of United States of America* **1995**, *92* (8), 3516–3520.

(52) Tomoyasu, T.; Gamer, J.; Bukau, B.; Kanemori, M.; Mori, H.; Rutman, A. J.; Oppenheim, A. B.; Yura, T.; Yamanaka, K.; Niki, H. *Escherichia coli* FtsH is a membrane-bound, ATP-dependent protease which degrades the heat-shock transcription factor sigma 32. *EMBO Journal* **1995**, *14* (11), 2551–2560.

(53) Blaszczak, A.; Georgopoulos, C.; Liberek, K. On the mechanism of FtsH-dependent degradation of the sigma 32 transcriptional regulator of *Escherichia coli* and the role of the DnaK chaperone machine. *Molecular Microbiology* **1999**, *31* (1), 157–166.

(54) Tomoyasu, T.; Ogura, T.; Tatsuta, T.; Bukau, B. Levels of DnaK and DnaJ provide tight control of heat shock gene expression and protein repair in *Escherichia coli*. *Molecular Microbiology* **1998**, *30* (3), 567–581.

(55) Thomanek, N.; Arends, J.; Lindemann, C.; Barkovits, K.; Meyer, H. E.; Marcus, K.; Narberhaus, F. Intricate crosstalk between lipopolysaccharide, phospholipid and fatty acid metabolism in *Escherichia coli* modulates proteolysis of LpxC. *Frontiers in Microbiology* **2019**, *9,* 3285.

(56) Gorzelak, P.; Klein, G.; Raina, S. Molecular basis of essentiality of early critical steps in the lipopolysaccharide biogenesis in *Escherichia coli* K-12: requirement of MsbA, cardiolipin, LpxL, LpxM and GcvB. *International Journal of Molecular Sciences* **2021**, *22* (10), 5099.

(57) Schäkermann, M.; Langklotz, S.; Narberhaus, F. FtsH-mediated coordination of lipopolysaccharide biosynthesis in *Escherichia coli* correlates with the growth rate and the alarmone (p)ppGpp. *Journal of Bacteriology* **2013**, *195* (9), 1912–1919.

(58) Führer, F.; Müller, A.; Baumann, H.; Langklotz, S.; Kutscher, B.; Narberhaus, F. Sequence and length recognition of the C-terminal turnover element of LpxC, a soluble substrate of the membrane-bound FtsH protease. *Journal of Molecular Biology* **2007**, *372* (2), 485–496.

(59) Mahalakshmi, S.; Sunayana, M. R.; SaiSree, L.; Reddy, M. YciM is an essential gene required for regulation of lipopolysaccharide synthesis in *Escherichia coli*. *Molecular Microbiology* **2014**, *91* (1), 145–157.

(60) Missiakas, D.; Betton, J.M.; Raina, S. New components of protein folding in extracytoplasmic compartments of *Escherichia coli* SurA, FkpA and Skp/OmpH. *Molecular Microbiology* **1996**, *21* (4), 871–884.

(61) Li, G.W.; Burkhardt, D.; Gross, C.; Weissman, J. S. Quantifying absolute protein synthesis rates reveals principles underlying allocation of cellular resources. *Cell* **2014**, *157* (3), 624–635.

(62) Lu, Y.H.; Guan, Z.; Zhao, J.; Raetz, C. R. H. Three phosphatidylglycerol-phosphate phosphatases in the inner membrane of *Escherichia coli*. *Journal of Biological Chemistry* **2011**, *286* (7), 5506–5518.

(63) Prince, C.; Jia, Z. An unexpected duo: rubredoxin binds nine TPR motifs to form LapB, an essential regulator of lipopolysaccharide synthesis. *Structure* **2015**, *23* (8), 1500–1506.

(64) Kelly, T. M.; Stachula, S. A.; Raetz, C. R. H.; Anderson, M. S. The *firA* gene of *Escherichia coli* encodes UDP-3-*O*-(*R*-3-hydroxymyristoyl)-glucosamine *N*-acyltransferase. The third step of endotoxin biosynthesis. *Journal of Biological Chemistry* **1993**, *268* (26), 19866–19874.

(65) Babinski, K. J.; Ribeiro, A. A.; Raetz, C. R. H. The *Escherichia coli* gene encoding the UDP-2,3-diacylglucosamine pyrophosphatase of lipid A biosynthesis. *Journal of Biological Chemistry* **2002**, *277* (29), 25937–25946.

(66) Babinski, K. J.; Kanjilal, S. J.; Raetz, C. R. H. Accumulation of the lipid A precursor UDP-2,3-diacylglucosamine in an *Escherichia coli* mutant lacking the *lpxH* gene. *Journal of Biological Chemistry* **2002**, *277* (29), 25947–25956.

(67) Ray, B. L.; Painter, G.; Raetz, C. R. H. The biosynthesis of Gram-negative endotoxin. Formation of lipid A disaccharides from monosaccharide precursors in extracts of *Escherichia coli*. *Journal of Biological Chemistry* **1984**, *259* (8), 4852–4859.

(68) Radika, K.; Raetz, C. R. H. Purification and properties of lipid A disaccharide synthase of *Escherichia coli*. *Journal of Biological Chemistry* **1988**, *263* (29), 14859–14867.

(69) Ray, B. L.; Raetz, C. R. H. The biosynthesis of Gram-negative endotoxin. A novel kinase in *Escherichia coli* membranes that incorporates the 4'-phosphate of lipid A. *Journal of Biological Chemistry* **1987**, *262* (3), 1122–1128.

(70) Brozek, K. A.; Hosaka, K.; Robertson, A. D.; Raetz, C. R. H. Biosynthesis of lipopolysaccharide in *Escherichia coli*. Cytoplasmic enzymes that attach 3-deoxy-D-*manno*-octulosonic acid to lipid A. *Journal of Biological Chemistry* **1989**, *264* (12), 6956–6966.

(71) Brozek, K. A.; Raetz, C. R. H. Biosynthesis of lipid A in *Escherichia coli*. Acyl carrier protein-dependent incorporation of laurate and myristate. *Journal of Biological Chemistry* **1990**, *265* (26), 15410–15417.

(72) Vorachek-Warren, M. K.; Ramirez, S.; Cotter, R. J.; Raetz, C. R. H. A triple mutant of *Escherichia coli* lacking secondary acyl chains on lipid A. *Journal of Biological Chemistry* **2002**, *277* (16), 14194–14205.

(73) Yethon, J. A.; Heinrichs, D. E.; Monteiro, M. A.; Perry, M. B.; Whitfield, C. Involvement of WaaY, WaaQ, and WaaP in the modification of *Escherichia coli* lipopolysaccharide and their role in the formation of a stable outer membrane. *Journal of Biological Chemistry* **1998**, *273* (41), 26310–26316.

(74) Genevaux, P.; Bauda, P.; DuBow, M. S.; Oudega, B. Identification of Tn*10* insertions in the *rfaG, rfaP,* and *galU* genes involved in lipopolysaccharide core biosynthesis that affect *Escherichia coli* adhesion. *Archives of Microbiology* **1999**, *172* (1), 1–8.

(75) Pradel, E.; Parker, C. T.; Schnaitman, C. A. Structures of the *rfaB, rfaI*, *rfaJ,* and *rfaS* genes of *Escherichia coli* K-12 and their roles in assembly of the lipopolysaccharide core. *Journal of Bacteriology* **1992**, *174* (14), 4736–4745.

(76) Yethon, J. A.; Vinogradov, E.; Perry, M. B.; Whitfield, C. Mutation of the lipopolysaccharide core glycosyltransferase encoded by *waaG* destabilizes the outer membrane of *Escherichia coli* by interfering with core phosphorylation. *Journal of Bacteriology* **2000**, *182* (19), 5620–5623.

(77) Müller-Loennies, S.; Lindner, B.; Brade, H. Structural analysis of oligosaccharides from lipopolysaccharide (LPS) of *Escherichia coli* K12 strain W3100 reveals a link between inner and outer core LPS biosynthesis. *Journal of Biological Chemistry* **2003**, *278* (36), 34090–34101.

(78) Wang, Z.; Wang, J.; Ren, G.; Li, Y.; Wang, X. Influence of core oligosaccharide of lipopolysaccharide to outer membrane behavior of *Escherichia coli*. *Marine Drugs* **2015**, *13* (6), 3325–3339.

(79) Samuel, G.; Reeves, P. Biosynthesis of *O*-antigens: genes and pathways involved in nucleotide sugar precursor synthesis and *O*-antigen assembly. *Carbohydrate Research* **2003**, *338* (23), 2503–2519.

(80) Polissi, A.; Georgopoulos, C. Mutational analysis and properties of the MsbA gene of *Escherichia coli*, coding for an essential ABC family transporter. *Molecular Microbiology* **1996**, *20* (6), 1221–1233.

(81) Zhou, Z.; White, K. A.; Polissi, A.; Georgopoulos, C.; Raetz, C. R. H. Function of *Escherichia coli* MsbA, an essential ABC family transporter, in lipid A and phospholipid biosynthesis. *Journal of Biological Chemistry* **1998**, *273* (20), 12466–12475.

(82) Doerrler, W. T.; Gibbons, H. S.; Raetz, C. R. H. MsbA-dependent translocation of lipids across the inner membrane of *Escherichia coli*. *Journal of Biological Chemistry* **2004**, *279* (43), 45102–45109.

(83) Karow, M.; Georgopoulos, C. The essential *Escherichia coli msbA* gene, a multicopy suppressor of null mutations in the *htrB* gene, is related to the universally conserved family of ATP-dependent translocators. *Molecular Microbiology* **1993**, *7* (1), 69–79.

(84) Meredith, T. C.; Aggarwal, P.; Mamat, U.; Lindner, B.; Woodard, R. W. Redefining the requisite lipopolysaccharide structure in *Escherichia coli*. *ACS Chemical Biology* **2006**, *1* (1), 33–42.

(85) Mamat, U.; Meredith, T. C.; Aggarwal, P.; Kühl, A.; Kirchhoff, P.; Lindner, B.; Hanuszkiewicz, A.; Sun, J.; Holst, O.; Woodard, R. W. Single amino acid substitutions in either YhjD or MsbA confer viability to 3-deoxy-D-*manno*-oct-2-ulosonic acid-depleted *Escherichia coli*. *Molecular Microbiology* **2008**, *67* (3), 633–648.

(86) Padayatti, P. S.; Lee, S. C.; Stanfield, R. L.; Wen, P.-C.; Tajkhorshid, E.; Wilson, I. A.; Zhang, Q. Structural insights into the lipid A transport pathway in *MsbA*. *Structure* **2019**, *27* (7), 1114-1123.

(87) Doshi, R.; Woebking, B.; Veen, H. W. van. Dissection of the conformational cycle of the multidrug/lipid A ABC Exporter MsbA. *Proteins: Structure, Function, and Bioinformatics* **2010**, *78* (14), 2867–2872.

(88) Ward, A.; Reyes, C. L.; Yu, J.; Roth, C. B.; Chang, G. Flexibility in the ABC transporter MsbA: alternating access with a twist. *Proceedings of the National Academy of Sciences of the United States of America* **2007**, *104* (48), 19005–19010.

(89) Ho, H.; Miu, A.; Alexander, M. K.; Garcia, N. K.; Oh, A.; Zilberleyb, I.; Reichelt, M.; Austin, C. D.; Tam, C.; Shriver, S.; Hu, H.; Labadie, S. S.; Liang, J.; Wang, L.; Wang, J.; Lu, Y.; Purkey, H. E.; Quinn, J.; Franke, Y.; Clark, K.; Beresini, M. H.; Tan, M.-W.; Sellers, B. D.; Maurer, T.; Koehler, M. F. T.; Wecksler, A. T.; Kiefer, J. R.; Verma, V.; Xu, Y.; Nishiyama, M.; Payandeh, J.; Koth, C. M. Structural basis for dual-mode inhibition of the ABC transporter MsbA. *Nature* **2018**, *557* (7704), 196–201.

(90) Doerrler, W. T.; Raetz, C. R. H. ATPase activity of the MsbA lipid flippase of *Escherichia coli*. *Journal of Biological Chemistry* **2002**, *277* (39), 36697–36705.

(91) Reynolds, C. M.; Raetz, C. R. H. Replacement of lipopolysaccharide with free lipid A molecules in *Escherichia coli* mutants lacking all core sugars. *Biochemistry* **2009**, *48* (40), 9627–9640.

(92) Douglass, M. V.; Cléon, F.; Trent, M. S. Cardiolipin aids in lipopolysaccharide transport to the Gram-negative outer membrane. *Proceedings of the National Academy of Sciences of the United States of America* **2021**, *118* (15), e2018329118.

(93) McGrath, B. C.; Osborn, M. J. Localization of the terminal steps of *O*-antigen synthesis in *Salmonella Typhimurium*. *Journal of Bacteriology* **1991**, *173* (2), 649–654.

(94) Cuthbertson, L.; Kos, V.; Whitfield, C. ABC transporters involved in export of cell surface glycoconjugates. *Microbiology and Molecular Biology Reviews* **2010**, *74* (3), 341–362.

(95) Greenfield, L. K.; Whitfield, C. Synthesis of lipopolysaccharide *O*-antigens by ABC transporter-dependent pathways. *Carbohydrate Research* **2012**, *356*, 12–24.

(96) Chng, S.-S.; Gronenberg, L. S.; Kahne, D. Proteins required for lipopolysaccharide assembly in *Escherichia coli* form a trans-envelope complex. *Biochemistry* **2010**, *49* (22), 4565–4567.

(97) Okuda, S.; Freinkman, E.; Kahne, D. Cytoplasmic ATP hydrolysis powers transport of lipopolysaccharide across the periplasm in *E. coli*. *Science* **2012**, *338* (6111), 1214–1217.

(98) Sperandeo, P.; Cescutti, R.; Villa, R.; Di Benedetto, C.; Candia, D.; Dehò, G.; Polissi, A. Characterization of *lptA* and *lptB*, two essential genes implicated in lipopolysaccharide transport to the outer membrane of *Escherichia coli*. *Journal of Bacteriology* **2007**, *189* (1), 244–253.

(99) Ruiz, N.; Gronenberg, L. S.; Kahne, D.; Silhavy, T. J. Identification of two inner-membrane proteins required for the transport of lipopolysaccharide to the outer membrane of *Escherichia coli*. *Proceedings of the National Academy of Sciences of the United States of America* **2008**, *105* (14), 5537–5542.

(100) Nikaido, H.; Pagès, J. M. Broad specificity efflux pumps and their role in multidrug resistance of Gram-negative bacteria. *FEMS Microbiology Reviews* **2012**, *36* (2), 340–363.

(101) Narita, S.; Tokuda, H. Biochemical characterization of an ABC transporter LptBFGC complex required for the outer membrane sorting of lipopolysaccharides. *FEBS Letters* **2009**, *583* (13), 2160–2164.

(102) Schultz, K. M.; Klug, C. S. Characterization of and lipopolysaccharide binding to the *E. coli* LptC protein dimer. *Protein Science* **2018**, *27* (2), 381–389.

(103) Wu, T.; McCandlish, A. C.; Gronenberg, L. S.; Chng, S. S.; Silhavy, T. J.; Kahne, D. Identification of a protein complex that assembles lipopolysaccharide in the outer membrane of *Escherichia coli*. *Proceedings of the National Academy of Sciences of the United States of America* **2006**, *103* (31), 11754–11759.

(104) Villa, R.; Martorana, A. M.; Okuda, S.; Gourlay, L. J.; Nardini, M.; Sperandeo, P.; Dehò, G.; Bolognesi, M.; Kahne, D.; Polissi, A. The *Escherichia coli* Lpt transenvelope protein complex for lipopolysaccharide export is assembled via conserved structurally homologous domains. *Journal of Bacteriology* **2013**, *195* (5), 1100–1108.

(105) Sperandeo, P.; Villa, R.; Martorana, A. M.; Šamalikova, M.; Grandori, R.; Dehò, G.; Polissi, A. New insights into the Lpt machinery for lipopolysaccharide transport to the cell surface: LptA-LptC interaction and LptA stability as sensors of a properly assembled transenvelope complex. *Journal of Bacteriology* **2011**, *193* (5), 1042–1053.

(106) Sperandeo, P.; Lau, F. K.; Carpentieri, A.; De Castro, C.; Molinaro, A.; Dehò, G.; Silhavy, T. J.; Polissi, A. Functional analysis of the protein machinery required for transport of lipopolysaccharide to the outer membrane of *Escherichia coli*. *Journal of Bacteriology* **2008**, *190* (13), 4460–4469.

(107) Chimalakonda, G.; Ruiz, N.; Chng, S.S.; Garner, R. A.; Kahne, D.; Silhavy, T. J. Lipoprotein LptE is required for the assembly of LptD by the beta-barrel assembly machine in the outer membrane of *Escherichia coli*. *Proceedings of the National Academy of Sciences of the United States of America* **2011**, *108* (6), 2492–2497.

(108) Li, X.; Gu, Y.; Dong, H.; Wang, W.; Dong, C. Trapped lipopolysaccharide and LptD intermediates reveal lipopolysaccharide translocation steps across the *Escherichia coli* outer membrane. *Scientific Reports* **2015**, *5* (1), 11883.

(109) Babu, M.; Arnold, R.; Bundalovic-Torma, C.; Gagarinova, A.; Wong, K. S.; Kumar, A.; Stewart, G.; Samanfar, B.; Aoki, H.; Wagih, O.; Vlasblom, J.; Phanse, S.; Lad, K.; Yu, A. Y. H.; Graham, C.; Jin, K.; Brown, E.; Golshani, A.; Kim, P.; Moreno-Hagelsieb, G.; Greenblatt, J.; Houry, W. A.; Parkinson, J.; Emili, A. Quantitative genome-wide genetic interaction screens reveal global epistatic relationships of protein complexes in *Escherichia coli*. *PLoS Genetics* **2014**, *10* (2), e1004120.

(110) Juncker, A. S.; Willenbrock, H.; von Heijne, G.; Brunak, S.; Nielsen, H.; Krogh, A. Prediction of lipoprotein signal peptides in Gram-negative bacteria. *Protein Science* **2003**, *12* (8), 1652–1662.

(111) Klein, G.; Raina, S. Regulated assembly of LPS, its structural alterations and cellular response to LPS defects. *International Journal of Molecular Sciences* **2019**, *20* (2), 356.

(112) Guo, L.; Lim, K. B.; Poduje, C. M.; Daniel, M.; Gunn, J. S.; Hackett, M.; Miller, S. I. Lipid A acylation and bacterial resistance against vertebrate antimicrobial peptides. *Cell* **1998**, *95* (2), 189–198.

(113) Bishop, R. E. The lipid A palmitoyltransferase PagP: molecular mechanisms and role in bacterial pathogenesis. *Molecular Microbiology* **2005**, *57* (4), 900–912.

(114) Bishop, R. E.; Gibbons, H. S.; Guina, T.; Trent, M. S.; Miller, S. I.; Raetz, C. R. H. Transfer of palmitate from phospholipids to Lipid A in outer membranes of Gram-negative bacteria. *EMBO Journal* **2000**, *19* (19), 5071–5080.

(115) Eguchi, Y.; Okada, T.; Minagawa, S.; Oshima, T.; Mori, H.; Yamamoto, K.; Ishihama, A.; Utsumi, R. Signal transduction cascade between EvgA/EvgS and PhoP/PhoQ two-component systems of *Escherichia coli*. *Journal of Bacteriology* **2004**, *186* (10), 3006–3014.

(116) Szczesny, M.; Beloin, C.; Ghigo, J. M. Increased osmolarity in biofilm triggers RcsB-dependent lipid A palmitoylation in *Escherichia coli*. *mBio* **2018**, *9* (4), e01415-18.

(117) Anandan, A.; Vrielink, A. Structure and function of lipid A–modifying enzymes. *Annals of the New York Academy of Sciences* **2020**, *1459* (1), 19–37.

(118) Groisman, E. A. The pleiotropic two-component regulatory system PhoP-PhoQ. *Journal of Bacteriology* **2001**, *183* (6), 1835–1842.

(119) Bader, M. W.; Sanowar, S.; Daley, M. E.; Schneider, A. R.; Cho, U.; Xu, W.; Klevit, R. E.; Le Moual, H.; Miller, S. I. Recognition of antimicrobial peptides by a bacterial sensor kinase. *Cell* **2005**, *122* (3), 461–472.

(120) Majdalani, N.; Gottesman, S. The Rcs phosphorelay: a complex signal transduction system. *Annual Review of Microbiology* **2005**, *59* (1), 379–405.

(121) Klein, G.; Stupak, A.; Biernacka, D.; Wojtkiewicz, P.; Lindner, B.; Raina, S. Multiple transcriptional factors regulate transcription of the *rpoE* gene in *Escherichia coli* under different growth conditions and when the lipopolysaccharide biosynthesis is defective. *Journal of Biological Chemistry* **2016**, *291* (44), 22999–23019.

(122) Bishop, R. E.; Kim, S.H.; El Zoeiby, A. Role of lipid A palmitoylation in bacterial pathogenesis. *Journal of Endotoxin Research* **2005**, *11* (3), 174–180.

(123) Trent, M. S.; Pabich, W.; Raetz, C. R.; Miller, S. I. A PhoP/PhoQ-induced lipase (PagL) that catalyzes 3-*O*-deacylation of lipid A precursors in membranes of *Salmonella Typhimurium. Journal of Biological Chemistry* **2001**, *276* (12), 9083–9092.

(124) Kawasaki, K.; Ernst, R. K.; Miller, S. I. 3-*O*-Deacylation of lipid A by PagL, a PhoP/PhoQ-regulated deacylase of *Salmonella Typhimurium*, modulates signaling through Toll-like receptor 4. *Journal of Biological Chemistry* **2004**, *279* (19), 20044–20048.

(125) Reynolds, C. M.; Ribeiro, A. A.; McGrath, S. C.; Cotter, R. J.; Raetz, C. R.H.; Trent, M. S. An outer membrane enzyme encoded by *Salmonella Typhimurium* LpxR that

removes the 3′-acyloxyacyl moiety of lipid A. *Journal of Biological Chemistry* **2006**, *281* (31), 21974–21987.

(126) Corcoran, C. P.; Podkaminski, D.; Papenfort, K.; Urban, J. H.; Hinton, J. C. D.; Vogel, J. Superfolder GFP reporters validate diverse new mRNA targets of the classic porin regulator, MicF RNA. *Molecular Microbiology* **2012**, *84* (3), 428–445.

(127) Inoue, K.; Matsuzaki, H.; Matsumoto, K.; Shibuya, I. Unbalanced membrane phospholipid compositions affect transcriptional expression of certain regulatory genes in *Escherichia coli*. *Journal of Bacteriology* **1997**, *179* (9), 2872–2878.

(128) Delihas, N.; Forst, S. MicF: An antisense RNA gene involved in response of *Escherichia coli* to global stress factors. *Journal of Molecular Biology* **2001**, *313* (1), 1–12.

(129) Carty, S. M.; Sreekumar, K. R.; Raetz, C. R. H. Effect of cold shock on lipid A biosynthesis in *Escherichia coli*. Induction at 12 degrees C of an acyltransferase specific for palmitoleoyl-acyl carrier protein. *Journal of Biological Chemistry* **1999**, *274* (14), 9677–9685.

(130) Tran, A. X.; Lester, M. E.; Stead, C. M.; Raetz, C. R. H; Maskell, D. J.; McGrath, S. C.; Cotter, R. J.; Trent, M. S. Resistance to the antimicrobial peptide polymyxin requires myristoylation of *Escherichia coli* and *Salmonella Typhimurium* lipid A. *Journal of Biological Chemistry* **2005**, *280* (31), 28186–28194.

(131) Hagiwara, D.; Yamashino, T.; Mizuno, T. A Genome-wide view of the *Escherichia coli* BasS–BasR two-component system implicated in iron-responses. *Bioscience, Biotechnology, and Biochemistry* **2004**, *68* (8), 1758–1767.

(132) Rubin, E. J.; Herrera, C. M.; Crofts, A. A.; Trent, M. S. PmrD Is required for modifications to *Escherichia coli* endotoxin that promote antimicrobial resistance. *Antimicrobial Agents and Chemotherapy* **2015**, *59* (4), 2051–2061.

(133) Zhou, Z.; Lin, S.; Cotter, R. J.; Raetz, C. R. H. Lipid A modifications characteristic of *Salmonella Typhimurium* are induced by NH_4VO_3 in *Escherichia coli* K12. Detection of 4-amino-4-deoxy-L-arabinose, phosphoethanolamine and palmitate. *Journal of Biological Chemistry* **1999**, *274* (26), 18503–18514.

(134) Herrera, C. M.; Hankins, J. V.; Trent, M. S. Activation of PmrA inhibits LpxT-dependent phosphorylation of lipid A promoting resistance to antimicrobial peptides. *Molecular Microbiology* **2010**, *76* (6), 1444–1460.

(135) Kato, A.; Chen, H. D.; Latifi, T.; Groisman, E. A. Reciprocal control between a bacterium's regulatory system and the modification status of its lipopolysaccharide. *Molecular Cell* **2012**, *47* (6), 897–908.

(136) Raina, S.; Missiakas, D.; Georgopoulos, C. The *rpoE* gene encoding the sigma E (sigma 24) heat shock sigma factor of *Escherichia coli*. *EMBO Journal* **1995**, *14* (5), 1043–1055.

(137) Tam, C.; Missiakas, D. Changes in lipopolysaccharide structure induce the σ^E-dependent response of *Escherichia coli*. *Molecular Microbiology* **2005**, *55* (5), 1403–1412.

(138) Coornaert, A.; Lu, A.; Mandin, P.; Springer, M.; Gottesman, S.; Guillier, M. MicA sRNA links the PhoP regulon to cell envelope stress. *Molecular Microbiology* **2010**, *76* (2), 467–479.

(139) Gogol, E. B.; Rhodius, V. A; Papenfort, K.; Vogel, J.; Gross, C. Small RNAs endow a transcriptional activator with essential repressor functions for single-tier control of a global stress regulon. *Proceedings of the National Academy of Sciences of the United States of America* **2011**, *108* (31), 12875–12880.

(140) Coornaert, A.; Chiaruttini, C.; Springer, M.; Guillier, M. Post-transcriptional control of the *Escherichia coli* PhoQ-PhoP two-component system by multiple sRNAs involves a novel pairing region of GcvB. *PLoS Genetics* **2013**, *9* (1), e1003156.

(141) Barreto, B.; Rogers, E.; Xia, J.; Frisch, R. L.; Richters, M.; Fitzgerald, D. M.; Rosenberg, S. M. The small RNA GcvB promotes mutagenic break repair by opposing the membrane stress response. *Journal of Bacteriology* **2016**, *198* (24), 3296–3308.

(142) Brabetz, W.; Müller-Loennies, S.; Holst, O.; Brade, H. Deletion of the heptosyltransferase genes *rfaC* and *rfaF* in *Escherichia coli* K-12 results in an Re-type lipopolysaccharide with a high degree of 2-aminoethanol phosphate substitution. *European Journal of Biochemistry* **1997**, *247* (2), 716–724.

(143) Kanipes, M. I.; Lin, S.; Cotter, R. J.; Raetz, C. R. H. Ca^{2+}-induced phosphoethanolamine transfer to the outer 3-deoxy-D-*manno*-octulosonic acid moiety of *Escherichia coli* lipopolysaccharide. A novel membrane enzyme dependent upon phosphatidylethanolamine. *Journal of Biological Chemistry* **2001**, *276* (2), 1156–1163.

(144) Moon, K.; Six, D. A.; Lee, H. J.; Raetz, C. R. H.; Gottesman, S. Complex transcriptional and post-transcriptional regulation of an enzyme for lipopolysaccharide modification. *Molecular Microbiology* **2013**, *89* (1), 52–64.

(145) Moon, K.; Gottesman, S. A PhoQ/P-regulated small RNA regulates sensitivity of *Escherichia coli* to antimicrobial peptides. *Molecular Microbiology* **2009**, *74* (6), 1314–1330.

(146) Mandin, P.; Gottesman, S. Integrating anaerobic/aerobic sensing and the general stress response through the ArcZ small RNA. *EMBO Journal* **2010**, *29* (18), 3094–3107.

(147) Klein, G.; Müller-Loennies, S.; Lindner, B.; Kobylak, N.; Brade, H.; Raina, S. Molecular and structural basis of inner core lipopolysaccharide alterations in *Escherichia coli*: incorporation of glucuronic acid and phosphoethanolamine in the heptose region. *Journal of Biological Chemistry* **2013**, *288* (12), 8111–8127.

(148) Makino, K.; Shinagawa, H.; Amemura, M.; Kawamoto, T.; Yamada, M.; Nakata, A. Signal transduction in the phosphate regulon of *Escherichia coli* involves phosphotransfer between PhoR and PhoB proteins. *Journal of Molecular Biology* **1989**, *210* (3), 551–559.

(149) Frirdich, E.; Lindner, B.; Holst, O.; Whitfield, C. Overexpression of the *waaZ* gene leads to modification of the structure of the inner core region of *Escherichia coli* lipopolysaccharide, truncation of the outer core, and reduction of the amount of O polysaccharide on the cell surface. *Journal of Bacteriology* **2003**, *185* (5), 1659–1671.

(150) Pradel, E.; Schnaitman, C. A. Effect of RfaH (SfrB) and temperature on expression of *rfa* genes of *Escherichia coli* K-12. *Journal of Bacteriology* **1991**, *173* (20), 6428–6431.

(151) Wang, L.; Jensen, S.; Hallman, R.; Reeves, P. R. Expression of the O antigen gene cluster is regulated by RfaH through the JUMPstart sequence. *FEMS Microbiology Letters* **1998**, *165* (1), 201–206.

(152) Artsimovitch, I.; Landick, R. The transcriptional regulator RfaH stimulates RNA chain synthesis after recruitment to elongation complexes by the exposed non-template DNA strand. *Cell* **2002**, *109* (2), 193–203.

(153) Belogurov, G. A.; Mooney, R. A.; Svetlov, V.; Landick, R.; Artsimovitch, I. Functional specialization of transcription elongation factors. *EMBO Journal* **2009**, *28* (2), 112–122.

(154) Bailey, M. J. A.; Hughes, C.; Koronakis, V. RfaH and the *ops* element, components of a novel system controlling bacterial transcription elongation. *Molecular Microbiology* **1997**, *26* (5), 845–851.

(155) Nieto, J. M.; Bailey, M. J. A.; Hughes, C.; Koronakis, V. Suppression of transcription polarity in the *Escherichia coli* haemolysin operon by a short upstream

element shared by polysaccharide and DNA transfer determinants. *Molecular Microbiology* **1996**, *19* (4), 705–713.

(156) Burmann, B. M.; Knauer, S. H.; Sevostyanova, A.; Schweimer, K.; Mooney, R. A.; Landick, R.; Artsimovitch, I.; Rösch, P. An *α*-helix to *β*-barrel domain switch transforms the transcription factor RfaH into a translation factor. *Cell* **2012**, *150* (2), 291–303.

(157) Raina, S.; Georgopoulos, C. The *htrM* gene, whose product is essential for *Escherichia coli* viability only at elevated temperatures, is identical to the *rfaD* gene. *Nucleic Acids Research* **1991**, *19* (14), 3811–3819.

(158) Missiakas, D.; Mayer, M. P.; Lemaire, M.; Georgopoulos, C.; Raina, S. Modulation of the *Escherichia coli* sigma E (RpoE) heat-shock transcription-factor activity by the RseA, RseB and RseC Proteins. *Molecular Microbiology* **1997**, *24* (2), 355–371.

(159) Alba, B. M.; Leeds, J. A.; Onufryk, C.; Lu, C. Z.; Gross, C. A. DegS and YaeL participate sequentially in the cleavage of RseA to activate the σ^E-dependent extracytoplasmic stress response. *Genes and Development* **2002**, *16* (16), 2156–2168.

(160) Collinet, B.; Yuzawa, H.; Chen, T.; Herrera, C.; Missiakas, D. RseB binding to the periplasmic domain of RseA modulates the RseA:σ^E interaction in the cytoplasm and the availability of σ^E•RNA polymerase. *Journal of Biological Chemistry* **2000**, *275* (43), 33898–33904.

(161) Cezairliyan, B. O.; Sauer, R. T. Inhibition of regulated proteolysis by RseB. *Proceedings of National Academy of Science of United States of America* **2007**, *104* (10), 3771–3776.

(162) Rouvière, P. E.; De Las Peñas, A.; Mecsas, J.; Lu, C. Z.; Rudd, K. E.; Gross, C. A. *rpoE*, the gene encoding the second heat-shock sigma factor, σ^E, in *Escherichia coli*. *EMBO Journal* **1995**, *14* (5), 1032–1042.

(163) Majdalani, N.; Heck, M.; Stout, V.; Gottesman, S. Role of RcsF in signaling to the Rcs phosphorelay pathway in *Escherichia coli*. *Journal of Bacteriology* **2005**, *187* (19), 6770–6778.

(164) Konovalova, A.; Mitchell, A. M.; Silhavy, T. J. A lipoprotein/*β*-barrel complex monitors lipopolysaccharide integrity transducing information across the outer membrane. *eLife 5*, e15276.

(165) Lima, S.; Guo, M. S.; Chaba, R.; Gross, C. A.; Sauer, R. T. Dual molecular signals mediate the bacterial response to outer-membrane stress. *Science* **2013**, *340* (6134), 837–841.

(166) Noor, R.; Murata, M.; Nagamitsu, H.; Klein, G.; Raina, S.; Yamada, M. Dissection of σ^E-dependent cell lysis in *Escherichia coli*: roles of RpoE regulators RseA, RseB and periplasmic folding catalyst PpiD. *Genes to Cells* **2009**, *14* (7), 885–899.

(167) Durand, P.; Golinelli-Pimpaneau, B.; Mouilleron, S.; Badet, B.; Badet-Denisot, M. A. Highlights of glucosamine-6P synthase catalysis. *Archives of Biochemistry and Biophysics* **2008**, *474* (2), 302–317.

(168) Connolly, J. P. R.; Finlay, B. B.; Roe, A. J. From ingestion to colonization: the influence of the host environment on regulation of the LEE encoded type III secretion system in enterohaemorrhagic *Escherichia coli*. *Frontiers in Microbiology* **2015**, *6*, 568.

(169) Göpel, Y.; Görke, B. Interaction of lipoprotein QseG with sensor kinase QseE in the periplasm controls the phosphorylation state of the two-component system QseE/QseF in *Escherichia coli*. *PLoS Genetics* **2018**, *14* (7), e1007547.

(170) Missiakas, D.; Raina, S. Protein misfolding in the cell envelope of *Escherichia coli*: new signaling pathways. *Trends in Biochemical Sciences* **1997**, *22* (2), 59–63.

(171) Connolly, L.; Peñas, A. D. L.; Alba, B. M.; Gross, C. A. The response to extracytoplasmic stress in *Escherichia coli* is controlled by partially overlapping pathways. *Genes and Development* **1997**, *11* (15), 2012–2021.

(172) Price, N. L.; Raivio, T. L. Characterization of the Cpx regulon in *Escherichia coli* Strain MC4100. *Journal of Bacteriology* **2009**, *191* (6), 1798–1815.

(173) Raivio, T. L.; Popkin, D. L.; Silhavy, T. J. The Cpx envelope stress response is controlled by amplification and feedback inhibition. *Journal of Bacteriology* **1999**, *181* (17), 5263–5272.

(174) Chao, Y.; Vogel, J. A 3' UTR-derived small RNA provides the regulatory noncoding arm of the inner membrane stress response. *Molecular Cell* **2016**, *61* (3), 352–363.

(175) Hunke, S.; Keller, R.; Müller, V. S. Signal integration by the Cpx-envelope stress system. *FEMS Microbiology Letters* **2012**, *326* (1), 12–22.

(176) Delhaye, A.; Collet, J.-F.; Laloux, G. Fine-tuning of the Cpx envelope stress response is required for cell wall homeostasis in *Escherichia coli*. *mBio* **2016**, *7* (1), e00047-16.

(177) Delhaye, A.; Laloux, G.; Collet, J.F. The lipoprotein NlpE is a Cpx sensor that serves as a sentinel for protein sorting and folding defects in the *Escherichia coli* envelope. *Journal of Bacteriology* **2019**, *201* (10), e00611-18.

(178) Ballouz, S.; Francis, A. R.; Lan, R.; Tanaka, M. M. Conditions for the evolution of gene clusters in bacterial genomes. *PLOS Computational Biology* **2010**, *6* (2), e1000672.

(179) Schnaitman, C. A.; Klena, J. D. Genetics of lipopolysaccharide biosynthesis in enteric bacteria. *Microbiology Reviews* **1993**, *57* (3), 655–682.

(180) Keseler, I. M.; Mackie, A.; Santos-Zavaleta, A.; Billington, R.; Bonavides-Martínez, C.; Caspi, R.; Fulcher, C.; Gama-Castro, S.; Kothari, A.; Krummenacker, M.; Latendresse, M.; Muñiz-Rascado, L.; Ong, Q.; Paley, S.; Peralta-Gil, M.; Subhraveti, P.; Velázquez-Ramírez, D. A.; Weaver, D.; Collado-Vides, J.; Paulsen, I.; Karp, P. D. The EcoCyc database: reflecting new knowledge about *Escherichia coli* K-12. *Nucleic Acids Research* **2017**, *45* (D1), D543–D550.

(181) Charoensuk, K.; Nagamitsu, H.; Raina, S.; Kosaka, T.; Oshima, T.; Ogasawara, N.; Yamada, M. Molecular strategy for survival at a critical high temperature in *Escherichia coli*. *PLoS One* **2011**, *6* (6):e20063.

(182) Karow, M.; Fayet, O.; Cegielska, A.; Ziegelhoffer, T.; Georgopoulos, C. Isolation and characterization of the *Escherichia coli htrB* gene, whose product is essential for bacterial viability above 33 degrees C in rich media. *Journal of bacteriology* **1991**, *173* (2), 741–750.

(183) Klena, J. D.; Ashford, R. S.; Schnaitman, C. A. Role of *Escherichia coli* K-12 *rfa* genes and the *rfp* gene of *Shigella dysenteriae* 1 in generation of lipopolysaccharide core heterogeneity and attachment of O antigen. *Journal of Bacteriology* **1992**, *174* (22), 7297–7307.

(184) Klein, G.; Raina, S. Small regulatory bacterial RNAs regulating the envelope stress response. *Biochemical Society Transactions* **2017**, *45* (2), 417–425.

(185) Ishihama, A. Prokaryotic genome regulation: multifactor promoters, multitarget regulators and hierarchic networks. *FEMS Microbiology Reviews* **2010**, *34* (5), 628–645.

(186) Baba, T.; Ara, T.; Hasegawa, M.; Takai, Y.; Okumura, Y.; Baba, M.; Datsenko, K. A.; Tomita, M.; Wanner, B. L.; Mori, H. Construction of *Escherichia coli* K-12 in-frame, single-gene knockout mutants: the Keio collection. *Molecular Systems Biology* **2006**, *2*, 2006.0008.

(187) Stothard, P.; Wishart, D. S. Circular genome visualization and exploration using CGView. *Bioinformatics* **2005**, *21* (4), 537–539.

(188) Biernacka, D.; Gorzelak, P.; Klein, G.; Raina, S. Regulation of the first committed step in lipopolysaccharide biosynthesis catalyzed by LpxC requires the essential protein LapC (YejM) and HslVU protease. *International Journal of Molecular Sciences* **2020**, *21* (23), 9088.

(189) Galloway, S. M.; Raetz, C. R. H. A mutant of *Escherichia coli* defective in the first step of endotoxin biosynthesis. *Journal of Biological Chemistry* **1990**, *265* (11), 6394–6402.

(190) Zhou, P.; Zhao, J. Structure, inhibition, and regulation of essential lipid A enzymes. *Biochimica et Biophysica Acta* **2017**, *1862* (11), 1424–1438.

(191) Kanemori, M.; Nishihara, K.; Yanagi, H.; Yura, T. Synergistic roles of HslVU and other ATP-dependent proteases in controlling *in vivo* turnover of σ^{32} and abnormal proteins in *Escherichia coli. Journal of Bacteriology* **1997**, *179* (23), 7219–7225.

(192) Missiakas, D.; Schwager, F.; Betton, J. M.; Georgopoulos, C.; Raina, S. Identification and characterization of HslV HslU (ClpQ ClpY) proteins involved in overall proteolysis of misfolded proteins in *Escherichia coli*. *EMBO Journal* **1996**, *15* (24), 6899–6909.

(193) Wu, W.-F.; Zhou, Y.; Gottesman, S. Redundant *in vivo* proteolytic activities of *Escherichia coli* Lon and the ClpYQ (HslUV) protease. *Journal of Bacteriology* **1999**, *181* (12), 3681–3687.

(194) De Lay, N. R.; Cronan, J. E. Genetic interaction between *the Escherichia coli* AcpT phosphopantetheinyl transferase and the YejM inner membrane protein. *Genetics* **2008**, *178* (3), 1327–1337.

(195) Clairfeuille, T.; Buchholz, K. R.; Li, Q.; Verschueren, E.; Liu, P.; Sangaraju, D.; Park, S.; Noland, C. L.; Storek, K. M.; Nickerson, N. N.; Martin, L.; Dela Vega, T.; Miu, A.; Reeder, J.; Ruiz-Gonzalez, M.; Swem, D.; Han, G.; DePonte, D. P.; Hunter, M. S.; Gati, C.; Shahidi-Latham, S.; Xu, M.; Skelton, N.; Sellers, B. D.; Skippington, E.; Sandoval, W.; Hanan, E. J.; Payandeh, J.; Rutherford, S. T. Structure of the essential inner membrane lipopolysaccharide-PbgA complex. *Nature* **2020**, *584* (7821), 479–483.

(196) Cian, M. B.; Giordano, N. P.; Masilamani, R.; Minor, K. E.; Dalebroux, Z. D. *Salmonella enterica* serovar Typhimurium uses PbgA/YejM to regulate lipopolysaccharide assembly during bacteremia. *Infection and Immunity* **2019**, *88* (1), e00758-19.

(197) Gabale, U.; Peña Palomino, P. A.; Kim, H.; Chen, W.; Ressl, S. The essential inner membrane protein YejM is a metalloenzyme. *Scientific Reports* **2020**, *10*, 17794.

(198) Guest, R. L.; Samé Guerra, D.; Wissler, M.; Grimm, J.; Silhavy, T. J. YejM modulates activity of the YciM/FtsH protease complex to prevent lethal accumulation of lipopolysaccharide. *mBio* **2020**, *11* (2), e00598-20

(199) Fivenson, E. M.; Bernhardt, T. G. An essential membrane protein modulates the proteolysis of LpxC to control lipopolysaccharide synthesis in *Escherichia coli*. *mBio* **2020**, *11* (3), e00939-20.

(200) Nguyen, D.; Kelly, K.; Qiu, N.; Misra, R. YejM controls LpxC levels by regulating protease activity of the FtsH/YciM complex of *Escherichia coli*. *Journal of Bacteriology* **2020**, *202* (18), e00303-20.

(201) Datsenko, K. A.; Wanner, B. L. One-step inactivation of chromosomal genes in *Escherichia coli* K-12 using PCR products. *Proceedings of the National Academy of Sciences of the United States of America* **2000**, *97* (12), 6640–6645.

(202) Kitagawa, M.; Ara, T.; Arifuzzaman, M.; Ioka-Nakamichi, T.; Inamoto, E.; Toyonaga, H.; Mori, H. Complete set of ORF clones of *Escherichia coli* ASKA library (a complete set of *E. coli* K-12 ORF archive): unique resources for biological research. *DNA Research* **2005**, *12* (5), 291–299.

(203) Müller-Loennies, S.; Brade, L.; MacKenzie, C. R.; Di Padova, F. E.; Brade, H. Identification of a cross-reactive epitope widely present in lipopolysaccharide from enterobacteria and recognized by the cross-protective monoclonal antibody WN1 222-5. *Journal of Biological Chemistry* **2003**, *278* (28), 25618–25627.

(204) Raina, S.; Missiakas, D.; Baird, L.; Kumar, S.; Georgopoulos, C. Identification and transcriptional analysis of the *Escherichia coli htrE* operon which is homologous to pap and related pilin operons. *Journal of Bacteriology* **1993**, *175* (16), 5009–5021.

(205) Klein, G.; Wojtkiewicz, P.; Biernacka, D.; Stupak, A.; Gorzelak, P.; Raina, S. Identification of substrates of cytoplasmic peptidyl-prolyl *cis/trans* isomerases and their collective essentiality in *Escherichia coli*. *International Journal of Molecular Sciences* **2020**, *21* (12), 4212.

(206) Rohrwild, M.; Coux, O.; Huang, H. C.; Moerschell, R. P.; Yoo, S. J.; Seol, J. H.; Chung, C. H.; Goldberg, A. L. HslV-HslU: a novel ATP-dependent protease complex in *Escherichia coli* related to the eukaryotic proteasome. *Proceedings of National Academy of Science of United States of America* **1996**, *93* (12), 5808–5813.

(207) Rohrwild, M.; Pfeifer, G.; Santarius, U.; Müller, S. A.; Huang, H.-C.; Engel, A.; Baumeister, W.; Goldberg, A. L. The ATP-dependent HslVU protease from *Escherichia coli* is a four-ring structure resembling the proteasome. *Nature Structural & Molecular Biology* **1997**, *4* (2), 133–139.

(208) Sousa, M. C.; Kessler, B. M.; Overkleeft, H. S.; McKay, D. B. Crystal structure of HslUV complexed with a vinyl sulfone inhibitor: corroboration of a proposed mechanism of allosteric activation of HslV by HslU. *Journal of Molecular Biolology* **2002**, *318* (3), 779–785.

(209) Ruiz-González, M. X.; Marín, I. Proteasome-related *hslU* and *hslV* genes typical of eubacteria are widespread in eukaryotes. *Journal of Molecular Evolution* **2006**, *63* (4), 504–512.

(210) Seol, J. H.; Yoo, S. J.; Shin, D. H.; Shim, Y. K.; Kang, M. S.; Goldberg, A. L.; Chung, C. H. The heat-shock protein HslVU from *Escherichia coli* is a protein-activated ATPase as well as an ATP-dependent proteinase. *European Journal of Biochemistry* **1997**, *247* (3), 1143–1150.

(211) Lee, J. W.; Park, E.; Bang, O.; Eom, S. H.; Cheong, G. W.; Chung, C. H.; Seol, J. H. Nucleotide triphosphates inhibit the degradation of unfolded proteins by HslV peptidase. *Molecules and Cells* **2007**, *23* (2), 252–257.

(212) Barb, A. W.; McClerren, A. L.; Snehelatha, K.; Reynolds, C. M.; Zhou, P.; Raetz, C. R. H. Inhibition of lipid A biosynthesis as the primary mechanism of CHIR-090 antibiotic activity in *Escherichia coli*. *Biochemistry* **2007**, *46* (12), 3793–3802.

(213) Barb, A. W.; Jiang, L.; Raetz, C. R.; Zhou, P. Structure of the deacetylase LpxC bound to the antibiotic CHIR-090: time-dependent inhibition and specificity in ligand binding. *Proceedings of National Academy of Science of United States of America* **2007**, *104* (47), 18433–18438.

(214) Dong, H.; Zhang, Z.; Tang, X.; Huang, S.; Li, H.; Peng, B.; Dong, C. Structural insights into cardiolipin transfer from the inner membrane to the outer membrane by PbgA in Gram-negative bacteria. *Scientific Reports* **2016**, *6*, 30815.

(215) Fan, J.; Petersen, E. M.; Hinds, T. R.; Zheng, N.; Miller, S. I. Structure of an inner membrane protein required for PhoPQ-regulated increases in outer membrane cardiolipin. *mBio* **2020**, *11* (1), e03277-19.

(216) Hirvas, L.; Nurminen, M.; Helander, I. M.; Vuorio, R.; Vaara, M. The lipid A biosynthesis deficiency of the *Escherichia coli* antibiotic-supersensitive mutant LH530 is suppressed by a novel locus, ORF195. *Microbiology (Reading)* **1997**, *143* (Pt 1), 73–81.

(217) Daley, D. O.; Rapp, M.; Granseth, E.; Melén, K.; Drew, D.; von Heijne, G. Global topology analysis of the *Escherichia coli* inner membrane proteome. *Science* **2005**, *308* (5726), 1321–1323.

(218) Mostafavi, M.; Wang, L.; Xie, L.; Takeoka, K. T.; Richie, D. L.; Casey, F.; Ruzin, A.; Sawyer, W. S.; Rath, C. M.; Wei, J. R.; Dean, C. R. Interplay of *Klebsiella pneumoniae* FabZ and LpxC mutations leads to LpxC inhibitor-dependent growth resulting from loss of membrane homeostasis. *mSphere* **2018**, *3* (5), e00508-18.

(219) Langklotz, S.; Schäkermann, M.; Narberhaus, F. Control of lipopolysaccharide biosynthesis by FtsH-mediated proteolysis of LpxC is conserved in enterobacteria but not in all Gram-negative bacteria. *Journal of Bacteriology* **2011**, *193* (5), 1090–1097.

(220) Karata, K.; Inagawa, T.; Wilkinson, A. J.; Tatsuta, T.; Ogura, T. Dissecting the role of a conserved motif (the second region of homology) in the AAA family of ATPases. Site-directed mutagenesis of the ATP-dependent protease FtsH. *Journal of Biological Chemistry* **1999**, *274* (37), 26225–26232.

(221) Tatsuta, T.; Tomoyasu, T.; Bukau, B.; Kitagawa, M.; Mori, H.; Karata, K.; Ogura, T. Heat shock regulation in the *ftsH* null mutant of *Escherichia coli*: dissection of stability and activity control mechanisms of σ^{32} *in vivo*. *Molecular Microbiology* **1998**, *30* (3), 583–593.

(222) Peruski, L. F.; Neidhardt, F. C. Identification of a conditionally essential heat shock protein *in Escherichia coli*. *Biochimica et Biophysica Acta* **1994**, *1207* (2), 165–172.

(223) Emiola, A.; Andrews, S. S.; Heller, C.; George, J. Crosstalk between the lipopolysaccharide and phospholipid pathways during outer membrane biogenesis in *Escherichia coli*. *Proceedings of National Academy of Science of United States of America* **2016**, *113* (11), 3108–3113.

(224) Baytshtok, V.; Fei, X.; Shih, T.-T.; Grant, R. A.; Santos, J. C.; Baker, T. A.; Sauer, R. T. Heat activates the AAA+ HslUV protease by melting an axial autoinhibitory plug. *Cell Reports* **2021**, *34* (3), 108639.

(225) Chang, C. Y.; Hu, H. T.; Tsai, C. H.; Wu, W. F. The degradation of RcsA by ClpYQ (HslUV) protease in *Escherichia coli*. *Microbiological Research* **2016**, *184*, 42–50.

(226) Barb, A. W.; Zhou, P. Mechanism and inhibition of LpxC: an essential zinc-dependent deacetylase of bacterial lipid A synthesis. *Current Pharmaceutical Biotechnology* **2008**, *9* (1), 9–15.

(227) Schweiger, R.; Soll, J.; Jung, K.; Heermann, R.; Schwenkert, S. Quantification of interaction strengths between chaperones and tetratricopeptide repeat domain-containing membrane proteins. *Journal of Biological Chemistry* **2013**, *288* (42), 30614–30625.

(228) Zeytuni, N.; Zarivach, R. Structural and functional discussion of the tetra-trico-peptide repeat, a protein interaction module. *Structure* **2012**, *20* (3), 397–405.

(229) Perez-Riba, A.; Itzhaki, L. S. The tetratricopeptide-repeat motif is a versatile platform that enables diverse modes of molecular recognition. *Current Opinion in Structural Biology* **2019**, *54*, 43–49.

(230) Qiu, N.; Misra, R. Overcoming iron deficiency of an *Escherichia coli tonB* mutant by increasing outer membrane permeability. *Journal of Bacteriology* **2019**, *201* (17), e00340-19.

(231) Lee, H. B.; Park, S. H.; Lee, C. R. The inner membrane protein LapB is required for adaptation to cold stress in an LpxC-independent manner. *Journal of Microbiology* **2021**, *59* (7), 666–674.

LIST OF FIGURES

LIST OF TABLES

International Journal of
Molecular Sciences

MDPI

Article

Regulation of the First Committed Step in Lipopolysaccharide Biosynthesis Catalyzed by LpxC Requires the Essential Protein LapC (YejM) and HslVU Protease

Daria Biernacka, Patrycja Gorzelak, Gracjana Klein * and Satish Raina *

Unit of Bacterial Genetics, Gdansk University of Technology, 80-233 Gdansk, Poland; darbiern@student.pg.edu.pl (D.B.); patrycja.gorzelak@gmail.com (P.G.)

* Correspondence: gracjana.klein@pg.edu.pl (G.K.); satish.raina@pg.edu.pl (S.R.); Tel.: +48-58-347-2618 (G.K. & S.R.)

Received: 5 November 2020; Accepted: 27 November 2020; Published: 29 November 2020

Abstract: We previously showed that lipopolysaccharide (LPS) assembly requires the essential LapB protein to regulate FtsH-mediated proteolysis of LpxC protein that catalyzes the first committed step in the LPS synthesis. To further understand the essential function of LapB and its role in LpxC turnover, multicopy suppressors of Δ*lapB* revealed that overproduction of HslV protease subunit prevents its lethality by proteolytic degradation of LpxC, providing the first alternative pathway of LpxC degradation. Isolation and characterization of an extragenic suppressor mutation that prevents lethality of Δ*lapB* by restoration of normal LPS synthesis identified a frame-shift mutation after 377 aa in the essential gene designated *lapC*, suggesting LapB and LapC act antagonistically. The same *lapC* gene was identified during selection for mutations that induce transcription from LPS defects-responsive *rpoE*P3 promoter, confer sensitivity to LpxC inhibitor CHIR090 and a temperature-sensitive phenotype. Suppressors of *lapC* mutants that restored growth at elevated temperatures mapped to *lapA*/*lapB*, *lpxC* and *ftsH* genes. Such suppressor mutations restored normal levels of LPS and prevented proteolysis of LpxC in *lapC* mutants. Interestingly, a *lapC* deletion could be constructed in strains either overproducing LpxC or in the absence of LapB, revealing that FtsH, LapB and LapC together regulate LPS synthesis by controlling LpxC amounts.

Keywords: lipopolysaccharide; LapB; LapC; YejM; LpxC; HslV/U protease; FabZ; RpoE

1. Introduction

The cytoplasm of Gram-negative bacteria, such as *Escherichia coli*, is surrounded by an inner membrane (IM), which is a phospholipid bilayer that separates an aqueous periplasmic compartment containing a thin layer of peptidoglycan from the outer membrane (OM). The OM of Gram-negative bacteria is an asymmetric bilayer in nature with phospholipids located in its inner leaflet, while the lipopolysaccharide (LPS) is located on the outer leaflet [1]. LPS is a complex glycolipid, essential for the bacterial viability and constitutes the major amphiphilic component of OM in most of the Gram-negative bacteria, including *E. coli* [1,2]. However, LPS is highly heterogeneous in the composition and comprised of a mixture of different glycoforms, whose synthesis and accumulation are controlled by various regulatory factors and growth conditions [3–7]. The preferential synthesis of certain glycoforms that determine the LPS composition involves the induction or activation of regulatory factors that include the main envelope stress-responsive regulator RpoE, two-component systems such as BasS/R, PhoP/Q and Rcs in addition to regulatory sRNAs [5,7–9]. Despite the heterogeneity in the composition of LPS, they in general share domains composed of a membrane-anchored bisphosphorylated and

acylated β(1→6)-linked GlcN disaccharide, termed lipid A, to which a carbohydrate moiety of varying size is attached [10–12]. The latter may be divided into a proximal core oligosaccharide and, in smooth-type bacteria, a distal *O*-antigen. The inner core usually contains residue(s) of 3-deoxy-α-D-*manno*-oct-2-ulosonic acid (Kdo) and L-*glycero*-D-*manno*-heptose (L,D-Hep). The lipid A part and the inner core are generally conserved in the structure, but often have nonstoichiometric modifications [2,5,8,11].

LPS biosynthesis begins with the acylation of UDP-GlcNAc by LpxA with *R*-3-hydroxymyristate derived from *R*-3-hydroxymyristoyl-ACP, which is also used by FabZ for the phospholipid synthesis. Thus, *R*-3-hydroxymyristoyl-ACP serves as a common precursor for the synthesis of phospholipids and LPS [3,13,14]. The second reaction of the lipid A biosynthesis is catalyzed by LpxC deacetylase, constituting the first committed step in the LPS synthesis, as the equilibrium constant for the first reaction catalyzed by LpxA is unfavorable due to reversible nature of reaction. The biosynthesis of LPS in *E. coli* proceeds in a discontinuous manner. First, the tetraacylated lipid A (lipid IV_A) precursor is synthesized, which requires six essential enzymes. After the synthesis of lipid IV_A precursor, the transfer of two Kdo residues constitutes an additional essential step in the LPS biosynthesis [3,9,15,16]. This Kdo addition ensures the incorporation of secondary lauroyl and myristoyl chains resulting in the synthesis of hexaacylated lipid A [11,16]. Following the synthesis of Kdo_2-lipid A, further sugars are sequentially transferred by membrane-associated glycosyltransferases for the completion of core biosynthesis. Thus, Kdo_2-lipid A constitutes the minimal LPS structure that is required for the viability of bacteria like *E. coli* under standard laboratory growth conditions [10,11]. However, viable strains synthesizing LPS composed of only glycosylation-free lipid IV_A precursor can be constructed, which can be propagated only under slow growth conditions at low temperatures with a narrow growth range around 23 °C, due to poor recognition by MsbA LPS flippase [11]. Furthermore, when the bacterial LPS synthesis is compromised at different steps of its biosynthesis, such as when the LPS is composed of minimal structures like Kdo_2-lipid A Δ*waaC*, Kdo_2-lipid IV_A or with only lipid IV_A precursor, such mutant bacteria exhibit severe permeability defects and the highly elevated RpoE-dependent envelope stress response [11]. Similarly, when the LPS assembly is compromised due to an imbalance in the synthesis of LPS and phospholipid as in Δ*lapB* strains, they too exhibit the super elevation in the RpoE-dependent stress response [17]. These LPS defects are sensed via the activation of Rcs two-component system that causes an induction of *rpoE* mRNA synthesis from its *rpoE*P3 promoter [18].

It is well established that the synthesis of LPS and phospholipids is tightly co-regulated and held at a nearly constant ratio of 0.15 to 1.0 [19]. Any alterations in the balance of phospholipid and LPS are not tolerated by bacteria and cause cell death. Thus, either the excess or reduction in the LPS synthesis in comparison to the phospholipid synthesis causes the lethality [17,20]. This balance is achieved by tightly regulated turnover of unstable LpxC enzyme to maintain the flux of common precursor *R*-3-hydroxymyristoyl-ACP for the utilization in either LPS or phospholipid biosynthesis. Thus, the key players in this pathway are FabZ and LpxC enzymes. The *fabZ* gene encodes the *R*-3-hydroxymyristoyl-ACP dehydratase, catalyzing the first step in the phospholipid biosynthesis [15]. Hence, the utilization of the fundamental common metabolic substrate of LpxC and FabZ, *R*-3-hydroxymyristoyl-ACP, constitutes an essential branch point in the biosynthesis of phospholipids and the lipid A part of LPS (Figure 1).

The turnover of LpxC enzyme is catalyzed by the essential IM-located, Zn-dependent metalloprotease FtsH in concert with another essential IM-anchored LPS assembly heat shock protein LapB (Figure 1) [17,20,21]. Although FtsH has several substrates, the essentiality of FtsH protease stems from its key role in proteolysis of LpxC to prevent excess build up in the LPS biosynthesis at the expense of synthesis of phospholipids [22]. The notion that FtsH and LapB work together to regulate LpxC proteolysis is based on biochemical data revealing their co-purification and the increased accumulation of LpxC in either *ftsH* or *lapB* mutants [17]. Thus, mutations in either the *ftsH* gene or the *lapB* gene result in the increased abundance of LpxC, which leads to excess of LPS over phospholipids due to depletion of the common precursor *R*-3-hydroxymyristoyl-ACP [17,20,23]. Consistent with their

role in regulating LpxC amounts, a deletion of either *ftsH* or *lapB* are tolerated in strains carrying either a hyperactive allele of the *fabZ* gene *sfhC21* or when the LPS synthesis is dampened due to mutations in either *lpxA* or *lpxD* genes [17,23].

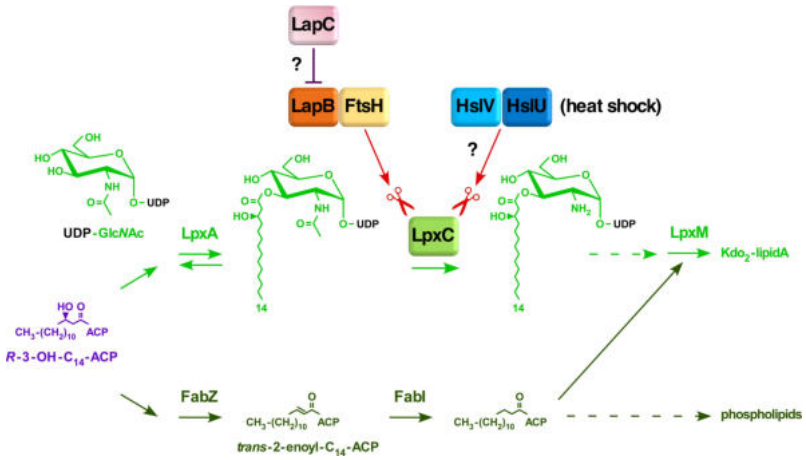

Figure 1. Model of regulation of balanced LPS and phospholipid biosynthesis: *R*-3-hydroxymyristoyl-ACP serves as a common metabolic precursor for the LpxC–dependent LPS biosynthesis and the FabZ-mediated phospholipid biosynthesis. LpxC stability is regulated by previously established FtsH/LapB and, from this study, via the negative regulation by LapC counteracting the LapB/FtsH pathway and also at high temperature by HslVU proteolysis of LpxC.

In addition, the lethal phenotype of Δ*lapB* or Δ(*lapA lapB*) can also be overcome, if either the LPS synthesis is impaired due to mutations in the gene encoding heptosyltransferase I (*waaC*) or when non-coding sRNA SlrA (MicL), a translational repressor of the most abundant Lpp protein, is overproduced [17]. Interestingly, *lapA* and *lapB* genes are co-transcribed from three promoters: the distal promoter located upstream of the *pgpB* gene, the middle promoter recognized by the heat shock sigma factor RpoH and the last one resembling house-keeping promoters [17]. Such a transcriptional organization suggests coupling of transcription of *lapA/B* genes with phospholipid metabolism using *pgpB* co-transcription. The *pgpB* gene encodes phosphatidylglycerophosphatase, an enzyme that is a part of the pathway of phosphatidylglycerol biosynthesis, and hence associated with phospholipid metabolism [24].

Although we showed that LapA and LapB proteins interact with FtsH and co-purify with LPS, it is unclear how LapB senses LPS to regulate LpxC proteolysis. Based on modelling prediction and subsequent crystal structure studies, it was shown that the LapB protein contains in its N-terminal domain nine tetratricopeptide repeats (TPR) and a C-terminal rubredoxin-like domain, both of which were found to be essential for its function and together provide a scaffold for the assembly and recruitment of LpxC and various LPS biosynthetic proteins [17,25].

It has been often reported that some unstable proteins can be substrates of multiple proteases. For example, the RpoH heat shock sigma factor is a substrate for FtsH and also the heat shock-inducible HslVU (ClpQY) protease [26–28]. Similarly, unstable SulA and RcsA proteins can be subjected to degradation by either Lon or HslVU proteases [29,30]. Thus, in this study, experiments were undertaken to further understand the molecular basis of the essentiality of LapB, address if additional interacting partners of LapB exist and if there is the possibility of alternative mechanism of LpxC proteolysis. We rationalized that if LapB is interacting with the additional protein(s), the deletion of such a gene could be lethal. However, point mutations in such a gene should exhibit the elevated transcriptional response of RpoE sigma factor quite like that observed with *lapB* mutants or in strains synthesizing the severely truncated LPS [11,17]. In parallel, a multicopy suppressor approach was utilized, asking if overexpression of any gene can rescue the lethal phenotype of either Δ*lapB* or Δ(*lapA lapB*) strains. Thus, in the first approach, Tn*10*-linked point mutations that simultaneously exhibited the elevated

*rpoE*P3 promoter activity, the sensitivity to the LpxC inhibitor CHIR090 to different extents and membrane permeability defects were analyzed leading to the identification of three point mutations: one having a frame-shift mutation resulting in truncation after 377 amino acid residue isolated three times, the second mutation introduces a stop codon after amino acid residue 190, another resulting into a single amino acid F349S substitution, in the essential *yejM* gene. During the completion of this work, YejM has been speculated to either maintain lipid homeostasis or be involved in the transport of cardiolipin or exhibit a metal-dependent phosphatase activity [31–37]. We designated this gene *lapC* based on identified genetic and biochemical interactions of LapC with LapB. Mutations in the *lapC* gene exhibited a nearly 2 to 8-fold increased expression of *rpoE*P3-*lacZ* fusion, with the inability to grow on rich medium above 37 °C, the sensitivity to the CHIR090 LpxC inhibitor and highly decreased amounts of LpxC and LPS. Suppressor analysis identified several mutations mapping to the *lapA/B* operon, *ftsH* and *lpxC* genes. In the second approach, we show that overexpression of *hslV* encoding the protease subunit can bypass the lethality of a Δ*lapB* derivative. Overexpression of *hslV* alone or *hslVU* was found to repress the elevated accumulation of LpxC in Δ*lapB* mutants, which was validated by pulse-chase experiments revealing an alternative pathway of LpxC degradation.

2. Results

2.1. Rationale

It is well established that LpxC constitutes the first rate-limiting step in the LPS biosynthesis and its amounts are tightly regulated by its proteolysis by the FtsH/LapB complex. However, it remains unknown, how LapB exerts its effect. Based on several lines of experimental evidence, LapB was proposed to act as a scaffold in the IM, where LPS biosynthetic enzymes, involved in lipid A and LPS core biosynthesis, are recruited [17]. During this process, LapB could monitor the accumulation of LPS in the IM and direct LpxC to proteolysis via FtsH to prevent unwanted excess of LPS biosynthesis. Consistent with this presumption, we have shown co-purification of LapB with LPS and FtsH [17]. However, it is unknown how LPS amounts are sensed and if FtsH is the sole protease that regulates LpxC turnover. Thus, we took several approaches: in one case, we sought to identify if additional proteases are involved in the degradation of LpxC using the multicopy suppressor approach to identify additional factors that can bypass the lethality of Δ*lapB* or Δ*lapA/B* mutants (Figure 2A). This multicopy suppressor approach identified the HslUV protease complex to participate in the turnover of LpxC and its overexpression circumvented the essentiality of LapB. Isolation of extragenic suppressors of strains lacking LapB, that restored normal LPS biosynthesis and bypassed LapB essentiality, identified a unique frame-shift mutation in the essential gene *yejM* causing truncation of its periplasmic domain and was designated *lapC* (Figure 2B). In a complementary approach, we sought temperature-sensitive point mutations that render *E. coli* sensitive to the LpxC inhibitor CHIR090, exhibit permeability defects (sensitivity to growth on MacConkey agar) and simultaneously induce transcription from the *rpoE*P3 promoter (Figure 2C). CHIR090 is a known inhibitor of LpxC and severe defects in LPS biosynthesis cause permeability defects and turn on transcription of the gene encoding the alternative sigma factor RpoE, which responds to defects in LPS and outer membrane protein maturation [11,17,18,38,39]. This approach further led to the isolation of several point mutations in the *lapC* gene establishing an essential role in the LPS assembly and sensing. LapC was shown to genetically and physically interact with LapB and found to control LpxC levels together with FtsH based on the identification of extragenic suppressors of *lapC* loss-of-function mutations.

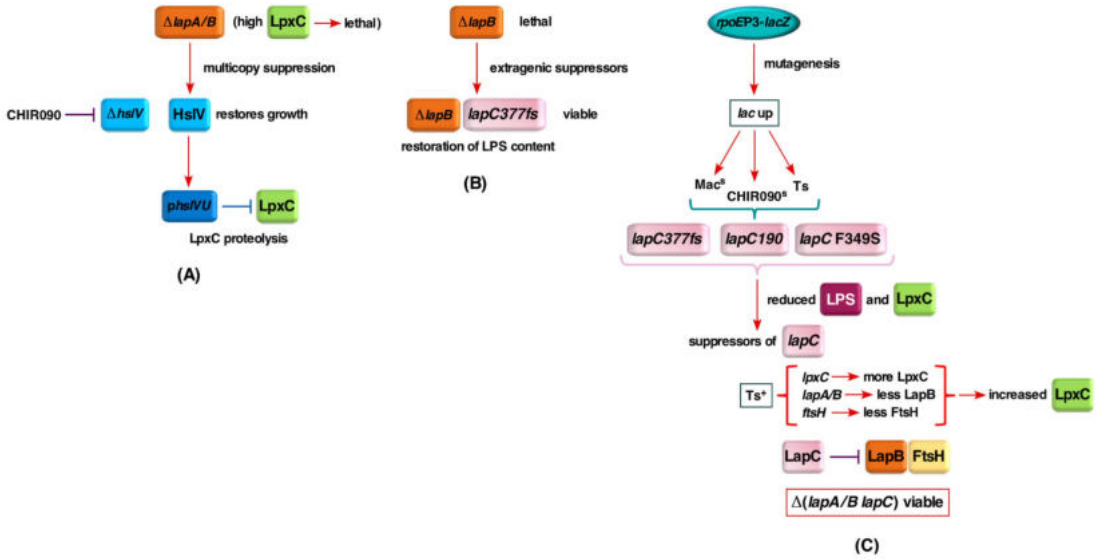

Figure 2. Schematic drawing illustrating three major approaches that identified additional players in the regulation of LpxC proteolysis. The multicopy suppressor approach led to discovery of the HslVU-dependent proteolysis of LpxC in the absence of LapB (**A**). In search of suppressors that bypass the lethality of a *lapB* deletion, the *lapC377fs* mutation was isolated that restored the normal LPS synthesis and the viability in the absence of LapB (**B**). In the third approach, based on mutagenesis, CHIR090- and temperature-sensitive mutants with defects in LPS identified the *lapC* gene. Suppressors of *lapC* mutants revealed that LapC works together with LapB/FtsH to regulate LpxC proteolysis and the essential *lapC* gene is dispensable in the absence of LapB (**C**).

2.2. Overexpression of Heat Shock Protein HslV Protease Can Bypass the Lethality Due to the Deletion of the lapB Gene, Whose Product Is Required for the Regulated Assembly of LPS

We previously showed that the *lapB* gene is essential for the viability of *E. coli* and its deletion can be very poorly tolerated only in few strain backgrounds at 30 °C on minimal medium unless an extragenic suppressor is present [17]. The essential function of LapB was shown to be due its role in LPS biosynthesis by regulating turnover of LpxC in concert with the essential Zn-dependent metalloprotease encoded by the *ftsH* gene. FtsH has been shown to be required for degradation of LpxC [17,20,21]. In this work, we sought to isolate factor(s) that bypass the lethality of Δ*lapB* mutants in order to identify, if any alternative back up proteolytic pathway exists in *E. coli* by using a multicopy suppressor approach. Thus, a complete library of all cloned ORFs, where genes are expressed from the IPTG-inducible P_{T5}-*lac* promoter from ASKA collection in the vector pCA24N [40], was introduced into the Δ(*lapA lapB*) strain SR17187 and plated on LA medium at 42 °C in the presence of 75 μM IPTG as an inducer for the gene expression. Plasmid DNA was isolated from such transformants and used to retransform the parental Δ(*lapA lapB*) strain to confirm the plasmid-mediated suppression. Such plasmid DNAs were sequenced and their analysis revealed that besides previously identified multicopy suppressors a set of plasmids contained the *hslV* gene, which encodes the catalytic subunit of ATP-dependent protease HslUV [27,41].

The *hslV* gene is co-transcribed as a part of heat shock-inducible operon *hslVU* also called *clpQY* [27,42]. HslVU comprises the prokaryotic counterpart of eukaryotic proteasome [43,44]. HslV exhibits homology to the β-subunits of the eukaryotic 20S proteosome, while HslU shows the high amino acid sequence homology to the ClpX protease [27]. HslV on its own exhibits the proteolytic activity, which is significantly enhanced by HslU in the presence of ATP [27,41]. We previously identified HslVU (ClpQY) on the basis of its overexpression repressing abnormally induced the heat shock gene expression or that induced by the addition of puromycin [27,45] and was indeed subsequently found to degrade the heat shock sigma factor RpoH [26].

Thus, we performed sets of controlled transductions, using bacteriophage P1 grown on Δ*lapA/B* and Δ*lapB* strains, into wild-type strain BW25113 derivatives transformed with either the vector alone or by the plasmid carrying either the *hslV* gene alone or with cloned *hslVU* genes in the presence of 75 μM IPTG. Results from such transductions convincingly demonstrate that the essential *lapB* gene can be deleted, when the *hslV* gene alone is overexpressed (Table 1). Furthermore, the transduction frequency was enhanced by approximately 3-fold, when *hslVU* genes were co-overexpressed (Table 1). It should be noted that Δ*lapB* transductants appear at a low frequency and are obtained after the prolonged incubation with small sized colonies, when the vector alone is present (Table 1). Taken together, we can conclude that the *lapB* gene becomes nonessential, when the *hslV* gene is overexpressed.

Table 1. Viable strains lacking the essential *lapB* gene can be constructed, when either the catalytic protease subunit of HslV or when HslUV is overproduced.

Number of Transductants with Selection for Kanamycin Resistance on Minimal Medium			
Donor	**Recipient**		
	BW25113 + vector	**BW25113 + p*hslV*$^+$**	**BW25113 + p*hslUV*$^+$**
P1 SR17187 Δ*lapA/B* Kan^R	35 Kan^R small colonies	1112 Kan^R	3230 Kan^R
P1 SR7753 Δ*lapB* Kan^R	43 Kan^R small colonies	1230 Kan^R	2980 Kan^R

2.3. Overexpression of Either hslV or hslUV Rescue the Lethality of LapB Deletion by Enhancing LpxC Degradation in a LapB-Independent Manner

To address the molecular basis of suppression of the lethality of either the *lapB* or *lapA/B* deletion by HslV or HslVU overproduction, we rationalized that the unstable LpxC could be a substrate for the HslV protease. We have earlier shown that LpxC is stabilized in the absence of LapB and its levels are enhanced in a Δ*lapA/B* derivative that leads to the increased synthesis of LPS and a consequent bacterial lethality. Thus, we measured levels of LpxC in a Δ*lapA/B* derivative transformed by the plasmid carrying the *hslV* gene expressed from a tightly regulated inducible P_{T5}-*lac* promoter using Western blotting technique. The expression of the *hslV* gene in the strain lacking *lapA/B* genes was induced by the addition of 75 μM IPTG and an equivalent amount of culture was withdrawn after 10 min intervals and proteins resolved by SDS-PAGE. Western blot analysis with anti-LpxC antibodies revealed a progressive reduction in amounts of LpxC, with less than 50% of LpxC present after 20 min incubation (Figure 3A, lane 3). After the prolonged incubation of 70 min, a barely detectable level of LpxC was observed (Figure 3A, lane 8). It should be noted that in the absence of LapB, LpxC is stable and its levels are elevated at all conditions [17]. Results from these experiments showed that LpxC can be subjected to proteolysis in the absence of LapB, which is known to work with FtsH, establishing an alternative mechanism of control of LpxC levels and helps to explain the identification of the *hslV* gene as a suppressor of lethality of Δ*lapB*.

As HslV is known to exhibit a weak peptidase activity, which is enhanced by HslU, we examined the impact of co-overexpression of *hslVU* genes in the wild-type background and analyzed the fate of LpxC in pulse chase experiments. A plasmid expressing both genes from the T7 promoter in pET24b was used for such studies. For these studies, the expression of *hslUV* genes was induced for 15 min and further transcription stopped by the addition of 200 μg/mL of rifampicin and incubated at 42 °C during chase. The equivalent amount of aliquots were collected at indicates intervals. Total proteins were resolved on SDS-PAGE and analyzed by the Western blotting technique, using LpxC-specific antibodies (Figure 3B).

As can be seen, LpxC amounts rapidly decline during the chase time, confirming that LpxC is a substrate for the HslUV protease that does not require FtsH protease (Figure 3B), since the complete host transcription was shut down by the addition of rifampicin. Following the 10 min chase itself, approximately only 20% of LpxC species that cross-react with anti-LpxC antibodies are observed (Figure 3B, lane 2). After 40 min, only the background level of LpxC can be detected (Figure 3B, lane 5).

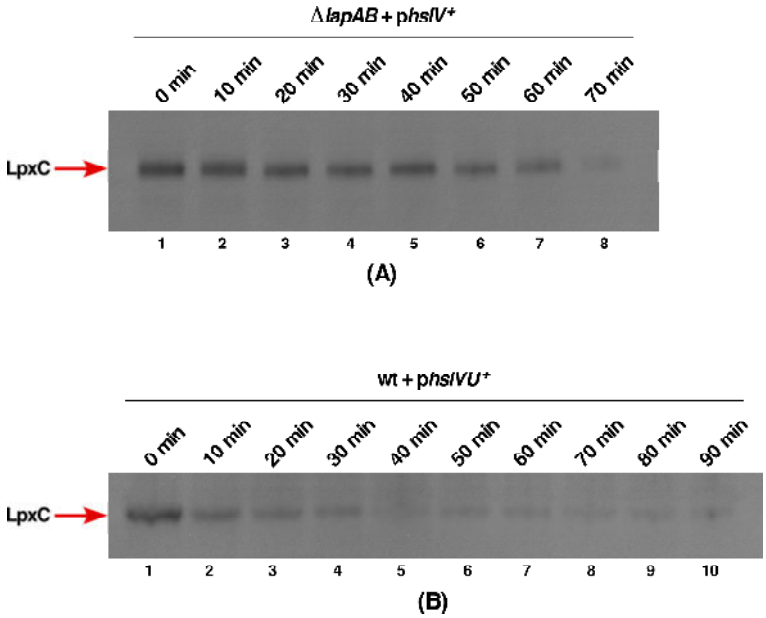

Figure 3. Overexpression of either the *hslV* gene alone or *hslVU* genes results in enhanced proteolysis of LpxC. (**A**) Cultures of Δ*lapA/B* strain carrying the inducible *hslV* gene on a plasmid were grown in M9 medium, adjusted to an OD_{595} of 0.2 in LB medium. Expression of the *hslV* gene was induced by the addition of 75 μM IPTG at 42 °C. An equivalent amount of total proteins from indicated time points were resolved by SDS-PAGE and LpxC levels were determined by immunoblot analysis using LpxC-specific antibodies, revealing a gradual decrease of LpxC. (**B**) Expression of *hslVU* genes from the pET24b vector in BL21 strain was induced by the addition of 75 μM IPTG at 30 °C for 15 min at an OD_{595} of 0.1. Cultures were washed and shifted to 42 °C and further host transcription stopped by the addition of rifampicin. LpxC levels were determined using the equivalent amount of total proteins by immunoblot analysis using LpxC-specific antibodies.

Thus, these results provide a convincing evidence that HslV can degrade LpxC in the absence of LapB/FtsH and this degradation is enhanced, when HslU is also present providing a rationale explanation for the identification of HslV as a multicopy suppressor of the *lapB* deletion and preventing the lethal accumulation of LpxC.

2.4. hslV and hslU Mutants Exhibit the Sensitivity to the LpxC Inhibitor CHIR090

It is well-established that the LpxC activity can be inhibited by the CHIR090 inhibitor, which binds near the Zn-binding domain of LpxC that determines its active site [39]. Mutations that confer resistance to CHIR090 are known to map to the *lpxC* gene [38]. Thus, we wondered if deletion derivatives of *hslV* and *hslU* genes exhibit any altered sensitivity to sub-lethal doses of CHIR090. Isogenic strains of wild type BW25113 and its derivatives lacking HslUV protease subunits were spot tested on LA agar with and without supplementation of CHIR090 at a concentration that is not deleterious to the wild-type strain. These experiments revealed that the deletion derivative of the *hslV* gene or a strain lacking both subunits exhibit a 100-fold reduction in the viability, when challenged with the sub-lethal concentration of CHIR090, and also a reduction in the colony size (Figure 4). Under the same conditions, Δ*hslU* mutants, although more sensitive than the parental strain, exhibit only a moderate sensitivity to CHIR090 (Figure 4). It should be however noted that the lack of HslUV does not confer the extreme sensitivity as observed with a *lapC* mutant expressing only its IM anchor (Figure 4 and see further below). Thus, we can conclude that consistent with a role for HslUV in the turnover of LpxC, removal of either both subunits of this protease complex or HslV catalytic subunit enhances the sensitivity to CHIR090, which is a specific inhibitor of LpxC.

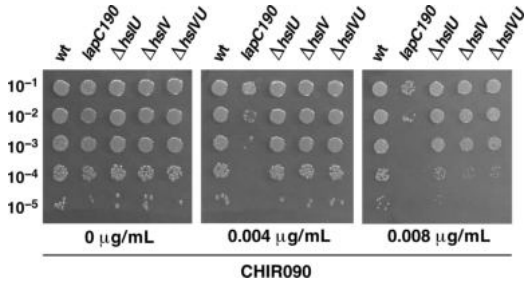

Figure 4. The absence of *hslV* and *hslVU* genes confers the sensitivity to the LpxC inhibitor CHIR090. Exponentially grown cultures of the wild type and its isogenic derivatives lacking genes encoding HslVU protease subunits were adjusted to an OD_{595} of 0.1 and serially spot diluted at 30 °C on LA agar supplemented with or without varying concentrations of CHIR090 as indicated. As a control, the isogenic CHIR090-sensitive strain with the *lapC190* mutation was included. Data presented are from one of the representative experiments.

2.5. An Extragenic Suppressor Mutation in the lapC Gene Restores the Normal LPS Synthesis and Prevents the Lethality in the Absence of LapB

In our earlier work, we reported that a *lapB* deletion could not be tolerated in *E. coli* W3110 strain unless a suppressor mutation was present [17]. To gain further understanding of LapB function, additional extragenic suppressors were sought by transducing Δ*lapB* in W3110 that allowed a deletion of the *lapB* gene. A novel mutation that allowed deletion of either the *lapB* gene or *lapA/B* genes was identified resulting into construction of SR8348 (Table S1). Marking of suppressor mutation and further transduction of this suppressor mutation was found to allow growth of Δ*lapA/B* strain also in BW25113 on LA medium at 30 °C and thus was not the strain-specific suppressor mutation. Complementation and DNA sequence analysis revealed that this suppressor mutation is due to a frame-shift mutation in the *yejM* essential gene [31,46] and based on further genetic interactions designated the *lapC* gene. This mutation causes an insertion of C residue at nt position 1133 resulting into frame-shift after 377 amino acid (*lapC377fs*), with the addition of 13 aa residues after Thr377, leading into the truncation of C-terminal periplasmic domain. LapC (YejM) structures have been described recently revealing five IM-spanning helices in the N-terminus and a large C-terminal globular domain connected by a linker domain [32,34,47,48].

To address the molecular basis of suppression by the *lapC377fs* mutation, LPS of the wild type, its Δ*lapB*, *lapC377fs* and (Δ*lapB lapC377fs*) derivatives was extracted from whole cell lysates treated with Proteinase K. Equivalent amount of extracts were resolved on a SDS-Tricine gel and LPS was revealed after silver staining. Comparison of LPS profile revealed an excess of LPS in Δ*lapB* and a reduced LPS content in *lapC377fs*, which is restored to wild-type levels in (Δ*lapB lapC377fs*) (Figure 5). Next, we used purified LPS and analyzed them by mass spectrometry. Consistent with previous results [17], spectra of Δ*lapB* derivative reveal that LPS is composed of mixture of complete and its precursor derivatives. This is evident from the presence of several prominent mass peaks (with mass ranging from 2428.9 to 3770.7 Da) that correspond to early intermediates of LPS as compared to their absence in the spectra of wild type strain (Figure 6). Some of these mass peaks representing early intermediates include the mass peak at 2815.4 Da in the LPS of Δ*lapB* with the predicted composition of LA_{penta} + Kdo_2 + Hep_2 + Hex_2 + *P*. Of significance is the absence of early intermediates of LPS and the restoration of accumulation of LPS with the complete core with hexaacylated lipid A in (Δ*lapB lapC377fs*) derivative (Figure 6C). Mass peaks of LPS of wild type and (Δ*lapB lapC377fs*) derivative, representing glycoforms with either 2 Kdo or 3 Kdo residues, are present in both spectra with *P*-EtN and L-Ara4N non-stochiometric modifications. The predicted composition of main mass peaks is marked (Figure 6). Thus, mass peaks at 3936.8 and its derivatives with mass peaks at 4139.9 and 4489.9 Da, corresponding to the glycoform with 2 Kdo residues with different additional non-stoichiometric substitutions, are present in spectra of the wild type and (Δ*lapB lapC377fs*). Furthermore, mass peaks corresponding to glycoforms IV and V derivatives with a third Kdo + Rhamnose (mass peaks such as 3948.8, 4071.7, 4202.8 and 4298.9 Da) are prominent

in the spectra of wild type and (Δ*lapB lapC377fs*), but absent in Δ*lapB* spectra, reflecting the suppression of Δ*lapB* LPS defect in the presence of *lapC377fs* suppressor mutation. Restoration of normal LPS composition in the Δ*lapB lapC377fs* derivative suggests that the truncation within the C-terminal domain of LapC could prevent the excessive synthesis of LPS in a Δ*lapB* background, which is consistent with the reduced LPS synthesis in *lapC* mutants (see below).

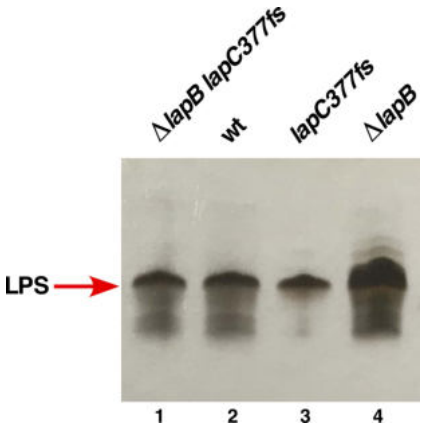

Figure 5. The *lapC377fs* mutation restores the wild-type LPS content in Δ*lapB*. Equivalent amounts of whole cell lysate treated with Proteinase K were resolved on a 14% SDS-Tricine gel and LPS revealed by silver staining. The arrow indicates the position of LPS and the relevant genotype of strains is depicted.

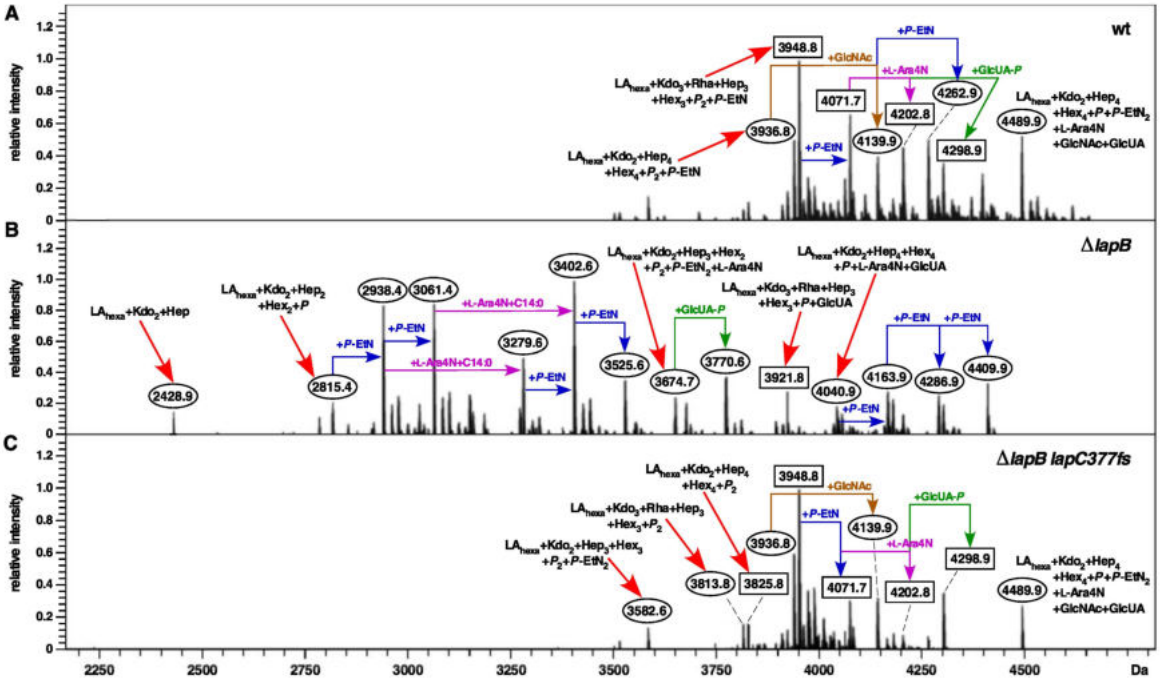

Figure 6. The *lapC377fs* mutation suppresses the accumulation of LPS precursors and restores the normal LPS synthesis in Δ*lapB*. Charge-deconvoluted mass spectra in the negative ion mode of LPS from the wild type (**A**), its Δ*lapB* (**B**) and Δ*lapB lapC377fs* (**C**) derivatives. Cultures were grown in phosphate-limiting medium at 30 °C. Mass numbers refer to monoisotopic peaks. Mass peaks with rectangular boxes correspond to the glycoform containing the third Kdo. Ovals—derivatives with two Kdo residues with either complete or incomplete core.

2.6. The C-Terminal Truncation of the Periplasmic Globular Domain in the Essential LapC Protein Results in the Induction of RpoE-Dependent Envelope Stress Response, a Temperature-Sensitive Phenotype and the Sensitivity to the LpxC Inhibitor CHIR090

In complementary studies, we sought to identify additional partners that could sense either the accumulation of LPS in the IM or defects in LPS biosynthesis and regulate LpxC amounts. As the major players identified thus far are essential for bacterial growth such as either the *lapB* gene or the *ftsH* gene, we reasoned that any previously unidentified partner protein could also be essential for the bacterial viability. To achieve this goal, temperature-sensitive (Ts) Tn*10*-linked point mutations that conferred the increased activity of single-copy *rpoE*P3-*lacZ* promoter were isolated. This promoter was chosen as its activity is specifically induced, when LPS biosynthesis or assembly is severely compromised [18]. Among such mutants, only those isolates that were sensitive to the CHIR090 inhibitor of LpxC and unable to propagate on MacConkey agar were retained (Figures 2 and 7). Mapping and complementation analysis of Tn*10*-linked mutations identified four independent Ts mutants with permeability defects defined by SR19041, SR19750, SR22861 and SR22862 with a mutation linked > than 95% to the *bcr* gene located at 49 min. Subcloning and further complementation approach led to the cloning of the *lapC* gene, which reversed the Ts phenotype, restored growth on MacConkey agar plates as well as restored the nearly wild-type activity of the *rpoE*P3-*lacZ* fusion. Next, we PCR amplified the *lapC* gene from the chromosomal DNA of four strains and their DNA sequence analysis revealed: SR19041 (*lapC190*) has a stop codon TGA replacing TGG (Trp190), SR19750 and SR22861 have a frame-shift *lapC377fs* mutation and SR22862 (*lapC* F349S) contains a single amino acid change resulting into 349F to 349S change (TTT to TCT). It is of interest, as described above (Section 2.5), that the *lapC377fs* mutation was independently identified as a suppressor mutation of the Δ*lapB* derivative.

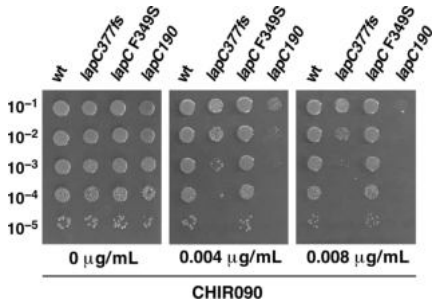

Figure 7. Truncation of the C-terminal periplasmic domain of LapC confers the sensitivity to the LpxC inhibitor CHIR090. Exponentially grown cultures of the wild type and its isogenic derivatives with point mutations in the *lapC* gene were adjusted to an OD_{595} of 0.1 and serially spot diluted at 30 °C on LA agar supplemented with or without varying concentrations of CHIR090 as indicated.

Among three Ts mutations, *lapC190* expresses only the IM anchor of LapC, comprising of five predicted TM helices but lacks the entire periplasmic domain. This mutation is identical to a mutation described in the strain LH530 exhibiting membrane permeability defects [31,46]. However, the most frequent mutation identified is *lapC377fs*. The F349 amino acid residue is highly conserved and located in the Mg^{++} ion-binding pocket in the pseudo-hydrolase domain and in the putative phosphatase active site [32,34]. Comparison of sensitivity of three isogenic *lapC* mutant derivatives to CHIR090 revealed that *lapC190* is extremely sensitive to this LpxC inhibitor, followed by the *lapC377fs* derivatives at the concentration, when growth of the parental strain is not affected (Figure 7, lanes 1, 3&4). However, the *lapC* F349S derivative showed only a small decrease in the colony size upon the exposure to CHIR090 and is consistent with a weaker induction of the *rpoE*P3-*lacZ* promoter fusion (Figure 8). Taken together, these results establish that LapC is required for the regulation of LpxC, since *lapC190* and *lapC377fs* mutations confer the hypersensitivity to the CHIR090 inhibitor and were further followed. To prevent read through of stop codon in the original *lapC190* derivative, for further comparative analysis and verification of results, we used a Δ*lapC190* derivative (GK6075) constructed by recombineering that

expresses only the N-terminal 190 amino acids defining the IM anchor and the periplasmic domain is replaced by an excisable antibiotic cassette.

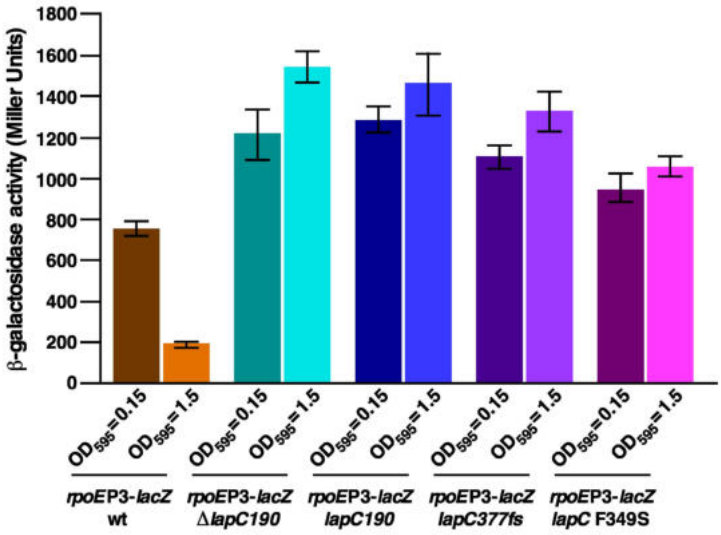

Figure 8. Mutations that cause truncation of periplasmic domain of LapC induce transcription from the *rpoE*P3 promoter, which specifically responds to severe defects in LPS. Exponentially grown isogenic strains of the wild type and its derivatives with various *lapC* mutations as indicated, carrying the single-copy chromosomal *rpoE*P3-*lacZ* fusion, were analyzed for the *β*-galactosidase activity. Cultures were adjusted to an OD_{595} of 0.05 and allowed to grow in LB medium at 30 °C. Aliquots of samples were drawn after different time intervals and used to measure the *β*-galactosidase activity. Error bars represent a S.E. of three independent measurements.

Measurement of *β*-galactosidase activity of *lapC* mutant bacteria revealed a 2 to 8-fold increase in the *rpoE*P3-*lacZ* activity as compared to the wild type depending upon the growth phase and the mutation in the *lapC* gene (Figure 8). As SR19041 (*lapC190*) and GK6075 (with the antibiotic cassette inserted in the coding region after the 190th amino acid) expresses only the intact IM N-terminal anchor region devoid of the C-terminal domain, both of these derivatives were used in this assay for comparison (Figure 8). Most striking results reveal a 6 to 8-fold induction of the *rpoE*P3-*lacZ* fusion in either *lapC190* or Δ*lapC190* and *lapC377fs* derivatives, when grown in the stationary phase (Figure 8). All of these derivatives are unable to propagate on MacConkey agar with a Ts phenotype. These results correlate very well with the sensitivity to the CHIR090 LpxC inhibitor of strains carrying either *lapC190* or *lapC377fs* mutations with a lower impact of the *lapC* F349S mutation. Thus, the induction of transcription from the *rpoE*P3 promoter that responds to LPS defects accompanied by the Ts phenotype, the sensitivity to the CHIR090 inhibitor and membrane permeability defects allows us to conclude that LapC is required for the cell envelope integrity and the regulation of LPS biosynthesis as illustrated by the suppression of lethality and the restoration of wild-type LPS content in Δ*lapB* by *lapC* loss-of-function mutations.

2.7. The lapC190 Mutation Resulting in the C-Terminal Truncation Causes the Reduction in Amounts of LpxC Leading to the Reduced Accumulation of LPS

As *lapC* mutant bacteria exhibit the extreme sensitivity to the sub-lethal concentration of the LpxC inhibitor CHIR090, have the elevated induction of *rpoE*P3 promoter that is activated in the response to severe defects in LPS and restore the LPS composition of a Δ*lapB* derivative, suggest that LapC has a specific role in the LPS assembly/biosynthesis. To further gain information about the function of LapC, firstly growth on LA and MacConkey agar was measured. Quantification of bacterial growth revealed that mutations in the C-terminal part of the *lapC* gene confer the temperature-sensitive phenotype

(Figure 9A). However, this Ts phenotype and the membrane permeability defect reflected by the sensitivity to MacConkey agar can be reversed by various suppressor mutations (see below).

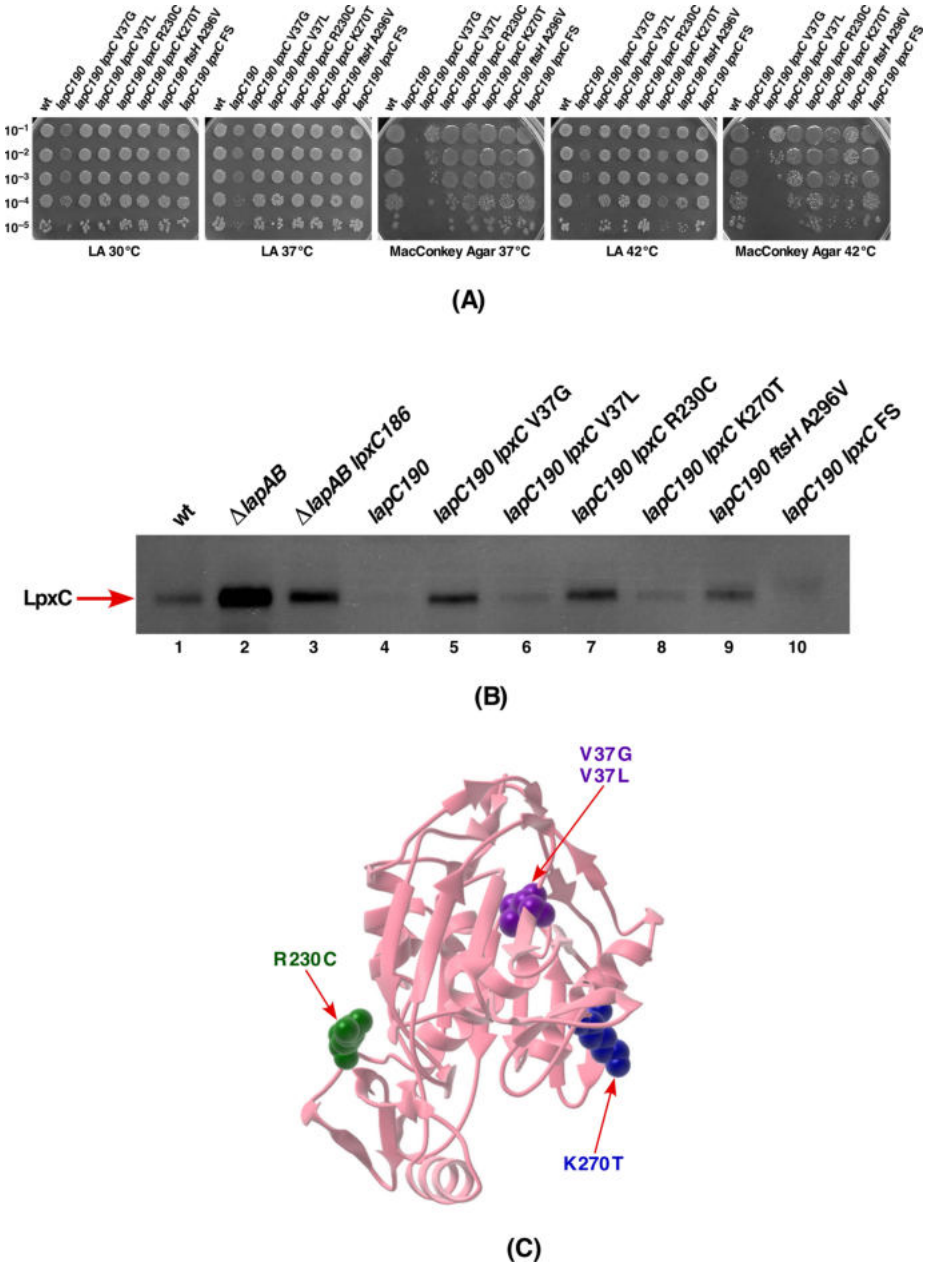

Figure 9. *lapC190* mutant bacteria exhibit a reduction in LPS amounts and the temperature-sensitivity (Ts) phenotype. (**A**) Exponentially grown cultures with indicated genotypes were adjusted to an OD_{595} of 0.1 and spot diluted on LA and MacConkey agar at different temperatures. (**B**) Exponentially grown cultures of the wild type, its *lapC190* derivative and strains with various suppressor mutations mapping to the *lpxC* gene were grown under permissive growth conditions. Equivalent amounts of total cellular proteins were resolved by SDS-PAGE and proteins transferred by Western blotting and subjected to immunoblotting, using LpxC-specific antibodies. (**C**) The position of amino acids residues in the structure of LpxC (PDB 4MQY, [49]), whose specific alterations suppress the Ts phenotype of a *lapC190* mutation and cause elevation of LpxC levels.

Next, we analyzed if LpxC amounts are affected and what is the status of LPS amounts. Since among three *lapC* mutations identified in this work a *lapC190* mutation confers a more stringent phenotype as reflected by the sensitivity to CHIR090, we measured levels of LpxC from cellular extracts obtained

from exponentially grown cultures of the isogenic wild type, its *lapC190* derivative and as controls Δ*lapA/B* and a strain carrying a suppressor mutation of *lapA/B* deletion mapping to the *lpxC* gene (Δ*lapA/B lpxC186*). Cultures for such experiments were grown under permissive growth conditions of M9 minimal medium at 30 °C and cell extracts analyzed by immunoblotting. Results from such a representative experiment reveal barely detectable levels of LpxC as compared to the isogenic parental strain in *lapC190* bacteria (Figure 9B, lanes 1&4, respectively). These results of highly diminished amounts of LpxC in the *lapC190* mutant are in sharp contrast to elevated LpxC levels in a Δ*lapA/B* derivative and its partial reduction in the *lpxC186* derivative of *lapAB* mutation (Figure 9B, lanes 2&3).

To correlate the reduction in LpxC amounts in *lapC190* mutants with the LPS accumulation, we directly measured LPS amounts using Proteinase K-treated whole cell lysates as described previously [11]. Samples were resolved on a SDS-Tricine gel and LPS was transferred by Western blotting. Amounts of LPS were revealed using a LPS-specific WN1 222-5 monoclonal antibody [50]. Results from immunoblots clearly show that the amount of LPS that cross reacted with WN1 222-5 monoclonal antibody in the *lapC190* mutant was significantly reduced as compared to that observed with the wild type (Figure 10, lanes 1&3), establishing a role for LapC in regulating LpxC amount and determining amount of LPS accumulation in line with results of restoration of LPS composition in a (Δ*lapB lapC377fs*) derivative (Figure 6).

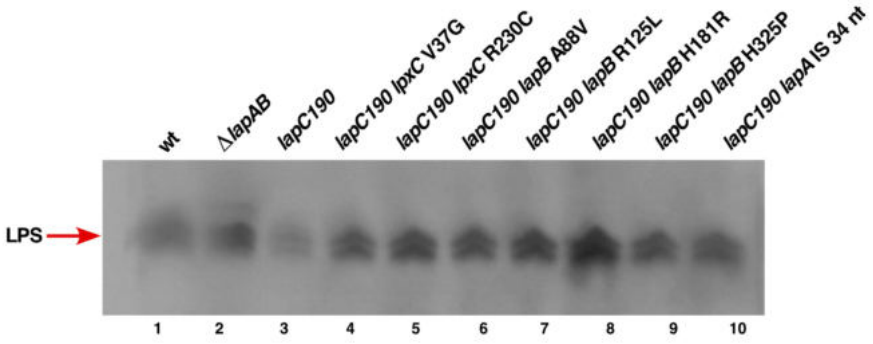

Figure 10. LPS levels are highly reduced in *lapC* mutants lacking the C-terminal periplasmic domain, which are restored by various suppressor mutations mapping to either *lpxC*, *lapA* or *lapB* genes. Isogenic bacterial cultures of the wild type and its derivatives with the indicated genotype were grown up to an OD_{595} of 0.5 at 30 °C. An equivalent portion of whole cell lysates were applied to a 14% SDS-Tricine gel and transferred by Western blotting. Relative amounts of LPS were revealed by immunoblotting with the LPS-specific monoclonal antibody WN1 222-5 using chemiluminescence detection kit.

2.8. Extragenic Suppressors That Restore LPS Levels in lapC190 Mutants Map to lpxC, lapA, lapB and ftsH

To further gain insights into the function of LapC, we took the advantage of Ts phenotype and the inability to grow on MacConkey agar of the *lapC190* and *lapC377fs* derivatives. Thus, we sought extragenic suppressors that either restored growth on LA agar at 42 °C or allowed growth on MacConkey agar by plating cultures under non-permissive growth conditions. Several spontaneous suppressors were isolated and 29 of them were marked with transposon Tn*10* as described earlier [17]. To map the suppressor mutation, linked Tn*10* insertion positions were obtained from recombinant cosmid clones by directly sequencing the Tn*10* insertion position. Out of 29 suppressors, 26 suppressor mutations could be grouped into three complementation groups (Table 2). Ten suppressors were found to be linked to *zab*::Tn*10*, 15 were linked to *pyrF*::Tn*10* and one was found to be linked to *greA*::Tn*10*. These map positions suggest that suppressor mutations linked to *zab*::Tn*10* could have a mutation in the *lpxC* gene, those linked to *pyrF*::Tn*10* mapping to the *lapA/B* locus and the last one linked to the *greA* gene could be having a mutation in the *ftsH* gene. Thus, we isolated chromosomal DNA from all 26 suppressor-containing mutants and directly sequenced the chromosomal DNA region spanning the coding and their flanking regions of *lpxC*, *lapA*, *lapB* and *ftsH* genes.

Table 2. Suppressors of *lapC190* and *lapC377fs* mutations map to *lpxC*, *lapA/B* and *ftsH* genes.

Gene	Mutation Position	Amounts of Isolates
lpxC	V37G (GTC → GGC)	4
	V37L (GTC → CTC)	1
	R230C (CGT → TGT)	3
	K270T (AAA → ACA)	1
	a frame-shift by the deletion of 2 nt TA from the stop codon resulting into the addition of 20 aa at the C-terminus	1
lapB	A88V (GCT → GTT) TPR2	2
	R115H (CGT → CAT) TPR3	1
	D124Y (GAC → TAC) TPR3	1
	R125L (CGC → CTC) TPR3	1
	H181R (CAT → CGT) TPR5	1
	H325L (CAC → CTC) TPR9	1
	H325P (CAC → CCC) TPR9	1
lapA	IS element after 34 nt	2
	IS element after 103 nt	1
	IS element after -107 nt - 2 nt after P2hs promoter of the *lapA* gene	1
	a frame-shift by the insertion of G after 69 nt (23 aa from LapA wt and 7 aa new followed by the stop codon)	1
	a frame-shift by the deletion of 137 nt C (45 aa from LapA wt and 12 aa new followed by the stop codon)	1
	LapA L8 (TTA → TGA) stop codon	1
ftsH	A296V (GCG → GTG) in the SRH domain	1

The results obtained from this DNA sequence analysis are presented in Table 2. Four independently isolated suppressor strains that restored growth at 42 °C on LA medium and also allowed growth to some extent on MacConkey agar contained a single amino acid exchange of V37G in the coding region of the *lpxC* gene (Figure 9A, Table 2). However, the strain with LpxC V37G suppressor grows poorly on MacConkey agar as compared to the LpxC V37L suppressor-containing strain in the *lapC190* background (Figure 9A). Similarly, three suppressor mutations that restored growth of either *lapC190* or *lpxC377fs* mutant strains had an exchange of R230 to C residue in the coding region of the *lpxC* gene (Figure 9A, Table 2). Sequence analysis of another suppressor-containing strain GK6094 revealed a frame-shift mutation due to the deletion of 2 nt in the stop codon that results in the extension of LpxC wild-type sequence by 20 amino acids. The C-terminal domain of LpxC is known to comprise the recognition domain for its proteolysis by FtsH protease [51]. Thus, this extension of LpxC by the unusual addition of 20 unrelated amino acids might prevent FtsH-mediated proteolysis, resulting into its stabilization and was verified by the examination of LpxC levels (see below).

Two other strains SR22738 and GK6078 with the suppressor mutation in the *lpxC* gene have single amino acid alterations resulting into V37L and K270T changes, respectively (Table 2, Figure 9C). The isolation of five independent isolates that lead to the substitution of Val37 residue is consistent with recent identification of LpxC V37G as a stable variant in *Klebsiella pneumoniae* [52]. Thus, we speculate that suppressor mutations that we identified in the *lpxC* gene render the encoding protein resistant to proteolysis and was investigated further.

2.9. Suppressors of lapC190 Mutation Mapping to the lpxC Gene Prevent Its Degradation and Lead to the Restoration of LPS Amounts

As LpxC and LPS amounts are limiting in strains carrying *lapC* mutations, we reasoned that suppressors mapping to the *lpxC* gene could act by stabilizing LpxC and restore LPS amounts to the wild-type levels. Thus, LpxC amounts were analyzed by Western blotting of cell extracts obtained from such suppressor-containing strains. As controls, the equivalent amount of total proteins from the parental wild type and its isogenic derivatives carrying either a Δ*lapA/B* mutation, the strain with the *lpxC186* suppressor mutation of *lapB* deletion and the derivative with the *lapC190* mutation were analyzed (Figure 9B). The most striking observation from the immunoblot analysis is the stabilization of LpxC in strains that carry the suppressor mutation in the *lpxC* gene. These results can explain the molecular basis of suppression and establish that LpxC is destabilized in *lapC* mutant derivatives with truncation of the periplasmic domain. All strains with *lpxC* suppressors accumulate more LpxC than even the wild type and the original *lapC190* mutant. The most prominent among them are strains with LpxC V37G, LpxC R230C and with a frame shift resulting into extension of LpxC by 20 amino acids, with a pronounced increase in the amounts of LpxC (Figure 9B). The Δ*lapA/B* strain, that served as a control, indeed accumulates lot more LpxC (Figure 9B, lane 2). Taken together, these results allow us to conclude that truncation of the C-terminal periplasmic domain destabilizes LpxC and suppressors mapping to the *lpxC* gene that restore growth at high temperature render LpxC more stable to balance the LPS synthesis.

To validate above results in the context of LPS synthesis and establish a role of LpxC degradation in the *lapC* mutant derivative and its stabilization in strains with the suppressor mutation, LPS amounts were analyzed by immunoblotting using the LPS-specific antibody. Whole cell lysates from two most prominent suppressor-containing strains with LpxC V37G and LpxC R230C mutations were analyzed in such comparative experiments. Results from such a representative experiment reveal the restoration of LPS synthesis as compared to the highly reduced LPS content in the *lapC190* derivative (Figure 10, lanes 4&5 vs. lane 3). These results provide a rationale explanation of decreased LPS synthesis due to destabilization of LpxC, when LapC function is impaired, and the restoration of LPS synthesis in the presence of suppressors mapping to the *lpxC* gene, which render LpxC more stable.

2.10. A Range of Suppressors of lapC190 Map to the lapA/lapB Operon That Could Either Disturb LapB Protein Structure or Dampen Its Abundance by Preventing Its Synthesis

The LapB protein is essential for bacterial growth due to its role in mediating LpxC degradation by either activating FtsH to recognize LpxC or its presentation to degradation pathway by acting as a scaffold for proteins involved in the LPS assembly/biosynthesis [17]. Consistent with this notion, we earlier demonstrated that LpxC is stabilized in the absence of LapB that leads to excess of build up LPS and causes the bacterial lethality [17]. Suppressors mapping to the *lpxC* gene, which reduce the LpxC synthesis or its accumulation, can allow a deletion of the *lapB* gene [17]. However, phenotypes of *lapC* mutants suggest an antagonistic action of LapC with LapB, as loss-of-function mutations have the opposite phenotype (less LPS and reduced LpxC stability) and (Δ*lapB lapC377fs*) combination restores the normal LPS synthesis. Thus, the isolation of suppressors of the *lapC190* and *lapC377fs* mutations mapping to the *lapA/B* operon should shed further light on how LapB and LapC operate. DNA sequence analysis revealed that 15 out of 26 suppressors had a mutation either in the coding region of the *lapB* structural gene or insertion sequence element (IS) in the *lapA* gene or in the promoter region of *lapA/B* operon, or a stop codon within the *lapA* gene (Table 2, Figure 11). Two additional mutations caused frame shifts in the *lapA* gene, disrupting the co-translation of downstream essential *lapB* gene (Figure 11C). It should be noted that *lapA* and *lapB* genes are transcribed as an operon and their translation is coupled [17]. The isolation of a number of IS elements in the *lapA* gene suggests that due to polarity such insertions could abrogate transcription of the *lapB* gene, thus prevent proteolysis of LpxC in the absence of LapB (Figure 11).

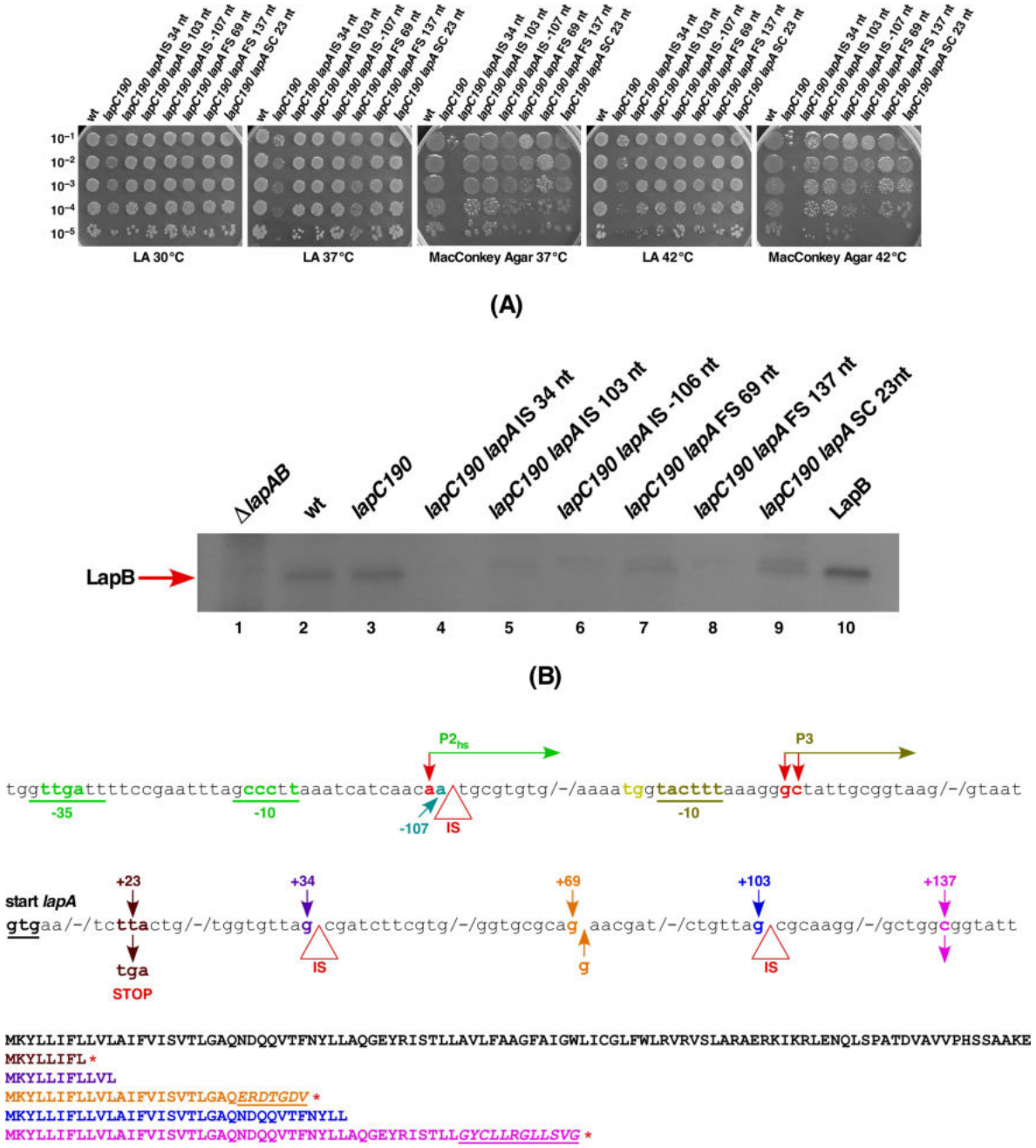

Figure 11. Suppressors of *lapC190* that restore growth at high temperature mapping either to the promoter region of the *lapA/B* operon or in the *lapA* gene reduce the LapB abundance. (**A**) Isogenic cultures of wild type, its *lapC190* derivative and *lapC190* with a specific suppressor mutation in the *lapA* gene or its promoter region were adjusted to an OD_{595} of 0.1, serially diluted, 5 µL aliquots spotted on either LA agar or MacConkey agar at various indicated temperatures and plates incubated for 24 h. (**B**) Immunoblots of whole cell lysates obtained from isogenic strains with indicated genotypes using LapB-specific antibodies. An equivalent amount of total proteins was loaded. As controls, extracts from Δ*lapA/B* and purified LapB (lanes 1&10) were applied. (**C**) The position of various suppressor mutations in the *lapA* gene is indicated. The presence of IS element in either the coding region or the promoter region is indicated by a triangle at the specific nt position. Other mutations causing frame shifts or introducing stop codons, resulting into either truncation of LapA or alterations in the amino acid sequence, are indicated and underlined with the indicated stop codon as * symbol.

To validate the isolation of suppressor mutations in the *lapA/B* operon that restore bacterial growth at high temperature of *lapC190* and *lapC377fs* mutant derivatives, we quantified the degree of suppression at various levels. Examination of growth of *lapC190* derivatives with suppressor mutations in either the *lapA* gene or in the promoter region of the *lapA/B* operon by spot dilution of isogenic cultures at different temperatures revealed restoration of growth of *lapC190* derivatives on LA medium at 37 and 42 °C (Figure 11A). Such suppressor-carrying strains also exhibited restoration of growth on MacConkey agar, which is very restrictive for a strain with a *lapC190* mutation (Figure 11A).

To address the molecular basis of suppression either due to the frame-shift mutation(s) or the presence of IS element in the *lapA* gene, we directly examined the comparative abundance of LapB in cell extracts of such suppressor-containing strains. To measure levels of LapB, the equivalent amount of total proteins from whole cell lysates of strains with various class of mutations in the *lapA* structural gene or its promoter region were examined by immunoblotting with anti-LapB antibodies (Figure 11B). As a control, we used the equivalent amount of total proteins from the isogenic Δ*lapA/B*, the wild type and *lapC190* derivatives. Purified LapB was used as a control to validate the cross-reactivity of anti-LapB antibodies. Examination of such an immunoblot showed that the presence of either IS element, or a frame-shift mutation in the *lapA* gene or the IS element after one of the major promoters of *lapA/B* operon either abolished the LapB synthesis or severely reduced its synthesis as compared to either the wild type or the *lapC190* derivative (Figure 11B,C). These results support the conclusions that transcription and translation of *lapA* and *lapB* mRNAs are coupled and suppressor mutations that restore growth of *lapC* mutant strains mapping to the *lapA* gene act by blocking the LapB synthesis. Thus, the IS element and frame-shift mutations in the *lapA* gene and promoter would as well result in reduced transcription of the *lapB* gene, which can cause an increased accumulation of LpxC and hence suppress *lapC* mutants, which have less LPS and less LpxC.

2.11. Suppressor Mutations in the Coding Region of the lapB Gene Map to Conserved Amino Acids in TPR Motifs that Result in the Reduced Abundance of LapB and Restoration of the LPS Synthesis

DNA sequence analysis revealed that eight suppressor-containing strains have single amino acid substitutions resulting into A88V, R115H, D124Y, R125L, H181R, H325L and H325P exchanges. All these amino acids in the *lapB*-coding sequence are highly conserved residues in tetratricopeptide repeats (TPR) elements (Table 2, Figure 12). Thus, the mutation of these residues could prevent interaction with proteins such as FtsH or interaction with the rubredoxin domain [17,25]. For example, the side-chain mutation H181R might result in the weaker rubredoxin-TPR binding (Figure 12).

Next, we systematically quantified the degree of suppression of *lapC190* mutation by above mentioned substitutions in the *lapB* gene by the spot dilution assay of strains with the suppressor mutation as compared to its parental strain. Consistent with their selection at 42 °C, all *lapB* substitutions restored growth of the parental *lapC190* strain on LA medium at 37 and 42 °C (Figure 12A). However, growth on MacConkey agar, reflecting the suppression of permeability defects, was restored only with suppressor D124Y, H181R and H325P mutations.

To further investigate how various substitutions impact the accumulation of LapB was addressed by Western blotting of total cellular proteins with anti-LapB antibodies. Examination of immunoblots revealed that most of mutations mapping to the *lapB* gene cause a severe reduction in the amounts of LapB as compared to its levels in the wild-type strain, with the exception of LapB D124Y substitution (Figure 12B). It is likely that D124Y substitution could cause the conformational change being located in the conserved TPR3 motif (Figure 12C). Consistent with this argument are the results of growth restoration of the *lapC190* mutation on LA as well as on MacConkey agar in the presence of D124Y substitution. Thus, we can conclude that amino acid substitutions in the *lapB* gene result in the loss of function or perturb folding of LapB protein, which could render it proteolytically sensitive and prevent its accumulation (Figure 12B).

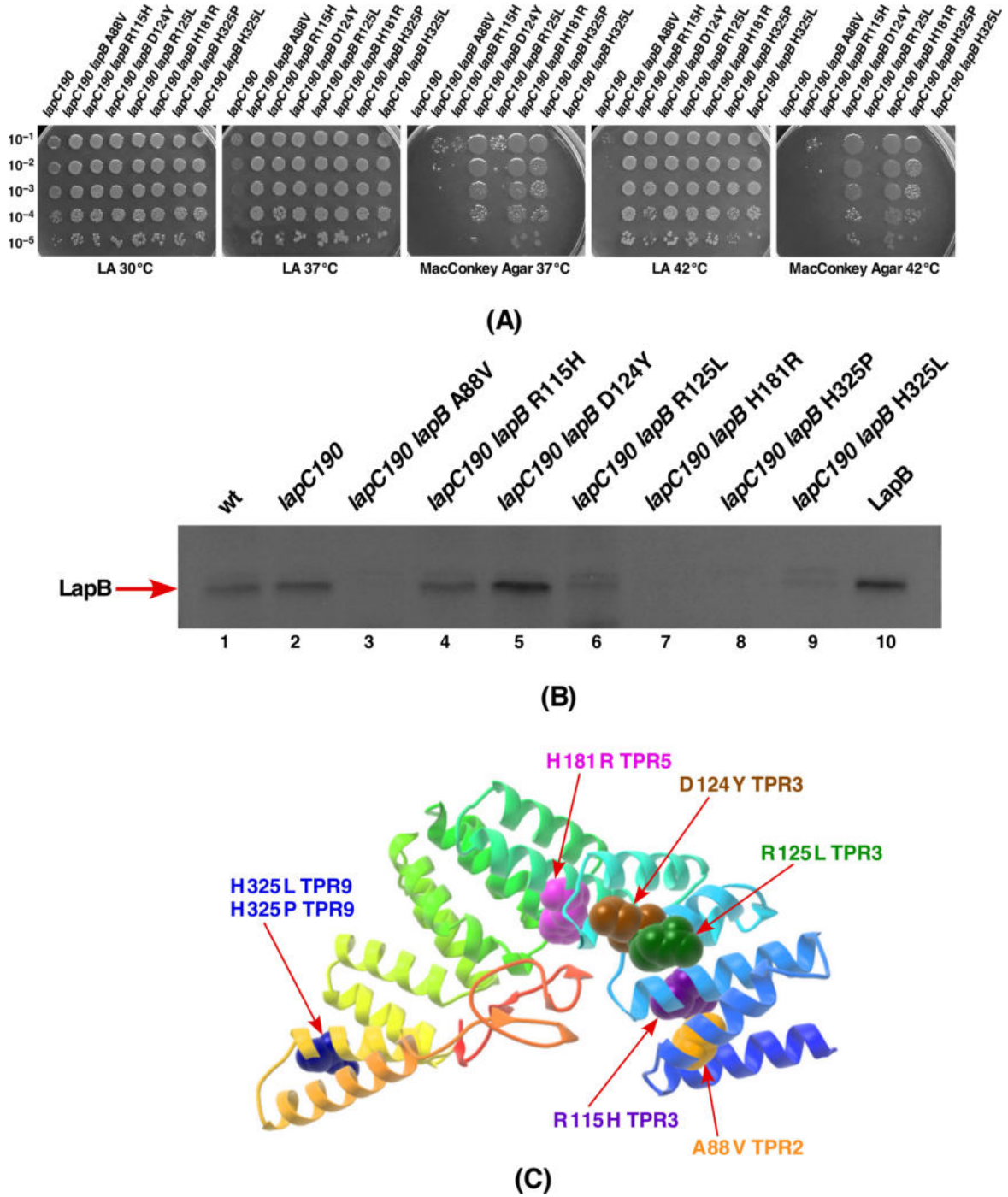

Figure 12. Suppressors mapping to the *lapB* gene that restore growth of *lapC* mutant bacteria reduce the LapB abundance. (**A**) Growth of isogenic cultures of strains with *lapC190* and with suppressor mutations in the *lapB* gene was quantified by spot dilution on LA and MacConkey agar at various temperatures. The genotype and incubation temperature are indicated. (**B**) Immunoblot of total cellular proteins from various strains, used in growth measurement, with LapB-specific antibodies. Purified LapB (lane 10) serves as a control to validate the cross-reactivity of LapB and its position on immunoblot. Equivalent amount of proteins were resolved by SDS-PAGE prior to immunoblotting. (**C**) The position of various mutations in LapB with the indicated relevant TPR motif are shown in the structure of LapB (PDB 4ZLH, [25]).

As LapB amounts determine amounts of the LPS synthesis and loss of LapB is lethal due to the increased synthesis of LPS causing depletion of pools of the *R*-3-hydroxymyristoyl-ACP

precursor for both phospholipid and LPS biosynthesis, we measured the accumulation of LPS in strains with suppressor mutations in either *lapA* or *lapB* genes as compared to the *lapC190* derivative. Measurement of LPS by immunoblots using the WN1 222-5 monoclonal antibody in parallel with strains with suppressor mutations in the *lpxC* gene clearly show that the synthesis of LPS is restored in all investigated variants of either LapA or LapB (Figure 10, lanes 6 to 10). These results provide the molecular basis of suppression of *lapC* derivative lacking the C-terminal periplasmic domain, as suppressor mutations exhibit the increased accumulation of LPS as compared to the highly reduced LPS content in *lapC* mutants. These results again support the isolation of another *lapC377fs* suppressor mutation that bypasses the lethality of Δ*lapB* derivatives (Figure 6). Thus, these results allow us to conclude that LapC and LapB jointly regulate the LPS synthesis by acting in an antagonistic manner.

2.12. Suppressor Mutation in the FtsH Gene Maps to the Conserved Region Required for Its ATPase Activity

Lastly, one of remaining suppressor mutation was found to map to the *ftsH* gene, which encodes the protease responsible for the LpxC degradation. This suppressor mutation causes exchange of conserved Ala296 by Val in the Second Region of Homology (SRH) domain (Figure 13). Mutations in the SRH domain are often associated with the loss of ATPase activity, which is critical for its proteolytic activity [53]. Consistent with its location in the SRH domain, *lapC190 ftsH* A296V derivative was found to accumulate more LpxC (Figure 9).

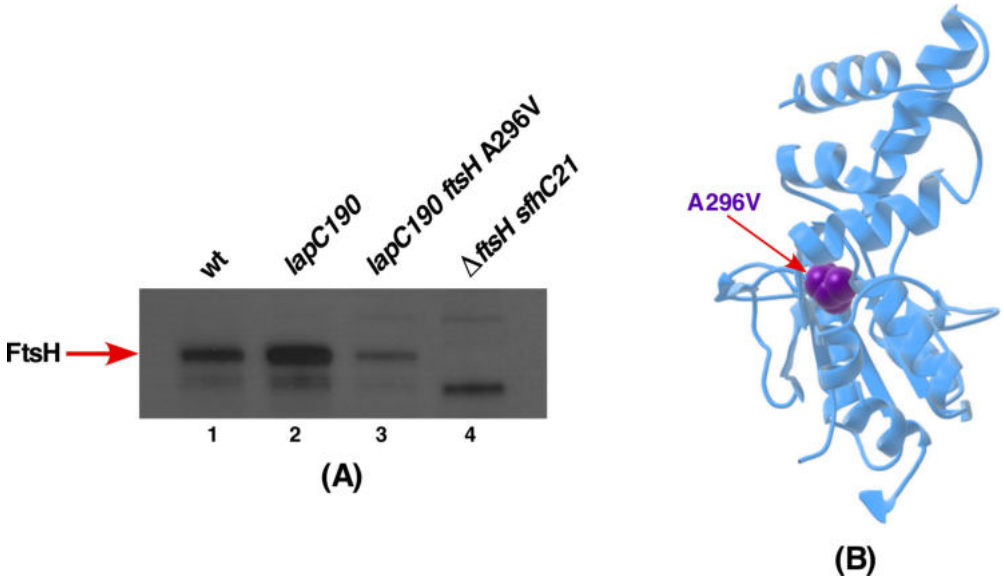

Figure 13. FtsH A296V suppressor mutation causes the reduction in FtsH levels. (**A**) Immunoblot analysis of total cellular extracts obtained from the wild type, its derivatives with *lapC190, lapC190 ftsH* A296V and as the negative control isogenic strain with Δ*ftsH sfhC21* mutation. An equivalent amount of proteins was resolved by SDS-PAGE and immunoblots were treated with a FtsH-specific antibody. Arrow indicates the position of FtsH. (**B**) The position of FtsH amino acid residue 296 on its crystal structure (PDB 1LV7 [54]) is shown.

As LapB and FtsH jointly regulate the LPS synthesis by regulating LpxC turnover, we examined levels of FtsH in the strain with *lapC190 ftsH* A296V using total cellular extracts. Western blot analysis revealed that FtsH levels are significantly reduced in the *lapC190 ftsH* A296V derivative as compared to the isogenic parental strain carrying the *lapC190* mutation (Figure 13A,B). As a negative control, total cell extracts from the Δ*ftsH* strain that is viable due to the *sfhC21* mutation, which encodes a hyperactive FabZ variant and lacks any cross-reacting FtsH were applied (Figure 13A). Thus, we can conclude that FtsH A296V in *lapC190* has the reduced amount of FtsH and due to its location in the ATPase-regulating domain could act by preventing LpxC degradation and restore the LPS synthesis.

2.13. The lapB Gene Is Dispenable in lapC Loss-of-Function Mutations and Overexpression of lpxC Can Bypass the Essentiality of the lapC Gene

Results presented in above sections revealed a reduced content of LPS in strains with either the *lapC190* or *lapC377fs* mutation and restoration of the LPS synthesis with either suppressor mutations mapping to the *lapA/B* operon or viability of Δ*lapB lapC377fs* derivatives prompted us to address in more detail if indeed the essential *lapB* gene is dispensable when LapC is dysfunctional. In line with such arguments, the suppressor mutation mapping to the *lpxC* gene render LpxC variants resistant to proteolysis and hence exhibit the increased accumulation of LpxC. Thus, we undertook genetic experiments using bacteriophage P1-mediated transductions to introduce either a Δ*lapA/B* or Δ*lapB* variants in either the *lapC190* or the *lapC377fs* backgrounds.

Results from transductions (Table 3) revealed that Δ*lapB* or Δ*lapA/B* can be readily introduced in strains carrying loss-of-function mutation in the *lapC* gene namely *lapC190* and *lapC377fs* as compared to the extremely low frequency of transduction with the parental BW25113 strain as a recipient. Furthermore, transductants in the wild-type strain form very small colonies and are obtained after the prolonged incubation. It should be noted that the *lapB* gene is essential in most of wild-type strains, however its deletion is tolerated poorly on M9 minimal medium at 30 °C and such strains grow very poorly [17] unless extragenic suppressor mutation(s) is present. These results are also consistent with the isolation of *lapC377fs* as an extragenic suppressor of Δ*lapB* (Figure 6) with the restoration of normal LPS synthesis. These results allow us to conclude that LapB is non-essential, when LapC is dysfunctional.

Table 3. The essential *lapB* gene is dispensable in either *lapC190* or *lapC377fs* backgrounds and the *lapC* gene becomes non-essential if LpxC is overproduced. ND denotes not done.

Number of Transductants with Selection for Kanamycin Resistance on Minimal Medium at 30 °C					
Donor	**Recipient**				
	BW25113	**BW25113 *lapC190***	**BW25113 *lapC377fs***	**BW25113 + p*lpxC*$^+$**	
				-IPTG	**50 μM IPTG**
Δ*lapA/B*Kan	33 Kan^R small colonies	2930 Kan^R normal size	3470 Kan^R normal size	ND	ND
Δ*lapB*Kan	36 Kan^R small colonies	3154 Kan^R normal size	3696 Kan^R normal size	ND	ND
Δ*lapC*Kan	None	ND	ND	None	754

As LpxC amounts are limiting in *lapC* mutants, with the same rationale as presented above, we performed transductions to introduce the Δ*lapC* mutation in the wild-type background transformed with a plasmid expressing the *lpxC* gene under the inducible P_{T5}-*lac* promoter. Firstly, the Δ*lapC* derivative, which served as a donor in P1 transductions, was constructed in a background where the Δ*lapC* derivative is maintained viable due to the expression of the *lapC* gene in a low-copy cosmid clone. Using controlled experiments, a Δ*lapC* mutation could be introduced when the *lpxC* gene is mildly induced by the addition of 50 μM IPTG (Table 3) but not in the absence of IPTG with supplementation of glucose (0.2%) when the *lpxC* expression is repressed. These results are consistent with the isolation of suppressor mutations of *lapC* mutants that accumulate more LpxC. Thus, we can conclude that LapC and LapB act antagonistically to maintain the balanced synthesis of LpxC and prevent its uncontrolled degradation and deletion of the *lapC* gene can be tolerated when either the *lpxC* gene is mildly overexpressed or in the absence of LapB.

2.14. Co-Purification of LapB and LapC

Given the genetic data presented in this work, all data point to the evidence of genetic interaction between the *lapB* and *lapC* genes. Thus, we performed pull-down experiments using the N-terminally His_{10}-tagged LapA. For this overexpression, different inducer concentrations of either 100 μM or 500 μM IPTG were used. Here, the plasmid used carries both *lapA* and *lapB* genes and hence are co-expressed. Purified IM fractions were subjected to Ni-NTA chromatography and eluted proteins

were identified by MALDI-TOF. Consistent with LapA and LapB co-purification, we also identified LapC as one of the proteins that could be part of this complex (Figure 14, lanes 1 and 3). In parallel, we could also pull-down LapB protein, when IM fractions from LapC induction were used for affinity purification (Figure 14, lane 2). Thus, co-purification of LapB and LapC provide the additional evidence of interaction of these proteins, supporting data of genetic interaction.

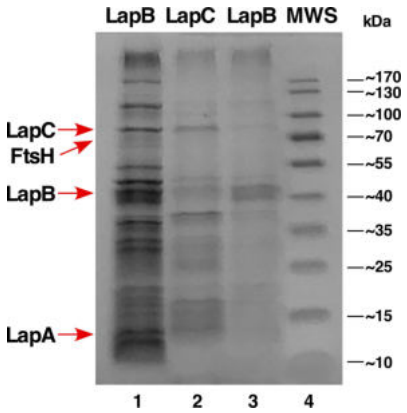

Figure 14. LapC and LapB show physical interaction. Purification profile of proteins from IM fractions after 100 μM and 500 μM IPTG addition to induce *lapA* and *lapB* transcription. Lanes 1 and 3 indicate co-purification of His-tagged LapA with LapB and LapC from IM fractions of total proteins. Lane 2 depicts elution profile of His_6-LapC and its co-elution with LapB. Proteins were resolved on a 12% SDS-PAGE. The identity of LapC, LapB, LapA and FtsH are shown by arrows.

2.15. The Expression of the lapC Gene Is Induced at High Temperatures

Although LapC is essential under all growth conditions, the synthesis of several genes is known to vary under stress conditions. For example, transcription of the *lapA/B* operon is heat shock inducible. As LapB and LapC interact, we further addressed if transcription of *lapC* is altered by a shift to high temperature. The relative abundance of *lapC* transcripts was measured by qRT-PCR using total RNA extracted from wild-type bacteria grown either at 30 °C or after a transient 15-min shift to 42 °C. Quantification of gene expression pattern revealed a significant 3.5-fold increase in the abundance of *lapC* transcripts after 15-min exposure to heat shock conditions (Figure 15).

Thus, *lapC* transcription is not only sustained at high temperature but is rather induced, consistent with its essentiality under all growth conditions. However, how the *lapC* transcription is induced at high temperature remains unknown (see Discussion).

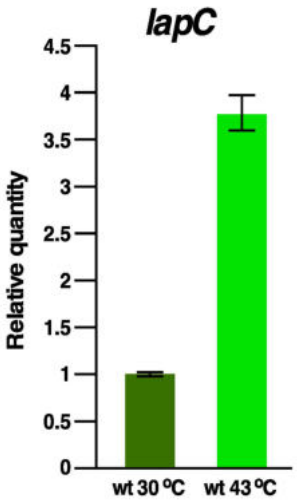

Figure 15. Transcription of the *lapC* gene is induced upon a shift to high temperature. qRT-PCR analysis of mRNA isolated from wild-type bacteria grown up to an OD_{595} of 0.2 in M9 minimal medium either at 30 °C or after a 15-min shift to 42 °C. Data presented are from RNA isolated from three biological replicates and error bars are indicated.

3. Discussion

It is well established that amounts of LpxC, which catalyzes the first rate-limiting step in LPS biosynthesis, are critical for determining a balanced biosynthesis of LPS and that of phospholipids [9,17,20,38]. LpxC is intrinsically unstable protein and its levels are tightly controlled by its turnover by two essential proteins: FtsH and LapB [17,20,23]. However, it is not known how LapB coordinates with FtsH in this process and if any additional protease is also involved in proteolytic control of LpxC. LapB and FtsH essentiality have been attributed to their role in regulating LpxC turnover. Consistent with such a notion, a deletion of either of these genes can be tolerated in the presence of hyperactive allele of the *fabZ* gene (*sfhC21*) that compensates by diverting common *R*-3-hydroxymyristoyl-ACP to phospholipid biosynthesis [7,17,20]. Alternatively, genetic backgrounds such as *lpxA101* or a Ts mutation in the *lpxD* gene or in genes whose products are required in the early steps of LPS core biosynthesis that reduce LPS biosynthesis or prevent the accumulation of LPS in the IM can rescue the deletion of *lapB* or *ftsH* genes [17,20]. A deletion of the *lapB* gene is lethal in most of the cases, however in certain backgrounds, like BW25113, the Δ*lapB* mutation can be poorly tolerated only on minimal medium at 30 °C but not on rich medium at any temperature. To gain further knowledge about the regulation of LpxC proteolysis and how LapB participates in this process, we employed multi-pronged approaches to address these issues. Firstly, multicopy suppressors were isolated that allow deletion of either *lapB* or *lapA/B* genes and restore growth at elevated temperatures of *lapB* mutant bacteria. These experiments, besides identifying previous multicopy suppressors, led to the cloning of the *hslV* gene. The *hslV* gene encodes the catalytic subunit of prokaryotic counterpart of proteosome and together with HslU has been shown to be involved in turnover of several unstable proteins such as RpoH, RcsA, SulA, dampen the elevated heat shock response and enhance the removal of puromycyl peptides [27,29,30]. Our data show that overexpression of the *hslV* gene alone can reduce elevated levels of LpxC and hence allow growth of either Δ*lapB* or Δ*lapA/B* derivatives. As HslU enhances the proteolytic activity of HslV, we also demonstrated in pulse chase experiments that they together synergistically enhance LpxC proteolysis at elevated temperatures. Thus, by 20 min LpxC amounts are barely detectable, under conditions when the synthesis of all host proteins, including FtsH, is blocked by the addition of rifampicin, with the exception of HslUV. Thus, our results for the first time demonstrate in vivo FtsH-independent degradation of LpxC by HslUV. Our conclusions draw support from computational and system biology-based approach that the predicted LpxC degradation could be regulated by an unidentified protease, whose activity is independent of the lipid A disaccharide

concentration [55]. Thus, our experiments establish that this speculated proteolytic activity is due to HslUV, also called ClpQY. Consistent with a role of HslUV protease complex in the regulation of LpxC levels, *hslV* mutants were found to be sensitive to CHIR090 antibiotic that inhibits the activity of LpxC.

The identification of HslUV-dependent proteolysis of LpxC is of relevance, particularly at high temperatures, since transcription of cognate genes is highly induced by the heat shock [27,42]. Interestingly, genome wide interaction studies have shown the interaction of LapA with HslV (UniProt). The HslUV-dependent proteolysis may also become more relevant at high temperature, since the LpxC degradation is inversely correlated with the doubling time [56]. It is likely that the HslUV-dependent degradation comes into play mostly at high temperature and that also draws a parallel between degradation of RpoH at high temperature by HslUV, although FtsH is the primary protease under normal growth conditions. These could also be reasons why HslUV are not essential for bacterial growth like FtsH. The HslUV-dependent proteolysis could also constitute a back-up mechanism to fine tune levels of LpxC under stress conditions. In support of synergistic roles of HslUV and FtsH proteases (Δ*ftsH* Δ*hslVU*) exhibit 10-fold more defect in survival as compared to Δ*ftsH* alone in *Pseudomonas aeruginosa* under carbon starvation conditions [57].

In the second approach, suppressor mutation(s) that allow introduction of Δ*lapB* in W3110 strain identified a novel frame-shift mutation in an essential gene *yejM* designated *lapC* upon further characterization of its genetic interactions. Quite interestingly, the *lapC* gene in certain bacteria is transcribed as a part of operon including the *waaC* gene [58]. We had previously shown that unlike BW25113, a Δ*lapB* mutation is not viable in W3110 a strain that has been widely used in elucidating LPS biogenesis and structural analysis in Raetz laboratory and in many other studies of relevance [4,5,13,14,17]. The frame-shift suppressor mutation in the *lapC* gene *lapC377fs* causes truncation within the periplasmic domain of IM-anchored LapC, highlighting a role for its periplasmic domain. Further characterization of LPS of (Δ*lapB lapC377fs*) derivative provided a significant explanation for LapC function in the regulation of LPS amounts. As previously shown, Δ*lapB* derivatives synthesize more LPS (hence toxicity) and accumulate precursor species of LPS that may not be targeted to the OM correctly [17]. Most importantly, mass spectrometry analysis of LPS of (Δ*lapB lapC377fs*) derivative revealed the restoration of normal LPS composition and suppression of accumulation of early intermediates as is observed in the spectra of LPS of strains lacking LapB. These results suggest that LapB and LapC could together regulate LpxC proteolysis to control the LPS accumulation and act in an antagonistic manner.

In another complementary approach, we set up genetic screens to identify mutations that cause LPS defects, induce the RpoE-dependent envelope stress response and render bacteria sensitive to the LpxC inhibitor CHIR090. RpoE is known to specifically respond to the cell envelope stress including defects in LPS, causing activation of promoters recognized by $E\sigma^E$ [18,59]. Rationale for the additional screen including the sensitivity to CHIR090 was based on its known inhibition of LpxC and mapping of CHIR090 resistant mutations in the *lpxC* gene [38,39]. Combination of these screens identified three mutations in the *lapC* (*yejM*) gene. The *yejM* gene is known to be essential for growth in *E. coli* and loss-of-function mutations in this gene exhibit an imbalance in phospholipid and LPS amounts, although the reasons are not fully understood [31,46]. Among three mutants, *lapC190* and *lapC377fs* conferred a tight Ts phenotype, the hypersensitivity to CHIR090 and the inability to grow on MacConkey agar. Of interest is that we had in an independent genetic approach already identified *lapC377fs* as a suppressor of Δ*lapB* lethality. We further characterized *lapC190* and *lapC377fs* mutations as they conferred a tighter phenotype. Examination of LPS of *lapC190* revealed a drastic reduction in LpxC and LPS amounts. To gain further insights in the function of LapC and its interacting partners, Ts^+ suppressors that could also restore growth on MacConkey agar albeit to different extents were analyzed further. Suppressors of *lapC190* or *lapC377fs* mutants mapped to the promoter region of the *lapA/B* operon and within the structural genes of *lapA*, *lapB*, *lpxC* and *ftsH* all resulting into the increased synthesis of LPS as well as the restoration of LpxC amounts. Based on the severe reduction in the amounts of LpxC in *lapC* mutant bacteria, it is suggested that LapC regulates proteolysis of LpxC. All of suppressor mutations that restored growth at high temperatures and on MacConkey agar mapping to

the *lpxC* gene were found to produce more LpxC, indicating these variants are resistant to degradation by FtsH. FtsH has been shown to recognize C-terminal residues in LpxC to initiate degradation [51]. Consistent with this pathway, one of the suppressor mutations exhibiting the increased accumulation of LpxC was found to have a frame-shift mutation at the stop codon resulting into the addition of 20 amino acids. Such a LpxC variant would obviously be not recognized by FtsH. Consistent with suppressors mapping to the *lpxC* gene leading to the stabilization of LpxC, the identification of five independent suppressors causing change of Val37 to Gly (4 out of 5 times) support such conclusions. Structural analysis predicts that this V37G substitution is a change from buried to exposed state and can cause structural damage. Not surprisingly, Val37 alteration in *Klebsiella pneumoniae* has been found to render LpxC more stable and resistant to the LpxC inhibitor [52]. Another variant of LpxC R230C as the suppressor of *lapC* mutants was also isolated three times that also resulted in elevated levels of LpxC. During the completion of this work, two independent studies also reported the isolation of suppressors of *lapC* that caused alterations of either V37 or R230 amino acids, respectively [35,36]. It is of interest that we isolated additional variants of LpxC that suppress *lapC190* and *lapC377fs* mutations, which were not reported in other complementary studies mentioned above, providing a broader model of LpxC regulation and help in understanding the function of LapC.

Consistent with our model that LapC, LapB and FtsH work together to regulate LpxC amounts by the controlled proteolysis and ensuring the balanced LPS synthesis as per demand, the vast majority of suppressors of *lapC* mutant bacteria belong to the category that reduce the LapB abundance or activity by either blocking its transcription or preventing its translation as is evident from the identification of IS elements in the *lapA*-coding region or its translational stop codon. It is worth remembering that *lapA* and *lapB* genes are co-transcribed and translation of LapB is coupled to the LapA synthesis as they have overlapping translational initiation and stop codons [17]. Examination of the LapB amount in all such mutants revealed a drastic reduction in the accumulation of LapB in strains with the IS element in the *lapA* gene or that prevent LapB translation. Regarding suppressor mutations within the coding region of the *lapB* gene, all of them are highly conserved residues in various TPR domains. TPR domains are known to mediate protein-protein interactions [60–62] and hence LapB derivatives isolated as suppressors of *lapC* mutants could either prevent the interaction with LapC and FtsH or could be improperly folded rendering LapB nonfunctional. Our modeling analysis suggests that A88V substitution in LapB disrupts all side-chain H-bonds. Another residue H181 in TPR5, whose exchange H181R suppresses the *lapC190* mutation and restores LPS levels, is of significance as H181 mutation was shown to be a loss-of-function mutation in earlier studies [25]. Thus, all such *lapB* variants result into its loss of function, since they mimic the phenotype of Δ*lapB* mutants with the synthesis of more LPS and the reduced accumulation of LapB. This supports our model, in which LapC and LapB act antagonistically and LapC could prevent either the interaction of LapB with FtsH or prevent LapB to act as an IM scaffold directing the LpxC degradation by FtsH. A direct proof for the LapB interaction with LapC was provided in this work based on their co-purification in reciprocal experiments supporting the data from genetic interactions described above. Thus, LapB interacts with FtsH, as demonstrated earlier, and with LapC. Consistent with our data of physical interaction of LapB with LapC, a recent finding published during the preparation of this manuscript have shown that LapC tagged with the FLAG epitope can pull-down LapB [32], consistent with our demonstration of LapB and LapC co-purification.

Since most of the suppressors mapping to the *lapA/B* operon synthesize very little LapB, we reasoned that LapB could be dispensable in the *lapC* mutant background. This was indeed established by the ability to transduce the *lapA/B* deletion into *lapC190* and *lapC377fs* mutant backgrounds. The absence of LapB would increase the LPS synthesis by stabilizing LpxC and compensate for the reduction in LPS levels in *lapC* mutants. Indeed, this could be shown by measuring the LPS content in various suppressor backgrounds revealing the elevation in the LPS accumulation despite the presence of *lapC190* mutation. Based on the same reasoning, we could show that the ectopic expression of LpxC can render LapC non-essential. Taken together, our findings support a model wherein LapC inhibits

the LapB/FtsH-mediated proteolysis allowing the accumulation of LpxC and this inhibition could be relieved, when higher levels of the LPS synthesis are not physiologically required.

However, under what circumstances the LapB interaction with LapC is promoted to direct LpxC to degradation or disrupted to enhance the LpxC synthesis remains to be fully understood. It is conceivable that under stress conditions, for example the exposure to high temperature when the *lapC* mRNA is made more, the LapB/FtsH activity is repressed when LapC is more. Supporting our results of increased accumulation of LapC at high temperature are independent proteomic analysis data of total *E. coli* proteome from high temperature or other stress conditions [63,64]. In line with such arguments are findings that LpxC is more rapidly degraded at lower temperatures than at higher temperatures correlating it with doubling time of *E. coli* [56]. This would allow the synthesis of more LPS under stress conditions. However, if at high temperature the FtsH-dependent proteolysis of LpxC is limiting, then HslVU protease, whose expression is highly induced at the elevated temperature, could rapidly shift this equilibrium back by the rapid removal of excess of LpxC to maintain the balanced synthesis of LPS.

Thus, in summary based on several lines of evidence we show that LapC is involved in regulating the LPS synthesis and together with FtsH and LapB it balances and regulates the LpxC degradation. As a safety mechanism, HslUV proteases prevent unwanted build-up of LpxC and LPS by promoting proteolysis of LpxC, which could be recruited at high temperatures. Furthermore, the unwarranted accumulation of LPS biosynthetic intermediates in the IM or prior to the LPS delivery to the OM via the Lpt system, when the LapB function is limiting, might relieve the inhibitory effect of LapC and restore the LpxC degradation allowing a balance between phospholipid and LPS biosynthesis.

4. Materials and Methods

4.1. Bacterial Strains, Plasmids and Media

The bacterial strains and plasmids used in this study are described in Table S1. Luria-Bertani (LB) broth, M9 (Difco, Franklin Lakes, NJ, USA) and M9 minimal media were prepared as described [5]. Whenever required, media were supplemented with ampicillin (100 μg/mL), kanamycin (50 μg/mL), tetracycline (10 μg/mL), chloramphenicol (20 μg/mL) and CHIR090 (0.004 or 0.008 μg/mL). The indicator dye 5-bromo-4-chloro-3-indolyl-*β*-D-galactopyranoside (X-Gal) was used at a final concentration of 40 or 60 μg/mL in the agar medium. Lactose-containing MacConkey agar (Difco) was supplemented with appropriate antibiotics when required. Deletion derivatives used in this study of *hslV*, *hslU*, Δ(*hslVU*), Δ*lapB* and Δ(*lapA/B*) have been previously described [17,27]. Δ*lapC190* strain was constructed using λ-Red mediated recombineering [65].

4.2. The Identification of Multicopy Suppressors Whose Overexpression Prevents Lethality of ΔlapA/B Bacteria

The genomic library of all predicted ORFs of *E. coli* cloned in pCA24N vector was used to transform Δ(*lapA lapB*) strain SR17187 [17]. Transformants were plated under non-permissive growth conditions of LA medium at 37 and 42 °C in the presence of 75 μM IPTG. Bacterial cultures were grown from such suppressing clones and used to retransform SR17187 to verify the suppression. DNA insert of all relevant plasmids that yielded reproducible results was sequenced. To further validate the suppression by overexpression of either the *hslV* gene alone or co-expression of *hslVU*, previously described plasmids were used [27]. For the induction of HslVU proteins, the minimal coding region of the operon was amplified by PCR using the chromosomal DNA from the wild-type BW25113 strain as a template and cloned in expression vectors such as pTTQ18 or pET24b (Table S1).

4.3. Identification of the lapC Gene Based on the Isolation of Mutations That Either Induce Transcription from the LPS-Responsive rpoEP3-lacZ Fusion or Suppressor a lapB Deletion

Saturated pools of mini-Tn*10* Kan transposon mutants were generated on LA medium at 30 °C as described previously [66]. A bacteriophage P1 was grown on such pools and transduced into

strains SR18868 and SR18987 [18] carrying derivatives of the chromosomal single-copy *rpoE*P3-*lacZ* promoter fusion and subjected to chemical mutagenesis. This promoter was chosen as it specifically responds to severe defects in LPS biosynthesis and is also activated by the Rcs two-component system [18]. Colonies that exhibited a Lac up phenotype (deep blue colonies) on X-Gal-supplemented plates were patched at 30 °C. Approximately more than 80,000 colonies were replica plated at 42 °C. Tn*10*-linked point mutations that conferred a concomitant temperature-sensitive phenotype (Ts) unable to grow at 42 °C and were simultaneously up-regulated for the activity of the *rpoE*P3-*lacZ* promoter fusion were retained. To make selection more stringent, Lac up and Ts isolates were streaked on MacConkey agar at 37 °C and on LA agar supplemented with 0.008 µg/mL of the LpxC inhibitor CHIR090 at 30 °C. Only those candidates that exhibited simultaneous Ts phenotype, unable or poor growth on MacConkey agar, sensitive to growth inhibition by the sub-lethal concentration of the CHIR090 inhibitor and increased the activity of *rpoE*P3-*lacZ* promoter fusion were further verified by bacteriophage P1-mediated transductions and measurement of *β*-galactosidase activity of the *rpoE*P3-*lacZ* fusion. To identify the mutated gene, the position of linked Tn*10* insertion was obtained by sequencing of chromosomal DNA using either inverse PCR as described earlier [17] or sub-cloning of Tn*10* from recombinant cosmid clones that complement the mutation causing LPS defects (see below). Tn*10* insertion or linked Tn*10* point mutations mapping to the main biosynthetic *waa* locus [67] or to other known LPS biosynthetic genes were not followed.

In parallel, we sought extragenic suppressors of a Δ*lapB* or Δ*lapA/B* derivative in W3110 strain. We have earlier reported that a Δ*lapB* derivative is not tolerated in W3110 unless an extragenic suppressor mutation is present. Most of those suppressors were found to synthesize deep-rough LPS (WaaC chemotype). Here we repeated several transductions and screened for Δ*lapB* derivatives in W3110 that synthesize normal amounts of LPS based on reactivity with WN1-225-5 antibody. One such suppressor mutation defined a strain SR8348 and was found by sequence analysis to have Δ*lapB lapC377fs* genotype and was further characterized.

4.4. Mapping and Complementation of MacConkey-Sensitive, rpoEP3 Hyperactive and Temperature-Sensitive Mutations

To perform complementation and identify mutated gene, a previously described cosmid library in the single-copy vector was used to transform Ts mutants. Complementing cosmids were obtained by the restoration of growth at 42 °C on MacConkey agar. Plasmids that could recombine mini-Tn*10* and restore growth of Ts mutants on MacConkey agar were used for subcloning and DNA sequencing of cloned inserts. Five Tn*10*-linked Ts mutants mapping at 49 min on the genetic map of *E. coli* with the *rpoE*P3-*lacZ* up phenotype and unable to grow on MacConkey agar that identified the *lapC* gene were further followed. To identify the mutation, the chromosomal DNA of the *lapC* gene and its adjoining regions was PCR amplified with appropriate oligonucleotides (Table S2) and its DNA sequence analyzed.

4.5. The Isolation of Extragenic Suppressors of lapC Mutants and Their Mapping

As *lapC* F349S, *lapC377fs* and *lapC190* bacteria exhibit the Ts phenotype (inability to grow above 42 °C), several independent cultures of each strain were grown in LB at 30 °C and portions of each plated at 43 °C to seek for temperature-resistant colonies. In parallel in a similar manner, suppressors that restore growth on MacConkey agar were selected by directly plating cultures of *lapC* mutant bacteria on such a selective medium. After verification for their growth at non-permissive growth conditions, mutations were marked with mini-Tn*10* Kan and verified that the Tn*10*-linked suppressor mutation breeds true. The abovementioned cosmid library was used to identify cosmid clones that can recombine linked Tn*10* Kan, which were used to group 26 out of 29 suppressors in three complementation groups. This was further substantiated by additional transductions with defined mutations in linked genes. To further validate this approach, chromosomal DNA of all 29 suppressor strains was isolated and used to PCR amplify candidate genes. In the first series of experiments, chromosomal DNA of 29 suppressors

served as a template to amplify the coding and adjoining regions covering the *lpxC* gene. Chromosomal DNA isolated from suppressors belonging to other two complementation groups were next used to PCR amplify the *lapA/lapB* operon, including the promoter region, and the *ftsH* gene. PCR products were sequenced using appropriate oligonucleotides listed in the Table S2.

4.6. Bacterial Growth Analysis and Measurement of β-Galactosidase Activity

For the quantification of bacterial growth, exponentially grown cultures were adjusted to an optical density OD_{595} of 0.1 and ten-fold dilutions were spot tested on agar plates at different temperatures. Five µL of each dilution was spotted and bacterial growth analyzed after incubation for 24 h at indicated temperatures. To measure the *β*-galactosidase activity, isogenic cultures of the wild type and its derivatives with a specific *lapC* mutation carrying *rpoE-lacZ* promoter fusions were grown overnight under permissive growth conditions. Cultures were adjusted to an optical density OD_{595} of 0.05, allowed to grow at 30 °C for another 45 min. Aliquots of cultures were taken after different intervals as indicated and analyzed for *β*-galactosidase activity as described previously [11]. For each assay, three independent cultures were used and average of each were plotted.

4.7. LPS Extraction, Mass Spectrometry and Measurement of LPS Levels

An equivalent amount of bacterial cultures grown up to an OD_{595} of 0.5 were harvested by centrifugation. Pellets were resuspended in 1X sample buffer, boiled for 10 min, followed by digestion with Proteinase K to obtain whole cell lysates. Equivalent portions of such whole cell lysates were applied to a 14% SDS-Tricine gel. After the electrophoresis LPS was transferred by Western blotting. Immunoblots were probed for LPS amounts using the WN1-222-5 monoclonal antibody [50] and revealed by chemiluminescence kit from Thermo Scientific (Warsaw, Poland).

Bacterial cultures (400 mL to 1 L) were grown in phosphate-limiting medium, harvested by centrifugation and pellets were lyophilized. For the LPS analysis, lyophilized material was dispersed in water by sonication and resuspended at a concentration of 2 mg/mL and LPS was extracted by the phenol/chloroform/petroleum ether procedure [68]. Electrospray ionization-Fourier transform ion cyclotron (ESI-FT-ICR)-mass spectrometry was performed on intact LPS in the negative ion mode using an APEX QE (Bruker Daltonics, Breman, Germany) equipped with a 7-tesla actively shielded magnet and dual ESI-MALDI. LPS samples were dissolved at a concentration of ~10 ng/µL and analyzed as described previously [11,69]. Mass spectra were charge deconvoluted, and mass numbers given refer to the monoisotopic peaks.

4.8. Immunoblotting to Measure Amounts of LpxC, LapB and FtsH

The isogenic bacterial culture of wild type and its derivatives carrying various extragenic suppressor mutations and as controls Δ*lapA/B*, Δ*ftsH sfhC21* were grown in either LB or M9 minimal medium at 30 °C to an OD_{595} of 0.5. Equivalent amounts of proteins were applied to a 12% SDS-PAGE and proteins transferred by Western blotting. Blots were probed with polyclonal antibodies against LpxC, FtsH and LapB as described previously. Custom made LapB-specific antibodies were made by Cusabio (Wuhan, China) and used at a dilution of 1:5000. The WN1-225 monoclonal antibody [50] was used at a dilution of 1:10,000. Blots were revealed by chemiluminescence kit from Thermo Scientific as per manufacturer's instructions.

4.9. Purification of LapC and LapB

To co-purify LapA and LapB proteins, the minimal coding region of *lapA/B* operon was cloned into the low-copy T7 promoter-based pDUET expression vector (Novagen, Warsaw, Poland) with in-frame deca-His tag at the N-terminus of LapA. The expression of *lapA/lapB* genes was induced in BL21 (DE3) derivative by the addition of either 100 or 500 µM IPTG at an OD_{600} 0.2 in 1-L culture medium. For the induction of LapC, the cloned gene in the T7 promoter-based pET28b vector was used and the expression induced with the addition of 200 µM IPTG. Cultures were harvested by

centrifugation at 12,000 rpm for 30 min. Pellets were resuspended in B-PER reagent (Pierce) containing 50 mM NaH_2PO_4, 300 mM NaCl, 10 mM imidazole. This mixture was supplemented with lysozyme to a final concentration of 200 µg/mL, a cocktail of protease inhibitors (Sigma) and 30 units of benzonase (Merck, Poznan, Poland). The mixture was incubated on ice for 45 min with gentle mixing. The lysate was centrifuged at 45,000× *g* for 30 min at 4 °C and pellets containing IM and OM proteins retained. LapA/B and LapC proteins were extracted using 2% octyl-*β*-D-glucoside for solubilization for IM proteins in the presence of PMSF and a cocktail of protease inhibitors. Solubilized IM proteins were applied over nickel-nitrilotriacetic acid beads (Qiagen, Geneva, Switzerland) and Lap proteins eluted essentially as described earlier [17].

4.10. RNA Purification and qRT-PCR Analysis

To measure the mRNA abundance at different temperatures, the bacterial culture of wild-type strain BW25113 were grown at 30 °C in LB rich medium to an OD_{600} of 0.1. For the heat shock, aliquots were immediately shifted to prewarmed medium held at 42 °C and incubated for another 15 min. Equivalent amounts of culture samples were collected from cultures grown at 30 °C and after the heat shock of 42 °C, and harvested by centrifugation. Total RNA was extracted by hot phenol extraction as described previously [70]. Purified total RNA was treated RQ1 DNase (Promega, Madison, WI, USA) to remove any genomic DNA and ethanol precipitated. Pellets were resuspended in DEPC-treated water. RNA amounts were quantified and RNA integrity verified by agarose gel electrophoresis. qRT-PCR was used to quantify changes in the *lapC* gene expression before and after the heat shock treatment. Routinely, 2 µg of purified mRNA was converted to cDNA using iScript Reverse Transcription Supermix from Bio-Rad (Warsaw, Poland). qRT-PCR was performed using CFX Connect Real-Time PCR Detection System (Bio-Rad) as described previously [71]. Data were analyzed by Bio-Rad CFX Maestro software.

Supplementary Materials: The following are available online at can be found at http://www.mdpi.com/1422-0067/21/23/9088/s1.

Author Contributions: Conceptualization, methodology, validation, writing, review and editing, S.R. and G.K.; investigation (G.K., D.B., P.G. and S.R.), supervision, S.R.; funding acquisition, S.R. All authors have read and agreed to the published version of the manuscript.

Funding: This research was funded by National Science Center (NCN) Grant 2017/25/B/NZ6/02021 to S.R.

Acknowledgments: We gratefully acknowledge S. Müller-Loennies, K. Ito, F. Narberhaus for kind gift of some of the antibodies used in this study and B. Lindner for mass spectrometric analysis.

Conflicts of Interest: The authors declare no conflict of interest.

Abbreviations

L-Ara4N	4-Amino-4-deoxy-L-arabinose
CHIR090	*N*-Aroyl-L-threonine hydroxamic acid
ESI	Electrospray ionization
FabZ	*R*-3-Hydroxymyristoyl acyl carrier protein dehydratase
FT-ICR	Fourier transform-ion cyclotron
Kdo	3-Deoxy-*α*-D-*manno*-oct-2-ulosonic acid
LPS	Lipopolysaccharide
LpxC	UDP-3-*O*-(*R*-3-hydroxymyristoyl)-*N*-acetylglucosamine deacetylase
P-EtN	Phosphoethanolamine
TPR	Tetratricopeptide repeat

References

1. Nikaido, H. Molecular basis of bacterial outer membrane permeability revisited. *Microbiol. Mol. Biol. Rev.* **2003**, *67*, 593–656. [CrossRef] [PubMed]
2. Raetz, C.R.H.; Whitfield, C. Lipopolysaccharide endotoxins. *Annu. Rev. Biochem.* **2002**, *71*, 635–700. [CrossRef] [PubMed]

3. Bohl, T.E.; Aihara, H. Current progress in the structural and biochemical characterization of proteins involved in the assembly of lipopolysaccharide. *Int. J. Microbiol.* **2018**, *2018*, 5319146. [CrossRef] [PubMed]
4. Müller-Loennies, S.; Lindner, B.; Brade, H. Structural analysis of oligosaccharides from lipopolysaccharide (LPS) of *Escherichia coli* K12 strain W3100 reveals a link between inner and outer core LPS biosynthesis. *J. Biol. Chem.* **2003**, *278*, 34090–34101. [CrossRef]
5. Klein, G.; Lindner, B.; Brade, H.; Raina, S. Molecular basis of lipopolysaccharide heterogeneity in *Escherichia coli*: Envelope stress-responsive regulators control the incorporation of glycoforms with a third 3-deoxy-α-D-*manno*-oct-2-ulosonic acid and rhamnose. *J. Biol. Chem.* **2011**, *286*, 42787–42807. [CrossRef]
6. Klein, G.; Müller-Loennies, S.; Lindner, B.; Kobylak, N.; Brade, H.; Raina, S. Molecular and structural basis of inner core lipopolysaccharide alterations in *Escherichia coli*. Incorporation of glucuronic acid and phosphoethanolamine in the heptose region. *J. Biol. Chem.* **2013**, *288*, 8111–8127. [CrossRef]
7. Klein, G.; Raina, S. Regulated control of the assembly and diversity of LPS by noncoding sRNAs. *Biomed. Res. Int.* **2015**, *2015*, 153561. [CrossRef]
8. Raetz, C.R.; Reynolds, C.M.; Trent, M.S.; Bishop, R.E. Lipid A modification systems in Gram-negative bacteria. *Annu. Rev. Biochem.* **2007**, *76*, 295–329. [CrossRef]
9. Klein, G.; Raina, S. Regulated assembly of LPS, its structural alterations and cellular response to LPS defects. *Int. J. Mol. Sci.* **2019**, *20*, 356. [CrossRef]
10. Gronow, S.; Brade, H. Lipopolysaccharide biosynthesis: Which steps do bacteria need to survive? *J. Endotoxin Res.* **2001**, *7*, 3–23. [CrossRef]
11. Klein, G.; Lindner, B.; Brabetz, W.; Brade, H.; Raina, S. *Escherichia coli* K-12 suppressor-free mutants lacking early glycosyltransferases and late acyltransferases: Minimal lipopolysaccharide structure and induction of envelope stress response. *J. Biol. Chem.* **2009**, *284*, 15369–15389. [CrossRef] [PubMed]
12. Raetz, C.R.; Brozek, K.A.; Clementz, T.; Coleman, J.D.; Galloway, S.M.; Golenbock, D.T.; Hampton, R.Y. Gram-negative endotoxin: A biologically active lipid. *Cold Spring Harb. Symp. Quant. Biol.* **1988**, *53*, 973–982. [CrossRef] [PubMed]
13. Anderson, M.S.; Bulawa, C.E.; Raetz, C.R.H. The biosynthesis of Gram-negative endotoxin. Formation of lipid A precursors from UDP-GlcNAc in extracts of *Escherichia coli*. *J. Biol. Chem.* **1985**, *260*, 15536–15541. [PubMed]
14. Anderson, M.S.; Bull, H.G.; Galloway, S.M.; Kelly, T.M.; Mohan, S.; Radika, K.; Raetz, C.R. UDP-N-acetylglucosamine acyltransferase of *Escherichia coli*. The first step of endotoxin biosynthesis is thermodynamically unfavourable. *J. Biol. Chem.* **1993**, *268*, 19858–19865. [PubMed]
15. Zhou, P.; Zhao, J. Structure, inhibition, and regulation of essential lipid A enzymes. *Biochim. Biophys. Acta Mol. Cell Biol. Lipids* **2017**, *1862*, 1424–1438. [CrossRef]
16. Reynolds, C.M.; Raetz, C.R.H. Replacement of lipopolysaccharide with free lipid A molecules in *Escherichia coli* mutants lacking all core sugars. *Biochemistry* **2009**, *48*, 9627–9640. [CrossRef]
17. Klein, G.; Kobylak, N.; Lindner, B.; Stupak, A.; Raina, S. Assembly of lipopolysaccharide in *Escherichia coli* requires the essential LapB heat shock protein. *J. Biol. Chem.* **2014**, *289*, 14829–14853. [CrossRef]
18. Klein, G.; Stupak, A.; Biernacka, D.; Wojtkiewicz, P.; Lindner, B.; Raina, S. Multiple transcriptional factors regulate transcription of the *rpoE* gene in *Escherichia coli* under different growth conditions and when the lipopolysaccharide biosynthesis is defective. *J. Biol. Chem.* **2016**, *291*, 22999–23019. [CrossRef]
19. Galloway, S.M.; Raetz, C.R. A mutant of *Escherichia coli* defective in the first step of endotoxin biosynthesis. *J. Biol. Chem.* **1990**, *265*, 6394–6402.
20. Ogura, T.; Inoue, K.; Tatsuta, T.; Suzaki, T.; Karata, K.; Young, K.; Su, L.H.; Fierke, C.A.; Jackman, J.E.; Raetz, C.R.; et al. Balanced biosynthesis of major membrane components through regulated degradation of the committed enzyme of lipid A biosynthesis by the AAA protease FtsH (HflB) in *Escherichia coli*. *Mol. Microbiol.* **1999**, *31*, 833–844. [CrossRef]
21. Fuhrer, F.; Langklotz, S.; Narberhaus, F. The C-terminal end of LpxC is required for degradation by the FtsH protease. *Mol. Microbiol.* **2006**, *59*, 1025–1036. [CrossRef] [PubMed]
22. Thomanek, N.; Arends, J.; Lindemann, C.; Barkovits, K.; Meyer, H.E.; Marcus, K.; Narberhaus, F. Intricate crosstalk between lipopolysaccharide, phospholipid and fatty acid metabolism in *Escherichia coli* modulates proteolysis of LpxC. *Front. Microbiol.* **2019**, *9*, 3285. [CrossRef] [PubMed]
23. Mahalakshmi, S.; Sunayana, M.R.; SaiSree, L.; Reddy, M. *yciM* is an essential gene required for regulation of lipopolysaccharide synthesis in *Escherichia coli*. *Mol. Microbiol.* **2014**, *91*, 145–157. [CrossRef]

24. Dillon, D.A.; Wu, W.I.; Riedel, B.; Wissing, J.B.; Dowhan, W.; Carman, G.M. The *Escherichia coli pgpB* gene encodes for a diacyl- glycerol pyrophosphate phosphatase activity. *J. Biol. Chem.* **1996**, *271*, 30548–30553. [CrossRef] [PubMed]
25. Prince, C.; Jia, Z. An unexpected duo: Rubredoxin binds nine TPR motifs to form LapB, an essential regulator of lipopolysaccharide synthesis. *Structure* **2015**, *23*, 1500–1506. [CrossRef] [PubMed]
26. Kanemori, M.; Nishihara, K.; Yanagi, H.; Yura, T. Synergistic roles of HslVU and other ATP-dependent proteases in controlling *in vivo* turnover of σ^{32} and abnormal proteins in *Escherichia coli*. *J. Bacteriol.* **1997**, *179*, 7219–7225. [CrossRef]
27. Missiakas, D.; Schwager, F.; Betton, J.M.; Georgopoulos, C.; Raina, S. Identification and characterization of HslV HslU (ClpQ ClpY) proteins involved in overall proteolysis of misfolded proteins in *Escherichia coli*. *EMBO J.* **1996**, *15*, 6899–68909. [CrossRef]
28. Tomoyasu, T.; Gamer, J.; Bukau, B.; Kanemori, M.; Mori, H.; Rutman, A.J.; Oppenheim, A.B.; Yura, T.; Yamanaka, K.; Niki, H.; et al. *Escherichia coli* FtsH is a membrane-bound, ATP-dependent protease which degrades the heat-shock transcription factor σ^{32}. *EMBO J.* **1995**, *14*, 2551–2560. [CrossRef]
29. Kanemori, M.; Yanagi, H.; Yura, T. The ATP-dependent HslVU/ClpQY protease participates in turnover of cell division inhibitor SulA in *Escherichia coli*. *J. Bacteriol.* **1999**, *181*, 3674–3680. [CrossRef]
30. Wu, W.F.; Zhou, Y.N.; Gottesman, S. Redundant in vivo proteolytic activities of *Escherichia coli* Lon and the ClpYQ (HslUV) protease. *J. Bacteriol.* **1999**, *181*, 3681–3687. [CrossRef]
31. De Lay, N.R.; Cronan, J.E. Genetic interaction between the *Escherichia coli* AcpT phosphopantetheinyl transferase and the YejM inner membrane protein. *Genetics* **2008**, *178*, 1327–1337. [CrossRef] [PubMed]
32. Clairfeuille, T.; Buchholz, K.R.; Li, Q.; Verschueren, E.; Liu, P.; Sangaraju, D.; Park, S.; Noland, C.L.; Storek, K.M.; Nickerson, N.N.; et al. Structure of the essential inner membrane lipopolysaccharide-PbgA complex. *Nature* **2020**, *584*. [CrossRef] [PubMed]
33. Cian, M.B.; Giordano, N.P.; Masilamani, R.; Minor, K.E.; Delabroux, Z.D. *Salmonella enterica* serovar Typhimurium uses PdgA/YejM to regulate lipopolysaccharide assembly during bacteremia. *Infect. Immun.* **2020**, *88*, e00758Ce19. [CrossRef]
34. Gabale, U.; Palomino, P.A.P.; Kim, H.A.; Chen, W.; Ressi, S. The essential inner membrane protein YejM is a metalloenzyme. *Sci. Rep.* **2020**, *10*, 17794. [CrossRef]
35. Guest, R.L.; Samé Guerra, D.; Wissler, M.; Grimm, J.; Silhavy, T.J. YejM modulates activity of the YciM/FtsH protease complex to prevent lethal accumulation of lipopolysaccharide. *mBio* **2020**, *11*, e00598-20. [CrossRef] [PubMed]
36. Fivenson, E.M.; Bernhardt, T.G. An essential membrane protein modulates the proteolysis of LpxC to control lipopolysaccharide synthesis in *Escherichia coli*. *mBio* **2020**, *11*, e00939-20. [CrossRef] [PubMed]
37. Nguyen, D.; Kelly, K.; Qiu, N.; Misra, R. YejM controls LpxC levels by regulating protease activity of the FtsH/YciM complex of *Escherichia coli*. *J. Bacteriol.* **2020**, *202*, e00303–e00320. [CrossRef]
38. Zheng, D.; Zhao, J.; Chung, H.S.; Guan, Z.; Raetz, C.R.H.; Zhou, P. Mutants resistant to LpxC inhibitors by rebalancing cellular homeostasis. *J. Biol. Chem.* **2013**, *288*, 5475–5486. [CrossRef]
39. Barb, A.W.; Zhou, P. Mechanism and inhibition of LpxC. An essential zinc-dependent deacetylase of bacterial lipid A synthesis. *Curr. Pharm. Biotech.* **2008**, *9*, 9–15. [CrossRef]
40. Kitagawa, M.; Ara, T.; Arifuzzaman, M.; Ioka-Nakamichi, T.; Inamoto, E.; Toyonaga, H.; Mori, H. Complete set of ORF clones of *Escherichia coli* ASKA library (a complete set of *E. coli* K-12 ORF archive): Unique resources for biological research. *DNA Res.* **2005**, *12*, 291–299. [CrossRef]
41. Rohrwild, M.; Coux, O.; Huang, H.C.; Moerschell, R.P.; Yoo, S.J.; Seol, J.H.; Chung, C.H.; Goldberg, A.L. HslV-HslU: A novel ATP-dependent protease complex in *Escherichia coli* related to the eukaryotic proteasome. *Proc. Natl. Acad. Sci. USA* **1996**, *93*, 5808–5813. [CrossRef]
42. Chuang, S.E.; Blattner, F.R. Characterization of twenty-six new heat shock genes of *Escherichia coli*. *J. Bacteriol.* **1993**, *175*, 5242–5252. [CrossRef] [PubMed]
43. Rechsteiner, M.; Hoffman, L.; Dubiel, W. The multicatalytic and 26 S proteases. *J. Biol. Chem.* **1993**, *268*, 6065–6068. [PubMed]
44. Bochtler, M.; Ditzel, L.; Groll, M.; Huber, R. Crystal structure of heat shock locus V (HslV) from *Escherichia coli*. *Proc. Natl. Acad. Sci. USA* **1997**, *94*, 6070–6074. [CrossRef] [PubMed]
45. Raina, S.; Georgopoulos, C. A new *Escherichia coli* heat shock gene, *htrC*, whose product is essential for viability only at high temperatures. *J. Bacteriol.* **1990**, *172*, 3417–3426. [CrossRef]

46. Hirvas, L.; Nurminen, M.; Helander, I.M.; Vuorio, R.; Vaara, M. The lipid A biosynthesis deficiency of the *Escherichia coli* antibiotic-supersensitive mutant LH530 is suppressed by a novel locus, ORF195. *Microbiology* **1997**, *143*, 73–81. [CrossRef]
47. Dong, H.; Zhang, Z.; Tang, X.; Huang, S.; Li, H.; Peng, B.; Dong, C. Structural insights into cardiolipin transfer from the inner membrane to the outer membrane by PbgA in Gram-negative bacteria. *Sci. Rep.* **2016**, *6*, 30815. [CrossRef]
48. Fan, J.; Petersen, E.M.; Hinds, T.R.; Zheng, N.; Miller, S.I. Structure of an inner membrane protein required for PhoPQ-regulated increases in outer membrane cardiolipin. *mBio* **2020**, *11*, e03277-19. [CrossRef]
49. Lee, C.J.; Liang, X.; Gopalaswamy, R.; Najeeb, J.; Ark, E.D.; Toone, E.J.; Zhou, P. Structural basis of the promiscuous inhibitor susceptibility of *Escherichia coli* LpxC. *ACS Chem. Biol.* **2014**, *9*, 237–246. [CrossRef]
50. Müller-Loennies, S.; Brade, L.; MacKenzie, C.R.; Di Padova, F.E.; Brade, H. Identification of a cross-reacting epitope widely present in lipopolysaccharide from enterobacteria and recognized by the cross-protective monoclonal antibody WN1 222-5. *J. Biol. Chem.* **2003**, *278*, 25618–25627. [CrossRef]
51. Langklotz, S.; Schäkermann, M.; Narberhaus, F. Control of lipopolysaccharide biosynthesis by FtsH-mediated proteolysis of LpxC is conserved in enterobacteria but not in all gram-negative bacteria. *J. Bacteriol.* **2011**, *193*, 1090–1097. [CrossRef] [PubMed]
52. Mostafavi, M.; Wang, L.; Xie, L.; Takeoka, K.T.; Richie, D.L.; Casey, F.; Ruzin, A.; Sawyer, W.S.; Rath, C.M.; Wei, J.R.; et al. Interplay of *Klebsiella pneumoniae fabZ* and *lpxC* mutations leads to LpxC inhibitor-dependent growth resulting from loss of membrane homeostasis. *mSphere* **2018**, *3*, e00508–e00518. [CrossRef] [PubMed]
53. Karata, K.; Inagawa, T.; Wilkinson, A.J.; Tatsuta, T.; Ogura, T. Dissecting the role of a conserved motif (the second region of homology) in the AAA family of ATPases. Site-directed mutagenesis of the ATP-dependent protease FtsH. *J. Biol. Chem.* **1999**, *274*, 26225–26232. [CrossRef] [PubMed]
54. Krzywda, S.; Brzozowski, A.M.; Verma, C.; Karata, K.; Ogura, T.; Wilkinson, A.J. The crystal structure of the AAA domain of the ATP-dependent protease FtsH of *Escherichia coli* at 1.5 Å resolution. *Structure* **2002**, *10*, 1073–1083. [CrossRef]
55. Emiola, A.; Andrews, S.S.; Heller, C.; George, J. Crosstalk between the lipopolysaccharide and phospholipid pathways during outer membrane biogenesis in *Escherichia coli*. *Proc. Natl. Acad. Sci. USA* **2016**, *113*, 3108–3113. [CrossRef]
56. Schäkermann, M.; Langklotz, S.; Narberhaus, F. FtsH-mediated coordination of lipopolysaccharide biosynthesis in *Escherichia coli* correlates with the growth rate and the alarmone (p)ppGpp. *J. Bacteriol.* **2013**, *195*, 1912–1919. [CrossRef]
57. Basta, D.W.; Angeles-Albores, D.; Spero, M.A.; Ciemniecki, J.A.; Newman, D.K. Heat-shock proteases promote survival of *Pseudomonas aeruginosa* during growth arrest. *Proc. Natl. Acad. Sci. USA* **2020**, *117*, 4358–4367. [CrossRef]
58. Fanelli, F.; Di Pinto, A.; Mottola, A.; Mule, G.; Chieffi, D.; Baruzzi, F.; Tantillo, G.; Fusco, V. Genomic characterization of *Arcobacter butzleri* isolated from shellfish: Novel insight into antibiotic resistance and virulence determinants. *Front. Microbiol.* **2019**, *10*, 670. [CrossRef]
59. Betton, J.M.; Boscus, D.; Missiakas, D.; Raina, S.; Hofnung, M. Probing the structural role of an αβ loop of maltose-binding protein by mutagenesis: Heat-shock induction by loop variants of the maltose-binding protein that form periplasmic inclusion bodies. *J. Mol. Biol.* **1996**, *262*, 140–150. [CrossRef]
60. Schweiger, R.; Soll, J.; Jung, K.; Heermann, R.; Schwenkert, S. Quantification of interaction strengths between chaperones and tetratricopeptide repeat domain-containing membrane proteins. *J. Biol. Chem.* **2013**, *288*, 30614–30625. [CrossRef]
61. Zeytuni, N.; Zarivach, R. Structural and functional discussion of the tetra-trico-peptide repeat, a protein interaction module. *Structure* **2012**, *20*, 397–405. [CrossRef] [PubMed]
62. Perez-Riba, A.; Itzhaki, L.S. The tetratricopeptide-repeat motif is a versatile platform that enables diverse modes of molecular recognition. *Curr. Opin. Struct. Biol.* **2019**, *54*, 43–49. [CrossRef] [PubMed]
63. Williamson, J.C.; Edwards, A.V.; Verano-Braga, T.; Schwämmle, V.; Kjeldsen, F.; Jensen, O.N.; Larsen, M.R. High-performance hybrid Orbitrap mass spectrometers for quantitative proteome analysis: Observation and implications. *Proteomics* **2016**, *16*, 907–914. [CrossRef] [PubMed]
64. Guzmán-Flores, J.E.; Steinemann-Hernández, L.; González de la Vara, L.E.; Gavilanes-Ruiz, M.; Romeo, T.; Alvarez, A.F.; Georgellis, D. Proteomic analysis of *Escherichia coli* detergent-resistant membranes (DRM). *PLoS ONE* **2019**, *14*, e0223794. [CrossRef]

65. Datsenko, K.A.; Wanner, B.L. One-step inactivation of chromosomal genes in *Escherichia coli* K-12 using PCR products. *Proc. Natl. Acad. Sci. USA* **2000**, *97*, 6640–6645. [CrossRef]
66. Dartigalongue, C.; Loferer, H.; Raina, S. EcfE, a new essential inner membrane protease: Its role in the regulation of heat shock response in *Escherichia coli*. *EMBO J.* **2001**, *20*, 5908–5918. [CrossRef]
67. Raina, S.; Georgopoulos, C. The *htrM* gene, whose product is essential for *Escherichia coli* viability only at elevated temperatures, is identical to the *rfaD* gene. *Nucleic Acids Res.* **1991**, *19*, 3811–3819. [CrossRef]
68. Galanos, C.; Lüderitz, O.; Westphal, O. A new method for the extraction of R lipopolysaccharides. *Eur. J. Biochem.* **1969**, *9*, 245–249. [CrossRef]
69. Kondakova, A.; Lindner, B. Structural characterization of complex bacterial glycolipids by Fourier-transform mass spectrometry. *Eur. J. Mass Spectrom.* **2005**, *11*, 535–546. [CrossRef]
70. Raina, S.; Missiakas, D.; Baird, L.; Kumar, S.; Georgopoulos, C. Identification and transcriptional analysis of the *Escherichia coli htrE* operon which is homologous to pap and related pilin operons. *J. Bacteriol.* **1993**, *175*, 5009–5021. [CrossRef]
71. Wojtkiewicz, P.; Biernacka, D.; Gorzelak, P.; Stupak, A.; Klein, G.; Raina, S. Multicopy suppressor analysis of strains lacking cytoplasmic peptidyl-prolyl cis/trans isomerases identifies three new PPIase activities in *Escherichia coli* that includes the DksA transcription factor. *Int. J. Mol. Sci.* **2020**, *21*, 5843. [CrossRef] [PubMed]

International Journal of
Molecular Sciences

MDPI

Article

Multicopy Suppressor Analysis of Strains Lacking Cytoplasmic Peptidyl-Prolyl *cis/trans* Isomerases Identifies Three New PPIase Activities in *Escherichia coli* That Includes the DksA Transcription Factor

Pawel Wojtkiewicz, Daria Biernacka, Patrycja Gorzelak, Anna Stupak, Gracjana Klein * and Satish Raina *

Unit of Bacterial Genetics, Gdansk University of Technology, Narutowicza 11/12, 80-233 Gdansk, Poland; pawwojtk1@student.pg.edu.pl (P.W.); darbiern@student.pg.edu.pl (D.B.); patrycja.gorzelak@gmail.com (P.G.); anna.stupak@pg.edu.pl (A.S.)

* Correspondence: gracjana.klein@pg.edu.pl (G.K.); satish.raina@pg.edu.pl (S.R.); Tel.: +48-58-347-2618 (G.K. & S.R.)

Received: 17 July 2020; Accepted: 13 August 2020; Published: 14 August 2020

Abstract: Consistent with a role in catalyzing rate-limiting step of protein folding, removal of genes encoding cytoplasmic protein folding catalysts belonging to the family of peptidyl-prolyl *cis/trans* isomerases (PPIs) in *Escherichia coli* confers conditional lethality. To address the molecular basis of the essentiality of PPIs, a multicopy suppressor approach revealed that overexpression of genes encoding chaperones (DnaK/J and GroL/S), transcriptional factors (DksA and SrrA), replication proteins Hda/DiaA, asparatokinase MetL, Cmk and acid resistance regulator (AriR) overcome some defects of Δ6*ppi* strains. Interestingly, viability of Δ6*ppi* bacteria requires the presence of transcriptional factors DksA, SrrA, Cmk or Hda. DksA, MetL and Cmk are for the first time shown to exhibit PPIase activity in chymotrypsin-coupled and RNase T1 refolding assays and their overexpression also restores growth of a Δ(*dnaK/J/tig*) strain, revealing their mechanism of suppression. Mutagenesis of DksA identified that D74, F82 and L84 amino acid residues are critical for its PPIase activity and their replacement abrogated multicopy suppression ability. Mutational studies revealed that DksA-mediated suppression of either Δ6*ppi* or Δ*dnaK/J* is abolished if GroL/S and RpoE are limiting, or in the absence of either major porin regulatory sensory kinase EnvZ or RNase H, transporter TatC or LepA GTPase or P_i-signaling regulator PhoU.

Keywords: prolyl isomerase; protein folding; RNA polymerase; DksA; heat shock proteins; DnaK/J; GroL/S; RpoE sigma factor; RNase H; LepA

1. Introduction

To be functionally active, all newly synthesized polypeptides must rapidly fold into their native three-dimensional structure. It is now established that, right from the synthesis of a polypeptide from its nascent chain stage until it achieves its native structure, its maturation is to a large extent dependent on several factors. In bacteria, e.g., *Escherichia coli*, as well as in other organisms, these factors are molecular chaperones and folding catalysts, whose requirements vary, depending on the individual functional or folding requirement of client protein(s). In the cytosol, despite the molecular crowding, productive folding in the cell is achieved via some common strategies. Partially folded protein segments are bound by molecular chaperones to prevent their aggregation/misfolding and critical slow folding steps are accelerated by folding catalysts such as peptidyl-prolyl *cis/trans* isomerases (PPIs) and

thiol-disulfide oxidoreductases, belonging to the protein disulfide isomerase (PDI) family, to reduce the accumulation of aggregation-prone folding intermediates [1,2].

Most of the peptide bonds in proteins are present in the *trans* configuration, since *trans* isomers are energetically more favorable than *cis* ones. However, proline is one exception, since it is an *N*-alkylated amino acid that creates an imidic peptide bond [3]. For the peptide bonds preceding proline, steric hindrance is comparable between two isomers. They are nearly isoenergetic (about 0.5 kcal/mol of free energy difference) and hence both conformations are thermodynamically possible [4,5]. Globally, around 7% proline residues are present in the *cis* conformation in different proteins in all three domains of life [6]. However, nonnative form of prolyl bond in a polypeptide chain can retard the completion of folding 10^3–10^6-fold [7]. PPIs are the only enzymes known thus far that can stabilize the transition state (high-energy state with ω around 90°) separated from the ground state by a difference in a torsional angle [3–7]. Thus, there is a requirement for PPIs to accelerate reactions that are rate-limited by the prolyl bond isomerization. PPIs are ubiquitous enzymes present in all organisms, virtually in all cell compartments and three families are known: the cyclophilins [8], the FK506-binding proteins (FKBPs) [9] and the parvulins [10]. The *E. coli* cytoplasm contains six PPIs, which cover all three families. However, their in vivo physiological requirement and specific substrates that require the PPIase activity have not been fully addressed.

We recently described the construction of strains devoid of all PPIs and showed that strains lacking all six cytoplasmic PPIs exhibit the synthetic lethality at high and low temperatures in rich medium [1]. Such Δ6*ppi* bacteria elicit a high propensity to accumulate proteins in the aggregation state and their identity revealed defects in folding of proteins involved in several essential processes. These include transcriptional-related proteins such as RNA polymerase subunits, the termination factor Rho, enzymes involved in metabolic processes and protein synthesis and those related to oxidative stress and DNA repair system. Several proteins that were identified to aggregate in Δ6*ppi* bacteria were found to be common to known aggregation-prone proteins in strains lacking the DnaK/J chaperone system [1]. Interestingly, measurement of the PPIase activity of a strain lacking all ten PPIs revealed a residual PPIase activity, suggesting the presence of some previously unknown PPI(s) [1].

In this work, we used stringent high temperature and cold sensitive phenotypes of Δ6*ppi* bacteria to isolate multicopy suppressors that rescue some of their phenotypic defects (Figure 1). The results of such experiments reveal that overexpression of major chaperone systems (GroL/S and DnaK/J), transcriptional factors (DksA and SrrA), the cytidylate kinase Cmk and the aspartokinase MetL restored the growth of Δ6*ppi* strains under non-permissive growth conditions (Figure 1). Interestingly, DksA, Cmk and MetL were shown to exhibit the PPIase activity as well as suppress growth defects of a Δ(*dnaK/J tig*) strain. This PPIase activity was inhibited by the FK506 macrolide and mutations abrogating DksA's PPIase activity were identified and shown to be defective in suppressing growth defects of Δ6*ppi* and Δ(*dnaK/J tig*) derivatives under non-permissive growth conditions. We further performed saturated mutagenesis in a *dksA*-overexpressing strain to isolate *trans*-acting mutations that block the multicopy suppression by DksA of Δ6*ppi* and Δ(*dnaK dnaJ*) strains, revealing a requirement for the intact GroL/S chaperone system, the RpoE sigma factor, the RNase H involved in genome integrity, the translation GTPase LepA and the TatC protein involved in protein translocation (Figure 1).

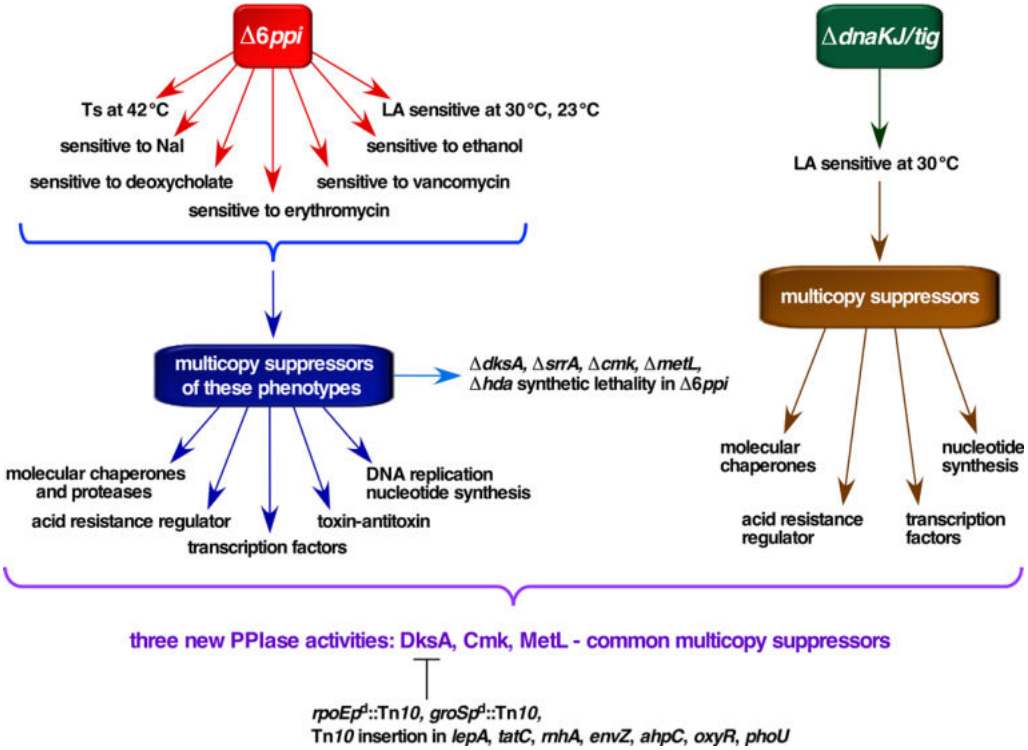

Figure 1. Schematic presentation of approach employed to identify factors that are limiting in Δ6*ppi* and Δ(*dnaK/J tig*) bacteria using multicopy suppressor approach. This identified several factors, whose overexpression can rescue their lethal phenotype. This identified transcription factor DksA, aspartokinase MetL and cytidylate kinase Cmk as common factors whose overproduction can restore growth and these factors also exhibit peptidyl *cis*/*trans* prolyl isomerase activity. Further, DksA-mediated suppression requires wild-type levels of GroL/S and RpoE, and it is abolished when either genome integrity is compromised in the absence of RNase H or in the absence of translational GTPase LepA or when cell envelope homeostasis is dysfunctional.

2. Results

2.1. Δ6ppi Mutant Bacteria Exhibit the Sensitivity towards Antibiotics, Membrane-Destabilizing Factors and the DNA-Damaging Agent Nalidixic Acid

It has been demonstrated that collectively the cytoplasmic PPIase activity is essential for the bacterial viability under optimal growth conditions [1]. To further understand the molecular basis of essentiality of cytoplasmic PPIs in *E. coli*, we examined growth properties and various defects exhibited by strains lacking six cytoplasmic PPIs. Besides cold- and temperature-sensitive phenotypes, Δ6*ppi* bacteria also reveal the sensitivity to mild challenge with ethanol (4%), membrane-destabilizing factors such as SDS (1%), deoxycholate (0.75%), vancomycin (60 μg/mL), erythromycin (12 μg/mL) and tetracycline (1.5 μg/mL) and aminoglycosides such as kanamycin (2 μg/mL) (Table 1). Quite strikingly, Δ6*ppi* bacteria exhibit hypersensitivity to the DNA-damaging agent nalidixic acid (Nal) (inability to grow above 2 μg/mL) on either M9 minimal medium or Luria Agar (LA) medium at 37 °C as compared to a Δ5*ppi* Δ(*ppiB fklB tig slyD ppiC*) strain (Figure 2). Nal is known to introduce both DNA-protein adducts and double-strand breaks by targeting the DNA gyrase and stabilizes gyrase-DNA cleavage complexes [11]. Such adducts can cause a barrier to DNA replication, transcription and chromosomal fragmentation [12]. The sensitivity of Δ6*ppi* bacteria to Nal suggests that PPIs might be required for folding of some components of the DNA replication/repair system and transcriptional apparatus. Overall, these results lead us to conclude that the PPIase activity is essential for the optimal growth and maintenance of the genome integrity.

Table 1. The sensitivity of a Δ6*ppi* derivative on M9 medium supplemented with different agents at 37 °C. Exponentially grown cultures were adjusted to an optical density OD_{600} of 0.2 and spot diluted. Numbers indicate the colony forming units of a Δ6*ppi* derivative as compared to the wild type.

Strain	Ethanol 4%	SDS 1%	Deoxycholate 0.75%	Vancomycin 60 μg/mL	Erythromycin 12 μg/mL	Tetracycline 1.5 μg/mL	Kanamycin 2 μg/mL
wild type	8×10^8	3×10^8	6×10^8	2×10^8	6×10^8	3×10^8	7×10^8
Δ6*ppi*	2×10^2	3×10^2	-	-	-	3×10^2	1×10^2

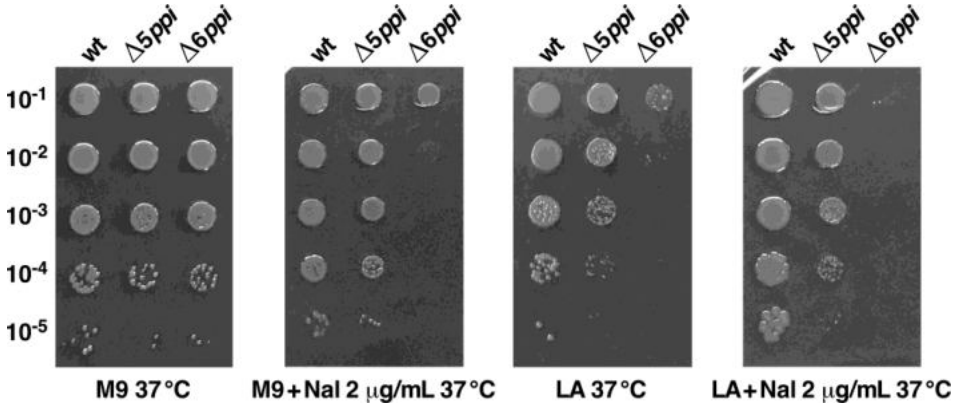

Figure 2. Δ6*ppi* bacteria exhibit the sensitivity to nalidixic acid (Nal) on either M9 minimal medium or Luria Agar (LA) medium. Exponentially grown cultures of the wild type and its isogenic Δ5*ppi* and Δ6*ppi* derivatives were adjusted to an optical density OD_{600} of 0.1 and serially spot diluted on M9 minimal medium and LA medium with or without supplementation with 2 μg/mL Nal. Plates were incubated at 37 °C for 24 h. Data presented are from one of the representative experiments.

2.2. Factors Limiting for the Viability of Δ6ppi Mutant Bacteria

We recently reported the construction of suppressor-free strains lacking all six cytoplasmic PPIs and showed that such bacteria are viable on M9 minimal medium at 37 °C, but unable to grow on rich medium at either low temperature (23 °C) or at temperatures above 37 °C [1]. To understand the molecular basis of growth defects of Δ6*ppi* mutant bacteria, a multicopy suppressor approach was undertaken in the Δ6*ppi* strain, using phenotypic defects such as the temperature-sensitive (Ts) phenotype and those with sensitivity towards detergents, ethanol, vancomycin and erythromycin. Two different multicopy libraries were employed. In one approach, plasmid DNA pools from the ASKA collection of single ORFs expressed from the tightly regulated IPTG-inducible P_{T5}-*lac* promoter in the vector pCA24N [13] were introduced into the Δ6*ppi* strain SR18292. Transformants were selected for the restoration of growth on LA medium supplemented by 75 μM IPTG at different non-permissive growth conditions. The concentration of IPTG used for the controlled induction of expression of different genes was optimized as reported earlier [14,15]. In the second approach, a plasmid library in a p15A-based vector was constructed and upon transformation used to select for multicopy suppressors [16]. This library was constructed from the genomic DNA of Δ6*ppi* bacteria and introduced into the strain SR18292, selecting for the restoration of growth under non-permissive growth conditions. The construction of this library was necessitated to enrich the selection and allow cloning of those genes, which are organized as operons and whose products work together. The plasmid DNA was isolated from obtained suppressing clones and used to retransform the parental Δ6*ppi* strain to confirm the restoration of growth under non-permissive growth conditions. DNA sequence analysis identified several genes, whose overexpression allowed the growth on rich medium (at either high or low temperature) and suppressed the sensitivity towards different agents albeit to a different extent (Table 2). The extent of suppression was quantified by spot-dilution assays under different growth conditions in the presence of 75 μM IPTG as an inducer of gene expression, when plasmids from

the ASKA collection were used (Figure 3). Some of the prominent genes encode well-characterized members of protein folding machinery (DnaK/J, GroL/S) (Table 2).

Table 2. Multicopy suppressors that restore the growth of Δ6*ppi* strains under different conditions.

	Growth conditions							
Gene	**LA 23 °C**	**LA 30 °C**	**LA 37 °C**	**LA 42 °C**	**LA 43.5 °C**	**V/Et/Er**	**M9 42 °C**	**Function**
metL	+ [a]	+	+	+	+	+ V/Er	+ sc	aspartokinase
dksA	-	-	± [b]	+	+	- [c]	+	transcription
srrA	-	+ sc	+	+	+	+ Et	+	transcription
yjfN	-	+ sc	+	+	+	+ Er	+	proteolytic
cmk	+	+	+	+	±	+ Et/Er/V	+	DNA synthesis
hda	+	+	+ sc	-	-	+ Et/Er	+	replication
diaA	+	+	+	-	-	+ Et/Er	+	replication
dnaK/J	+	+	+	+	±	NT	-	chaperone
groL/S	-	± sc	+	+	±	NT	+	chaperonin
mqsA	-	+	+	+	±	+ Er	+	antitoxin
yceD	-	±	+	-	-	+ V	±	stress response
ariR	+	+	+	+	+	+ Er	+ sc	stress response
pepA	+	+	+	+	+ sc	-	±	proteolytic
bcr	+	+	+	-	-	+ Et/Er	-	peptide transport
cspC	-	±	+	+ sc	+ sc	-	+	stress response
hha	-	-	-	-	-	+ Er	+	transcription with *mqs*
mppA	+	+	± sc	-	-	+ V/Er	-	murein binding
ycaD	+	+	+ sc	-	-	+ V/Er	-	transport
murI	+ sc	±	+	-	-	+ Et/Er/V	-	peptidoglycan
nudE	-	+	+	-	-	+ Et/Er	-	nudix
nudJ	+	+	±	-	-	-	-	nudix
yigB	+	+	-	-	-	-	-	riboflavin
ycjW	-	-	+	-	-	+ Er	-	transcription
gadW	± sc	±	± sc	-	-	+ Er	-	acid resistance
ydgC	+	+	+	±	-	+ Er	-	GlpM family
yhaM	-	-	+	-	-	-	-	cysteine detoxification
preT	-	-	+	-	-	-	-	pyrimidine metabolism

Additional suppressors, which restored the growth by 10-fold on LA at 37 °C (±), include *hchA*, *hslO*, *ilvB*, *rluB*, *cspH*, *argA*, *msyB*, *ddpF* and *intQ*. However, the *msyB* gene was also isolated as a multicopy suppressor for the growth on M9 minimal medium with glycerol as the sole carbon source. +[a] indicates the wild type-like growth efficiency of plating close to 1. ±[b] indicates up to 50% growth as compared to the wild type. -[c] indicates the inability to support the colony forming capacity. Note overexpression of *dnaK/J* and *groS/L* genes restores the growth at 42 °C, but not above 43 °C. sc, small colonies; NT, not tested; V, vancomycin (75 μg/mL); Et, ethanol (4.5%); Er, erythromycin (15 μg/mL).

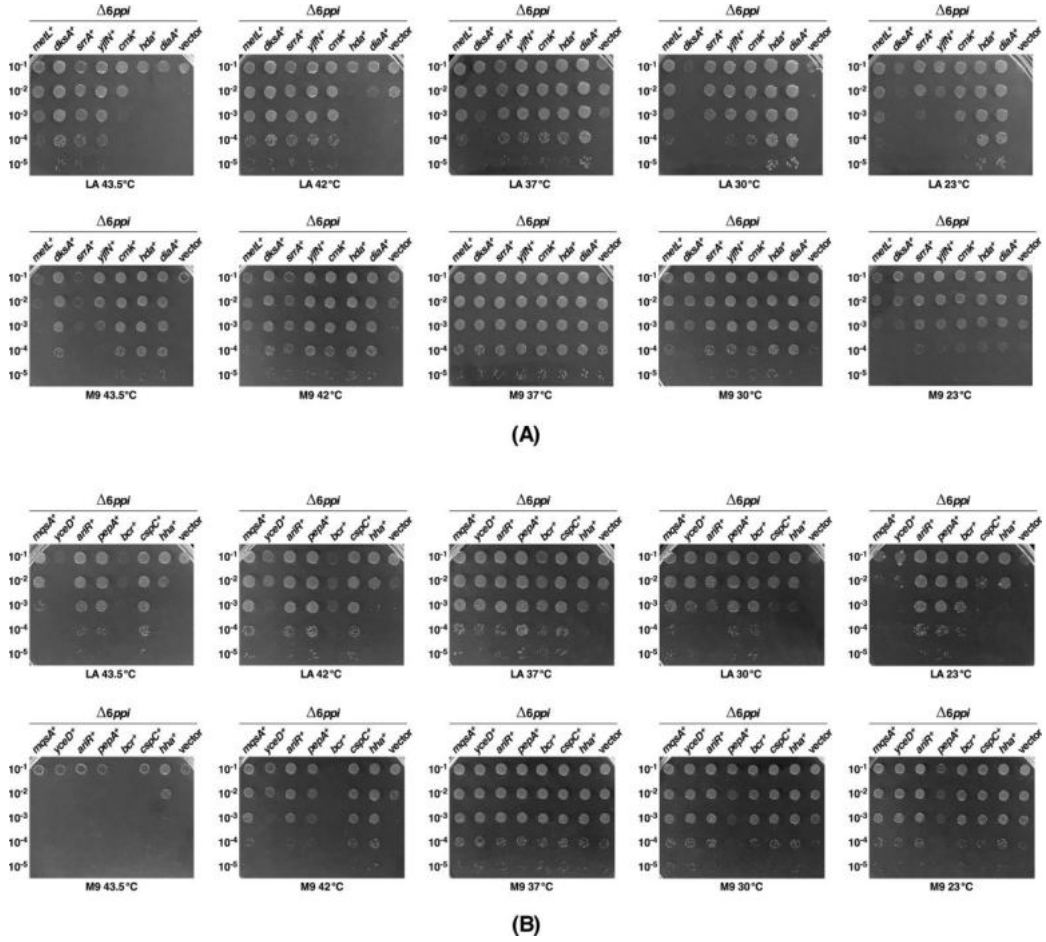

Figure 3. Identification of genes whose overexpression can restore the growth of Δ6*ppi* bacteria at different temperatures. Exponentially grown cultures of the wild type and its isogenic Δ6*ppi* derivatives transformed with either the vector pCA24N or the same vector expressing a specific gene under the control of IPTG-inducible promoter were grown at 37 °C in M9 minimal medium. Cultures were washed and adjusted to an optical density OD_{600} of 0.1 and serially spot diluted on M9 minimal medium and LA medium in the presence of 75 μM IPTG. (**A**,**B**) The growth of different strains expressing a specific gene with the indicated genotype, whose overexpression confers a varying degree of suppression depending upon temperature of incubation and growth medium.

Other multicopy suppressor-encoding genes include predicted or known transcription regulators [*dksA*, *srrA* (*yheO*), *ariR*, *ycjW*], an antitoxin *mqsA* and its potential interacting partner *hha*, while others are involved in DNA replication (*diaA*, *hda*), DNA/RNA synthesis (*cmk*), stress response and acid resistance (*ariR*, *gadW*, *yceD*, *cspC*), amino acid biosynthesis (*metL*), proteolytic turnover (*yjfN*, *pepA*), peptide transport (*bcr*, *mppA*, *ddpF*), peptidoglycan biosynthesis (*murI*) and nudix protein-encoding genes *nudE* and *nudG* (Table 2, Figure 3 and Supplementary Figure S1). At high temperature (42 °C), *dnaK/J* and *groS/L* operons, *dksA*, *srrA*, *yjfN*, *mqsA*, *ariR*, *pepA* and *cspC* were found to be major suppressors, whose overexpression restored the growth on rich medium with the efficiency of plating nearly to the wild-type level as determined by spot-dilution assays (Table 2, Figures 3 and 4A).

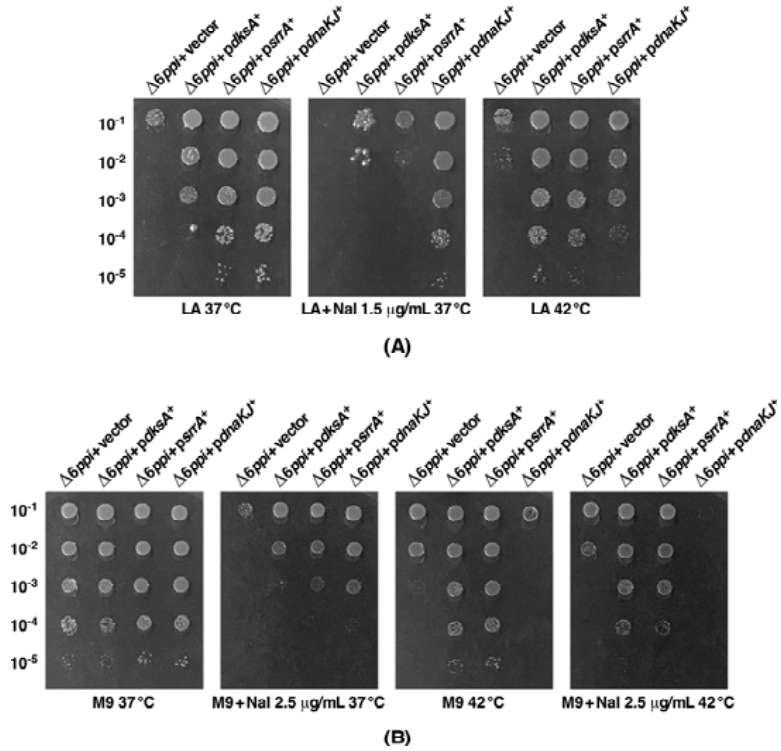

Figure 4. Overexpression of either the *dksA* gene or the *srrA* gene or the *dnaK/J* operon can rescue the sensitivity of Δ6*ppi* bacteria to nalidixic acid (Nal) to varying levels depending upon growth conditions. Exponentially grown cultures of the wild type and its isogenic Δ6*ppi* derivatives transformed with the vector pCA24N alone, the plasmid expressing either the *dksA* gene or the *srrA* gene or the *dnaK/J* operon were grown as described in the legend to Figure 3 and the bacterial growth measured on either LA medium (**A**) or on M9 medium (**B**) at indicated temperature. The concentration of Nal, when added to growth medium, is depicted. For the induction of gene expression, 75 μM IPTG was added.

Among these, overexpression of *dksA*, *srrA*, *metL*, *cspC* and *yjfN* restored the wild type-like growth even up to 43.5 °C, conditions at which overexpression of either the *dnaK/J* or the *groS/L* genes confer only a partial suppression (Figure 3, Table 2 and Supplementary Table S1). Among various multicopy suppressors, overexpression of the *metL* gene encoding the aspartokinase II uniquely restored the wild type-like growth at low and high temperatures on LA medium (Figure 3). However, on M9 minimal medium at 43.5 °C, the *metL* overexpression does not provide the same relief as was observed on LA medium, although at 42 °C the restoration of growth of Δ6*ppi* bacteria was nearly to the wild-type level in either LA or M9 medium. The *srrA* gene is annotated as the *yheO* ORF with the unknown function. However, sequence examination of its coding sequence predicts it to be a DNA-binding transcriptional regulator and was designated SrrA (Stress Response Regulator A) based upon further characterization. It is worth noting that in multicopy the *dksA* gene does not exert any noTable Suppression at 37 °C or below, although it restores the growth at 43.5 °C with the efficiency of plating close to the wild type (Table 2 and Figures 3 and 4). At low temperatures such as 23 or 30 °C, overexpression of *diaA*, *hda*, *ariR*, *pepA* and *ydgC* genes restored the wild type-like growth (Figure 3 and Supplementary Figure S1). Other multicopy suppressors that partially overcome the conditional lethality of Δ6*ppi* bacteria include products of heat shock genes such as Hsp33 and HchA, the cysteine detoxification protein YhaM and the RluB pseudouridine synthase (Table 2).

Regarding the suppression of sensitivity to erythromycin (15 μg/mL), ethanol (4.5%) and vancomycin (75 μg/mL), a multicopy plasmid library was used as described above, selecting for the restoration of growth of Δ6*ppi* bacteria on M9 minimal medium at 37 °C in the presence of either of these agents. DNA sequence analysis of suppressing clones after retransformation revealed that overexpression of *cmk*, *srrA*, *hda*, *diaA*, *bcr*, *murI* and *ddpF* nearly restored the wild type-like growth of

Δ6*ppi* bacteria on M9 minimal medium at 37 °C in the presence of supplemented ethanol (4.5%) in the growth medium (Table 2). Interestingly, *metL*, *hda*, *srrA*, *cmk*, *yjfN* and *bcr* genes were again identified in the independent selection of multicopy suppressors for the restoration of growth in the presence of erythromycin antibiotic, in addition to *ariR*, *gadW*, *ycjW*, *mppA* and *murI* genes (Table 2). Concerning the selection of multicopy suppressors for the vancomycin sensitivity, *diaA*, *srrA*, *cmk*, *metL*, *yceD*, *mppA* and *murI* were cloned in this selection (Table 2). Interestingly, we also cloned the *eptB* gene, whose product is required for the modification of inner core of lipopolysaccharide by phosphoethanolamine [17], as a multicopy suppressor for the suppression of vancomycin sensitivity. Thus, several genes such as *srrA*, *hda*, *diaA*, *metL* and *cmk* were cloned in multiple approaches that overcome several defects of Δ6*ppi* bacteria and hence identify factors that are limiting in such PPIs-lacking bacteria.

2.3. Overexpression of Either the srrA Gene or the dksA Gene Suppresses the Sensitivity of Δ6ppi Bacteria to Nal

As Δ6*ppi* bacteria exhibit hypersensitivity to Nal, we tested if any of the major multicopy suppressors can also restore the growth on medium supplemented with Nal. Towards this goal, we mainly tested the effect of overexpression of *dksA*, *srrA* and *dnaK/J*, since they are among the most prominent multicopy suppressors of growth defects of Δ6*ppi* bacteria (Figures 3 and 4A and Table 2). At 37 °C, overexpression of either *dnaK/J* or *srrA* genes restored the growth of Δ6*ppi* bacteria on M9 medium supplemented with 2.5 μg/mL of Nal nearly to the wild-type level, thereby suppressing the Nal-sensitivity phenotype (Figure 4B). In LA medium, when supplemented with 1.5 μg/mL of Nal, only overexpression of *dnaK/J* was able to suppress the Nal sensitivity at 37 °C (Figure 4A). However, at 42 °C, overexpression of either the *dksA* or the *srrA* gene could rescue the growth on M9 medium supplemented with Nal (Figure 4B). These results thus allow us to conclude that the Nal sensitivity can be overcome by overexpression of either *dksA* or *srrA* genes and only partly by overexpressing *dnaK/J* genes up to a temperature of 37 °C.

2.4. The Essentiality of DksA, SrrA, MetL and Hda for the Viability of Δ6ppi Bacteria and Synthetic Growth Defects with Δcmk and ΔhchA

If indeed any of the products of genes encoding different multicopy suppressors identified in above studies are limiting for the growth of Δ6*ppi* bacteria was investigated by introducing deletion mutations of their cognate genes in the Δ6*ppi* strain. The results of such experiments reveal that *dksA*, *srrA*, *metL* and *hda* genes are indispensable for the growth of Δ6*ppi* bacteria such as SR18292 as their deletion combinations were lethal (Table 3). The deletion of either the *dksA* gene or the *srrA* gene or the *hda* gene or the *metL* gene could be introduced in Δ6*ppi* bacteria on LA medium at 37 °C only if the wild-type copy of the corresponding gene was present on the plasmid. However, it is worth noting that a deletion of the *metL* gene can be tolerated on M9 minimal medium (supplemented by 0.2% casamino acids), but not of either the *srrA* gene or the *dksA* gene in the Δ6*ppi* background. Supplementation of casamino acids was necessary, since Δ*dksA* bacteria being auxotrophic do not grow on minimal medium without amino acids. A Δ*hchA* mutation could be introduced into SR18292 on M9 minimal medium. Even on M9 minimal medium Δ(6*ppi hchA*) bacteria form small colonies and further exhibit synthetic growth defects (attenuated growth on LA medium with small colonies after the prolonged incubation of more than 24 h at 37 °C) (Table 3). Among other deletion derivatives of multicopy-suppressing genes, Δ(6*ppi cmk*) transductants were obtained only after the incubation of more than 48 h (Table 3) and hence Cmk is also a limiting factor. The lack of either Hda or Cmk in Δ6*ppi* bacteria could exacerbate DNA replication/synthesis defects and can account for the lethality and synthetic growth defects.

Table 3. The essentiality of *dksA*, *srrA*, *hda*, *cmk*, *metL* genes and a partial requirement for HchA in Δ6*ppi* strains.

Number of Transductants in Δ6*ppi* Strains Obtained Either in the Presence or Absence of Covering Wild-Type Plasmid-Born Gene		
Gene	BW25113 LA/M9 + CAA 37 °C	MC4100 LA/M9 + CAA 37 °C
Δ*hda*	9	6
Δ*hda* +p*hda*$^+$	1234	1146
Δ*dksA*	8 *	small non-viable colonies
Δ*dksA*+p*dksA*$^+$	1436	1598
srrA	7	455 small colonies after 48 h, cold sensitive at 23 °C and 30 °C
srrA+p*srrA*$^+$	1255	1376
metL	11 *	23
metL+p*metL*$^+$	1830	1941
cmk	136 small colonies after 48 h	254 small colonies after 48 h
cmk+p*cmk*$^+$	1575	945
hchA	312 small colony size	380 after 48 h (however, viable on M9)
hchA+p*hchA*$^+$	1174	1470

* Additional non-viable transductants obtained when either Δ*dksA* or Δ*metL* were introduced, which do not grow upon streaking. Note viable very small colony-sized transductants were obtained at the normal frequency, when Δ*ariR*, Δ*cspC*, Δ*pepA* or Δ*ycjW* were introduced in the Δ6*ppi* background after 24 h incubation. The comparable transductional frequency with or without covering the plasmid obtained when either Δ*diaA* or Δ*yjfN* were introduced. CAA indicates supplementation of minimal medium by 0.2% casamino acids.

To reinforce the results of the essentiality of the *dksA* gene in Δ6*ppi* bacteria, a strain SR20355 (*dksA*::cm *htrE*::tet) was constructed. This strain served as a donor in bacteriophage P1-mediated transductions to score for co-transduction of *dksA* and *htrE* null alleles in the wild type and its Δ6*ppi* derivative SR18292. The *htrE* gene is >90% linked to the *dksA* gene [18]. The deletion of the *htrE* gene does not confer any growth phenotype at 37 °C in either the wild type or its Δ6*ppi* derivative and could be transduced at the same frequency in both strains (Table 4). However, none of the *htrE*::tet^R transductants were found to carry *dksA*::cm in Δ6*ppi*, while >90% of tet^R transductants in the wild type were of the (*htrE*::tet^R *dksA*::cm) genotype (Table 4). These genetic experiments unambiguously prove that the *dksA* gene is indispensable for the viability of Δ6*ppi* bacteria.

Table 4. The essentiality of the *dksA gene* in Δ6*ppi* as determined by the linked *htrE* mutation.

Number of Transductants with Selection for Tetracycline Resistance		
Donor	**Recipient**	
	BW25113	Δ6*ppi*
htrE::tet	873 tet^R	912 tet^R
htrE::tet *dksA*::cm	940 tet^R	922 tet^R
	(870 cm^R)	(0 cm^R)

Interestingly, Δ*diaA* and Δ*yjfN* could be transduced into Δ6*ppi* strains without any additional deleterious phenotype. Concerning other candidates, the majority of remaining genes, whose overexpression restores the growth of Δ6*ppi* bacteria, were also found to be required for the optimal growth, since their null combination derivatives conferred a small colony size morphology. However, in such combinations, the transduction frequency in a Δ6*ppi* strain is comparable to that

when the parental wild-type strain was used as a recipient. Such a synthetic growth defect was specifically observed, when null alleles of *ariR*,r *pepA*, *ycjW* or *cspC* were introduced into the Δ6*ppi* strain SR18292. However, it should be noted that in MC4100 Δ6*ppi* derivatives (GK4649 or SR18255) the requirement of some of the genes that act as multicopy suppressors is not very stringent (Table 3). For example, a deletion of the *srrA* gene that was conditional as Δ(6*ppi srrA*) confers a cold-sensitive phenotype at 30 °C or below, but is viable at 37 °C, although the colony size is severely diminished on minimal medium. Thus, in summary, we can conclude that functions of DksA, SrrA, MetL and Hda are essential for the survival of Δ6*ppi* bacteria, and Δ*hchA* and Δ*cmk* deletions are very poorly tolerated in Δ6*ppi* derivatives; hence, HchA and Cmk proteins are limiting in Δ6*ppi* bacteria.

2.5. Overexpression of Either the dksA Gene or the cmk Gene or the metL Gene Also Restore the Growth of a Δ(dnaK dnaJ tig) Strain

It has been previously reported that strains that simultaneously lack the ribosome-associated PPI Tig and the chaperones encoded by *dnaK* and *dnaJ* genes exhibit the synthetic lethality on rich medium (LA) at 30 °C and above [19,20]. This phenotype is reminiscent of the synthetic lethality exhibited by Δ6*ppi* bacteria at 30 °C on LA medium [1]. Furthermore, the majority of proteins that aggregate in Δ6*ppi* bacteria are common to strains lacking DnaK/J chaperones [1]. This prompted us to construct Δ(*dnaK dnaJ tig*) derivatives under permissive growth conditions of M9 minimal medium at either 23 °C or 30 °C and seek multicopy suppressors that restore the growth of such a strain on LA medium at 30, 34 or 37 °C. Using the complete library of plasmids from the ASKA collection of single ORFs [13], a Δ(*dnaK dnaJ tig*) strain was transformed and used to identify genes which, when overexpressed upon the addition of 75 μM IPTG as the inducer, can restore the growth of such an attenuated strain under non-permissive growth conditions (LA medium 30, 34 or 37 °C). As the plasmid library contains all the protein-coding genes, this selection for suppressors is saturated. After the retransformation in a Δ(*dnaK dnaJ tig*) strain, plasmids that bred true were sequenced to identify the gene whose overexpression can restore the growth of a Δ(*dnaK dnaJ tig*) strain. This DNA sequence analysis identified fifteen genes (*dksA*, *cmk*, *metL*, *ariR*, *trmU*, *groL*, *ghoS*, *rplJ*, *aegA*, *ytfH*, *glpB*, *glyQ*, *greB*, *cohE* and *murI*), whose overexpression restored the growth on LA rich medium albeit to different extents at 30 °C. Out of these genes, the most promising multicopy suppressors of a Δ(*dnaK dnaJ tig*) strain on LA medium at 34 °C are: *metL*, *trmU*, *cmk*, *dksA*, *cohE*, *groL* and *ytfH* (Figure 5). However, overexpression of the *ariR* gene can also effectively restore the growth of a Δ(*dnaK dnaJ tig*) strain at 30 °C, but not at 34 °C (Figure 5A). At 37 °C, overexpression of *metL*, *cmk*, *dksA* or *cohE* gene were the only ones that could restore the colony-forming ability of Δ(*dnaK dnaJ tig*) derivative (Figure 5). Among 15 multicopy suppressors, overexpression of the *greB* gene offered only a weaker suppression on LA medium at 30 °C, but not at higher temperatures. Of interest is the re-cloning of *cmk*, *metL*, *dksA*, *groL* and *ariR* as multicopy suppressors of a Δ(*dnaK dnaJ tig*) strain, which in above studies were isolated as multicopy suppressors of the growth defect of Δ6*ppi* bacteria (Figure 3). These results allow us to conclude that there exists an overlap in the function of major chaperones and cytoplasmic PPIs in *E. coli* and both pathways are dedicated to ensure correct folding of proteins in the cell, consistent with the accumulation of several common proteins that aggregate in Δ6*ppi* and Δ(*dnaK dnaJ tig*) derivatives [1]. However, not all multicopy suppressors are common to Δ6*ppi* and Δ(*dnaK dnaJ tig*) bacteria, suggesting some limiting factors are unique to either of such derivatives.

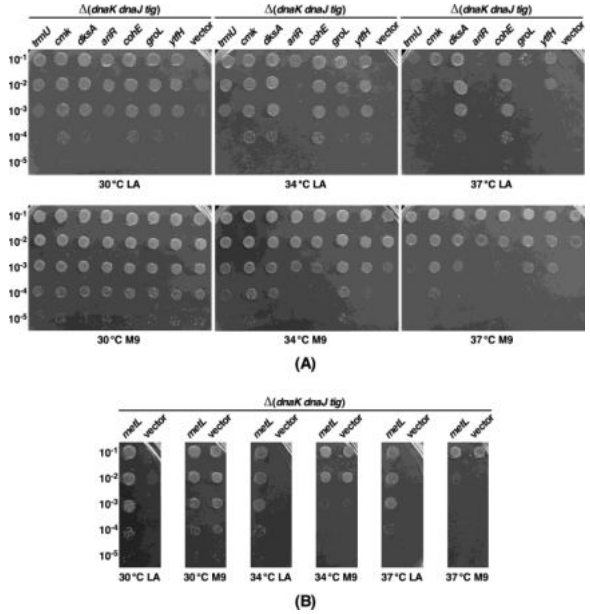

Figure 5. Overexpression of either the *cmk* gene or the *dksA* gene (**A**) or the *metL* gene (**B**) that act as multicopy suppressors of Δ6*ppi* bacteria can restore the growth of a Δ(*dnaK/J tig*) strain under non-permissive growth conditions. Exponentially grown cultures of the wild type and its isogenic Δ(*dnaK dnaJ tig*) derivative transformed with either the vector pCA24N alone or the plasmid expressing the indicated gene were grown in minimal medium at 30 °C. Cultures were washed and adjusted to an optical density OD_{600} of 0.1 and serially spot diluted on M9 minimal medium and LA medium at different temperatures in the presence of 75 μM IPTG.

2.6. DksA, Cmk and MetL Exhibit the PPIase Activity, Explaining Their Mode of Suppression

We previously reported that Δ10*ppi* bacteria still retain a weak residual activity, implying that some unidentified PPI(s) could still exist explaining their viability [1]. We rationalized that multicopy suppressors that restore the bacterial growth under non-permissive growth conditions of either a Δ6*ppi* strain or Δ(*dnaK/J tig*) bacteria might identify such unknown PPI(s), since the multicopy suppression mechanism can often act by bypassing a requirement of missing factor, if a similar activity is encoded by a suppressing factor. Thus, we purified several proteins, which were identified in above experiments, whose high dosage compensated for the absence of six cytoplasmic PPIs and also restored the growth of Δ(*dnaK/J tig*) bacteria. Such purified proteins were tested at the biochemical level for the presence of any PPIase activity in the classical chymotrypsin-coupled assay. All proteins were purified from cell extracts obtained from a Δ6*ppi* strain to prevent contamination from well-characterized highly active six cytoplasmic PPIs. Measurement of PPIase activity revealed that DksA, Cmk and MetL indeed exhibit the PPIase activity (Figures 6–8). Among the multicopy suppressors, DksA, Cmk and MetL in high dosage are common to both sets of strains in the suppression of growth defects. However, the PPIase activity of DksA, MetL or Cmk is weaker than that of well characterized PPIs such as FklB with k_{cat}/K_M 10^6 M^{-1} s^{-1} (Figures 6–8). Nevertheless, the relative PPIase activity of DksA and FkpB are comparable (Figure 6A). The catalytic efficiency of DksA turns out to be k_{cat}/K_M 0.7×10^3 M^{-1} s^{-1} as compared to 1.25×10^3 M^{-1} s^{-1} for FkpB, which is comparable to previously reported activity of FkpB [21]. The relatively weaker PPIase activity of these multicopy suppressing factors can explain why DksA, MetL and Cmk have not been previously identified as PPI enzymes. However, this activity provides a rational explanation for their multicopy suppressing ability. Identification of PPIase activity of DksA can in part explain the previously unknown mechanism of suppression of the growth phenotype of strains lacking DnaK/J chaperones and, in the present study, the restoration of growth of Δ(*dnaK/J tig*) and Δ6*ppi* strains and the synthetic lethality exhibited by Δ(*dksA* 6*ppi*), Δ(*cmk* 6*ppi*) and Δ(*metL* 6*ppi*) combinations.

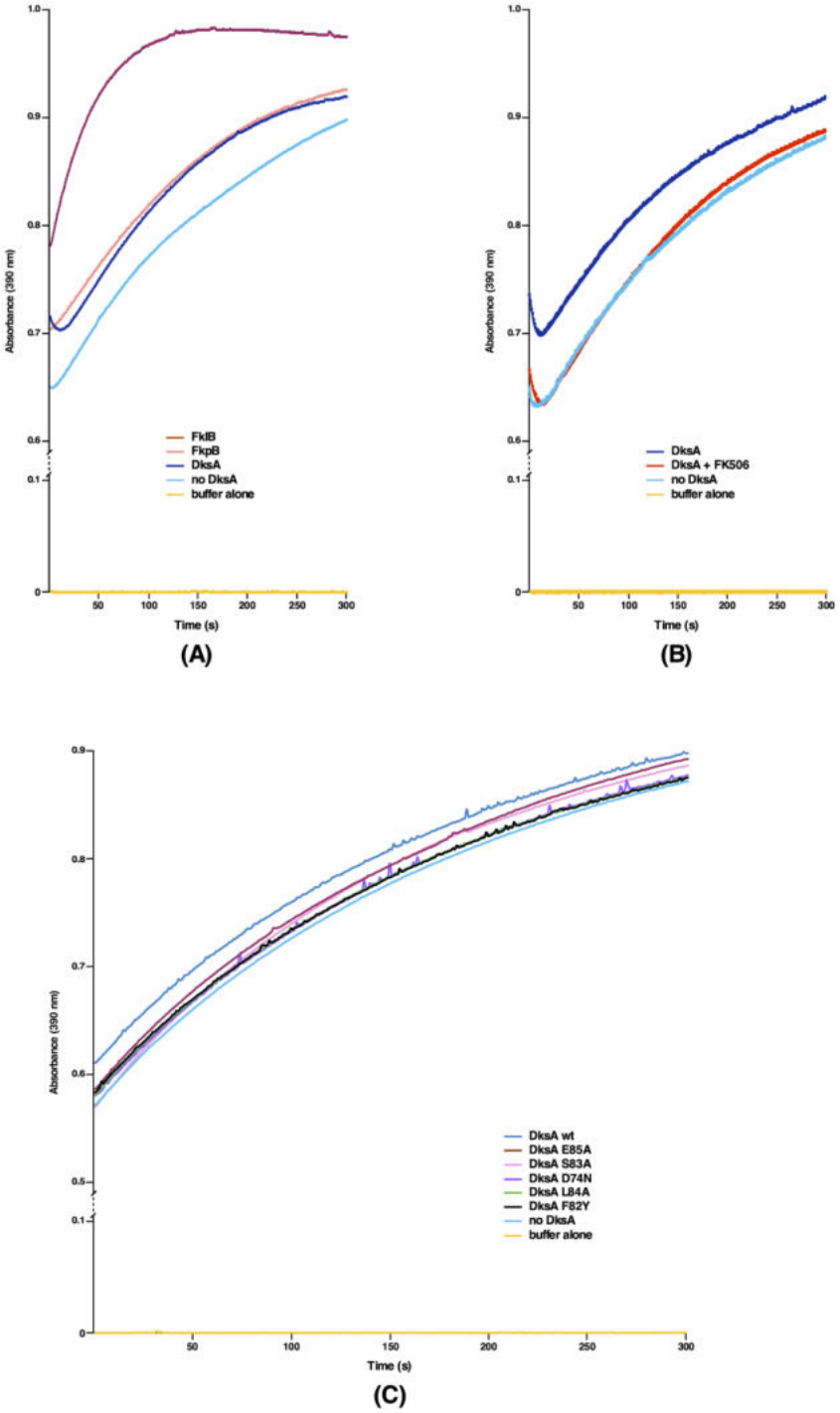

Figure 6. The RNA polymerase-binding protein DksA exhibits a PPIase activity that is comparable to that of FkpB and is inhibited by FK506. The PPIase activity was measured in the chymotrypsin-coupled assay using *N*-Suc-Ala-Ala-*cis*-Pro-Phe-*p*-nitroanilide as the substrate. (**A**) The comparative PPIase activity of FkpB, FklB and DksA proteins. (**B**) DksA was incubated with a two-fold molar excess of FK506 for 5 min at 10 °C prior to the PPIase activity measurement. The PPIase activity of DksA in the presence or absence of FK506, along with uncatalyzed reaction are plotted. (**C**) Measurement of PPIase activity of wild-type DksA and its variants. Proteins were used at a concentration of 5 μM each.

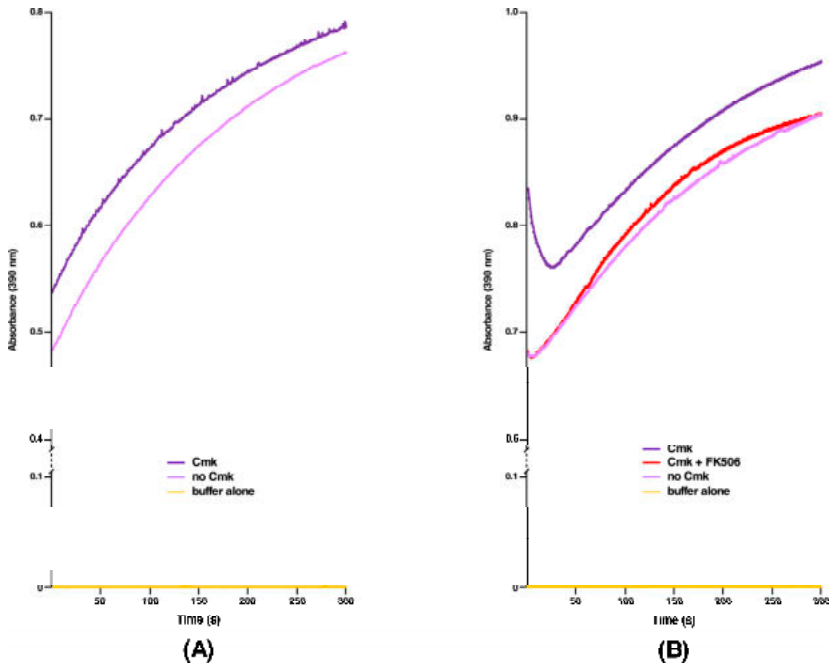

Figure 7. Multicopy suppressor of Δ6*ppi* the cytidylate kinase Cmk exhibits the PPIase activity. (**A**) Measurement of PPIase activity of Cmk in the chymotrypsin-coupled assay, using 5 μM of protein in the assay buffer. (**B**) Measurement of inhibition of the PPIase activity of Cmk by the two-fold molar excess of FK506. The PPIase activity in the presence or absence of FK506 and the uncatalyzed reaction without any enzyme are plotted in the light violet color.

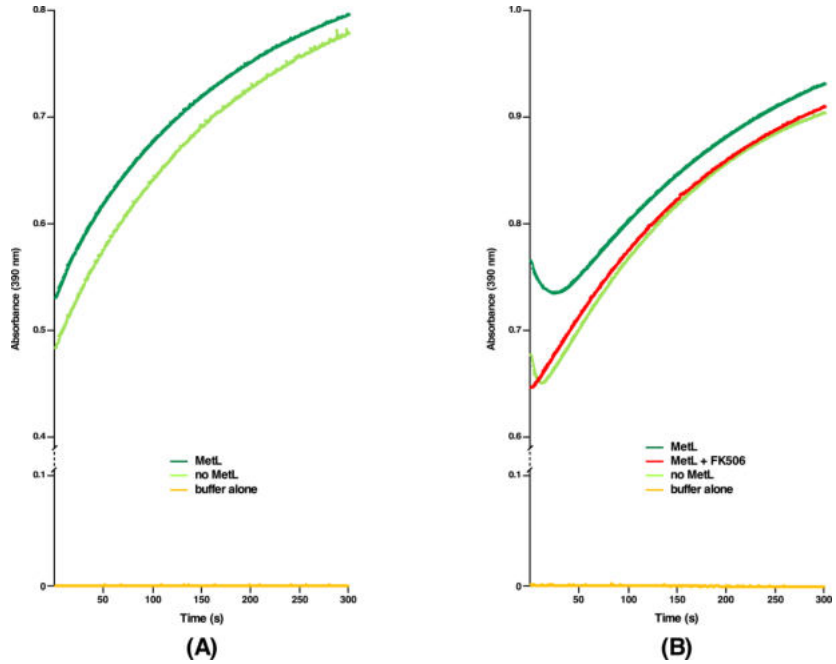

Figure 8. Multicopy suppressor of Δ6*ppi* the asparatokinase kinase II MetL exhibits the PPIase activity. (**A**) Measurement of the PPIase activity of MetL in the chymotrypsin-coupled assay, using 5 μM of protein in the assay buffer. (**B**) Measurement of inhibition of the PPIase activity of MetL by the two-fold molar excess of FK506. The PPIase activity in the presence or absence of FK506 and spontaneous reaction without any enzyme are plotted.

2.7. The PPIase Activity of DksA, Cmk and MetL Is Inhibited by FK506

Three distinct families of PPIs are classified on the basis of their specific inhibition. Thus, cyclophilins are inhibited by the cyclosporin A, FKBPs by the FK506 macrolide and parvulins by juglon [22]. However, the sensitivity to the inhibitor is known to vary depending upon the origin of PPIs. Since DksA, Cmk and MetL are not known to belong to any of these three families at structural level, we set out experiments to examine if any of three inhibitors of PPIs can also inhibit our the newly discovered PPIase activity. Interestingly, sequence alignment predicts some similarity in amino acid sequences between DksA and FkpB (see below). Thus, we measured the PPIase activity of DksA, Cmk and MetL proteins in the chymotrypsin-coupled assay in the presence or absence of FK506. Quantification of these data reveals that FK506 can effectively inhibit the PPIase activity of these enzymes. In these experiments, a two-fold molar excess of FK506 was used according to the established protocol [23] in the chymotrypsin-coupled assay with the *N*-Suc-Ala-Ala-*cis*-Pro-Phe-*p*-nitroanilide tetrapeptide as a test substrate to measure the PPIase activity (Figures 6, 7 and 8B). These results thus provide a conclusive evidence showing that DksA, Cmk and MetL exhibit the PPIase activity and hence define a new class of PPIs, whose activity is inhibited by FK506. Thus, the identification of their PPIase activity establishes the molecular basis of multicopy suppression upon their overexpression in Δ6*ppi* bacteria.

2.8. DksA, Cmk and MetL Can Catalyze the PPIase-Dependent Refolding of RNase T1

Next, we measured the PPIase activity in the RNase T1 refolding assay. The RNase T1 enzyme is a well-established protein substrate of PPIs, since the folding of RNase T1 is rate-limited by the *cis/trans* isomerization of two prolyl bonds (Tyr38-Pro39 and Ser54-Pro55) [24]. The PPIase-dependent refolding of RNase T1 after denaturation with 8 M urea was monitored after 40-fold dilution of urea in the presence or absence of DksA, Cmk or PpiB by measuring the increase in tryptophan fluorescence at 320 nm. All of these test proteins contain a single tryptophan residue. The results of such experiments reveal an enhanced emission of fluorescence as compared to buffer alone when RNase T1 was refolded in the absence of any added enzyme (Figure 9). However, the kinetics of refolding in the presence of DksA and Cmk are slower as compared to the PpiB PPI. In these experiments of RNase T1 refolding, we did not include MetL, since it contains multiple tryptophan residues giving a very high signal. Overall, these results are consistent with the presence of the PPIase activity associated with DksA and Cmk in measurements using the chymotrypsin-coupled assay, although to a reduced extent as compared to the PpiB protein, which is not surprising.

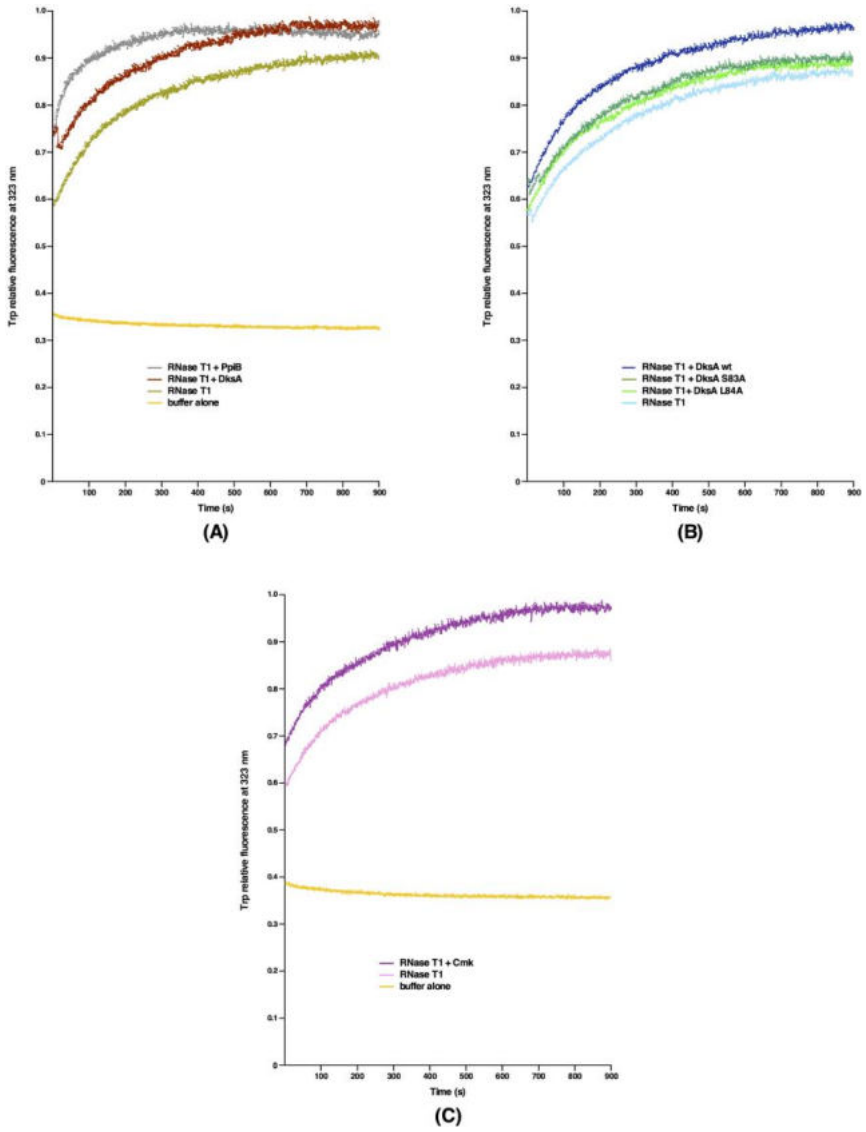

Figure 9. Catalysis of PPIase-dependent refolding of RNase T1. (**A**) The increase in fluorescence at 320 nm is depicted as a function of time of refolding of RNase T1 in the presence of DksA and PpiB. (**B**) Measurement of refolding of RNase T1 in the presence of wild-type DksA and different DksA mutants. (**C**) Refolding of RNase T1 catalyzed by the addition of Cmk as measured by the increase in fluorescence at 320 nm. Reaction when buffer alone is added is depicted in (**A**,**C**).

2.9. Identification of Amino Acid Residues That Are Critical for the PPIase Activity of DksA and Its Multicopy Suppression

The DksA protein is the very well characterized global transcriptional factor, which binds in the secondary channel of RNA polymerase (RNAP). DksA alters transcription by binding to RNAP and allosterically modulates its activity upon amino acid starvation [25]. Strains lacking the *dksA* gene are known to exhibit an auxotrophic growth phenotype and hence are unable to form colonies on minimal medium [26]. Δ*dksA* mutants are also characterized by an increased expression of rRNA promoters such as *rrnB*P1 [26]. Based on the structural analysis and mutagenesis of various residues in the DksA protein, it has been proposed that the coiled-coil domain of DksA inserts into the secondary channel of RNAP and that residues at the tip of the coiled-coil of DksA are important for its activity [27,28]. It has been shown that RNAP β subunit Sequence Insertion 1 (β-SI1) is the binding site for DksA and the tip of DksA interacts with the highly conserved substrate-binding region of the β subunit active site.

Thus, we mutated conserved residues in the DksA's tip motif, particularly those that show limited homology to FkpB of *E. coli* (Figure 10A). Specific single amino acid mutations introduced in the coding sequence of the *dksA* gene are D74N, F82Y, S83A, L84A and E85A (Figure 10B). These variants were cloned in the same expression vector, which carries the wild-type Hexa-His-tagged *dksA* gene. The expression in all cases is regulated by the IPTG-inducible P_{T5}-*lac* promoter and were examined: (*a*) for the complementation of auxotrophic phenotype of a Δ*dksA* strain; (*b*) if they can restore the growth of either the Δ6*ppi* bacteria or a Δ*dnaK/J* strain when overexpressed; (*c*) the suppression of transcriptional activity of test promoter such as the *rrnB*P1 promoter, whose activity is known to be repressed by overexpression of the wild-type DksA; and (*d*) the relative PPIase activity as compared to the wild-type DksA protein. The results of these experiments are summarized in Table 5. Briefly, overexpression of none of the DksA variants complemented the auxotrophic phenotype of a Δ*dksA* strain, with only F82Y conferring a partial growth on minimal medium (Table 5). Notably, when either the DksA-D74N or the DksA-L84A variant was overexpressed in the Δ*dksA* derivative, they conferred a very tight auxotrophic phenotype on minimal medium. Concerning the ability to repress the *rrnB*P1 promoter activity, overexpression of DksA-L84A variant in Δ*dksA* exhibited the same *β*-galactosidase activity from a single-copy chromosomal *rrnB*P1-*lacZ* fusion as was observed when the vector alone was present in the Δ*dksA* strain (Figure 10C). Furthermore, overexpression of DksA-D74N, DksA-S83A or DksA-E85A caused a significantly milder reduction in the *rrnB*P1-*lacZ* fusion activity as compared to that when the expression of the wild-type *dksA* gene was induced (Figure 10C). Overexpression of only DksA-F82Y variant was found to reduce the *rrnB*P1 promoter activity close to that observed with overexpression of the wild-type *dksA* gene. The activity of *rrnB*P1 promoter has been used as the reporter in several studies and its activity is known to be inhibited by overexpression of the wild-type DksA [27]. Consistent with previous study [27], DksA-D74N variant in our experiments revealed that its overexpression does not complement the auxotrophic phenotype of a Δ*dksA* strain and the activity of the *rnnB*P1 promoter is not repressed to the same extent as when the wild-type DksA is overexpressed. Next, we measured the PPIase activity of various DksA mutants, using purified proteins in the chymotrypsin-coupled assay. Most of the DksA mutants exhibited the relatively reduced PPIase activity as compared to the wild-type DksA (Figure 6C). Interestingly, DksA-F82Y and DksA-L84A substitutions abrogated the PPIase activity of DksA. However, the PPIase activity of DksA-E85A is reduced to a lower extent as compared to other DksA mutants. We further investigated the PPIase activity of DksA-S83A and DksA-L84A variants in the RNase T1 refolding assay. Both mutants exhibited the reduced PPIase activity in this assay as compared to the wild-type DksA (Figure 9C). These results are consistent with the results of PPIase activity measurement of DksA mutants in the chymotrypsin-coupled experiments.

Table 5. Properties of various DksA mutants in terms of suppression of auxotrophic phenotype of a Δ*dksA* strain, the suppression of Ts phenotype and impact on the PPIase activity.

Strain	Auxotrophy	*rrnB*P1 Activity	Δ*dnaK/J*	Δ(*dnaK/J tig*)	Δ6*ppi*	PPIase Activity
wild type DksA	+[a]	repressed	+	+	+	+
DksA D74N	-[b]	not repressed	-[e]	-[e]	-	reduced
DksA F82Y	± [f] sc	repressed	-[e]	-[e]	-	highly reduced
DksA S83A	-[c]	weakly repressed	-[e]	-[g]	-	reduced
DksA L84A	-[b]	not repressed	-[e]	-[e]	-	reduced
DksA E85A	-[c]	weakly repressed	-	-[g]	-[d]	marginal reduction

+[a] indicates the complementation of auxotrophic growth on minimal medium of Δ*dksA* bacteria. -[b] indicates no growth at all on minimal medium, the tight auxotrophic phenotype. -[c] indicates the background growth, but no single colonies on minimal medium. -[d] indicates a leaky small colony phenotype at 43.5 °C after the prolonged incubation of transformants of Δ6*ppi*. -[e] indicates no suppression of Ts phenotype of Δ*dnaK/J* mutant bacteria at 42 °C. -[f] indicates small colonies after 48 h incubation and sc indicates small colonies. -[g] indicates small colonies after 48 h incubation of Δ(*dnaK/J tig*) bacteria at 30 °C.

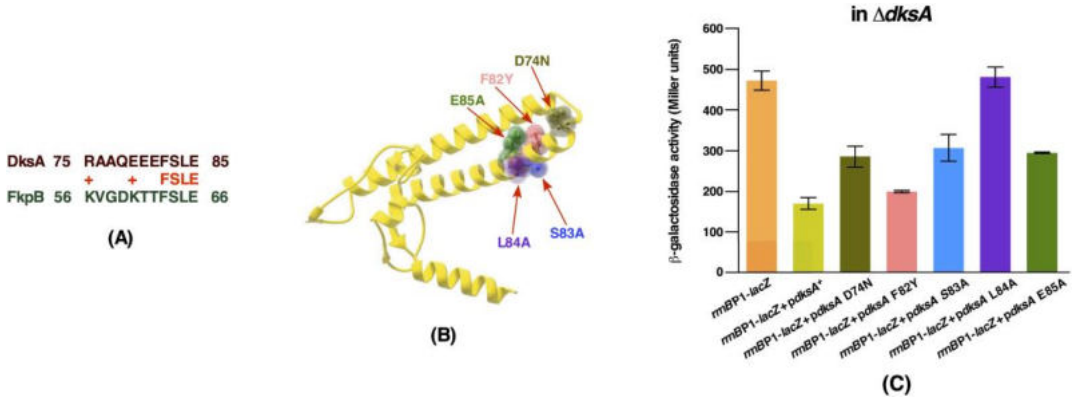

Figure 10. Mutational analysis of amino acid residues critical for the DksA PPIase activity and impact on the transcriptional activity of the *rrnB*P1 promoter. (**A**) Alignment of conserved amino acid residues of DksA and FkpB. (**B**) The position of amino acid residues that were mutated mapping to the coiled-coil tip and adjacent residues in the structure of DksA (PDB 1TJL). (**C**) Measurement of the *β*-galactosidase activity from a single-copy chromosomal *rrnB*P1-*lacZ* fusion in Δ*dksA* derivatives with either the vector alone or its isogenic strains transformed with either the plasmid carrying the wild-type *dksA* gene or plasmids with *dksA* variants. Data are presented from a representative experiment with cultures sampled at OD_{600} 4.0 in the stationary phase. Error bars represent a S.E. of three independent measurements.

Regarding the suppression of Ts phenotype, none of the variants could restore the growth of a Δ6*ppi* derivative, although the plasmid expressing DksA-E85A mutant protein conferred a leaky phenotype with the appearance of small colonies after a prolonged incubation. Similarly, we also tested the ability of these mutants to suppress the Ts phenotype of a Δ*dnaK*/J strain upon their overexpression. D74N and F82Y substitutions in the DksA protein also totally abrogated the multicopy suppressing ability of Δ*dnaK*/J strain (Table 5). DksA D74N variant has also been reported to be defective in the suppression of Ts phenotype of a Δ*dnaK*/J strain, which supports our results [29]. However, in the previous study, the DksA mutants other than D74N that we describe in this work were not available [29]. Overexpression of S83, L84 and E85 DksA variants also abolished the restoration of growth of a Δ*dnaK*/J strain at 42 °C. Thus, we can conclude that, while the F82Y alteration has the wild type-like ability to repress the *rrnB*P1 promoter activity, its PPIase activity is highly attenuated and does not suppress the Ts phenotype of either a Δ6*ppi* strain or that of Δ*dnaK*/J strain.

Next, the ability of these plasmid-born DksA variants to support the growth of a Δ(*dnaK/J tig*) strain was examined. None of these variants restored the growth of a Δ(*dnaK/J tig*) strain on LA medium at 34 °C upon overexpression, although a leaky growth phenotype at 30 °C was observed for with E85A derivative (Table 5). Taken together, our data show that the PPIase-dependent activity of DksA is required for the suppression of growth defects of either Δ6*ppi* or Δ(*dnaK/J tig*) strains.

2.10. The DksA-Mediated Multicopy Suppression of Either Δ6ppi or ΔdnaK/J Mutant Bacteria Requires the Wild-Type Expression of GroL/S and RpoE Essential Proteins

Our work thus far established that overexpression of the secondary channel RNA polymerase-binding protein DksA can efficiently suppress a Ts phenotype of Δ6*ppi* strains and also restore the growth of a Δ(*dnaK/J tig*) strain on LA medium up to 37 °C. The *dksA* gene was originally identified as the multicopy suppressor of a Ts phenotype of the Δ*dnaK/J* strain at 42 °C [30]. In the above experiments, we showed that DksA has a PPIase activity, which is necessary for DksA's multicopy suppression. In the next series of experiments, we identified *trans*-acting factors that are required for DksA's multicopy suppression. This was achieved by the isolation of Tn*10* transposon insertion mutants in a Δ6*ppi* derivative carrying the *dksA* gene on a plasmid that were unable to grow at 43 °C from a saturated screen of mutants. Those Tn*10* mutants that bred true were transduced into the wild type to eliminate mutations that conferred a Ts phenotype at 43 °C even in the wild-type background. Out of these, 18 Tn*10* insertions

were found to be Ts in the wild type, while the remaining were specific to the Δ6*ppi* strain. Among Ts mutants, nine independently isolated mutants carried the Tn*10* insertion in the *degP* gene (Table 6). The *degP* gene is required for the bacterial growth at temperatures above 42 °C and is a member of the *rpoE* regulon [31–33]. Interestingly, Δ(*degP dksA*) confers a Ts phenotype above 39 °C, unlike a single Δ*degP* or Δ*dksA*, which are viable under such conditions (Table 6). Concerning the remaining Ts mutants, one of them has the insertion in the *cydA* gene and other has it in the *ftsX* gene (Table 6). The *cydA* gene encodes the cytochrome *bd*-1 ubiquinol oxidase subunit I, which is essential for the bacterial growth at temperatures above 37 °C [34]. Furthermore, a (*cydA*::Tn*10* Δ*dksA*) strain exhibits growth defects even at 30 °C and Δ*dksA ftsX*::Tn*10* was found to be synthetically lethal (Table 6).

Table 6. Tn*10* insertions that block the multicopy suppression by DksA of Δ6*ppi*, their suppression of Δ*dnaK/J* strains as determined by colony forming units, the synthetic phenotype in the Δ*dksA* background and the lack of *ppk* requirement for the DksA-mediated suppression of Δ6*ppi*.

Gene	Tn*10* Position	Δ*dnaK/J*+p*dksA*$^+$		wt	Δ6*ppi*	Δ*dksA*	Function
		40 °C	42 °C	43 °C	M9 37 °C	43 °C	
rpoEp [d]	−90	-	-	+[a] sc	+	+ sc	sigma factor
groSp [d] *1*	−101	-	-	-	+ sc	-	chaperone
groSp [d] *2*	−101	-	-	+ sc	+	+	chaperone
degP	12/112 *	-	-	-	+	- Ts >39 °C	periplasmic protease
lepA	702	± sc	-	±[b] sc	+ sc	-[c]	translational GTPase
ahpC	94	-	-	+	+ sc	+	oxidative stress
rnhA	59	-	-	+	+ sc	± sc	ribonuclease HI
tatC	23	-	-	+	+	- sc	transport of folded proteins
tolA	299	± sc	-	+	± sc	± vsc	cell envelope integrity
mrcB	1186	± sc	-	+	+	+	peptidoglycan synthesis
oxyR	518	± sc	-	+	+	+	oxidative stress regulator
cpxR	474	+	± sc	+	+	+ sc	envelope stress regulator
cydA	20	-	-	-	+	-	cytochrome *d* terminal oxidase
clsA	533	± sc	-	+	+	+	cardiolipin synthase
ftsX	166	-	-	± sc	± sc	-	cell division
nudB	369	+	±	+	+	± sc	folate biosynthesis
envZ	291	± sc	-	+	+	+	regulation of *ompF/C* expression
phoU	655	-	-	+sc	+sc	- vsc	P_i signalling
Δ*ppk*	deletion	+	-	+	+	+	polyphosphate kinase

+[a] indicates the normal growth. ±[b] indicates the partial temperature sensitivity. -[c] indicates the inability to support the colony-forming ability. * indicates the Tn*10* insertion position in the *degP* gene determined for two out of nine mutants. sc, small colonies; vsc, very small colonies after the prolonged incubation.

The remaining mutants that do not confer a Ts phenotype in the wild-type background identified 15 genes whose products/amounts of encoded proteins are crucial for the DksA-mediated suppression. Out of these, two insertions mutations identified GK5109 and GK5578 strains have Tn*10* inserted at the identical position in the promoter region of the essential chaperonin-encoding *groSL* operon. This Tn*10* insertion in the *groSL* operon is located 3 nt downstream of the −35 heat shock promoter element, which is 101 nt upstream of the translational initiation codon (Figure 11A). Although both insertions abolish the DksA-mediated suppression of Δ6*ppi*, the insertion in GK5109 strain also confers the small colony morphology at 40 °C and the inability to grow at 43 °C in the wild type as compared to the nearly normal growth of GK5578 derivatives. To address differences in growth properties exhibited by two strains with the identical position of Tn*10* insertion in the *groSL* promoter, the amount of GroL was measured from total cell extracts. Thus, cultures of wild-type bacteria and its derivatives GK5109 and GK5578 (Δ6*ppi* + p*dksA*) *groS101::*Tn*10* were grown under permissive conditions and

subjected to a 15-min heat shock treatment at 42 °C. The relative abundance of GroL was analyzed using Western blot technique. Such experiments revealed that the amount of GroL is significantly reduced in the strains with the Tn*10* insertion in the promoter region of *groSL* and the induction of GroL at higher temperature is impaired, which is consistent with the disruption of −35 element of RpoH-regulated heat shock promoter (Figure 11B). Furthermore, the amount of GroL is higher in the strain GK5578 as compared to the strain GK5109, explaining the differences in the growth phenotype of these strains (Figure 11B). Thus, transcription of the *groSL* operon in these strains is independent of the RpoH-regulated heat shock promoter and is driven from the promoter generated by the insertion element. This interesting difference with the similar position of insertion elements in the promoter region synthesizing different levels of GroL and the degree of suppression can be explained by the potential creation of promoter of different strength within the insertion element that drive *groSL* transcription. Such differences arising due to changes in transcription due to identical insertion elements in the promoter region is not without precedence and has been reported previously within the *groSL* promoter [35]. Significantly, these *groSL* promoter mutations also abolished the multicopy suppression of a Δ*dnaK/J* mutation (Table 6). The isolation of mutations in the promoter region of the *groSL* operon that allow their constitutive expression with the dysfunctional heat shock promoter suggests that at high temperature DksA overexpression cannot suppress either a Δ6*ppi* or a Δ*dnaK/J* mutation, since GroL and GroS proteins are not heat shock induced and hence they become limiting. Thus, the DksA multicopy suppression requires wild-type levels of GroL/S chaperonins and their heat shock induction.

Two other Tn*10* insertions of significance were located at the position 90 nt upstream of the translational initiation codon of the essential *rpoE* gene that totally abolished the multicopy suppression by the *dksA* gene (Table 6, Figure 11B). This Tn*10* insertion is located 3 nt upstream of the −10 *rpoE*P6 promoter element. This *rpoE* promoter is the most proximal promoter, which is transcribed by $E\sigma^E$ [15]. As the *rpoE* gene is essential for the viability of *E. coli*, we wondered if its expression is abolished by this Tn*10* insertion. DNA sequencing of the *rpoE* gene and its adjoining region revealed that an extra copy of the intact *rpoE* gene from −90 nt until its end had been duplicated at the Tn*10* insertion site in the same orientation (Figure 11C). Further analysis of the *rpoE* gene expression by quantitative reverse transcription PCR (qRT-PCR) revealed that this Tn*10* insertion leads to a 10-fold reduction of its transcription, which is further reduced when the *dksA* gene is overexpressed (Figure 11D). As a control, total mRNA from the Δ*rpoE* strain SR8691 was included in this qRT-PCR experiment, which did not show any *rpoE*-specific amplification products (Figure 11D). Thus, the DksA-mediated multicopy suppression requires full RpoE functionality. This allele for brevity is called *rpoEp*^{d} (down mutation). Consistent with our previous results, a Δ6*ppi* strain exhibits a reduction in the expression of the *rpoE* gene under permissive growth conditions [1] (Figure 11D) and could hence become severely limiting in the presence of *rpoEp*^{d} mutation. Interestingly, the *rpoEp*^{d} mutation also abrogated the multicopy suppression by the *dksA* gene of the Ts phenotype of a Δ*dnaK/J* strain at either 40 or 42 °C (Table 6 and Figure 12). Taken together, the DksA-mediated multicopy suppression of either a Δ6*ppi* or a Δ*dnaK/J* strain requires the wild-type level expression of the *rpoE* gene and *groS/L* genes.

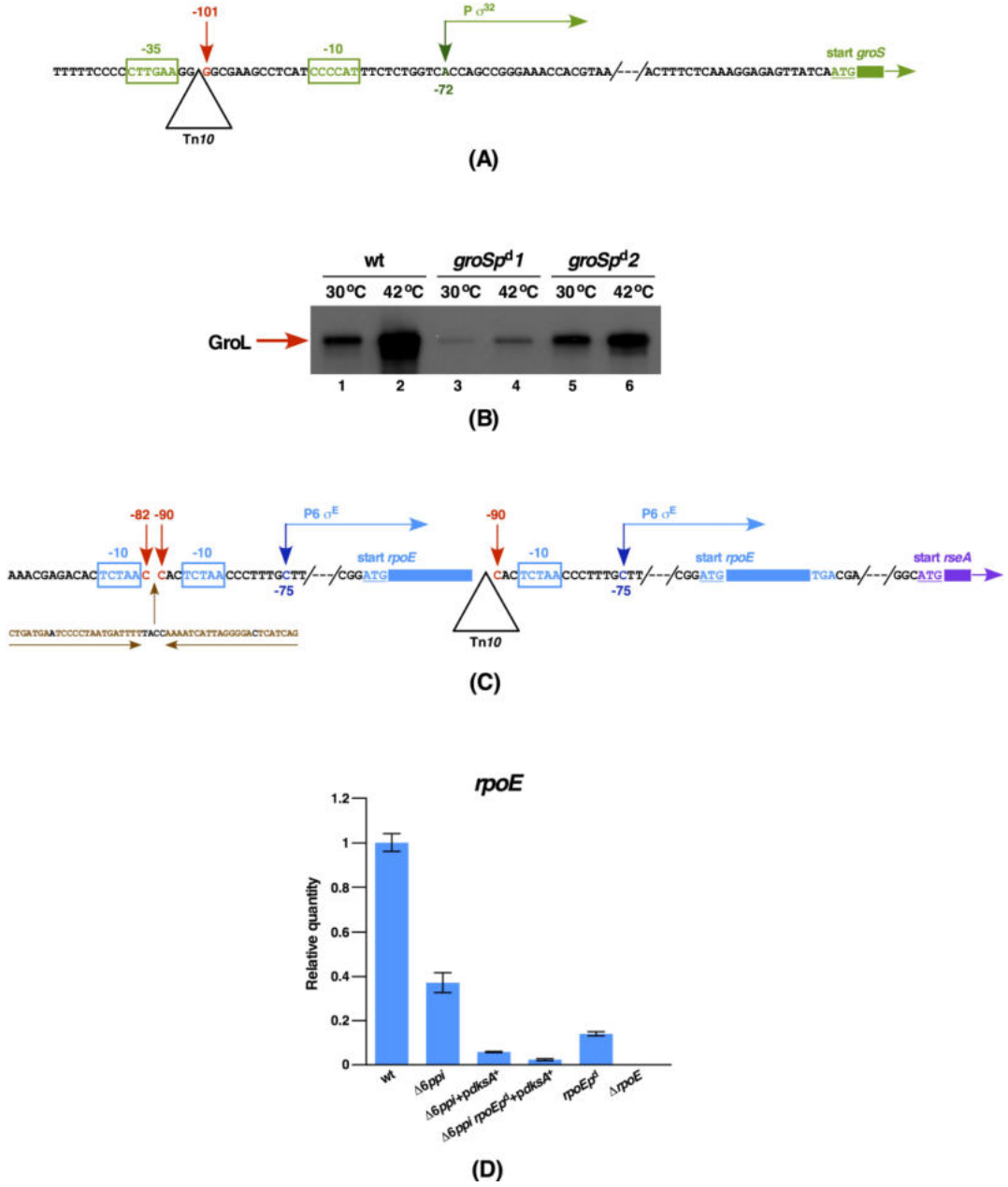

Figure 11. Wild-type expression of GroL and RpoE are required for the DksA-mediated suppression of either Δ6*ppi* or Δ*dnaK/J* bacteria. (**A**) Schematic drawing of the Tn*10* insertion position in the promoter region of the *groS/L* operon. Boxes indicate the location of −10 and −35 heat shock elements recognized by RpoH. (**B**) Western blot analysis of total cell extracts obtained from the wild type (wt) and its two isogenic derivatives carrying *groSp*^{d}*1* and *groSp*^{d}2 mutation with or without a heat shock of 15 min at 42 °C. Equivalent amounts of proteins were applied and resolved on 12.5% SDS-PAGE and transferred by Western Blotting. Blots were probed using GroL-specific antibodies and revealed by chemiluminescence. (**C**) The position of the Tn*10* insertion at the nt position −90 in the *rpoE*P6 promoter is indicated. The duplication and the orientation of the intact *rpoE* gene and the disruption of the *rpoE*P6 promoter is shown by an arrow. (**D**) Quantification of the *rpoE* mRNA by qRT-PCR using the total RNA isolated from the isogenic wild type (wt), SR18292 (Δ6*ppi*), SR20561 (Δ6*ppi* + p*dksA*$^{+}$), GK5165 (Δ(6*ppi rpoEp*^{d}) + p*dksA*$^{+}$), GK5347 (wt *rpoEp*^{d}) and SR8691 (Δ*rpoE*) strains. For RNA isolation, cultures were grown under permissive growth conditions of M9 at 37 °C.

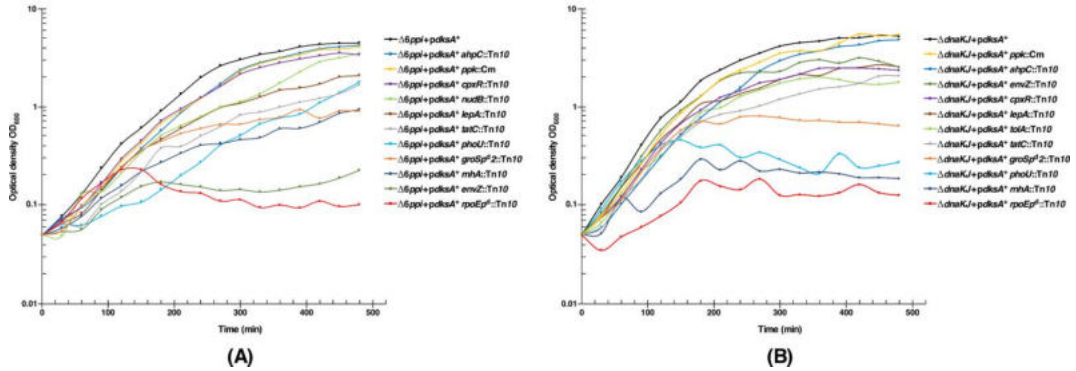

Figure 12. Wild-type levels of RpoE, GroL/S and intact copies of RNase H, TatC and LepA are required for the DksA-mediated suppression of Ts growth of either Δ6*ppi* or Δ*dnaK/J* strains. (**A**) Isogenic cultures of Δ6*ppi* + p*dksA*$^{+}$ and its derivatives with either the Tn*10* insertion or deletion were grown overnight in M9 medium at 37 °C. Culture were adjusted to $OD6_{00}$ of 0.05 in 10 mL of prewarmed LB medium at 43.5 °C. Aliquots of samples were drawn at different intervals and the bacterial growth monitored by measuring OD_{600}. (**B**) Isogenic cultures of Δ*dnaK/J* + p*dksA*$^{+}$ and its derivatives with gene disruptions were grown in M9 medium at 30 °C and analyzed for the bacterial growth in LB medium at 41 °C by measuring OD_{600}. Data presented are from a representative experiment.

2.11. The DksA-Mediated Multicopy Suppression Requires Cell Envelope Homeostasis, the Genome Integrity, the Ribosome Assembly, Translocation of Folded Proteins and Factors Combating Oxidative Stress

Mapping and characterization of remaining Tn*10* insertions that prevent the multicopy suppression by DksA can be grouped in four functional categories: (*i*) the cell envelope composition and its integrity (*cpxR*, *envZ*, *tolA*, *mrcB* and *clsA*); (*ii*) the genome integrity and repair (*rnhA* and *nudB*); (*iii*) translation and transport systems (*lepA* and *tatC*); (*iv*) phosphate uptake and phosphate sensing system (*phoU* and *pstS*); and (*v*) genes whose products are related to the oxidative stress responsive pathway (*ahpC* and *oxyR*) (Table 6). This mutagenesis is saturated, since Tn*10* insertions in some of these genes were obtained multiple times (three each in *envZ* and *tolA* and two each in *clsA* and *ahpC*). Furthermore, the introduction of *rnhA*::Tn*10*, *lepA*::Tn*10*, *phoU*::Tn*10*, *ahpC*::Tn*10*, *oxyR*::Tn*10*, *tolA*::Tn*10*, *tatC*::Tn*10* and *envZ*::Tn*10* also abrogated the multicopy suppression of Δ*dnaK/J* by DksA at either 40 °C or 42 °C on LA medium, although to a variable extent (Table 6). Consistent with these results, a synthetic growth phenotype was observed with Δ(*dksA degP*), Δ(*dksA lepA*), Δ(*dksA tatC*), Δ(*dksA rnhA*) and Δ(*dksA phoU*) combinations (Table 6).

To validate the requirement of above-mentioned genes, whose products are required for the DksA-mediated multicopy suppression of either a Δ6*ppi* or a Δ*dnaK/J* derivative, kinetics of the bacterial growth was measured in aerobically shaken cultures. Isogenic bacterial cultures of SR20561 (Δ6*ppi* + p*dksA*$^{+}$) alone and its derivatives with the Tn*10* insertion in the specific gene were grown under the permissive growth condition of M9 minimal medium at 37 °C and shifted to LB medium at 43.5 °C. Measurement of optical density OD_{600} at different intervals confirmed that there exists an acute requirement for the adequate expression of either the *groSL* operon or the *rpoE* gene for the DksA-mediated multicopy suppression of Δ6*ppi* bacteria (Figure 12A). A similar dependence for the presence of intact RpoE and GroL/S was found for the multicopy suppression by DksA of a Δ(*dnaK dnaJ*) derivative in the liquid culture (Figure 12B). However, the requirement for the intact *rpoE* gene is more stringent as the *rpoEp*^{d} mutation in the SR20561 (Δ6*ppi* + p*dksA*$^{+}$) background was much more severely affected. It should be noted that for the growth analysis with the Tn*10* insertion in the *groS* promoter we used the *groSp*^{d}*2* derived strain, since this mutation does not confer the Ts phenotype per se as the *groSp*^{d}*1* mutation (Figures 11B and 12 and Table 6).

Concerning the quantitative growth measurement of other Tn*10* insertions in the SR20561 (Δ6*ppi* + p*dksA*$^{+}$) background, the order of severity of the growth inhibition after the *rpoEp*^{d} mutation is *envZ*::Tn*10* > *rnhA*::Tn*10*, *groSp*^{d}*2*::Tn*10*, *phoU*::Tn*10*, *tatC*::Tn*10* and *lepA*::Tn*10* at 43.5 °C in LB

medium (Figure 12A and Supplementary Table S2). Surprisingly, the Tn*10* insertion in the c*pxR* gene, the *ahpC* gene or the *nudB* gene exhibited only a minor detrimental growth effect in the liquid culture (Figure 12) and hence the multicopy suppression by the *dksA* gene does not absolutely require such genes in all growth conditions. Similarly, no significant growth inhibition in the liquid culture was observed, when *clsA*::Tn*10* or *mrcB*::Tn*10* were introduced in the strain SR20561 (Δ6*ppi*+p*dksA*$^+$). As *tolA*::Tn*10* derivatives in (Δ6*ppi* + p*dksA*$^+$) grew quite poorly in liquid culture, such a strain was not analyzed for growth properties. In summary, we can conclude that, besides a requirement for RpoE and GroS/L chaperonins, the genome integrity (RnhA), the outer membrane protein homeostasis (EnvZ), the balanced translational process (LepA), the Tat-dependent translocation of folded proteins and appropriate regulation of phosphate regulon are required for the DksA-mediated multicopy suppression of Δ6*ppi* bacteria.

For the measurement of growth of Δ*dnaK/J* + p*dksA*$^+$ derivatives with Tn*10* insertions in various genes that block the DksA-mediated suppression of Δ6*ppi*, all such Tn*10* insertions were transduced in a Δ*dnaK/J* strain SR20733. Isogenic cultures were grown under permissive growth condition (M9 minimal medium at 30 °C) and shifted to LB medium at either 40.5 or 41 °C. Data are presented from a representative set of experiments from growth conditions at 41 °C. Measurement of optical density OD_{600} at different growth intervals and determination of growth rate confirmed the inability of DksA-mediated suppression with the *rpoEp*^{d} mutation, with the order Ts growth inhibition following the *rpoE* mutation as *rnhA*::Tn*10* > *phoU*::Tn10, *groSp*^{d}2::Tn*10*, *tolA*::Tn10, *tatC*::Tn*10* and *lepA*::Tn*10* (Supplementary Table S2). In contrast to a requirement for the EnvZ function in Δ6*ppi* bacteria, no such dependence was observed in the Δ*dnaK/J* background for the suppression by DksA. Again, no stringent requirement was observed for the presence of either the *cpxR* gene or the *ahpC* gene in the growth in the liquid culture (Figure 12B). Thus, besides a requirement for RpoE and GroL/S, the genome integrity maintenance by RnhA, protein synthesis/translocation (LepA and TatC), the outer membrane integrity (TolA) and phosphate sensing/regulation of phosphate uptake are needed for the multicopy suppression by DksA of either Δ6*ppi* or Δ*dnaK/J* derivatives.

2.12. The ppk Gene Encoding Polyphosphate Kinase Is Not Required for the DksA-Mediated Multicopy Suppression of a Δ6ppi Strain and Only a Marginal Requirement for a Δ(dnaK/J) Derivative

Next, we addressed, if the *ppk* gene encoding the polyphosphate kinase is required for the DksA-mediated multicopy suppression. This experiment was included, since Ppk has a chaperone-like function and was identified as a substrate of PpiC and FklB PPIs [1]. Thus, a non-polar deletion of the *ppk* gene was constructed and introduced into SR20561 (Δ6*ppi* + p*dksA*$^+$) and SR20733 (Δ*dnaK/J* + p*dksA*$^+$) strains under permissive growth conditions on M9 minimal medium and examined for growth properties. On LA medium, Δ(6*ppi ppk*) + p*dksA*$^+$ grew nearly to the same extent as its parental strain SR20561 (Δ6*ppi* + p*dksA*$^+$) at 43.5 °C (Table 6). Similarly, in the liquid culture, the Δ(6*ppi ppk*) + p*dksA*$^+$ derivative grew nearly to the same level as its isogenic strain SR20561 (Δ6*ppi* + p*dksA*$^+$) at 43.5 °C, with only a minor growth reduction (Figure 12A). These results thus establish that the *ppk* gene is not essential for the DksA-mediated multicopy suppression of a Δ6*ppi* derivative. Regarding the comparative growth of a Δ(*dnaK/J ppk*) + p*dksA*$^+$ derivative with its isogenic parental strain SR20733 (Δ*dnaK/J* + p*dksA*$^+$) on LA medium, a similar growth was obtained at 40 °C on LA medium (Table 6). However, on LA medium at elevated temperature of 42 °C, which is the uppermost limit for the growth of a Δ*dnaK/J* + p*dksA*$^+$ strain, no viable single colonies were obtained when a Δ(*dnaK/J ppk*) + p*dksA*$^+$ derivative was tested (Table 6). Furthermore, only a minor growth difference was obtained between SR20733 (Δ*dnaK/J* + p*dksA*$^+$) and SR22300 Δ(*dnaK/J ppk*) + p*dksA*$^+$ derivative as compared to the drastic growth inhibition when Tn*10* insertions in *lepA*, *rnhA*, *tatC*, *envZ* genes or *rpoEp*^{d} mutation were examined (Figure 12B). Thus, we can conclude that Ppk is not required for the DksA-mediated multicopy suppression of Δ6*ppi* bacteria and only a minor growth reduction is observed when the *ppk* gene is absent when the *dksA* gene is overexpressed in strains lacking *dnaK/J* at temperatures around 42 °C, but not at either 40 or 40.5 °C on LA medium or up to 41 °C in liquid culture.

3. Discussion

PPIs are universally conserved enzymes that catalyze the *cis*/*trans* isomerization of peptide bonds that precede the proline amino acid. PPIs accelerate this rate-limiting step in protein folding of the *cis*/*trans* isomerization of the peptide bond by a factor of 10^3–10^6 [36,37]. PPIs have been classified into three families depending on the sensitivity to specific inhibitors. The cytoplasm of *E. coli* contains six such enzymes representing all three families. However, their substrates were only recently described [1]. Although individually all six cytoplasmic PPIs are non-essential for bacterial viability, collectively the removal of all such enzymes confers synthetic lethality, which is manifested by the inability of such Δ6*ppi* bacteria to grow on rich medium and the temperature sensitivity (Ts) on rich as well as minimal medium [1]. In this work, we further characterized various growth defects of Δ6*ppi* bacteria and show that they exhibit highly pleiotropic phenotypes. These include the inability to grow under fast-growing conditions of rich medium, and the sensitivity to: (*i*) DNA-damaging agents such as nalidixic acid indicating that the genome integrity of Δ6*ppi* bacteria is compromised; (*ii*) cell envelope-destabilizing agents; and (*iii*) the exposure to ethanol and the inability to grow on minimal medium, when glycerol was used as the sole carbon source. Taking advantage of such growth defects, multicopy suppressors that restore the viability of Δ6*ppi* bacteria under non-permissive growth conditions were isolated to identify factors that are limiting for the viability of such bacteria. We also reasoned that potentially some multicopy suppressors could compensate growth defects of Δ6*ppi* bacteria by possessing a PPIase activity, explaining the presence of the residual PPIase activity in strains lacking all *E. coli*'s known PPIs.

Isolation of multicopy suppressors identified cellular factors that are limiting in Δ6*ppi* bacteria and the reasons for the essentiality of PPIase activity. Consistent with the role of PPIs in protein folding, several prominent suppressors identified are: (*i*) major cytosolic chaperones; (*ii*) transcriptional factors such as DksA or SrrA; (*iii*) antitoxin MqsA and toxin Hha; (*iv*) the modulator of the proteolytic activity; (*v*) those involved in combating oxidative stress/acid resistance or detoxification of cysteine; (*vi*) the aspartokinase II MetL involved in the amino acid synthesis; and (*vii*) factors that modulate the chromosomal replication initiation via regulating the activity of initiator protein DnaA (DiaA and Hda). Isolation of DnaK/J and GroL/S as multicopy suppressors is consistent with our previous identification of several proteins that are substrates of these chaperones and PPIs [1]. Thus, PPIs and the molecular chaperone network are together required for folding of cellular proteins. Other multicopy suppressors such as transcriptional factors could act by the enhancing transcription of genes, whose products are needed to maintain proteostasis or by the repressing transcription of genes, whose products become toxic in Δ6*ppi* bacteria.

Next, we systematically removed individual genes, which in multicopy suppressed growth defects of Δ6*ppi* bacteria, other than *dnaK*/*dnaJ* and *groL*/*groS* genes. These studies revealed that Δ6*ppi* bacteria require DksA, MetL, SrrA and Hda for their viability as their deletion combinations in the Δ6*ppi* background turns out to be lethal. Since Δ6*ppi* bacteria exhibit the sensitivity towards DNA-damaging agents could be one of the reasons for the synthetic lethality with Δ*hda*. In support of these data, it has been reported that *hda* mutations increase the cellular level of ATP-DnaA and cause the over initiation of replication, which results in the inhibition of cell division and cell growth [38]. This can help to explain the synthetic lethality of Δ(6*ppi hda*) combination. A requirement for survival of Δ6*ppi* bacteria on the presence of Cmk was also observed, since Δ(6*ppi cmk*) exhibited exacerbated synthetic growth defects. The function of SrrA is at present unknown. Homology searches predict it to be a putative transcriptional factor with the predicated N-terminal PAS domain and the C-terminal helix-turn-helix motif. As overexpression of the *srrA* gene not only restores the growth of Δ6*ppi* strains on rich medium at elevated temperatures, but also can suppress the Nal sensitivity, we believe that SrrA plays an important role in stress response.

Given some of the phenotypes exhibited by Δ6*ppi* and Δ(*dnaK/J tig*) bacteria such as the inability to grow on LA medium and the vast number of proteins that aggregate in such mutants show an overlap, we also undertook the multicopy suppressor approach with a Δ(*dnaK/J tig*) strain. Quite significantly, we identified a set of genes such as *dksA*, *cmk*, *metL*, *groL*, *ariR* whose overexpression resulted in the

restoration of growth of a Δ(*dnaK/J tig*) strain, although to different degrees depending on the growth temperature. As these genes were already identified as multicopy suppressors of Δ6*ppi* bacteria suggested that their mechanism of suppression could operate by providing a function related to the protein folding process. The MetL aspartokinase II is a bifunctional enzyme known to be required for the synthesis of amino acids such as a threonine, lysine and methionine [39]. However, overexpression of the *metL* gene offers a better suppression on LA medium than on M9 medium for both either Δ6*ppi* or Δ(*dnaK/J tig*) bacteria arguing an additional function other than its requirement in the amino acid biosynthesis pathway. Using a different plasmid DNA library, an independent study also reported that overexpression of the *dksA* gene can rescue growth defects of a Δ(*dnaK/J tig*) strain [40]. However, in that study [38], certain other genes whose products are involved in metabolic processes such as *ldhA*, *lpd*, *talB*, *tpx*, *ackA*, *nagB*, *pykF* and *sseA* were identified as multicopy suppressors of a Δ(*dnaK/J tig*) strain that restore the growth on rich medium above 33 °C. Thus, we used a controlled overexpression of such genes [40], whose products are involved in metabolic functions, using plasmids from the ASKA library [13]. However, their overexpression did not restore the growth of a Δ(*dnaK/J tig*) strain and hence those results could not be validated. This explains why such genes were not identified in our multicopy selection using the complete genomic library that could identify *dksA*, *metL*, *groL*, *cmk*, *cohE* and *ariR* as validated multicopy suppressors.

Based on the identification of multicopy suppressors that restore the growth of either Δ6*ppi* or Δ(*dnaK/J tig*) bacteria, two most significant findings of this work are: (*a*) the identification of three new PPIase activities that can explain in part the pathway of suppression; and (*b*) the identification of factors that are required for the DksA-mediated multicopy suppression. We rationalized that products of multicopy suppressors could identify function(s) missing in strains that are compromised in protein folding, when PPIs are absent. Thus, we purified products of all major 15 multicopy suppressors other than GroL/S and DnaK/J protein folding chaperons. Among these DksA, Cmk and MetL proteins exhibited a PPIase activity in the chymotrypsin-coupled assay and in the protein substrate RNase T1, whose folding is limited by the *cis/trans* proline isomerization. Furthermore, this PPIase activity of DksA, Cmk and MetL could be inhibited by FK506 establishing them as bona fide PPIs. It should be noted that, although the PPIase activity of DksA is 1000-fold less than classical PPIs such as FklB [k_{cat}/K_M 0.7 x 10^3 M^{-1} s^{-1} for DksA vs. k_{cat}/K_M 10^6 M^{-1} s^{-1} for FklB (Figure 6A)], it is still comparable to the PPIase activity of FkpB—a well characterized PPI with the low PPI activity with several substrates [1,21]. However, more experiments will be required to identify the binding affinity of these proteins with FK506, the contact regions where FK506 can bind and exact residues involved in catalysis.

Although on the basis of sequence homology none of these proteins exhibit the significant structural homology to any of three classes of PPIs, a segment in DksA (amino acid residues 75–85) located near the coiled-coil tip that protrudes in the secondary channel of RNAP aligns with FkpB amino acid residues 56–66. DksA and other secondary channel binding proteins such as GreA and GreB have a similar fold in the coiled-coil tip domain, but they are not similar at the amino acid sequence level [41,42]. Interestingly, GreA and GreB C-terminal domains exhibit the structural similarity with FKBPs [43]. However, this C-terminal domain is absent in the sequence of DksA. Based on the amino acid alignment of DksA with FkpB and the importance of coiled-coil tip and nearby residues, we constructed D74N, F82Y, S83A, L84A and E85A substitutions, purified such proteins and tested their PPIase activity. All such variants other than E85A exhibited the reduced PPIase activity and did not complement the auxotrophic phenotype of Δ*dksA* and were unable to restore the growth of either a Δ6*ppi* or a Δ*dnaK/J* or a Δ(*dnaK/J tig*) derivative. However, D74N and L84A are much tighter as far as the auxotrophic phenotype is concerned. Quite interestingly, the repression of the *rrnB*P1 promoter activity by DksA variants does not match with the multicopy suppression phenotype of Δ6*ppi* bacteria. For example, the F82Y variant represses the *rrnB*P1 promoter activity quite similar to the wild-type DksA (Figure 10C), but it has the lowest PPIase activity and also cannot rescue the growth of either Δ6*ppi* or Δ*dnaK/J* bacteria (Figure 6C and Table 5). Such results suggest that the PPIase activity of DksA

matches with its ability to perform the rescue of growth defects of Δ6*ppi*. It is of interest that D74N variant of the DksA protein has been very well-characterized [27,28]. DksA D74N mutant protein has been shown to bind RNA polymerase, but was defective in the transcription initiation [27,28] and unable to suppress the Ts phenotype of a Δ*dnaK/J* mutant [29]. It has been suggested that the D74 amino acid residue in the coiled-coil tip of DksA is important for the substrate binding of the active site of RNA polymerase and electrostatic charge of carboxyl group is critical for D74 function [27,28]. Amino acid residues R678 and R1106 in the β subunit of RNAP are presumed to interact with D74 of DksA [27,28]. DksA L84 and DksA F82 are also predicted to interact with β′ subunit and L84 could be cross-linked to R744-M747 amino acid residues [28] and hence can impact DksA function, explaining the inability of DksA F82Y and L84A to suppress growth defects of a Δ6*ppi* bacteria. At present, however, we do not know if the PPIase activity is directly required for the DksA-RNAP interaction and future studies are needed to address this vital issue. In the structure of RNA polymerase α, β and β′ subunits, *cis* proline residues are known to be present [1] and DksA's PPIase activity may be required for the isomerization of their prolyl residues. Furthermore, DksA could prevent the aggregation of RNAP major subunits in Δ6*ppi* and Δ*dnaK/J* mutants, which are known to aggregate in such strains. Thus, finding the natural cellular substrates of DksA, Cmk and MetL requires further extensive studies.

DksA has been structurally and functionally well-studied, yet the mechanism of suppression of the Ts phenotype of Δ*dnaK/J* has remained elusive [29]. As DksA turned out to be an effective suppressor of Ts phenotype of Δ6*ppi* and Δ(*dnaK/J tig*) bacteria, and exhibits a PPIase activity, we also identified genes whose products are required for its multicopy suppressor phenotype. Thus, we showed that the DksA-mediated multicopy suppression is abolished when the expression of either RpoE sigma factor or chaperonins (GroL/S) are reduced. Thus, a unique mutation *rpoEp*^{d} that caused a disruption of the promoter element of the *rpoE* gene, even though its structural gene was duplicated, abolished the suppression by DksA not only of Δ6*ppi* but also of Δ*dnaK/J* bacteria. RpoE responds to the cell envelope stress and positively regulates the expression of many genes, whose products are involved in folding and assembly of outer membrane proteins (OMPs) and sRNAs that act in the feedback mechanism to repress synthesis of major components of the cell envelope such as OMPs and lipoproteins to maintain the cellular homeostasis [44]. Examination of transcription of the *rpoE* gene revealed that its expression is repressed in Δ6*ppi* at permissive growth conditions and is further reduced in a *rpoEp*^{d} background. Thus, when the *dksA* gene is expressed from a plasmid, it further decreases the *rpoE* transcription that could lead to abolishing of the DksA-mediated restoration of growth. This also explains the isolation of mutations in *envZ* and *tol*A genes that abolish the suppression of Δ6*ppi* and Δ*dnaK/J* bacteria at high temperature by DksA. Since *tolA* mutants exhibit the enhanced RpoE induction and hypervesiculation [45,46] is consistent with the DksA-mediated suppression being sensitive to hyperinduction of the RpoE regulon. Thus, connection between the DksA-mediated restoration of growth of either Δ*dnaK/J* or Δ6*ppi* is highly dependent on maintenance of homeostasis of extracytoplasmic components and balanced signaling of envelope stress. Supporting this pathway is also isolation of the *cpxR*::Tn*10* insertion that abolish the multicopy suppression by DksA. The activation of CpxR/A two-component system induces the expression of several periplasmic folding factors including *degP, ppiD* and *dsbA* [47,48]. The importance of GroL/S abundance for survival of either Δ6*ppi* or Δ(*dnaK/J tig*) derivatives is further highlighted in this work, since (*a*) *groS/L* overexpression suppresses growth defects of such strains and (*b*) the isolation of *groSL* promoter mutations reducing transcription of this operon also abolished the multicopy suppression by DksA. Interestingly, the isolation of Tn*10* insertion located 101 nt upstream of the initiation codon is similar to the previously isolated insertion element as a suppressor mutation of the *rpoH* deletion that creates a new promoter, allowing the constitutive expression of the *groSL* operon [35]. It is well established that *groS/L* genes are essential for bacterial growth under all growth conditions [49,50].

The isolation of *rnhA*::Tn*10* that totally abolished the suppression by DksA of either Δ*dnaKJ* or Δ6*ppi* is in line with the DksA's important role in DNA damage repair [11]. The RnhA function is crucial in the removal of RNA-DNA hybrids and prevention of the lethality due to the R-loop

formation [51]. Thus, RnhA and DksA are both important in this process of maintaining the genomic integrity and this appears to be impaired in Δ6*ppi* bacteria. In support of these conclusions, we have shown that Δ6*ppi* bacteria exhibit the sensitivity towards DNA-damaging agents such as nalidixic acid—a phenotype shared with *rnhA* and *dksA* mutants. This role of DksA for DNA repair system draws further support, since overexpression of the *dksA* gene can suppress the sensitivity of Δ6*ppi* bacteria to Nal. It is likely that the SrrA-mediated suppression of Nal sensitivity operates via the same pathway as DksA. The suppression by DksA was also found to require the functional Tat system of protein translocation. The insertion mutation in the *tatC* gene will abrogate the export of folded proteins that require the Tat system. TatC is the first protein to interact with the N-region of Tat signal peptide [52]. Interestingly, SlyD and DnaK have been shown to bind Tat signal sequences [53,54] and the Tat system could recruit PPIs in assisting translocation. Other prominent insertion defines the LepA requirement for the DksA suppression. Consistent with our results, a synthetic growth defect of Δ*lepA* and Δ*dksA* has also been reported [55]. The *lepA* gene encodes an elongation factor EF4 GTPase with a role in the biogenesis of 30S subunit of ribosomes and the translational initiation [56]. These results explain abrogation of DksA-mediated suppression when either the translational apparatus or the genome integrity are compromised.

We also addressed whether there is any requirement for the Ppk polynucleotide kinase for the DksA-mediated multicopy suppression, since it was identified as one of the prominent co-eluting proteins during the purification of PPIs [1]. However, Δ(6*ppi ppk*) + p*dksA*$^+$ and Δ6*ppi* + p*dksA*$^+$ derivatives grew nearly to the same extent at 43.5 °C either on LA or LB medium, ruling out any requirement for the Ppk function. Even Δ(*dnaK/J ppk*) + p*dksA*$^+$ and Δ*dnaK/J* + p*dksA*$^+$ grew nearly similarly up to 41.0 °C. However, no viable colonies were observed at 42 °C, which is the temperature limit at which DksA can exert the suppression of Ts phenotype of a *dnaK/J* deletion, suggesting only a minor requirement. During this manuscript preparation, it was reported that Ppk is required for the DksA-mediated restoration of growth a *dnaK* Ts mutant strain at 40.5 °C [57]. However, we did not observe any such requirement at the same growth temperature. We showed that a *phoU*::Tn*10* insertion abolishes the DksA-mediated multicopy suppression, which further reinforces the notion that Ppk may not be needed for the multicopy suppression phenotype, since it has been reported that *phoU* mutants have elevated levels of polyphosphates [58].

It is intriguing why overexpression of the *dksA* gene does not suppress growth defects of Δ6*ppi* bacteria at 37 °C but shows a good suppression at elevated temperatures in contrast to the suppression of Δ(*dnaK/J tig*) at 30 or 37 °C. This suggests that the transcription induction or repression of specific gene(s) at elevated temperatures is a requirement for the DksA-mediated suppression for Δ6*ppi* bacteria. At high temperature, mainly RpoH and RpoE regulons are induced. Hence, we propose a model that the DksA suppression depends on the heat shock induction of GroL/S chaperonins and the RpoE induction, consistent with the isolation of transposon insertions in their promoter regions that renders their transcription independent of heat shock promoters and abolish the multicopy suppression by DksA. As DnaK/J negatively regulate the heat shock response, Δ(*dnaK/J tig*) mutants have already elevated levels of GroL/S chaperonins. Consistent with this idea is the isolation of GroL as a multicopy suppressor of (Δ(*dnaK/J tig*) bacteria. The DksA-mediated suppression could be to maintain proper folding in the cytoplasm and extracytoplasm via the transcriptional regulation, sensing oxidative stress and due to its PPIase activity. The regulation of extracytoplasmic stress response could be the essential pathway, since insertions that could elevate the RpoE activation abolish the DksA suppression and DksA was also shown to suppress a lethal phenotype of null mutation of the gene encoding the periplasmic Prc (Tsp) protease [59]. The identification of common insertion mutations that abolish the suppression by DksA in strains lacking either PPIs or DnaK/J chaperones strongly suggests that various aspects of cellular defects are presumably common to strains lacking these protein folding factors and hence a similar requirement for DksA.

In summary, this work shows that cytoplasmic PPIs are crucial for the viability of *E. coli* under conditions that impact either protein folding or perturb the outer membrane. The viability of strains

lacking PPIs requires the presence of DksA and SrrA transcriptional factors, the component of replication/nucleic acid synthesis system Hda/Cmk and MetL. Overexpression of *metL*, *dksA*, *srrA*, *cmk*, *hda*, *diaA*, chaperone systems encoded by *dnaK/J* and *groS*/L and *yjfN* elevates growth defects of Δ6*ppi* bacteria. Importantly, MetL, Cmk and DksA were shown to exhibit the PPIase activity that is inhibited by FK506 and also suppress the conditional lethal phenotype of Δ(*dnaK/J tig*) strains. The identification of these three new PPIs provides a sound explanation for the molecular basis of suppression of growth defects of Δ6*ppi* and in part for suppression of Δ(*dnaK/J tig*) bacteria. The multicopy suppression by DksA was shown to require adequate levels of GroL/S and RpoE, the intact Tat translocation system and is abolished if either genome integrity or envelope stress responsive pathways are compromised. Furthermore, the coiled-coil domain is not only important for the DksA interaction with RNAP, but also for its PPIase activity as the substitution of conserved residues not only abolished its PPIase activity, but also the ability to exert the multicopy suppression with an acute requirement for D74, F82 and L84 residues of DksA.

4. Materials and Methods

4.1. Bacterial Strains, Plasmids and Media

The bacterial strains and plasmids used in this study are described in Supplementay Table S3. Luria–Bertani (LB) broth, M9 (Difco, MD, USA) and M9 minimal media were prepared as previously described [17]. When required, media were supplemented with ampicillin (100 μg/mL), kanamycin (50 μg/mL), tetracycline (10 μg/mL), spectinomycin (50 μg/mL) and chloramphenicol (20 μg/mL). For transductions or evaluating growth properties involving either Δ*dksA* derivatives or different cloned *dksA* mutants, M9 minimal medium with or without supplementation of casamino acids was used.

4.2. Generation of Null Mutations in Various Genes, Whose Products in the High Dosage Suppress Growth Defects of Δ6ppi Strains and the Construction of Δ(dnaK/J tig) Deletion Derivatives

Non-polar antibiotic-free deletion mutations of various genes, whose overexpression restored the growth of Δ6*ppi* strains, were constructed by using the λ Red recombinase/FLP-mediated recombination system as described previously [14,60]. The antibiotic cassette was amplified using pKD3 and pKD13 as templates [60]. PCR products from such amplification reactions were electroporated into BW25113 containing the λ Red recombinase-encoding plasmid pKD46 (GK1942). Each deletion was verified by PCR amplification and sequencing of PCR products. Such deletions were transduced into parental wild-type strains and Δ6*ppi* strains by bacteriophage P1-mediated transduction. Multiple null combinations were constructed as described previously, followed by the removal of *aph* or *cat* cassettes using the pCP20 plasmid and confirmed to be non-polar [17,60]. When required, additional deletion derivatives were constructed using *ada* cassette for gene replacement using the pCL1920 plasmid as a template in PCR amplification reactions, followed by gene replacement as described above. A non-polar deletion derivative of the *ppk* gene was also constructed in the same manner and verified by its >95% linkage with the *hda* gene. To construct strains simultaneously lacking major chaperones encoded by *dnaK/dnaJ* genes and trigger factor PPI encoded by the *tig* gene, previously constructed the deletion strain Δ(*dnaK dnaJ*) GK3078 [14] served as a recipient for the introduction of either *tig*<>*cat* or *tig*<>*ada* deletions by bacteriophage P1-mediated transduction, resulting into the strains SR21830 and SR21836, respectively. Similarly, SR18157 (*dnaK/J*)<>*ada* strain served as a recipient to bring in the *tig*<>*aph* mutation, resulting into the construction of Δ(*dnaK dnaJ tig*) strain SR21842. Transductions were performed on M9 minimal medium at 23 and 30 °C to prevent the accumulation of extragenic suppressors and verified for the inability to plate the bacteriophage λ and also the synthetic lethality on LA medium at 30 °C and above.

4.3. The Identification of Multicopy Suppressors, Whose Overexpression Restores the Growth of Either Δ6ppi or Δ(dnaK/J tig) Derivatives under Non-Permissive Growth Conditions

The complete genomic library of all predicted ORFs of *E. coli* cloned in pCA24N (ASKA collection) [13] was used to transform the Δ6*ppi* derivative SR18292. As this strain exhibits a stringent growth phenotype on LA medium at all temperatures, LA resistant transformants were selected at 23, 30, 37 and 43 °C in the presence of IPTG (75 μM). DNA insert of all relevant plasmids that restored the growth upon retransformation on LA rich medium at one of these temperatures was sequenced. Since the Δ6*ppi* derivative SR18292 also exhibits the temperature-sensitive phenotype on minimal medium at 43 °C, multicopy suppressors were directly selected for the restoration of growth. In parallel, we used the same genomic library for the isolation of multicopy suppressors that restore the growth on M9 minimal medium with glycerol as the sole carbon source (non-permissive for Δ6*ppi* bacteria) or when supplemented with either 4.5% ethanol or erythromycin (15 μg/mL) or vancomycin (75 μg/mL). Since the ASKA library is a collection of cloned single genes, it is likely that some genes, which are organized as operons and whose products work together, will be missed, the whole genomic plasmid library was constructed after partial digestion of chromosomal DNA of Δ6*ppi* strain by Sau3A I and cloned in a p15-based medium-copy number plasmid as described previously [14].

To isolate multicopy suppressors of Δ(*dnaK/J tig*), deletion derivatives SR21836 and SR21842 were transformed with the above-mentioned genomic library containing all ORFs and plated at 30 and 34 °C on LA medium in the presence of 75 μM IPTG. The plasmid DNA was isolated from cultures obtained from such suppressing clones and used to retransform SR21836 and SR21842 strains to verify the reproducibility of suppression. The identity of gene, which when overexpressed suppresses a Δ(*dnaK/J tig*) derivative, was obtained from DNA sequencing.

4.4. The Isolation of Chromosomal Transposon Insertion Mutations That Prevent the Multicopy Suppression by the dksA Gene

As overexpression of the *dksA* gene restores the growth of Δ6*ppi* bacteria, chromosomal gene disruptions were isolated to understand the pathway of DksA-mediated suppression. Thus, the strain SR20561 Δ6*ppi* derivative from SR18292 carrying the *dksA* gene in pBR322 (pSR9332) was used as a host to isolate Tn*10* insertions. In this plasmid, the expression of the full-length *dksA* gene is driven from its own promoters and has an identical insert of the suppressing clone originally isolated as a suppressor of the *dnaKJ* deletion. More than 50,000 transposon insertion mutants were isolated on M9 medium at 37 °C using λTn*10* mutagenesis as described previously [15]. Transductants were screened for a Ts phenotype on LA medium at 42 and 43 °C (lack of suppression). A bacteriophage P1 was grown on such mutants individually and such P1 lysates were used to validate a Ts phenotype in the strain SR20561 (Δ6*ppi* + p*dksA*) by retransduction. Those mutations that bred true were introduced into the wild-type strain BW25113 for further characterization and preparation of chromosomal DNA. The position of Tn*10* was determined by the inverse PCR with nested primers and sequenced using the Tn*10* primer as described previously [14]. Alternatively, the Tn*10* insertion and the flanking chromosomal regions were cloned in a medium-copy vector pMBL18/19 using chromosomal DNA fragments generated by partial digestion by Sau3A I. The position of Tn*10* was determined by sequencing DNA insert using appropriate primers. Temperature sensitive mutations mapping to the *degP* gene were identified either by sequencing the junction of Tn*10* insertion or by P1 transductions using SR8703 (a well characterized *degP*::Tn*10* tet^R) as a donor. For the analysis of suppression of a Δ*dnaK/J* strain, GK3078 [14] was transformed with the *dksA*-expressing plasmid pSR9332 resulting in SR20733. SR20733 served as a recipient for transductions that were performed on M9 minimal medium at 30 °C. Transductants were subsequently tested for the Ts phenotype at 40 and 42 °C on LA medium.

4.5. Cloning of Various Genes for Complementation Studies

For routine complementation, the expression of corresponding genes was induced from clones in the expression vector pCA24N [13]. For the analysis of multicopy suppression by overexpression of

the *dksA* gene, the wild type gene was cloned in pBR322 using chromosomal DNA cloned in λ phage from the Kohara library 15A7DNA. Recombinant plasmids carrying the *dksA* gene were selected on the basis of restoration of the growth of either the Δ6*ppi* derivative SR18292 at 43.5 °C on LA medium or that of *dnaKJ* deletion at 42 °C on LA medium. This plasmid pSR9332 is thus identical to the original *dksA* derivative that identified the *dksA* gene [30]. For the complementation of Δ*dnaK/J*, the minimal coding region of the *dnak dnaJ* operon with its native promoter was PCR amplified and cloned in the p15A-based vector, resulting into plasmid pSR21593.

4.6. RNA Purification and qRT-PCR Analysis

Exponentially grown cultures of the wild-type strain BW25113, its Δ6*ppi* derivative SR18292, SR20561 (Δ6*ppi* + p*dksA*$^+$), GK5165 [(Δ6*ppi* + p*dksA*$^+$)::*rpoE*^{d}Tn*10*], SR8691 Δ*rpoE* were grown at 37 °C in M9 minimal medium and adjusted to an optical density OD_{600} of 0.05. Culture were allowed to grow up to an OD_{600} of 0.2 and harvested by centrifugation. RNA was purified by the hot phenol extraction procedure as previously described [61]. RNA was precipitated with ethanol and resuspended in 100 µL of DEPC-treated water. RNA amounts were quantified and RNA integrity verified by agarose gel electrophoresis. Quantitative Real Time PCR (qRT-PCR) was used to quantify changes in the *rpoE* gene expression, using the gene-specific primer (Supplementary Table S4). Purified mRNA (2 µg) was converted to cDNA and qRT-PCR was performed using CFX Connect Real-Time PCR Detection System (Bio-Rad, Poland) under conditions described previously [1]. Data were analyzed by software Bio-Rad CFX Maestro. For each experiment, three biological replicates were used.

4.7. Protein Purification of Wild-Type and dksA Mutants

For the protein induction, the minimal coding sequence of the *dksA* gene was cloned with an in-frame cleavable N-terminal His_6 affinity tag in the T7 polymerase-based pET28b expression vector. Specific mutations were introduced by the gene synthesis and Gibson cloning. For the purification, hexa-His-tagged wild-type DksA or its variants cloned in the pET28b expression vector, gene expression was induced in the *E. coli* T7 express derivative lacking all six PPIs (SR21984) at 33 °C at an optical density of 0.1 at 600 nm in a 1-l culture by the addition of 0.3 mM IPTG and grown for 4 h. For the purification of Cmk and MetL, the plasmid DNA from JW0893 and JW3911 [13] were used to transform the Δ6*ppi* strain SR18292 to induce the expression of proteins by the addition of 0.3 mM IPTG. After the induction, cells were harvested by centrifugation at 12,000 rpm for 30 min. The pellet was resuspended in B-PER reagent (Pierce) and adjusted to contain 50 mM NaH_2PO_4, 300 mM NaCl, 10 mM imidazole (buffer A), supplemented with lysozyme to a final concentration of 200 µg/mL, a cocktail of protease inhibitors (Sigma, Poznan, Poland) and 30 units of benzonase (Merck, Poznan, Poland). The mixture was incubated on ice for 45 min with gentle mixing. The lysate was centrifuged at 45,000× *g* for 30 min at 4 °C. Soluble proteins were applied over nickel-nitrilotriacetic acid beads (Qiagen, Geneva, Switzerland), washed and eluted with buffer A with a linear gradient (50 mM–500 mM) of imidazole.

4.8. The PPIase Assay and the PPIase-Dependent Refolding of RNase T1

For the measurement of PPIase activity with purified individual wild-type or mutant protein, PPIs were used at a concentration in the range of 0.1 to 5 µM. All purified proteins were obtained from Δ6*ppi* strains. The PPIase activity was measured in a chymotrypsin-coupled enzymatic assay [23,36] using 8 mM *N*-Suc-Ala-Ala-*cis*-Pro-Phe-*p*-nitroanilide as the substrate. The PPIase activity was determined in 35 mM HEPES pH 8.0 as assay buffer and the activity was measured at 10 °C. The reaction was initiated by the addition of chymotrypsin (300 µg/mL) and change in the absorbance at 390 nm was recorded using Specord 200 Plus spectrophotometer equipped with the Peltier temperature control system. When required, the FK506 inhibitor (Sigma, Poznan, Poland) was added in a 2-fold molar excess. FK506 and purified DksA, MetL and Cmk were incubated at 10 °C for 5 min prior to the addition of chymotrypsin.

The proline-limited folding of ribonuclease T1 (RNase T1) was analyzed using the procedure [23] with few modifications. The purified RNase T1 was purchased from Worthington (USA). To unfold RNase, T1 was incubated at 64 μM concentration in a buffer containing 100 mM Tris-HCl, pH 8.0 and 8 M urea for 2 h at 25 °C. The refolding was initiated by 40-fold dilution of urea in a buffer containing 100 mM Tris-HCl, pH 8.0 with the final concentration of 0.33 mM RNase T1. The folding catalyst was added to the reaction mixture at a 10 μM concentration prior to the urea dilution. The tryptophan fluorescence was measured with the emission wavelength of 320 nm (20-nm bandwidth) and the excitation wavelength of 268 nm (20-nm bandwidth) using a Tecan Spark 10M spectrofluorophotometer. The measurement was performed for 15 min with interval time of 1 s.

4.9. β-Galactosidase Activity Assay and Measurement of GroL Levels

For the quantification of activity of the *rrnB*P1 promoter, a single-copy promoter fusion was constructed. To achieve this, the minimal *rrnB*P1 promoter region was cloned in the promoter probe vector pRS415 and transferred to the chromosome using bacteriophage λ derivative λRS45 to generate a single copy *rrnB*P1-*lacZ* fusion in BW25113, using previously described procedure [61,62]. This resulted in the construction of SR22123 strain, which subsequently served as a host to introduce the null allele of the *dksA* gene (SR22415) and various plasmids carrying either the wild-type *dksA* gene or its different mutant derivatives. For the measurement of *β*-galactosidase activity, isogenic cultures were grown in LB medium at 37 °C. Exponentially grown cultures were adjusted to an OD_{600} of 0.05 and aliquots of samples were used to measure the *β*-galactosidase activity as described [15]. For the measurement of GroL levels, overnight cultures of the wild-type strain and its isogenic derivatives carrying either *groSp*^{d}*1* or *groSp*^{d}2 mutation were grown at 30 °C in M9 minimal medium. Cultures were adjusted to an OD_{600} of 0.05 in M9 medium and allowed to reach an OD_{600} of 0.2. One-milliliter aliquots were shifted to prewarmed tubes held at 42 °C and incubated for 15 min. Proteins were precipitated by TCA (10%) and analyzed on 12.5% SDS-PAGE, followed by immunoblotting with anti-GroL antibodies.

Supplementary Materials: Supplementary materials can be found at http://www.mdpi.com/1422-0067/21/16/5843/s1. Table S1. Overexpression of *groS/L* genes can rescue growth of Δ6*ppi* bacteria up to 42 °C on LA medium; Table S2. Growth rate per hour (μ) of strains carrying Tn*10* insertions in various genes that prevent the DksA-mediated suppression to different extents in Δ6*ppi* and Δ*dnaK/J* derivatives carrying the plasmid expressing the *dksA* gene; Table S3. Bacterial strains and plasmids used in this study; Table S4. Primers; Figure S1. Overexpression of the *nudJ* and *ydgC* genes can restore the wild type-like growth of Δ6*ppi* bacteria on LA medium at either 23 or 30 °C.

Author Contributions: Conceptualization, methodology and validation, S.R. and G.K.; investigation, S.R., G.K., P.W., D.B., A.S. and P.G.; writing—original draft preparation, review and editing, S.R. and G.K.; supervision, S.R.; and funding acquisition, S.R. All authors have read and agreed to the published version of the manuscript.

Funding: This research was funded by National Science Center (NCN) Grant 2017/25/B/NZ6/02021 to S. R.

Conflicts of Interest: The authors declare no conflict of interest.

Abbreviations

PPI	peptidyl-prolyl *cis*/*trans* isomerase
FKBP	FK506-binding protein
RNAP	RNA polymerase

References

1. Klein, G.; Wojtkiewicz, P.; Biernacka, D.; Stupak, A.; Gorzelak, P.; Raina, S. Identification of substrates of cytoplasmic peptidyl-prolyl *cis/trans* isomerases and their collective essentiality in *Escherichia coli*. *Int. J. Mol. Sci.* **2020**, *21*, 4212. [CrossRef] [PubMed]
2. Okumura, M.; Kadokura, H.; Hashimoto, S.; Yutani, K.; Kanemura, S.; Hikima, T.; Hidaka, Y.; Ito, L.; Shiba, K.; Masui, S.; et al. Inhibition of the functional interplay between endoplasmic reticulum (ER) oxidoreductin-1α (Ero1α) and protein-disulfide isomerase (PDI) by the endocrine disruptor bisphenol A. *J. Biol. Chem.* **2014**, *289*, 27004–27018. [CrossRef] [PubMed]

3. Fischer, G.; Aumüller, T. Regulation of peptide bond *cis/trans* isomerization by enzyme catalysis and its implication in physiological processes. *Rev. Physiol. Biochem. Pharmacol.* **2003**, *148*, 105–150. [CrossRef] [PubMed]
4. Grathwohl, C.; Wüthrich, K. The X-Pro peptide bond as an NMR probe for conformational studies of flexible linear peptides. *Biopolymers* **1976**, *15*, 2025–2041. [CrossRef]
5. Cheng, H.N.; Bovey, F.A. *Cis-trans* equilibrium and kinetic studies of acetyl-L-proline and glycyl-L-proline. *Biopolymers* **1977**, *16*, 1465–1472. [CrossRef]
6. Stewart, D.E.; Sarkar, A.; Wampler, J.E. Occurrence and role of *cis* peptide bonds in protein structures. *J. Mol. Biol.* **1990**, *214*, 253–260. [CrossRef]
7. Schmidpeter, P.A.M.; Koch, J.R.; Schmid, F.X. Control of protein function by prolyl isomerization. *Biochim. Biophys. Acta* **2015**, *1850*, 1973–1982. [CrossRef]
8. Lang, K.; Schmid, F.X.; Fischer, G. Catalysis of protein folding by prolyl isomerase. *Nature* **1987**, *329*, 268–270. [CrossRef]
9. Siekierka, J.J.; Hung, S.H.; Poe, M.; Lin, C.S.; Sigal, N.H. A cytosolic binding protein for the immunosuppressant FK506 has peptidyl-prolyl isomerase activity but is distinct from cyclophilin. *Nature* **1989**, *341*, 755–757. [CrossRef]
10. Rahfeld, J.U.; Schierhorn, A.; Mann, K.; Fischer, G. A novel peptidyl-prolyl *cis/trans* isomerase from *Escherichia coli*. *FEBS Lett.* **1994**, *343*, 65–69. [CrossRef]
11. Myka, K.K.; Küsters, K.; Washburn, R.; Gottesman, M.E. DksA-RNA polymerase interactions support new origin formation and DNA repair in *Escherichia coli*. *Mol. Microbiol.* **2019**, *111*, 1382–1397. [CrossRef] [PubMed]
12. Malik, M.; Zhao, X.; Drlica, K. Lethal fragmentation of bacterial chromosomes mediated by DNA gyrase and quinolones. *Mol. Microbiol.* **2006**, *61*, 810–825. [CrossRef] [PubMed]
13. Kitagawa, M.; Ara, T.; Arifuzzaman, M.; Ioka-Nakamichi, T.; Inamoto, E.; Toyonaga, H.; Mori, H. Complete set of ORF clones of *Escherichia coli* ASKA library (a complete set of *E. coli* K-12 ORF archive): Unique resources for biological research. *DNA Res.* **2005**, *12*, 291–299. [CrossRef] [PubMed]
14. Klein, G.; Kobylak, N.; Lindner, B.; Stupak, A.; Raina, S. Assembly of lipopolysaccharide in *Escherichia coli* requires the essential LapB heat shock protein. *J. Biol. Chem.* **2014**, *289*, 14829–14853. [CrossRef]
15. Klein, G.; Stupak, A.; Biernacka, D.; Wojtkiewicz, P.; Lindner, B.; Raina, S. Multiple transcriptional factors regulate transcription of the *rpoE* gene in *Escherichia coli* under different growth conditions and when the lipopolysaccharide biosynthesis is defective. *J. Biol. Chem.* **2016**, *291*, 22999–23019. [CrossRef]
16. Missiakas, D.; Georgopoulos, C.; Raina, S. Identification and characterization of the *Escherichia coli* gene *dsbB*, whose product is involved in the formation of disulfide bonds in vivo. *Proc. Natl. Acad. Sci. USA* **1993**, *90*, 7084–7088. [CrossRef]
17. Klein, G.; Lindner, B.; Brade, H.; Raina, S. Molecular basis of lipopolysaccharide heterogeneity in *Escherichia coli*: Envelope stress-responsive regulators control the incorporation of glycoforms with a third 3-deoxy-α-D-*manno*-oct-2-ulosonic acid and rhamnose. *J. Biol. Chem.* **2011**, *286*, 42787–42807. [CrossRef]
18. Raina, S.; Missiakas, D.; Baird, L.; Kumar, S.; Georgopoulos, C. Identification and transcriptional analysis of the *Escherichia coli htrE* operon which is homologous to Pap and related pilin operons. *J. Bacteriol.* **1993**, *175*, 5009–5021. [CrossRef]
19. Teter, S.A.; Houry, W.A.; Ang, D.; Tradler, T.; Rockabrand, D.; Fischer, G.; Blum, P.; Georgopoulos, C.; Hartl, F.U. Polypeptide flux through bacterial Hsp70: DnaK cooperates with trigger factor in chaperoning nascent chains. *Cell* **1999**, *97*, 755–765. [CrossRef]
20. Deuerling, E.; Schulze-Specking, A.; Tomoyasu, T.; Mogk, A.; Bukau, B. Trigger factor and DnaK cooperate in folding of newly synthesized proteins. *Nature* **1999**, *400*, 693–696. [CrossRef]
21. Geitner, A.J.; Weininger, U.; Paulsen, H.; Balbach, J.; Kovermann, M. Structure-based insights into the dynamics and function of two-domain SlpA from *Escherichia coli*. *Biochemistry* **2017**, *56*, 6533–6543. [CrossRef] [PubMed]
22. Hennig, L.; Christner, C.; Kipping, M.; Schelbert, B.; Rücknagel, K.P.; Grabley, S.; Küllertz, G.; Fischer, G. Selective inactivation of parvulin-like peptidyl-prolyl *cis/trans* isomerases by juglone. *Biochemistry* **1998**, *37*, 5953–5960. [CrossRef] [PubMed]
23. Fischer, G.; Wittmann-Liebold, B.; Lang, K.; Kiefhaber, T.; Schmid, F.X. Cyclophilin and peptidyl-prolyl *cis-trans* isomerase are probably identical proteins. *Nature* **1989**, *337*, 476–478. [CrossRef] [PubMed]

24. Schmid, F.X.; Frech, C.; Scholz, C.; Walter, S. Catalyzed and assisted protein folding of ribonuclease T1. *Biol. Chem.* **1996**, *377*, 417–424. [PubMed]
25. Gourse, R.L.; Chen, A.Y.; Gopalkrishnan, S.; Sanchez-Vazquez, P.; Myers, A.; Ross, W. Transcriptional responses to ppGpp and DksA. *Annu. Rev. Microbiol.* **2018**, *72*, 163–184. [CrossRef]
26. Paul, B.J.; Barker, M.M.; Ross, W.; Schneider, D.A.; Webb, C.; Foster, J.W.; Gourse, R.L. DksA: A critical component of the transcription initiation machinery that potentiates the regulation of rRNA promoters by ppGpp and the initiating NTP. *Cell* **2004**, *118*, 311–322. [CrossRef]
27. Lee, J.H.; Lennon, C.W.; Ross, W.; Gourse, R.L. Role of the coiled-coil tip of *Escherichia coli* DksA in promoter control. *J. Mol. Biol.* **2012**, *416*, 503–517. [CrossRef]
28. Parshin, A.; Shiver, A.L.; Lee, J.; Ozerova, M.; Schneidman-Duhovny, D.; Gross, C.A.; Borukhov, S. DksA regulates RNA polymerase in *Escherichia coli* through a network of interactions in the secondary channel that includes sequence insertion 1. *Proc. Natl. Acad. Sci. USA* **2015**, *112*, E6862–E6871. [CrossRef]
29. Chandrangsu, P.; Wang, L.; Choi, S.H.; Gourse, R.L. Suppression of a *dnaKJ* deletion by multicopy *dksA* results from non-feedback-regulated transcripts that originate upstream of the major *dksA* promoter. *J. Bacteriol.* **2012**, *194*, 1437–1446. [CrossRef]
30. Kang, P.J.; Craig, E.A. Identification and characterization of a new *Escherichia coli* gene that is a dosage-dependent suppressor for a *dnaK* deletion mutation. *J. Bacteriol.* **1990**, *172*, 2055–2064. [CrossRef]
31. Lipinska, B.; Sharma, S.; Georgopoulos, C. Sequence analysis and regulation of the *htrA* gene of *Escherichia coli*: A σ32-independent mechanism of heat-inducible transcription. *Nucleic Acids Res.* **1988**, *16*, 10053–10067. [CrossRef] [PubMed]
32. Baird, L.; Lipinska, B.; Raina, S.; Georgopoulos, C. Identification of the *Escherichia coli sohB* gene, a multicopy suppressor of the HtrA (DegP) null phenotype. *J. Bacteriol.* **1991**, *173*, 5763–5770. [CrossRef] [PubMed]
33. Dartigalongue, C.; Missiakas, D.; Raina, S. Characterization of the *Escherichia coli* σ^E regulon. *J. Biol. Chem.* **2001**, *276*, 20866–20875. [CrossRef] [PubMed]
34. Goldman, B.S.; Gabbert, K.K.; Kranz, R.G. The temperature-sensitive growth and survival phenotypes of *Escherichia coli cydDC* and *cydAB* strains are due to deficiencies in cytochrome *bd* and are corrected by exogenous catalase and reducing agents. *J. Bacteriol.* **1996**, *178*, 6348–6351. [CrossRef]
35. Kusukawa, N.; Yura, T. Heat shock protein GroE of *Escherichia coli*: Key protective roles against thermal stress. *Genes Dev.* **1988**, *2*, 874–882. [CrossRef]
36. Kofron, J.L.; Kuzmič, P.; Kishore, V.; Colón-Bonilla, E.; Rich, D.H. Determination of kinetic constants for peptidyl prolyl *cis-trans* isomerases by an improved spectrophotometric assay. *Biochemistry* **1991**, *30*, 6127–6134. [CrossRef]
37. Park, S.T.; Aldape, R.A.; Futer, O.; DeCenzo, M.T.; Livingston, D.J. PPIase catalysis by human FK506-binding protein proceeds through a conformational twist mechanism. *J. Biol. Chem.* **1992**, *267*, 3316–3324.
38. Fujimitsu, K.; Su'etsugu, M.; Yamaguchi, Y.; Mazda, K.; Fu, N.; Kawakami, H.; Katayama, T. Modes of overinitiation, *dnaA* gene expression, and inhibition of cell division in a novel cold-sensitive *hda* mutant of *Escherichia coli*. *J. Bacteriol.* **2008**, *190*, 5368–5381. [CrossRef]
39. Falcoz-Kelly, F.; van Rapenbusch, R.; Cohen, G.N. The methionine-repressible homoserine dehydrogenase and aspartokinase activities of *Escherichia coli* K12. Preparation of the homogeneous protein catalyzing the two activities. Molecular weight of the native enzyme and of its subunits. *Eur. J. Biochem.* **1969**, *8*, 146–152. [CrossRef]
40. Anglès, F.; Castanié-Cornet, M.P.; Slama, N.; Dinclaux, M.; Cirinesi, A.M.; Portais, J.C.; Létisse, F.; Genevaux, P. Mutilevel interaction of the DnaK/DnaJ(HSP70/HSP40) stress-responsive chaperone machine with the central metabolism. *Sci. Rep.* **2017**, *7*, 41341. [CrossRef]
41. Laptenko, O.; Lee, J.; Lomakin, I.; Borukhov, S. Transcript cleavage factors GreA and GreB act as transient catalytic components of RNA polymerase. *EMBO J.* **2003**, *22*, 6322–6334. [CrossRef] [PubMed]
42. Opalka, N.; Chlenov, M.; Chacon, P.; Rice, W.J.; Wriggers, W.; Darst, S.A. Structure and function of the transcription elongation factor GreG bound to bacterial RNA polymerase. *Cell* **2003**, *114*, 335–345. [CrossRef]
43. Lamour, V.; Rutherford, S.T.; Kuznedelov, K.; Ramagopal, U.A.; Gourse, R.L.; Severinov, K.; Darst, S.A. Crystal structure of *Escherichia coli* Rnk, a new RNA polymerase-interacting protein. *J. Mol. Biol.* **2008**, *383*, 367–379. [CrossRef] [PubMed]
44. Klein, G.; Raina, S. Small regulatory bacterial RNAs regulating the envelope stress response. *Biochem. Soc. Trans.* **2017**, *45*, 417–425. [CrossRef] [PubMed]

45. Bernadac, A.; Gavioli, M.; Lazzaroni, J.C.; Raina, S.; Lloubès, R. *Escherichia coli tol-pal* mutants form outer membrane vesicles. *J. Bacteriol.* **1998**, *180*, 4872–4878. [CrossRef]
46. Vinés, E.D.; Marolda, C.L.; Balachandran, A.; Valvano, M.A. Defective *O*-antigen polymerization in *tolA* and *pal* mutants of *Escherichia coli* in response to extracytoplasmic stress. *J. Bacteriol.* **2005**, *187*, 3359–3368. [CrossRef]
47. Missiakas, D.; Raina, S. Signal transduction pathways in response to protein misfolding in the extracytoplasmic compartments of *E. coli*: Role of two new phosphoprotein phosphatases PrpA and PrpB. *EMBO J.* **1997**, *16*, 1670–1685. [CrossRef]
48. Dartigalongue, C.; Raina, S. A new heat-shock gene, *ppiD*, encodes a peptidyl-prolyl isomerase required for folding of outer membrane proteins in *Escherichia coli*. *EMBO J.* **1998**, *17*, 3968–3980. [CrossRef]
49. Fayet, O.; Ziegelhoffer, T.; Georgopoulos, C. The *groES* and *groEL* heat shock gene products of *Escherichia coli* are essential for bacterial growth at all temperatures. *J. Bacteriol.* **1989**, *171*, 1379–1385. [CrossRef]
50. Shewmaker, F.; Kerner, M.J.; Hayer-Hartl, M.; Klein, G.; Georgopoulos, C.; Landry, S.J. A mobile loop order-disorder transition modulates the speed of chaperonin cycling. *Protein Sci.* **2004**, *13*, 2139–2148. [CrossRef]
51. Wimberly, H.; Shee, C.; Thornton, P.C.; Sivaramakrishnan, P.; Rosenberg, S.M.; Hastings, P.J. R-loops and nicks initiate DNA breakage and genome instability in non-growing *Escherichia coli*. *Nat. Commun.* **2013**, *4*, 2115. [CrossRef] [PubMed]
52. Cléon, F.; Habersetzer, J.; Alcock, F.; Kneuper, H.; Stansfeld, P.J.; Basit, H.; Wallace, M.I.; Berks, B.C.; Palmer, T. The TatC component of the twin-arginine protein translocase functions as an obligate oligomer. *Mol. Microbiol.* **2015**, *98*, 111–129. [CrossRef] [PubMed]
53. Graubner, W.; Schierhorn, A.; Brüser, T. DnaK plays a pivotal role in Tat targeting of CueO and functions beside SlyD as a general Tat signal binding chaperone. *J. Biol. Chem.* **2007**, *282*, 7116–7124. [CrossRef] [PubMed]
54. Pérez-Rodríguez, R.; Fisher, A.C.; Perlmutter, J.D.; Hicks, M.G.; Chanal, A.; Santini, C.L.; Wu, L.F.; Palmer, T.; DeLisa, M.P. An essential role for the DnaK molecular chaperone in stabilizing over-expressed substrate proteins of the bacterial twin-arginine translocation pathway. *J. Mol. Biol.* **2007**, *367*, 715–730. [CrossRef] [PubMed]
55. Balakrishnan, R.; Oman, K.; Shoji, S.; Bundschuh, R.; Fredrick, K. The conserved GTPase LepA contributes mainly to translation initiation in *Escherichia coli*. *Nucleic Acids Res.* **2014**, *42*, 13370–13383. [CrossRef] [PubMed]
56. Gibbs, M.R.; Fredrick, K. Roles of elusive translational GTPases come to light and inform on the process of ribosome biogenesis in bacteria. *Mol. Microbiol.* **2018**, *107*, 445–454. [CrossRef]
57. Gray, M.J. Interactions between DksA and stress-responsive alternative sigma factors control inorganic polyphosphate accumulation in *Escherichia coli*. *J. Bacteriol.* 2020. [CrossRef]
58. Morohoshi, T.; Maruo, T.; Shirai, Y.; Kato, J.; Ikeda, T.; Takiguchi, N.; Ohtake, H.; Kuroda, A. Accumulation of inorganic polyphosphate in *phoU* mutants of *Escherichia coli* and *Synechocystis* sp. strain PCC6803. *Appl. Environ. Microbiol.* **2002**, *68*, 4107–4110. [CrossRef]
59. Bass, S.; Gu, Q.; Christen, A. Multicopy suppressors of *prc* mutant *Escherichia coli* include two HtrA (DegP) protease homologs (HhoAB), DksA, and a truncated R1pA. *J. Bacteriol.* **1996**, *178*, 1154–1161. [CrossRef]
60. Datsenko, K.A.; Wanner, B.L. One-step inactivation of chromosomal genes in *Escherichia coli* K-12 using PCR products. *Proc. Natl. Acad. Sci. USA* **2000**, *97*, 6640–6645. [CrossRef]
61. Raina, S.; Missiakas, D.; Georgopoulos, C. The *rpoE* gene encoding the σ^E (σ^{24}) heat shock sigma factor of *Escherichia coli*. *EMBO J.* **1995**, *14*, 1043–1055. [CrossRef] [PubMed]
62. Simons, R.W.; Houman, F.; Kleckner, N. Improved single and multicopy *lac*-based cloning vectors for protein and operon fusions. *Gene* **1987**, *53*, 85–96. [CrossRef]

International Journal of
Molecular Sciences

MDPI

Article

Identification of Substrates of Cytoplasmic Peptidyl-Prolyl *Cis/Trans* Isomerases and Their Collective Essentiality in *Escherichia Coli*

Gracjana Klein *, Pawel Wojtkiewicz †, Daria Biernacka †, Anna Stupak, Patrycja Gorzelak and Satish Raina *

Unit of Bacterial Genetics, Gdansk University of Technology, 80-233 Gdansk, Poland; pawwojtk1@student.pg.edu.pl (P.W.); darbiern@student.pg.edu.pl (D.B.); anna.stupak@pg.edu.pl (A.S.); patrycja.gorzelak@gmail.com (P.G.)

* Correspondence: gracjana.klein@pg.edu.pl (G.K.); satish.raina@pg.edu.pl (S.R.); Tel.: +48-58-347-2618 (G.K. & S.R.)

† These authors contributed equally to this work.

Received: 15 May 2020; Accepted: 9 June 2020; Published: 13 June 2020

Abstract: Protein folding often requires molecular chaperones and folding catalysts, such as peptidyl-prolyl *cis/trans* isomerases (PPIs). The *Escherichia coli* cytoplasm contains six well-known PPIs, although a requirement of their PPIase activity, the identity of their substrates and relative enzymatic contribution is unknown. Thus, strains lacking all periplasmic and one of the cytoplasmic PPIs were constructed. Measurement of their PPIase activity revealed that PpiB is the major source of PPIase activity in the cytoplasm. Furthermore, viable Δ*6ppi* strains could be constructed only on minimal medium in the temperature range of 30–37 °C, but not on rich medium. To address the molecular basis of essentiality of PPIs, proteins that aggregate in their absence were identified. Next, wild-type and putative active site variants of FkpB, FklB, PpiB and PpiC were purified and in pull-down experiments substrates specific to each of these PPIs identified, revealing an overlap of some substrates. Substrates of PpiC were validated by immunoprecipitations using extracts from wild-type and PpiC-H81A strains carrying a 3xFLAG-tag appended to the C-terminal end of the *ppiC* gene on the chromosome. Using isothermal titration calorimetry, RpoE, RseA, S2, and AhpC were established as FkpB substrates and PpiC's PPIase activity was shown to be required for interaction with AhpC.

Keywords: prolyl isomerase; protein folding; heat shock proteins; protein aggregation; RpoE sigma factor; PpiB; PpiC; FkpB; FklB; AhpC

1. Introduction

Cellular protein concentration in the cytoplasm is relatively very high, which leads to macromolecular crowding and exposure of hydrophobic surfaces that can cause protein aggregation [1]. Thus, in vivo, the process of folding can compete with the formation of aberrant aggregates, which can lead to severe cellular defects. Hence, in order to carry out their biological functions, most polypeptide chains must fold rapidly into the stable three-dimensional conformation. This is achieved with the help of conserved group of molecular machines to maintain cellular protein homeostasis. In vivo partially folded polypeptides are bound by chaperones to prevent their aggregation or misfolding and critical slow rate-limiting folding steps are accelerated by folding catalysts, such as peptidyl-prolyl *cis/trans* isomerases (PPIs) and thiol-disulfide oxidoreductases (PDIs). PPIs are ubiquitous enzymes, found in all organisms and they catalyze the slow *cis/trans* isomerization of prolyl peptide Xaa-Pro bonds. Due to the relatively high energy barrier (14–24 kcal/mol), the uncatalyzed isomerization is

a slow process with an exchange time constant on the order of several minutes [2]. Hence, PPIs reduce the energy barrier between *cis* and *trans* states and hence accelerate the isomerization [3]. PPIs were initially identified as targets of two immunosuppressive drugs: cyclosporine A (CsA) or FK506 and were hence called cyclophilins and FK506-binding proteins (FKBPs), respectively, and are collectively known as immunophilins [4]. The third family of PPIs is called parvulins, which are distinct from cyclophilins and FKBPs, since their PPIase activity is neither inhibited by cyclosporine nor FK506 [5].

The model bacterium *Escherichia coli* contains ten PPIs that cover all three families of PPIs. Out of these, six PPIs are present in the cytoplasm. These six *E. coli* cytoplasmic PPIs include the cyclophilin PpiB, the FKBPs {trigger factor (Tig), SlyD, FkpB, FklB} and the parvulin PpiC. Although the PPIase activity for each of six cytoplasmic PPIs have been demonstrated, the relative contribution towards the cellular pool has not been reported. Similarly, there is a lack of information about the cellular function of most of PPIs in *E. coli* other than Tig and to some extent for SlyD. Tig is an abundant ribosome-associated protein, consisting of an N-terminal ribosome-binding domain, a PPIase domain and a C-terminal domain [6]. Ribosome profiling studies have revealed that the Tig protein interacts with all nascently synthesized polypeptides with the highest interaction for β-barrel outer membrane proteins (OMPs) [7]. Another cytoplasmic PPI SlyD has been shown to be a two-domain protein functioning as a molecular chaperone, a prolyl *cis/trans* isomerase, and a nickel-binding protein [8,9]. However, its PPIase activity may not be required for its function for the nickel insertion in [NiFe]-hydrogenase [10]. Regarding other cytoplasmic PPIs, on the basis of co-purification the alkyl hydroperoxide reductase subunit C (AhpC) has been suggested as a substrate of PpiC [11]. The FkpB also has a two-domain architecture like SlyD. Using pull-down experiments some ribosomal proteins were found to co-elute with FkpB [12]. However, a complete spectrum of substrates with mutational comparisons in PPI-encoding genes remains unknown in most of the cases.

To gain a better understanding of function of cytoplasmic PPIs, suppressor-free Δ6*ppi* strains were constructed and characterized for their defects in protein folding. Several proteins were identified that aggregate in Δ6*ppi* strains, some of which are essential for bacterial growth. Further, in vivo substrates were identified by pull-down and immunoprecipitations experiments using wild-type and putative active site variants of different PPIs. Among various substrates, an interaction of AhpC with FkpB and PpiC was shown and the essential sigma factor RpoE and its cognate anti-sigma factor RseA established as clients of FkpB using isothermal titration calorimetry.

2. Results

2.1. The Peptidyl-Prolyl Cis/Trans Isomerase Activity Is Required for Optimal Growth

E. coli genome contains six genes, whose products represent all three known families of folding catalysts with the peptidyl-prolyl *cis/trans* isomerase activity in the cytoplasm. To gain insights about their function, strains with a single non-polar gene disruption were constructed and transduced into commonly used *E. coli* K-12 strain BW25113 and tested for any perceivable defects in the colony size, motility, cellular morphology and sensitivity towards antibiotics or factors that cause defects in protein folding and growth properties at different temperatures. Individually all the genes were found to be dispensable; however, Δ*fkpB* derivatives exhibited significant growth defects reminiscent of phenotypes ascribed to *lytB* (*ispH*) mutants [13] such as hypersensitivity to ampicillin (1.5 μg/mL) and to ethanol (4%). Sequence examination of *fkpB* and *ispH* coding regions revealed that their transcription and translation is coupled. Thus, a new non-polar deletion of the *fkpB* gene was constructed and such a (Δ*fkpB ispH*^{C}) strain exhibited growth similar to the wild type and was further used to construct strains lacking all six cytoplasmic PPIs (for simplicity referred as Δ6*ppi*) using bacteriophage P1-mediated transductions. All transductions were carried in parallel on M9 minimal and Luria Agar (LA) rich medium at 30 and 37 °C. Strains lacking five out of six PPIs exhibited a reduction in the colony size (Figure 1). Hence, to obtain a six-deletion strain and assess any essentiality, Δ5*ppi* strains were transformed with either the vector alone or the plasmid carrying the wild-type copy of gene to be

deleted. When Δ5*ppi* derivatives were used as recipients, viable transductants were obtained on M9 medium at 30 °C as well as 37 °C, but not on LA medium when the vector alone was present (Table 1). For further studies, we used a Δ6*ppi* derivative in BW25113 (SR18292) without the vector after verification by PCR the absence of all six *ppi* genes. In the absence of plasmid vector, a Δ6*ppi* derivative forms small colonies on LA at 37 °C with a reduction of colony forming ability by 10^3 as compared to the wild type, but is not viable at either 43 or 23 °C (Table 1, Figure 1). Further, such bacteria were unable to grow even at 30 or 37 °C when glucose was replaced by glycerol as the carbon source. Overall, these results lead us to conclude that the PPIase activity is essential for optimal growth.

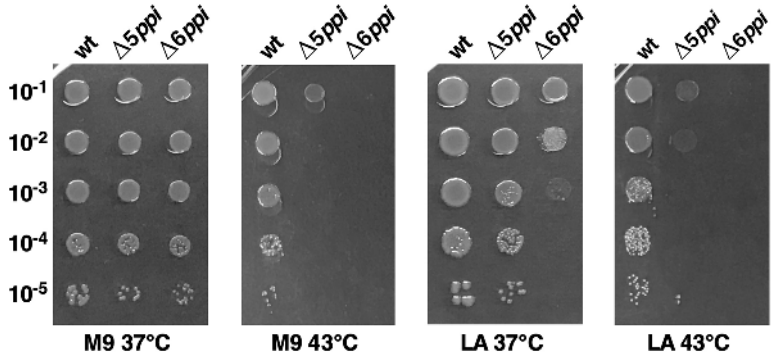

Figure 1. Δ6*ppi* bacteria are unable to grow at either 37 or 43 °C on LA medium. Exponentially grown cultures of the wild type and its isogenic Δ5*ppi* and Δ6*ppi* derivative were adjusted to an optical density OD_{600} 0.1 and serially spot diluted on M9 minimal medium and LA medium. Data presented are from one of the representative experiments.

Table 1. The essentiality of peptidyl-prolyl *cis/trans* isomerases (PPIs) in the wild-type strain BW25113 in Luria Agar (LA) medium as revealed by bacteriophage P1-mediated transductional efficiency criteria. Numbers indicate obtained transductants/mL of recipient. Data are from one of the representative experiments with several repeats.

	23 °C		30 °C		37 °C		43 °C	
	M9	**LA**	**M9**	**LA**	**M9**	**LA**	**M9**	**LA**
Δ(*fklB slyD fkpB tig ppiB*) + vector x Δ*ppiC*	434	8	2369	27	2460	47	–	–
Δ(*fklB slyD fkpB tig ppiB*) + p*ppiC*$^+$ x Δ*ppiC*	1740	1630	2280	1973	2710	2432	838	1140
Δ(*fklB slyD tig ppiB ppiC*) + vector x Δ*fkpB*	342	10	1732	37	1562	35	–	–
Δ(*fklB slyD tig ppiB ppiC*) + p*fkpB*$^+$ x Δ*fkpB*	2314	2640	1948	2100	1980	2013	954	901
Δ(*fklB slyD tig ppiC fkpB*) + vector x Δ*ppiB*	425	5	1420	24	1830	48	–	–
Δ(*fklB slyD tig ppiC fkpB*) + p*ppiB*$^+$ x Δ*ppiB*	1451	1620	1830	1723	2620	2534	1031	977

2.2. Protein Folding Defects—Accumulation of Various Proteins in Aggregation Fractions in Δ6ppi Bacteria

To investigate the cellular function of cytoplasmic PPIs in protein folding, protein folding defects were examined in the Δ6*ppi* strain SR18292 in comparison to its parental wild-type strain BW25113. Exponentially grown cultures in M9 minimal medium at 37 °C (permissive growth conditions) were washed and shifted to Luria-Bertani (LB) medium at 30 °C for 2 h (conditions poorly tolerated by Δ6*ppi* bacteria). Protein aggregates were obtained after careful removal of membrane proteins using previously established procedure [14]. At 30 °C, as expected, wild-type bacteria did not show any significant amount of protein aggregates. However, under the same conditions, extracts from the Δ6*ppi* strain showed a significant increase in the accumulation of protein aggregates accounting for more than 10% of total proteins. Proteins that aggregated in the Δ6*ppi* strain were resolved by SDS polyacrylamide gel electrophoresis (SDS-PAGE) and analyzed by 2-dimensional electrophoresis. The identity of major protein spots, corresponding to aggregation-prone proteins present in the Δ6*ppi* strain and absent in

the parental wild type, was obtained by MALDI-TOF (Table S1). Several proteins that were found to aggregate include major subunits of RNA polymerase and associated factors (RpoB, RpoC, RpoA, Rho), several proteins involved in DNA replication and repair (DnaE, RecB, GyrA, RecA, RuvB, SeqA, LexA), RNA degradation pathway-related proteins (HrpA, CsrD, RhlB, DeaD, Eno), cell division proteins (FtsZ, ZapD, FtsX), those involved in the protein translation (TufA, TufB, InfB, PrfC), proteins required in various metabolic pathways and sugar uptake, transcription factors (Crl, Lrp, Crp, NarL, ArcA, OmpR, ModE), tRNA modifying enzymes, some proteins needed in early steps of lipid A biosynthesis and fatty acid metabolism (LpxA, LpxC, FabA, FabB, FabZ), protein folding and degradation machinery components (IbpB, HslU, ClpX, FtsH), proteins related to cellular redox homeostasis such as alkyl hydroperoxide reductase subunits (AhpC, AhpF), osmotic stress-related proteins (OtsA, BetB, ProP), many ribosomal proteins, including S2, and proteins such as Der, which are required for the ribosomal stability/integrity (Table S1). Interestingly, several of proteins that aggregate in Δ6*ppi* bacteria are essential for the bacterial viability and can help to explain the collective essentiality of cytoplasmic PPIs for the viability under standard laboratory growth conditions. Proteins that were found to aggregate in Δ6*ppi* bacteria were analyzed using the available protein database (PDB server) revealing that some of them indeed contain either known or predicted *cis* proline residues, while many are proline rich suggesting a requirement of PPIs in the catalysis of proline isomerization (Table S1).

2.3. The PpiB Protein Is the Major Contributor of PPIase Activity in the Cytoplasm

Up to now, the relative contribution of each cytoplasmic PPI to the total enzymatic pool has not been reported. To measure only the PPIase activity of cytoplasmic PPIs, a strain that lacks four periplasmic PPIs was constructed to introduce different null alleles of genes encoding cytoplasmic PPIs to quantify their PPIase activity in a single copy. Measurement of the PPIase activity of soluble cell extracts obtained from such strains revealed that among cytoplasmic PPIs PpiB contributes the bulk of peptidyl-prolyl *cis/trans* isomerase activity (Figure 2A). The relative order of PPIase activity is PpiB > FklB > SlyD > Tig > PpiC > FkpB. Surprisingly, the strain lacking four periplasmic PPIs and the *tig* gene consistently showed the higher PPIase activity than its parental strain. As Tig is an abundant ribosome-associated protein with a chaperone-like activity, suggested that the expression of one or more cytoplasmic PPIs might be up-regulated in a *tig*-deleted strain. Thus, an individual null allele of rest of five cytoplasmic PPI-encoding genes were introduced into a SR20072 derivative lacking the *tig* gene and analyzed for the PPIase activity. Among such strains, the deletion derivative of the *fkpB* gene alone showed the significantly reduced PPIase activity that can be attributed to Tig (Figure 2B). Thus, we can conclude that the observed lack of reduction in the PPIase activity in Δ(*ppiA surA ppiD fkpA tig*) as compared to Δ(*ppiA surA ppiD fkpA*) is due to the increased contribution from FkpB, when the Tig protein is absent, and the major contributor to the cytoplasmic pool of the PPIase activity activity is from the PpiB protein (Figure 2A).

Further, we sought to identify major contributors to the overall pool of total cellular PPIase activity. Thus, several double deletion combinations were constructed and used for the PPIase activity measurement. Among these, the most striking is a drastic reduction in the PPIase activity in Δ(*ppiA ppiB*) (Figure 2B). PpiA located in the periplasm and PpiB in the cytoplasm are highly homologous proteins and both belong to the cyclophilin family. Furthermore, we also constructed strains devoid of all ten PPIs, revealing only the presence of a very little residual PPIase activity (Figure 2B). However, it is pertinent to point out that strains lacking all ten PPIs exhibit severe growth defects with doubling time of 270 min and are unable to reach an OD_{600} above 0.3 at 37 °C. Such a phenotype highlights the importance of this class of folding catalysts for the bacterial viability. Taken together, we can conclude that PpiA and PpiB are the main contributors to the PPIase activity.

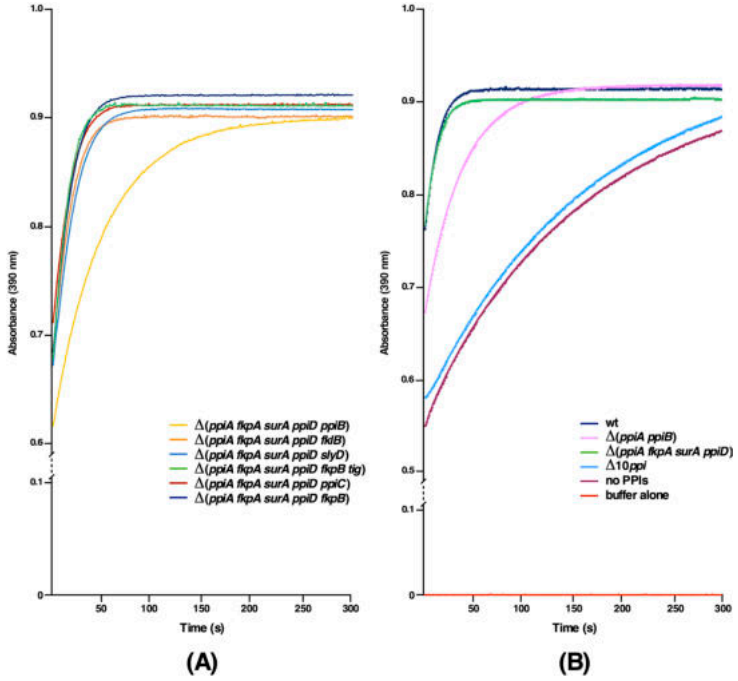

Figure 2. PpiB is the major contributor of PPIase activity in the cytoplasm. (**A**) The PPIase activity in soluble extracts obtained from six sets of strains lacking periplasmic PPIs and one of the cytoplasmic PPI were used to measure the PPIase activity, revealing that the absence of PpiB leads to highly reduced PPIase activity. In all cases, total protein concentration was 10 mg/mL and N-Suc-Ala-Ala-cis-Pro-Phe-p-nitroanilide was used as the substrate. The PPIase activity was measured in a chymotrypsin-coupled assay. (**B**) Under similar conditions, extracts from the wild type, Δ(*ppiA ppiB*), Δ(*ppiA fkpA surA ppiD*), Δ10*ppi* strain lacking all PPIs were used to measure the PPIase activity.

2.4. Δ6ppi Bacteria Exhibit the Constitutive Induction of RpoH-Regulated Heat Shock Response

It is well established that accumulation of misfolded proteins and overall defects in protein folding process induces cellular stress responsive pathways that can mitigate such stresses. *E. coli* uses two such stress combative pathways that leads to the induction of heat shock response. As Δ6*ppi* bacteria exhibited gross defects in terms of growth, extensive protein aggregation and also many transcription factors were found enriched during the analysis of proteins that accumulate in aggregation fractions, we analyzed the fate of major stress responsive pathways, such as the RpoH-regulated heat shock response and the RpoE-controlled envelope stress response. Thus, quantitative real-time polymerase chain reaction (qRT-PCR) analysis of well-known RpoH-regulated heat shock genes was performed, using total cellular mRNA isolated with or without temperature upshift. mRNA was also extracted from isogenic wild-type and Δ6*ppi* bacteria after shift from M9 30 °C or 37 °C to LB 37 °C. Data from qRT-PCR of highly conserved heat shock genes *dnaK* and *ibpA* are presented, revealing increased abundance of transcripts of these heat shock genes in Δ6*ppi* bacteria as compared to the wild type even under permissive growth conditions of either 30 or 37 °C (Figure 3A,B). Noteworthy is the hyperinduction of transcription of the *ibpA* heat shock gene at 37 °C. These data are consistent with a role of IbpA in binding to protein aggregates. A 15 min transient shift of culture of Δ6*ppi* bacteria from 30 °C to 42 °C in M9 minimal medium also resulted in the increased expression of all major heat shock genes in the wild type as well as in Δ6*ppi* bacteria (Figure 3). Thus, these data show that in the absence of PPIs heat shock response under the control of the *rpoH* gene is constitutively induced under permissive growth conditions in Δ6*ppi* strains and they exhibit an elevated induction of transcription of heat shock genes after temperature shift to 42 °C.

Concerning the RpoE-regulated stress response, the basal level transcriptional activity of the *rpoE* gene, which regulates the envelope stress response, is reduced in Δ6*ppi* bacteria at 30 °C and

is unaltered at 37 °C. Regarding the *degP* gene, whose transcription is subjected to dual control by RpoE and CpxR/A systems [15], its transcriptional activity is also reduced at 30 °C, although its transcription at 37 °C remains unaltered (Figure 3C,D), which is in contrast to the constitutively enhanced activity of RpoH-dependent heat shock regulon. However, a 15 min shift to 42 °C causes the induction of transcription of the *rpoE* as well as the *degP* genes in Δ6*ppi*, which is comparable with their induction in the parental wild-type strain. Thus, we can conclude that while the RpoH-regulated heat shock response is constitutively induced in Δ6*ppi* bacteria even under permissive growth conditions, the RpoE-regulated transcription under similar growth conditions is rather dampened.

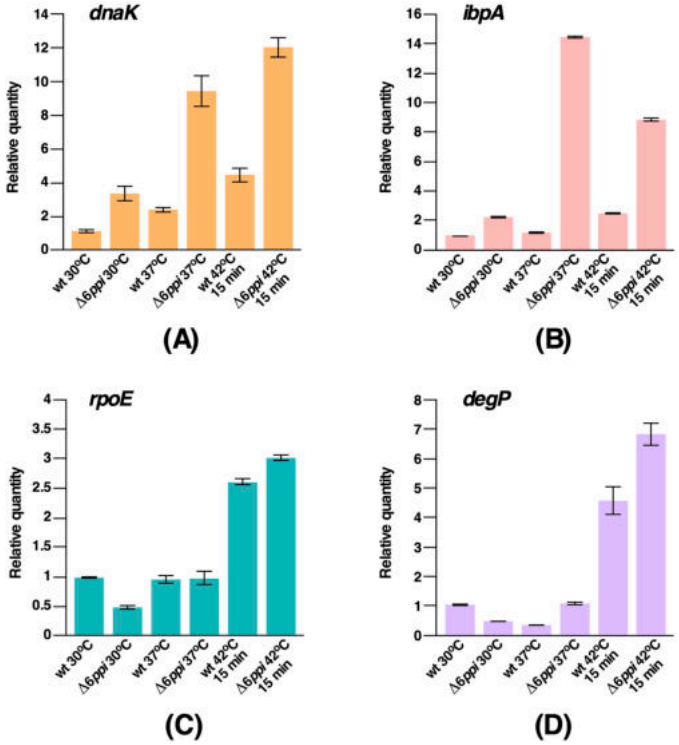

Figure 3. Δ6*ppi* bacteria exhibit constitutive elevated transcription of RpoH-regulated heat shock genes but reduced level of RpoE-transcribed genes at 30 and 37 °C. qRT-PCR analysis of mRNA isolated from the wild type (wt) and its Δ6*ppi* derivative bacteria grown up to an OD_{600} of 0.2 in M9 medium at either 30 or after shift to LB at 37 °C. In parallel, total RNA was extracted after heat shock for 15 min at 42 °C. Quantification of data for the *dnaK* gene (Panel **A**), the *ibpA* gene (Panel **B**), the *rpoE* gene (Panel **C**) and the *degP* gene (Panel **D**).

2.5. Identification of Substrates of the PpiC Protein Reveals a Role in Oxidative Stress, Transcriptional and Essential Metabolic Processes

Up to now, no systematic study has been carried out to identify substrates of individual cytoplasmic PPIs. Multipronged strategies were employed to identify in vivo substrates of PpiC. Firstly, the wild-type *ppiC* gene and its variants with single amino acid substitutions in residues predicted to correspond to either the potential active site or the substrate-binding site based on the available solution structure were cloned in the T7 polymerase-based expression plasmid pET24b. We chose highly conserved amino acids Met57 and Phe81 and replaced them with Ala, since they are predicted to form a part of substrate-binding and catalytic domains of PpiC, respectively [11]. In each plasmid construct, the coding region was appended in-frame with a C-terminal cleavable Hexa-His tag and used to transform SR21984 lacking all six PPIs to prevent the presence of other PPIs during purification. After the induction with IPTG (100 μM), proteins were purified using linear gradient of imidazole in Ni-NTA affinity chromatography and eluting protein fractions resolved by SDS-PAGE. The identity of co-eluting proteins with His-tagged PPIs in such pull-down experiments was revealed by MALDI-TOF.

Comparison of co-elution profiles of the wild-type Hexa-His-tagged PpiC and Hexa-His-tagged PpiC mutant derivatives revealed that most prominent substrates of PpiC include the BipA GTPase, the translational factor EttA, YrdA, FabH, RbsB, transcription-related proteins (NusG, SuhB, Rho, RpoA), the RNA chaperone ProQ, the GlmY/GlmS sRNA-binding protein RapZ, OxyR, RpsB, RbsC (S2/S3) ribosomal proteins. Other substrates identified include the polyP kinase Ppk, the essential lipid A transporter LptB and AhpC/AhpF subunits of alkyl hydroperoxide reductase. All these co-eluting proteins identified with the wild-type PpiC were either absent or with highly reduced amounts in PpiC F81A and PpiC M57A variants in such pull-down experiments (Figure 4A). Most prominent differences in the co-elution profile are observed when proteins from pull-down experiments from the wild-type PpiC vs. PpiC M57A are compared. This comparison reveals the absence of NusG, YrdA and AhpC proteins in M57A variant (Figure 4A).

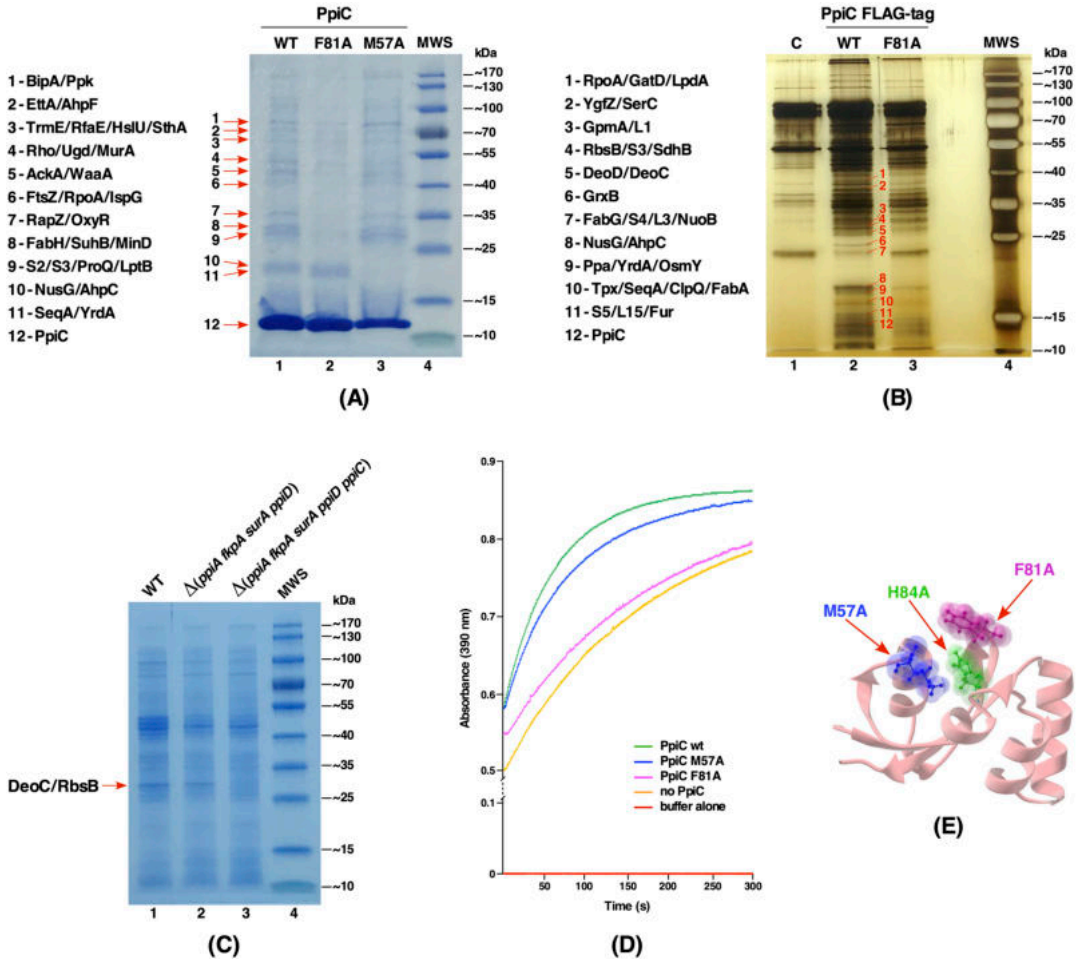

Figure 4. (**A**) Purification profile of wild-type PpiC, PpiC F81A and PpiC M57A after the induction in a Δ6*ppi* derivative with 100 μM IPTG. Proteins were resolved on a 12.5% SDS-PAGE. Co-eluting proteins are indicated by arrows with their identity marked. MWS indicates the molecular weight standard (Thermo Scientific). (**B**) Proteins identified after immunoprecipitation with an anti-FLAG M2 monoclonal antibody of extracts from the wild-type strain without FLAG tag as a control (lane marked C) and strains with a chromosomal FLAG-tagged PpiC wt and PpiC F81. Immunoprecipitated proteins are indicated. (**C**) Soluble proteins from equivalent amounts of cells from the wild type (wt), its isogenic strain derivatives lacking four periplasmic PPIs and its derivative strain additionally lacking PpiC, were resolved on a 12.5% SDS-PAGE. Missing proteins in the absence of Δ*ppiC* derivative are indicated by arrow. (**D**) The PPIase activity in the chymotrypsin-coupled assay with 0.5 μM purified wt PpiC and its mutants with either M57A or F81A are plotted. Controls without enzyme and buffer are also plotted. (**E**) Position of M57, F81 and H84 residues in the structure of PpiC (PDB 1JNT).

In a complementary and more sensitive second approach, the wild-type chromosomal copy of the *ppiC* gene was epitope-tagged with 3xFLAG using recombineering. In parallel, PpiC F81A mutation was introduced and thus an isogenic strain with an appended in-frame C-terminal 3xFLAG epitope with a chromosomal mutation in the putative catalytic site was generated. Total cell extracts from such FLAG-tagged wild-type PpiC and its mutant F81A were immunoprecipitated with an anti-FLAG M2 monoclonal antibody and bound substrates after elution were revealed by silver-staining after SDS-PAGE. This analysis revealed common substrates that were identified as co-eluting proteins in pull-down studies like RpoA, AhpC, YrdA, SeqA, NusG and RpsC, validating them as clients of PpiC (Figure 4B). Interestingly, many substrates like GrxB, AhpC, YrdA, NusG, and SeqA were not immunoprecipitated when extracts from the strain carrying PpiC F81A::3xFLAG were used, consistent with pull-down experiments as compared to their presence in immunoprecipitated extracts from the wild-type FLAG-tagged PpiC (Figure 4A,B). Some additional substrates, revealed with immunoprecipitations in the case of wild-type PpiC::3xFLAG, were proteins such as GrxB, Ppa, GpmA, YgfZ, DeoC, and RbsB, which were missing in pull-down experiments. As immunoprecipitations were performed with cell extracts from FLAG-tagged strains carrying a single-copy wild-type and its F81A derivative, without any overexpression, such results are physiologically more relevant than using overexpressing systems. Due to limitations of current recombineering techniques, a chromosomal M57A mutation in a FLAG-tag system could not be constructed. Finally, in the third approach, we compared the profile of total soluble proteins obtained from isogenic strains lacking all periplasmic PPIs Δ(*surA ppiD ppiA fkpA*) (SR20072) and its derivative SR20098 Δ(*surA ppiD ppiA fkpA ppiC*) additionally lacking the *ppiC* gene (Figure 4C). MALDI-TOF analysis of missing protein(s) in SR20098 identified DeoC and RbsB to be absent when the Δ*ppiC* mutation was introduced (Figure 4C). These results further reinforce their identification in either pull-down or immunoprecipitation studies, validating them as PpiC substrates.

To correlate the identification of substrates and gain better insight in the function of PpiC in relationship with its PPIase activity and relevance of substrate-binding site, purified wild-type PpiC, PpiC M57A and PpiC F81A proteins were obtained after rifampicin treatment and used to measure their activity in chymotrypsin-coupled assay. Results from these measurements revealed that PpiC F81A mutant protein has lost its PPIase activity, while PpiC M57A still retains a substantial PPIase activity (Figure 4D). Based on the structural analysis, Met57 is located in the putative substrate- binding domain of PpiC [11] (Figure 4E) and thus helps to explain the inability to recognize some of the substrates as revealed by pull-down studies. Similarly, the absence of several substrates, when PpiC F81A::3xFLAG was used in immunoprecipitations, implies a dependence of several substrates, such as GrxB, AhpC, NusG (Figure 4) on the PPIase activity of PpiC. Thus, we can conclude that both substrate-binding and PPIase active site residues are required for PpiC's function.

2.6. Substrates of FkpB Include the RpoE Sigma Factor, Proteins Related to Cell Shape/Division and Lipopolysaccharide (LPS) Transport

The FkpB PPIase of *E. coli* exhibits structural similarity with the SlyD protein [8,12]. However, its cellular substrates and physiological function remains to be elucidated. Thus, as with PpiC, we identified substrates using pull-down experiments with FkpB. To achieve this, the minimal coding region of the *fkpB* gene with a C-terminal in-frame Hexa-His tag was cloned in the T7 polymerase-based expression plasmid pET24b and protein expression induced in the Δ6*ppi* derivative as described above. In the case of FkpB, some of the prominent co-eluting proteins using pull-down experiments are: RpoE (envelope stress response regulator sigma E), LptB (cytoplasmic ATPase component of LPS ABC transport complex), the RseA anti-sigma factor specific to RpoE, RpsB and RpsC (S2 and S3, respectively) ribosomal proteins, the RNA chaperone ProQ, Rho transcriptional terminator factor, the GapA protein which is involved in glycogenesis, putative methyl transferase YfiF related to RNA processing, the cell shape determining protein MreB, an alkyl hydroperoxide reductase subunit C AhpC and also some proteins that are involved in the phospholipid/fatty acid synthesis such as

FabF. To gain insights in the structure-function analysis of FkpB, single amino acid substitutions include E86A, N126A, P128A, and a H126A N127A double mutant were constructed on plasmids. Such Hexa-His-tagged FkpB mutant proteins were purified and the profile of co-eluting proteins were analyzed in comparison with co-eluted proteins obtained from the wild-type His-tagged FkpB (Figure 5A). All the mutated residues were selected on the basis of their location in the putative active site of FkpB (Figure 5) [12]. Examination of co-eluting proteins with substitution of E86A in FkpB yielded a profile quite similar to that of the wild-type. However, quite importantly the co-elution of RpoE was diminished in FkpB N127A, P128A variants and abolished in FkpB N126A H127A double mutant. These results were further validated by analysis of co-eluting proteins upon two-dimensional (2D) gel electrophoresis. As is evident, the protein spot corresponding to RpoE was visualized and its identity established by MALDI-TOF analysis using co-eluted proteins from His-tagged wild-type FkpB (Figure 5B). However, the protein spot corresponding to RpoE is missing in the 2D gel when the co-eluted proteins from His-tagged FkpB H126A N127A double mutant were applied (Figure 5C). It is worth noting an overlap of substrates between PpiC and FkpB for ribosomal proteins S2 and S3, and AhpC, LptB, Rho, and ProQ which are also common substrates. Some of these substrates were validated by in vitro binding assays (see below).

Next, we measured the PPIase activity of wild-type FkpB and its variants that were tested in pull-down studies using the standard chymotrypsin-coupled assay. This analysis revealed a significantly reduced PPIase activity of FkpB H126A N127A double mutant protein as compared to the wild-type (Figure 5D,E). Furthermore, FkpB P128A mutant protein was also found to be defective in the catalysis of the prolyl isomerization, while E86A variant still retains the PPIase activity although reduced as compared to the wild type (Figure 5D,E). These results are consistent with a predicted role of H126, N127, and P128 residues in the catalysis of prolyl isomerization.

2.7. The PpiB Protein Has Larger Number of Substrates That Require Its PPIase Activity

The PpiB protein was the first cytoplasmic *E. coli* PPIase identified and biochemically its activity elucidated [16,17]. As shown in this work, PpiB is the major source of PPIase activity in the cytoplasm of *E. coli*. However, little information is available concerning its cellular substrates. Thus, in this study we cloned the wild-type and putative active site variant of the *ppiB* gene with appended His-tag at the C-terminal end of its coding sequence and expressed from the T7 promoter-based expression vector pET24b. Pull-down experiments with His-tagged PpiB revealed largest number of co-eluting polypeptides as compared to similar experiments with other PPIs (Figure 6A). While the identity of several proteins could be obtained, we focused more on those proteins which do not co-purify with PpiB R43A variant. PpiB R43A substitution was constructed, since its counterpart R55 residue in human Cyp18 is known to have a very low PPIase activity [18]. Examination of purification profile of PpiB R43A variant revealed that the vast majority of co-eluting proteins observed in the case of wild-type His_6-tagged PpiB were either absent or their abundance is reduced (Figure 6A). Some of the co-purifying proteins observed with the wild-type PpiB, but with a reduced abundance with His_6-tagged PpiB R43A, are: components of RNA polymerase β and β′ subunits, transcription factors Rho, CytR and NtrC, tRNA modification enzymes MiaB, MnmG, the RNA helicase DeaD, Eno, which is a part of RNA degradosome, catalase subunits HPI and HPII (KatE and KatG, respectively), enzymes related to DNA replication/recombination like GyrB, RecA, several proteins related to energy metabolism such as AcnB, GlpD, LpdA, and SthA, components of biotin-carboxyl carrier protein assembly which are also involved in the fatty acid synthesis like AccA and AccC, stress-related proteins like ClpX, HslU and UspG (Figure 6A). Additionally, in pull-down studies proteins involved in cell division/cell shape (FtsZ, MreB and MinD) were observed as well as ribosomal proteins like RpsB/C (S2 and S3 proteins) and RplV (Figure 6A). Thus, PpiB substrates are quite broad in function and most of these proteins were only identified during purification of the wild-type PpiB but not with PpiB R43A.

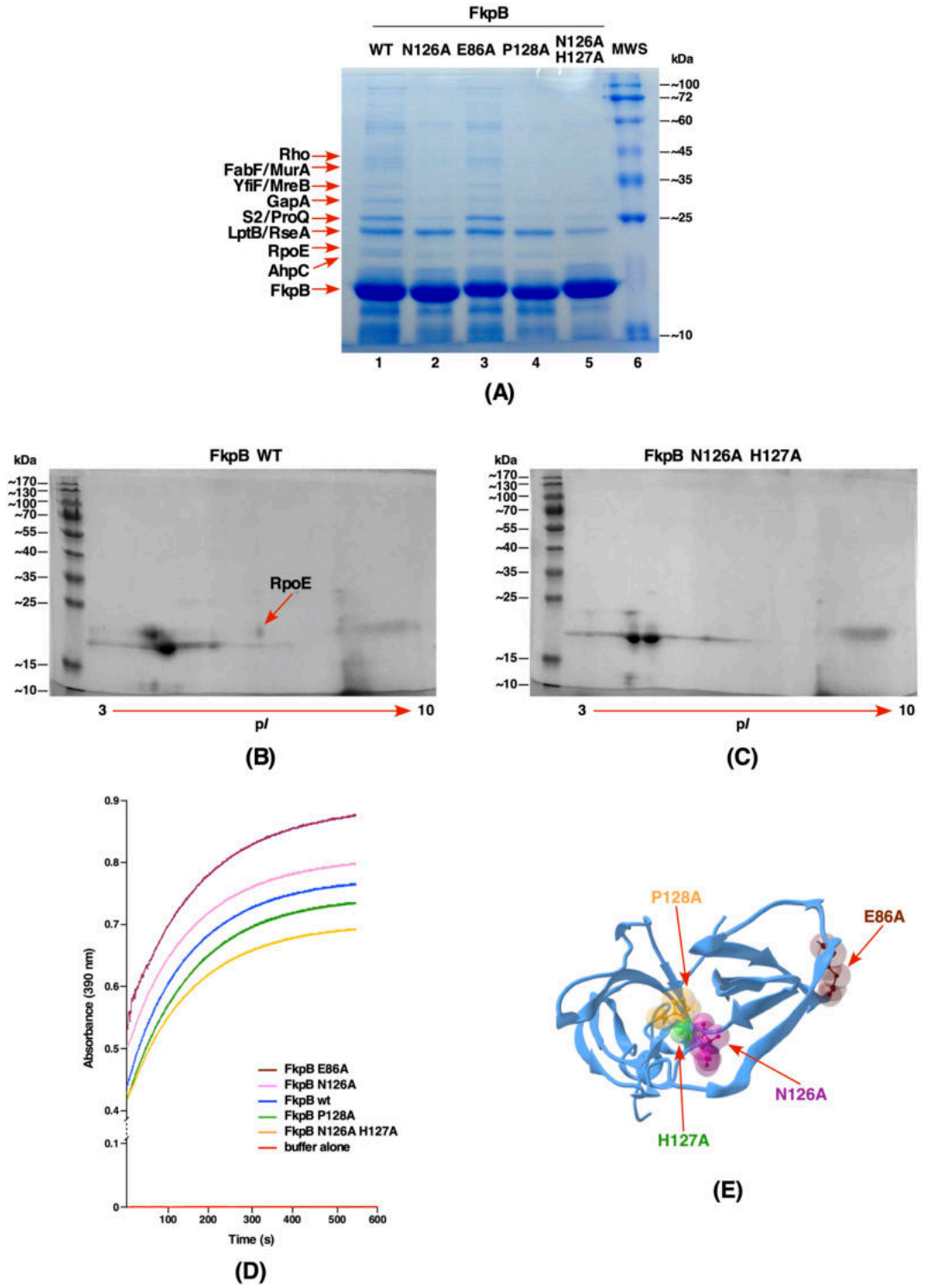

Figure 5. The RpoE sigma factor is one of the substrates of FkpB. (**A**) Co-purification profile of the wild-type FkpB protein and its derivatives N126A, P128A, E86A and with N126A H127 double mutation after the induction in a Δ6*ppi* derivative with 100 µM IPTG. Proteins were resolved on a 12.5% SDS-PAGE and co-eluting proteins are indicated and their identity shown. (**B**) Picture of dried 2-D gels of purified FkpB and co-eluting RpoE. The identity of the spot corresponding to RpoE was obtained from MALDI-TOF and is indicated. (**C**) 2-D gel of purified FkpB variant N126A H127. (**D**) The PPIase activity in the chymotrypsin-coupled assay with 0.5 µM purified of above mentioned FkpB variants in comparison to the wild type is plotted. (**E**) Position of various FkpB residues, which were mutated, is indicated in the structure of FkpB (PDB 4DT4).

Next, we verified if indeed PpiB R43A mutant protein is defective in its PPIase activity. As shown, this mutation nearly abolished the PPIase activity of PpiB (Figure 6B), consistent with observations with corresponding Cyp18 R55 variant. Taken together, we can conclude that most of the substrates identified in these studies require PpiB's PPIase activity for their interaction.

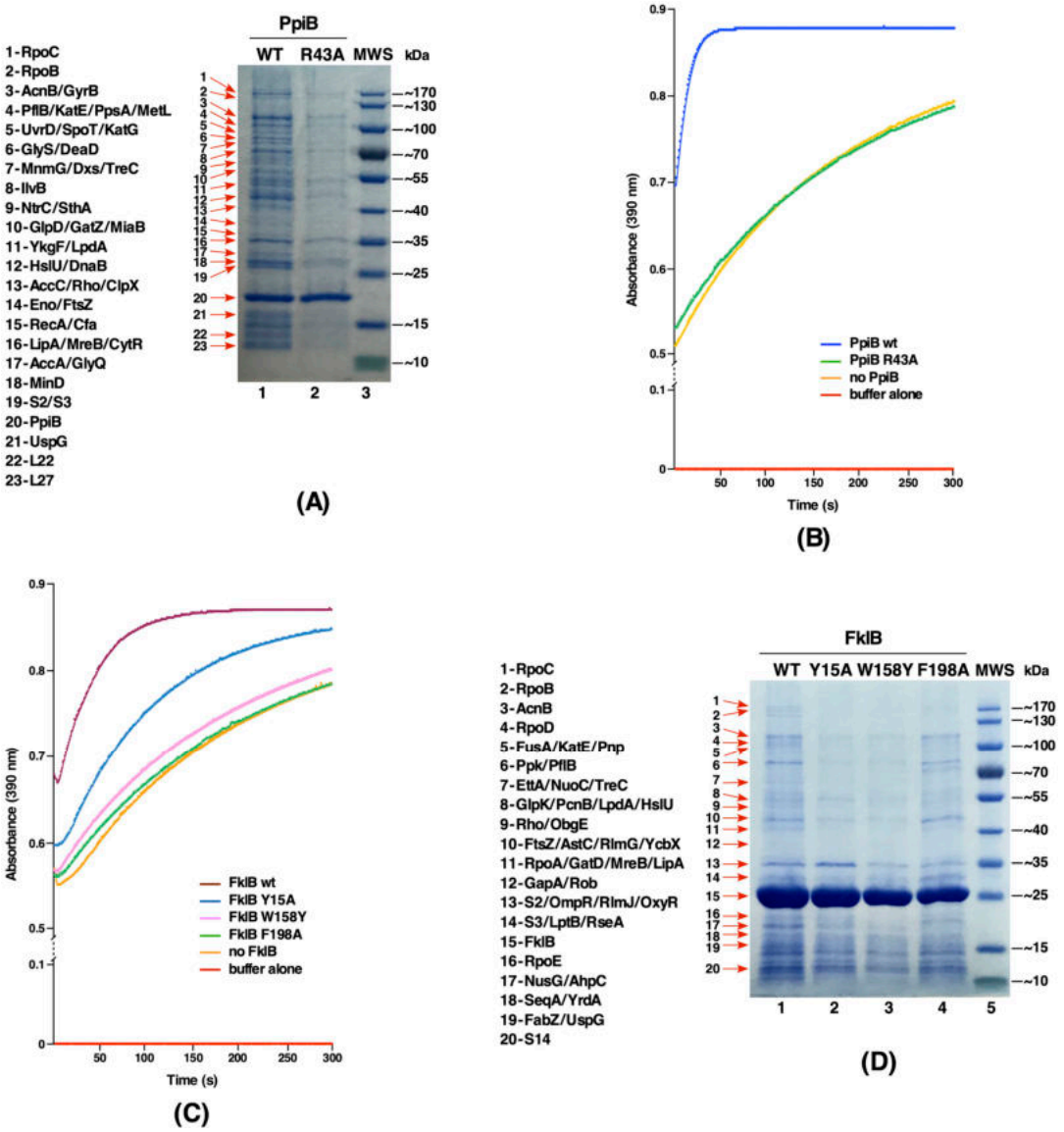

Figure 6. Identification of substrates of PpiB and FklB. (**A**) Co-purification profile of wild-type PpiB and PpiB R43A proteins. Co-eluting proteins present in the wild-type that are either absent or with reduced abundance are indicated. (**B**) The PPIase activity in the chymotrypsin-coupled assay with purified wt PpiB and PpiB R43A (0.5 μM each) is indicated. Controls without enzyme and buffer are also plotted. (**C**) The PPIase activity in the chymotrypsin-coupled assay with 0.5 μM purified FklB variants in comparison to the wild-type FklB, without enzyme and buffer alone are plotted. (**D**) Co-purification profile of wild-type FklB, and its derivatives Y15A, W158Y and E86A. Proteins were resolved on a 12.5% SDS-PAGE and co-eluting proteins are indicated and their identity shown.

2.8. Identification of Active Site Residues of the FklB Protein and Identification of its Substrates Reveal Certain Unique and Some with an Overlap with Other PPIs

No substrate of FklB has been reported thus far in *E. coli* and its biochemical studies are limited, although it has been shown to be a dimeric protein [19]. To investigate the function of FklB, experiments

were undertaken to identify its binding partners and determine the importance of highly conserved amino acid residues predicted to impact its PPIase and substrate-binding activity. Hence, we generated single amino acid substitutions based on homology modeling with FKBP22 of *Shewanella* sp. [20]. Homology data suggest *E. coli* FklB to be a V-shaped dimer, with the N-terminal domain required for dimerization and the C-terminal domain to constitute the catalytic domain. Thus, mutations in FklB with Y15A, W158Y and F198A substitutions were generated and cloned in pET28b expression vector. Such *fklB* mutants and the wild type were expressed in the Δ6*ppi* derivative SR21984 and proteins were purified under identical conditions. Substitutions like Y15A in the N-terminal domain should render FklB in the monomeric state [20,21], while substitutions in C-terminal residues W158 and F198 can affect the PPIase and the chaperone-like activity. Measurement of the PPIase activity using *N*-Suc-Ala-Ala-*cis*-Pro-Phe-*p*-nitroanilide peptide as a substrate revealed a severe reduction of PPIase activity in the case of FklB W158Y and a loss of PPIase activity with FklB F198A mutants (Figure 6C). However, Y15A mutation in the N-domain retained the PPIase activity, although it is reduced as compared to the wild type. In parallel, pull-down experiments revealed a substantial reduction in the number of co-eluting proteins, when FklB Y15A and W158Y variants were subjected to affinity purification (Figure 6D). However, when FklB F198A was purified, many proteins that co-elute with the wild-type Hexa-His-tagged FklB were also observed, although certain proteins were reduced in abundance. These results suggest that both the dimeric nature and the PPIase activity are required for the FklB function. However, all substrates may not require FklB's PPIase activity.

Identification of potential substrates of FklB from co-eluting proteins revealed some unique interacting partners like the transcriptional regulator Rob, which is involved in regulation of antibiotic resistance and stress response [22,23], the transcriptional factor Crl regulating RpoS expression/activity, *ompF/C* transcriptional regulator OmpR, the plasmid copy number regulator PcnB, proteins related to translational process like the ribosome assembly-related GTP-binding protein ObgE, ribosomal proteins and RlmG/RlmJ involved in methylation of 23S rRNA (Figure 6D). However, many co-purifying proteins were common with FkpB, PpiC and PpiB. These include proteins like AhpC, OxyR, TreC, NusG, Rho, RpoA, and RpoE. However, higher overlap is observed with FkpB, suggesting redundancy in substrate usage by different cytoplasmic PPIs.

2.9. Validation of RpoE, RseA, and S2 Proteins as Client Proteins of FkpB

Based on pull-down experiments, several proteins were identified as potential substrates of FkpB. These include the S2 ribosomal protein, the RpoE sigma factor and the anti-sigma factor RseA. The RpoE sigma factor is an alternative sigma factor that in the complex with RNA polymerase initiates transcription of several genes whose products are involved in either folding and assembly of various components of the OM including major OMPs and lipopolysaccharide or transcription of sRNAs that negatively regulate the synthesis of OMPs and the abundant envelope murein lipoprotein Lpp (reviewed in [24]). RseA acts as the anti-sigma factor for RpoE and regulates the RpoE availability in response to envelope stress [25,26].

To further investigate the interaction between RpoE and RseA with FkpB, binding affinity measurements were performed with isothermal titration calorimetry (ITC) using various peptides spanning different segments of RpoE and RseA. The best binders were peptides P2 (KVASLVSRYVPSGDV) and P4 (AAIMDCPVGTVRSRI) that were derived from the most conserved regions 2 and 4 of RpoE. The titration of FkpB into peptides P4 and P2 was exothermic (Figure 7A,B). The binding curves were fit to a single binding-site mode (n = 1), revealing a binding affinity with a K_d of 10.69 μM for P2 peptide and with a K_d of 10.31 μM for P4 peptide (Figure 7A,B). Another peptide designated P3 (FRAREAIDNKVQPLIRR) again covering the conserved region 4 that includes amino acid like R178 shown previously critical for RpoE and RseA interaction and the RpoE activity [15,27], when titrated with FkpB also revealed a high binding affinity with a K_d of 18.99 μM (Figure 7C). Similarly, fitting the data to a single-site binding model (n = 1) with peptide P1 (YLVAQGRRPPSSDVD) corresponding to the C-terminal end of conserved region 2.4 of RpoE, also yielded thermodynamically favorable interaction,

although with a relatively modest binding affinity with a K_d of 38.14 μM (Figure 7D). Taken together, ITC measurements of affinities between RpoE-base peptides with FkpB are driven by a favorable change in enthalpy.

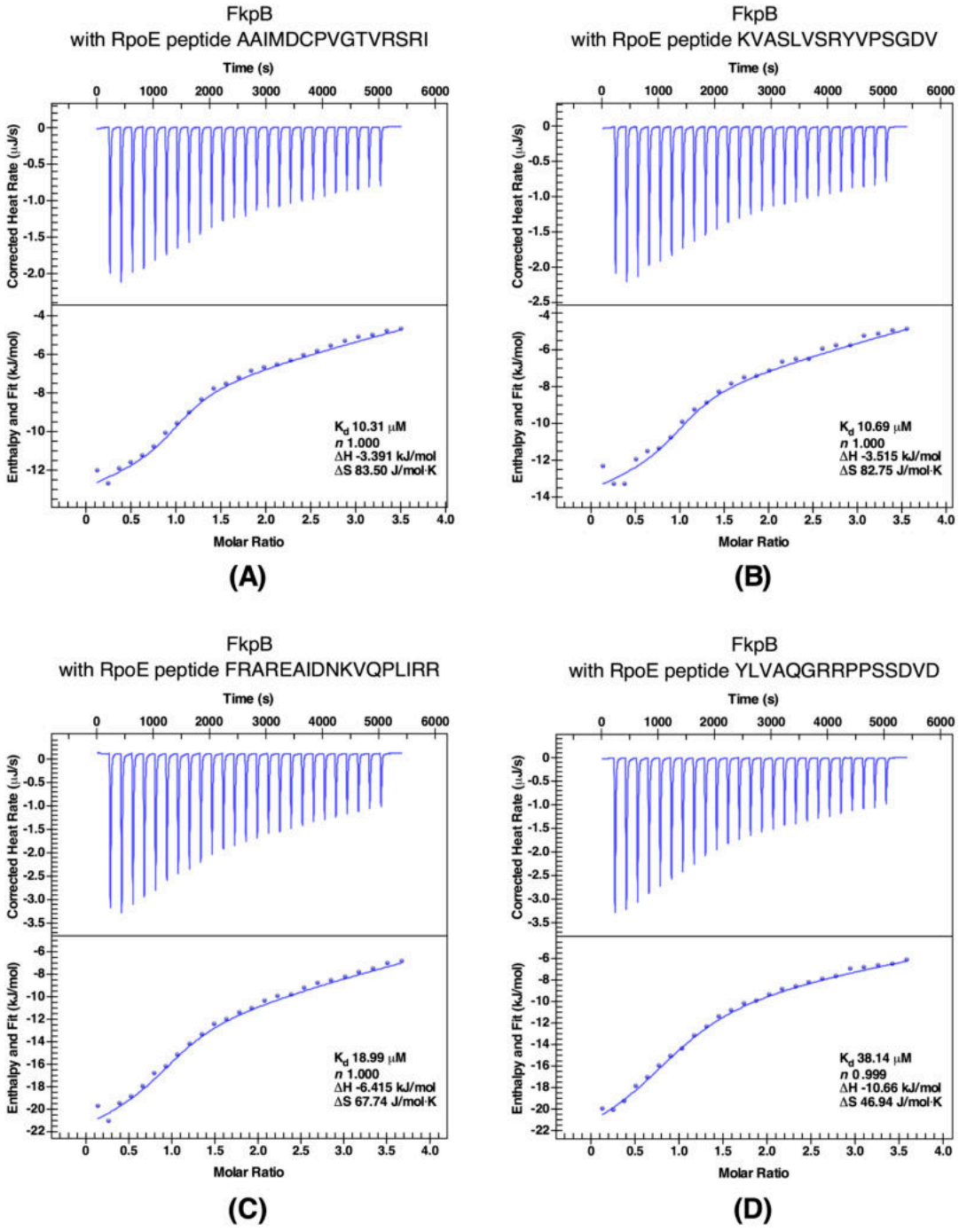

Figure 7. Quantification of binding affinity of FkpB with four different peptides derived from RpoE (Panel **A**–**D**). FkpB was titrated into peptides indicated on the top of each panel in ITC cell. Raw data (top half of each panel) and integrated heat measurements enthalpy (bottom part) are shown. The calculated stoichiometry (n) and dissociation constant (K_d) are indicated in insets.

Since the anti-sigma factor RseA also co-elutes with FkpB, binding affinities were measured using ITC with peptides covering the most conserved regions in the N-terminal domain of RseA. Thermograms of two best binders are presented (Figure 8B,C). Peptide Rse1 corresponding to amino

acid 2-29 of N-RseA binds to FkpB with a K_d of 15.08 μM and with a stoichiometric value (n) of 1.002 (Figure 8B). Similarly, a high affinity binding with a K_d of 13.02 μM was observed with peptide Rse3 (IIEEEPVRQPATL) (Figure 8C). Furthermore, interaction of peptides Rse1 and Rse3 with FkpB were exothermic and driven by favorable change in enthalpy with ΔH being −9.102 and −6.213 kJ/mol, respectively.

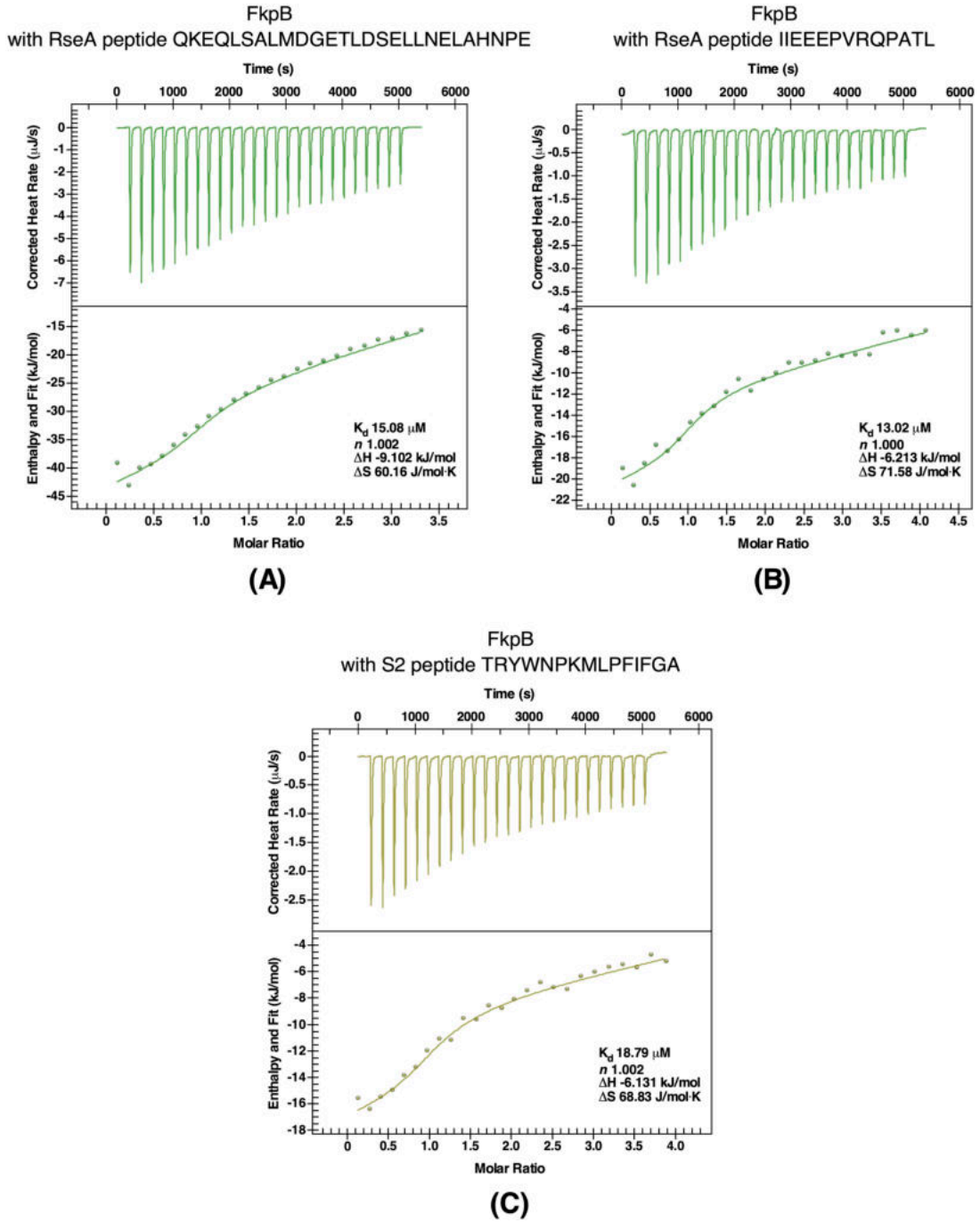

Figure 8. Quantification of binding affinity of FkpB with peptides from RseA (Panel **A**,**B**) and the peptide from the S2 ribosomal protein (Panel **C**). Heat rates and fit for ITC experiment, where FkpB is injected into above-mentioned peptides. The calculated stoichiometry (n) and dissociation constant (K_d) are indicated in insets.

As shown in the analysis of accumulation of proteins that tend to aggregate in a Δ6*ppi* mutant strain even under permissive growth conditions, the S2 ribosomal protein (RpsB) was enriched in aggregation fractions (Table S1). Furthermore, the S2 ribosomal protein is one of the prominent proteins that co-elutes with FkpB. The S2 ribosomal protein was also in earlier independent studies identified as a potential substrate of FkpB and a peptide containing a *trans* Pro residue derived from the S2 ribosomal protein was used in such studies to show favorable interaction with FkpB [12]. Thus, we validated binding of the same S2-derived peptide using ITC. Measurement of binding affinity by ITC to this peptide gave a binding affinity with a K_d of 18.79 μM (Figure 8A), which is similar to that reported earlier [12], thus reinforcing our results obtained with pull-down experiments. Thus, taken together, ITC experiments validated the RpoE sigma factor, the anti-sigma factor RseA and the ribosomal protein S2 as binding partners of FkpB PPIase. These results also draw support from co-purification of these client proteins with FkpB.

2.10. AhpC as a Client Protein of PpiC and FkpB

As shown above, AhpC protein was identified as one of the aggregation-prone proteins in Δ6*ppi* bacteria and as a potential partner of PPIs, since AhpC was also found to co-purify with PpiC and FkpB. Such purified proteins were used to study their interaction with a peptide from AhpC (RATFVVDPQGI) using ITC. This peptide was chosen, since it is present in one of three segments of AhpC as a potential PpiC binder [11]. Measurement of binding constants revealed that wild-type PpiC and FkpB proteins bind with stoichiometric value (n) of 0.99 in each case, indicating that one molecule of these catalysts binds to the AhpC peptide with high affinity (K_d values of 30 μM and 47 μM, respectively) validating AhpC as their substrate (Figure 9A,B). Reactions in both cases were again exothermic with wild-type PpiC and FkpB with favorable changes in enthalpy.

Since our PPIase measurements established PpiC F81A to have lost its PPIase activity and in immunoprecipitation experiment PpiC F81A::3xFLAG could not show interaction with several substrates identified in pull-down experiments including AhpC, we tested interaction by ITC with the AhpC peptide used in above studies. In parallel, the interaction between another mutant PpiC M57V with the AhpC peptide was analyzed. This analysis revealed that unlike exothermic reaction upon the interaction of wild-type PpiC with the AhpC peptide, the titration of PpiC mutants defective in the PPIase activity and substrate binding into the AhpC peptide yielded endothermic reactions (Figure 9C,D respectively) with unfavorable thermodynamic changes. Thus, comparison of thermodynamic parameters and nature of only exothermic reaction with the wild-type PpiC but not with PpiC mutants, leads us to conclude that defects in the PPIase activity (PpiC F81A) and substrate binding (PpiC M57A) disrupts interaction between AhpC and PpiC. Hence, the PPIase activity of PpiC is required for interaction with AhpC, which is also supported by immunoprecipitation experiments.

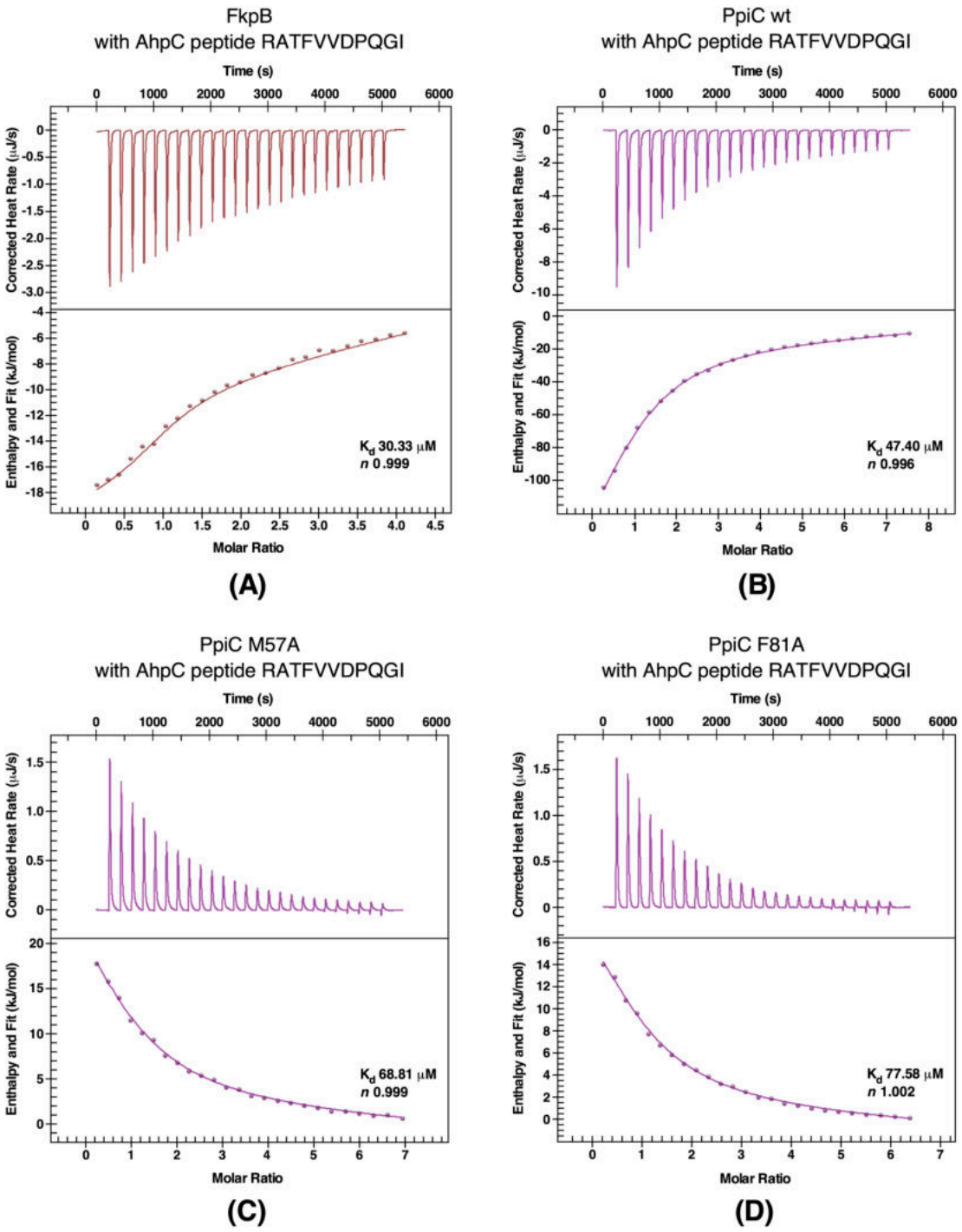

Figure 9. ITC experiments with the AhpC-derived peptide and FkpB (Panel **A**) and PpiC wild-type (Panel **B**) and PpiC M57A (Panel **C**) and PpiC F81 (Panel **D**). Heat rates and fit for ITC experiment, and the calculated stoichiometry (n) and dissociation constant (K_d) are indicated in insets.

3. Discussion

It is well established that the kinetics of the Xaa-Pro bond isomerization is intrinsically slow due to the partial double bond nature of the peptide bond [28] and hence is a rate-limiting step in protein folding. Peptidyl-prolyl *cis*/*trans* isomerases (PPIs) constitute a unique ubiquitous group of universally conserved protein folding catalysts that accelerate the catalysis of this rate-limiting step of isomerization around Xaa-Pro bonds. However, in *E. coli* their physiological requirement,

the identification of interacting partners and which substrates require their PPIase activity has not been addressed. This is partly due to: (i) the transient nature of PPI-substrate interactions, (ii) the overlap in substrates that masks the phenotype of individual *ppi* deletion, (iii) the absence of systematic studies that address the individual contribution of any PPI to overall enzymatic activity, since no strains have been reported that lack all six PPIs, (iv) the polar effect of gene disruptions in some PPIs-encoding genes on downstream essential gene(s) like the polarity effect of gene disruption of *fkpB* and *ppiB* genes on *ispH* and *lpxH* genes, respectively. Thus, in this work, we for the first time report the construction and characterization of strains that lack all six cytoplasmic PPIs. All deletion derivatives were non-polar and transduced into the wild-type *E. coli* strain BW25113. Such Δ6*ppi* deletion derivatives were found to exhibit highly pleiotropic phenotypes. These include the inability to grow under fast growing conditions of rich medium and severe defects in protein folding as manifested by the accumulation of protein aggregates. Examination of protein that aggregate in Δ6*ppi* bacteria revealed that more than 10% cytoplasmic proteins accumulated in the aggregation state. Among various proteins that were identified to aggregate in Δ6*ppi* bacteria, some of them are involved in transcription and RNA processing, translational process, many ribosomal proteins, DNA synthesis/repair/replication enzymes, oxidative stress-related proteins and enzymes that play a key role in central metabolism like TCA cycle, glycerol uptake and its catabolic process and ubiquinone biosynthesis. Consistent with these results, Δ6*ppi* strains cannot utilize glycerol as the sole carbon source. Other aggregation-prone proteins are involved in the assembly and biosynthesis of two essential components of cell envelope: LPS and phospholipids. Synthesis of these components in the cell is tightly regulated and coupled [14] and can contribute to the collective essentiality of PPIs. Although a diverse set of proteins were found to aggregate, yet one can conclude that major defects in Δ6*ppi* bacteria can be attributed to aggregation of proteins related to translation, transcription, maintenance of cell envelope homeostasis and factors related to combating oxidative stress and DNA repair processes. Indeed, during our ongoing studies, we have found that Δ6*ppi* bacteria are super sensitive to oxidative stress, factors that interfere with protein translation/synthesis and protein folding process, variety of DNA and cell envelope damaging agents. Some of these aggregation-prone proteins related to oxidative stress like AhpC and AhpF or ribosomal proteins were indeed again identified during pull-down studies and ITC experiments as bona fide substrates of PPIs. A vast number of proteins that were shown to aggregate in Δ6*ppi* bacteria have also been reported to aggregate when DnaK/J chaperones are absent [29,30]. These results suggest an overlap in substrates between major cytosolic chaperones and PPIs, further reinforcing the importance of PPIs in protein folding. However, now the major task is to identify which of these aggregation-prone proteins require a specific PPI for their in vivo folding. Towards this goal several strategies were undertaken, results of which are further discussed below.

In this work, our major focus has been on the identification of substrate using multiple approaches besides monitoring aggregation of proteins in the absence of PPIs. To identify physiologically relevant client proteins of PPIs, single-amino acid substitutions were introduced in predicted active and substrates-binding domains and used comparative pull-down studies to identify substrates of PpiB, PpiC, FklB and FkpB. Major highlights are: (i) A good correlation exists between aggregation-prone substrates observed in Δ6*ppi* bacteria with interacting partners in pull-down studies. This common set of proteins that aggregate as well as appear as co-purifying proteins with PPIs cover those involved in transcription (RNA polymerase subunits and transcription factors like Rho), translation-associated proteins, particularly enrichment of ribosomal proteins in all sets as well as ribosome-associated GTPases, cell division proteins FtsZ and MinD, the heat shock protein HslU and proteins involved in oxidative stress like subunits of alkyl hydroperoxide reductase (AhpC and AhpF). (ii) Importantly, based on co-purification studies, PpiB emerged with largest number of interacting partners. Interestingly, this interaction was lost with majority of interacting proteins when PpiB PPIase inactive variant PpiB R43A was used as a bait. Our biochemical data clearly show that PpiB R43A mutant quite like its human Cyp18 R55 counterpart lacks the PPIase activity. It has been shown that Cyp18 R55A replacement leads to less than 1% of the PPIase activity [18], which is consistent with our results with

PpiB R43A. Thus, we can conclude that interaction of PpiB with majority of its binding partners requires its PPIase activity. (iii) In the case of PpiC, we employed several strategies to identify its substrates such as immunoprecipitations using the single-copy chromosomal 3xFLAG-tagged wild-type PpiC and PpiC F81A, comparative pull-down studies using the His-tagged wild type, active site variant F81A and with a substitution of M57A, and at the proteomic level by comparison between strains lacking all periplasmic PPIs and with additional deletion of the *ppiC* gene. We could show that M57A substitution in the substrate-binding domain [11], while retaining its PPIase activity albeit to a reduced level, can still interact with some potential client proteins but not all. However, PPIase defective F81A in immunoprecipitation experiments does not form the complex with majority of substrates that immunoprecipitated with the wild type. Previously, it had been reported that PpiC interacts with the AhpC protein [11]. In this work, we showed that the PpiC folding catalyst has several substrates including AhpC, AhpF, Ppk, NusG, Ppa, SeqA, Rho, the BipA GTPase, GrxB, FabH, and RbsB. Co-elution of transcription-related proteins (NusG, Rho, SuhB, and RpoA) and those involved in oxidative stress (AhpC/AhpF and OxyR) suggest enrichment of substrates, which are involved in regulation of transcription and oxidative stress as primary clients of PpiC. Quite importantly for PpiC, we could establish a requirement for its interaction with AhpC, but not when the PPIase activity is abrogated. These conclusions draw further support from the measurement of binding affinity using ITC. The dissociation constant with the wild-type PpiC is of the magnitude with K_d of 47.4 μM with a favorable enthalpy. Furthermore, the negative enthalpy of the interaction (exothermic) of wild-type PpiC with the AhpC peptide, suggests the noncovalent interactions (hydrogen bonds and van der Waals interactions) for its binding. However, of interest is that this interaction between AhpC and PpiC variants M57A (in the substrate-binding site) and PPIase deficient F81A is endothermic, suggesting disruptions of the energetically favorable noncovalent interactions [31]. Thus, PpiC interaction requires its substrate-binding domain as well as the PPIase catalytic domain for its in vivo and in vitro interactions. (iv) Finally, FklB and FkpB show a significant overlap in terms of partner proteins that include ribosomal proteins and the essential sigma factor RpoE.

Pull-down experiments using FklB monomeric variant Y15A revealed reduced substrate interactions as only few proteins were observed to co-elute, although it still retained substantial PPIase activity. These results imply the importance of dimeric shape for binding to its interacting partner proteins. PPIase deficient FklB F198A still showed interacting ability suggesting that the PPIase activity may not be essential for the substrate recognition as has been observed in related FKBP22 from *Shewanella* sp. [20]. However, another FklB variant with W158Y mutation exhibited a reduced PPIase activity and was also impaired in its interaction in pull-down studies. It is likely that W158Y alteration might also cause structural perturbations as has been proposed in the corresponding mutation in *Shewanella* sp. [20]. Thus, some client proteins may need both chaperone-like activity provided via its dimeric structure and while certain other proteins may need both PPIase and chaperone-like activity.

Our work highlights a major role of PPIs in functions related to protein translation process, since many ribosomal proteins either aggregate in the absence of PPIs or co-purify with PPIs. In support of these conclusions, we also show that the EttA protein (Energy-dependent Translational Throttle A) is a substrate of PpiC and FklB, since it was identified during pull-down studies. EttA is a translational factor that has been suggested to modulate the movement of ribosome and tRNA that are required for protein elongation [32]. Similarly, various components of rRNA modification, the RNA helicase DeaD, ribosome assembly factors like BipA and ObgE GTPases were identified as binding partners of various PPIs. BipA and ObgE are known to impact the ribosome assembly [33,34]. Concerning ribosomal proteins such as S2 and S3, they not only aggregate in Δ6*ppi* bacteria, but were also identified as co-eluting partner proteins with PpiB, PpiC, FklB, and FkpB. It had been earlier suggested that ribosomal proteins could specifically be substrates of FkpB [12]. However, our study shows that PPIs exhibit a redundancy so far their interaction with ribosomal proteins is concerned and overall PPIs are intricately related to various components of the translation process.

It is of significance that RpoE and RseA that act as sigma and anti-sigma factors, respectively were identified as specific clients of FkpB and FklB. RpoE and RseA are present in minor quantities in the cell [35] and their amounts and activities are tightly regulated at transcriptional and post-transcriptional level [24,25,36]. RpoE is essential for the cellular viability and regulates transcription of genes whose products are involved in folding and assembly of main cell envelope components like outer membrane proteins and lipopolysaccharide [24,37,38]. We chose to measure the binding affinity of specific peptides derived from RpoE and RseA amino acid sequence with FkpB by ITC, since analysis of peptide coverage in MALDI-TOF analysis of various substrates was much higher for FkpB than with FklB. Additionally, RpoE specifically was observed in the pull-down studies with the wild-type FkpB but not with the active site variant that has lost its PPIase activity. RpoE and the N-terminal domain of RseA are known to physically interact, with specific contacts of N-RseA with the region 2 and the region 4 of RpoE [39]. We had earlier identified essential residues in the conserved region 4 of RpoE and in the N-terminal domain of RseA that are required for their interaction, which is further supported by the co-crystal structure of RpoE and N-RseA [25,27,39]. Thus, specific peptides were chosen that cover such essential domains in RpoE and RseA. Analysis of binding affinities with peptides from the region 2 (−10 binding domain) and the region 4 of RpoE (−35 recognition) and N-RseA domain using ITC studies revealed tight binding with K_d ranging from 10 μM to 18.9 μM with favorable enthalpy changes suggesting that all complex formations were driven by the establishment of noncovalent interactions (van der Waals contacts, hydrogen bonds). For FkpB, the positive $T\Delta S$ showed that the association was entropically driven, which suggests a burial of solvent-accessible surface area upon binding a scenario similar to what has been observed with cyclophilin-substrate interactions [40]. Consistent with RpoE being a client of PPIs like FkpB and FklB, qRT-PCR analysis showed a reduction in mRNA levels of RpoE regulon members and the *rpoE* gene itself in Δ6*ppi* bacteria as compared to the wild type. This is in contrast to the constitutively up-regulated induction of RpoH regulon members (heat shock regulon) under the same conditions. Since RpoE senses maturation/folding status of OMPs and balance between phospholipids and LPS in the outer membrane (OM), it will be interesting to address, which specific factors are impaired in this signal transduction. If LPS translocation is impacted is under current investigation, since LptB an essential ATPase component of LPS transport system [14] was identified in pull-down studies with PpiC, FkpB and FklB. However, dampening of RpoE induction could as well be due to overall reduction of synthesis/maturation of major abundant OMPs in Δ6*ppi* bacteria.

Although the PPIase activity of all *E. coli* PPIs has been measured, yet the relative contribution is unknown. In this work, we thus undertook systematic studies to measure relative contribution of each PPI towards overall cellular enzymatic activity without using recombinant proteins. We could show that PpiB and PpiA are the major contributors of PPIase activity. PpiA and PpiB are homologous proteins located in the periplasm and the cytoplasm, respectively. Although PpiB was found to be the major contributor towards the cytoplasmic PPIase activity, yet a Δ*ppiB* strain exhibits no growth phenotype defect under standard laboratory growth conditions, exhibits wild-type like bacterial motility and cellular morphology and overexpression of the *ppiB* gene also does not confer any phenotypic defect. The lack of any major growth defect is best explained by a significant overlap of substrates with other PPIs as shown in this study with pull-down experiments. Further, we note that a Δ*ppiB* strain JW0514 from deletion set of all ORFs exhibits hypermotility and the cell division phenotype. However, this phenotype was found to be unrelated to PpiB function as transduction of Δ*ppiB* mutation from JW0514 into the wild-type *E. coli* confers a wild-type like phenotype for motility and cell morphology and plasmids carrying the wild-type copy of *ppiB* gene do not complement any phenotype of JW0514 (Table S2 and Materials and Methods). Hence, the conclusions concerning the negative regulation of bacterial motility and cell division by PpiB/FklB [41] could not be validated.

In this study, we also constructed a strain lacking all ten PPIs to measure its PPIase activity. However, such a Δ10*ppi* derivative grows extremely poorly. Most importantly, a small residual PPIase activity above the background level was observed. Thus, intensive studies are ongoing to identify potential new PPIs that can explain this residual activity and explain the viability of strains lacking

currently known PPIs. It is of interest that several stress-related proteins with an adaptive function, such as polyphosphate kinase (Ppk), the heat shock protein HslU and UspG were identified as putative clients of PPIs [22,42,43], suggesting a co-operation between PPIs and factors in maintaining cellular homeostasis. Furthermore, the identification of several proteins that may require PPIs for their folding or activity has laid a fertile ground for future investigations. Our ongoing studies indeed reveal the PPIase activity-dependent and independent interactions with substrates like FabH, NusG, OxyR, GrxB, YgfZ, Ppk, Ppa, RpoA, ProQ, RapZ, and YrdA (manuscript in preparation).

4. Materials and Methods

4.1. Bacterial Strains, Plasmids and Media

The bacterial strains and plasmids used in this study are described in supporting Table S2. Luria-Bertani (LB) broth, M9 (Difco) and M9 minimal media were prepared as described [44]. When required, media were supplemented with ampicillin (100 μg/mL), kanamycin (50 μg/mL), tetracycline (10 μg/mL), spectinomycin (50 μg/mL), chloramphenicol (20 μg/mL).

4.2. Generation of Null Mutations and the Construction of Δ6*ppi* Derivatives

Non-polar antibiotic-free deletion mutations of various PPIs-encoding genes or genes whose overexpression restored growth of various Δ6*ppi* strains were constructed by using the λ Red recombinase/FLP-mediated recombination system as described previously [14,45]. The antibiotic cassette was amplified using pKD3 and pKD13 as templates [45]. PCR products from such amplification reactions were electroporated into BW25113 containing the λ Red recombinase-encoding plasmid pKD46 (GK1942). Each deletion was verified by PCR amplification and sequencing of PCR products. Such deletions were transduced into BW25113 wild-type strain by bacteriophage P1-mediated transduction. Multiple null combinations were constructed as described previously, followed by the removal of *aph* or *cat* cassettes using the pCP20 plasmid and confirmed to be non-polar [44,45]. When required, additional deletion derivatives were constructed using *ada* cassette for gene replacement using pCL1920 plasmid as a template in PCR amplification reactions, followed by gene replacement as described above. Transductants were plated in parallel on M9 and LA medium at various temperatures. To validate obtaining of suppressor-free Δ6*ppi* derivatives, deletion derivatives carrying up to five deletion combinations were transformed with either the vector alone or the plasmid carrying the sixth PPI-encoding gene under the control of P_{T5}-*lac* promoter. Such six strains then served as a recipient to bring in the last deletion by bacteriophage P1-mediated transductions to construct Δ6*ppi* derivatives and verified as described above. Since deletion derivatives of *ppiB* and *fkpB* genes from the library of gene disruptions in the Keio collection exhibit a polar phenotype, new gene disruptions were constructed using the λ Red-mediated recombineering. In these cases, the *aph* cassettes were introduced using oligonucleotides that contain a ribosome-binding site to allow a constitutive induction of downstream essential genes (*lpxH* in the case of *ppiB* gene and *ispH* in the case of *fkpB* gene, respectively). Furthermore, since the Δ*ppiB* derivative in Keio collection JW0154 exhibits a hypermotility phenotype, this Δ*ppiB* mutation was transduced into wild-type BW25113 and BW30270 strains resulting into SR19818 and SR19840, which exhibited wild-type like cell morphology and wild-type like bacterial motility (Table S2).

4.3. Construction of Chromosomal Wild-Type and Single-Copy Mutants of ppiC FLAG Derivatives

To construct chromosomal C-terminal 3xFLAG-tagged genes, pSUB11 plasmid [46] was used as template for PCR amplification as described earlier [14,44]. PCR reactions were carried out using appropriate oligonucleotides. To introduce single amino acid substitutions in the *ppiC* on the chromosome with C-terminal 3xFLAG, mutations were introduced in the forward oligonucleotides. Verification of the introduced mutations in the concerned gene was done on the basis of DNA sequencing of PCR amplification products using chromosomal DNAs as templates.

4.4. The Isolation of Aggregated Proteins

Aggregation of cellular proteins was analyzed using isogenic wild-type BW25113 and its Δ6*ppi* derivative. Fifty ml bacterial cultures were grown in M9 medium at 37 °C up to an OD_{600} of 0.3, washed and shifted to LB medium at 30 °C. Cultures were harvested by centrifugation. Pellets were resuspended in 600 µL of B-PER reagent (Pierce, Warsaw, Poland), supplemented with 1 mg/mL lysozyme, a cocktail of protease inhibitors (Sigma, Poznan, Poland), PMSF and 30 U of benzonase and incubated for 90 min on ice with gentle mixing and subjected to fractionation into soluble, membrane and aggregates as described [14]. This procedure is based on previously described method [47] to isolate protein aggregates with modifications that allow better removal of membrane proteins. The pellet fraction containing outer membrane and aggregated proteins were resuspended in 40 µL of 10 mM Tris buffer. Soluble and aggregates were analyzed by gel electrophoresis. To identify protein by MALDI-TOF, 2D electrophoresis was undertaken using 300 µg of protein from aggregate samples. Proteins were incubated in rehydration buffer as per protocol from Bio-Rad (Warsaw, Poland). The mixture was added to hydration tray chamber and incubated in 7 cm immobilized pH gradient (IPG) strip gels. Isoelectric focusing was carried out in PROTEAN i12 (Bio-Rad) IEF cell at 20 °C. For the second dimension, strips were applied to 12.5% SDS-PAGE.

4.5. Co-immunoprecipitation with 3xFLAG-tagged PpiC Protein

Isogenic cultures of 3xFLAG-tagged wild-type *ppiC* and its PpiC F81A::3xFLAG derivative (5 mL each) were grown to an OD_{600} of 0.5 and harvested by centrifugation at 12,000× *g* for 20 min at 4 °C. Pellet was resuspended in 100 µL of lysis buffer (Sigma FLAGIPT1), supplemented by a cocktail of protease inhibitors (Sigma), PMSF, benzonase and lysozyme as per manufacturer's instructions. Samples were incubated with shaking at 4 °C and incubated with 30 µL of washed ANTI-FLAG gel suspension. Samples were shaken for 12 h at 4 °C and centrifuged at 7000× *g* for 30 s and washed. FLAG-fusion protein was eluted under native conditions with 3xFLAG peptide. Equivalent amounts of eluted samples were resolved on a 12% SDS-PAGE and proteins visualized by silver staining.

4.6. Protein Purification of Wild-Type and Ppi Mutants

For the protein induction, the minimal coding sequence of *ppi* genes were cloned with either a C-terminal or N-terminal His_6 affinity tag in the T7 polymerase-based expression vectors (pET24b or pET28b). Specific mutations were introduced by gene synthesis and Gibson cloning. For the purification of hexa-His-tagged PPIs, their cognate genes cloned in pET expression vectors were induced in the *E. coli* T7 express derivative lacking all six PPIs (SR21984) at 33 °C at an optical density of 0.1 at 600 nm in a 1 L culture by the addition of either 0.1 mM or 0.3 mM IPTG. Lower concentration of IPTG was used to identify co-eluting proteins, whereas higher concentration of IPTG 0.3 mM to obtain pure proteins. This strain contains a chromosomal copy of the phage T7 RNA polymerase gene, whose expression is controlled by IPTG inducible *lac* promoter and also carries $lacI^q$ and *lysY* to prevent basal level expression. When only pure protein was needed cultures after 2 h incubation with IPTG, rifampicin was added to prevent the synthesis of host proteins and shaken for another 2 h, as described previously [14]. After the induction, cells were harvested by centrifugation at 12,000 rpm for 30 min. The pellet was resuspended in B-PER reagent (Pierce) and adjusted to contain 50 mM NaH_2PO_4, 300 mM NaCl, 10 mM imidazole (buffer A), supplemented with lysozyme to a final concentration of 200 µg/mL, a cocktail of protease inhibitors (Sigma) and 30 units of benzonase (Merck, Poznan, Poland). The mixture was incubated on ice for 45 min with gentle mixing. The lysate was centrifuged at 45,000× *g* for 30 min at 4 °C. Soluble proteins were applied over nickel-nitrilotriacetic acid beads (Qiagen, Geneva Switzerland), washed and eluted with buffer A with a linear gradient (50 mM–500 mM) of imidazole.

4.7. PPIase Assay

Total cell lysates were obtained from the wild type, its derivative lacking all four periplasmic PPIs and its isogenic derivatives lacking one of cytoplasmic PPIs or strain lacking all ten PPIs. Cultures (250 mL) were grown at 37 °C in LB or M9 medium up to an OD_{600} of 0.4 and harvested by centrifugation. Pellets were resuspended in B-PER reagent, supplemented with lysozyme to a final concentration of 200 µg/mL, cocktail of protease inhibitors and 30 units of benzonase and incubated on ice for 30 min with mixing. The lysate was centrifuged at 45,000× *g* for 90 min at 4 °C to obtain soluble proteins. For each sample, 10 mg/mL protein was used to measure the PPIase activity in a chymotrypsin-coupled enzymatic assay [48,49] using 8 mM *N*-Suc-Ala-Ala-*cis*-Pro-Phe-*p*-nitroanilide as the test peptide. The PPIase activity was determined in 35 mM HEPES pH 8.0 as assay buffer and the activity was measured at 10 °C. The reaction was initiated by the addition of chymotrypsin (300 µg/mL) and change in absorbance at 390 nm recorded using Specord 200 Plus spectrophotometer equipped with the Peltier temperature control system. For measurement of the PPIase activity with purified individual wild-type or mutant protein, PPIs were used at a concentration of 0.1 µM.

4.8. RNA Purification and qRT-PCR Analysis

Isogenic bacterial cultures were grown at either 30 or 37 °C in either M9 minimal medium or LB rich medium in the presence of appropriate antibiotics to an OD_{600} of 0.2. For heat shock, aliquots were immediately shifted to pre-warmed medium held at 43 °C and incubated either for 15 min or 90 min. Samples were collected at times indicated above, and harvested by centrifugation. Pellets were flash frozen in liquid nitrogen and stored at −80 °C. RNA was purified using GenElute Total RNA Purification Kit as per manufacturer instructions for Gram-negative bacteria. RNA was eluted in 50 to 100 µL of DEPC-treated water. RNA amounts were quantified and RNA integrity verified by agarose gel electrophoresis. Moreover, qRT-PCR was used to quantify gene expression changes in Δ6*ppi* mutants as compared to the wild type before and after heat shock treatment. For each target gene, gene-specific primers (Table S3) were used to amplify DNA fragments of ≈100 bp. Purified mRNA (2 µg) was converted to cDNA using iScript Reverse Transcription Supermix from Bio-Rad. qRT-PCR was performed using CFX Connect Real-Time PCR Detection System (Bio-Rad). Reactions were carried out for 40 cycles in an optical 96 well plate with 20 µL reaction volumes containing 10 µL PowerUp SYBR® Green PCR Master Mix (ThermoFisher Scientific, Poznan, Poland), 0.5 µL cDNA, 0.6 µL each of the 10 µM forward and reverse primers, and 8.3 µL of RNase-free water. In addition, samples lacking cDNA in above reaction served as a control for any DNA contamination. Data were analyzed by software Bio-Rad CFX Maestro.

4.9. Isothermal Titration Calorimetry (ITC) Measurements

The experiments were conducted using a Nano ITC instrument (TA instruments, Utah USA). Purified proteins were dialyzed against ITC buffer (20 mM sodium phosphate pH 7.5 and 100 mM NaCl). For these experiments, peptides used were used at a concentration of 200 µM in the calorimetric cell and titrated with 2 mM of various protein at 20 °C. Typically for each experiment, 25 injections (2 µL of protein sample) at 200 s intervals were performed. Binding isotherms were analyzed according to 1:1 binding model using NanoAnalyze software.

Supplementary Materials: The following are available online at http://www.mdpi.com/1422-0067/21/12/4212/s1, Table S1. Proteins that specifically accumulate in aggregation fractions in Δ6*ppi* strains under permissive growth conditions, Table S2. Bacterial strains and plasmids used in this study, Table S3. Primers for qRT-PCR.

Author Contributions: Conceptualization and methodology, S.R., and G.K.; validation, S.R., and G.K.; investigation, S.R., G.K., P.W., D.B., A.S., and P.G.; writing—original draft preparation, review and editing, S.R. and G.K.; supervision, S.R.; funding acquisition, S.R. All authors have read and agreed to the published version of the manuscript.

Funding: This research was funded by the National Science Center (NCN) Grant 2017/25/B/NZ6/02021 to S.R.

Acknowledgments: We wish to thank G. Fischer and C. Schiene-Fischer for several suggestions and H. Mori for gift of strains. We also thank present and past members of our laboratory, including M. Arendt and P. Sulima.

Conflicts of Interest: The authors declare no conflict of interest.

Abbreviations

PPI	peptidyl-prolyl *cis/trans* isomerase
FKBP	FK506-binding protein
OMP	outer membrane protein
ITC	isothermal titration calorimetry

References

1. Ellis, R.J. Protein misassembly: Macromolecular crowding and molecular chaperones. *Adv. Exp. Med. Biol.* **2007**, *594*, 1–13. [CrossRef]
2. Grathwohl, C.; Wüthrich, K. NMR studies of the rates of proline *cis-trans* isomerization in oligopeptides. *Biopolymers* **1981**, *20*, 2623–2633. [CrossRef]
3. Nicholson, L.K.; Lu, K.P. Prolyl *cis-trans* isomerization as a molecular timer in Crk signaling. *Mol. Cell* **2007**, *25*, 483–485. [CrossRef]
4. Fischer, G.; Aumüller, T. Regulation of peptide bond *cis/trans* isomerization by enzyme catalysis and its implication in physiological processes. *Rev. Physiol. Biochem. Pharmacol.* **2003**, *148*, 105–150. [CrossRef]
5. Rahfeld, J.U.; Schierhorn, A.; Mann, K.; Fischer, G. A novel peptidyl-prolyl *cis/trans* isomerase from *Escherichia coli*. *FEBS Lett.* **1994**, *343*, 65–69. [CrossRef]
6. Ferbitz, L.; Maier, T.; Patzelt, H.; Bukau, B.; Deuerling, E.; Ban, N. Trigger factor in complex with the ribosome forms a molecular cradle for nascent proteins. *Nature* **2004**, *431*, 590–596. [CrossRef]
7. Oh, E.; Becker, A.H.; Sandikci, A.; Huber, D.; Chaba, R.; Gloge, F.; Nichols, R.J.; Typas, A.; Gross, C.A.; Kramer, G.; et al. Selective ribosome profiling reveals the cotranslational chaperone action of trigger factor *in vivo*. *Cell* **2011**, *147*, 1295–1308. [CrossRef]
8. Hottenrott, S.; Schumann, T.; Plückthun, A.; Fischer, G.; Rahfeld, J.U. The *Escherichia coli* SlyD is a metal ion-regulated peptidyl-prolyl *cis/trans*-isomerase. *J. Biol. Chem.* **1997**, *272*, 15697–15701. [CrossRef]
9. Knappe, T.A.; Eckert, B.; Schaarschmidt, P.; Scholz, C.; Schmid, F.X. Insertion of a chaperone domain converts FKBP12 into a powerful catalyst of protein folding. *J. Mol. Biol.* **2007**, *368*, 1458–1468. [CrossRef]
10. Zhang, J.W.; Leach, M.R.; Zamble, D.B. The peptidyl-prolyl isomerase activity of SlyD is not required for maturation of *Escherichia coli* hydrogenase. *J. Bacteriol.* **2007**, *189*, 7942–7944. [CrossRef]
11. Malešević, M.; Poehlmann, A.; Hernandez Alvarez, B.; Diessner, A.; Träger, M.; Rahfeld, J.U.; Jahreis, G.; Liebscher, S.; Bordusa, F.; Fischer, G.; et al. The protein-free IANUS peptide array uncovers interaction sites between *Escherichia coli* parvulin 10 and alkyl hydroperoxide reductase. *Biochemistry* **2010**, *49*, 8626–8635. [CrossRef] [PubMed]
12. Quistgaard, E.M.; Nordlund, P.; Löw, C. High-resolution insights into binding of unfolded polypeptides by the PPIase chaperone SlpA. *FASEB J.* **2012**, *26*, 4003–4013. [CrossRef] [PubMed]
13. Potter, S.; Yang, X.; Boulanger, M.J.; Ishiguro, E.E. Occurrence of homologs of the *Escherichia coli lytB* gene in gram-negative bacterial species. *J. Bacteriol.* **1998**, *180*, 1959–1961. [CrossRef] [PubMed]
14. Klein, G.; Kobylak, N.; Lindner, B.; Stupak, A.; Raina, S. Assembly of lipopolysaccharide in *Escherichia coli* requires the essential LapB heat shock protein. *J. Biol. Chem.* **2014**, *289*, 14829–14853. [CrossRef]
15. Raina, S.; Missiakas, D.; Georgopoulos, C. The *rpoE* gene encoding the σ^E (σ^{24}) heat shock sigma factor of *Escherichia coli*. *EMBO J.* **1995**, *14*, 1043–1055. [CrossRef]
16. Compton, L.A.; Davis, J.M.; Macdonald, R.; Bächinger, H.P. Structural and functional characterization of *Escherichia coli* peptidyl-prolyl *cis-trans* isomerases. *Eur. J. Biochem.* **1992**, *206*, 927–934. [CrossRef]
17. Hayano, T.; Takahashi, N.; Kato, S.; Maki, N.; Suzuki, M. Two distinct forms of peptidylprolyl-*cis-trans*-isomerase are expressed separately in periplasmic and cytoplasmic compartments of *Escherichia coli* cells. *Biochemistry* **1991**, *30*, 3041–3046. [CrossRef]
18. Zydowsky, L.D.; Etzkorn, F.A.; Chang, H.Y.; Ferguson, S.B.; Stolz, L.A.; Ho, S.I.; Walsh, C.T. Active site mutants of human cyclophilin A separate peptidyl-prolyl isomerase activity from cyclosporin A binding and calcineurin inhibition. *Protein Sci.* **1992**, *1*, 1092–1099. [CrossRef]

19. Rahfeld, J.U.; Rücknagel, K.P.; Stoller, G.; Horne, S.M.; Schierhorn, A.; Young, K.D.; Fischer, G. Isolation and amino acid sequence of a new 22-kDa FKBP-like peptidyl-prolyl *cis/trans*-isomerase of *Escherichia coli*. Similarity to Mip-like proteins of pathogenic bacteria. *J. Biol. Chem.* **1996**, *271*, 22130–22138. [CrossRef]
20. Budiman, C.; Tadokoro, T.; Angkawidjaja, C.; Koga, Y.; Kanaya, S. Role of polar and nonpolar residues at the active site for PPIase activity of FKBP22 from *Shewanella* sp. SIB1. *FEBS J.* **2012**, *279*, 976–986. [CrossRef]
21. Polley, S.; Chakravarty, D.; Chakrabarti, G.; Chattopadhyaya, R.; Sau, S. Proline substitutions in a Mip-like peptidyl-prolyl *cis-trans* isomerase severely affect its structure, stability, shape and activity. *Biochim. Open* **2015**, *1*, 28–39. [CrossRef] [PubMed]
22. Missiakas, D.; Schwager, F.; Betton, J.M.; Georgopoulos, C.; Raina, S. Identification and characterization of HslVHslU (ClpQ ClpY) proteins involved in overall proteolysis of misfolded proteins in *Escherichia coli*. *EMBO J.* **1996**, *15*, 6899–6909. [CrossRef] [PubMed]
23. Martin, R.G.; Rosner, J.L. Genomics of the *marA/soxS/rob* regulon of *Escherichia coli*: Identification of directly activated promoters by application of molecular genetics and informatics to microarray data. *Mol. Microbiol.* **2002**, *44*, 1611–1624. [CrossRef] [PubMed]
24. Klein, G.; Raina, S. Regulated assembly of LPS, its structural alterations and cellular response to LPS defects. *Int. J. Mol. Sci.* **2019**, *20*, 356. [CrossRef] [PubMed]
25. Missiakas, D.; Mayer, M.P.; Lemaire, M.; Georgopoulos, C.; Raina, S. Modulation of the *Escherichia coli* σ^E (RpoE) heat-shock transcription-factor activity by the RseA, RseB and RseC proteins. *Mol. Microbiol.* **1997**, *24*, 355–371. [CrossRef] [PubMed]
26. De Las Peñas, A.; Connolly, L.; Gross, C.A. The σ^E-mediated response to extracytoplasmic stress in *Escherichia coli* is transduced by RseA and RseB, two negative regulators of σ^E. *Mol. Microbiol.* **1997**, *24*, 373–385. [CrossRef]
27. Tam, C.; Collinet, B.; Lau, G.; Raina, S.; Missiakas, D. Interaction of the conserved region 4.2 of σ^E with RseA anti-sigma factor. *J. Biol. Chem.* **2002**, *277*, 27282–27287. [CrossRef]
28. Fanghänel, J.; Fischer, G. Insights into the catalytic mechanism of peptidyl prolyl *cis/trans* isomerases. *Front. Biosci.* **2004**, *9*, 3453–3478. [CrossRef]
29. Deuerling, E.; Patzelt, H.; Vorderwülbecke, S.; Rauch, T.; Kramer, G.; Schaffitzel, E.; Mogk, A.; Schulze-Specking, A.; Langen, H.; Bukau, B. Trigger Factor and DnaK possess overlapping substrate pools and binding specificities. *Mol. Microbiol.* **2003**, *47*, 1317–1328. [CrossRef]
30. Zhao, L.; Vecchi, G.; Vendruscolo, M.; Körner, R.; Hayer-Hartl, M.; Hartl, F.U. The Hsp70 chaperone system stabilizes a thermo-sensitive subproteome in *E. coli*. *Cell Rep.* **2019**, *28*, 1335–1345.e6. [CrossRef]
31. Du, X.; Li, Y.; Xia, Y.L.; Ai, S.M.; Liang, J.; Sang, P.; Ji, X.L.; Liu, S.Q. Insights into protein-ligand interactions: Mechanisms, models, and methods. *Int. J. Mol. Sci.* **2016**, *17*, 144. [CrossRef] [PubMed]
32. Chen, B.; Boël, G.; Hashem, Y.; Ning, W.; Fei, J.; Wang, C.; Gonzalez, R.L., Jr.; Hunt, J.F.; Frank, J. EttA regulates translation by binding the ribosomal E site and restricting ribosome-tRNA dynamics. *Nat. Struct. Mol. Biol.* **2014**, *21*, 152–159. [CrossRef] [PubMed]
33. Dewachter, L.; Deckers, B.; Martin, E.; Herpels, P.; Gkekas, S.; Versées, W.; Verstraeten, N.; Fauvart, M.; Michiels, J. GTP binding is necessary for the activation of a toxic mutant isoform of the essential GTPase ObgE. *Int. J. Mol. Sci.* **2019**, *21*, 16. [CrossRef] [PubMed]
34. Choi, E.; Jeon, H.; Oh, J.I.; Hwang, J. Overexpressed L20 rescues 50S ribosomal subunit assembly defects of *bipA*-deltion in *Escherichia coli*. *Front. Microbiol.* **2020**, *10*, 2982. [CrossRef] [PubMed]
35. Ishihama, A. Functional modulation of *Escherichia coli* RNA polymerase. *Annu. Rev. Microbiol.* **2000**, *54*, 499–518. [CrossRef] [PubMed]
36. Klein, G.; Stupak, A.; Biernacka, D.; Wojtkiewicz, P.; Lindner, B.; Raina, S. Multiple transcriptional factors regulate transcription of the *rpoE* gene in *Escherichia coli* under different growth conditions and when the lipopolysaccharide biosynthesis is defective. *J. Biol. Chem.* **2016**, *291*, 22999–23019. [CrossRef] [PubMed]
37. Dartigalongue, C.; Missiakas, D.; Raina, S. Characterization of the *Escherichia coli* σ^E regulon. *J. Biol. Chem.* **2001**, *276*, 20866–20875. [CrossRef]
38. Ades, S.E. Regulation by destruction: Design of the σ^E envelope stress response. *Curr. Opin. Microbiol.* **2008**, *11*, 535–540. [CrossRef]
39. Campbell, E.A.; Tupy, J.L.; Gruber, T.M.; Wang, S.; Sharp, M.M.; Gross, C.A.; Darst, S.A. Crystal structure of *Escherichia coli* σ^E with the cytoplasmic domain of its anti-sigma RseA. *Mol. Cell* **2003**, *11*, 1067–1078. [CrossRef]

40. Daum, S.; Schumann, M.; Mathea, S.; Aumüller, T.; Balsley, M.A.; Constant, S.L.; de Lacroix, B.F.; Kruska, F.; Braun, M.; Schiene-Fischer, C. Isoform-specific inhibition of cyclophilins. *Biochemistry* **2009**, *48*, 6268–6277. [CrossRef]
41. Skagia, A.; Zografou, C.; Vezyri, E.; Venieraki, A.; Katinakis, P.; Dimou, M. Cyclophilin PpiB is involved in motility and biofilm formation via its functional association with certain proteins. *Genes Cells* **2016**, *21*, 833–851. [CrossRef]
42. Rao, N.N.; Kornberg, A. Inorganic polyphosphate supports resistance and survival of stationary-phase *Escherichia coli*. *J. Bacteriol.* **1996**, *178*, 1394–1400. [CrossRef]
43. Bochkareva, E.S.; Girshovich, A.S.; Bibi, E. Identification and characterization of the *Escherichia coli* stress protein UP12, a putative in vivo substrate of GroEL. *Eur. J. Biochem.* **2002**, *269*, 3032–3040. [CrossRef]
44. Klein, G.; Lindner, B.; Brade, H.; Raina, S. Molecular basis of lipopolysaccharide heterogeneity in *Escherichia coli*: Envelope stress-responsive regulators control the incorporation of glycoforms with a third 3-deoxy-α-D-*manno*-oct-2-ulosonic acid and rhamnose. *J. Biol. Chem.* **2011**, *286*, 42787–42807. [CrossRef] [PubMed]
45. Datsenko, K.A.; Wanner, B.L. One-step inactivation of chromosomal genes in *Escherichia coli* K-12 using PCR products. *Proc. Natl. Acad. Sci. USA* **2000**, *97*, 6640–6645. [CrossRef] [PubMed]
46. Uzzau, S.; Figueroa-Bossi, N.; Rubino, S.; Bossi, L. Epitope tagging of chromosomal genes in *Salmonella*. *Proc. Natl. Acad. Sci. USA* **2001**, *98*, 15264–15269. [CrossRef] [PubMed]
47. Tomoyasu, T.; Mogk, A.; Langen, H.; Goloubinoff, P.; Bukau, B. Genetic dissection of the roles of chaperones and proteases in protein folding and degradation in the *Escherichia coli* cytosol. *Mol. Microbiol.* **2001**, *40*, 397–413. [CrossRef]
48. Fischer, G.; Wittmann-Liebold, B.; Lang, K.; Kiefhaber, T.; Schmid, F.X. Cyclophilin and peptidyl-prolyl *cis-trans* isomerase are probably identical proteins. *Nature* **1989**, *337*, 476–478. [CrossRef] [PubMed]
49. Kofron, J.L.; Kuzmič, P.; Kishore, V.; Colón-Bonilla, E.; Rich, D.H. Determination of kinetic constants for peptidyl prolyl cis-trans isomerases by an improved spectrophotometric assay. *Biochemistry* **1991**, *30*, 6127–6134. [CrossRef]

THE JOURNAL OF BIOLOGICAL CHEMISTRY VOL. 291, NO. 44, pp. 22999–23019, October 28, 2016

Multiple Transcriptional Factors Regulate Transcription of the *rpoE* Gene in *Escherichia coli* under Different Growth Conditions and When the Lipopolysaccharide Biosynthesis Is Defective*[S]

Received for publication, July 18, 2016, and in revised form, September 11, 2016 Published, JBC Papers in Press, September 14, 2016, DOI 10.1074/jbc.M116.748954

Gracjana Klein[‡1], **Anna Stupak**[‡1], **Daria Biernacka**[‡], **Pawel Wojtkiewicz**[‡], **Buko Lindner**[§], **and Satish Raina**[‡2]

From the [‡]*Unit of Bacterial Genetics, Gdansk University of Technology, Narutowicza 11/12, 80-233, Gdansk, Poland and the* [§]*Research Center Borstel, Leibniz-Center for Medicine and Biosciences, Parkallee 22, 23845 Borstel, Germany*

The RpoE σ factor is essential for the viability of *Escherichia coli*. RpoE regulates extracytoplasmic functions including lipopolysaccharide (LPS) translocation and some of its non-stoichiometric modifications. Transcription of the *rpoE* gene is positively autoregulated by $E\sigma^E$ and by unknown mechanisms that control the expression of its distally located promoter(s). Mapping of 5′ ends of *rpoE* mRNA identified five new transcriptional initiation sites (P1 to P5) located distal to $E\sigma^E$-regulated promoter. These promoters are activated in response to unique signals. Of these P2, P3, and P4 defined major promoters, recognized by RpoN, RpoD, and RpoS σ factors, respectively. Isolation of *trans*-acting factors, *in vitro* transcriptional and gel retardation assays revealed that the RpoN-recognized P2 promoter is positively regulated by a QseE/F two-component system and NtrC activator, whereas the RpoD-regulated P3 promoter is positively regulated by a Rcs system in response to defects in LPS core biosynthesis, overproduction of certain lipoproteins, and the global regulator CRP. Strains synthesizing Kdo_2-LA LPS caused up to 7-fold increase in the *rpoE*P3 activity, which was abrogated in Δ(*waaC rcsB*). Overexpression of a novel 73-nucleotide sRNA *rirA* (RfaH interacting RNA) generated by the processing of 5′ UTR of the *waaQ* mRNA induces the *rpoE*P3 promoter activity concomitant with a decrease in LPS content and defects in the *O*-antigen incorporation. In the presence of RNA polymerase, RirA binds LPS regulator RfaH known to prevent premature transcriptional termination of *waaQ* and *rfb* operons. RirA in excess could titrate out RfaH causing LPS defects and the activation of *rpoE* transcription.

The cell envelope of Gram-negative bacteria, including *Escherichia coli*, contains two distinct membranes, an inner (IM) and an outer (OM) membrane separated by the periplasm, a hydrophilic compartment that includes a layer of peptidoglycan. The OM is an asymmetric lipid bilayer with phospholipids forming the inner leaflet and LPS forming the outer leaflet. LPSs are highly heterogeneous in composition. However, they share a common architecture composed of a membrane-anchored phosphorylated and acylated β(1→6)-linked GlcN disaccharide, termed lipid A, to which a carbohydrate moiety of varying size is attached (1, 2).

During the analyses of signals that induce the RpoE-dependent extracytoplasmic stress response, we showed that strains synthesizing heptoseless LPS due to the absence of either GmhD (RfaD/HtrM) or WaaC exhibited a constitutive induction of RpoE (3–6). Such strains also display constitutive synthesis of exopolysaccharide that is regulated by the Rcs two-component system (5, 7, 8). Subsequently, we showed that strains synthesizing the minimal LPS structure composed of either Kdo_2-lipid IV_A or only free lipid IV_A exhibited hyperelevated levels of the RpoE activity (6). The activity of RpoE is highly induced when the LPS assembly is severely compromised or when there is an imbalance between LPS and phospholipids (9). Lack of many LPS core biosynthetic genes also leads to defects in survival at high temperatures (5, 6, 10).

The RpoE synthesis is positively regulated at the transcriptional level and negatively at the post-transcriptional level by the IM-anchored anti-σ factor RseA and the periplasmic sensor RseB (Fig. 1) (3, 11–16). There is an intricate link between the LPS assembly, its non-stoichiometric modifications, and the RpoE-mediated control exerted via its regulon members (17, 18). Elevated levels of RpoE with intact core biosynthetic enzymes lead to global alterations in the LPS composition. Under such conditions, LPS is primarily composed of glycoforms with a third Kdo, phosphoethanolamine (P-EtN) on the second Kdo and rhamnose on the third Kdo (Fig. 2) (19). The synthesis of such LPS glycoforms is controlled by the RpoE-regulated RybB and EptB (19). RpoE also positively regulates transcription of *micA* and *slrA* (*micL*) sRNAs (9, 20, 21). MicA negatively regulates the PhoP expression by direct translational inhibition of the *phoP* mRNA (22), thus further linking the PhoP/Q two-component system, known to regulate LPS non-stoichiometric alterations, with the RpoE control. The LPS syn-

* This work was supported by National Science Grants 2011/03/B/NZ1/02825 and 2013/11/B/NZ2/02641 (to S. R.). The authors declare that they have no conflicts of interest with the contents of this article.
[S] This article contains supplemental Tables S1 and S2.
[1] Both authors contributed equally to this work.
[2] To whom correspondence should be addressed: Unit of Bacterial Genetics, Gdansk University of Technology, Narutowicza 11/12, 80-233 Gdansk, Poland. Tel.: 48-58-347-2618; E-mail: satish.raina@pg.gda.pl.
[3] The abbreviations used are: IM, inner membrane; OM, outer membrane; RNAP, RNA polymerase; TSS, transcription start site; Kdo, 3-deoxy-α-D-*manno*-oct-2-ulosonic acid; P-EtN, phosphoethanolamine; L-Ara4N, 4-amino-4-deoxy-L-arabinose; ESI-FT-ICR MS, electrospray ionization Fourier transform-ion cyclotron mass spectrometry; *ops*, operon polarity suppression; Tricine, *N*-[2-hydroxy-1,1-bis(hydroxymethyl)ethyl]glycine; nt, nucleotide(s); IPTG, isopropyl 1-thio-β-D-galactopyranoside; CRP, cyclic AMP receptor protein; sRNA, small RNA.

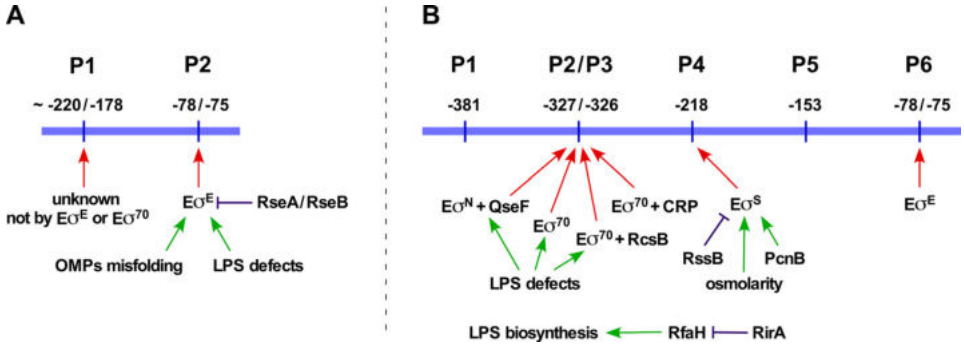

FIGURE 1. **Transcriptional regulation of the *rpoE* gene.** Schematic drawing of previously identified transcriptional start sites of the *rpoE* gene (3, 16) (*A*) and those identified in this work (*B*). Major regulators and factors controlling the *rpoE* transcription are indicated.

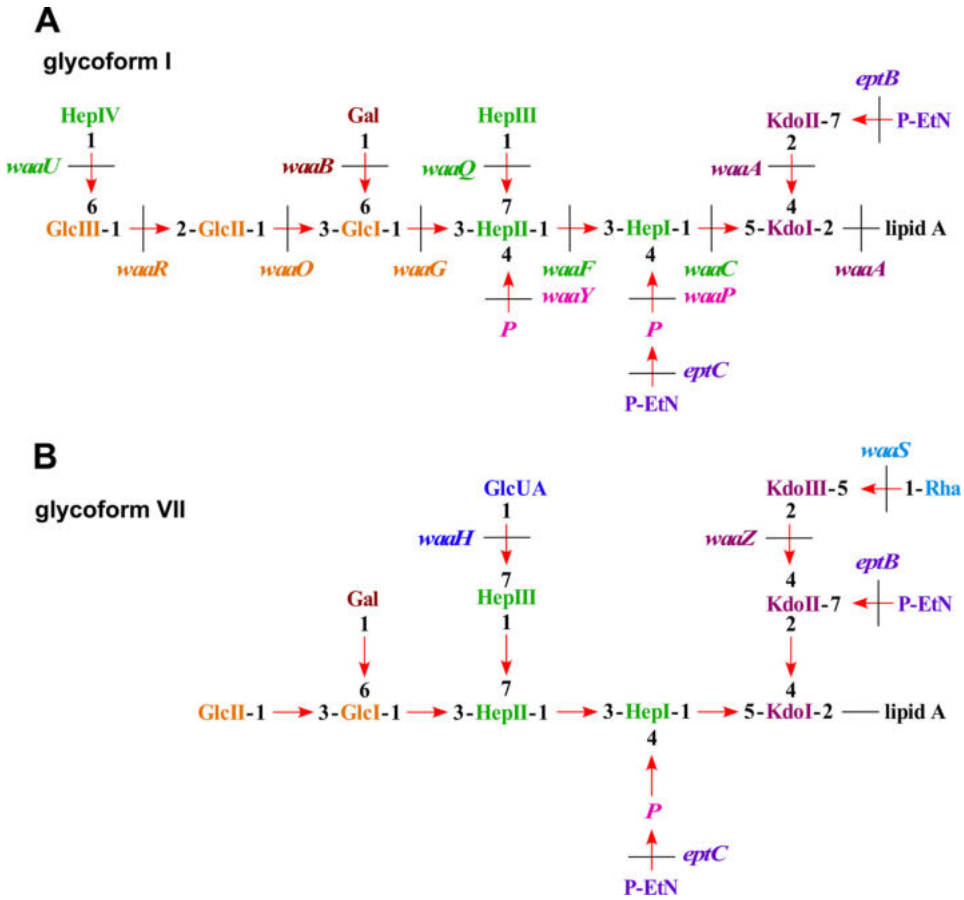

FIGURE 2. **Proposed LPS structure of major glycoforms observed in *E. coli* K-12.** Schematic drawing of LPS glycoforms I (*A*) and VII (*B*) with the indicated genes whose products are involved in the LPS core biosynthesis and non-stoichiometric modifications.

thesis is further regulated by the transcriptional factor RfaH. RfaH strongly inhibits the Rho-dependent termination of *waaQ* and *rfb* operons, which contain *ops* (operon polarity suppression) sites in their 5′ UTR and also binds to the ribosome to activate translation (23–25). Thus, the synthesis of LPS, like many key cellular components, is regulated by various transcriptional factors including two-component systems and σ factors.

Interestingly, some two-component systems that regulate LPS modifications, like BasS/R and envelope stress responsive Rcs phosphorelay systems, are also linked with quorum sensing Qse systems by phosphorylation of the response regulator by a non-cognate kinase (26–28). Similarly, at the transcriptional level, the synthesis of different σ factors is interlinked due to the presence of multiple promoters adding additional layers of regulation. For example, the gene encoding the housekeeping σ factor RpoD is transcribed from two promoters and one of them is the RpoH-regulated heat shock promoter (29). Similarly, the *rpoH* gene is transcribed from multiple promoters whose transcription is regulated by different σ factors (3, 30). The presence of multiple promoters endows them the ability to respond to different signals. Such a mode of complex transcriptional regulation allows linking of different stress responsive pathways.

Despite numerous strides in the post-transcriptional regulation of the *rpoE* gene, its transcriptional regulation has not been

TABLE 1

Impact of non-polar deletion mutations or overexpression of various regulators that alter the activity of the *rpoE*P1-P5-*lacZ* transcriptional fusion

Values correspond to average of four independent samples from cultures grown in LB or in M9 minimal medium at A_{600} 0.2 to 0.4.

	Function	Effect	Specificity
Genotype			
Wild-type SR7917 (*rpoE*P1-P5-*lacZ*)		393 ± 26	
Δ*waaC*	Heptosyltransferase I	2630 ± 168	*rpoE*P3 in Rcs-dependent manner, also induces the Eσ^E-regulated *rpoE*P6 promoter that is only partially dependent on the Rcs system
Δ*waaF*	Heptosyltransferase II	1052 ± 65	*rpoE*P3
Δ*waaG*	LPS glucosyltransferase I	837 ± 46	*rpoE*P3
Δ*waaP*	LPS core HepI kinase	894 ± 51	*rpoE*P3
Δ*rfaH*	Transcriptional anti-terminator	1505 ± 93	*rpoE*P3
Δ*cya*	Adenylate cyclase	230 ± 16	*rpoE*P3
Δ*crp*	Transcriptional dual regulator	215 ± 18	*rpoE*P3
Δ(*ecfLM*)	RpoE regulon member, DedA family member	870 ± 85	*rpoE*P3
Δ*rssB*	Regulator of RpoS	531 ± 37	*rpoE*P4
Δ*arcA*	Transcriptional dual regulator	831 ± 65	*rpoE*P4
Δ*arcB*	Sensory histidine kinase	1120 ± 90	*rpoE*P4
Δ*rpoS*	RpoS σ factor	193 ± 14	*rpoE*P4
Δ*rpoN*	RpoN σ factor	302 ± 25	*rpoE*P2, lack of RpoN in Δ*waaC*, reduces *rpoE*P2 induction that is QseF-dependent
Δ(*rpoN waaC*)		1290 ± 90	
Δ*ntrC*	Transcriptional dual regulator	312 ± 27	*rpoE*P2
Multicopy expression that alters the transcription			
qseG	Part of *qseE/F* operon	6920 ± 335	*rpoE*P2
yhdV and six other genes encoding lipoproteins	Lipoprotein	1063 ± 68	*rpoE*P3 (Rcs-dependent)
rirA	sRNA	786 ± 52	*rpoE*P3
pcnB	Poly(A) polymerase I	540 ± 38	*rpoE*P4
fliZ	DNA-binding transcriptional regulator	249 ± 21	*rpoE*P4

fully addresses. In *E. coli*, two promoters were initially identified, one distally located with unknown regulation and a second promoter recognized by σ^E itself (Fig. 1*A*) (3, 16). However, transcription from the upstream promoter(s) is sustained under several stress and non-stress conditions (3). The RpoE activity is also induced by stresses like exposure to high osmolarity, cold shock conditions, and entry into the stationary phase (31, 32). Some of these factors, like the absence of RpoS, do not alter the LPS composition (19) and hence how these diverse signals are sensed is unknown. Thus, several single-copy chromosomal *rpoE*P-*lacZ* promoter fusions, devoid of DNA sequence covering the promoter recognized by Eσ^E, were constructed to identify *trans*-acting factors that regulate *rpoE* transcription, followed by mapping of transcription start sites and verification by *in vitro* run-off assays. This analysis revealed five new transcription start sites that are utilized by different regulatory factors in response to distinct signals (Fig. 1*B*).

Results

LPS Defects and Signals Regulating RpoS, RpoN, and CRP Alter the Transcriptional Activity of the rpoE Gene

As the regulation of the *rpoE* promoter region distal to its Eσ^E-transcribed promoter is unknown, a single-copy *lacZ* promoter fusion was constructed that contains the 529-bp region upstream of this autoregulated promoter. For simplicity, such a fusion derivative is referred to as *rpoE*P-*lacZ*. Strains with this promoter fusion (MC4100 derivative SR4245 and SR7917-based on BW25113) served as a host for saturated random transposon mutagenesis to identify mutations that alter the activity of this transcriptional region. The rationale of using two strains rules out any strain specificity. It is worth mentioning that the host strain BW25113 is also the parental strain for the Keio collection of gene knockouts (33) and hence its usage. Mapping and sequencing of Tn*10* mutations conferring a Lac up phenotype revealed that the majority of them had insertion in LPS biosynthetic/LPS regulatory genes and a few in other loci (supplemental Table S1). A similar spectrum of mutants was obtained in SR4245 and SR7917. Among these, 12 Tn*10* insertions were mapped to the *waaC* gene, three to the *waaF* gene, and one each was located in *rfaH* and *waaQ* genes. Furthermore, two Tn*10* insertions were mapped to the *rssB* gene (both with Tn*10* insertion at nucleotide position 240), one Tn*10* insertion in the *arcA* gene (nucleotide position 72 within the coding region), and one at nucleotide position −78 upstream of the initiation codon of the *ecfL* gene. Mapping of Lac down mutations identified one mutation each in *glnG* (*ntrC*), *glnA*, and *cya* genes, indicating that their products could play positive regulatory roles. The introduction of defined non-polar dele-

TABLE 2

Supplementation of growth medium that alter the activity of the *rpoE*P1-P5-*lacZ* transcriptional fusion using strain SR7917

Cultures were grown in either LB medium adjusted to an A_{600} 0.05, followed by challenge with specific reagent as indicated, or in nitrogen-limiting minimal medium containing 3 mM ammonium chloride as the nitrogen source. Values correspond to an average of four independent samples after a 30–60-min shift.

Supplementation of growth medium that alter the transcription activity		
Sucrose (0.25 M)	1410 ± 110	*rpoE*P4
Glucose (0.5%)	219 ± 15	*rpoE*P3
25 mM Ammonium metavanadate	1540 ± 90	*rpoE*P2/P3
0.25 μg of Polymyxin B (A_{600} 0.05)	1503 ± 77	*rpoE*P3
0.25 μg of Polymyxin B (A_{600} 0.4)	410 ± 29	No induction
3 mM Ammonium chloride	575 ± 37	*rpoE*P2

tion of various genes (33) confirmed the above results. This analysis identified additional genes that either down-regulate or induce transcription of *rpoE*P-*lacZ*. Thus, a Δ*arcB* mutation led to an increase in transcription, whereas Δ*rpoS* and Δ*crp* caused a decrease in the activity (Tables 1 and 2). All such deletion derivatives carrying the *rpoE*P-*lacZ* fusion in SR7917 were used for measurement of the β-galactosidase activity revealing involvement of several regulatory pathways (Tables 1 and 2).

In a complementary approach, pools of plasmids with all ORFs of *E. coli* genome under control of the tightly regulated IPTG-inducible promoter (34) were introduced in SR4245 and SR7917 and screened for a Lac up or down phenotype in growth medium supplemented with 50 μM IPTG. This collection of cloned genes expresses only individual ORFs. Thus, one might miss genes whose products require the expression of whole operons or regulatory sRNAs. To overcome such limitations, a previously described complete genomic library in a medium-copy p15A vector (9, 35) was introduced to identify clones that exhibit a Lac up or down phenotype. These multicopy approaches identified *qseG* and several genes encoding lipoproteins (*csgG*, *pgaB*, *spr*, *yhdV*, *yceB*, *yddW*, and *yghB*), which, when overexpressed, increase the *rpoE*P-*lacZ* activity (Tables 1 and 2). Furthermore, DNA subcloning identified a novel sRNA located between *waaQ* and *waaA* ORFs, whose overexpression also induces the *rpoE*P-*lacZ* activity. Detailed analysis revealed that this sRNA is generated by the processing of 5′ UTR of the *waaQ* mRNA (see below). Additionally, overexpression of the *pcnB* gene encoding poly(A) polymerase I (PAP I) (36) also increases the *rpoE*P-*lacZ* activity (Tables 1 and 2). Among genes, whose induction repressed the *rpoE*P-*lacZ* activity, the *fliZ* gene was identified whose product could act as a negative regulator.

The quantification of the β-galactosidase activity of strains carrying the *rpoE*P-*lacZ* fusion under different growth conditions revealed that it is induced in the stationary growth phase, exposure to high osmolarity, limiting nitrogen conditions, upon challenge with either cationic antimicrobial peptide polymyxin B or ammonium metavanadate and repressed in glucose-supplemented medium (catabolite repression) (Tables 1 and 2). Ammonium metavanadate is a nonspecific phosphatase inhibitor (37) and hence can activate the expression of several two-component systems. The addition of ammonium metavanadate induces lipid A modifications (37, 38) and the PhoB/R-dependent incorporation of glucuronic acid (GlcUA) by WaaH in the inner core of LPS (39). Concerning the effect of polymyxin B, the *rpoE* transcriptional induction was observed when challenged at A_{600} of 0.05, but not when bacterial cultures were treated at or above an A_{600} of 0.4. Overall, these results revealed that transcription of the *rpoE* distal promoter region responds to diverse signals generated by defects in LPS, overproduction of certain lipoproteins, activators of RpoN and factors that influence the RpoS stability/activity. Such distinct signals could be sensed via multiple pathways. This could require recruitment of different σ factors, two-component systems, and hence potentially the presence of multiple promoters. As subsequent analysis indeed confirmed the presence of multiple promoters, multicopy libraries were once again introduced to identify genes whose overexpression modulates activity of specific *rpoE* promoters. Such additional approaches confirmed most of the above results and identified a specific mechanism of regulation of individual promoters recruiting different σ factors in each case (Tables 1 and 2).

Identification of 5′ Ends of the rpoE mRNA

Previous studies identified two promoters, out of them the initiation from the second promoter required $E\sigma^E$, whereas *in vitro* neither $E\sigma^{70}$ nor $E\sigma^E$ could initiate transcription of the upstream promoter (Fig. 1) (3, 16). Thus, the transcriptional initiation from the upstream promoter region was examined using 5′ rapid amplification of cDNA ends. In parallel, total RNA extracted from the strain overexpressing the *qseG* gene was also used for mapping of transcription initiation site(s). This overexpressing strain was chosen, because the *qseG* was identified as a multicopy inducer of the *rpoE* transcription. These analyses revealed the utilization of five major new transcriptional initiation sites designated P1 (−381), P2 (−327), P3 (−327/−326), P4 (−218), and P5 (−153) (Fig. 3*A*). The frequency of usage of the P2 promoter (−327) was significantly pronounced when RNA was extracted from the strain overexpressing the *qseG* gene. However, when RNA from the Δ*waaC* strain was used, both −327 and −326 initiation sites were identified in addition to the −218 site corresponding to the P4 promoter. Plasmids bearing the 5′ end of the P4 promoter were enriched when RNA was extracted from bacterial cultures harvested in the late stationary growth phase. Additional initiation sites located at −336, −321, and −319 were also identified (Fig. 3*A*). Of these, −321 and −319 could be secondary mRNA sites arising due to processing as the number of plasmid clones bearing these initiation sites was significantly reduced when mRNA was treated with calf intestinal phosphatase.

Examination of the DNA sequence upstream of the P2 TSS showed that it contains at −12 (GC) and −24 (GG) motifs characteristic of RpoN recognition sites (Fig. 3*A*) and a very good match was observed with the promoter region of the RpoN-regulated genes (Fig. 3*B*). Transcription initiation sites −327 or −326 also define the P3 promoter. It is likely that the −326 site is generated by the processing of mRNA, because the overlapping *rpoE*P3 initiation site corresponding to the −327-nt position contains a high degree of similarity to consensus −10 and −35 elements of housekeeping promoters and the extended −10 promoter. Of interest is the presence of conserved −7T and −11A nucleotide residues that are critical in the −10 promoter element (40). Examination of the DNA sequence upstream of the −327 site also revealed the presence of consensus regions for binding to CRP and RcsB activators for the P3 promoter (Fig. 3*A*). The initiation site corresponding to the *rpoE*P1 promoter located at nucleotide position −381 overlaps with the promoter region of the divergently transcribed *nadB* gene. The DNA sequence in the −10 and −35 regions upstream of the initiation site corresponding to the P4 promoter suggests consensus sequences that could be recognized by either $E\sigma^{70}$ or $E\sigma^S$. The frequency of plasmids containing the 5′ end of the P5 promoter was the lowest of all. Next, DNA sequences covering five individual promoters were cloned in promoter probe vectors and transferred in a single-copy on the chromosome for

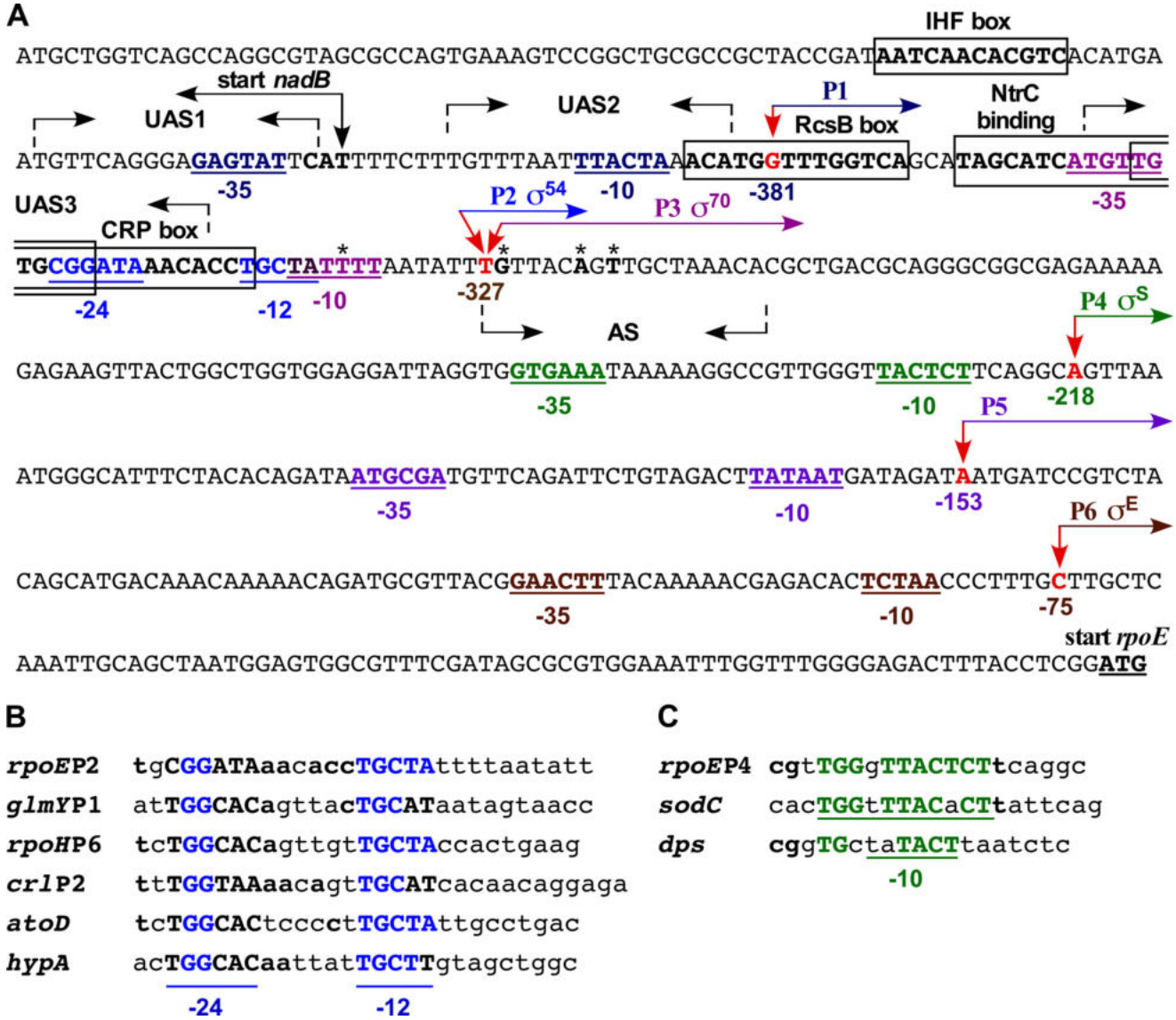

FIGURE 3. **Transcriptional regulation of different promoters of the *rpoE* gene.** *A,* nucleotide sequence of the promoter region of the *rpoE* gene. *Arrows* in *red* indicate the position of transcription start sites. The shared TSS at −327 is utilized by RpoN and RpoD. The P4 start site represents the initiation site recognized by RpoS. The −10 and −35 elements of the RpoD (*pink*) and RpoS recognized promoter (*green*) and −12 and −24 elements of RpoN (*blue*) are indicated. The P6 initiation site corresponds to the Eσ^E-regulated promoter. Nucleotides marked with *boxes* correspond to IHF, RcsB, NtrC, and CRP recognition sites. Three palindromic regions marked with *inverted arrows* correspond to UAS1, UAS2, and UAS3 representing QseF-binding sites required for the P2 promoter. Nucleotides marked with *asterisks* (*) correspond to putative processing sites. *B,* the alignment of −12 and −24 regions of the *rpoE*P2 promoter with well characterized RpoN-regulated promoters. *C,* the alignment of −10 and extended −10 elements of the *rpoE*P4 promoter with well known RpoS-regulated promoters.

further analyses (supplemental Table S1). Among these five promoters, *rpoE*P1 and *rpoE*P5 were not followed as no specific growth conditions/regulatory factors could be identified that alter their activity. Taken together, these data reveal the existence of multiple functional promoters that regulate transcription of the *rpoE* gene.

In Vitro Transcriptional Run-off Assays

Regulation of the P4 Promoter Is RpoS-dependent—As the 5′ rapid amplification of cDNA ends analysis revealed the existence of multiple transcriptional initiation sites that could utilize different σ factors, *in vitro* run-off assays were performed to validate these results/predictions. One template contained 45 bp downstream of the −218 transcription initiation site corresponding to the P4 promoter. Examination of its −10 and −35 regions suggests the similarity with promoters recognized by Eσ^{70} and Eσ^S. Thus, run-off assays were undertaken using the RNAP core supplemented with either σ^{70} or σ^S (Fig. 4*A*, *lanes 2* and *3*). Only Eσ^S was able to initiate transcription from the P4 promoter and gave the transcript size as expected of 45 nt (Fig. 4*A*). Supplementation of Eσ^{70} with RcsB did not result in any transcription initiation from this promoter (Fig. 4*A*, *lane 4*). The −10 and extended −10 regions of the P4 promoter indeed contain a high degree of similarity to the counterpart promoter regions of well known Eσ^S-transcribed genes like *dps* (Fig. 3*C*). Consistent with these *in vitro* experiments with the *rpoE*P4 promoter revealing Eσ^S-dependent transcriptional initiation, genetic data also support such results (see below) and allow us to conclude that this promoter is indeed regulated by RpoS.

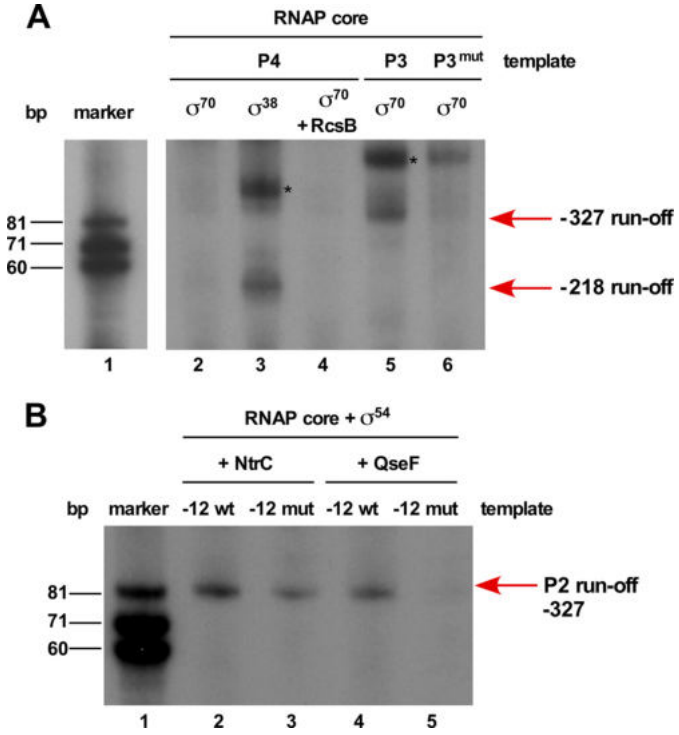

FIGURE 4. ***In vitro* transcription run-off assays showing selective recruitment of different promoters of the *rpoE* gene with various forms of RNA polymerase.** *A*, RpoS (σ^{38}) and RpoD complexed with the RNAP core initiate transcription from −218 TSS and TSS at −327, respectively. *Lane 1* corresponds to the size standard. For *lanes 2–4*, a DNA template of 105 bp was used. *Lane 2* shows the incubation reaction with Eσ^{70}, *lane 3* the incubation with Eσ^{38} resulting in the synthesis of expected 45-nt product marked with the *arrow*. *Lane 4* was incubated with Eσ^{70} in the presence of phosphorylated RcsB. *Lanes 5* and *6* show RNA transcripts synthesized from DNA template of 170 bp. An expected size of 85-nt RNA product was observed when Eσ^{70} was incubated with the wild-type DNA template (*lane 5*), whereas only a weak signal was visible when Eσ^{70} was used with template with mutation at −7T(C) and −11A(G) in the −10 element (*lane 6*). Bands marked with an *asterisk* (*) symbol in *lanes 3* and *5* indicate nonspecific end-to-end transcription reaction products. *B*, RpoN (σ^{54}) complexed with the core RNAP in the presence of either NtrC or QseF can initiate transcription from the *rpoE*P2 promoter using the −327 TSS. *Lane 1* corresponds to size standard, *lanes 2* and *4* corresponds to reactions with the wild-type DNA template in the presence of either NtrC or QseF. *Lanes 3* and *5* correspond to the RNA transcript produced with DNA template containing mutations at −12 (GC to AT) and −24 (GG to GA).

P2 and P3 Promoters are Regulated by RpoN and RpoD Using the Same Initiation Start Site—DNA sequence examination of the promoter region corresponding to the −327 TSS suggested that transcription initiation could be mediated by RNA polymerase containing either RpoN or housekeeping σ factor RpoD or subjected to a dual usage. Eσ^{N} cannot transcribe on its own, because it requires ATP-dependent activators like NtrC belonging to the AAA family (41). NtrC is known to act as an enhancer-like protein for many RpoN-regulated promoters (41, 42). A consensus matching the RpoN-regulated promoter is located in the −12 and −24 regions and a recognition site for NtrC is also present (Fig. 3). Thus, *in vitro* run-off assays with reconstituted RNA polymerase, containing RpoN and either NtrC or QseF (GlrR) as activators, were performed. The rationale for using QseF is based on our results that showed that the QseE/F two-component system positively regulates the *rpoE*P2 promoter in response to overexpression of the *qseG* gene (see below). QseF, like NtrC, belongs to the family of AAA activators and contains a response regulator domain (42) with a key conserved aspartate residue and an RpoN-interaction domain including the GAFTGA motif (amino acid residues 211 to 216).

Thus, for *in vitro* run-off experiments, DNA template covering the P2 promoter region and 85 bp downstream of the initiation site located at −327 was used. In multiround transcription assays, the expected size of the transcript was observed when RpoN was supplemented with either NtrC or QseF (Fig. 4*B*, *lanes 2* and *4*). To validate recognition of the P2 promoter by RpoN, specific mutations in the −12 (GC to AT) and −24 (GG to GA) RpoN recognition sites were introduced in the template for *in vitro* run-off assays. Transcription reaction with the RNAP core containing RpoN + QseF using such a mutated DNA template resulted in a significant inhibition in the initiation of transcription, as compared with the same reaction with the wild-type DNA template (Fig. 4*B*, *lane 5*). RpoN + NtrC also recognized such a mutated template less efficiently as compared with the wild-type, although the reduction is not as severe as observed with the RpoN + QseF reaction (Fig. 4*B*, *lane 3*). These results thus confirm that RpoN recognizes the *rpoE*P2 promoter and QseF acts as the main activator/enhancer.

The initiation site corresponding to the −327 TSS has also a good similarity for the −10 and −35 promoter elements recognized by RpoD (σ^{70}) (Fig. 3*A*). Accordingly, the wild-type DNA template used for *in vitro* run-off assay with RpoN also served as a template for reaction with Eσ^{70}. This assay showed that Eσ^{70} without any activator efficiently initiates transcription (Fig. 4*A*, *lane 5*). The size of transcript was similar to that obtained with RpoN. Thus, it is quite likely the −327-nt residue defines the initiation site for P2 (RpoN-regulated) and P3 (RpoD-regulated) promoters. As the −10 element corresponding to the P3 promoter contains conserved −7T- and −11A-nt residues, they were mutated to −7C and −11G, respectively. Next, such a mutated DNA template was used in *in vitro* run-off assays with the RNAP core and RpoD. Unlike the wild-type template, the mutated template could not be recognized efficiently by the RNAP core and RpoD to initiate transcription (Fig. 4*A*, *lane 6*). This mutated P3 promoter was cloned in the promoter probe vector pRS551 (pGK4838) and transferred in a single-copy to the chromosome (SR19089). *In vivo* such a fusion did not respond to signals that activate the *rpoE*P3 promoter and exhibited reduced activity (see below). Thus, we can conclude that RpoN and RpoD recognize P2 and P3 promoters, respectively, and they share the same initiation start site located at −327 nt upstream of the *rpoE* translational start site.

QseF (GlrR) Positively Regulates the RpoN-recognized P2 Promoter

To understand the mechanism of transcriptional regulation of various *rpoE* promoters, genes whose overexpression induces the *rpoE* transcription were sought using multicopy libraries. Subsequently, such an overexpression-induced transcription was analyzed for specificity toward individual promoters. One of the genes, whose overexpression specifically induced the *rpoE*P2 promoter activity, identified *yfhG* (*qseG*), whose product could mediate signal transduction. The *qseG* gene encodes an OM α-helical protein and has been characterized in enterohemeorrhagic *E. coli* (EHEC) and *Edwardsiella*

tarda (28, 43). The *qseG* gene is co-transcribed within the *qseE* (*glrK*) *qseF* (*glrR*) operon. The QseEFG system regulates key virulence factors and cross-talks with other regulatory systems, such as PhoP/Q and RcsB/C (28). QseG and its other operon members are involved in the formation of attaching pedestal and responding to phosphate and sulfate sources (28, 44). In *E. coli* K-12, the QseE/F two-component system positively regulates transcription of the *glmY* sRNA, located upstream of the *qseE* gene, in an RpoN-dependent manner and hence usage of Glr terminology in that study (42). The quantification of the β-galactosidase activity revealed approximately a 20-fold increase in the *rpoE*P2 promoter activity upon the overexpression of the *qseG* gene (Fig. 5*A*). This induction of the *rpoE*P2 promoter by QseG overproduction requires the QseF response regulator. This was shown by near abrogation of *rpoE*P2-*lacZ* induction upon *qseG* overexpression in a Δ*qseF* derivative (Fig. 5*A*).

As the *in vitro* run-off assay demonstrated that RpoN-dependent transcription from the P2 promoter requires QseF, this was also examined *in vivo*. Thus, the plasmid expressing the *qseG* gene was introduced in the isogenic strain carrying the mutated single-copy *rpoE*P2*-*lacZ* promoter fusion (−12 and −24 mutations). This *rpoE*P2*-*lacZ* derivative could not be induced upon *qseG* overexpression as compared with the wild-type (Fig. 5*A*). Hence, we can conclude that the RpoN-regulated *rpoE*P2 promoter can recruit QseF as an activator providing a link between RpoN and RpoE via a Qse two-component system.

QseF Binds to Upstream Elements of the rpoEP2 Promoter

The results presented in above sections established the presence of the active RpoN-dependent P2 promoter that recruits QseF as the activator. To further confirm the role of QseF in recognition of the *rpoE*P2 promoter, binding of purified QseF was analyzed by electrophoretic mobility shift assays (EMSAs). Two DNA fragments of 529 and 265 bp, containing 329 and 65 bp, respectively, upstream of the transcriptional start site for the P2 promoter, were used in EMSAs. Up to now, the only known promoter regulated by RpoN together with QseF is that of the *glmY* gene in *E. coli* K-12 (42). It was proposed, based on the alignment of the *glmY* promoter region, that the QseF-binding site located upstream of about 100 bp (up to three sites) contains a conserved palindromic sequence of $TGTCN_{10}GACA$. Examination of the DNA sequence revealed the presence of three such sequence elements upstream of the P2 TSS with a similar palindromic sequence and similar distance between two half-sites. These sequence elements are designated UAS1, UAS2, and UAS3 (upstream activator sequence) (Fig. 3*A*). The UAS1 is located −100 nt upstream of the P2 TSS. A similar palindromic sequence is also present immediately downstream of the P2 TSS (Fig. 3*A*). A DNA fragment of 529 bp contains all three UAS elements, whereas the 265-bp fragment contains only UAS3. These DNA fragments were incubated with increasing concentrations of QseF and their complexes analyzed by a native polyacrylamide gel electrophoresis. As shown in Fig. 5*B*, the longer DNA fragment containing UAS1 to UAS3 was shifted much more efficiently as compared with the shorter fragment containing only UAS3. Thus, we can conclude

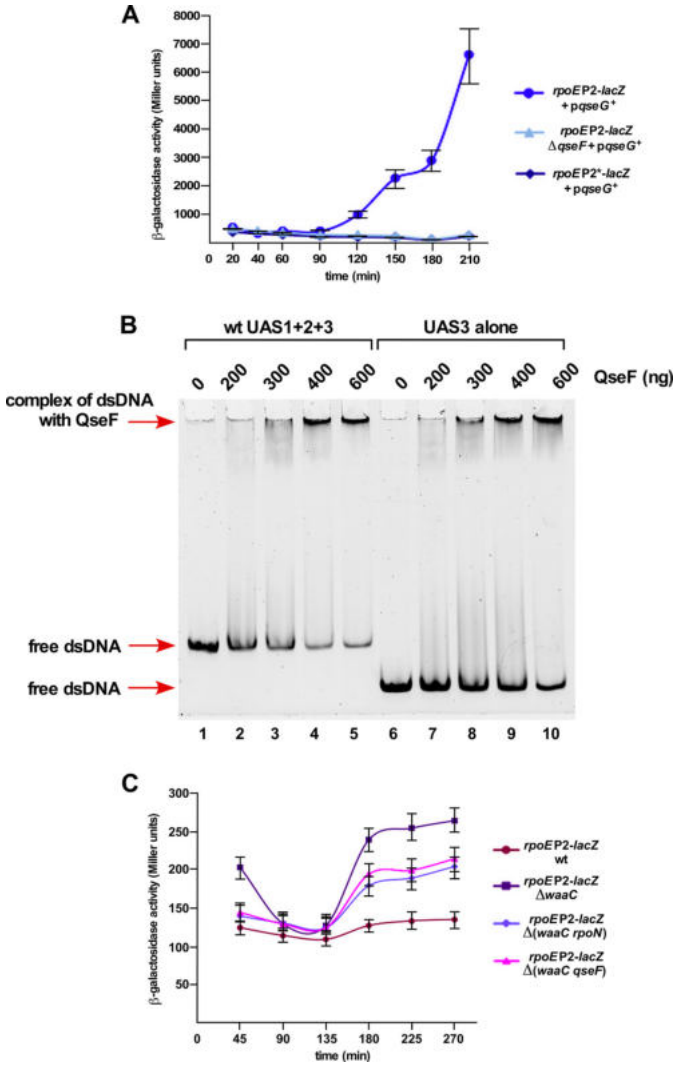

FIGURE 5. **The positive regulation of the *rpoE*P2 promoter by the QseF activator.** *A*, four independent cultures of wild-type and its Δ*qseF* derivative carrying either the wild-type *rpoE*P2 promoter fusion or with *rpoE*P2* promoter fusion with mutations in the −12 and −24 regions expressing the cloned *qseG* gene were analyzed for β-galactosidase activity after different growth intervals in the presence of 50 μM IPTG. *B*, the QseF-DNA interaction at the P2 promoter. Thirty-five ng of the wild-type DNA fragment covering QseF binding sites UAS1 + 2+3 (*lanes 2–5*) were incubated with increasing concentrations of QseF and analyzed by EMSA. A DNA probe containing only UAS3 was also incubated with QseF as indicated. *Lanes 1* and *6* serve as a control with DNA alone. Samples were analyzed as described under "Experimental Procedures." *C*, the RpoN-regulated *rpoE*P2 promoter also senses LPS defects. Isogenic cultures of SR19089 and its Δ*waaC*, Δ(*waaC rpoN*), and Δ(*waaC qseF*) were analyzed for β-galactosidase activity after different growth intervals and averages of four independent derivatives are plotted.

that QseF binds DNA located upstream of the *rpoE*P2 TSS and based on *in vitro* assays acts as an activator for RpoN-dependent *rpoE*P2 transcription.

Modulators of RpoS Regulate the rpoEP4 Promoter

To identify signals and regulators of individual promoters, various mutations in different genes that caused activation of the *rpoE* transcription (Tables 1 and 2) were introduced into strain SR18874 carrying the *rpoE*P4-*lacZ* fusion. Thus, a Δ*rpoS* mutation resulted in ~60% reduction as compared with the wild-type (Fig. 6). Furthermore, introduction of the Δ*rssB* caused more than 35% increase in the *rpoE*P4 promoter activity

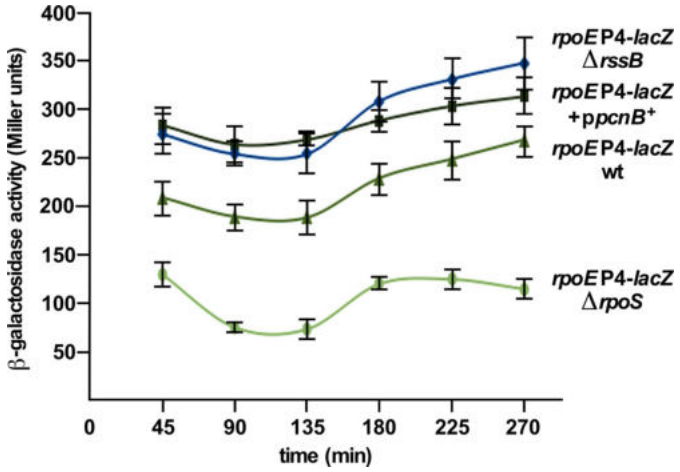

FIGURE 6. **The *rpoE*P4 promoter is regulated positively by RpoS and responds to its modulators.** Cultures of SR18874 carrying the *rpoE*P4 promoter fusion, its Δ*rpoS* or Δ*rssB* derivatives, and derivative carrying the cloned *pcnB* gene were grown in LB medium at 30 °C either in the presence of 50 μM IPTG for strain with plasmid or without IPTG for plasmid-free derivatives. Samples from four independent cultures at different growth intervals in each case were analyzed for the β-galactosidase activity.

consistent with the isolation of Tn*10* mutations in the *rssB* gene (Fig. 6). RssB acts as an adapter protein in the pathway of the ClpXP-dependent proteolysis of RpoS and hence *rssB* mutants exhibit elevated RpoS levels (45, 46). Thus, the isolation of Tn*10* mutations in the *rssB* gene that increase *rpoE*P4 promoter activity and the reduction of P4 activity in Δ*rpoS* is overall consistent with results from *in vitro* run-off assays establishing that this promoter is uniquely transcribed by $E\sigma^S$.

Among various growth conditions that were identified to induce the *rpoE* transcription, the exposure to increased osmolarity (addition of 0.25 M sucrose or 0.5 M NaCl) also caused a 2–3-fold induction in *rpoE*P4 promoter activity (Tables 1 and 2). An increase in osmolarity increases RprA-dependent RpoS translation (47). Thus, *in vivo* the P4 promoter behaves in a typical RpoS-dependent manner.

Next, cloned genes, whose overexpression altered the *rpoE* transcription, were introduced in SR18874. Among these, overexpression of the *pcnB* gene caused an ~40% increase in the *rpoE*P4 activity (Fig. 6). However, a mild induction of the *fliZ* gene repressed the P4 promoter activity by 40% (Tables 1 and 2). The *pcnB* gene encodes PAP I and in its absence the RssB-dependent proteolysis of RpoS is enhanced (36). The negative effect on the activity of the *rpoE*P4 promoter upon *fliZ* overexpression can be rationalized, because FliZ behaves as a repressor of RpoS by acting as its antagonist due to overlapping DNA-binding properties (48). Thus, overall these results support our conclusions that the *rpoE*P4 promoter is regulated by RpoS and conditions that either stabilize RpoS (PAP I) or destabilize it (RssB) alter the activity of the *rpoE*P4 promoter in accordance with its positive regulation by RpoS.

Defects in Early Steps of the LPS Core Biosynthesis Induce the rpoEP3 Transcription

As the majority of *trans*-acting Tn*10* mutations that increased the *rpoE*P-*lacZ* activity mapped to the *waaC* gene and some other genes in the *waa* locus (supplemental Table S1) suggested that defects in LPS activate the *rpoE* transcription from distally located promoter(s). The second largest number of Tn*10* insertion mutations were mapped to the *waaF* gene. The *waaC* gene encodes heptosyltransferase I transferring L-*glycero*-α-D-*manno*-heptopyranose (Hep) to Kdo. The second Hep transfer to the HepI requires heptosyltransferase II WaaF (1, 2). To avoid any effect of polarity, non-polar deletion derivatives of various *waa* genes were constructed and transduced into strains carrying the *lacZ* fusion to the P2, P3, and P4 promoter to identify which of these promoters is specifically induced when LPS synthesis is defective. Such isogenic strains were used to measure the β-galactosidase activity and also verified for their LPS composition.

As the P2 and P3 promoter use the same TSS, two different promoter fusions were constructed in a single-copy to distinguish between modes of activation of these promoters. One such construct SR18987 contains mutations in RpoN recognition sites for the P2 promoter in −12 and −24 regions, but with intact −10 and −35 elements for the P3 promoter recognized by RpoD. Another strain, SR19089, carries the mutation in the −10 element of the RpoD-regulated P3 promoter with mutated −7- and −11-nt residues. Thus, SR18987 reflects mainly the activity of the P3 promoter, whereas the promoter fusion in SR19089 shows the RpoN-dependent P2 promoter activity. Into these strains, different null alleles of various *waa* genes were introduced and quantified for the promoter-specific transcriptional activity. Such an analysis revealed up to a 7-fold increase in the *rpoE*P3-*lacZ* promoter activity with Δ*waaC* as compared with its basal activity in the wild-type (Fig. 7*A*). However, the Δ*waaC* derivative of *rpoE*P2-*lacZ* fusion exhibited only 70% to a 2-fold increase upon entry into the stationary phase (Fig. 5*C*). No induction of the RpoS-regulated P4 promoter was observed when the Δ*waaC* mutation was introduced. Next, impact of the individual non-polar deletion of other genes within the *waa* locus on the *rpoE*P3-*lacZ* activity was addressed. A Δ*waaF* derivative exhibited a nearly 2–3-fold increase in the *rpoE*P3-*lacZ* activity (Fig. 7*A*). Similarly, Δ*waaG*, Δ*waaP*, and Δ*waaO* mutants exhibited a more than 2-fold increase in the *rpoE*P3 promoter activity (Fig. 7*A*). WaaG glycosyltransferase mediates the incorporation of GlcI, whereas WaaP is required for the phosphorylation of HepI (49, 50). Induction of the P3 promoter in Δ*waaG* and Δ*waaP* reflects the importance of phosphorylation in OM integrity (50). Deletion derivatives of *waaQ*, *waaS*, *waaY*, and *waaZ* did not result in any major induction of the *rpoE*P3 promoter or other *rpoE* promoters (data not shown). The above results allow us to conclude that severe LPS defects in the most conserved part of the inner core and the lack of GlcI induce the activity of the RpoD-dependent P3 promoter.

waaC and waaF Mutants Incorporate P-EtN on the Second Kdo Rather Than in the Lipid A

To validate the authenticity of different *waa* mutants and impact on LPS modifications, LPS was obtained from isogenic strains grown under conditions that induce lipid A and inner core modifications (6, 19, 39). As LPS defects due to mutations like Δ*waaC* and Δ*waaF* caused a significant induction of the *rpoE* transcription, this should be reflected in the modification

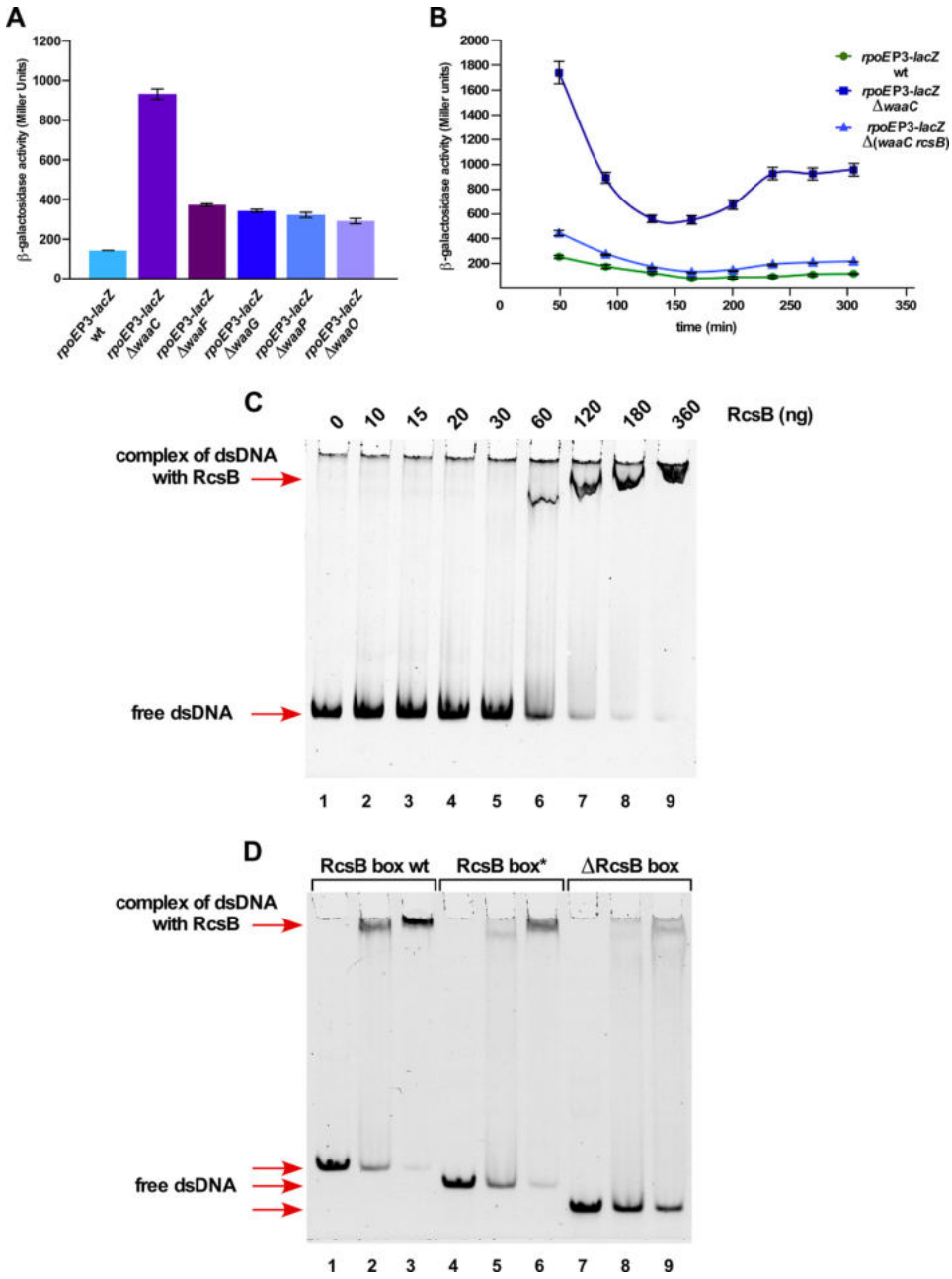

FIGURE 7. **The Eσ^{70}-recognized *rpoE*P3 promoter is positively regulated by the Rcs two-component system in response to LPS defects in an RcsB-dependent manner.** *A,* cultures of SR18987 carrying the *rpoE*P3 promoter fusion and its derivatives with non-polar deletion in various *waa* genes were grown in LB medium at 30 °C and analyzed for β-galactosidase activity after different intervals. Four independent derivatives in each case were analyzed and averaged data are presented after a 250-min incubation. *B,* cultures of SR18987, its Δ*waaC* and Δ(*waaC rcsB*) derivatives were grown in LB medium at 30 °C and analyzed for β-galactosidase activity after different intervals of growth. Averages from four cultures in each case are plotted. *C,* the RcsB-DNA interaction at the P3 promoter. Thirty-five ng of a 280-bp wild-type DNA fragment that includes a putative RcsB recognition site was incubated with increasing concentrations of phosphorylated RcsB and analyzed by EMSA on a 4% native gel. *D,* specificity of RcsB-DNA interaction at the P3 promoter. Three DNA probes included a 81-bp DNA fragment with the wild-type RcsB sequence (*lanes 2* and *3*), a second 78-bp DNA fragment lacking conserved CAT trinucleotide residues of RcsB consensus (*lanes 5* and *6*), and a third 71-bp probe lacking nucleotides CATGGTTTGG of RcsB consensus (*lanes 8* and *9*) were incubated with 120 and 180 ng of RcsB for each probe, respectively. *Lanes 1*, *4,* and *7* serve as control with DNA alone. After incubation the reaction mixtures were analyzed on a 6% native gel.

of Kdo by the EptB-dependent incorporation of the P-EtN residue. Mass spectrometric analysis of LPS of the Δ*waaC* strain revealed the mass peak at 2,237.3 Da (Fig. 8*A*). This is in agreement with the predicted composition of the Kdo_2-lipid A_{hexa} 1,4′-bisphosphate. The spectra of LPS obtained from a Δ*waaF* derivative contains the mass peak at 2,429.4 Da reflecting the incorporation of one heptose with a predicted composition of Kdo_2-lipid A_{hexa} + Hep_1 (Fig. 8*B*). Additional mass peaks in the spectra of Δ*waaC* at 2,360.3 and 2,491.4 Da correspond to the addition of P-EtN and an additional 4-amino-4-deoxy-L-arabinose (L-Ara4N) residue, respectively (Fig. 8). Similarly, mass peaks at 2,560.5 and 2,683.5 Da present in the spectra of LPS of Δ*waaF* can be explained to arise due to the incorporation of L-Ara4N and an additional P-EtN residue, respectively (Fig. 8). The mass spectrometric analysis of LPS obtained from the Δ*waaG* strain revealed mass peaks at 2,621.5 and 2,824.4 Da.

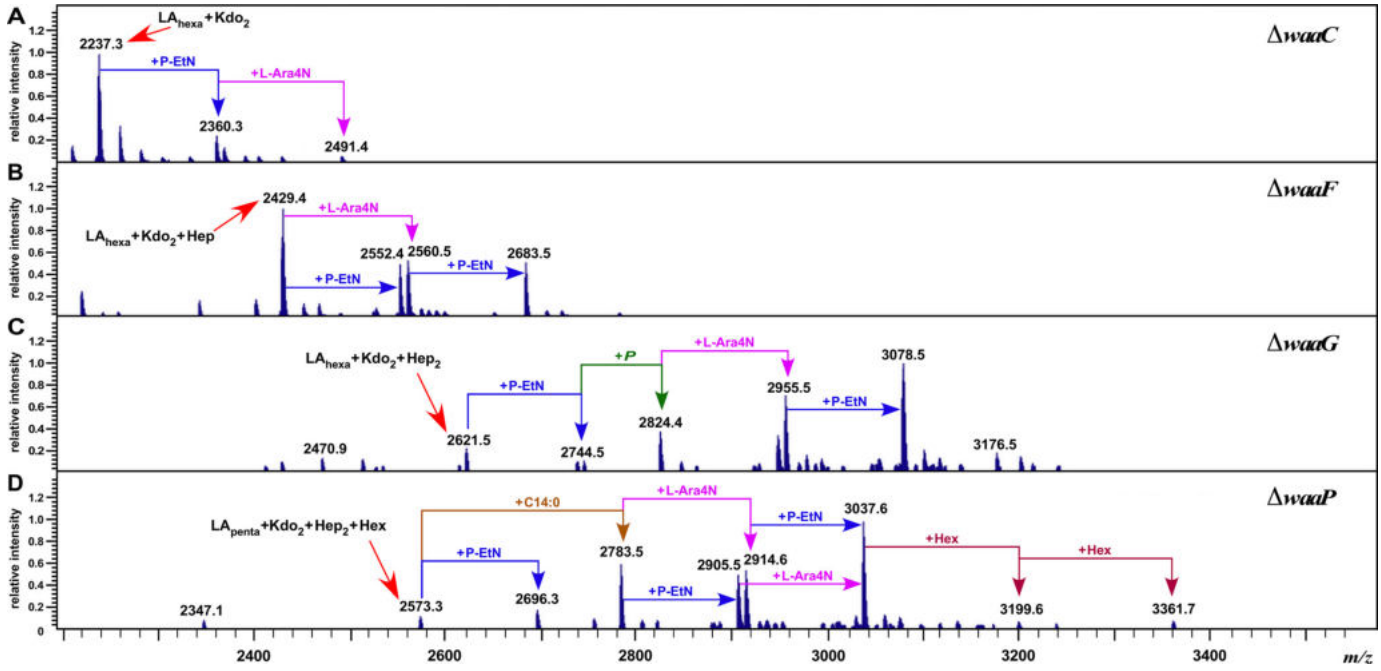

FIGURE 8. **The LPS composition of derivatives with specific mutations causing LPS truncation leading to the induction of the *rpoE*P3 transcription.** Charge deconvoluted ES FT-ICR mass spectra in the negative ion mode of native LPS obtained from isogenic deletion derivatives of the wild-type strain carrying the Δ*waaC* mutation (*A*), Δ*waaF* (*B*), Δ*waaG* (*C*), and Δ*waaP* (*D*) grown in phosphate-limiting medium at 30 °C. Mass numbers refer to monoisotopic peaks. The mass peaks corresponding to additional substitutions with P-EtN and/or L-Ara4N are indicated.

These mass peaks correspond to the predicted structure composed of LA_{hexa} + Kdo_2 + Hep_2 and LA_{hexa} + Kdo_2 + Hep_2 + *P* + *P-EtN*$_1$, respectively (Fig. 8*C*), similar to previously described structural analysis of LPS from the *waaG* mutant in the *E. coli* strain with the R1 core type (49) reflecting partial phosphorylation of HepI. Additional mass peaks at 3,078.5 Da can be attributed to the mass composition of LA_{hexa} + Kdo_2 + Hep_2 + *P* + *P-EtN*$_2$ + L-Ara4N$_1$. The mass spectrometric analysis of LPS of a Δ*waaP* derivative revealed the presence of pentaacylated (LA_{penta} + Kdo_2 + Hep_2 + Hex, the mass peak at 2,573.3 Da) and derivatives of hexaacylated species (2,783.5 and 3,037.6 Da). These mass peaks can be explained to be composed of LA_{hexa} + Kdo_2 + Hep_2 + Hex_1 and LA_{hexa} + Kdo_2 + Hep_2 + Hex_1 + *P-EtN*$_1$ + L-Ara4N$_1$, respectively. Further mass peaks at 3,199.6 and 3,361.7 Da correspond to the addition of one and two Hex residues, respectively (Fig. 8*D*). No mass peaks corresponding to phosphorylated derivatives of Hep residues are present, consistent with the lack of WaaP kinase due to the Δ*waaP* mutation. The presence of two P-EtN residues reveals modification of Kdo as well as lipid A by P-EtN in Δ*waaP*.

The analysis of lipid A revealed the incorporation of L-Ara4N represented by the mass peak at 1,928.3 Da in the spectra of all mutants (Fig. 9). In *E. coli* K-12, the most preferred position of L-Ara4N in lipid A is at the 4′-phosphate (51). Interestingly, Δ*waaC* and Δ*waaF* derivatives did not reveal any P-EtN incorporation in the lipid A part. Thus, the mass peak at 2,360.3 Da in Δ*waaC* and at 2,552.4 Da in Δ*waaF* corresponding to the incorporation of P-EtN is predicted to have P-EtN on the Kdo, which is EptB-dependent (Fig. 8, *A* and *B*). These results are consistent with previous detailed fragmentation analysis of LPS obtained from various derivatives of *waaC* mutants (6). The EptB-dependent P-EtN modification of Kdo in Δ*waaC*, Δ*waaF*, and Δ*waaP* derivatives is consistent with the activation of the *rpoE* transcription due to LPS defects and the RpoE-dependent regulation of the *eptB* gene. These structural alterations of LPS upon the hyper-induction of the *rpoE* transcription in Δ*waaC* and Δ*waaF* derivatives indicate the preferential modification of Kdo by P-EtN at the expense of its incorporation in the lipid A part.

The Transcriptional Induction of the rpoE Gene Due to LPS Defects Requires Qse and Rcs Two-component Systems

Results presented above established that defects in LPS biosynthesis induce transcription of *rpoE*P2/P3 promoters. To address the molecular mechanism of the activation of the *rpoE* transcription when LPS is defective, panels of double deletion strains lacking various regulators in the Δ*waaC* background were analyzed. Among these, the Δ(*waaC rpoN*) derivative showed ~40–45% reduction in the *rpoE*P2-*lacZ* activity as compared with the isogenic Δ*waaC* mutant (Fig. 5*C*). These results of RpoN dependence could require recruitment of the QseF activator based on the *in vitro* run-off assays. Consistent with these data, activation of the *rpoE*P2-*lacZ* fusion in a Δ(*waaC qseF*) derivative was reduced by more than 30% as compared with the parental Δ*waaC* strain (Fig. 5*C*).

Severe defects in LPS are known to induce the Rcs two-component system leading to overproduction of colanic acid (7). In the Rcs two-component system, RcsB acts as the major response regulator (8). Thus, a Δ*rcsB* mutation was transduced into Δ*waaC* derivatives carrying *rpoE*P3-*lacZ* fusion. Strikingly, activation of *rpoE*P3-*lacZ* fusion in a Δ(*waaC rcsB*) derivative is nearly abrogated as compared with highly elevated levels of the *rpoE*P3-*lacZ* activity in Δ*waaC* (Fig. 7*B*). These data suggest that Rcs and Qse systems regulate the *rpoE* transcrip-

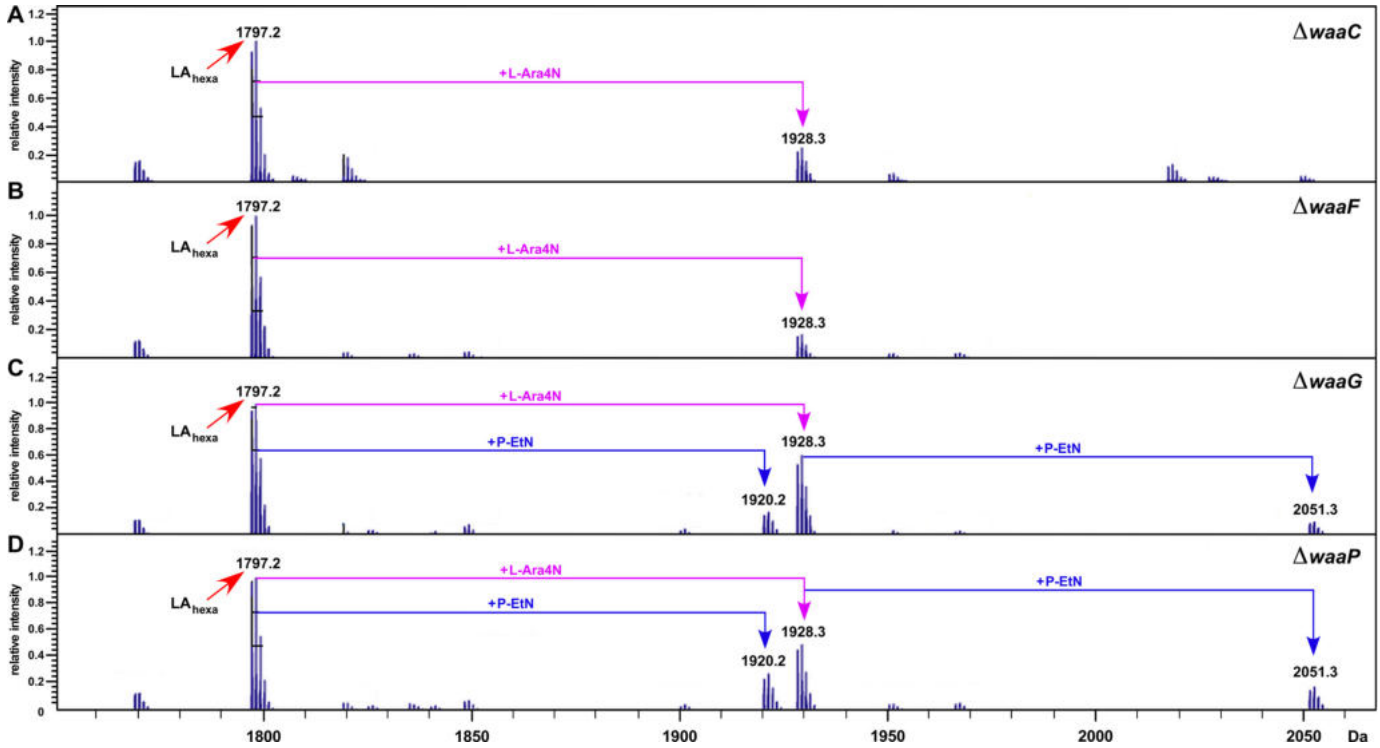

FIGURE 9. **Defects in the lipid A biogenesis of Δ*waa* mutants exhibiting increased *rpoE*P3 transcriptional activity.** Charge deconvoluted ESI FT-ICR mass spectra of isogenic Δ*waaC* (*A*), Δ*waaF* (*B*), Δ*waaG* (*C*), and Δ*waaP* (*D*) in the negative ion mode depicting the lipid A composition and its modifications from the LPS obtained from cultures grown in phosphate-limiting medium at 30 °C. Part of the negative ion mass spectra of the native LPS after unspecific fragmentation, leading to the cleavage of the labile lipid A-Kdo linkage, is presented. The mass peaks corresponding to the hexaacylated lipid A part and substitutions with P-EtN and/or L-Ara4N are indicated.

tion in response to LPS defects with the Rcs system playing the major role.

In Vitro RcsB Binds in the P3 Promoter Region

To establish the role of RcsB in regulation of the *rpoE*P3 promoter, the ability of RcsB to bind DNA containing the region upstream of this promoter was tested by EMSA. A 280-bp DNA fragment was incubated with increasing concentrations of RcsB. Indeed, such a DNA fragment could efficiently shift in the presence of RcsB (Fig. 7*C*). Examination of DNA sequence upstream of the P3 promoter revealed that it contains a DNA sequence element with similarity to the RcsB box proximal to the −35 region of the P3 promoter (Fig. 3*A*). The specificity of RcsB binding to the RcsB box was examined using a smaller 81-bp DNA fragment with the intact RcsB box, a 78-bp fragment lacking three conserved nucleotides marked as asterisks and a 71-bp fragment lacking RcsB box. The 78-bp fragment with a deletion of 3 bp was shifted much less efficiently and this mobility shift was further reduced with the 71-bp lacking the conserved RcsB box (Fig. 7*D*). Thus, these results of RcsB binding upstream of the P3 promoter region support *in vivo* results of involvement of the Rcs two-component system in regulating the *rpoE* transcription from its P3 promoter.

Defects in the LPS Assembly Also Induce the rpoEP3 Promoter

Previously, we showed that the balanced biosynthesis of LPS requires the essential LapB protein and in its absence transcription of the *rpoE* gene is significantly induced (9). Δ*lapB* mutants synthesize excess LPS with a significant proportion of LPS comprised of precursor forms and also have a dysfunctional Lpt translocation system (9). Thus, Δ*lapB* derivatives were constructed under permissive growth conditions in strains carrying *rpoE*P1-P5-*lacZ* and *rpoE*P3-*lacZ* (with mutated RpoN recognition site) fusions in the wild-type background and Δ*rcsB*. The Δ(*lapA lapB*) derivative exhibited more than a 5-fold increase in the *rpoE*P1-P5-*lacZ* activity and a 3-fold induction of the *rpoE*P3-*lacZ* activity when the Rcs system is intact (Fig. 10, *A* and *B*). However, this activation in the absence of Lap proteins was significantly diminished in strains lacking RcsB (Fig. 10*A*). Thus, these results demonstrate that transcriptional activation of the *rpoE* gene caused by severe defects in the LPS synthesis is driven from the *rpoE*P3 promoter and this signal activation requires the RcsB response regulator.

Multicopy Inducers of the rpoEP3 Promoter Identify a Novel RfaH-interacting sRNA RirA

One of the approaches, using a multicopy plasmid library, led to the identification of a novel sRNA, whose overexpression induced the *rpoE*P1-P5-*lacZ* activity. Subcloning identified a minimal clone carrying DNA overlapping the 5′ UTR of the *waaQ* mRNA. Further analysis revealed ~2-fold induction of the *rpoE*P3 promoter when this sRNA was expressed in a medium-copy plasmid from its own promoter (Fig. 11*B*). Mapping of the 5′ and 3′ ends revealed that this sRNA shares its 5′ end with the known 5′ end of the *waaQ* mRNA and is a 73-nt sRNA (Fig. 11, *A* and *C*). This sRNA could arise due to processing of the 5′ end of the *waaQ* mRNA. Examination of its nucleotide sequence revealed that it contains the conserved JUMPstart

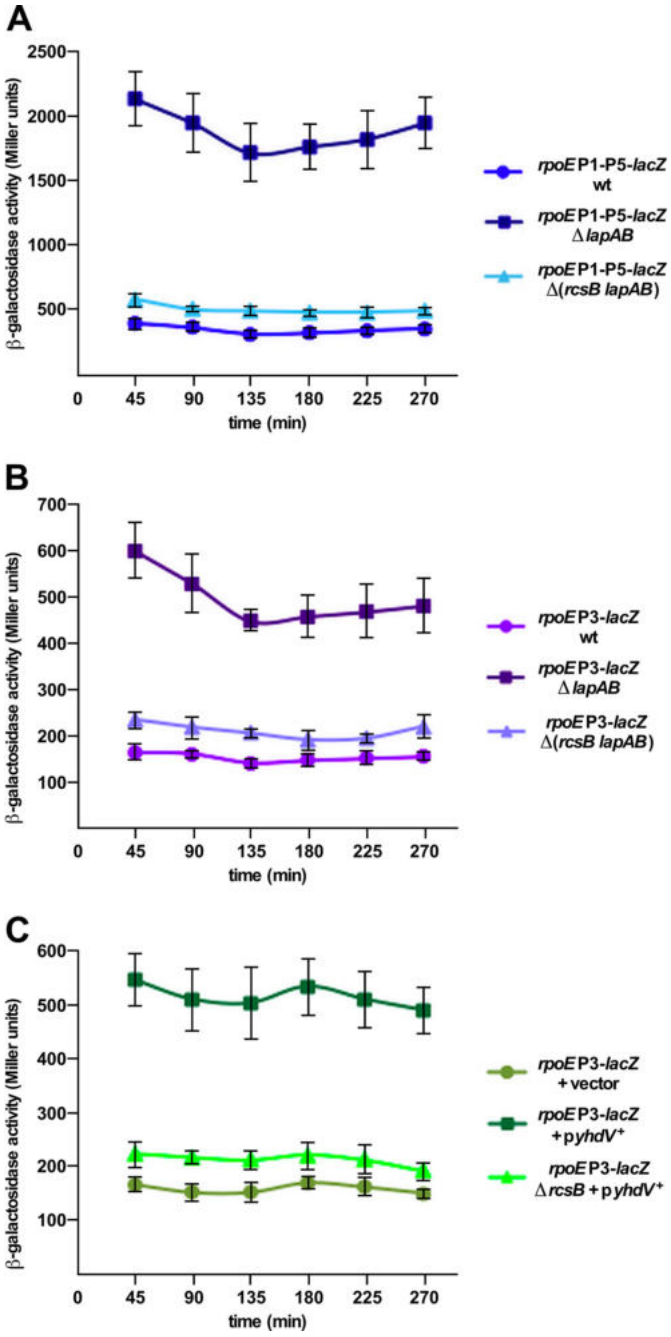

FIGURE 10. **The absence of LapAB proteins or overexpression of lipoprotein encoded by the *yhdV* gene induces the *rpoE*P3 transcription.** *A,* overnight cultures of SR7917 (carrying chromosomal *rpoE*P1-P5-*lacZ* fusion), its Δ(*lapA lapB*) and Δ(*rcsB lapA lapB*) derivatives, and *B,* SR18987 (*rpoE*P3-*lacZ*), its isogenic Δ(*lapA lapB*) and Δ(*rcsB lapA lapB*) derivatives, were grown in M9 medium at 30 °C and analyzed for β-galactosidase activity after different intervals. Data averaged from four independent samples are presented for *panels A* and *B*. *C,* cultures of SR18987 carrying *rpoE*P3-*lacZ* fusion with empty vector, its derivative with the cloned *yhdV* gene, and its Δ*rcsB* derivative with the *yhdV* gene on the plasmid were analyzed for β-galactosidase activity after the addition of 50 μM IPTG. Data from four replicates are plotted.

and the *ops* site (GGCGGTAG) located between nt 40 and 60 recognized by the RfaH transcriptional factor (Fig. 11*A*). Based on biochemical evidence and the observed interaction with RfaH, this sRNA is designated RirA (RfaH interacting RNA). The −10 promoter region of the *rirA* gene contains similarity to RpoD-recognized promoters (Fig. 11*A*). It also contains TGA nucleotides next to the −10 element resembling the extended −10 promoter.

RfaH is an operon-specific transcription factor belonging to the NusG family of proteins (25). RfaH is known to regulate the expression of genes transcribed as long operons encoding the LPS core, capsule, *O*-antigen biosynthesis, hemolysin, and conjugation system (23–25). RfaH functions by binding to the *ops* site located in the 5′ region of non-template DNA of these operons and prevents premature transcriptional termination by Rho. This is achieved by RfaH simultaneous contacts with RNA polymerase and coupling with translating ribosome by interaction with the S10 protein (25). We wondered if the *rirA* mRNA would bind RfaH. This was addressed by EMSA wherein RfaH was incubated with RirA alone and in the presence of the RNAP core. RfaH could efficiently gel shift RirA in the presence of RNAP, but not when incubated with RfaH alone (Fig. 12*A*). As RirA contains the conserved *ops* site, we tested if the interaction between RirA and RfaH requires the core *ops* element. Hence, gel shift assays were performed using synthetic wild-type RirA or RirA* with mutated *ops* site RNAs. EMSA experiments revealed that RirA with the mutated *ops* site does not bind RfaH (Fig. 12*B*). Thus, we can conclude that RirA indeed interacts with RfaH in the presence of RNA polymerase. Furthermore, this interaction is dependent on the presence of the *ops* site within RirA.

Because overexpression of the *rirA* gene induces the *rpoE*P3 activity, a Δ*rfaH* mutant was also tested for influence on the *rpoH*P3 activity. A 4-fold induction of *rpoE*P3 promoter activity was observed (Fig. 11*B*). These results are consistent with isolation of a *rfaH*::Tn*10* mutation conferring an increase in the *rpoE* transcriptional activity (supplemental Table S1). To address the basis of induction of the *rpoE*P3 by RirA, the effect of the *rirA* overexpression on the LPS content was examined. Whole cell lysates were prepared from isogenic strains with and without overexpression of RirA. The overexpression of RirA caused a reduction in the total amount of LPS (Fig. 12*C*). As the conserved *ops* site is also located in front of the *O*-antigen gene cluster, the wild-type *E. coli* K-12 strain BW25113 was transformed with plasmid pMF19 (expressing the *wbbL* gene (52)) to restore *O*-antigen biosynthesis. Next, this strain was transformed with the compatible vector alone or its derivative carrying the *rirA* gene and examined for the LPS profile. A quite robust reduction in the *O*-antigen was observed, when the *rirA* gene is present on the plasmid (Fig. 12*D*). It should be noted that the cloned *rirA* gene was expressed from its own promoter. These results suggest that RirA in excess could cause titration of RfaH and limit its availability to bind *in vivo ops* sites. This could lead to decreased expression of LPS core biosynthetic genes transcribed from the *waaQ* operon and other operons with the *ops* site in the 5′ UTR like *O*-antigen biosynthetic genes. Defects in the *O*-antigen presence upon the *rirA* overexpression can be due to an additive effect of reduction in the *rfb* operon expression and reduced number of sites for *O*-antigen incorporation.

To further understand the molecular basis of reduction of LPS upon RirA overexpression, the expression of RfaH-regulated *waaQ* and *rfb* operons was monitored. Western blot anal-

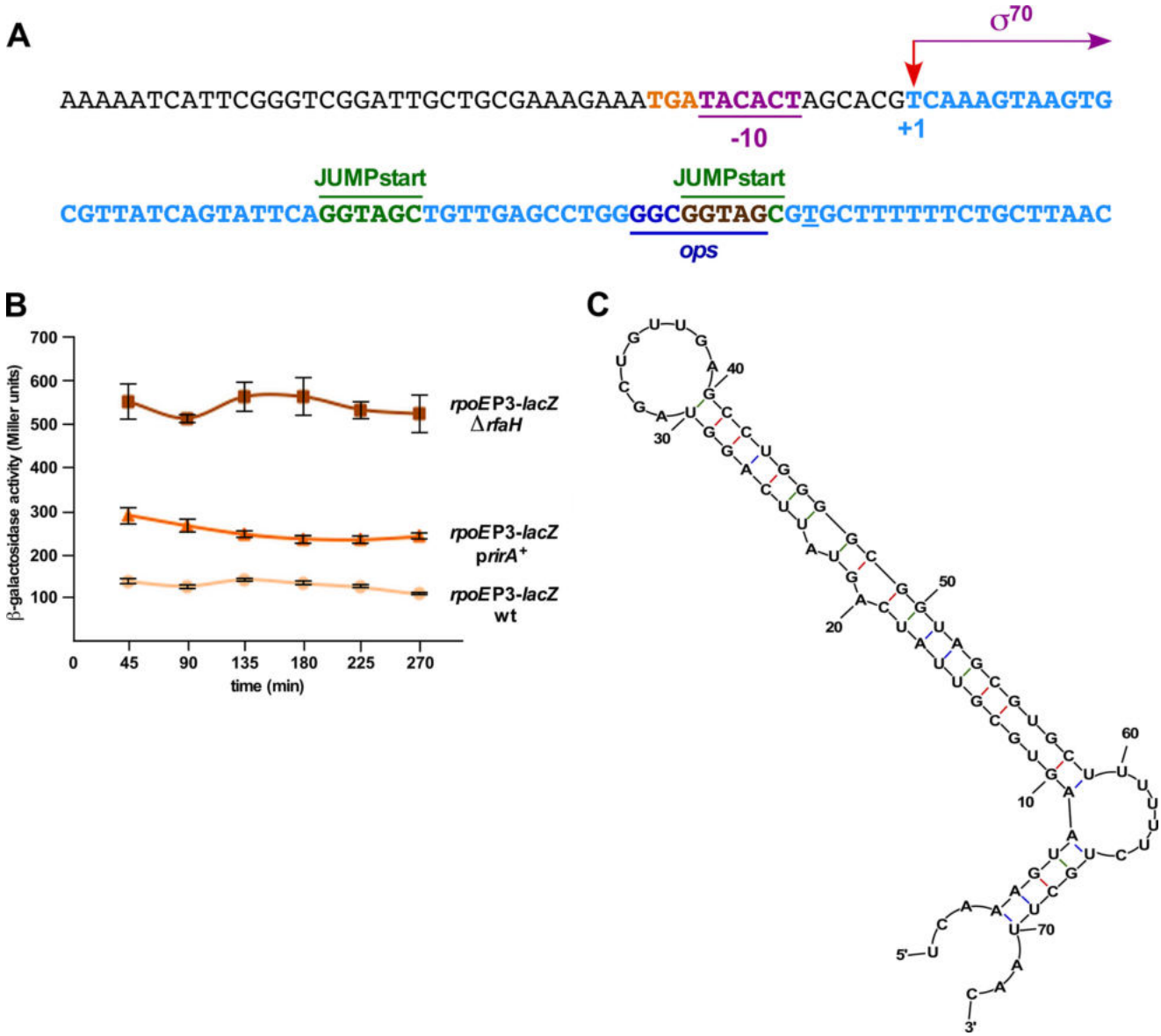

FIGURE 11. **A novel sRNA *rirA* in multicopy induces the *rpoE* transcriptional activity and controls LPS biosynthesis.** *A,* nucleotide sequence of the gene encoding the *rirA* sRNA and its promoter region. The *arrow* indicates the TSS of the *rirA* sRNA. The −10 and extended −10 promoter elements, the conserved JUMPstart, and *ops* sites are depicted. *B,* either overexpression of the *rirA* gene or the absence of RfaH induces the *rpoE*P3 promoter activity. Cultures of SR18987 with the vector pRS551, its Δ*rfaH* derivative, or when the *rirA* gene is expressed from its own promoter in pRS551 were grown in LB medium at 30 °C and analyzed for the β-galactosidase activity after different growth intervals. Average of four independent samples are presented. *C,* model of RirA generated using M-fold.

ysis revealed that the WaaO-FLAG and RfbB-FLAG amounts are reduced, whereas as a control WaaC-FLAG levels were unaltered (Fig. 12*E*). The *waaO* gene is transcribed as a part of the *waaQ* operon and the *rfbB* gene also contains the *ops* site in the 5′ UTR. The *waaC* gene is transcribed as a part of the *gmhD waaF waaC* operon lacking the *ops* site. Taken together, these results establish that RirA sRNA acts as a novel sRNA that interacts with RfaH and its excess reduces LPS amounts by the potential sequestration model that limits the availability of RfaH.

The overexpression of Genes Encoding Lipoproteins Induces the rpoEP3 Promoter

The most prominent class of multicopy inducers of the *rpoE*P1-P5 transcription identified genes encoding lipoproteins (Tables 1 and 2). From these, impact of overexpression of the *yhdV* gene was analyzed, because it was repeatedly isolated as inducer of the *rpoE*P1-P5-*lacZ* or specifically the *rpoE*P3-*lacZ* transcriptional activity. Measurement of the *rpoE*P3-*lacZ* activity revealed a nearly 3.4-fold increase (Fig. 10*C*). Most of the genes encoding lipoproteins identified in this work encode proteins of low abundance like YhdV, YddW, and YghB, and Spr is in the bottom 25% range (based on pax-db.org), making their isolation physiologically relevant. We reasoned that the increased synthesis of lipoprotein could cause limitation of the Lol system required for sorting of lipoproteins. Defective lipoprotein is known to induce the Rcs pathway (53). Thus, we tested if the mechanism of activation of the *rpoE*P3 promoter was also Rcs-dependent. Accordingly, expression of the *yhdV* gene was induced in the wild-type and its Δ*rcsB* derivative. This analysis revealed a reduction in the activation of the *rpoE*P3

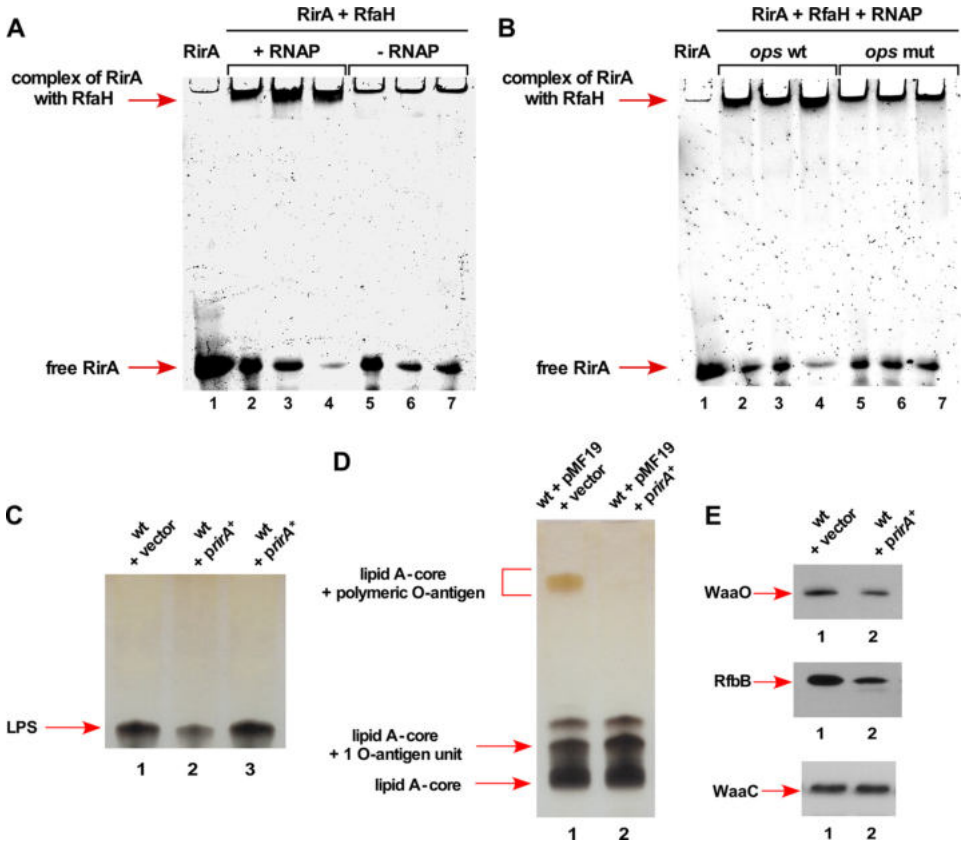

FIGURE 12. **RirA sRNA binds to RfaH and its overexpression causes defects in the LPS synthesis.** *A,* interaction of RirA with RfaH in the presence or absence of RNAP. Fifty ng of RirA were incubated at 37 °C with 150, 300, and 450 ng of RfaH in the presence of 50 μg of RNA polymerase core (*lanes 2–4*) or in the absence of RNAP (*lanes 5–7*). *Lane 1* corresponds to RirA alone. Samples were analyzed on a 6% native polyacrylamide gel. *Arrows* indicate the position of complex and free RirA. *B,* the replacement of the 8-nt *ops* site by 8 A nt in RirA abolishes interaction with RfaH + RNAP core. Fifty ng of wild-type RirA (*lanes 2–4*) and RirA with mutated *ops* site (*lanes 5–7*) were analyzed for the complex formation with RfaH in the presence of RNAP and resolved by native gel electrophoresis. *C,* a portion of whole cell lysate obtained from the wild-type *E. coli* K-12 strain BW25113 with vector pRS551 (*lane 1*), its derivative expressing the wild-type *rirA* gene in pRS551 (*lane 2*), and *rirA* with 8-nt *ops* site replaced by 8 A residues *rirA** (*lane 3*) were applied on a 16.5% SDS-Tricine gel and LPS was revealed after silver staining. The *arrow* indicates the position of the LPS core. *D,* a portion of whole cell lysates after proteinase K treatment obtained from isogenic strains with pMF19 and vector pRS551 alone (*lane 1*) and its derivative expressing the *rirA* gene from its own promoter in pRS551 with pMF19 (*lane 2*) were resolved on a 14% SDS-Tricine gel and LPS was revealed after silver staining. *Arrows* indicate the position of the lipid A-core, lipid A-core + 1 *O*-antigen unit, and lipid A-core + polymeric *O*-antigen. *E,* isogenic cultures carrying vector pRS551 alone (*lane 1*) or expressing the wild-type *rirA* gene (*lane 2*) in the strain with chromosomal *waaO*, *rfbB*, or *waaC* genes epitoped at the C-terminal end with 3× FLAG were grown in LB medium at 30 °C up to an A_{600} of 0.2. An equivalent amount of total protein was analyzed on 12% SDS-PAGE, followed by immunoblotting using anti-FLAG monoclonal antibody.

promoter by more than 50% (Fig. 10*C*). A similar dependence was observed for the lipoprotein-induced *rpoE*P3 activity for the presence of RcsF (data not shown). Hence, these results establish that the Rcs two-component system senses imbalances in the OM due to either LPS defects or overexpression of lipoproteins causing activation of the *rpoE*P3 transcription. However, these results do not show if the overexpression of every lipoprotein will induce the *rpoE*P3 transcription.

The rpoEP3 Promoter Is Subjected to Catabolite Repression

During the quantification of transcription, we repeatedly observed that the activity of the *rpoE*P1-P5 promoter is higher when glycerol is used as the sole carbon source as compared with glucose-supplemented medium (Tables 1 and 2). After the identification of multiple promoters regulating the *rpoE* transcription, this effect was observed more specifically for the *rpoE*P3 promoter. Its activity is also severely repressed upon the addition of glucose to LA medium, like well known CRP-cAMP-regulated genes. It is well established that in the presence of glucose cAMP levels are low, resulting in reduced or lack of expression of promoters that require CRP binding (54). These observations are consistent with the identification of a Tn*10* insertion in the *cya* gene (supplemental Table S1) and an observed 50% reduction in the activity of the *rpoE*P3 promoter in Δ*crp* (Fig. 13*A*). Thus, direct binding of the CRP protein in the presence of cAMP was examined by EMSA using 118-bp DNA fragments that contain nucleotides upstream of the P3 TSS. This DNA template is efficiently shifted in the presence of activated CRP (Fig. 13*B*) consistent with the presence of DNA sequences that match the CRP-binding site (Fig. 3*A*). Overall, these results establish cAMP-CRP-mediated control of *rpoE*P3 transcription.

The RpoE-regulated ecfLM Operon Influences the rpoE Transcription

During the mutagenesis screen for Tn*10* insertion(s) that in *trans* alter the *rpoE* transcription, one mutation mapped to the *ecfL* gene (supplemental Table S1). *ecfL* and *ecfM* genes are transcribed as an operon with a RpoE-dependent transcription (31). Non-polar deletion of either the *ecfL* gene alone or the

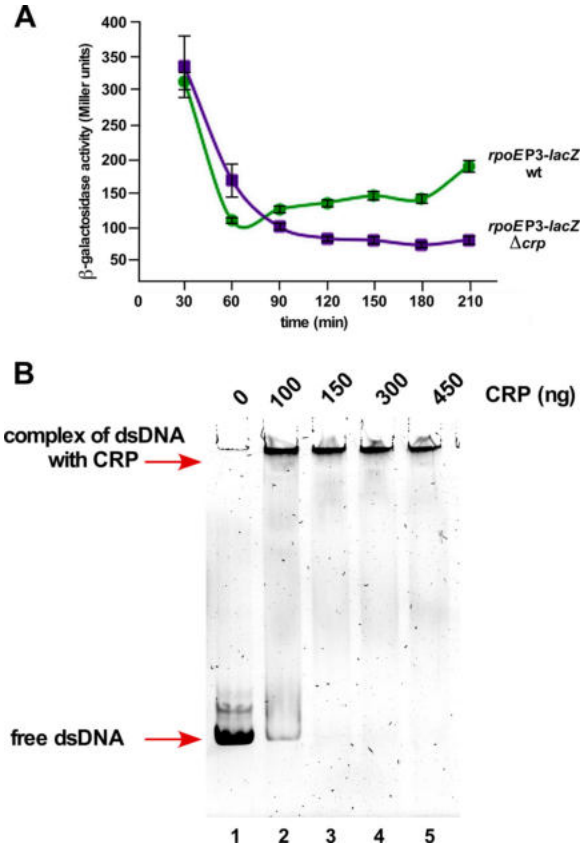

FIGURE 13. **The *rpoE*P3 promoter is positively regulated by the CRP activator protein.** *A,* cultures of the wild-type strain carrying the *rpoE*P3 promoter fusion and its four independent Δ*crp* transductants were grown in LB medium at 30 °C and analyzed for β-galactosidase activity after different intervals. *B,* interaction of CRP with DNA containing the P3 promoter and upstream DNA region. A 118-bp DNA fragment covering the P3 promoter region was incubated with increasing concentrations of CRP activated by cAMP (*lanes 2–5*) and complexes were resolved on a 6% native gel. *Lane 1* serves as a negative control with DNA alone. *Arrows* show the position of free dsDNA and CRP-DNA complex.

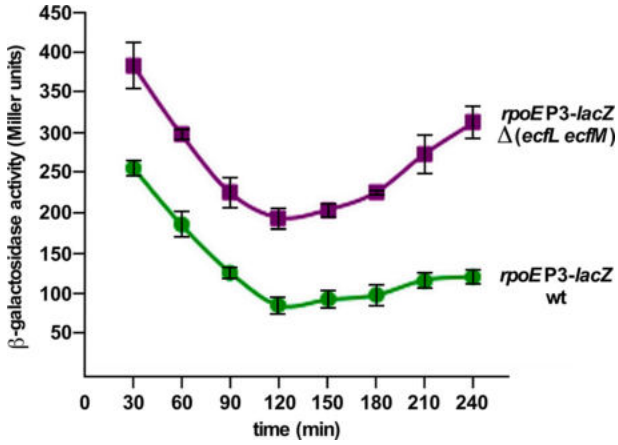

FIGURE 14. **The *rpoE*P3 promoter activity is induced in the absence of *ecfLM* genes.** Isogenic cultures of the wild-type and its Δ(*ecfL ecfM*) derivative carrying the *rpoE*P3 promoter fusion were grown in LB medium at 37 °C and analyzed for the β-galactosidase activity.

ecfM gene alone does not alter the transcriptional activity of any *rpoE* promoters. However, a total deletion of the *ecfLM* operon does increase the *rpoE*P3 activity by a 2–3-fold (Fig. 14). EcfL belongs to the family of conserved DedA IM proteins (31). Consistent with our data, it has been recently reported that multiple deletion combinations of *ecfL* orthologs, including *ecfL*, cause an increase in the *rpoE* transcriptional activity (55). EcfM, also called MzrA (56), could act as a connector protein in cross-talk among two-component systems and needs more studies.

Discussion

In this work, we addressed the transcriptional regulation of the *rpoE* gene, encoding the extracytoplasmic function σ factor. Several members of its regulon have dedicated functions, particularly whose products are involved in the assembly of OM, including components of LPS translocation, OM protein maturation, and some sRNAs that maintain homeostasis of OM components (31). Despite the wealth of knowledge about the function of RpoE and its negative regulation by the anti-σ factor RseA, transcriptional regulation of the *rpoE* gene has not been fully understood. Previously, we and others showed that transcription of the *rpoE* gene is autoregulated by $E\sigma^E$ from one of its promoters (3, 16). However, the regulation of transcription from its distal promoter remained elusive for more than two decades.

The construction of various transcriptional fusions and the identification of *trans*-acting factors that modulate the *rpoE* transcription revealed that the distal promoter region responds to several divergent stimuli. Factors that alter the *rpoE* transcription from the distal promoter region include activation by (i) severe defects in LPS, (ii) the addition of ammonium metavanadate, (iii) entry into the stationary phase, (iv) a shift to high osmolarity, (v) growth phase-dependent challenge with polymyxin B, (vi) a shift to nitrogen-limiting growth conditions, and (vii) overexpression of certain genes encoding lipoproteins. However, transcription is repressed in glucose-supplemented medium. Significantly, no single transposon insertion or any defined deletion could be identified that totally abolished transcription from this promoter region. These results suggested that either an essential transcriptional factor regulates expression of the *rpoE* gene from the upstream region or multiple transcriptional factors are involved in mediating the transcriptional control.

To address possibilities of the existence of multiple regulatory controls, 5′ ends of the *rpoE* mRNA were mapped. This led to the identification of at least five new transcriptional start sites located upstream of the $E\sigma^E$-transcribed promoter. The presence of multiple authentic promoters was confirmed by *in vitro* run-off assays and the construction of the single-copy promoter fusion to individual promoters. Of five promoters, P2 and P3 promoters share the same TSS located at −327. The P2 promoter shares homology to RpoN-regulated promoters with the presence of conserved −12 and −24 RpoN recognition sites. Interestingly, the P2 promoter is strongly activated by QseF, which also contains extensive homology to the NtrC family of activators (42). QseF activation of the *rpoE*P2 promoter occurs via RpoN and requires RpoN-recognition motifs (−12 and −24) as shown by mutagenesis and *in vitro* run-off assays. A role for QseF in regulating the *rpoE*P2 promoter was first observed by a nearly 20-fold induction upon overexpression of the OM protein QseG. The *qseG* gene is co-transcribed with

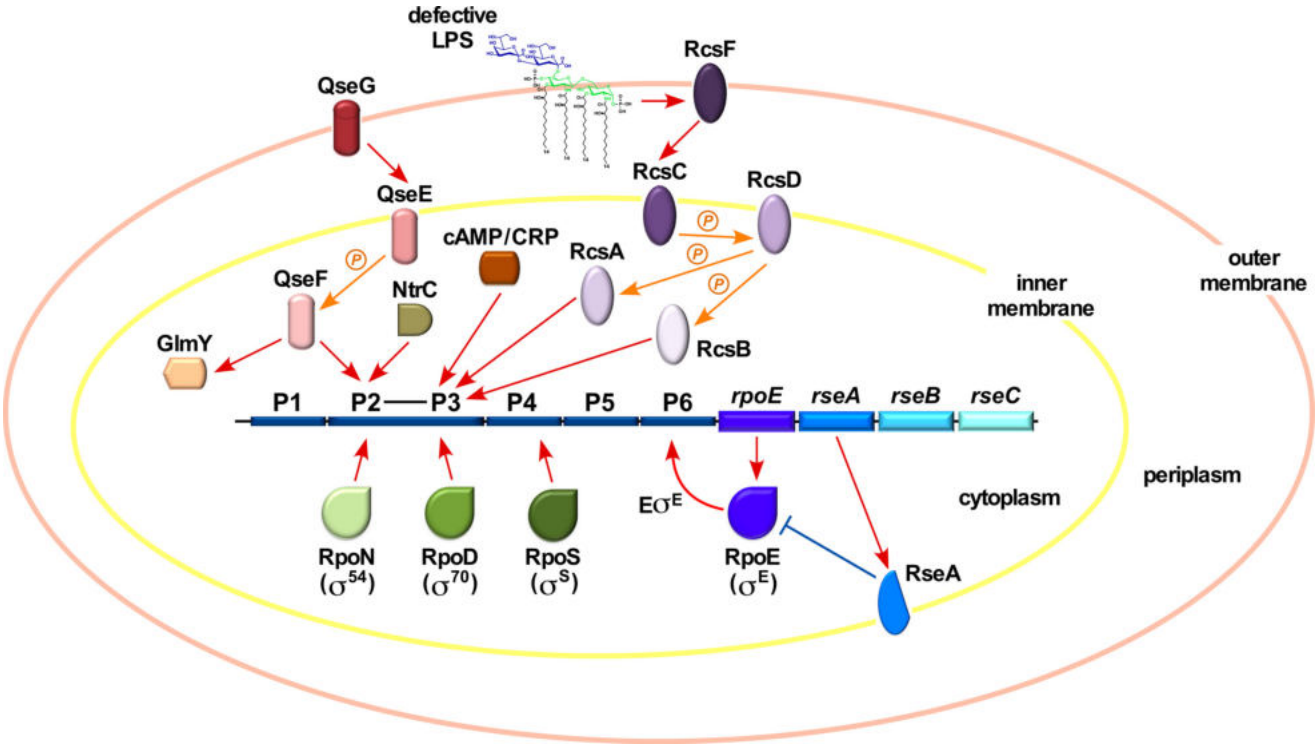

FIGURE 15. **Co-integration of multiple signaling pathways and recruitment of different transcriptional factors in the regulation of the transcription of the *rpoE* gene in response to specific stimuli.** A schematic drawing of the promoter region of the *rpoE* gene, depicting the organization of six promoters designated P1 to P6. The transcription from *rpoE*P6 is initiated by Eσ^E and responds to OM protein defects via the RseA. P2 and P3 promoters utilize the same TSS. The *rpoE*P2 is recognized by σ^{54} and can recruit either NtrC or QseF as activators. The QseE/F system can be activated by QseG. QseE/F-regulated transcription of the *rpoE*P2 and *glmY* sRNA can co-integrate signals of cell envelope constituents like LPS and peptidoglycan synthesis to *rpoE* transcription. The *rpoE*P3 is recognized by σ^{70} and its transcription is specifically induced when LPS biosynthesis is compromised (lack of assembly protein LapB, titration of RfaH by RirA sRNA, or when the inner core of LPS is truncated). LPS defects could the transmit signal from the RcsF OM lipoprotein leading to the activation of the RcsB response regulator. The P2 promoter can also be induced in response to LPS defects albeit to a lower extent than the *rpoE*P3 promoter. The global regulator CRP protein in response to cAMP levels also positively regulates the *rpoE*P3 promoter. The *rpoE*P4 promoter is recognized by the stationary phase σ factor RpoS and is activated in response to diverse stresses like challenge with high osmolarity and factors that regulate transcription of the *rpoS* gene and the stability of σ^S.

qseE and *qseF* genes. QseE and QseF constitute a two-component system that positively regulates the expression of the promoter of the *glmY* sRNA in an RpoN-dependent manner (42). GlmY regulates the synthesis of GlmS in response to amounts of glucosamine 6-phosphate (GlcN6P). GlcN6P is the precursor for the synthesis of UDP-GlcNAc and hence, it constitutes the first rate-limiting step in LPS and peptidoglycan synthesis (17, 42). QseG interaction with the QseE kinase could trigger phosphorylation of the QseF response regulator. Indeed, activation of the *rpoE*P2 promoter by overexpression of *qseG* is solely dependent on the presence of QseF. Examination of the DNA sequence upstream of the *rpoE*P2 promoter identified three QseF-binding sites in the upstream region, which were verified by gel-retardation assays. A fourth QseF binding-like motif is also present in the downstream region of the *rpoE*P2 promoter.

The predicted −10 promoter element of *rpoE*P3 contains a consensus for RpoD-recognized promoters, with the presence of conserved −7T and −11A residues and an extended −10 TGC (Fig. 3). Mutation of −7T(C) and −11A(G) severely repressed the *rpoE*P3 promoter activity. This allowed us to establish that the −327 TSS is used by RpoD and RpoN. The −326 TSS could arise due to *in vivo* processing of the 5′ end or may be used *in vivo* under specific conditions. The RpoD-regulated P3 promoter is further subjected to catabolite repression and activated specifically when the LPS has truncation in the inner core region or the LPS assembly is dysfunctional.

As the *rpoE* gene is essential in *E. coli* under all growth conditions, the presence of multiple promoters regulated by RpoN (P2), RpoD (P3), and RpoS (P4) ensures that the basal level of transcription is sustained even when the OM integrity is not compromised (Fig. 15). Furthermore, each of these promoters fine-tunes transcription under specific conditions. Thus, the induction of the *rpoE* transcription upon entry into the stationary phase could recruit RpoS via the initiation from the P4 promoter. The P4 promoter utilization could integrate diverse signals that regulate the activity of RpoS. RpoS is induced not only in the stationary phase, but also upon challenge with high osmolarity, carbon starvation, oxidative stress, and in response to stringent growth conditions. We also observed that *rpoE*P4 is induced upon the shift to high osmolarity. In support of the RpoS-mediated transcription of the P4 promoter, our genetic analyses also identified factors that control the RpoS transcription/stability, like ArcA/B, RssB, and PcnB affecting the *rpoE*P4 activity.

The Mechanism of Sensing of LPS Alterations and the Overexpression of Lipoproteins—As the maximal number of mutations that induce transcription from the *rpoE* proximal promoter caused LPS defects, the mode of signal transduction was

addressed. LPS defects significantly induce the RpoD-regulated *rpoE*P3 promoter that was dependent on the activation of the Rcs two-component system. Thus, the induction of this promoter was mitigated in the absence of either the OM protein RcsF or the response regulator RcsB when either were challenged with polymyxin B or when the LPS synthesis was defective. This mode of the *rpoE*P3 promoter activation via the Rcs system was demonstrated using strains with truncation of the LPS inner core or strains lacking LPS regulators like RfaH or LapA/B proteins. However, some signals due to LPS defects are also transmitted to the P2 promoter in the RpoN-QseF dependent manner. To distinguish between the activation of P2 and P3 promoters, mutations were introduced in either RpoN recognition sequences or in the −10 conserved element recognized by RpoD. Usage of such mutated promoter fusions confirmed that both P2 and P3 promoters can be activated when LPS is defective, with the main signal activation mediated by the Rcs system to the RpoD-regulated P3 promoter. Observed binding of RcsB and QseF upstream of the P2/P3 TSS further supports these conclusions.

The molecular basis of RpoE induction due to specific LPS defects and participation of any specific signal relay system, like Rcs or other two-component systems, has not been addressed. Two models have been proposed, suggesting sensing of acylation defects in lipid A and a trade-off between the lipopolysaccharide transporter LptA and RpoE negative regulator RseB (38, 57). However, as shown here, the Rcs system can independently sense LPS defects. Our data of signal transduction via multiple systems are compatible with additional modules like RseB and sensing involving additional pathways like the QseGEF system that can signal LPS defects. In support of such a model, we still observed a nearly 2-fold induction of the Eσ^E-regulated promoter of the *rpoE* gene in Δ(*waaC rcsB*) and also involvement of RpoN-mediated Qse-dependent control. Utilization of multiple pathways could make the system to launch rapid response and make it more robust.

One of the novel findings from this work is the identification of a new 73-nt sRNA located in the 5′ UTR of *waaQ* mRNA. This sRNA shares the same start site as the *waaQ* mRNA and contains the *ops* site recognized by RfaH. This sRNA, designated RirA, binds RfaH in the presence of the RNAP core. The *rirA* gene was cloned, because its overexpression induces the *rpoE* transcription via the P3 promoter. Based on the LPS profile, a mild overexpression of the *rirA* sRNA caused severe reduction in the incorporation of *O*-antigen. When RirA was overexpressed in a wild-type *E. coli* K-12, which does not synthesize *O*-antigen, the overall LPS amount was reduced. RfaH regulates the expression of many long operons including *waaQ* and *rfb* operons by preventing transcription termination and enhancing translation of their mRNAs. RfaH is known to bind to *ops* sites and our model of reduction of the LPS amount and severe decrease in the *O*-antigen incorporation upon the *rirA* overexpression posits that an excess of RirA could titrate RfaH. This could make RfaH limiting and reduce the expression of operons that require RfaH, like *rfb* and *waaQ* operons. Thus, the induction of *rpoE* transcription upon *rirA* overexpression can be attributed to limiting amounts of LPS or an imbalance with other components of the OM. Hence, not only LPS defects, but also any imbalance (excess of LPS as with *lapAB* mutants or its reduction when RirA is in extra copies) are sensed by the *rpoE*P3-dependent transcriptional response. It is tempting to speculate that an accumulation of RirA sRNA under regulated mRNA processing of the *waaQ* UTR might constitute an internal checkpoint to balance the LPS synthesis.

Furthermore, it was noticed that overexpression of genes encoding some lipoproteins causes an induction of the *rpoE*P3 promoter. Mislocalization of lipoproteins has been shown to cause induction of the Rcs pathway (53). Consistent with the positive regulation of the *rpoE*P3 promoter by the Rcs system, its activation by overexpression of the lipoproteins is also Rcs-dependent. Among the genes encoding lipoproteins identified in this work that induce the *rpoE*P3 transcription, *yhdV*, *yghG*, *spr*, and *yceB* were previously shown to induce the transcription of the *rpoE*-regulated *degP* promoter (58). Some of the lipoproteins are known to show significant genetic interactions with several components of LPS biosynthesis (59). For example, *yceB* shows interactions with many genes whose products are involved in LPS and phospholipid biosynthesis. Thus, an excess of such lipoproteins could alter the delicate balance in the cell envelope leading to induction of *rpoE* transcription.

In summary, we have shown that in addition to autoregulation by RpoE, transcription of the *rpoE* gene is further regulated by RpoS, RpoD, and RpoN σ factors that specifically respond to different stimuli to sustain its transcription under all growth conditions (Fig. 15). Additional recruitment of envelope responsive two-component systems (QseE/F and Rcs) and global regulator CRP further modulate transcriptional of the *rpoE*P2 and P3 promoters linking several networks to regulate the expression of RpoE. This mode of interlinked regulatory control allows integration of several signals to rapidly respond to a variety of stress conditions and cell envelope defects including LPS alterations.

Experimental Procedures

Bacterial Strains, Plasmids, and Media—The bacterial strains and plasmids used in this study are described in supplemental Table S1. Luria-Bertani (LB) broth, M9 (Difco), and 121 phosphate-limiting minimal media were prepared as described (19, 60). For assays monitoring response to nitrogen concentrations, minimal medium was supplemented with either 3 or 10 mM NH_4Cl. When required, media were supplemented with ampicillin (100 μg ml^{-1}), kanamycin (50 μg ml^{-1}), tetracycline (10 μg ml^{-1}), spectinomycin (50 μg ml^{-1}), or chloramphenicol (20 μg ml^{-1}). The indicator dye 5-bromo-4-chloro-3-indolyl-β-D-galactopyranoside (X-Gal) was used at final concentrations of 20 or 40 μg ml^{-1} in the agar medium. Ammonium metavanadate was added at a final concentration of 25 μg ml^{-1} to LB or LA media. Polymyxin B (Sigma) was added to LB medium at concentrations ranging from 0.2 to 0.3 μg ml^{-1}. Lactose-containing MacConkey agar (Difco) was supplemented with appropriate antibiotics when required.

The Isolation of Trans-acting Mutations—The MC4100-derived bacterial strain SR4245 and the BW25113 derivative SR7917 were used as parental strains to isolate Tn*10* insertion mutants. Each of these strains carries an identical single-copy chromosomal transcriptional *rpoE*P-*lacZ* fusion at the λ

attachment site as bacteriophage λ lysogen. Given the essentiality of the *rpoE* gene, a chromosomal replacement of the wild-type *rpoE* gene with such *rpoE*P-*lacZ* fusion was not attempted. More than 50,000 transposon insertion mutants were isolated on LA medium at 30 °C and screened for Lac up or down phenotypes as described previously (3, 61). Bacteriophage P1 or T4 lysates were prepared on individual Lac up candidates and transduced back into SR4245 or SR7197. The position of Tn*10* was determined by the inverse PCR with nested primers and sequenced using the Tn*10* primer as described previously (9).

The Identification of Trans-acting Factors Whose Overexpression Alters the rpoE Transcription—The complete genomic library of all predicted ORFs of *E. coli* cloned in pCA24N (33) was used to transform SR4245, SR7917 (carrying *rpoE*P1-P5-*lacZ* fusion), SR18874 (*rpoE*P4-*lacZ*), and SR18868 (*rpoE*P2/P3-*lacZ*). The plasmid carrying the *lacZ* gene was omitted to reduce the background noise. Lac up or Lac down transformants were isolated at 30 °C in the presence of IPTG (50 μM) based on X-Gal phenotype. DNA insert of all relevant plasmids that yielded reproducible results was sequenced. In parallel, previously described whole genomic libraries obtained from the wild-type *E. coli* K-12, cloned in medium-copy plasmids (9, 35), were used in similar screens to identify genes whose overexpression alters the *rpoE* transcriptional activity. The minimal genomic DNA fragment cloned in the same plasmid was obtained by standard subcloning.

Generation of Null Mutations and the Construction of Their Combinations—Non-polar antibiotic-free deletion mutations of various genes used in this study were constructed by using the λ Red recombinase/FLP-mediated recombination system as described previously (9, 39, 62). PCR products from such amplification reactions were electroporated into BW25113 containing the λ Red recombinase-encoding plasmid pKD46 (GK1942). Each deletion was verified by PCR amplification and sequencing of PCR products. Such deletions were transduced into BW25113 by bacteriophage T4-mediated transduction. Multiple null combinations were constructed as described previously, followed by the removal of *aph* or *cat* cassettes using the pCP20 plasmid and confirmed to be non-polar. The construction of deletion derivatives of *waaC*, *waaO* genes, and the Eσ^E-regulated *rpoE-lacZ* fusion were previously described (3, 9, 19).

Cloning of Various Genes for Their Overexpression and Complementation Studies—For protein induction, the minimal coding sequences of *rpoS*, *ntrC*, *qseF*, *rcsA*, *rcsB*, and *crp* genes of *E. coli* were cloned in different expression vectors. The minimal coding region of each relevant gene was PCR-amplified, digested with specific restriction endonucleases, and cloned in expression vectors. *rcsA* and *rcsB* genes were cloned in pET22b (NdeI-XhoI), resulting in plasmids pGK4661 and pGK4662. In parallel, *crp* and *rpoS* genes with the C-terminal His_6 tag were cloned in pET22b and pET24b (NdeI-XhoI), resulting in plasmids pSR16739 and pSR16691, respectively. These plasmids were verified to retain wild-type properties of the respective genes by confirming the complementation of strain Δ*crp* (GK2986) and Δ*rpoS* (GK2876). *qseF* and *ntrC* genes with the C-terminal His_6 tag were cloned in pET28b (NdeI-XhoI) (pSR13036 and pSR18976, respectively). For the induction of RpoN and RfaH, the expression of corresponding genes was induced from clones in the expression vector pCA24N (34).

For LPS analysis and quantification of changes in the *rpoE* transcription, the *rirA* gene with its own promoter was subcloned into the pRS551 vector (pSR9446). The minimal coding region of *rirA* sRNA was PCR-amplified from the chromosomal DNA obtained from the wild-type strain BW25113 using specific oligonucleotides (supplemental Table S2).

RNA Purification and Mapping of 5′ Ends—For the identification of the transcription start site(s) of *rpoE* and *rirA* mRNAs, total RNA was extracted from wild-type strain BW25113 and its Δ*waaC* derivative or in the presence of multicopy inducers of the *rpoE* transcription. Cultures were grown in LB medium at 30 °C until an absorbance of 0.2 at 600 nm (exponential phase) or after entry into the stationary phase. RNA was purified according to the manufacturer's protocol (Bioline UK) and digested with RQ1 DNase (Promega) to remove any chromosomal DNA, followed by phenol extraction and RNA precipitation.

The GeneRacer from Invitrogen was used to obtain 5′ ends of cDNA according to the manufacturer's protocol as described previously (9). RNA with and without treatment with calf intestinal phosphatase was used to identify primary and processed products according to the manufacturer's instructions. The cDNA was amplified by PCR using 2 pmol of reverse gene-specific primers (supplemental Table S1) and the GeneRacer 5′ primer. An additional round of nested PCR was employed, using GeneRacer-nested and gene-specific oligonucleotides (supplemental Table S2). PCR products from the second round nested PCR were purified and cloned into the pCR-4-TOPO vector. From each reaction, at least 10 independent plasmids were isolated and sequenced using the M13 forward primer (−21 universal).

In Vitro Run-off Assays—For the identification of the transcription initiation site with specific forms of RNA polymerase, DNA template (50 ng) was incubated with the core RNAP and the specific σ factor at a molar ratio of 4:1. Twenty μl of reaction was carried in buffer containing 40 mM Tris-HCl, pH 7.5, 150 mM KCl, 10 mM $MgCl_2$, 1 mM DTT, 0.5 mM each of ATP, GTP, CTP, and 0.1 mM UTP plus 3.7 kBq of [α-^{32}P]UTP. The reaction was allowed to proceed for 20 min at 37 °C, as described previously (3), and terminated by the addition of formamide stop solution. For *in vitro* assays with RpoN, NtrC, and QseF, the wild-type template and the template with mutations in the −12 and −24 elements were used. After the open complex formation in reactions with RpoN + NtrC and RpoN + QseF, 5 mM ATP was added and further incubated at 37 °C for 5 min before the addition of nucleotides. RNA samples (4 μl) labeled with [α-^{32}P]UTP were electrophoresed as described previously (3).

Gel Retardation Assays—EMSAs were performed on PCR-generated probes containing various sizes of DNA. When required, mutations were introduced using specific oligonucleotides during PCR (supplemental Table S2). Binding reactions were performed by incubating 35 ng of various DNA probes with an increasing amount of purified RcsB or RcsA or CRP or QseF, using binding buffer (Invitrogen). Whenever required, RcsB and QseF were phosphorylated with acetyl-phosphate at 30 °C for 30 min. Similarly, the CRP-cAMP complex was gen-

erated by the incubation of purified CRP with 1 mM cAMP in buffer containing 10 mM Tris-HCl (pH 7.8 at 4 °C), 150 mM NaCl, and 3 mM $Mg(OAc)_2$. Products were analyzed on 4 or 6% native acrylamide gel and visualized after staining with SYBR Green (Invitrogen).

β-Galactosidase Assays—To measure the activity of *rpoE* promoters, single-copy chromosomal promoter fusions to the *lacZ* gene were constructed and used to monitor their β-galactosidase activity. DNA sequences located upstream of the known RpoE-autoregulated promoter were amplified by PCR, using specific oligonucleotides (supplemental Table S2). After PCR amplification, gel-purified DNA was digested with EcoRI and BamHI, cloned into either pRS415 or pRS551 vector, and transferred to the chromosome in a single-copy by recombination with λRS45 (63). Lysogens were selected either on the basis of Lac^+ phenotype or by directly selecting for Kan-resistant lysogens as described previously (3, 6, 9). Mutations in the −12 and −24 regions of the RpoN-regulated P2 promoter were introduced by PCR using mutagenic oligonucleotides (supplementalTableS2), cloned into pRS551 and transferred to the chromosome to generate single-copy promoter fusion (SR18987). Nucleotide changes corresponding to the −7T and −11A residues of the *rpoE*P3 promoter were constructed similarly with mutagenic oligonucleotides and cloned in pRS551. Such single-copy lysogens carrying *lacZ* fusions with mutated promoter regions were directly selected for Kan resistance (SR19089) and verified. Null alleles in different genes studied in this work were transduced into strains carrying various *rpoE-lacZ* promoter fusions in a single-copy on the chromosome. To measure the β-galactosidase activity, isogenic bacterial strains carrying promoter fusions were grown in LB or M9 medium with appropriate antibiotics at 30 °C, adjusted to an A_{600} of 0.05 and allowed to grow further. The β-galactosidase activity was measured in Miller units at different growth intervals from four independent cultures in each case as described previously (6, 9).

Protein Purification—The expression of His_6-tagged RpoN, RfaH was induced in the *E. coli* BW25113 strain at an optical density of 0.1 at 600 nm in a 1-liter culture by the addition of 0.5 mM IPTG. For the purification of His_6-tagged RpoS, CRP, RcsB, RcsA, NtrC, and QseF, their cognate genes cloned in pET expression vectors were induced in *E. coli* BL21(DE3) strain at 28 °C. After induction (4 h-5 h at 28 °C), cells were harvested by centrifugation at 12,000 rpm for 20 min. The pellet was resuspended in B-PER reagent (Pierce) and adjusted to contain 50 mM NaH_2PO_4, 300 mM NaCl, 10 mM imidazole (buffer A), supplemented with lysozyme to a final concentration of 200 μg ml^{-1}. A mixture of protease inhibitors (Sigma) was added as per the manufacturer's instructions. The mixture was incubated on ice for 15 min with gentle mixing. To this lysate, 30 units of benzonase (Merck) was added and incubated with gentle mixing at 4 °C for another 15 min. The mixture was centrifuged at 45,000 × *g* for 30 min at 4 °C. Soluble proteins were applied over nickel-nitrilotriacetic acid beads (Qiagen), washed, and eluted with buffer A with a linear gradient (50 mM- 500 mM) of imidazole.

LPS Extraction—LPS was extracted by the phenol/chloroform/petroleum ether procedure (64) from cultures grown in phosphate-limiting medium and lyophilized. For the LPS analysis, lyophilized material was dispersed in water by sonication and resuspended at a concentration of 2 mg ml^{-1}. For detection of the chemotype, an equivalent portion of whole cell lysate treated with proteinase K was applied to a 16.5% Tricine gel. To detect *O*-antigen, cultures of BW25113 carrying the vector alone (pRS551) or its derivative carrying the *rirA* sRNA expressed in pRS551, were transformed with the plasmid pMF19 (to restore the *O*-antigen biosynthesis). In these experiments, samples were applied on 14% Tricine gel. Gels were silver-stained for the LPS analysis.

Mass Spectrometry—Electrospray ionization-Fourier transform ion cyclotron (ESI-FT-ICR)-mass spectrometry was performed on intact LPS in the negative ion mode using an APEX QE (Bruker Daltonics) equipped with a 7-tesla actively shielded magnet and dual ESI-MALDI. LPS samples were dissolved at a concentration of ~10 ng μl^{-1} and analyzed as described previously (6, 19). For the nonspecific fragmentation, the DC offset (collision voltage) of the quadruple interface was set from 5 to 30 V. Under these conditions, the labile linkage between lipid A and the core oligosaccharide is cleaved. Mass spectra were charge deconvoluted, and mass numbers given refer to the monoisotopic peaks.

Author Contributions—S. R. and G. K. designed the study and performed *in vitro* run-off assays and wrote the manuscript. G. K., A. S., P. W., and D. B. conducted genetic screens, quantified promoter strengths, and purified various proteins used in this study. G. K. purified LPS and B. L. performed MS analysis. All authors analyzed the results and approved the final version of the manuscript.

Acknowledgments—We thank D. Missiakas, G. Storz, M. Valvano, M. Yamada, and H. Brade for helpful suggestions and D. Clark and H. Mori for the gift of strains. We also acknowledge contributions made by Y. Yun, P. Sulima, A. Przeslakiewicz, J. Barski, D. Polak, P. Gorzelak, and M. Grygorewicz.

References

1. Raetz, C. R., and Whitfield, C. (2002) Lipopolysaccharide endotoxins. *Annu. Rev. Biochem.* **71,** 635–700
2. Gronow, S., Xia, G., and Brade, H. (2010) Glycosyltransferases involved in the biosynthesis of the inner core region of different lipopolysaccharides. *Eur. J. Cell Biol.* **89,** 3–10
3. Raina, S., Missiakas, D., and Georgopoulos, C. (1995) The *rpoE* gene encoding the σ^E (σ^{24}) heat shock σ factor of *Escherichia coli*. *EMBO J.* **14,** 1043–1055
4. Missiakas, D., Betton, J. M., and Raina, S. (1996) New components of protein folding in extracytoplasmic compartments of *Escherichia coli* SurA, FkpA and Skp/OmpH. *Mol. Microbiol.* **21,** 871–884
5. Raina, S., and Georgopoulos, C. (1991) The *htrM* gene, whose product is essential for *Escherichia coli* viability only at elevated temperatures, is identical to the *rfaD* gene. *Nucleic Acids Res.* **19,** 3811–3819
6. Klein, G., Lindner, B., Brabetz, W., Brade, H., and Raina, S. (2009) *Escherichia coli* K-12 suppressor-free mutants lacking early glycosyltransferases and late acyltransferases: minimal lipopolysaccharide structure and induction of envelope stress response. *J. Biol. Chem.* **284,** 15369–15389
7. Parker, C. T., Kloser, A. W., Schnaitman, C. A., Stein, M. A., Gottesman, S., and Gibson, B. W. (1992) Role of the *rfaG* and *rfaP* genes in determining the lipopolysaccharide core structure and cell surface properties of *Escherichia coli* K-12. *J. Bacteriol.* **174,** 2525–2538
8. Majdalani, N., and Gottesman, S. (2005) The Rcs phosphorelay: a complex signal transduction system. *Annu. Rev. Microbiol.* **59,** 379–405

9. Klein, G., Kobylak, N., Lindner, B., Stupak, A., and Raina, S. (2014) Assembly of lipopolysaccharide in *Escherichia coli* requires the essential LapB heat shock protein. *J. Biol. Chem.* **289,** 14829–14853
10. Murata, M., Fujimoto, H., Nishimura, K., Charoensuk, K., Nagamitsu, H., Raina, S., Kosaka, T., Oshima, T., Ogasawara, N., and Yamada, M. (2011) Molecular strategy for survival at a critical high temperature in *Escherichia coli*. *PLoS ONE* **6,** e20063
11. Missiakas, D., Mayer, M. P., Lemaire, M., Georgopoulos, C., and Raina, S. (1997) Modulation of the *Escherichia coli* σ^E (RpoE) heat-shock transcription-factor activity by the RseA, RseB and RseC proteins. *Mol. Microbiol.* **24,** 355–371
12. De Las Peñas, A., Connolly, L., and Gross, C. A. (1997) The σ^E-mediated response to extracytoplasmic stress in *Escherichia coli* is transduced by RseA and RseB, two negative regulators of σ^E. *Mol. Microbiol.* **24,** 373–385
13. Missiakas, D., and Raina, S. (1998) The extracytoplasmic function σ factors: role and regulation. *Mol. Microbiol.* **28,** 1059–1066
14. Ades, S. E. (2008) Regulation by destruction: design of the σ^E envelope stress response. *Curr. Opin. Microbiol.* **11,** 535–540
15. Noor, R., Murata, M., Nagamitsu, H., Klein, G., Raina, S., and Yamada, M. (2009) Dissection of σ^E-dependent cell lysis in *Escherichia coli*: roles of RpoE regulators RseA, RseB and periplasmic folding catalysts PpiD. *Genes Cells* **14,** 885–899
16. Rouvière, P. E., De Las Peñas, A., Mecsas, J., Lu, C. Z., Rudd, K. E., and Gross, C. A. (1995) *rpoE*, the gene encoding the second heat-shock σ factor, σ^E, in *Escherichia coli*. *EMBO J.* **14,** 1032–1042
17. Klein, G., and Raina, S. (2015) Regulated control of the assembly and diversity of LPS by noncoding sRNAs. *Biomed. Res. Int.* **2015,** 153561
18. Needham, B. D., and Trent, M. S. (2013) Fortifying the barrier: the impact of lipid A remodeling on bacterial pathogenesis. *Nat. Rev. Microbiol.* **11,** 467–481
19. Klein, G., Lindner, B., Brade, H., and Raina, S. (2011) Molecular basis of lipopolysaccharide heterogeneity in *Escherichia coli*: envelope stress-responsive regulators control the incorporation of glycoforms with a third 3-deoxy-α-D-*manno*-oct-2-ulosonic acid and rhamnose. *J. Biol. Chem.* **286,** 42787–42807
20. Johansen, J., Rasmussen, A. A., Overgaard, M., and Valentin-Hansen, P. (2006) Conserved small non-coding RNAs that belong to the σ^E regulon: role in down-regulation of outer membrane proteins. *J. Mol. Biol.* **364,** 1–8
21. Guo, M. S., Updegrove, T. B., Gogol, E. B., Shabalina, S. A., Gross, C. A., and Storz, G. (2014) MicL, a new σ^E-dependent sRNA, combats envelope stress by repressing synthesis of Lpp, the major outer membrane lipoprotein. *Genes Dev.* **28,** 1620–1634
22. Coornaert, A., Lu, A., Mandin, P., Springer, M., Gottesman, S., and Guillier, M. (2010) MicA sRNA links the PhoP regulon to cell envelope stress. *Mol. Microbiol.* **76,** 467–479
23. Creeger, E. S., Schulte, T., and Rothfield, L. I. (1984) Regulation of membrane glycosyltransferases by the *sfrB* and *rfaH* genes of *Escherichia coli* and *Salmonella typhimurium*. *J. Biol. Chem.* **259,** 3064–3069
24. Marolda, C. L., and Valvano, M. A. (1998) Promoter region of the *Escherichia coli* O7-specific lipopolysaccharide gene cluster: structural and functional characterization of an upstream untranslated mRNA sequence. *J. Bacteriol.* **180,** 3070–3079
25. Burmann, B. M., Knauer, S. H., Sevostyanova, A., Schweimer, K., Mooney, R. A., Landick, R., Artsimovitch, I., and Rösch, P. (2012) An α helix to β barrel domain switch transforms the transcription factor RfaH into a translation factor. *Cell* **150,** 291–303
26. Yamamoto, K., Hirao, K., Oshima, T., Aiba, H., Utsumi, R., and Ishihama, A. (2005) Functional characterization *in vitro* of all two-component signal transduction systems from *Escherichia coli*. *J. Biol. Chem.* **280,** 1448–1456
27. Guckes, K. R., Kostakioti, M., Breland, E. J., Gu, A. P., Shaffer, C. L., Martinez, C. R., 3rd, Hultgren, S. J., and Hadjifrangiskou, M. (2013) Strong cross-system interactions drive the activation of the QseB response regulator in the absence of its cognate sensor. *Proc. Natl. Acad. Sci. U.S.A.* **110,** 16592–16597
28. Reading, N. C., Rasko, D., Torres, A. G., and Sperandio, V. (2010) A transcriptome study of the QseEF two-component system and the QseG membrane protein in enterohaemorrhagic *Escherichia coli* O157:H7. *Microbiology* **156,** 1167–1175
29. Taylor, W. E., Straus, D. B., Grossman, A. D., Burton, Z. F., Gross, C. A., and Burgess, R. R. (1984) Transcription from a heat-inducible promoter causes heat shock regulation of the σ subunit of *E. coli* RNA polymerase. *Cell* **38,** 371–381
30. Janaszak, A., Nadratowska-Wesołowska, B., Konopa, G., and Taylor, A. (2009) The P1 promoter of the *Escherichia coli rpoH* gene is utilized by σ^{70}-RNAP or σ^S-RNAP depending on growth phase. *FEMS Microbiol. Lett.* **291,** 65–72
31. Dartigalongue, C., Missiakas, D., and Raina, S. (2001) Characterization of the *Escherichia coli* σ^E regulon. *J. Biol. Chem.* **276,** 20866–20875
32. Bianchi, A. A., and Baneyx, F. (1999) Hyperosmotic shock induces the σ^{32} and σ^E stress regulons of *Escherichia coli*. *Mol. Microbiol.* **34,** 1029–1038
33. Baba, T., Ara, T., Hasegawa, M., Takai, Y., Okumura, Y., Baba, M., Datsenko, K. A., Tomita, M., Wanner, B. L., and Mori, H. (2006) Construction of *Escherichia coli* K-12 in-frame, single-gene knockout mutants: the Keio collection. *Mol. Syst. Biol.* 2006.0008
34. Kitagawa, M., Ara, T., Arifuzzaman, M., Ioka-Nakamichi, T., Inamoto, E., Toyonaga, H., and Mori, H. (2005) Complete set of ORF clones of *Escherichia coli* ASKA library (a complete set of *E. coli* K-12 ORF archive): unique resources for biological research. *DNA Res.* **12,** 291–299
35. Missiakas, D., Georgopoulos, C., and Raina, S. (1993) Identification and characterization of the *Escherichia coli* gene *dsbB*, whose product is involved in the formation of disulfide bonds *in vivo*. *Proc. Natl. Acad. Sci. U.S.A.* **90,** 7084–7088
36. Santos, J. M., Freire, P., Mesquita, F. S., Mika, F., Hengge, R., and Arraiano, C. M. (2006) Poly(A)-polymerase I links transcription with mRNA degradation via σ^S proteolysis. *Mol. Microbiol.* **60,** 177–188
37. Zhou, Z., Lin, S., Cotter, R. J., and Raetz, C. R. (1999) Lipid A modifications characteristic of *Salmonella typhimurium* are induced by NH_4VO_3 in *Escherichia coli* K12. Detection of 4-amino-4-deoxy-L-arabinose, phosphoethanolamine and palmitate. *J. Biol. Chem.* **274,** 18503–18514
38. Tam, C., and Missiakas, D. (2005) Changes in lipopolysaccharide structure induce the σ^E-dependent response of *Escherichia coli*. *Mol. Microbiol.* **55,** 1403–1412
39. Klein, G., Müller-Loennies, S., Lindner, B., Kobylak, N., Brade, H., and Raina, S. (2013) Molecular and structural basis of inner core lipopolysaccharide alterations in *Escherichia coli*: incorporation of glucuronic acid and phosphoethanolamine in the heptose region. *J. Biol. Chem.* **288,** 8111–8127
40. Feklistov, A., and Darst, S. A. (2011) Structural basis for promoter-10 element recognition by the bacterial RNA polymerase σ subunit. *Cell* **147,** 1257–1269
41. Syed, A., and Gralla, J. D. (1997) Isolation and properties of enhancer-bypass mutants of σ^{54}. *Mol. Microbiol.* **23,** 987–995
42. Reichenbach, B., Göpel, Y., and Görke, B. (2009) Dual control by perfectly overlapping σ^{54}- and σ^{70}-promoters adjusts small RNA GlmY expression to different environmental signals. *Mol. Microbiol.* **74,** 1054–1070
43. Xiao, J., Chen, T., Yang, M., Zhang, Y., and Wang, Q. (2012) Identification of *qseGF* genetic locus and its roles in controlling hemolytic activity and invasion in fish pathogen *Edwardsiella tarda*. *Lett. Appl. Microbiol.* **55,** 91–98
44. Reading, N. C., Rasko, D. A., Torres, A. G., and Sperandio, V. (2009) The two-component system QseEF and the membrane protein QseG link adrenergic and stress sensing to bacterial pathogenesis. *Proc. Natl. Acad. Sci. U.S.A.* **106,** 5889–5894
45. Muffler, A., Fischer, D., Altuvia, S., Storz, G., and Hengge-Aronis, R. (1996) The response regulator RssB controls stability of the σ^S subunit of RNA polymerase in *Escherichia coli*. *EMBO J.* **15,** 1333–1339
46. Pratt, L. A., and Silhavy, T. J. (1996) The response regulator SprE controls the stability of RpoS. *Proc. Natl. Acad. Sci. U.S.A.* **93,** 2488–2492
47. Madhugiri, R., Basineni, S. R., and Klug, G. (2010) Turn-over of the small non-coding RNA RprA in *E. coli* is influenced by osmolarity. *Mol. Genet. Genomics* **284,** 307–318

48. Pesavento, C., and Hengge, R. (2012) The global repressor FliZ antagonizes gene expression by σ^S-containing RNA polymerase due to overlapping DNA binding specificity. *Nucleic Acids Res.* **40,** 4783–4793
49. Yethon, J. A., Vinogradov, E., Perry, M. B., and Whitfield, C. (2000) Mutation of the lipopolysaccharide core glycosyltransferase encoded by *waaG* destabilizes the outer membrane of *Escherichia coli* by interfering with core phosphorylation. *J. Bacteriol.* **182,** 5620–5623
50. Whitfield, C., and Trent, M. S. (2014) Biosynthesis and export of bacterial lipopolysaccharides. *Annu. Rev. Biochem.* **83,** 99–128
51. Zhou, Z., Ribeiro, A. A., and Raetz, C. R. (2000) High-resolution NMR spectroscopy of lipid A molecules containing 4-amino-4-deoxy-L-arabinose and phosphoethanolamine substituents. Different attachment sites on lipid A molecules from NH_4VO_3-treated *Escherichia coli versus kdsA* mutants of *Salmonella typhimurium*. *J. Biol. Chem.* **275,** 13542–13551
52. Feldman, M. F., Marolda, C. L., Monteiro, M. A., Perry, M. B., Parodi, A. J., and Valvano, M. A. (1999) The activity of a putative polyisoprenol-linked sugar translocase (Wzx) involved in *Escherichia coli* O antigen assembly is independent of the chemical structure of the O repeat. *J. Biol. Chem.* **274,** 35129–35138
53. Tao, K., Narita, S., and Tokuda, H. (2012) Defective lipoprotein sorting induces *lolA* expression through the Rcs stress response phosphorelay system. *J. Bacteriol.* **194,** 3643–3650
54. Browning, D. F., and Busby, S. J. (2004) The regulation of bacterial transcription initiation. *Nat. Rev. Microbiol.* **2,** 57–65
55. Sikdar, R., Simmons, A. R., and Doerrler, W. T. (2013) Multiple envelope stress response pathways are activated in an *Escherichia coli* strain with mutations in two members of the DedA membrane protein family. *J. Bacteriol.* **195,** 12–24
56. Gerken, H., Charlson, E. S., Cicirelli, E. M., Kenney, L. J., and Misra, R. (2009) MzrA: a novel modulator of the EnvZ/OmpR two-component regulon. *Mol. Microbiol.* **72,** 1408–1422
57. Lima, S., Guo, M. S., Chaba, R., Gross, C. A., and Sauer, R. T. (2013) Dual molecular signals mediate the bacterial response to outer-membrane stress. *Science* **340,** 837–841
58. Miyadai, H., Tanaka-Masuda, K., Matsuyama, S., and Tokuda, H. (2004) Effects of lipoprotein overproduction on the induction of DegP (HtrA) involved in quality control in the *Escherichia coli* periplasm. *J. Biol. Chem.* **279,** 39807–39813
59. Babu, M., Díaz-Mejía, J. J., Vlasblom, J., Gagarinova, A., Phanse, S., Graham, C., Yousif, F., Ding, H., Xiong, X., Nazarians-Armavil, A., Alamgir, M., Ali, M., Pogoutse, O., Pe'er, A., Arnold, R., *et al*. (2011) Genetic interaction maps in *Escherichia coli* reveal functional crosstalk among cell envelope biogenesis pathways. *PLoS Genet.* **7,** e1002377
60. Torriani, A. (1960) Influence of inorganic phosphate in the formation of phosphatases by *Escherichia coli*. *Biochim. Biophys. Acta* **38,** 460–469
61. Klein, G., Dartigalongue, C., and Raina, S. (2003) Phosphorylation-mediated regulation of heat shock response in *Escherichia coli*. *Mol. Microbiol.* **48,** 269–285
62. Datsenko, K. A., and Wanner, B. L. (2000) One-step inactivation of chromosomal genes in *Escherichia coli* K-12 using PCR products. *Proc. Natl. Acad. Sci. U.S.A.* **97,** 6640–6645
63. Simons, R. W., Houman, F., and Kleckner, N. (1987) Improved single and multicopy *lac*-based cloning vectors for protein and operon fusion. *Gene* **53,** 85–96
64. Galanos, C., Lüderitz, O., and Westphal, O. (1969) A new method for the extraction of R lipopolysaccharides. *Eur. J. Biochem.* **9,** 245–249